Time-Dependent Eco-Efficiency Assessment in the Production of Composite Structures

Case study from manufacturing aircraft ribs made of fiber-reinforced polymer (FRP)

Von der Fakultät für Maschinenbau
der Technischen Universität Carolo-Wilhelmina zu Braunschweig

zur Erlangung der Würde

eines Doktor-Ingenieurs (Dr.-Ing.)

genehmigte Dissertation

von: Ali Al-Lami
aus (Geburtsort): Baghdad

eingereicht am: 18. Januar 2021
mündliche Prüfung am: 31. März 2021

Gutachter: Prof. Dr.-Ing. Michael Sinapius
Prof. Dr. Thomas S. Spengler

2021

***„It's not what happens to you, but how you react to it that matters*“**
Epictetus

Declaration

I hereby declare that except where specific reference is made to the work of others, the contents of this dissertation are original and have not been submitted in whole or in part for consideration of any other degree or qualification in this, or any other university. This dissertation is the result of my own work and includes nothing which is the outcome of work done in collaboration, except where specifically indicated in the text.

Ali Al-Lami
January 2021

Acknowledgements

This thesis has been carried out during my work as a research associate at the German Aerospace Center (DLR) between 2015 and 2020 in the Institute of Composite Structures and Adaptive Systems.

First, I would like to acknowledge the unlimited support of my family especially my father and mother. Their continuous encouragement has enabled me to accomplish this milestone inter alia. I am thankful for my supportive siblings as well as my lovely nephews and niece.

The targets of this thesis could only be achieved with the great support and assistance from the Institute of Composite Structures and Adaptive Systems at DLR and the Institute of Mechanics and Adaptronics (former: Institute of Adaptronic and Functional Integration) at the Technical University in Braunschweig. I would like to express my appreciation to Prof. Dr.-Ing. Michael Sinapius, my doctoral supervisor and director of the Institute of Mechanics and Adaptronics, for giving me the opportunity and continuous support to write this thesis. His unlimited advisement and available guidance have not only motivated me to carry out this work but also encouraged me to achieve its current level. I am very thankful to Prof. Dr. Thomas Spengler, the head of the Institute of Automotive Management and Industrial Production at the Technical University in Braunschweig, and his team for the cooperative work they carried out to assist me in covering the economic aspects in this work.

It is my pleasure to work in the Institute of Composite Structures and Adaptive Systems under the supervision of Prof. Dr.-Ing. Martin Wiedemann the head of the institute, whom unlimited support and inducement have enabled the realization of the associated concepts, systems, and experiments in this thesis. Many thanks to the specialist advisor of my thesis Dr.-Ing. Philipp Hilmer for the continuous support and assistance he provided me with. Thanks a lot for his useful advice, suggestions, and help, which had a significant effect in achieving the aimed targets of this thesis as well as several previous scientific works. For facilitating the accomplishment of many thesis related projects and milestones, I am also very thankful for the great support I received from Dr.-Ing. Markus Kleineberg the head of my department.

Special thanks go to our EVo-team in Stade especially Sven Torstrick-von der Lieth and Ricardo Carneiro. For the assistance in reviewing the multidisciplinary fields in this thesis, I am grateful for the efforts of Dr.-Ing. Christian Willberg, Dr.-Ing. Nico Liebers, and Dr.-rer.-nat. Michael Rose. I am thankful for the efforts of my students including Hans-Christian Rudolf, Sven Leitsch, Andreas Schachinger, and Vivek Barthwal. I would like here to thank the laboratory staff in Branschweig including Kathrin Löbel, Konstantin Schmidt, Eric Bünger, and Gezim Bajrami for their continuous cooperation. Furthermore, many thanks to DLR library staff especially Katrin Bosselmann and Ann-Kathrin Christann.

Abstract

Nowadays, technologies are continuously developed to efficiently produce structures made of fiber-reinforced polymers (FRPs) in several industries including aerospace. This necessitates assessing the eco-efficiency of process variants to identify the drivers of their economic and ecological impacts. Therefore, play the decision support systems (DSSs) for assessment a crucial role in shaping the future of FRPs production. In practice, such assessment DSSs should be based on collected process data and they have to be adaptable to relevant process scenarios. Moreover, decision-making should be performed in a timely manner within modern production. Therefore, time-dependent assessment capabilities are a key in covering these process variants and providing the timely decision-making.

In literature, there is a wide range of frameworks and concepts that serve only particular aspects of time-dependent eco-efficiency assessment in FRP production. Not only frameworks for life-cycle assessment (LCA), modeling, and Industry 4.0, but also selected concepts and works for time-dependent assessment and real-time data collection are considered in the literature review.

Based on these conventional approaches, a comprehensive framework for a time-dependent eco-efficiency assessment in FRP production has been introduced in this thesis. To realize this framework, the previously developed eco-efficiency assessment model (EEAM) is enhanced and implemented in assessing parametrized FRPs production. Moreover, the concept of smart-work-station (SWS) is established to provide process data in real-time. Similar to the framework, the SWS concept is developed to be adaptable to a variety of associated FRP products and process scenarios within defined system boundaries. The SWS concept includes the determination of required sensor nodes to gather the relevant initial data. The introduced time-dependent approach in this thesis is a key not only in realizing the assessment and comparison of process and product variants but also in facilitating the eco-efficiency estimation in the early development phases.

As a case study, the highly-automated manufacturing of vertical stabilizer ribs in a commercial aircraft is selected to examine the framework, realize the data collection concept of SWS, and validate the results of EEAM. The results of assessing this case study show a direct cost of around 221.3 €/kg and the carbon footprint of around 105.7 kg CO_2/kg from the considered preparing, cutting, preforming, and trimming unit processes (UPs). These time-dependent economic and ecological impacts are allocated to their drivers in each UP and validated.

Kurzfassung

Heutzutage unterliegen Technologien zur effizienten Produktion von Strukturen aus faserverstärkten Polymeren in verschiedenen Industriezweigen einschließlich der Luftfahrt einer ständigen Weiterentwicklung. Dies macht es erforderlich, die Ökoeffizienz von Prozessvarianten zu bewerten, um die Treiber ihrer ökonomischen und ökologischen Auswirkungen aufzuspüren. Daher spielen Entscheidungsunterstützungswerkzeuge zur Prozessbewertung eine entscheidende Rolle bei zukünftiger Produktion der Strukturen aus faserverstärkten Polymeren. In der Praxis sollten solche Bewertungsunterstützungssysteme auf gesammelten Prozessdaten basieren und sie müssen für relevante Prozessszenarien anpassbar sein. Darüber hinaus ist diese Entscheidungsfindung ein zeitgemäßer Ansatz in moderner Produktion. Deshalb ist die zeitabhängigen Bewertungsfähigkeit ein Schlüssel zur Abdeckung dieser Prozessvarianten und zur rechtzeitigen Entscheidungsfindung.

In der Literatur gibt es eine Vielzahl von Rahmenwerken und Konzepten, die nur bestimmten Aspekten der zeitabhängigen Ökoeffizienz-Bewertung in der Produktion von Strukturen aus faserverstärkten Polymeren dienen. In der Literaturübersicht dieser Arbeit sind nicht nur Rahmenwerke für die Ökobilanzierung, Modellierung und Industrie 4.0, sondern auch ausgewählte Konzepte und Studien zur zeitabhängigen Bewertung und Echtzeit-Datenerfassung betrachtet.

Basierend auf diesen konventionellen Ansätzen wurde in dieser Arbeit ein umfassender Rahmen für die zeitabhängige Ökoeffizienzbewertung in der Produktion von Strukturen aus faserverstärkten Polymeren eingeführt. Um diesen Rahmen zu realisieren, wird das zuvor entwickelte Ökoeffizienz-Bewertungsmodell, das als Eco-Efficiency Assessment Model (EEAM) benannt wurde, erweitert und für die Bewertung der parametrisierten Produktion implementiert. Darüber hinaus wurde das Konzept der Smart-Work-Station (SWS) etabliert, um Prozessdaten in Echtzeit bereitzustellen und die Prozesse zu parametrisieren. Ähnlich wie das Rahmenwerk wurde das SWS-Konzept so entwickelt, dass es für eine Vielzahl zugehöriger Produkte und Prozessszenarien innerhalb definierter Systemgrenzen anpassbar ist. Es umfasst die Bestimmung der erforderlichen Sensorknoten für die Messung der zugehörigen initialen Daten. Die in dieser Arbeit eingeführte zeitabhängige Ökoeffizienzbewertung ist ein Schlüssel nicht nur zur Durchführung der Bewertung und des Vergleichs von Produktions- und Produktvarianten, sondern auch zur Erleichterung der Abschätzung in frühen Entwicklungsphasen.

Als Fallstudie ist die hochautomatisierte Fertigung von Seitenleitwerksrippen in Verkehrsflugzeugen ausgewählt, um den Rahmen zu untersuchen, das Datenerfassungskonzept der SWS zu realisieren und die Ergebnisse aus EEAM zu validieren. Die Ergebnisse der Bewertung dieser Fallstudie zeigen direkte Kosten von rund 221,3 €/kg und einen Kohlenstoffdioxid-Fußabdruck von etwa $105,7\,\mathrm{kg}\,CO_2/\mathrm{kg}$ aus den betrachteten Vorbereitungs-, Zuschnitt-, Vorform- und Trimmteilprozessen. Diese zeitabhängigen ökonomischen und ökologischen Auswirkungen werden in jedem Teilprozess ihren Treibern zugeordnet und validiert.

Contents

Nomenclature

Symbols

[]	Column vector
[]	Matrix
{}	Row vector
$\hat{F}$	Process global function
$\hat{F}_i$	UP global function
f	Production activity function
i	Index of UP sequence
j	Index of elementary flow type
α	Elementary flow
α_j	Elementary flow of type j
α_{ij}	Elementary flow of type j in UP i
α_{Γ_l}	Elementary flow of type l in subset Γ
$\alpha_{\Gamma_{lin}}$	Flow of type l in input subset Γ
$\alpha_{\Gamma_{lout}}$	Flow of type l in output subset Γ
v	Input elementary flow
u	Output elementary flow
m	Maximum index of UP sequence
ρ	Index of input elementary flow type
τ	Index of output elementary flow type
$v_{i\rho}$	Input elementary flow of type ρ in UP i
$u_{i\tau}$	Output elementary flow of type τ in UP i
t_a	Start time point
t_b	End time point
$t^{[\alpha_{ij}]}$	Temporal allocation of α_{ij}
Δt_{tot}	Process total time
$\min_{v_\rho} t_a^{[v_\rho]}$	Lowest time point in process
$\max_{u_\tau} t_b^{[u_\tau]}$	Highest time point in process
t	Temporal allocation point
s	Spatial allocation spot
$s^{[\alpha_{ij}]}$	Spatial allocation of α_{ij}
Δt	Temporal difference
Δs	Spatial difference
I	Information flow
I_a	Input information flow
I_b	Output information flow
J	Universal set
V	Input representative superset
U	Output representative superset
ϵ	Energy set
μ	Matter set
N	Maximum index of flow types
N_{in}	Maximum index of input flow types
N_{out}	Maximum index of output flow types
n	Maximum index of flow types in a subset
n_{in}	Maximum index of flow types in input subset
n_{out}	Maximum index of flow types in output subset
$V^{[\epsilon]}$	Input energy flows set
$V^{[\mu]}$	Input matter flows set
$U^{[\epsilon]}$	Output energy flows set
$U^{[\mu]}$	Output matter flows set
Γ	Category type of flows subset
$[\Upsilon^{[\Gamma]}]$	Category matrix
$\{\Upsilon_i^{[\Gamma]}\}$	Category vector in UP i
l	Index of elementary flows in a category
l_{in}	Index of flows in input category
l_{out}	Index of flows in output category
Γ_l	Elementary flow types in a category
p	Maximum index of categories
$[X]$	Input matrix
$[Y]$	Output matrix
$[Z]$	Process matrix
$[\hat{Y}]$	Intermediate matrix
$\{X_i\}$	UP input vector
$\{Y_i\}$	UP output vector
$\{Z_i\}$	UP vector
$\{\hat{Y}_i\}$	UP intermediate vector
$[A]$	Elementary flows matrix
$\{A_i\}$	UP elementary flows vector
$[\hat{\Lambda}]$	Characterization factors matrix
$[\Lambda]$	Characterization factors column vector
$[\check{\Lambda}^{[A]}]$	Economic factors column vector for $[A]$
$[\check{\check{\Lambda}}^{[A]}]$	Ecological factors column vector for $[A]$
F	Fiber category index
M	Matrix (Resin) category index
C	Core material category index
R	Ancillaries category index
T	Electricity category index
Q	Equipment category index
L	Labor category index

S	FRP structure category index
P	Semi-finished structure category index
K	Rejected FRP structure category index
W	FRP waste category index
G	Fiber waste category index
D	Matrix waste category index
N	Core material waste category index
O	Ancillaries waste category index
B	Ancillaries reusable category index
H	Thermal energy category index
$\mathbb{R}$	Real numbers
λ	Characterization factor
γ	Economic characterization factor
ε	Ecological characterization factor
r	Retained earnings
sr	Sales revenue
c	Indirect and other costs
k	Sales revenue excluding (other) costs
η	Efficiency
θ	Global impact of CSF
θ_i	UP i impact of CSF
θ_j	elementary flow j impact of CSF
θ_{ij}	flow j impact of CSF in UP i
θ_Γ	Category impact of CSF
θ_t	Time-dependent impact of CSF
δ	Direct cost
β	Carbon footprint
ξ	Eco-efficiency
€	European euro
°C	Degree Celsius
m	Meter
m^2	Square meter
s	Second
kW	Kilowatt
kWh	Kilowatt hours
kg	Kilogram
kg_{eq}	Kilogram equivalent

Abbreviations

AI	Artificial intelligence
CFRP	Carbon fiber-reinforced polymer
CO_2	Carbon dioxide
CPPS	Cyber-physical production system
CSF	Critical success factor
DB	Database
DIKW	Knowledge pyramid
DLR	Deutsches Zentrum für Luft- und Raumfahrt
DMAIC	Design-measure-analyze-improve-control
DoA	Degree-of-automation
DSS	Decision support system
EEAM	Eco-efficiency assessment model
EVo	Endkonturnahe Volumenbauteile
FRP	Fiber-reinforced polymer
GFRP	Glass fiber-reinforced thermoset polymer
GHG	Greenhouse gas
GUI	Graphical user interface
ID	Identification number
IoT	Internet of things
IR	Infrared
KDD	Knowledge discovery in databases
KPI	Key performance indicator
KRI	Key result indicator
LCA	Life-cycle assessment
LCC	Life-cycle cost
LCCA	Life-cycle cost analysis
LCI	Life-cycle inventory analysis
LCIA	Life-cycle impact assessment
MI	Method of identification
MM	Method of magnitude measuring
PI	Performance indicator
PwC	PricewaterhouseCoopers International
QR	Quick response
RAMI 4.0	Reference architectural model industry 4.0
RI	Result indicator
RTM	Resin transfer molding
SD	Sustainable developments
SI	Sensor node for identification
SM	Sensor nodes for magnitude measuring
SWS	Smart-work-station
TRL	Technology readiness level
UP	Unit process
VSM	Value stream mapping
WS	Work station
WSP	Workspace

Chapter 1

Introduction

Composite structures are applied nowadays in many industries such as aerospace, automotive, wind energy, marine, and construction. In aerospace industry, such composite structures in general and the fiber-reinforced polymers (FRPs) in specific decrease the vehicle empty weight. Therefore, they reduce both economic and ecological impacts throughout the vehicle operation due to the consequently reduced fuel consumption. As a result, the application of these FRP structures is rapidly growing in this industry, which argues enhancing the eco-efficiency throughout their entire life-cycle. However, there is still a significant potential for eco-efficiency enhancement in the production of these structures.

While the social aspect is excluded from this thesis, both economic and ecological aspects are considered within the eco-efficiency as the only sustainability representative here [270]. On the one hand, the economic aspect is crucial for shaping the FRPs future in aerospace industry [334]. As a decisive part of the economic aspect, the direct cost reduction is demanded by the decision-makers on different managerial levels to achieve higher retained earnings. On the other hand, there are several ecological damage categories that may be relevant for the eco-efficiency. As one of the most crucial and urgent challenges the mankind ever faced, the climate change is a significant ecological damage category that is affiliated with the man-made global warming [308]. While limiting the global warming is an international goal, several industries including aerospace are participating in this effort [179, 257]. Technically, the man-made global warming is associated with the carbon dioxide (CO_2) as the primarily emitted greenhouse gas (GHG) [159]. Here, the ecological impact for global warming can be assessed by what is known as the carbon footprint [148].

Besides serving the direct cost reduction in the economic aspect, direct applications should be implemented to decrease the carbon footprint under what is known as the sustainable developments (SDs). After establishing the proper assessment capabilities, the economic and ecological impacts of the assessed product system may be reduced together or separately through the implementation of proper technical or managerial SDs. However, this thesis aims to enhance the assessment capabilities to recognize and define the eco-efficiency impacts in a process [288], while all other decision-making steps including selecting the proper SDs are beyond the scope of it. To carry out the decision-making in a timely manner, there is a need for establishing a time-dependent eco-efficiency assessment based on the realization of a real-time data collection. Nowadays, Industry 4.0 offers a wide range of advanced solutions with a significant implementation potential in the aimed time-dependent decision support systems (DSSs). Especially in the production stage within a product life-cycle, Industry 4.0 aims to transform the traditional factory into a smart factory to fulfill the dynamic demand patterns, such as the case of mass customization. Practically, such factory should provide timely decision-making and sustainable production [68, 78, 206]. In it, a data-based process control is essential, while the realization of an eco-efficiency control in the future necessitates establishing time-dependent assessment capabilities for relevant product variants and process scenarios.

Although several scholars have discussed the eco-efficiency of FRP structures in different life-cycle stages, there is a lack of studies that cover the time-dependent eco-efficiency assessment in FRPs production. While frameworks for implementing Industry 4.0 already exist in literature, a framework for assisting the decision-makers in performing eco-efficiency assessments with the help of advanced Industry 4.0 solutions is still needed. Moreover, the literature review has shown the need for a comprehensive time-dependent assessment framework and a real-time data collection concept that are adaptable for FRPs production variants. However, the framework of life-cycle assessment (LCA) includes systematic stages for goal and scope definition, life-cycle inventory analysis (LCI), life-cycle impact assessment (LCIA), and their interpretation. In previous works, the LCA framework has been integrated with the process modeling to establish an eco-efficiency assessment framework [9, 10]. Based on that framework, the eco-efficiency assessment model (EEAM) has been developed [13]. Although there are varieties of assessment models and associated software solutions, the EEAM is adopted and enhanced in this work as a DSS for the LCIA peculiarly in FRPs production [13].

Therefore, the required assessment framework and data collection concept are introduced in this thesis to realize the aimed time-dependent assessment DSSs. Moreover, a novel concept is introduced in this thesis to serve a real-time data collection within the LCI, which is known as the smart-work-station (SWS). The SWS concept suggests implementing specific sensor nodes and advanced solutions in data collection and processing as a part of the real-time LCI to serve the EEAM as a DSS for the time-dependent eco-efficiency LCIA. The generated assessment DSSs of SWS and EEAM lean on adopting suitable conceptual, mathematical, and computerized modeling. Based on a set of working hypotheses, these modeling stages are realized within clear system boundaries and cut-off-criteria. Moreover, this modeling framework consists of systematic validation steps that are applied throughout this work.

The communicating DSSs of SWS and EEAM provide the results in novel statistical and visualized forms. From the initial collected data by the SWS up to the generated knowledge by the EEAM, the targeted decision-making steps are served sufficiently by these data-based DSSs. These results identify and measure the drivers of both economic and ecological impacts as well as their associated eco-efficiency impact as the main studied critical success factors (CSFs) in this work. These impacts are allocated on different CSF levels not only as the key result indicators (KRIs) but also to their unit processes (UPs) by a systematic discretization approach. This novel time-dependent eco-efficiency assessment assists the decision-makers not only in identifying the impact driving elementary flows, flow categories, and UPs but also determining the associated techniques in the UPs as well as the technologies in their activities. However, the time-dependent eco-efficiency assessment model describes the temporal impact status of a non-transient process with no consideration of the possible back-coupling impacts. As a simplified representation of the production process, only selected UPs from the FRPs manufacturing are covered by the case study in this thesis.

Chapter 2

Research Objectives and Thesis Outlines

2.1 Hypotheses

The research hypothesis claims that the eco-efficiency and its associated impacts in FRPs production can be assessed in a time-dependent manner by a real-time sensor-based data collection. This main hypothesis is then apportioned into a set of working hypotheses.

- It is assumed that the complex product system can be described through discretized conceptual as well as mathematical models of its flows.
- An assessment model can be likewise established, while identical elementary flows for both economic and ecological aspects are hypothesized.
- The possibility of having generic methods and sensor nodes to collect all relevant elementary flows in real-time is also assumed.
- Based on such DSS for real-time data collection within LCI, time-dependent assessment capabilities by a DSS for LCIA are also hypothesized.

2.2 Thesis Objectives, Contributions, and Outlines

In FRPs manufacturing, there is a wide range of process variants as a result of different structure applications, designs, manufacturing techniques, as well as degrees-of-automation (DoA). This thesis aims to provide a framework that offers eco-efficiency assessment capabilities to cover these process variants. This is realized through a time-dependent eco-efficiency assessment that has generic frameworks and concepts for DSSs. These DSSs serve the operational, tactical, and strategic managerial levels in general and the first one of them in specific. While some scholars provide solutions for particular aspects, this thesis has the goal of introducing a comprehensive solution based on a literature review.

This thesis realizes a time-dependent eco-efficiency assessment that is based on real process data. Here, the required data is gathered from production work stations (WSs). This work contributes to the research and development attempts to enhance the sustainability in production. Moreover, the SWS offers technical solutions for data collection through suggested real-time capable sensor nodes. When it comes to process control, this thesis contributes to the stages of defining, measuring, analyzing, and indirectly controlling the process, while the improving stage is considered to be beyond the scope of this thesis. This thesis suggests a new approach in determining the ecological impact of a product based on the real-time LCI realized by the SWS. In this approach, the ecological impact is categorized similarly to the economic one, while the same elementary flows

are considered in both aspects. To validate it, this time-dependent eco-efficiency assessment is applied to a selected FRP manufacturing technique and a predefined product. Therefore, a conceptual model is generated for the selected UPs in their WSs. By developing process matrices for these UPs, they are mathematically modeled. In the era of Industry 4.0, this thesis suggests a novel concept for the target oriented data collection and processing based on a generic parametrization mathematical model. The time-dependent LCIA is then realized through the EEAM as a computerized model. The generated DSSs in this work enable the future realization of an individualized LCIA and an automated LCI for various process scenarios and produced structures in FRPs production.

Based on the objectives and contributions of this thesis, its outlines are illustrated in Fig. 2.1.

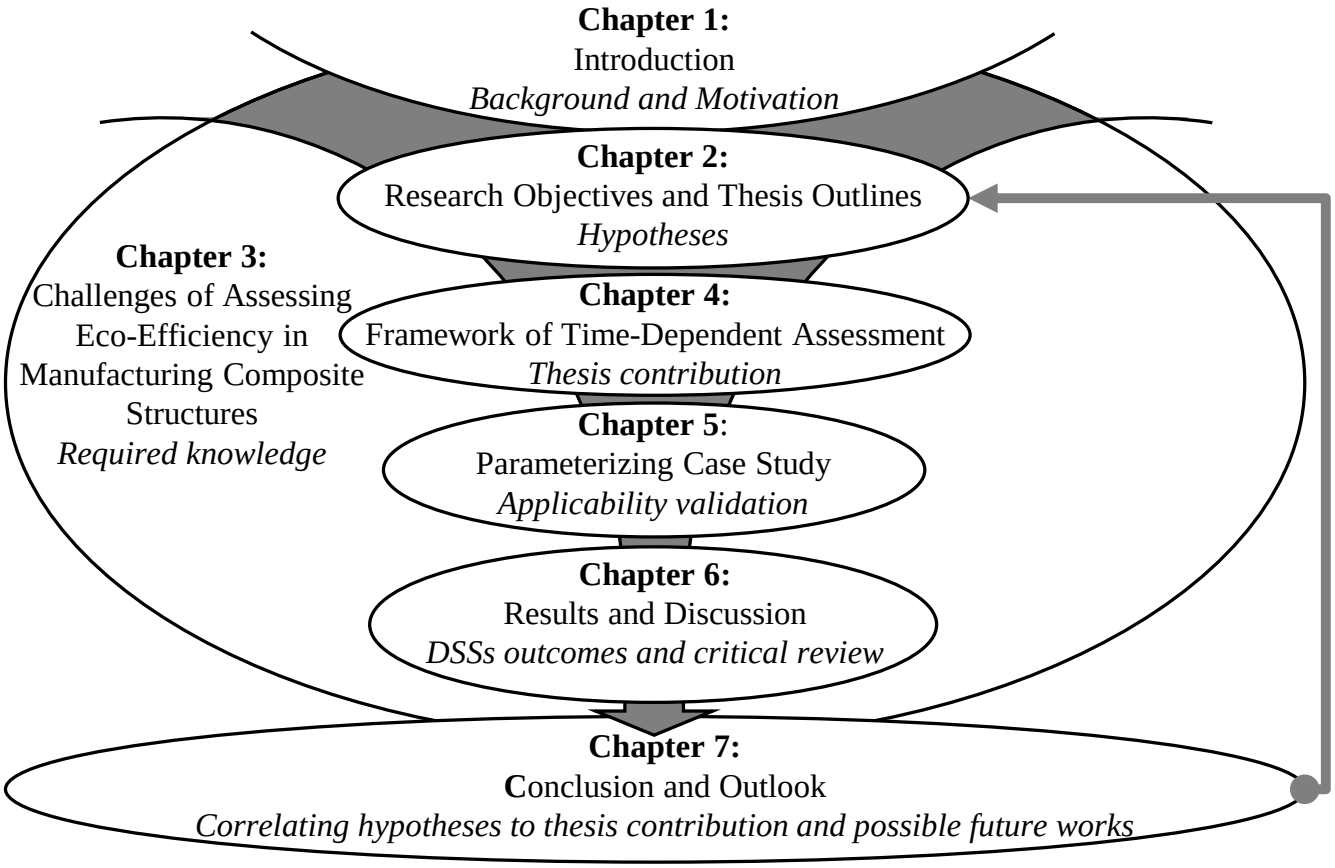

Figure 2.1 Thesis outline

In chapter 1, the growing demands for time-dependent eco-efficiency assessment, real-time data collection, FRP structures, and sustainability enhancement especially in aerospace are discussed as the main motivation for carrying out this thesis. While chapter 2 is summarizing the objectives and contribution of this thesis, the state-of-the-art is discussed for the associated subjects in chapter 3. This review has an impact on the entire thesis in general and chapter 1, chapter 4, chapter 5, chapter 6, as well as chapter 2 in specific. In chapter 4, the framework of time-dependent eco-efficiency assessment is introduced. To validate it, chapter 5 provides a case study for the parametrization of suggested generic models. The concluded results are then discussed and validated within chapter 6, which are related to the thesis hypotheses in chapter 2 as Fig. 2.1 shows. Based on these results, conclusions and outlooks are stated in chapter 7.

Chapter 3

Challenges of Assessing Eco-Efficiency in Manufacturing Composite Structures

Determining the scope of this thesis and its contribution requires understanding the state-of-the-art of different subjects. This thesis combines various science fields to provide the sufficient DSSs. Therefore, it is essential to understand the subject of decision-making and all associated aspects. Especially in the production, the implementation potential of Industry 4.0 in the decision-making steps is significant nowadays, which necessitates reviewing the relevant solutions. The scope of eco-efficiency must be clarified in such work as well, while it may include a wide range of possibly adoptable frameworks for diverse coverable aspects. Then, it is essential to understand the special features of FRPs and their production processes, to which the aimed DSSs are applied. After that, selected modeling approaches are reviewed as a cornerstone in bringing all these fields together. Finally, a comprehensive comparison is carried out between studies related to the time-dependent assessment especially in the FRPs manufacturing.

3.1 Decision Support Systems (DSSs)

To understand the relevant DSSs, the management framework is reviewed as the environment where they are implemented. Next, the decision-making in general and its frameworks are studied, whereas this is the most relevant part of management. Finally, the production management and control as well as the Industry 4.0 and its implementation in modern DSSs are discussed here.

3.1.1 Management Framework and DSSs

It is essential to have an adequate insight into the management in general. As a part of the management framework, decision-making has a temporal perspective that is discussed here too. While the management is applied in the entire life-cycle of a product, the production is focused on in this work.

Management definition and objectives

In his work, Chang has addressed the efficiency as a major management function, where task outputs are optimized with the minimized utilized resources [54]. Linguistically, management is the manner of handling, administrating, directing, and controlling [337]. According to Drucker, management is practiced by professionals who focus on effective communication, decision-making, and strategic planning [82]. In general, decision is defined by Beer to be the way of realizing a belief [33]. Bellman and Zadeh have defined the decision to be the intersection between the associated goals and constrains [34]. To execute any change, there is a need to understand the process or as it is also called the product system subjected to that change.

An enterprise has strategic goals and missions, that may be quantified by economic, environmental, as well as social CSFs [238]. In practice, such goals should be specific, determinable, reasonable for the decision-making, realistic to achieve, and time-dependent [117]. However, there is a need to measure each goal value in order to identify what is required to achieve the targeted one. For decision support, the DSSs evaluate the CSFs and inform the decision-makers on different managerial levels about the associated ones [288].

Therefore, the CSFs are classified in levels, while the ones on the highest level are called the KRIs [238]. KRIs refer to the degree in which the enterprise goals have been addressed. KRIs include for instance the net enterprise profit, as well as customer and employees satisfaction. These KRIs are derived from the key performance indicators (KPIs), which refer to the degree of success, performance, or utilization on the lowest assessed level [138].

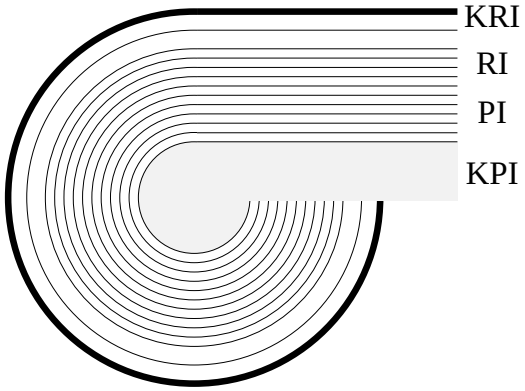

Figure 3.1 CSF levels, affiliated with [238]

In Fig. 3.1, KRIs represent the outer peel as global results. On most inner level, KPIs are the locally observed performance indicators. In between, there are result indicators (RIs), which inform about the decisions that have been brought to action. The next level includes the performance indicators (PIs) which illuminate decision-makers about how to identify the next required SDs [238]. Still, CSFs are subjected to the defined system boundary and open to interpretation. In this thesis, the main concern is to provide DSSs to realize time-dependent assessment of eco-efficiency KRIs by real-time measuring of specific KPIs in FRP manufacturing. The considered KRIs in this work are the direct cost and carbon footprint as the assessed economic and ecological impacts.

Management framework and perspectives

In order to achieve the aimed value of KRIs, processes should be defined, measured, analyzed, improved and then controlled within what is known under the acronym of (DMAIC) approach [9, 32, 167]. While this framework can be applied for various purposes, it is implemented to control the eco-efficiency KRIs in this work.

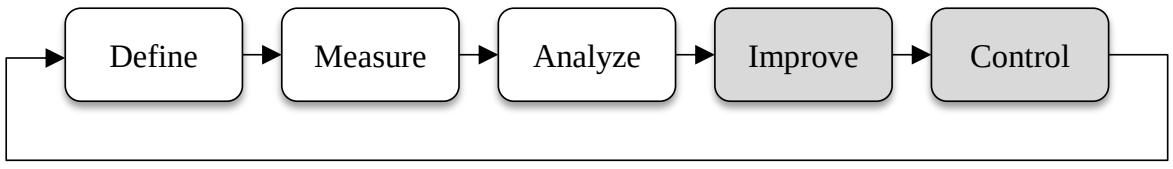

Figure 3.2 DMAIC framework, adapted from [9, 32, 167]

On the first stage of defining in Fig. 3.2, problems are described and project goals are identified. For the assessed process as a product system, its function, space, time, and associated input/output flows are to be defined [24]. In the second stage, KPIs are measured from the collected data [9, 167]. Then, this collected data is to be analyzed and converted into knowledge about KRIs relevant to the described problems in order to generate suitable solutions. Within the fourth improving stage, actions are taken and direct applications are executed as SDs [9, 110]. Finally, the impact of these SDs on KRIs or KPIs is evaluated and iteratively managed in the control stage [9]. Theoretically, controlling here contains all previous stages except defining, while the problem is known in it. Based on the evaluation of these CSFs in this stage, decision-makers decided whether a next DMAIC loop is required or not. Although this thesis serves mainly the unshaded stages in Fig. 3.2, it contributes indirectly to the control as well, while controlling contains logically activities from the first stages.

In this thesis, controlling and planning are distinguished, while decision-maker is a term that combines the performers of both [283]. The difference between planning and controlling is correlated with the course of time in which decision-making is carried out. Yet, there is a need for evaluating the considered system or process in both planning and controlling [18, 341]. However, frameworks such as DMAIC are handling an existing process, where a measurement is possible. This is inapplicable in planning, where the planned product system is still totally or partially virtual [9, 32, 167].

Although KRIs, such as eco-efficiency, are ideally planned and controlled throughout the entire life-cycle of a product from cradle-to-grave, management on a single life-cycle stage is common. While this thesis is dedicated to production, management tasks are simplified in either unrepeatable planning or iterative controlling. However, planning is an iterative approach in reality, while it may be also considered as a preventive controlling from the perspective of higher management level. In this work, any planning activity is assumed to be prior to the product system establishment, while any controlling activity is handling an existing process, even when controlling activities contain the planning perspectives as well.

Regarding the course of time, production management may be split into strategic, tactical, and operational management horizons [85]. They are distinguished regarding their objectives, the medium with which the process can be manipulated, and the managed CSFs of each level in Tab. 3.1.

Table 3.1 Management horizons, adapted from [85]

Horizon	Objectives	Medium	CSFs
Strategic (years)	Competition plans, supply chain ...	Product concept, resources concept ...	Enterprise sustainability, cost options, competition ...
Tactical (months, weeks, days)	Final plans of product and process concepts ...	Product portfolio, supply chain structure ...	Domestic facility sustainability impact ...
Operational (hours, minutes, real-time)	Realization and results controlling ...	Products quantity, components ...	UPs eco-efficiency, delivery, processing times ...

Moreover, the top-down and bottom-up are two different but also combinable management approaches [172]. On the one hand, a top-down approach adopts the perspective of strategic level for the entire organization based on gained summarized wisdom. On the other hand, a bottom-up approach depends on operational expanded data to create the knowledge required for decision-making. However, distinguishing these approaches is difficult in some cases, while decision-makers may build their decision based on mixing their wisdom with some data from lower management levels [85, 172].

While it means finding something value, evaluation can be classified into several types that might have some commons [283]. A main distinguishing criterion is the existence of the evaluated system. Therefore, it is essential to differentiate between evaluating a planned process and an existing one [56, 87, 191, 283]. From this simplified understanding, it is clear that the forecasting evaluation prior to establishing a system or process is an estimation as a part of planning. On the other hand, controlling contains the evaluation of existing process [56], or as it is called assessment in this thesis. Hence, an assessment provides a descriptive hindsight for decision-makers [163]. Nonetheless, estimation may be carried out for existing systems as well, whenever assessment is technically difficult or costly. Moreover, assessment term is utilized in literature for describing the evaluation of non-existing systems as well. In practice, estimation credibility depends on the availability and accuracy of the used data, its maturity degree, as well as its model transparency [110, 191]. Estimation is a multidisciplinary approach, whereas a wide range of factors within the different life-cycle stages is to be considered and their impacts are to be determined. Despite the definition diversity in literature, assessment is appointed solely for the evaluation of existing product systems to serve controlling in this work, while estimation is evaluating the non-existing or unreachable ones as a part of planning.

The data maturity degree may be classified by the (DIKW) knowledge pyramid into data, information, knowledge, and wisdom. Based on historical data collected from previous process assessments of specific KRIs, such KRIs may be estimated for the future processes within comparable system boundaries. In this thesis, the assessment of existing processes is considered, while the enhancement of estimation capabilities is discussed only as an outlook. One of the main challenges here is to orient the CSFs appropriately to serve a single or multiple management horizons.

3.1.2 Decision-Making and DSSs

The DSS is a core issue in this thesis. Therefore, its terminology and typology are briefly discussed here. After that, the decision-making framework is studied.

DSS and relevant decision maturity levels

DSS is a term used to describe a wide range of applications in a specific area of information systems. These applications serve the enhancement of managerial process in decision-making [20]. A DSS offers a specific guidance level to assist the decision-makers in selecting or developing optimum solutions as direct applications with minimum possible efforts [67]. Still, a decision generator, or as it is known as the decision-maker, is required. Decision-makers are individuals or teams, who are responsible to perform the strategic planning, priority setting, as well as product and process control, design, or redesign. They can serve the industry, government, or non-government organizations [151]. In this thesis, the targeted decision-makers are the shareholders and managers from different enterprise hierarchy levels in general and from the operational production management in specific. In some cases, decision-making may be performed as a result of human intelligence, artificial intelligence (AI), or a combination of them [83, 151, 267].

To examine the possibility of establishing a computer-based DSS, decisions or actions are distinguished into programmable and nonprogrammable ones [219]. However, it may be impossible to differentiate them in some cases. On the one hand, a programmable decision has a definable routine approach that repeats itself each time it is required. On the other hand, a nonprogrammable decision has a high novelty and no assured repeatability or iteration [290].

In general, rational decisions are associated with knowledge, while such decisions are assumed to be knowledge based. For better understanding of the decision evolution, decision maturity levels have been described in Fig. 3.3, whereas the relevant levels for this thesis are unshaded.

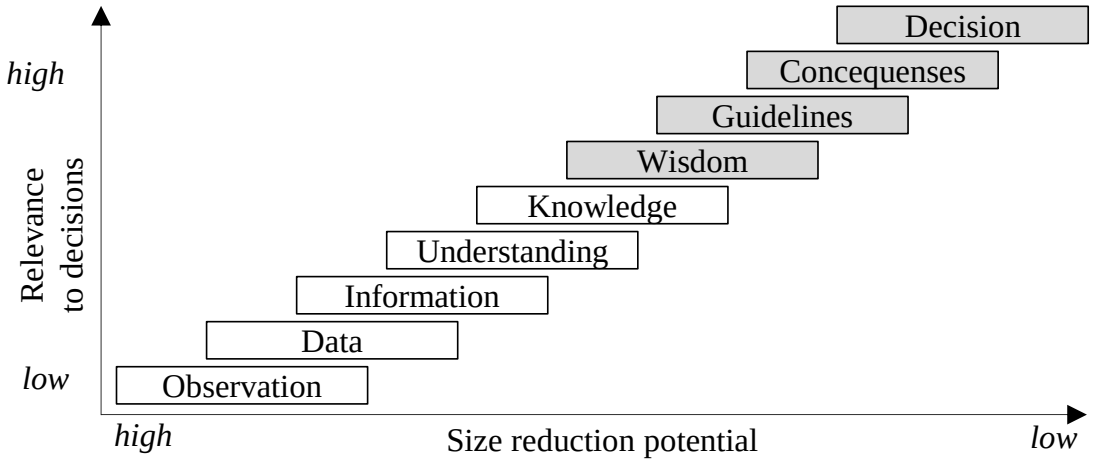

Figure 3.3 Decision maturity levels, adapted from [62]

As Fig. 3.3 shows, a rational decision is built upon the processing of initial data or as it is also called observation. This initial data is converted into data, information, understanding, and knowledge about the problem. After assessing the problem in reality, alternatives are to be predicted based on the generated wisdom. Moreover, guidelines for selecting proper alternatives are to be modeled. Based on the consequences of each alternative, the proper one has to be selected and a decision about that is to be taken [62]. As it is shown in Fig. 3.3, an observation has the largest size and the least direct affiliation with the decision.

Decision-making framework

In general, a rational decision should be concluded in systematic steps. They start by recognizing a problem, then defining it by gaining the required knowledge about it. After generating or gathering the alternative solutions, they should be rated to select the proper ones and implement them. Moreover, the effectiveness of them is to be controlled [207, 219, 291], as Fig. 3.4 shows.

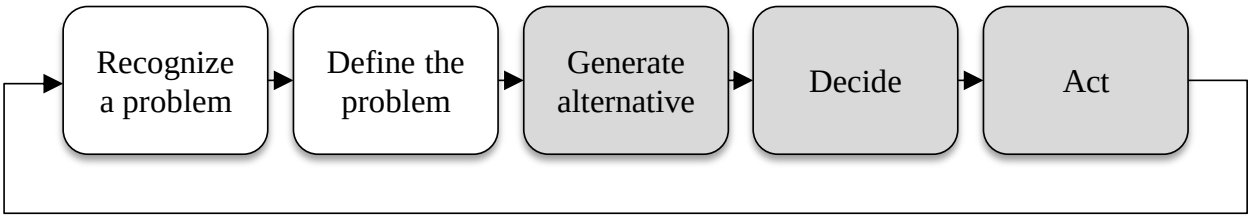

Figure 3.4 Decision-making steps, based on [288]

In this thesis, only the first steps of problem recognition and definition are considered. As Fig. 3.4 shows, these steps consist of repetitive routines for assessing the targeted KRIs continuously.

In another definition, da Silva et al. have split the decision support into two phases within what is called the learning-search-oriented concept. In the learning-oriented phase, DSSs can assist the decision-makers in understanding the problem. This phase is then followed by the search-oriented phase in which a comprehensive evaluation for the possible solutions and their consequences is performed [67]. Again, the developed DSSs in this thesis serve the learning-oriented phase only.

Generally, the DSSs facilitate the decision-making steps, while they can be split into several types such as the personal DSSs, group support systems, and executive support systems [20]. An executive support system assists decision-makers with data collection and processing to extract the information from big data [15, 331]. From understanding the different types of DDS, the time-dependent eco-efficiency assessment in this thesis serves mainly as an executive support system. They offer a computerized access to their outcomes and reports in appropriate illustration forms. Such DSSs should be user-friendly and require no or very limited operating and interpreting efforts [331]. Here, it is challenging to distinguish between the decision maturity levels from Fig. 3.3 and to adopt a proper assessment framework to serve exact levels by the developed DSSs, while such approach is rarely discussed in literature.

3.1.3 Production Management and Control

Production management should address the aimed product characteristics qualitatively and quantitatively within the temporal and cost boundaries of the customer demand [85, 134]. In this section, the production and a framework of system control within it are briefly reviewed.

Production definition, characteristics, and scenarios

First, clear definitions of the production and its processes as a distinguishable part of product life-cycle in general and FRP structures in specific are required. In his paper, Solow has defined production function as a technical change over time that transforms the inputs into outputs [296]. This life-cycle stage can be split into its main processes such as manufacturing, assembling, and finishing [334]. These main processes may be also discretized into UPs, which they themselves contain clusters of activities. While the discretization is associated with different criteria, it is essential to have a clear system boundary in it and to provide a comprehensive non-redundant modeling. In practice, the production should consist of all required factors to create the aimed product. For instance, FRP structures are manufactured by turning semi-finished raw materials into ready-for-assembling finished structures. Then, assembling is the process of combining a set of structures into one assembly, whereas finishing is a term that describes the process of preparing the assembly for further installation in the aircraft. However, manufacturing may include its own finishing UP to prepare the structure for assembling.

Second, production characteristics depend on its system boundaries. Here, any process or as it is also called product system must have technical, temporal, and spatial boundaries [24, 152]. Process equilibrium theory is a crucial characteristic, that assumes a physical balance between both input and output flows in a process. On the one side, mass conservation principle states that mass is an uncreatable, an indestructible, and a conserved property in a process [48]. Thus, mass conservation principle expresses that mass change rate is the mass crossing the system boundary of a control volume [57, 237]. Like the mass-energy equivalence, process equilibrium lays under the special theory of relativity. In that theory, energy and matter are flowing within temporal and spatial dimensions or as they are also called the space-time dimensions [237, 294].

Techniques and technologies as well as their DoA, technology readiness level (TRL), and process maturity are decisive in forming a production scenario. In this thesis, technology is the term that describes a technical approach of performing a single activity or a part of it within production, while each technology has distinguishable technical characteristics and elements. Practically, such definition is subjected to interpretation and perspectives, while multiple new technologies can occur within a single previous one. For instance, draping has been carried out traditionally as a simple manual technology, while the modern automated draping contains

various novel sensing, actuating, and controlling technologies. Theoretically, the DoA may be evaluated qualitatively based on rating the dominance of automation technologies in the studied process [95]. Therefore, the simplified levels of manual activities, low-, semi-, highly-, and fully-automated activities are considered to evaluate the DoA in this work.

In practice, technologies and their DoA vary between the case studies of FRPs production [241]. In its simplified meaning, automation is relying on equipment instead of people. Therefore, understanding the overall equipment effectiveness is required as a method to measure equipment productivity in a percentage form in an automated process [26, 245]. Other aspects, such as takt-time, availability, machine useful life, downtime, active operation time, changeover time, and availability loss may be considered by the overall equipment effectiveness [312]. Moreover, production can be distinguished based on its discretization into either batch, continuous, or discrete process [332]. While UPs can be discretized with timely repeatable activities, both FRPs production in general and their manufacturing in specific are considered as batch processes. In this work, the term technique describes a set of technologies that serves an entire UP or multiple of them. In Appx. A, a wide range of FRP manufacturing techniques is discussed.

TRL is an industrial system to determine how far any technology stays from its final full-scale industry application. Including nine levels, TRL tracks the technology development from a basic principle up to an approved one in industrial operation. Although the selected case study includes some on-going developments, the assessed UPs in this work are assumed to have the highest TRL for simplicity. Similar to the TRL, process maturity can be classified into five levels. An initial process such as first experiments in research and development is considered to be on the lowest maturity level. On the next level, there is the reproducible process. This is followed by the defined process, where a systematic documentation, such as procedures, exists. Controlled process is a level higher, in which outputs are modifiable based on a clear definition and a possible manipulation of the process inputs. On the highest level according to Scheer comes the optimized process [273]. Still, optimization is a continuous effort.

In this work, process variants can be described as the scenarios by which the production is carried out. Here, the process scenario is a combination of various technologies in the selected techniques with consideration of their TRLs, DoA, as well as process maturity. For decision-makers, several other aspects play the role in selecting proper scenarios, such as product size, quality, and complexity, as well as production volume [141, 173, 317]. Moreover, some economic aspects such as process cost, time to market, and certification are carefully considered in selecting the appropriate manufacturing technique [4, 8]. The configurations of each technique and its scenario differ between the industries, manufacturers, as well as products.

Endkonturnahe Volumenbauteile (EVo), which is a German term to describe a facility for high volume production of components close to the final contour, is a platform that has been developed by the German aerospace center (DLR). Due to the accessibility, data availability, and its relatively high overall TRL, DoA, and process maturity, the EVo-platform is selected as the case study in this thesis. Although this is not the common situation of technology development platforms, the EVo-platform is assumed to carry out an optimized process. In other words, an ideal problem-free process is considered by the selected case study for simplification.

System control framework

In production, the framework of system control is a widely implemented optimization approach. Similar to controlling, seeking sustainability by applying SDs is an iterative approach. This is a result of correlating the targeted outputs to their inputs, that are dynamically changing due to continuous developments in the various associated sectors. From management perspective, seeking sustainability is similar to process closed-loop

controlling [54]. Considering the main elements of a closed-loop control system, there is the process to which the change is applied, there is the sensor that gathers the required feedback from this product system, there is the controller which may be a decision-maker as well, and finally there is the actuator to turn decisions into actions in the process, as they are all shown in Fig. 3.5.

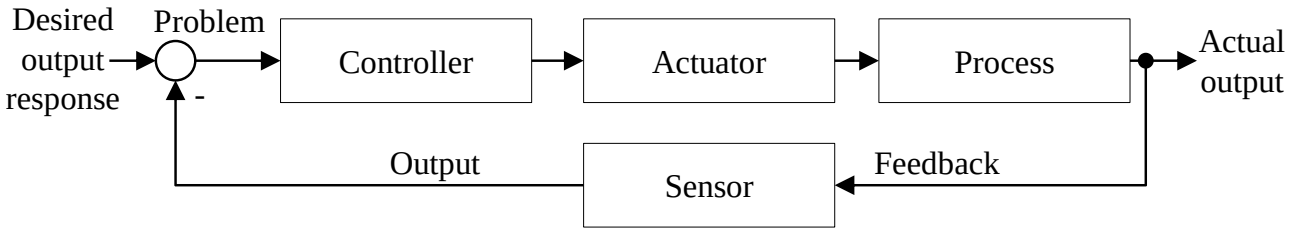

Figure 3.5 Closed-loop control system, adapted from [77]

While controlling, actuating, and sensing can be performed artificially by a device or manually by a human, controlled variables can be physical, economic, ecological, social, or political [77]. In production, decisions can be split into arrangements, or as they are also called transactions, and real-time oriented ones. On the one hand, arrangement direct applications are controlled directly or indirectly by a decision-maker, whereas the decision time is less critical for this type. On the other hand, real-time direct applications are performed by integrated AI and cyber-physical production systems (CPPSs) automatically within a defined time slot [203]. This thesis is associated with sensing the production eco-efficiency, while all other closed-loop steps are beyond the scope of it. Nonetheless, it aims to serve future arrangement as well as real-time control systems. However, this requires a clear understanding of AI and CPPS as a part of Industry 4.0. Besides the difficulty of distinguishing different production aspects, implementing the control system framework in eco-efficiency assessment is a challenging approach for decision-makers, while this type of decision support is uncommonly considered as sensor-based approach.

3.1.4 Industry 4.0 and Modern DSSs

In this section, a definition for Industry 4.0 and its solutions is selected from the various available ones. Moreover, selected frameworks of it as well as solutions from it are reviewed.

Terminology and Typology of Industry 4.0

As any novel concept, Industry 4.0 has variety of definitions in literature, while there is some confusion in interpreting the true meaning of it. The term Industry 4.0 describes the latest major leap in modern industry, which has occurred after mechanization, electric power-train, and automation [282]. Moreover, eco-efficiency is anticipated to be the next industrial significant leap [218].

Technically, connecting both real and virtual environments is one of the major features of Industry 4.0. It contains several advanced solutions such as CPPS, Internet of things (IoT), AI, and big data [71, 213, 282]. The sensor nodes within a CPPS enable the realization of an open real-time data connection and communication between both real physical objects from the production process and their virtual models or as they are known as the digital twins. In general, IoT is an interface between physical and virtual worlds. It provides descriptions of the correlation protocols between all types of assets including people, products, services, and machines. IoT, which is realized through linking various platforms and technologies, is also known as „*internet of all things*“ [282]. Moreover, AI helps in understanding the human intelligent entities and imitates their functionalities

within man-made computerized models [267]. Finally, big data is a term that is used to describe the act of seeking the business advantage through intelligence. Such intelligence may be derived from high size and complexity data [98, 217]. It enhances high accuracy decisions based on more sufficient data, while data collection activities for big data are to be further automated in Industry 4.0 [282]. The impact of big data is not limited to increasing the decision accuracy, it also shapes the future expertise by changing the management practice and defining a new value for experience [217].

These advanced solutions are associated with data collecting and processing frequency [37, 212]. In practice, time interval is crucial for near real-time processing capabilities, which may be also called a real-time process due to its reduced timestamps [59, 157]. These solutions of Industry 4.0 may be implemented in various sectors for different life-cycle stages, while this thesis is focused on the FRPs production.

Frameworks of Industry 4.0 in production

Practically, the production process is taking a place within a spatial centered facility that fulfills the required attributes for performing it, which is known as the factory [85]. By implementing Industry 4.0, a conventional facility is converted into a so called smart factory [205]. Such smart, digital, or as it is also called integrated factory aims to enhance efficiency and to enable production flexibility by mastering the process complexity [161], while these are the cornerstones of realizing the mass customization [68, 326]. Within a smart factory, implementing Industry 4.0 is shaping the entire production process and not only a single aspect of it. Historically, the description of such smart factory exists already since the late eighties of the last century [72, 79, 338]. Yet, recent novel Industry 4.0 solutions are featuring the globalization and decentralization of communicating information in the smart factory [71, 279, 282]. Open real-time data connection and communication between both physical assets and their virtual models are significant attributes of CPPS in a smart factory. From the real world, the data is gathered by advanced solutions such as specialized sensor nodes. The collected data is communicated with the virtual world via advanced connection software and hardware solutions, while it may be structured within configured databases (DBs) [205]. In practice, advanced information technologies such as cloud platforms may be implemented for such structured DBs [80].

In order to convert a traditional production factory into a smart one, a systematic framework is essential to assure both successful transition and competitive outcomes. However, Industry 4.0 is not a single solution or even a set of generically definable ones. Therefore, there is a significant effort to establish systematic frameworks and standards to facilitate the implementation of Industry 4.0 [244]. In this thesis, selected frameworks from two institutions are briefly discussed, including the approaches of PricewaterhouseCoopers International (PwC) and Plattform Industrie 4.0 [128, 244].

The PwC study discusses a framework that covers the transition into Industry 4.0 for the entire value-chain. This value-chain includes all value-added activities that are carried out by the enterprise throughout the product life-cycle. In this framework, the business value-chain is covered starting from the establishment of a new business model up to the marketing and sale stage by a two dimensional integration. Considering its relevance to the production, a vertical integration is discussed in this framework, while it contains all product development processes within the enterprise. On the other hand, the horizontal integration covers further key aspects of the value-chain outside the enterprise. Advanced technology applications and DSSs such as end-to-end product life management, the realization of digital factory, the machine automation enhancement, as well as the advanced management systems are considered by this framework as cornerstones for addressing Industry 4.0 in production [244].

In the reference architectural model industry 4.0 (RAMI 4.0), three model dimensions are suggested. Similar to PwC framework, RAMI 4.0 includes the entire value-chain phases [3]. The first dimension represents the stages of product life-cycle, as Fig. 3.6 shows.

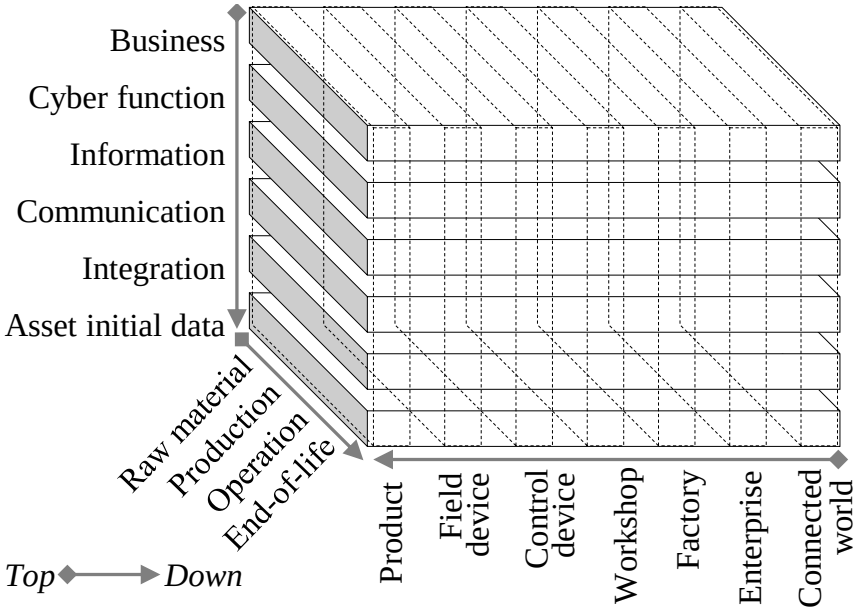

Figure 3.6 RAMI 4.0 with simplified product life-cycle, adapted from [128]

The other dimension in RAMI 4.0 describes the architecture of enterprise process. On the lowest layer in the vertical axis within Fig. 3.6, the assets are all physical systems and non-physical systems that configure the production such as labors, hardware, software, as well as procedures [128]. Integration represents the layer, where accurate and reliable data from the entire life-cycle is collected by sensors and provided on a computerized level [3, 42, 188]. On the communication layer, the collected data is unified, while its mining is performed on the information layer to cluster the data and establish its structure. On the cyber function layer, asset functionalities are described, while this layer includes the horizontal integration between these functions based on virtual models. The business layer connects mainly the different actions from these layers [3, 78]. It may be concluded that these layers combine the DIKW pyramid with the architecture for CPPS implementation [3, 110, 188].

As it is shown in the horizontal axis within Fig. 3.6, RAMI 4.0 includes seven hierarchy levels, that are particularized for the production to include the product in production, the field device, the control device, the workshop where the process takes a place, the facility, the entire enterprise, as well as the connection between it and the outside world. This multilevel and multidisciplinary framework in Fig. 3.6 is describing the possible contribution of Industry 4.0 to both bottom-up and top-down approaches as well as the combination of them in the related DSSs. In RAMI 4.0, each local transition among these levels is associated with existing suggested standards. Still, there is no target oriented path in RAMI 4.0 or in PwC framework where the purpose of implementing Industry 4.0 is clarified, such as the case of implementing it to assess and enhance the eco-efficiency.

In practice, the data development toward knowledge in DIKW goes through data processing steps in what is called the knowledge discovery in databases (KDD) [100]. As Fig. 3.7 shows, these steps start from the targeted data selection out of gathered initial data. Then, data is processed after it is collected from the sensor nodes as signals. Here, it may be filtered and compressed in order to transform it into clustered distinguishable information [100, 323], In the transformation, data may be clustered, summarized, and regulated. After that, data mining activities are carried out to determine the patterns and establish the proper data models [84, 100].

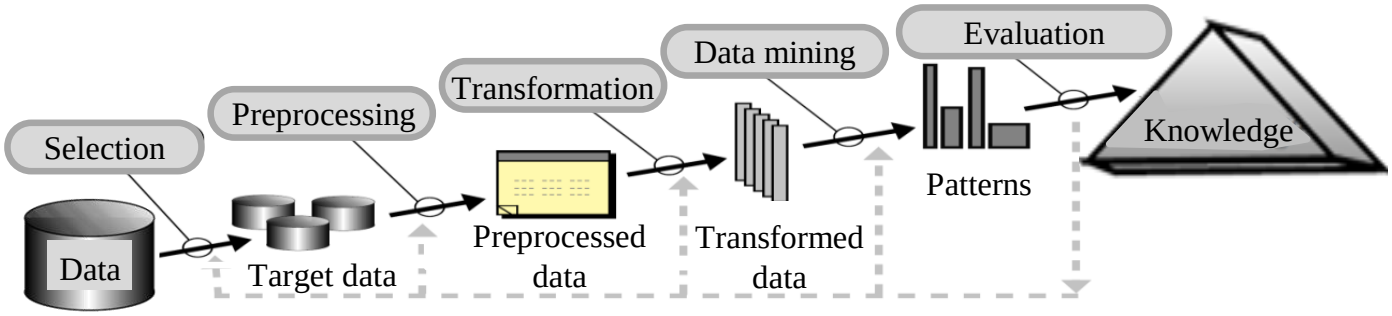

Figure 3.7 KDD steps, adapted from [100]

Finally, the evaluation and interpretation are taking a place in order to achieve the aimed knowledge [100]. However, KDD exclude the stage of initial data collection, while it focuses on the data handling when data already exists. From analyzing both frameworks of RAMI 4.0 in Fig. 3.6 and KDD in Fig. 3.7, a clear correlation and a possible combination can be sensed, as it is introduced later in chapter 4.

Based on real-time factory information, advanced systems such as manufacturing execution systems may be implemented to control the CSFs [332], as Fig. 3.8 shows.

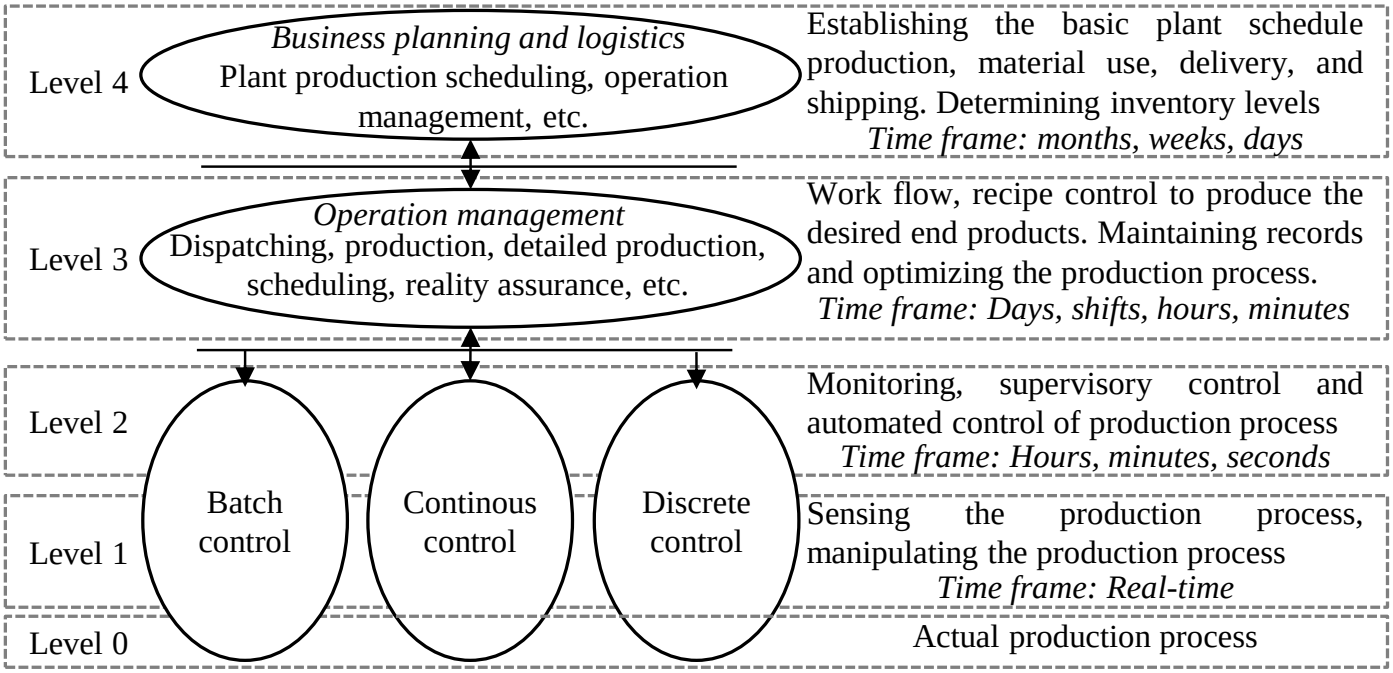

Figure 3.8 Manufacturing execution systems hierarchy in smart factory, based on [332]

This hierarchy for manufacturing execution systems in Fig. 3.8 starts from the existing production process with its associated assets on level 0. By the data collection and communication from the assigned sensor nodes in level 1, the assets are monitored in level 2. Based on that, these assets are controlled in level 3, while production planning is realized through level 4 [332]. The approach in Fig. 3.8 illuminates the importance of considering the course of time in such manufacturing execution systems, while it includes similar levels to RAMI 4.0 in Fig. 3.6.

Nowadays, there is an attempt to have a human centered Industry 4.0 [309]. This necessitates the establishment of DSSs that serve the relevant process scenarios with various DoA such as the ones suggested later in this thesis. The challenge here is to implement Industry 4.0 solutions for the eco-efficiency assessment, while these solutions are handled as the aimed goals themselves in many studies.

3.2 Eco-Efficiency Assessment

In an assessment, it is essential to define the considered impacts in order to determine all relevant data. After reviewing the terminology and typology of eco-efficiency, its framework is discussed in this section. Finally, some modern DSSs of eco-efficiency are briefly studied.

3.2.1 Terminology and Aspects of Eco-Efficiency

Here, terminologies of the eco-efficiency and its assessment are discussed, while both economic and ecological aspects are reviewed.

Terminology of eco-efficiency and its assessment

Although the term eco-efficiency describes the efficiency in both economic and ecological aspects [270], the variety of definitions for eco-efficiency in literature may generate some confusion about its meaning [147]. According to Ehrenfeld, eco-efficiency has been introduced for the first time by Schaltegger and Sturm in 1989 [89, 147, 272]. Since then, this term has been often used to describe various things such as the eco-efficiency as a concept and as an indicator [147]. On the one hand, the term is implemented to describe a management philosophy that enhances both economic and ecological objectives simultaneously. Eco-efficiency means achieving higher benefits in both aspects with less undesirable impacts on both of them [209, 269]. As a concept, the eco-efficiency of a system is achieved by a cost competitive product that has a reduced environmental impact to serve the current generation and the next generations [75, 272].

In addition, the eco-efficiency can be described as an indicator that is equal to the ratio of useful output over useful input [89, 269]. Others define eco-efficiency for specific cases as the ratio of economic value-added outcomes over the ecological burden [74]. Therefore, eco-efficiency is a crucial KRI for the decision-makers in both product and process developments [225]. From these various definitions, it is concluded that eco-efficiency is a target oriented philosophy that can be realized through a concept and assessed by an indicator. Hence, the decision-makers should not only assess this indicator, but they must also enhance the eco-efficiency philosophy on the various managerial levels. This may be realized through applying an appropriate assessment framework as well as DSSs to select and generate the suitable SDs.

Generally, it is essential to distinguish between the efficiency and eco-efficiency. On the one hand, efficiency is the correlation between homogeneous outputs to inputs that both represent a single CSF in a unified unit. On the other hand, eco-efficiency is the correlation between two CSFs. It describes a ratio of economic benefit or as it is also called retained earnings to ecological burden, while they are described by heterogeneous monetary and physical units respectively. Nonetheless, process efficiency is affecting the eco-efficiency, while enhancing efficiency may be achieved by SDs that serve increasing the economic benefit as retained earnings, reducing ecological burden, or combining both.

Economic and ecological aspects of eco-efficiency as parts of sustainability

Since the earth summit in Rio de Janeiro in 1992, sustainability has been announced as the targeted development for the mankind future [298]. Sustainability is considered nowadays as a set of principles that is adopted by shareholders as well as decision-makers [104]. From general sustainable perspective, economic sustainability is achieved when the economy reaches sufficient level of stability and invulnerability against collapses and

discontinuities. On the other hand, ecological sustainability should lead to the capability of avoiding any decline in the life condition of human and the surrounding environmental segments [63].

In order to achieve these goals completely or partially, SDs need to be applied [269]. The SD has been defined as the development methods, techniques, and applications that fulfill the requirements of the current and future generations. An ideal SD serves all sustainability aspects by protecting the environment, developing the economy, and assuring the social equity [65, 269, 340], as Fig. 3.9 shows.

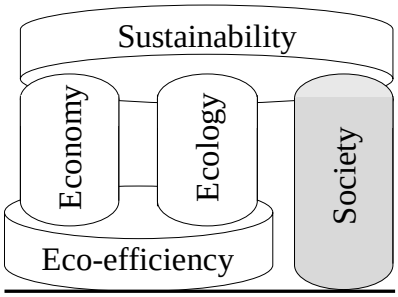

Figure 3.9 Sustainability pillars, adapted from [104, 270]

In general, eco-efficiency is to be considered as a part of a comprehensive sustainable philosophy [209]. Translated into SDs, eco-efficiency direct applications should have positive impacts on both economic and ecological aspects [275]. According to Finkbeiner, life-cycle sustainability assessment is the approach that evaluates all associated aspects to realize the sufficient SDs [104]. In practice, such comprehensive sustainability assessment can be performed through the combination of different specialized approaches [175], while each of them is dedicated to a specific sustainability aspect from the pillars in Fig. 3.9.

From global economic management perspective, a profitable business aims to win customers for its products by satisfying their demands [82]. This demand oriented management is applicable for both industrial as well as customer products [165]. Still, inconsistency and unpredictability in the shareholder demands, in the product life-cycle definitions, in the nature of business competition, as well as in the technology developments are challenging aspects for every business in addressing its customers satisfaction.

By narrowing these challenges down to the project management level, it is difficult to agree on universal CSFs for all projects, while the project success has different meaning from the various point of views [52, 197]. However, three criteria including cost, time, and quality have been addressed in what is called the iron triangle [22], which is illustrated on the left side within Fig. 3.10. Furthermore, sustainability aspects have been also considered as success criteria for project management in what is called the star methodology [22, 88], as it is shown on the right side of Fig. 3.10.

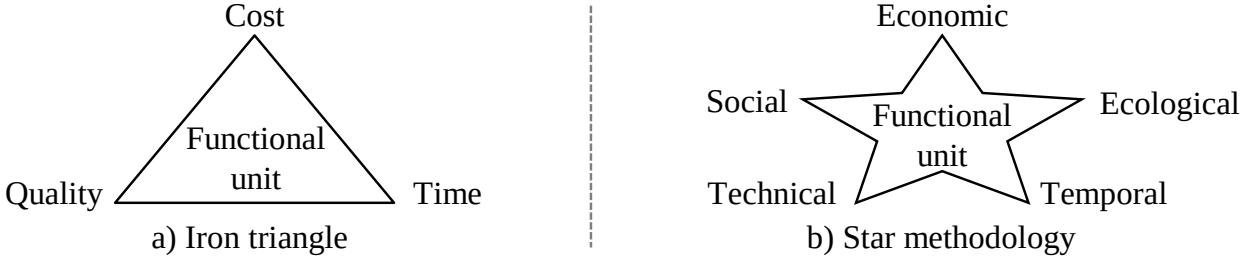

Figure 3.10 Success criteria in project management, adapted from [22, 88]

Each criterion in Fig. 3.10 may be represented by a single CSF or a set of multiple ones. However, it is essential to distinguish between the different levels of CSF and to have a clear differentiation between the

reasons and results of them. Yet, this thesis is about both economic and ecological aspects as parts of the eco-efficiency.

Economic aspect

In any assessment, it is essential to define the scope and goals of it, whereas the scope includes a clear definition of the assessed CSFs and their levels. The economic aspect contains a wide range of terms, while some of them are implemented to describe different parameters from various perspectives. To avoid such confusion in this work, the assessed CSFs are clearly allocated to the levels within their global aspect later in chapter 4.

In practice, every success criterion is crucial for addressing shareholder demands [88]. This thesis focuses on the direct cost as an economic aspect, while cost competitiveness is a cornerstone in eco-efficiency [275]. In literature, there are various ways to distinguish between economic substances and cluster them. For instance, the terms of price, cost, and profit are commonly used as simplifications of the sophisticated economic parameters. According to Helminen, the net value-added of a process output on the enterprise level can be calculated by Eq. 3.1 [132].

$$sr - Bo - Dp + Inv = Wa + Int + Di + Ta + Mo + r \tag{3.1}$$

With sr = sales revenue; Bo = bought-in materials and services; Dp = depreciation; Inv = change in inventories; Wa = wages; Int = interest; Di = dividends; Ta = taxes; Mo = equity of monitoring shareholders in subsidiaries net income; r = retained earnings, all in the monetary unit of (€).

For simplification, these monetary values can be clustered under three terms from producer point of view, which are the total production costs ToC, sales revenue sr as the price of production output, and the retained production earnings r [64, 153, 345].

$$r = sr - ToC \tag{3.2}$$

For instance, the total production costs ToC of an aircraft structure represent what the producer or supplier pays to build it. Its production price as sales revenue sr is describing how much an aircraft original equipment manufacturer pays that supplier to get it. Now, the sales revenue sr is a market oriented value, which depends on several external aspects such as the lowest possible expenses and the available competing offers. In practice, decision-makers on operational production level have no impact on the market sales revenue sr. Technically, it is a fixed value from production point of view, while it is considered as a predefined constant in this thesis. In this work, sr is assumed based on the most competitive price offers of the assessed UPs, whereas analyzing the possible deviation in price estimation is beyond the work scope. While sales revenue sr is beyond the production scope, the retained earnings r as the economic process output are controllable only by manipulating the total production cost ToC.

After distinguishing the different types of monetary values, the cost itself can be further classified under different criteria. From global eco-efficiency perspectives, economic aspects are to be considered throughout the entire life-cycle [104]. In his study, Klöpffer explains that all costs caused before the assessed life-cycle stage are self-evidently considered within the economic assessment of that stage [175]. Therefore, economic assessment is a cradle-to-gate or cradle-to-grave and not a gate-to-gate approach in its nature. However, this point of view is sufficient only for cumulative total costs ToC, when the retained earnings r are excluded or predefined. However, all economic impacts are parts of their global summation throughout product entire life-cycle under whats known as the life-cycle cost (LCC).

The LCC sums costs of producing, purchasing, operating, maintaining, and disposing a product [94]. Not to be mixed with life-cycle costing, which is an assessment method [289], the LCC in this thesis refers to the cumulative costs throughout the entire life-cycle of the assessed product as a functional unit [66, 247]. According to Roskam, the LCC for the example of an aircraft can be split into four main costs [261], as it is simplified in Eq. 3.3.

$$LCC = C_{RDTE} + C_{ACQ} + C_{OPS} + C_{DISP} \tag{3.3}$$

With C_{RDTE} = research, development, test and evaluation cost; C_{ACQ} = acquisition cost; C_{OPS} = operation cost; C_{DISP} = disposal cost, all in the monetary unit of (€); As it is shown in Fig. 3.11, this LCC can be broken down to include lists of contained sub-costs under each main cost from Eq. 3.3 [66, 324].

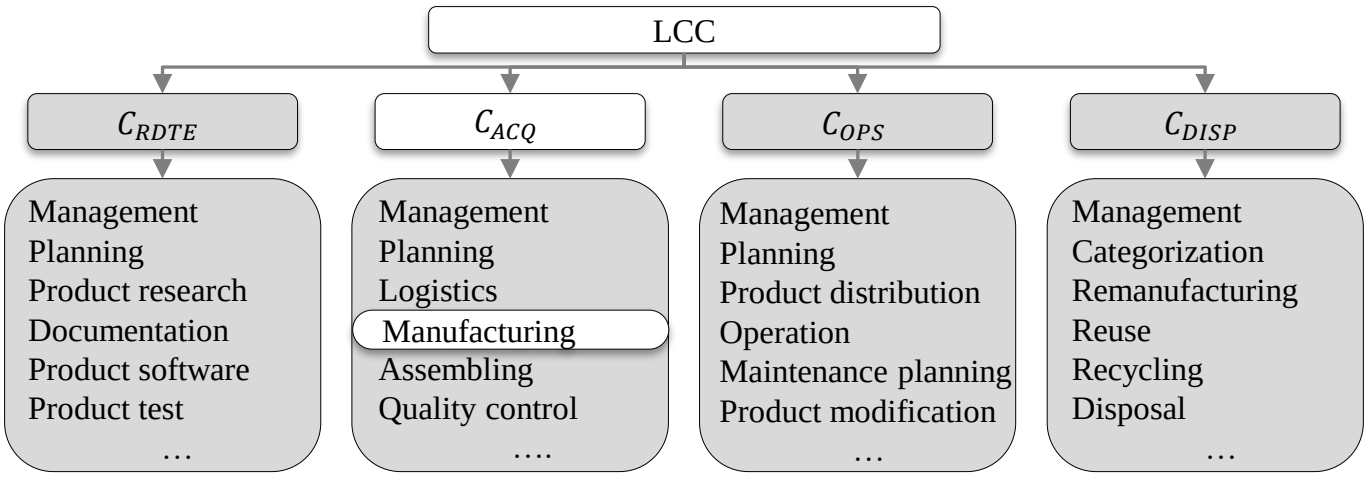

Figure 3.11 LCC structure, adapted from [66, 202, 253, 261, 325]

Despite the variation of LCC break-down structures in literature, the LCC is generally sorted under the different life-cycle stages on its upper level. Regardless of the description and orientation of selected sub-costs, LCC must include all affiliated sub-costs in unified real or theoretical monetary values through the life-cycle [21, 66, 202, 253, 261, 269, 324, 325]. The case study in this thesis is about the manufacturing of a selected FRP structure, as it is unshaded in Fig. 3.11. Although Fig. 3.11 provides a comprehensive visualization of the LCC, these lists may differ based on the differences in assessment goals and scopes. Moreover, each of these sub-costs has a unique significance based on the assessed product as well as assessment goal and scope.

Theoretically, the LCC in general and manufacturing cost in specific can be classified under a set of intercorrelated cost categories [319]. They include direct, indirect, recurring, nonrecurring, fixed, as well as variable costs [66, 320]. Still, there is a lack of a comprehensive description of manufacturing cost categories. Therefore, such an illustration is introduced in this thesis within chapter 4.

Ecological aspect

Similar to the economic one, the ecological aspect consists of various categories and impacts, which should be clearly defined to select the targeted CSFs and their KRIs. Before simplifying this ecological aspect into assessable phenomena, it has a complex net of correlations between the studied system and other ones [258]. One of the sufficient approaches to such simplification is achieved by defining the ecological categories that should be considered and handled in the decision-making. Decision-makers should plan the resource depletion to not exceed the natural resource reproduction. Moreover, they are responsible for producing ecologically

absorbable wastes and emissions side-by-side with avoiding eco-system degrading activities [86]. To serve these objectives, a set of ecological damage categories may be determined. In literature, there are several definitions for impact categories as well as their associated indicators.

In their study, Jolliet et al. have summarized the major four damage categories to include human health, ecosystems quality, climate change, and resources, as they are shown on the right side in Fig. 3.12. These main categories of ecological damage are affiliated with so called midpoint categories. The reference substances in Fig. 3.12 facilitate the normalization of ecological assessment [159].

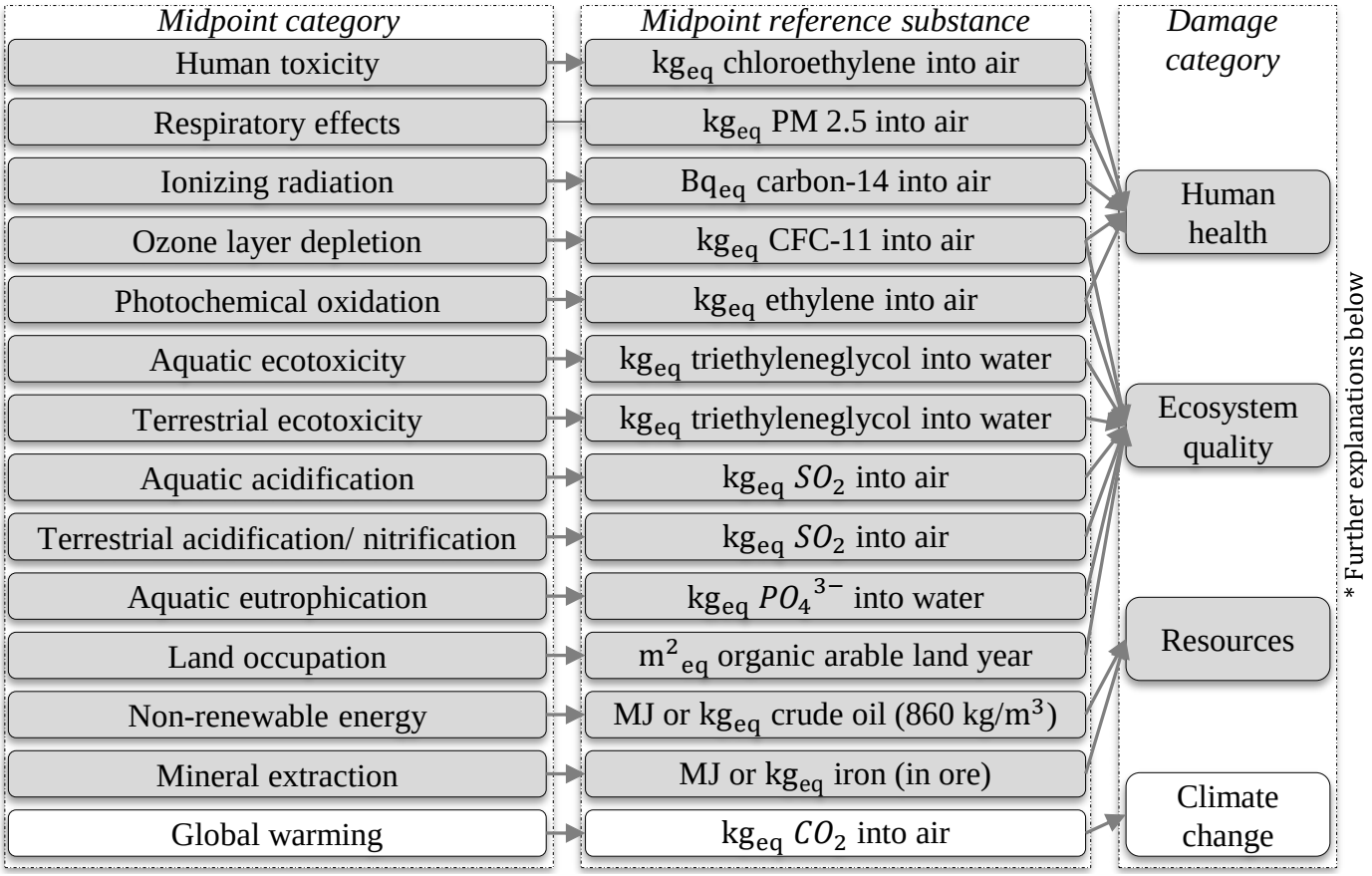

Figure 3.12 Ecological damage and midpoint categories as well as reference substances, adapted from [159]

* kg: kilogram eq: equivalent PM: particle matter Bq: becquerel radioactivity unit carbon-14: radiocarbon CFC-11: trichlorofluoromethane SO_2: sulfur Dioxide PO_4^{3-}: eutrophication CH_4: methane MJ: mega joule

Although all damage categories are significant for the ecological aspect of eco-efficiency, climate change is ranked as one of the most crucial challenges the mankind ever faced [308]. As it is unshaded in Fig. 3.12, the global warming and the affiliated climate change phenomena are solely considered in this thesis. From studying the terminology of both climate change and global warming, these terms are interchangeably implemented in media, politics, and literature [281]. On the one hand, climate change can be defined as a temporal fluctuation of climate patterns due to unforced natural variability or external forcing mechanisms by human activity [129, 145]. On the other hand, global warming brings attention to the temperature increase in specific rather than all the general aspects of climate change [281]. According to Hansen et al., this means that the temperature increase is a response to different types of natural and man-made radiative forcing. Such radiative forcing inflicts the global radiation balance of the earth [129]. According to a recent report from the intergovernmental panel on climate change, the temperature increase has reached 1.5 °C above the preindustrial level [142].

Due to their concentration disorder, gases can generate radiative forcing directly and indirectly [144]. The GHGs are relatively active gases in the atmosphere that absorb sun emitted as well as earth and oceans

re-emitted radiations [144, 222]. These GHGs such as CO_2 trap some of the emitted and re-emitted radiations with thermal, terrestrial, or infrared (IR) wavelengths in the atmosphere, in what is called greenhouse effect [144, 222]. Besides CO_2, GHGs have been defined to include several gases such as methane, nitrous oxide, hydrofluorocarbons, perfluorocarbons, and sulphur hexafluoride [41, 308]. For the ecological assessment, global warming potential is an indicator for the decision-makers to determine the trapped heat by GHGs on earth surface as well as in its troposphere [199].

Considering the global warming as the midpoint category, its reference substance is calculated by the damage unit of kg_{eq} CO_2 into air [148], as Fig. 3.12 shows. Yet, carbon footprint is a term that refers to the emissions amount in kg_{eq} CO_2 caused by the assessed system [97, 159, 335]. Still, the carbon footprint may be implemented to describe the summation of all emissions from the different GHGs [154]. Compared to a unit of CO_2, these equivalents are defined to be factor 21 for methane, 310 for nitrous oxide, and 23.900 in the case of sulphur hexafluoride. However, the impacts of both hydrofluorocarbons and perfluorocarbons vary based on the specific gas [96, 308]. In this thesis, these impacts of various GHGs are covered in the CO_2 equivalent by the adopted characterization factors, while the assessment is carried out by determining the kg_{eq} CO_2 equivalents of all involved process elementary flows and not the directly emitted GHGs from that process.

3.2.2 Frameworks for Eco-Efficiency Assessment

There are several frameworks for assessing the eco-efficiency or a single aspect of it. Frameworks of life-cycle cost analysis (LCCA) and LCA are the main approaches in assessing economic and ecological impacts respectively. In a previous work, a combination of both LCCA and LCA has been integrated with a modeling framework to realize the eco-efficiency assessment in FRPs manufacturing [10]. In this section, the main phases of these frameworks including the LCI and LCIA are reviewed. Moreover, the implementations of Industry 4.0 solutions in executing relevant frameworks as well as examples of computer-based DSSs are briefly studied.

Relevant assessment frameworks

It is essential to briefly review the main frameworks for assessing economic, ecological, as well as both eco-efficiency aspects. On the one hand, the LCCA is implemented to calculate the total product LCC [176]. On the other hand, the LCA framework provides the required development guidelines for decision-makers from an ecological perspective. In this framework, the impact results should be gathered for a defined selection of ecological impact categories [151]. These frameworks guide the decision-makers to select suitable SDs by affording comparable non-absolute values for different product systems, while executing and controlling such SDs are beyond the scope of these assessment frameworks [135, 152]. Practically, the framework of LCA can be implemented in performing LCCA. Furthermore, collected data about process parameters may be used for both economic and ecological assessments [152].

As it is illustrated in Fig. 3.13, the LCA is performed through an iterative framework that includes sequential phases with an internal interaction [151]. The first phase in this framework includes defining the goal and scope of the assessment as well as its system boundary. The second phase is accomplished by performing the LCI for the assessed process. The LCIA is the third phase in this framework, while it concludes the assessment results based on the collected data from LCI. In the final interpretation phase, all previous phases are evaluated and the required modifications in each one are performed [152]. Considering the cost assessment, there are other bottom-up approaches, which might be implemented in undertaking the LCCA such as material flow cost accounting and activity-based costing [278, 342], while their DSSs are discussed later in this chapter.

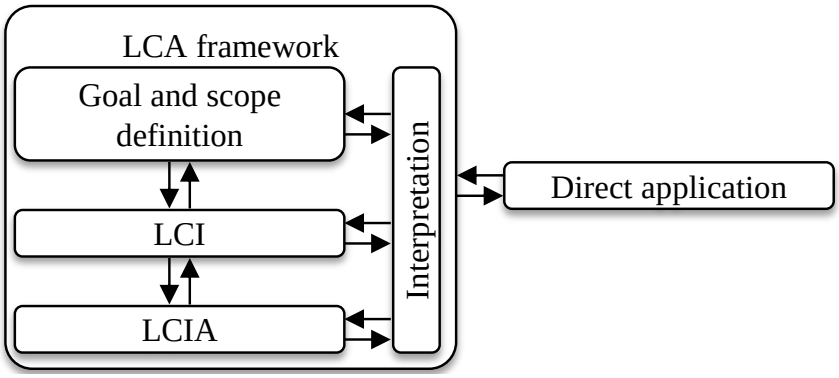

Figure 3.13 LCA Framework [152]

Within their study, Witik et al. have introduced a framework that combines both LCCA and LCA for an economic and ecological assessment of FRPs [343]. Although the LCCA is based on the LCA [151], Norris differentiates between ecological LCA and economic LCCA. Still, both LCA and LCCA are key tools in promoting the eco-efficiency of a product system [232]. Technically, the LCA guides decision-makers to select the suitable direct applications by comparing different scenarios. It provides comparable non-absolute values within what is called a consequential LCA [135, 232]. On the other hand, cost models are mainly implemented to determine exact values within what can be considered as an attributional LCCA [39]. Such attributional assessment aims to understand the impact behavior regarding product system flows. Moreover, there are three levels of LCA implementation,which are product micro-level such as carbon footprint and labeling, meso-macro level that serves policy making and global improvement potential identification, and finally an accounting LCA that monitors the product and process on various levels [91].

In Tab. 3.2, differences and similarities between the phases of LCCA and LCA are compared.

Table 3.2 Comparison of LCA and LCCA, adapted from [10, 152, 232]

Framework phase	LCCA	LCA
Goal and scope definition	Evaluating and/or comparing products or processes economically	Evaluating and/or comparing products or processes ecologically
LCI	Measuring relevant elementary flows	Measuring relevant elementary flows
LCIA	Determining economic impacts such as direct cost	Determining ecological impacts such as carbon footprint
Interpretation	Evaluating both framework and results by economic norms	Evaluating both framework and results by environmental norms
Direct applications	Cost effective SDs	Environmentally friendly SDs

Tab. 3.2 explains the different goals and scopes of LCA and LCCA and illuminates the miscellaneous results, which are compiled from the various indicators. Furthermore, these results lead decision-makers to address direct applications for different intentions. The LCA and eco-efficiency assessment have several common characteristics such as comprehensiveness, transparency, as well as iteration [269]. From understanding Tab. 3.2, there is a possibility to unify the measured elementary flows in the LCI, which is an uncommon approach in literature.

Similar to the one for LCA, an eco-efficiency framework is shown in Fig. 3.14. As Fig. 3.14 shows, the eco-efficiency framework is similar to the LCA one except for the specified considerations of both economic

and ecological aspects in it, which is followed by the eco-efficiency assessment. However, this framework integrates the LCI as an obvious part of the LCIA within the assessment phases in Fig. 3.14.

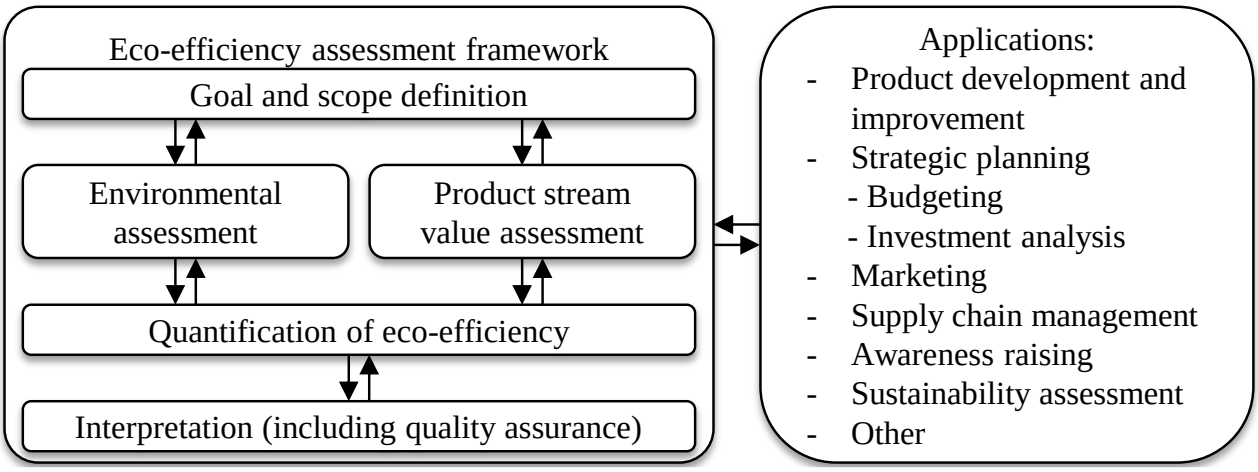

Figure 3.14 Eco-efficiency framework [269]

In practice, both LCCA and LCA can serve consequential or attributional assessments based on their goal and scope definition, while combining them to perform an attributional assessment is adopted in this work. Theoretically, the eco-efficiency assessment includes the time dimension in its core, whereas the temporal system boundaries have been focused on in several works [152]. However, the necessary time interval of assessment iteration is still the main question, while a recent assessment at least is always suggested.

Framework phases

The first phase in LCA framework is to identify the assessment goal and scope. This can be firmed up by the definition of assessment objectives. Then the assessment motivations and the served decision-makers are to be defined [151]. In this thesis, the target objective is not only to assess a process, but also to achieve the capability of time-dependent eco-efficiency assessment for different production scenarios of relevant FRP structures. Furthermore, the motivation is explicitly elucidated within the introduction, while the targeted group from implementing the novel time-dependent eco-efficiency assessment includes the decision-makers from FRPs sector in general and especially from the operational management level in the FRPs production.

The second step in the first phase is about defining the assessment scope to assure that the outcomes can address the goals sufficiently. This includes determining the product system as well as the functional unit. It also implies defining the system boundaries, impacts allocation, data quality, identifying the data requirements in order to gather the available parameters, as well as selecting the work limitations and assumptions. Now, the impact categories and allocation procedures should define the cut-off criteria. As a part of that, the cut-off-criteria can be defined as the elementary flows, their impacts and characterization factors, and the containing activities or UPs, which are excluded from the assessment scope [151].

In practice, some of the system boundary aspects can be illustrated as a part of the process modeling, whereas their definition is an iterative approach [151]. Such definition clarifies where, when, and which system is assessed, within what are know as the geographical, temporal, and technical boundaries respectively [24, 300]. The geographical boundary allocates the assessment parameters to their countries or regions. This includes several relevant aspects such as the ecosystems sensitivity to environmental impacts, the energy sources, and the waste management in that selected region. Moreover, the time horizon boundary is related to the study temporal aspects including the assessment year at least. This thesis introduces a novel approach for time-dependent

assessment that gives special attention to the time horizon aspects. Finally, the technical boundary describes the applied technologies and techniques, which is substantial to have a clear allocatable and interpretative assessment results in both consequential and attributional approaches. Moreover, the introduced time-dependent eco-efficiency assessment later in chapter 4 necessitates a clear definition of this technical boundary in order to assign the results to their reasons in chapter 6.

After the goal and scope definition, LCI is the phase where the relevant data about process inputs as well as outputs is collected. Conventionally, the data about material and energy flows is either manually measured in production or estimated based on available research. In the case of unavailable data, assumptions based on the technical knowledge of field experts may be implemented [152]. Therefore, data availability and quality are crucial to the reliability of LCI and consequently the LCIA [139, 166].

Practically, the LCI may be realized through the systematic procedures suggested in Fig. 3.15.

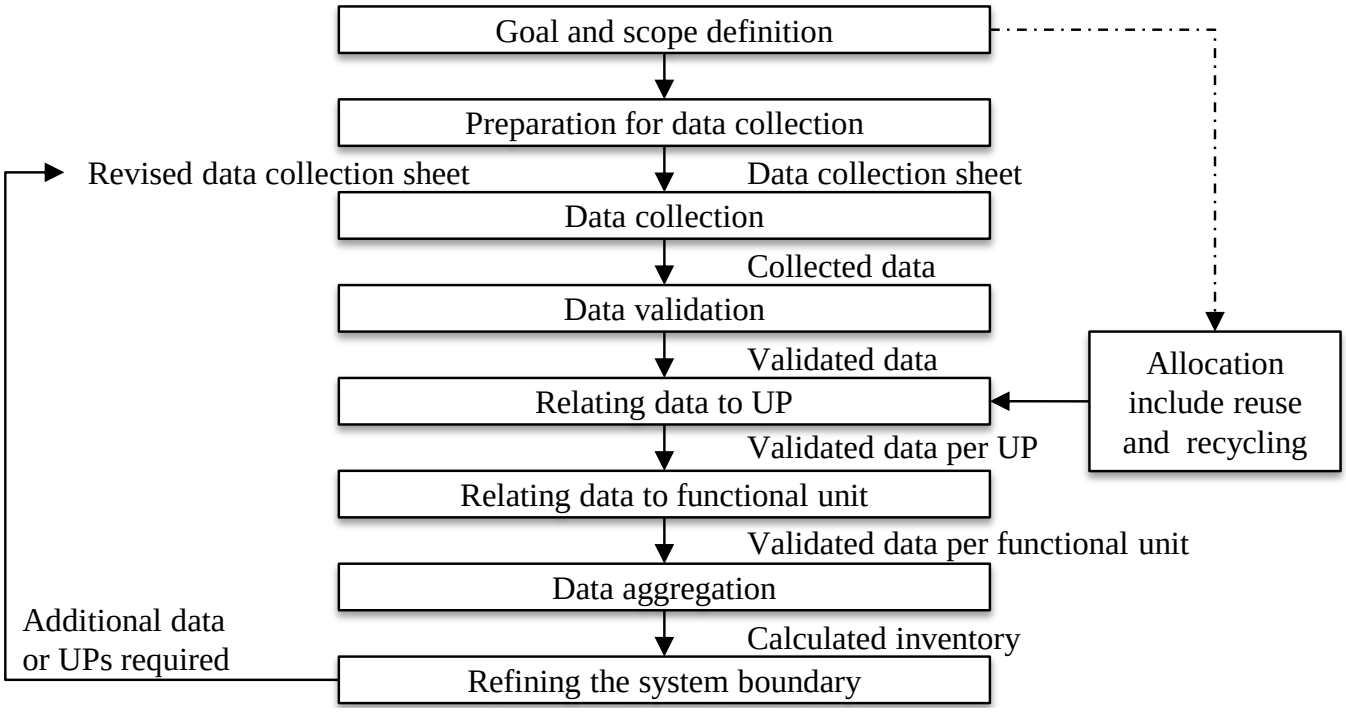

Figure 3.15 LCI simplified procedures, based on [151]

The first step of goal and scope definition is common in both LCA and eco-efficiency frameworks in Fig. 3.13 and Fig. 3.14 respectively as well as LCI procedures in Fig. 3.15. However, this step in LCI procedures is meant to cover only the LCI goal and scope. The second step is to prepare for the data collection by establishing the proper setups, while data sheets are common forms to collect data in conventional LCI [10]. After collecting the data, it should be validated and related to its UP and functional unit.

The data targeted by LCI can be classified under two main parameter groups. On the one hand, there are the parameters which are associated with the process itself. These elementary flow parameters can be gathered from the process. On the other hand, there are the parameters related to the impact equivalents of these flows, which are known as the characterization factors. These so called resource parameters depend on various aspects beyond the process itself. For instance, the magnitude of used material in a process is an elementary flow parameter, while the price of that material is a characterization factor. Here, the characterization factors represent the studied impacts of used elementary flows per each unit of them applied in the assessed product system.

In his thesis, Hilmer listed the main steps of LCI for assessing the eco-efficiency of producing FRP structures [138], as they are shown in Fig. 3.16.

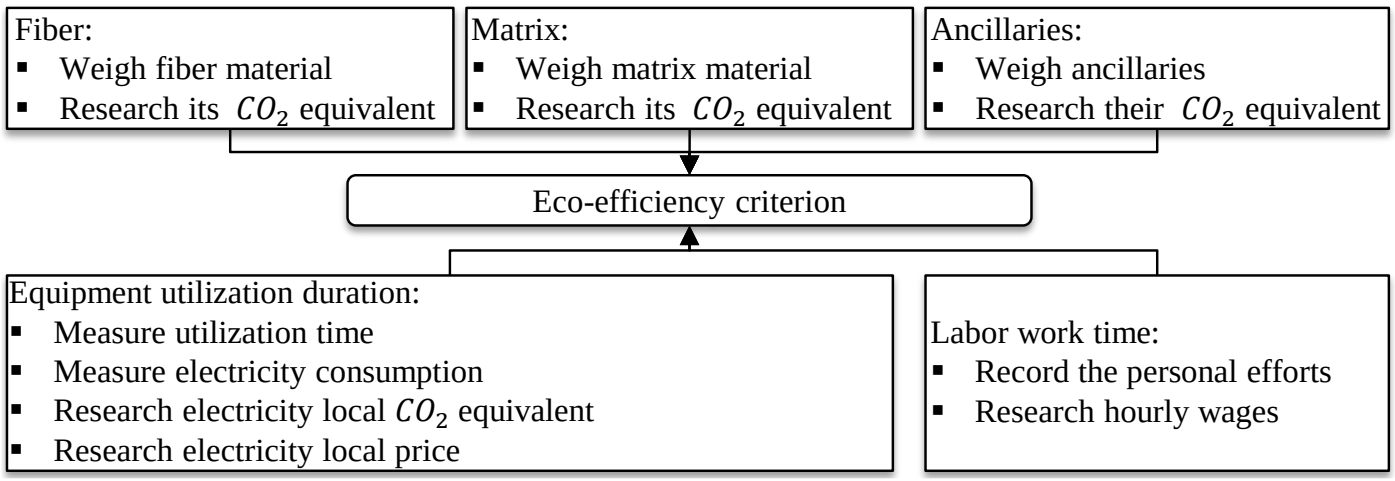

Figure 3.16 Data collection for eco-efficiency, based on [138]

As Fig. 3.16 shows, the main elementary flow categories within the FRPs manufacturing have been defined to include the fiber, matrix, ancillaries, labor, equipment, and electricity. In his thesis, Hilmer suggests two main LCI steps which are the elementary flow measurement and the characterization factor research [138].

Although the time-dependency in LCI is not covered in the previously discussed frameworks, it has attracted some attention lately. For the ecological aspects, several works have introduced dynamic data collection approaches [49, 304]. On the one hand, Tao et al. suggest the implementation of advanced technologies for collecting the ecological data from product systems throughout the entire life-cycle of a functional unit [304]. On the other hand, the characterization factors have been calculated dynamically in Levasseur et al. study [193]. For the eco-efficiency, a LCIA assesses the potential of product economic and ecological impacts during the life-cycle within defined impact categories. Technically, it provides supplemental information that explains a long term economic and ecological perspectives [151]. However, the review of LCIA is partially included within this thesis, while simplified LCIA concept and approach have been discussed for the development of EEAM in previous works [10, 13].

However, there is no clear distinguish between the life-cycle of the assessed functional unit and the life-cycles of implemented elementary flows in literature. Therefore, a clear definition of the included life-cycle stages of each characterization factor is required in order to define the assessment coverage of product life-cycle, while such coverage may be a cradle-to-gate, gate-to-gate, gate-to-grave, or cradle-to-grave. Such combined illustration of product and elementary flows life-cycles is introduced later in this thesis within chapter 4.

Industry 4.0 and eco-efficiency frameworks

Based on a thorough literature review and field questionnaires, Varela et al. detect a clear correlation between Industry 4.0 and sustainability in general. Although their study concludes that Industry 4.0 is impacting all sustainability pillars, the study provides no clear framework to achieve that [322]. The idea of implementing advanced solutions from Industry 4.0 in eco-efficiency assessment has attracted some attention recently [49, 302, 304]. Despite the direct and indirect benefits of applying it, reviewing the Industry 4.0 here aims to clarify that the transition into it is not the goal itself, but it is all about achieving eco-efficient and sustainable industry by its implementation [22, 42, 218]. Especially for the production process, Tao et al., Al-Lami et al., Cerdas et al., Tan et al., and several others have studied the implementation of Industry 4.0 technologies in the different aspects of the eco-efficiency from different perspectives [11, 49, 302, 304].

In their work, Tao et al. have introduced a comprehensive approach for the implementation of solutions such as IoT in LCA throughout the entire life-cycle of a product. They discuss the possible usage of automated data collection in achieving a real-time LCA especially in the production stage. Besides the real-time energy data collection, the materials can be tracked by the bill of material and measured by advanced technologies such as radio-frequency identification according to them. Other sensor nodes such as electricity meters, water meters, gas meters, temperature sensors, as well as fiber optical sensors are also mentioned in that study [304]. However, the bill of material is an inventory that represents only the overall inputs, whereas the wastes description is not identifiable by it [301]. Moreover, Tao et al. work superficially covers only energy and material flows as it focuses on the ecological impact of the process, while labor work and equipment operation are not specifically considered in that work. When it comes to the data quality, it is not systematically assured in that framework, whereas there is no clear classification of assumed and measured data.

The utilization of AI for data collection and processing in eco-efficiency assessment has been discussed by Cortés et al. in their work. Although that work provides a clear framework for the ecological DSSs in Fig. 3.17, it has no clear perspective of the entire life-cycle stages in handling the environmental issues [62].

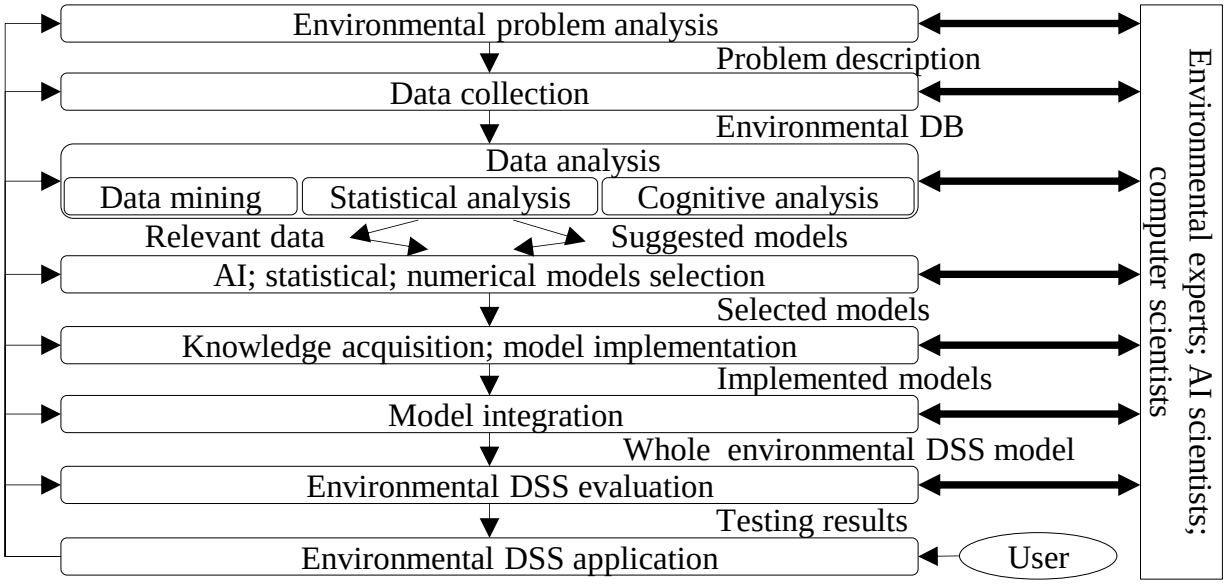

Figure 3.17 Framework of implementing AI in ecological DSSs, based on [62]

Now, the framework in Fig. 3.17 is more data oriented, while there is no clear modeling approach. Moreover, this framework lacks a clear description of the involved LCA stages such as the LCI and LCIA, while AI solutions can be applied to enhance a single stage or multiple ones in practice. On the other hand, their framework has the advantage of considering detailed data processing steps [62].

In Fig. 3.18, Thiede et al. have suggested a realization of DMAIC framework through a human centered approach. This control oriented framework in Fig. 3.18 provides clear correlations between the physical world, the data collection, the cyber world, and the control systems for processes with different DoA [309]. Although these stages are discussed through steps within them, the framework lacks a clear concept of data collecting capabilities. In other words, achieving the proper temporally and spatially allocated data is not an obvious approach, while a detailed real-time capable data collection concept is not covered here.

Furthermore, the study of Tan et al. provides a framework of applying solutions from Industry 4.0 to enhance the energy efficiency in production facility [302]. This study; however, provides no description of data collection concept for the various elementary flows or generic approach of data processing.

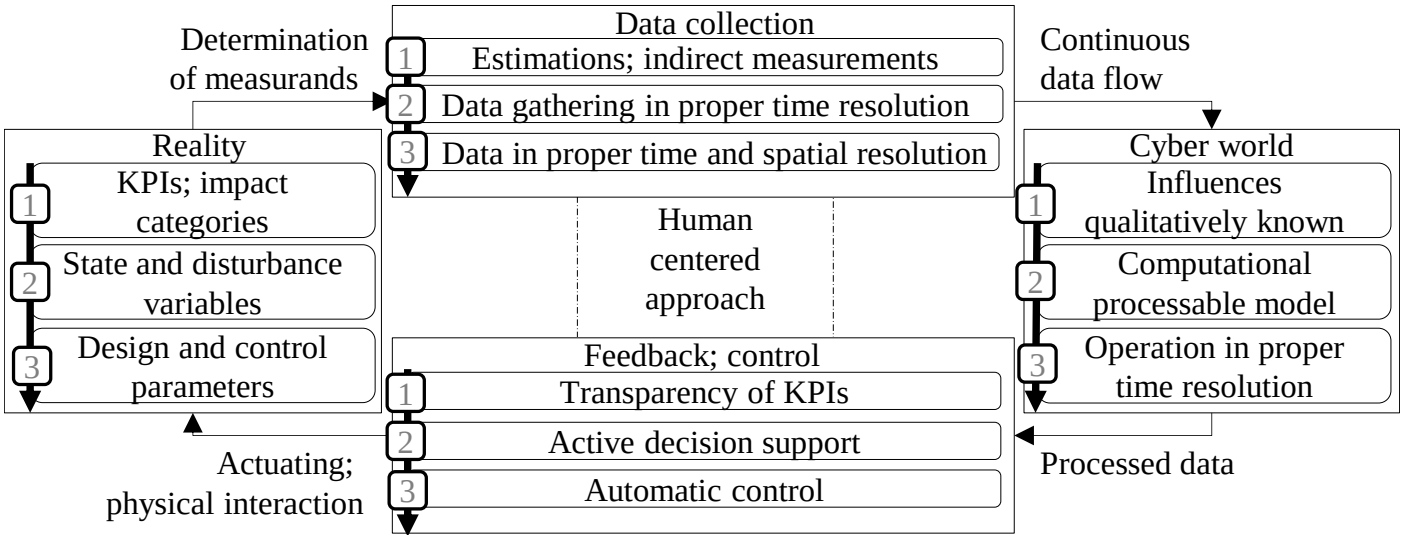

Figure 3.18 Implementing CPPS in learning factories, based on [309]

In conclusion, no concept from implementing Industry 4.0, that enables the realization of real-time data collection system as a set of predefined sensor nodes and covers all associated elementary flows, has been introduced by any of these studies. Such a concept should illustrate the methods of selecting, assigning, and allocating the sensor nodes. Moreover, there is no Industry 4.0 framework for time-dependent eco-efficiency assessment that includes such concept in literature. Therefore, a goal oriented framework that starts from establishing a conceptual model and ends by a computerized model to generate the aimed knowledge based on clearly defined data collection concept is still required.

Eco-efficiency computer-based DSSs

When it comes to the review of existing computer-based DSSs, there is a difficulty in finding published works that describe the functionalities of these tools. In practice, such software DSSs are treated as confidential properties of their developing organizations. Nonetheless, there are still some published studies about DSSs that serve assessing the process eco-efficiency or a single aspect of it. In this work, the terms of software, computerized model, and computer-based DSS refer to the same codes operating on a computer. However, a computer-based tool with a graphical user interface (GUI) is supposed to be more than a program code, while it has a user-friendly interface for non-programmers.

Nowadays, several computerized models are developed and implemented in assessing the direct cost of production processes. Starting from simple calculation tools developed internally by facility managers ending with professional commercially available ones, such DSSs exist to serve various managerial levels through bottom-up and top-down approaches. Moreover, these DSSs can be distinguished to assessment tools that are based on process parameters and estimation ones that are based usually on product parameters. While there is a large magnitude of cost analyses tools, the focus here is on the ones related to the FRPs production. As an example, the SEER-MFG is a cost estimation tool for product management in general that is utilized for the production of FRPs structures as well. In his thesis, Nills has discussed a design-based software solution that is specialized for cost estimation of FRPs structures, while similar tool has been introduced by Hagnell et al. [124, 230]. In literature, the discussed DSSs for cost analyses in FRPs production are clearly focusing on the estimation rather than the assessment.

In FRPs productions, decision-makers lean on the available universal ecological assessment tools to assess their processes, while there is a lack of specialized ones with proper ecological DBs. Similar to the case

of economic computer-based DSSs, there is a wide range of universal ecological assessment tools that are applicable for different life-cycle stages of various functional units. Some of these computer-based DSSs are commercially available, while others are internally used by their developing organizations. However, open-source ones that serve this aspect may still be found. In practice, some of these tools are provided as software packages that depend on universal ecological DBs. These DBs are continuously updated based on the results that are generated from associated assessments [25]. Such tools may cover the entire life-cycle as well as a wide range of ecological impact categories such as climate change, human health, resources, and ecosystem quality [159]. For instance, GaBi is a computer-based DSS that is developed by the University of Stuttgart in Germany. This tool provides ecological assessment for the entire life-cycle of a product [25]. SimaPro is another worldwide known LCA tool that covers the entire life-cycle as well [116]. Another example is Umberto software solution that assesses both ecological and economic impacts. Within Umberto, a production can be modeled to allocate the associated elementary flows [233, 255, 277]. As it is discussed later in chapter 4, the EEAM is a bottom-up computer-based assessment DSS that is also developed to assess both economic and ecological aspects in FRPs production [10, 13]. However, the data collection is commonly excluded from all previously discussed computer-based DSSs, while they focus on serving LCIA more than LCI. Therefore, comprehensive DSSs for both LCI and LCIA are still required.

3.3 Fiber-Reinforced Polymers (FRPs)

Composites in general and FRPs in specific are considered as leading materials in sustainability enhancement efforts. In aerospace industry, economic and ecological reasons motivate decision-makers to implement FRPs. The weight reduction potential is attracting commercial aircraft operators to encourage the original equipment manufacturers in utilizing more of such materials. However, the manufacturing of structures made of these materials has a significant development potential in the technical, economic, and ecological aspects [228]. In practice, a variety of possible techniques, technologies, structures, and industry applications is forming a wide range of process scenarios. These process variants are challenging the realization of an adaptable time-dependent eco-efficiency assessment. In this section, the FRP structures, their industry applications, and their manufacturing techniques especially in aerospace are briefly reviewed.

3.3.1 Structures Made of FRPs

It is essential to define the terminology and typology of FRPs as well as the characteristics of these materials. While the adopted case study structure comes from it, aerospace industry is also briefly discussed here.

Terminology and typology of FRPs

In general, the term composite refers to the combination of heterogeneous substances [114]. Technically, it consists of two or more ultimately separated constituent materials with different properties, which are bound together to achieve a new product with optimized physical properties [46]. However, this term is implemented in describing ancient and modern combinations of heterogeneous substances in several sectors [226]. In reference to the matter types, composites include several possibly combined substances within a non-atomic level such as metal matrix composites, ceramic matrix composites, carbon carbon composites, and polymer matrix composites, which are also known as FRPs [4, 185].

In their work, Callister et al. split composites into three types of substance architecture [46], which are shown in Fig. 3.19.

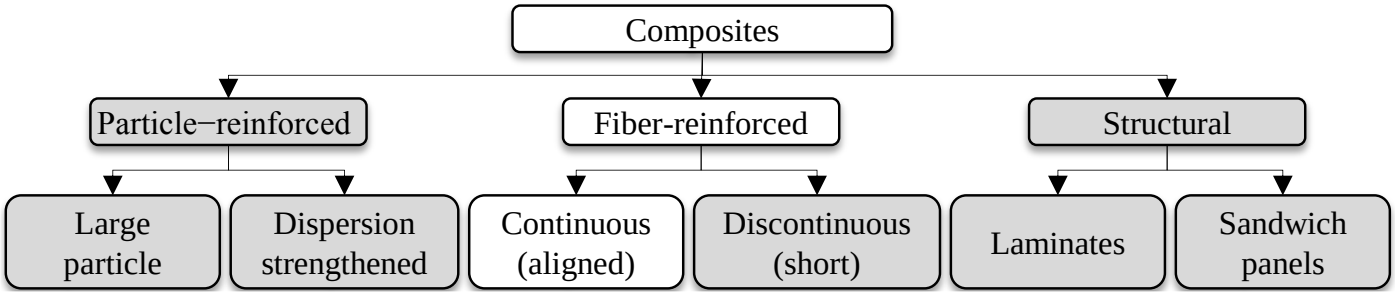

Figure 3.19 Composites categorization, adapted from [46]

In Fig. 3.19, fiber-reinforced composites are split into two main categories, which are the continuous as aligned fiber and the discontinuous with short aligned or randomly oriented fiber [46]. Such continuous fiber can be formed in several dimensions and orientations to provide the aimed properties [4]. As it is shown in Fig. 3.19, the shadowed categories are irrelevant to the case study in this work. Therefore, no further explanation about them is provided in this literature review.

FRPs characteristics

Their properties such as high stiffness, strength, lightweight, as well as corrosion and fatigue resistance are attracting various industries toward using the FRPs in different applications. In practice, the FRP is a high-performance material in aerospace, marine, and many other industries [185].

On the one hand, the fibers provide the macroscopic stiffness and strength to withstand the mechanical loads [4]. Technically, these fibers can be made of materials such as carbon, glass, and aramid [164]. In FRPs industry, carbon fiber-reinforced polymers (CFRPs) and glass fiber-reinforced polymers (GFRPs) are the most popular structures [4]. As an input to the FRPs manufacturing, the fiber can be processed in different maturity scales. As it is explained by Hoa, single filaments may be converted into a fiber tow, while the sets of tows construct a tape, woven fabric, braid, knit, or a mat. Finally a stack of fiber layers can be produced by any of these tow maturity scales [141]. For many structures, non-crimp fabric is a commonly used type of fiber in aerospace applications. Based on the selected manufacturing technique and the aimed structure characteristics, fiber material from a suitable maturity scale must be selected.

On the other hand, the matrix can be metal, ceramic, or polymer [141]. However, only the FRPs are discussed in this thesis, while polymer matrix can be thermoset, thermoplastic, or elastomers. The matrix of polymer resin is applied to fix the fibers together and form the surface of the combination as desired. Moreover, the mechanical functionality of the cured resin is to withstand both compression and shear. Due to the chemical characteristics of these matrix types, thermoset and elastomer are unmeltable, swellable, and insoluble after curing. Technically, a cured thermoplastic is meltable and soluble. Considering the production process, thermosets are invariably formed after curing. Unlike thermosets, a thermoplastic is thermos-formable matrix that can be re-melted and welded [349]. Elastomers can elastically reform under tension and back to its original form after that. However, like thermosets elastomers cannot be re-melted after curing. Technically, matrix viscosity plays a decisive role in the manufacturing process especially in the selection of proper relevant techniques, as Appx. A shows. A high viscosity matrix can be also pre-impregnated in fiber as a semi-finished product, which is also known as the prepreg [173].

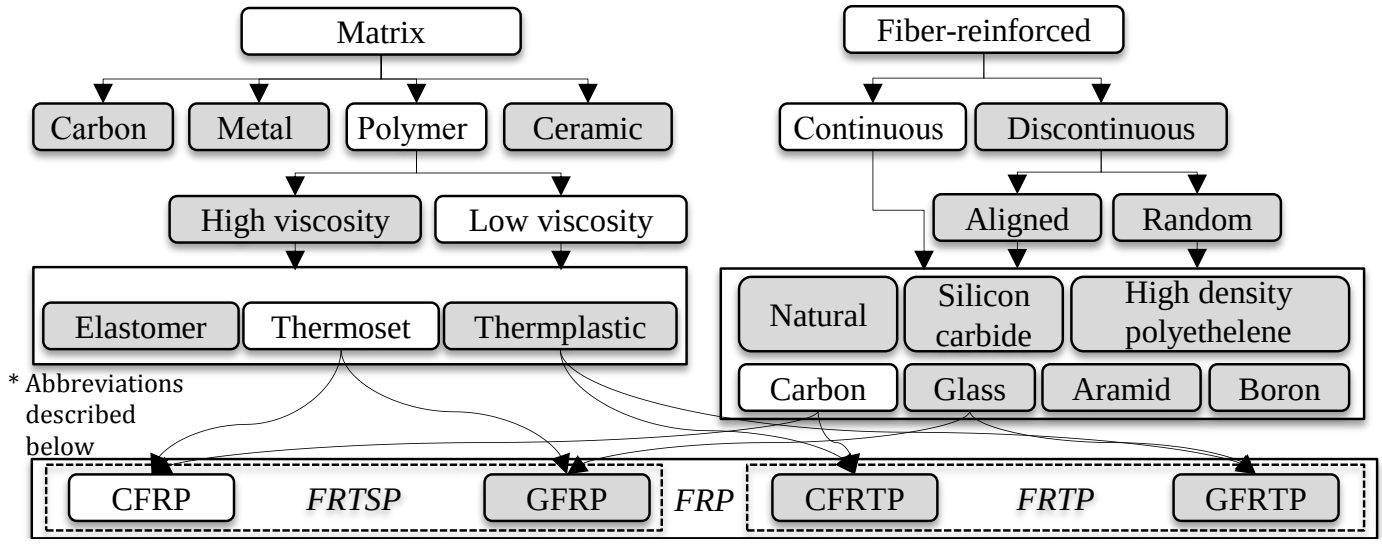

Figure 3.20 Types of FRP, adapted from [36, 46, 114]

* FRP: fiber-reinforced polymer FRTSP: fiber-reinforced thermoset polymer CFRP: carbon fiber-reinforced thermoset polymer GFRP: glass fiber-reinforced thermoset polymer FRTP: fiber-reinforced thermoplastic polymer CFRTP: carbon fiber-reinforced thermoplastic polymer GFRTP: glass fiber-reinforced thermoplastic polymer

As it is shown in Fig. 3.20, the selected matrix and reinforcement combinations of FRP may include carbon fiber-reinforced thermoset polymer referred to as CFRP, glass fiber-reinforced thermoset polymer referred to as GFRP, carbon fiber-reinforced thermoplastic polymer referred to as CFRTP, and glass fiber-reinforced thermoplastic polymer referred to as GFRTP [36, 46, 114]. According to Kraus et al., thermoset polymers dominate the matrix market revenue worldwide with about 77 % against 23 % for thermoplastic in all industrial applications of FRPs [178]. As it is unshaded in Fig. 3.20, the case study in this work is about the continuous carbon fiber-reinforced thermoset polymer. Although other physical and chemical properties of both fiber and matrix are crucial in configuring the production process as well as defining the industrial applications, these properties are beyond the scope of this thesis.

FRP applications in aerospace

Structures made of FRPs are applied in various industries with different scales. For several industrial applications, composites are opening the door for further advanced products through their reduced weight, advanced mechanical characteristics, as well as the possibility of function integration [334]. Nowadays, industries such as aerospace and energy are leading this trend. Practically, the direct cost and carbon footprint of a composite structure depend heavily on its design and consequently the selected manufacturing technique as well as the adopted process scenario. However, some scholars provide rough estimations for the value ranges of both economic and ecological equivalents. After considering the inflation rates to have the equivalent costs in 2019, composite structures cost around 22 €/kg in automotive, around 496 €/kg in a commercial aircraft within aerospace industry, and around 5366 €/kg in the space applications [8]. According to internal cost studies, CFRP structures for aerospace applications cost around 516 €/kg to 608 €/kg. The carbon footprints of these aerospace structures are in the range of 199 kg CO_2/kg to 109 kg CO_2/kg respectively [13, 138].

Linguistically, aerospace includes the atmosphere as well as the space ahead of it [337]. However, this work focuses on the sector of commercial passengers aircraft. In aerospace industry, several materials have been implemented to build the aircraft structures including metal, wood, and composite ones [247], while metals and composites are the most relevant ones in a modern commercial aircraft.

Considering the holistic life-cycle of composite structures as a part of their containing aircraft, an achievable eco-efficiency benefit has been anticipated from their implementation. On the one hand, fuel consumption is to be reduced by 1 % to 3 % through implementing primary composite structures. On the other hand, implementing secondary composite structures can save another 1 % of that consumption [149]. Generally, any aircraft structure can be either primary or secondary. While the primary structures are the load-bearing ones that are critical to the flight capabilities such as the wing box and its structures, the secondary structures are the ones installed to enhance the flight performance such as leading edge fairings.

As common examples of FRPs in aerospace, structures made of CFRPs such as wing ribs offer around 50 % weight reduction compared to the conventional aluminum made ones [13, 69], while implementing such structures aims to decrease the CO_2 emissions by around 20 % from each aircraft [310]. When it comes to aerospace industry on both sides of the Atlantic, composite applications are expanding in the new aircraft generations, as the examples in Tab. 3.3 clearly show.

Table 3.3 Example of composite applications in commercial aircraft

Aircraft	Examples of composite structures	Mass %
Airbus A350 XWB	Fairings, nacelles, empennage, control surfaces and wings [214]	53 % [214]
Boeing 787 Dreamliner	Fuselage and wing [228]	50 % [204]
Airbus A380	Horizontal stabilizer, center box, pylons, spoilers, and ailerons[141]	25 % [228]
Boeing 777	Fin, stabilizer, thrust reverser cowl, and inlet cowl inner barrel [292]	12 % [292]
Airbus A310	In spoiler, rudder, and vertical stabilizer [228]	7 % [228]
Boeing 767	In doors, rudders, elevators, ailerons, spoilers, fairings [259]	3 % [259]

Listed in Tab. 3.3 from the newest to oldest for both Airbus and Boeing respectively, these selected commercial aircraft types show increasing composite applications. In these examples, composite materials are implemented in various structures, which are made of CFRP, GFRP, hybrid, and other composite materials. Although composite materials may be implemented in different aircraft systems, this thesis focuses on the airframe, which may be split into components such as empennage, fuselage, wings, landing gears, and pylons. In a commercial aircraft, each of these components contains assemblies of structures. Later in chapter 5, the selected case study of a vertical stabilizer rib is a primary structure from the empennage or as it is also called the tail structure.

3.3.2 Challenging Characteristics in Manufacturing FRP Structures

Nowadays, aircraft producers lean on suppliers to provide a wide range of aircraft structures. In their study, Reed and Walsh illuminate this trend of outsourcing manufacturing activities in aerospace industry [250]. This increases the competition between these suppliers to achieve more eco-efficient processes. After defining what composite materials are, this section illuminates how to manufacture structures made of them.

FRP Manufacturing concept

In general, production process depends on the design architecture or as it is called the build-philosophy. Thus, the characterizations of both manufacturing and assembling are influenced by whether the structure integral or differential is [215]. While this work focuses on the manufacturing process of FRP structures, the assembling

process is not studied any further. Regardless of the implemented materials, manufacturing can be additive, net shape, subtractive, or a combination of these processes [121]. Except for the process of 3-dimensional printing, which is an additive process, the FRPs manufacturing contains steps that serve the net shape and subtractive processes in general.

In FRPs manufacturing, both product material properties and product geometry are dimensioned concurrently [334]. Therefore, this manufacturing consists of activities for geometrical preforming and combined substances curing [202]. Based on this simplification, relevant activities can be clustered in generic manufacturing steps. First, the fiber orientation is set, while fiber mechanical characteristics are influenced by this fiber orientation. In this step, the fiber or pre-impregnated fiber is to be formed in the aimed geometrical specification. Second, the matrix is to be impregnated in the fiber with specified volume fraction. This step is irrelevant for pre-impregnated fiber if no additional matrix is required. Finally, this combination of oriented fiber and in it impregnated matrix is cured into stable consolidated structure.

These steps, or as they are called in this thesis UPs, have been introduced by Fig. 3.21 for the techniques of single-line infusion and autoclave curing in a previous work [13].

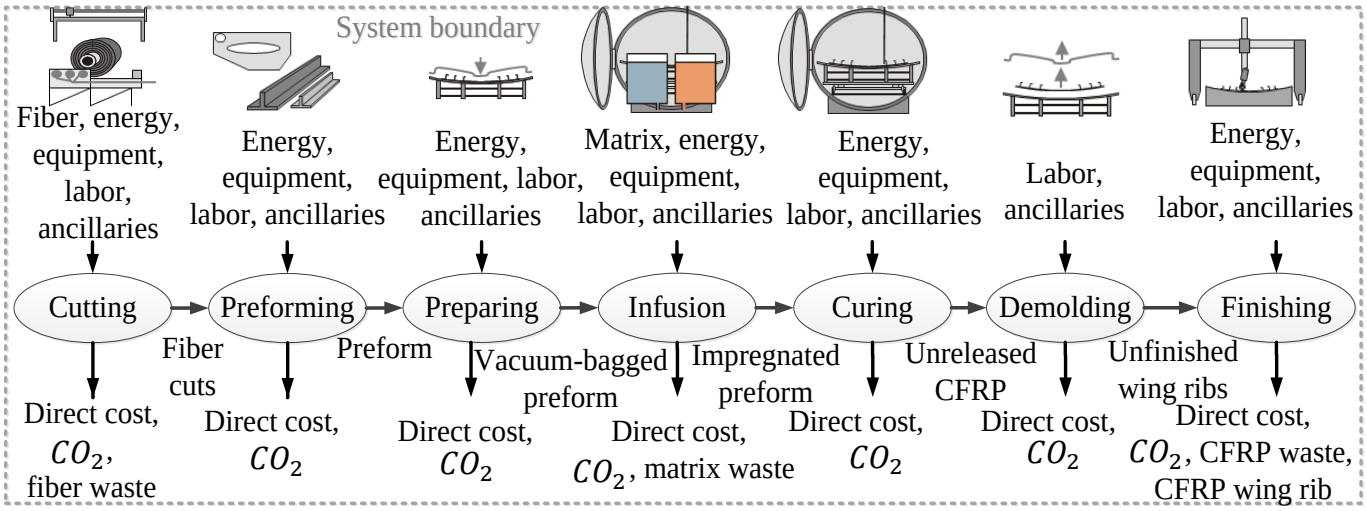

Figure 3.21 UPs of single-line infusion and autoclave curing techniques, based on [13]

Moreover, the relevant eco-efficiency elementary flow categories have been also visualized in Fig. 3.21. While finishing is considered as a separated production main process that comes after assembling, some finishing activities such as machining are carried out after the structure demodling. Moreover, no trimming UP is applied in that work [13].

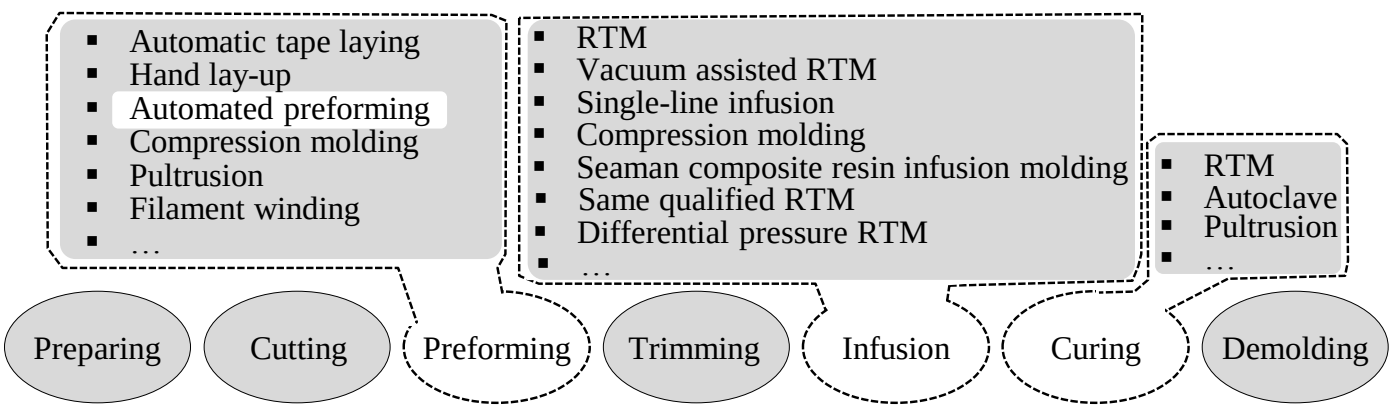

Figure 3.22 Overview of selected FRPs manufacturing techniques, adapted from [13, 228]

Technically, each of these main steps of preforming, infusion, and curing may be carried out through one of different possible techniques. The selected techniques in Fig. 3.22 are associated with the arguably main steps in FRP manufacturing. Starting from preparing and ending with demolding, the UPs in Fig. 3.22 sum up all the activities that are required to manufacture the desired FRP structures. However, these steps are not necessarily sequential in this order. Now, preforming brings the fabric to the final desired pattern or close to it as this fabric is still formable. In this step, selecting the preforming technique depends on various aspects such as fiber maturity scale. Based on the structure design, the selection of that scale is crucial for both FRP structure as well as its manufacturing techniques. Moreover, the preforming technique may be distinguished based on its DoA [317]. From the manual hand lay-up as an example of a low DoA technique to the automatic tape laying, automatic fiber placement, and automated preforming as examples of high DoA, these preforming techniques vary in their DoA. From understanding the common approaches in preforming, manual and automated ones are all carried out by applying vacuum or low pressure from locally used tools or devices. Automatic fiber placement and tape laying as well as filament winding are associated with the applied moderate pressure. If no separated preforming is applied, the fabric is preformed as a part of the consolidation step in some approaches, which is the case in the techniques of pultrusion, compression molding, extrusion, and sheet forming. Not to be mixed with the automatic fiber placement and tape laying, the automated preforming is a high DoA version of the manual lay-up, where cuts with various geometries are preformed by special devices instead of labors. In addition to the applied pressure and vacuum, heat application is also crucial to the preforming.

In Fig. 3.22, the infusion may be performed by various techniques. Technically, FRPs manufacturing depends on the matrix viscosity and the stage of fiber [173]. For instance, resin transfer molding (RTM) is a common technique that provides high manufacturing capacity as well as wide process variants. Therefore, developing RTM technique for large scale manufacturing is of interest to many industries in general and to automotive and aerospace in particular [344]. However, infusion and curing are beyond the scope of the selected UPs in the case study within chapter 5, while further details about these techniques are provided in Appx. A. As it is shown in Fig. 3.22, preparing, cutting, trimming, and demolding are the UPs that contain no unique techniques. In practice, the techniques of these UPs are universal and not FRP specific. As it is unshaded in Fig. 3.22, only the automated preforming technique is relevant for the selected case study in this thesis.

Realized in the EVo-platform, the automated preforming consists of four activities, which are the handling, draping and lay-up, hot-forming, and non-destructive inspection, as they are illustrated in Fig. 3.23.

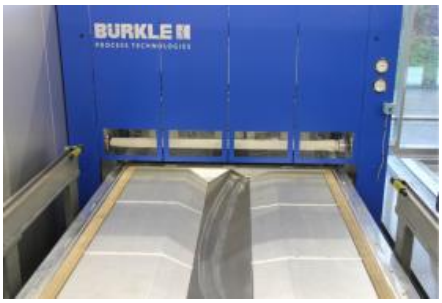

Main activities:

- Handling (Automated)
- Lay-up (Automated)
- Hot-Forming (Automated)
- Non-destructive inspection (Automated)

Figure 3.23 Automated preforming in the EVo-platform, adapted from [315]

The fully-automated preforming technique in the EVo-platform contains various technologies, that are developed partially or completely by DLR, as Fig. 3.23 shows. These technologies are realized in two main machines, which are the draping robot and the membrane press. By an articulated robot on a fixed track, handling and lay-up are automatically carried out. The membrane press applies vacuum, pressure, and heat to

consolidate the cuts into preforms. Moreover, this UP includes a non-destructive inspection system to assure the preforms quality. With all the possible scenarios that may be generated from combining these techniques from Fig. 3.22 and technologies such as the example in Fig. 3.23, it is challenging to find or establish the proper DSSs that are capable of covering the process and product variants in FRPs manufacturing.

3.4 Process Modeling and DSSs Complication in FRP Manufacturing

In this section, modeling is defined as a part of the management and decision-making. Then, modeling frameworks in management are briefly discussed. Finally, relevant stages are studied, while a collection of associated studies in eco-efficiency assessment is briefly reviewed.

3.4.1 Modeling in Management

In this work, the modeling approach intends to unify the different perspectives of the various relevant fields on an understandable level. Now, clear conceptual, mathematical, and computerized models provide a compromise for the multidisciplinary decision-makers from these fields in understanding the assessment results. To have a clear understanding of them, system and model classifications are discussed here. Then, modeling frameworks and types are briefly reviewed. Finally, a selection of modeling DSSs examples is discussed.

System and model classification

The nature of decision is associated with the problem to be solved and the containing system that needs to be assessed. Therefore, it is essential to understand the complexity of that system, in which the problem occurs. In their work, Snowden and Boone differentiate the system complexity levels to be either complex, complicated, simple, chaotic, or disorder [109, 293]. As they are shown in Fig. 3.24, these categories are distinguishable based on their characteristics and the unique way of dealing with them.

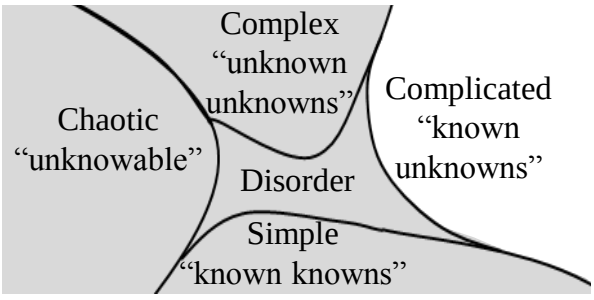

Figure 3.24 System complexity classification, based on [109, 293]

In Fig. 3.24, a complex system has no valid comprehensive representing model other than itself, while the cause-and-effect relationship can be only predicted by probe. The parameters of such a system can be; therefore, considered as „*unknown unknowns*“. Unlike the complex system, a complicated one can have a valid model to represent it, while its parameters are „*known unknowns*“. Therefore, decision-makers are able to analyze the sophisticated cause-and-effect relationship in such system. A simple system has a clear cause-and-effect relation, that is based on „*known knowns*“ parameters. Solving a problem in such a system requires mainly the categorization of associated facts. In a chaotic system, the cause-and-effect relationship is undefinable, while the parameters of such system are unknowable. Therefore, decision-makers have to act for the transformation of chaotic system into complex, complicated, or simple one in order to sense it. The disorder system appears when

decision-makers fail to sort the system under any of the previous categories. These types of systems have a direct impact on the adopted modeling approach and its generated models. In this thesis, the discussed product system is considered to be an ordered complicated one with model-able cause-and-effect pattern based on its „*known unknowns*“ parameters. For the assessment, the complex system of process reality may be described by a relatively simplified isolated model based on clear description of system boundary definitions [150, 152]. Thus, this assessment model may be considered as a complicated one that represents a complex reality.

Another aspect in modeling is the type of model regarding its transparency. Theoretically, a system can be described through either a white-box, gray-box, or black-box model [169]. The first type depends on the bottom-up data in establishing a thorough transparent description of the system in what is called a white-box model. On the other hand, a top-down approach of illustrating a system can be realized through what is called black or gray-box models. In a black-box model, the relation of cause-and-effect is hidden from the decision-makers. However, that relationship is partially traceable in what is called the gray-box model. While there is no straightforward correlation between the outcomes and their reasons in black-box models, white-box models are associated with costly data collection and processing [122]. In practice, distinguishing between black-, gray-, and white-box models by decision-makers is open to some degree of interpretation, while there is no quantitative barriers between them.

Production modeling and validation approaches

Any process can be described by words, mathematical symbols, graphical visualizations, or a combination of them to achieve an understandable illustration of that process [115, 248]. In Schlesinger et al. framework, modeling can be split into two stages, which are the conceptual and computerized models. Based on analyzing the reality, a conceptual model aims to describe it within a correlation map. In the next stage, a computerized model converts the conceptual model into a programmed computer-based code [274]. Moreover, an alternative approach is suggested by Dyckhoff and Spengler specifically for the decision modeling in production [85], as Fig. 3.25 shows.

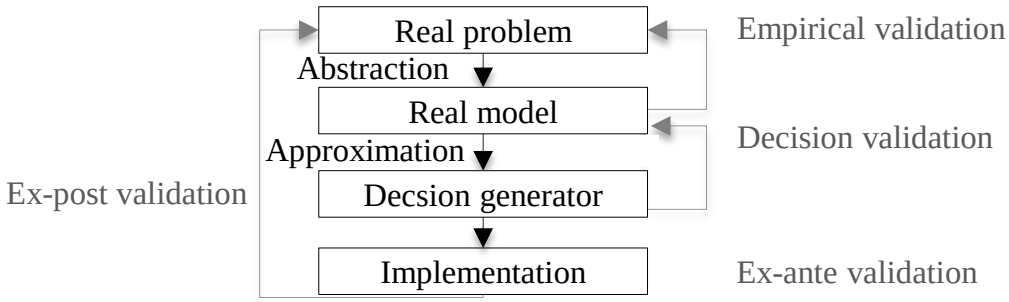

Figure 3.25 Decision modeling in production, based on [85]

In this approach within Fig. 3.25, a model, that conceptually represents this problem, is abstracted from the definition of the real problem. Then a mathematical model is to be established for this real model through the relaxation. Based on this model outcomes, decisions are to be implemented. In this process, a set of validation stages is applied to enhance the decision quality throughout the process [85].

A major question, that faces any DSS developer, is about the confidence in their models and credibility of their results [234]. Therefore, it is essential to perform an evaluation of the DSSs and a validation of their results in a systematic framework. In addition, the transparency of the validation outcomes in general and the uncertainty quantification in specific are essential to have the acceptable credibility. In their work,

Schlesinger et al. have introduced a validation framework for the computerized models [274], as Fig. 3.26 shows.

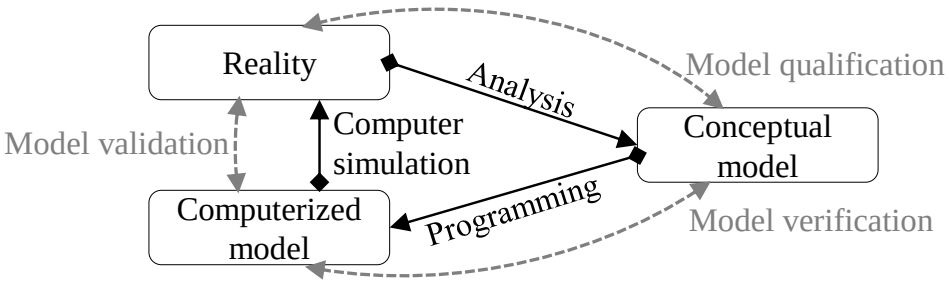

Figure 3.26 Model validation framework, based on [234, 274]

Based on reality, this framework in Fig. 3.26 includes the conceptual model generation and its qualification after that. Then, a computerized model is to be programmed and verified with that conceptual one. Finally, the computer-based model is validated with the initial system in reality. For the sake of validation, interpretation checks have been specified within the LCA framework from Fig. 3.13, as Fig. 3.27 suggests.

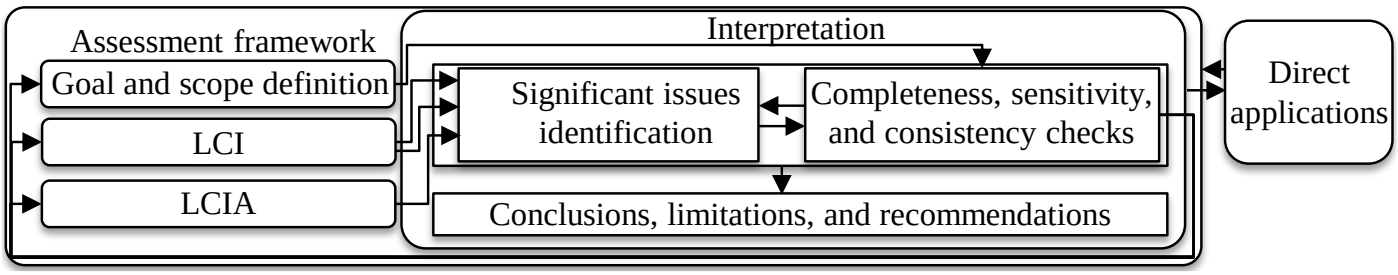

Figure 3.27 Interpretation checks in assessment framework, based on [151]

Besides the previously discussed stages of LCA framework in Fig. 3.13, Fig. 3.27 suggests interpretation steps such as completeness, sensitivity, and consistency checks. Based on that, the validation outcomes may lead to modifying the framework stages including the interpretation itself in an iterative approach. In this interpretation, the completeness check examines the availability and entirety of the data that is required to perform the interpreting evaluation. The sensitivity check includes ensuring the reliability of final results by evaluating the data allocation and calculation methods including issues such as the uncertainty. However, the uncertainty analysis is beyond the defined goal and scope of this work. In the consistency check, the appropriation of applied methodologies, the collected data, as well as the assumptions is ensured. Moreover, differences of temporal, technical, and geographical boundaries are to be checked. Based on the final results of all checks, sets of conclusions, limitations, and recommendations are to be reported [151], which are introduced in chapter 6 and chapter 7 after presenting the work results. Again, both model complexity and transparency classifications are significant aspects in such modeling and validation frameworks.

Examples of modeling DSSs

As an approach as well as realized DSSs based on it, the product life management provides a comprehensive knowledge exchange platform for the decision-makers [90]. Recently, the importance of product life management to Industry 4.0 has been intensively discussed, while many experts see it as an indispensable tool in realizing Industry 4.0 [31]. Moreover, in their study Ciroth et al. have suggested the integration of both LCA and product life management to enable data exchange between them [58]. Technically, LCA, LCCA, and

product life management intend to provide a comprehensive assessment throughout the entire product life-cycle in general and aim to enhance the eco-efficiency within its value-chain in specific.

Moreover, business process re-engineering is defined as fundamental and radical redesign and rethinking in the business process. It aims to achieve the required developments by measuring performance indicators including cost, quality and time [51]. However, business process re-engineering associated models can be either static or dynamic. On the one hand, static models depict the processes „*as is*“ with actual process environment. On the other hand, dynamic models foresee the process behaviors under modified environment in what is called „*what if*“ simulation environment [28]. In their nature, economic and ecological assessments have to be dynamic [62]. Now, dynamically collected data can serve the „*as is*“ process variants and reflect their time-dependency aspect as well, which is relevant to this thesis. In practice, information technologies have been implemented in digitalizing such models in business process re-engineering [23].

In production modeling, value stream mapping (VSM) is implemented widely in process representation [78, 280]. The VSM illustrates the material, energy, and information flows including the coherence between them [280]. However, the VSM lacks the capability of representing dynamic production process such as the case of mass customization and it has no indication of the CSFs. Therefore, an advanced VSM, that enables handling not only static processes such as mass production but also dynamic ones such as mass customization, has been introduced by Schönemann et al. in his work. In that study, VSM is performed as a simulation that focuses on energy VSM in particular, while data collection for this simulation is realized manually [280]. Although some articles trickle down the correlation between Industry 4.0 and VSM, no data collection approaches are explicitly suggested. In general, VSM may be described as a simulation tool that serves process estimation mainly [120]. Therefore, it may be hypothesized that VSM as a simulation tool can be validated only based on collected process data such as the one provided by this thesis.

The bill of material is originally developed as a tool for estimating material cost in the early design phase. However, it may be further implemented for material planning purposes, whenever the value-chain aspects are considered in it [195]. Moreover, a traditional bill of material is not sufficient in orienting the flows to the various products or assemblies for instance [321]. Therefore, patents about integrating the bill of material in product planning with the computer-aided design have been published [102, 103]. However, elementary flows other than materials, such as energy, facility, equipment, and labor work, are decisive for the eco-efficiency assessment. In addition, wasted materials in FRPs manufacturing have significant direct cost and carbon footprint. In literature, wasted fiber can reach up to 50 % from the initial material amount in cutting alone. In a previous study, the fiber waste alone has caused around 17 % from the total direct cost and 36 % of the total carbon footprint [13].

Furthermore, material flow cost accounting determines the wastes, emissions, and non-value-added elementary flows [177]. Such waste determination is more advantageous for the eco-efficiency assessment in comparison to the bill of material. This tool enables the eco-efficiency assessment by linking both physical and monetary information for integrated economic and ecological activities [301]. Similar to the material flow cost accounting, material flow analysis is a life-cycle analysis from material rather than product point of view. This material flow analysis is a tool to quantify matter flows between the different processes [24]. Other similar DSSs are the technical cost model and activity-based costing. On the one hand, the technical cost model analyzes the direct costs resulted from direct material, labor, equipment, energy, and facility elementary flows [318]. On the other hand, activity-based costing monitors the efficiency within a production line by allocating the costs to their causing activities to identify the non-value-adding ones [210, 301].

3.4.2 Modeling Examples and Relevant Assessment Research

After reviewing the system and model classification as well as modeling and validation approaches especially for the production, model examples for both life-cycle and production are discussed here. Moreover, a selection of relevant assessment studies is briefly listed to illuminate the thesis contribution to the state-of-the-art.

Life-cycle and production modeling examples

In literature, the generic product life-cycle has been modeled variously to include a flexibly defined set of stages, which may cause a confusion in understanding it. Despite this definition variety, it is crucial to clearly distinguish between all life-cycle stages in general and the studied ones in specific. Therefore, a generic model for the life-cycle of aircraft structures has been developed in a previous work [13], as Fig. 3.28 shows.

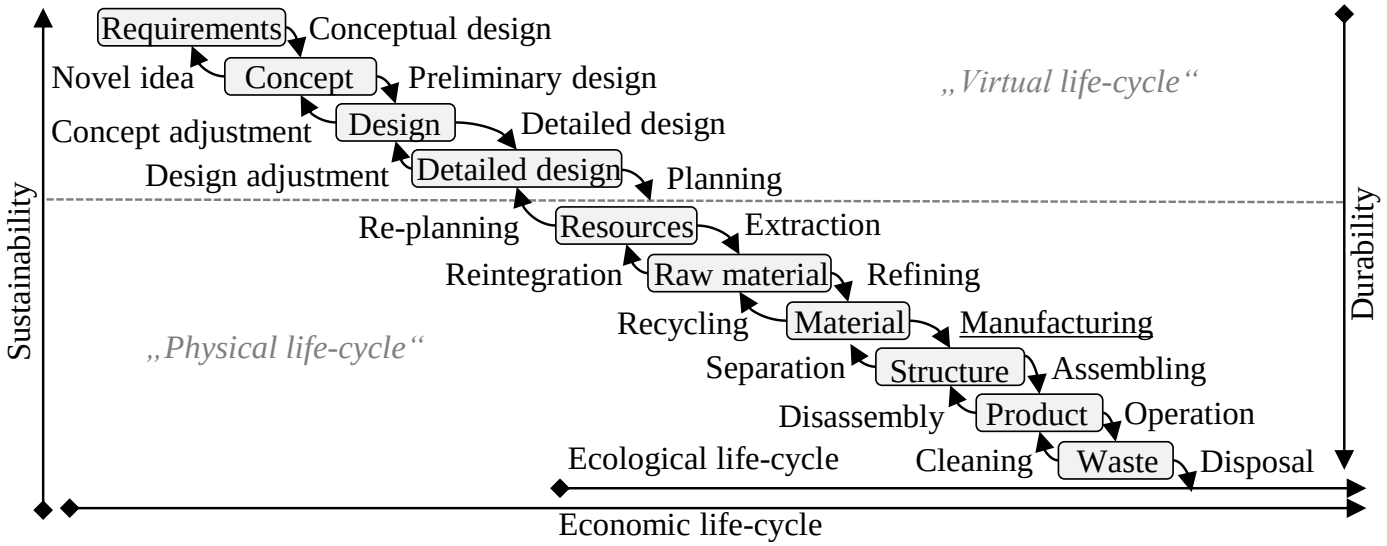

Figure 3.28 Eco-efficiency product life-cycle, based on [13]

However, the detailed life-cycle model in Fig. 3.28 is still a simplification of the complex reality, whereas its stages are barely distinguishable and have hidden interaction influences. Generally, a product life-cycle includes all stages from raw material acquisition to final disposal. This physical life-cycle, which is also known as the ecological cradle-to-grave, can be split into several gate-to-gate stages [151, 232]. On the other hand, economic life-cycle is defined to include two phases of virtual as well as physical ones [128]. The virtual phase includes the developing and planing activities before product creation, which has a significant economic impact on any product in general and the commercial aircraft in specific [261]. However, this phase is rarely considered or even mentioned in the ecological studies. On the other hand, the physical phase starts by extracting the portion of resources required to realize the product. This part is covered by both economic and ecological studies due to its importance for both. In the case of series production, virtual life-cycle is nonrecurring, whereas physical one is recurring for each product. To put it more simply, planning and designing activities in virtual life-cycle are carried out commonly for more than a product, while it is difficult to distinguish the portion of each product from the total efforts in these activities. On the other hand, the activities, which are associated with the examples of extraction and production processes in physical life-cycle, may be assigned to a single product. In Fig. 3.28, a comprehensive description of the eco-efficiency life-cycle is illustrated by combining both stages.

As it is illustrated in Fig. 3.28, a product life-cycle has two possible paths of implementing SDs, which are durability and sustainability. In this illustration, the life-cycle stages are shown in boxes, while durability

and sustainability transitions between these stages are represented by arrows. On the one side, durability path represents the temporal life-cycle of the product starting from the conceptual design ending with the waste disposal. In durability, the product itself and its fulfillment of the customer demands are the dominant goals. However, SDs may still be applied all the way in this durability path. On the other side, sustainability path should include SDs, which are applied to enhance the eco-efficiency all the way from waste cleaning to re-establishing novel sustainable ideas. However, not all steps of sustainability path are applied in reality, while most of durability ones are common industrial steps. In DSSs, the life-cycle can be either totally covered in what is called the cradle-to-grave or a selection of its stages is handled in a gate-to-gate approach [152]. Logically, a gate-to-gate study that starts from the life-cycle beginning may be called a cradle-to-gate, while the ones start from any gate and end at the grave stage can be called a gate-to-grave. Despite this distinguishing approach between durability and sustainability in Fig. 3.28, the term sustainability is a common one to describe the activities that serve both, while it is used to describe the aspects regarding production in this thesis.

In process modeling, a set of model types is generated to describe the different levels. One of the common generic production conceptual models is the one describing the input and output correlation [85], as Fig. 3.29 shows.

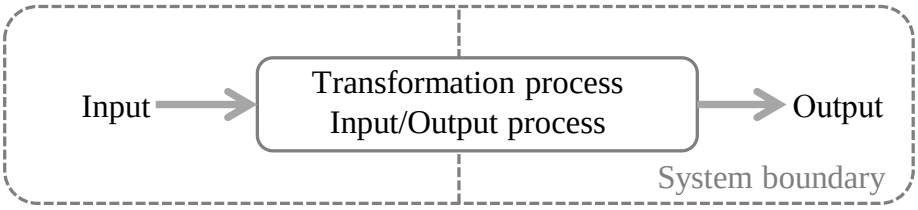

Figure 3.29 Production process as inputs and outputs correlation, based on [85]

Especially in batch production, an industrial process consists of various UPs [85]. Therefore, not only the UPs illustration is required but also the clear definition of UPs input, output, and intermediate flows [151]. As it is shown in Fig. 3.29, production outputs including the product itself depend entirely on the process inputs [115]. In another approach, Anderson has introduced the production model, which covers the associated resources based on material processing, waste generation, and energy utilization [17].

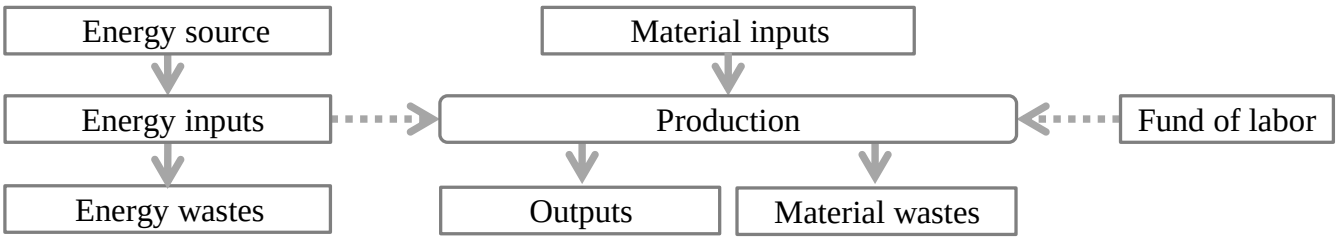

Figure 3.30 Production model and its main inputs and outputs, based on [17]

Fig. 3.30 suggests the forms of inputs and outputs as well as their relations. On the one hand, there are energy and labor inputs, which flow to the production as the dashed arrows in Fig. 3.30 show. On the other hand, there are the material inputs to the production, which are distinguished by solid arrows. With regard to the production outcomes, Fig. 3.30 illustrates three main classes, which include outputs, materials wastes, as well as energy wastes. Moreover, the physical equilibrium is expected for matter and energy between both sides of production inputs and outputs [17]. However, the production may be a multilevel process with higher complexity than the simplified model in Fig. 3.30, as the hierarchical model in Fig. 3.31 suggests [134].

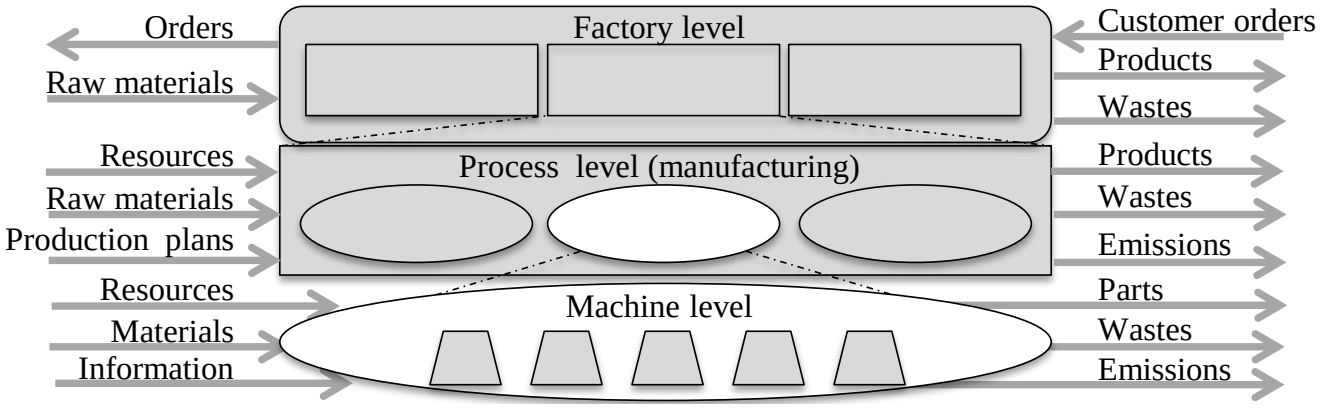

Figure 3.31 Hierarchical production model and its main inputs and outputs, based on [134]

On each level in Fig. 3.31, there are inputs and outputs, which are associated with other flows on the different levels. As it is previously shown in Fig. 3.8, such hierarchal modeling is common in decision-making on factory level. However, Fig. 3.31 illustrates the input and output flows, which are crucial for evaluating various levels of CFSs. In addition to the material and energy in Fig. 3.30, Fig. 3.31 discusses the information flow. Including orders, customer orders, and production plans, these information forms are crucial to any production process. Unlike Fig. 3.30, Fig. 3.31 distinguishes between wastes and emissions, while each of the referenced studies discusses the production process model from its unique perspective [17, 134]. To put it more simply, the same production process may be modeled differently to illuminate specific aspects among others.

Review of relevant works

Based on the comprehensive knowledge gained in this chapter, a selection of related works is listed and analyzed in Tab. 3.4. In it, the associated criteria are shown with scaled comparison for the different selected studies. To address the purpose of this thesis, which is serving a time-dependent eco-efficiency assessment in FRPs manufacturing, associated aspects such as the framework stages and considered elementary flows must be covered. The concept of sensor nodes for data collection in production, detailed modeling stages, capabilities of real-time data collection and time-dependent assessment, coverage of both eco-efficiency aspects, and an iterative interpretation and validation strategy are additional significant criteria. Therefore, a simplified (Y) for yes or (N) for no answer is assigned to each case. However, the simplified answer of (Y) as positive rating is only assigned when that criterion is undoubtedly studied and thoroughly handled in that work. For better visualization, the criteria in Tab. 3.4 are represented by numbers, which are defined here from (1) to (13).

- (1) What are the considered input elementary flows? In FRPs manufacturing they may include: (F) Fiber: as a part of structural core materials; (M) Matrix: as a part of structural core materials; (C) Core materials: as a part of structural core materials; (R) Ancillaries: as materials that are used in process but not within the product; (T) Energy: as all energy forms used to operate equipment and facility (except manual labor work); (Q) Equipment: as machines, tools, and molds utilization; (L) Labor: as direct work performed by employees; (Δs) Facility: as place temporal and spatial utilization. However, some frameworks include all associated input elementary flows without specification, while in such approaches the term ((All) Indirectly) is used.
- (2) Does it include goal and scope definition? Logically, goal and scope definition is an obvious first step in any framework. However, (Y) is only given if the goal and scope definition is clearly discussed in the framework. Here, it should include a clear system boundary definition as a part of that.

- (3) Does it include data collection concept in production? It must have a clear definition of all required sensor nodes to automatically collect relevant data about the covered elementary flows. Data collection by a „*data collection clerk*“ such as controller or consultant is theoretically always possible, but it is still not considered as a novel data collection concept. Therefore, only a sensor-based automated date collection concept is considered with a positive (Y) answer here. In some studies, this is only partially discussed, while a (Y) is given here for a clear sensor assignment for every input flow, similar to the detailed one suggested later in chapter 4.
- (4) Does it include a knowledge processing concept? It has to have a clear approach to wisdom and decision-making in knowledge stages. Here, it is essential to find a clear distinguishable knowledge evolution stages within the framework, otherwise a letter (N) is assigned.
- (5) Does it include an inventory analysis? In which a data mining must be considered as a part of gathering associated data, that is required for the assessment. Unlike the criterion (4), here these activities may be applied to a single knowledge level.
- (6) Does it include a process conceptual model? It should be clearly stated that such model is a part of the framework to assign a (Y) answer.
- (7) Does it include a process mathematical model? Unless such model is provided within the studied work a letter (N) is considered. Here, it is essential to distinguish between an assessment model and the mathematical model that describes the assessed process, while both are meant here.
- (8) Does it include an assessment computerized model? Computer-based codes themselves are rarely published in scientific works due to confidentiality and the fact that codes are not scientific results. Therefore, a clear mentioning of their existence is sufficient to notate this criterion with a (Y).
- (9) Does it include an impact assessment? While some frameworks are generic, they are not necessarily including assessing an impact. Unless the framework is clearly containing this stage, a (N) is considered.
- (10) Does it include a real-time data collection? While data may be collected automatically with or without temporal assignment, providing a real-time data collection is the most possible updating form of time-dependency. Not to be mixed with criterion (3), this one is about the temporal manner of automated data collection.
- (11) Does it include a time-dependent assessment? This is associated with criterion (9), while an assessment might be time-independent or time-dependent. Here a (Y) is considered only if the second type is clearly applied.
- (12) Does it cover eco-efficiency? Although the implementation of several frameworks for the eco-efficiency assessment is thinkable in many cases, a (Y) is stated only if a framework is clearly applied for that purpose in the discussed work.
- (13) Does it include an iterative interpretation? While a framework should be repeatable to correct its stages and to validate its outcomes, only a clear consideration of that will be notated by a (Y).

While some of these works in Tab. 3.4 are pure scientific theoretical approaches, others are based on industrial publications of implemented solutions. When it comes to the rating within Tab. 3.4, the assignments of positive and negative in any criterion are subjected to perspectives and interpretations. Still, other scholars may be considered and further studied in future works.

Table 3.4 Relevant works for time-dependent eco-efficiency assessment

Framework	1	2	3	4	5	6	7	8	9	10	11	12	13
Activity based costing [210]	F, M, C, R	N	N	N	Y	Y	N	Y	Y	N	N	N	N
Bill of material [102, 103]	F, M, C, R	N	N	N	Y	N	N	Y	Y	N	N	Y	N
Business process re-engineering [29, 140]	All (Indirectly)	Y	N	N	N	Y	N	N	N	N	N	N	Y
CPPS [309]	T, Q	N	N	N	N	Y	N	Y	Y	Y	Y	Y	Y
Data envelopment analysis [183]	All (Indirectly)	N	N	N	N	N	N	N	Y	N	N	Y	N
Dynamic LCA [60, 240]	F, M, C, R, T	Y	N	N	Y	Y	Y	Y	Y	Y	Y	N	Y
DMAIC [167]	All (Indirectly)	Y	N	N	Y	Y	N	N	Y	N	N	N	Y
Environmental DSS [62]	All (Indirectly)	N	N	Y	Y	N	N	Y	Y	N	N	N	Y
Energy efficiency [302]	F, M, C, T	N	N	N	Y	Y	N	Y	Y	Y	Y	Y	N
Eco-efficiency analysis [269]	All (Indirectly)	Y	N	N	Y	Y	N	Y	Y	N	N	Y	Y
Energy-saving [304]	F, M, C, R, Q, T	Y	N	Y	Y	Y	N	Y	Y	Y	Y	Y	Y
Energy VSM [280]	T	N	N	N	Y	Y	N	Y	Y	N	N	N	Y
KDD [100]	All (Indirectly)	N	N	Y	Y	N	N	N	N	N	N	N	Y
LCA [151]	F, M, C, R, T	Y	N	N	Y	Y	N	N	Y	N	N	N	Y
LCCA [174]	All (Indirectly)	Y	N	N	Y	Y	N	N	Y	N	N	N	Y
Material flow analysis [24]	F, M, C, R, T	Y	N	Y	Y	Y	N	Y	Y	N	N	Y	Y
Material flow cost accounting [177, 278]	F, M, C, R	Y	N	N	Y	Y	Y	Y	Y	N	N	N	N
Model validation [234, 274]	All (indirectly)	N	N	N	N	Y	Y	Y	N	N	N	N	Y
Motion tracing [208]	L	N	Y	N	Y	Y	N	Y	N	Y	Y	N	Y
Maynard sequencing [119, 350]	Q, L	N	N	N	Y	Y	N	Y	N	N	N	N	Y
Multi-relationship evaluation [332]	Q, L	Y	N	N	Y	Y	Y	Y	Y	Y	N	N	Y
Methods-time measurement [186]	L	Y	N	N	Y	Y	N	Y	N	N	N	N	Y
Overall equipment effectiveness [26, 245]	Q	Y	N	N	Y	Y	N	Y	N	Y	Y	N	N
Product life management [16, 90]	All (Indirectly)	Y	N	Y	Y	Y	N	Y	Y	N	N	Y	Y
RAMI 4.0 [2, 78, 128]	All (Indirectly)	N	N	Y	Y	N	N	Y	Y	Y	Y	N	N
Shop-floor LCA [49]	R, T, Q	Y	N	N	Y	Y	N	Y	Y	Y	Y	Y	Y
Technical cost model [318, 343]	All	N	N	N	Y	Y	N	N	Y	N	N	Y	N
VSM [280, 285]	F, M, C, R, T	N	N	N	Y	Y	N	Y	Y	N	N	Y	Y
Wireless sensor networks [196]	F, M, C, R, T	N	N	Y	Y	N	N	Y	Y	Y	Y	Y	N

The relevance here can be interpreted qualitatively from the matched criteria of each study. However, each criterion may be met with different relevance, while the LCA, LCCA, eco-efficiency analysis, KDD, DMIAC, RAMI 4.0, model validation, business process re-engineering, VSM, activity based costing, and dynamic LCA are respectively seen as the most relevant frameworks to the one introduced in this thesis. On the other hand, the CPPS, method-time measurement, shop-floor LCA, material flow analysis, motion tracing, and wireless sensor nodes are ranked respectively as the most relevant works for the LCI as well as LCIA and consequently the SWS and EEAM in this work. As Tab. 3.4 shows, it is challenging to find a work that satisfies all mentioned criteria in the time-dependent eco-efficiency assessment of all relevant elementary flows in FRP manufacturing. Therefore, this thesis aims to exceed the state-of-the-art in order to fulfill the hypotheses from chapter 2.

Chapter 4

Framework of Time-Dependent Assessment

Based on understanding the state-of-the-art from chapter 3 as well the hypotheses in chapter 2, an integrated framework for eco-efficiency assessment and DSSs for real-time LCI and time-dependent LCIA are introduced in this chapter.

4.1 Integrated Framework for Eco-Efficiency Assessment

In order to establish a time-dependent assessment framework, frameworks from decision support, eco-efficiency, FRPs manufacturing, and process modeling are considered. Then conceptual as well as mathematical models are developed according to that framework to enable the establishment of computerized DSSs. To facilitate understanding that modeling approach, a case study from FRP manufacturing is illustrated. This includes introducing process equilibrium theory within conceptual models as well as the resulted mathematical ones.

4.1.1 Integrated Framework

After thoroughly investigating the state-of-the-art regarding decision support, eco-efficiency, FRPs manufacturing, and process modeling, a framework for realizing the time-dependent eco-efficiency assessment by appropriate DSSs is introduced. The idea here is to establish a generic approach that is applicable for various life-cycle stages or other products in general and the production variants in specific. As a consequence of establishing this framework, the capability of iterative time-dependent assessment with minimized efforts can enable assessing and comparing various production scenarios in future works. By the DSSs in such framework, impacts are allocated temporally in order to evaluate the studied techniques and technologies. Still, this necessitates clear models that illuminate the process discretization, system boundaries, relevant elementary flows, and their characterization factors.

While several frameworks have been developed and optimized in literature, a sufficient framework is established as a result of combining existent ones. It includes clear stages for the assessment such as goal and scope definition, LCI, LCIA, and their iterative interpretation, which are adopted from the LCA framework. Now, these generic stages are realized through clear modeling structure including conceptual, mathematical, and computerized forms. Realized through DSSs, this framework leads to visual and statistical results that sufficiently serve the targeted decision-makers on various management levels. In this context, approaches such RAMI 4.0 should be acknowledged and have been integrated to address the data mining and communicating aspects. Unlike the initial LCA framework, the established one clearly illuminates the correlation between physical and virtual worlds by distinguishing the relevant decision-media. Moreover, a systematic validation approach is considered in every stage to enhance the results accuracy and DSSs reliability.

In this work, both LCI and LCIA stages are served by the SWS and EEAM respectively. On the one hand, the novel concept of SWS offers real-time data collection and processing in LCI. This concept describes the possible methods and sensor nodes for identification, magnitude measurement, as well as spatial and temporal allocations of each relevant elementary flow. Consequently, capabilities of a time-dependent LCIA are developed in the EEAM. While traditional DSSs for these stages of LCI and LCIA contain manually performed data collection and processing by data collection clerks, the developed SWS and EEAM automate these tasks. It is hypothesized here that unified process models are sufficiently representing all elementary flows for both economic and ecological aspects. When it comes to the characterization factors, a novel understanding of their life-cycle stages and their correlation with cradle-to-gate, gate-to-gate, gate-to-grave, as well as cradle-to-grave spectra is suggested in this thesis. To have an achievable work scope, these DSSs are modeled and parameterized for the assessment of manufacturing a selected FRP structure regarding the KRIs of eco-efficiency, direct cost, and carbon footprint including their associated levels of CSFs.

The integrated framework is developed in two main phases. The first phase is to establish a sufficient integration of modeling and eco-efficiency assessment for the case of FRP manufacturing. While such integrated framework establishes a generic correlation between the associated assessment stages, there is a need for a parametrization approach. Therefore, the frameworks of Industry 4.0 from Fig. 3.6 and KDD from Fig. 3.7 are merged to address the parametrization requirements in the second phase. Finally, it is essential to understand the correlation between different associated fields or media in order to have a clear perspective of the served decision-makers by the generated DSSs from this integrated framework.

Integrated assessment and modeling framework

The first step in establishing the combined framework is to integrate the frameworks of modeling and LCA. For the eco-efficiency assessment, a modeling framework is required to enable the development of a computer-based model. Although process modeling is a core dimension of the LCA, the LCA framework contains only general guidelines for the assessment procedures and system boundary modeling [152]. Therefore, the LCA framework has been integrated with the modeling framework. This facilitates the combination of various eco-efficiency aspects in one comprehensive process model. It also enables process modification and redesign to evaluate the direct applications in future works. Based on that, an integrated framework, that includes the LCA, production decision support, and modeling from Fig. 3.13, Fig. 3.25, and Fig. 3.26 respectively, is introduced in Fig. 4.1.

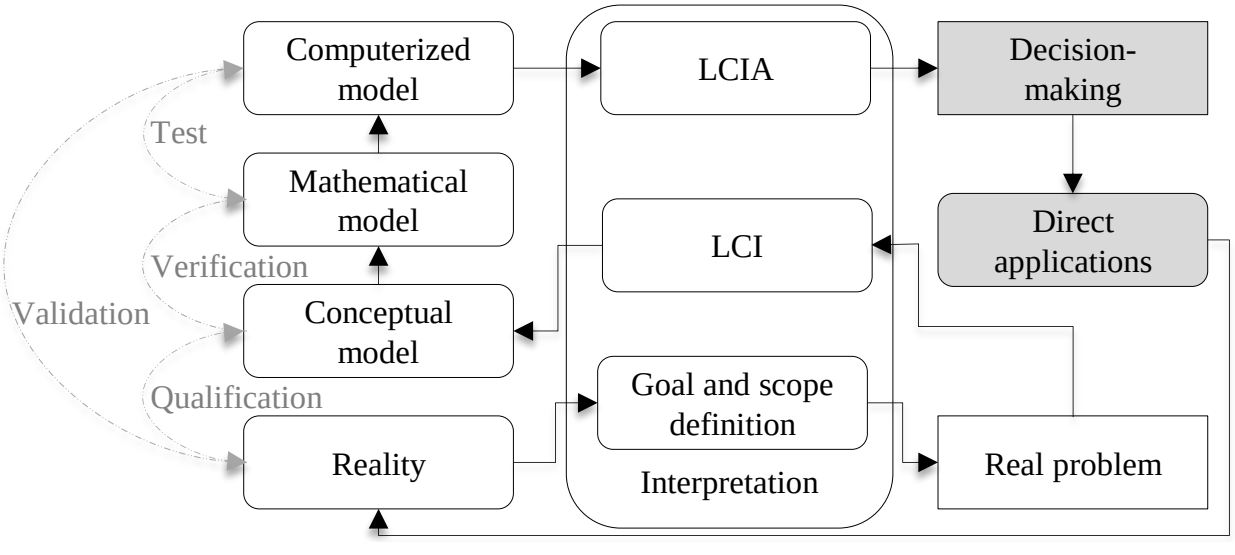

Figure 4.1 Integrated framework for assessment DSSs, adapted from [85, 152, 234]

This framework in Fig. 4.1 aims to facilitate the establishment and enhancement of eco-efficiency assessment DSSs particularly for the production process. Establishing the aimed DSSs starts from defining their goals and scopes including the definition of the targeted CSFs and their levels. This is; however, associated with the real problem or demand that any DSS intends to handle. Furthermore, the reality, as the environment in which that problem exists, is affecting that goal and scope definition as well [85, 152]. Such clear goal and scope definition illuminates the real problem, which has to be solved by suitable SDs. Consequently, reality itself is impacted later by such direct applications [152]. Therefore, aspects associated with the discussed CSFs in this real problem are analyzed by the LCI. Here, the goal is to build a sufficient conceptual model that represents these aspects virtually [274]. Based on this conceptual model, a mathematical model is to be relaxed. From this model, a computerized model is formulated [85]. This computer-based DSS contains the previous modeling stages to deduct the LCIA results and represent them properly. Based on these results, decisions are to be generated by the decision-makers, while these decision-makers may exist in the form of either human or AI [188]. As it is mentioned previously, decisions are to be implemented in reality as direct applications [152]. This framework consists of validation stages that are shown with dashed lines in Fig. 4.1. Similar to the implemented original frameworks, this one inherits the nature of being continuous and iterative. As it is shaded in Fig. 4.1, both decision-making itself and its direct applications are not included in the scope of aimed time-dependent DSSs in this thesis.

This framework from Fig. 4.1 is integrated with the frameworks of decision maturity levels, Industry 4.0, and KDD implementation to enable the DSS of time-dependent eco-efficiency assessment. This thesis in general and the introduced framework in specific serve the attributional micro-level assessment mainly, that investigates the time-dependent impacts of elementary flows on their lowest discretized level. Nonetheless, implementing the approach of time-dependent eco-efficiency assessment in future studies enhances not only the attributional accounting and meso-macro levels of assessment but also the consequential SDs comparisons based on the real-time data collected and time-dependent assessment of their scenarios in reality.

Integrated framework of decision maturity levels, KDD, RAMI 4.0, and eco-efficiency assessment

As it is discussed previously, the real-time data collection and processing solutions from Industry 4.0 can be implemented in facilitating the parametrization of computerized models. In its current version, the RAMI 4.0 framework offers an adequate explanation for how to apply Industry 4.0 within an enterprise. However, it is unclear how to assess the impacts of implementing Industry 4.0 and how to measure the achievements of such purposes in that framework. Therefore, there is a need for an integrated framework of Industry 4.0 and eco-efficiency assessment.

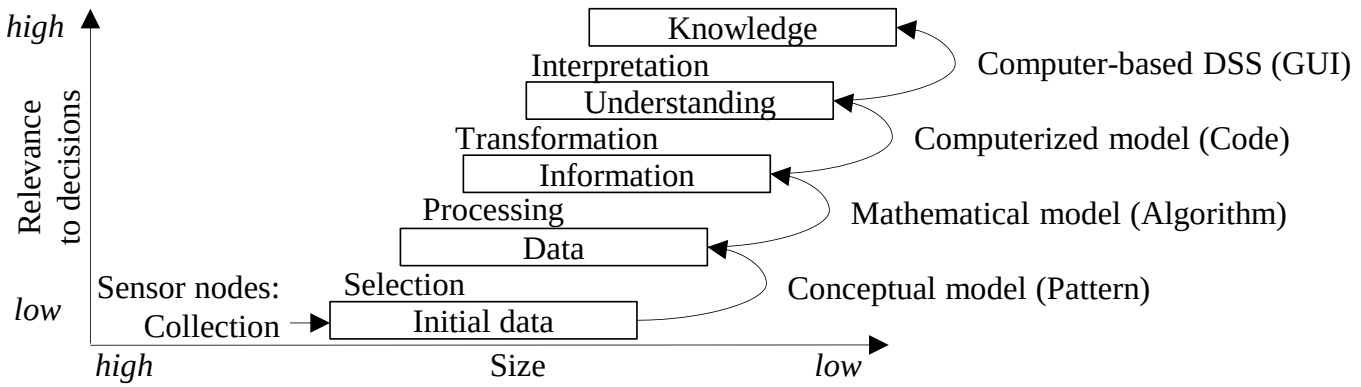

Figure 4.2 Decision maturity in combined RAMI 4.0 and KDD, adapted from [2, 62, 100, 188]

From Fig. 3.3, Fig. 3.6, and Fig. 3.7 respectively, the decision maturity levels, RAMI 4.0, and KDD are combined in Fig. 4.2 for a comprehensive knowledge evolution and modeling approach. Fig. 4.2 describes the data layers, their size, and their relevance to the decision. It suggests that the relevant initial data is gathered from assets and communicated instantly through suitable interfaces. Based on the predefined parametrization requirements and patterns in the conceptual model, the assessment associated data is selected from initial one. Then, the data is processed through the mathematical model into information. The computerized model is developed to transform the information into a clear understanding. Moreover, this understanding is interpreted to provide a clear knowledge about the aimed CSFs by the computer-based DSS. With such DSS, the knowledge is presented to the decision-makers by understandable visualization as a part of the computer-based GUI.

Such GUI assists the decision-makers in gaining the aimed business wisdom by multilevel and adaptable visual as well as statistical results representations. After applying these iterative stages shown in Fig. 4.2, the computer-based DSS contains functionalities of all other model development stages in order to represent them in its final version. This includes visualization of conceptual model and coverage of the mathematical one. As it is shown on the axes in Fig. 4.2, data size as well as data relevance to the decision varies among these data layers. While initial data has the highest size, that level contains the lowest direct relevance to the decision. On the other hand, the knowledge has the lowest data size and the highest relevance to the decision-makers. Therefore, DSSs, that convert initial data all the way to knowledge about the impacts, are established in this work to assist the decision-making.

Although the aimed DSSs are serving the operational management level directly, enhancing other levels is also achievable. As it is shown in Fig. 4.3, correlations between the various DSSs from different model types are expected in a sufficient management framework.

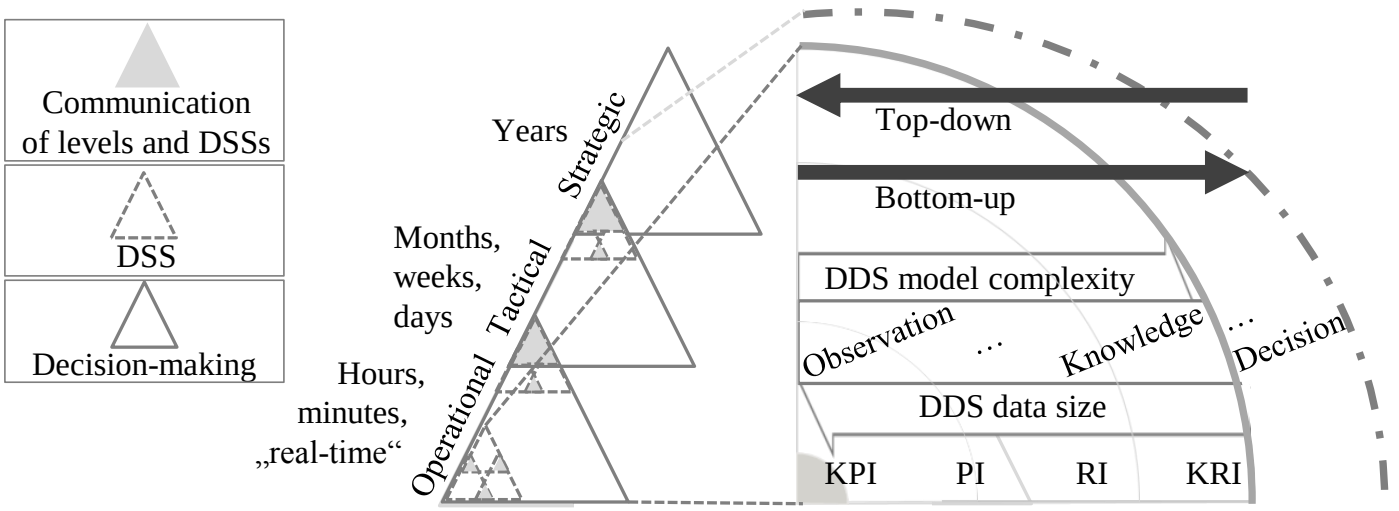

Figure 4.3 DDSs in various management levels and their correlation and categorization

For the three management levels in Fig. 4.3, a temporal horizon is shown on the left side based on Tab. 3.1. Although real-time and time-dependent DSSs are logically associated with the operational level, their contribution may exceed that level. As it is discussed previously in chapter 3, DSSs may also have categories due to their approaches of a bottom-up, a top-down, or a mixture of them. As Fig. 4.3 shows, the decision generation phases and data magnitude, which are presented previously in Fig. 3.3, are relevant for the CSF levels and model complexity. Nonetheless, the relation between CSFs and decision generation phases in Fig. 4.3 is adjustable and unnecessarily quantifiable, which is subjected to the decision-making goal and scope.

For instance, the assessment in this thesis is limited to the knowledge generation as it is previously illustrated in Fig. 3.3 within chapter 3. While any combination of decision generation phases can be selected to handle any

single or multiple CSF levels, the scope of this thesis is defined to include all of these CSF levels by defining the relevant KRIs, RIs, PIs, and KPIs for the studied case. On the right side of Fig. 4.3, the top-down as well as bottom-up approaches, CSF levels, data sizes, decision generation phases, and DSSs model complexity levels are applicable for all three management levels. However, these aspects are existing with the same manner in each single level as well, while this illustration mainly serves the operational management in this work. As the legend on Fig. 4.3 left side shows, each decision-making triangle represents a level that consists of various DSSs. These DSSs may communicate with each other on the same or on another level, as the shaded triangles in Fig. 4.3 show. Such correlation may be established between the introduced DSSs from this work and other correlated DSSs. Other suggestions for advanced DSSs implementations, such as estimation and planning on other managerial levels within this management framework, are briefly mentioned as outlooks in chapter 7.

In this thesis, the DSS for time-dependent assessment can be achieved by a connected DSS for real-time data collection, which serves the LCI within the integrated framework. Therefore, both frameworks from Fig. 4.1 and Fig. 4.2 are integrated to achieve the time-dependency. As a part of this work, the real-time data collection in the LCI is covered by the SWS concept. Moreover, the LCIA is realized through the EEAM, while the EEAM is further enhanced in this work to address the SWS and time-dependency requirements. Considering the data layers, both SWS and EEAM can be integrated to carry out the phases of suggested framework, as they are shown in Fig. 4.4.

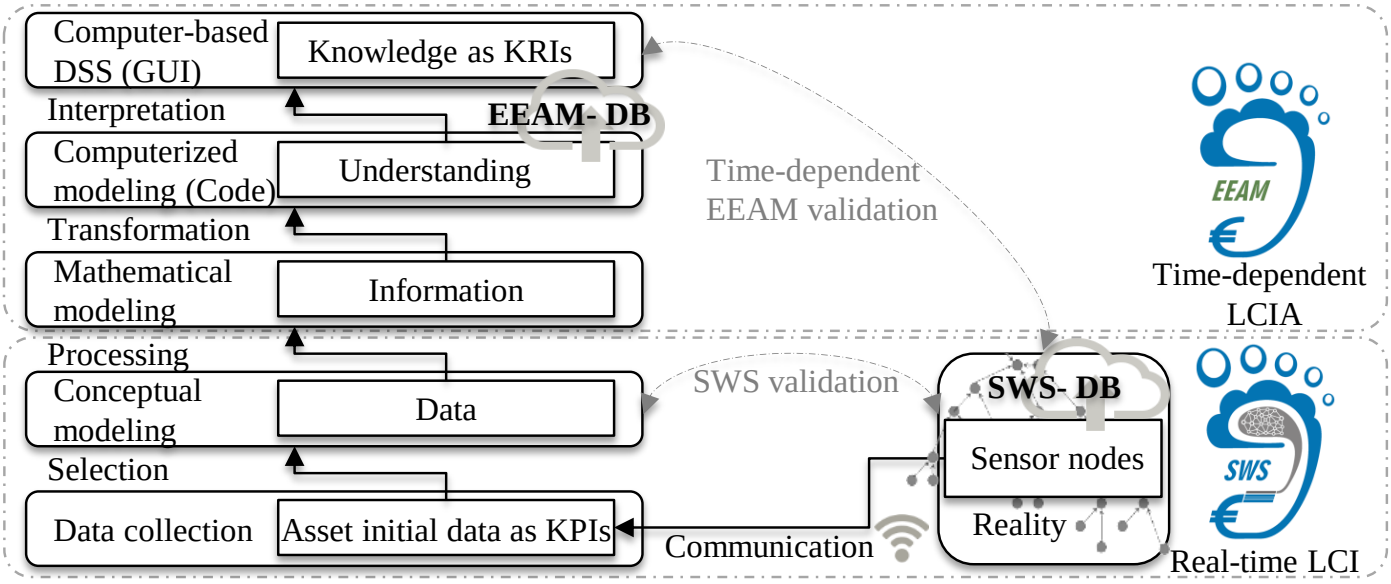

Figure 4.4 Implementation of SWS and EEAM in the integrated framework

In Fig. 4.4, Industry 4.0 is implemented to achieve the goals and to fulfill the scope of eco-efficiency assessment. Based on Fig. 3.6 in chapter 3, a single hierarchy level, that covers only the factory, is considered here. It includes all WSs as well as their assets, which are the relevant interfaces between real and virtual worlds. Based on the factory specification and situation in reality, the assessment goal and scope are to be defined. This includes the definition of all associated UPs, their system boundaries, as well as their elementary flows [152]. After defining the scope and system boundaries for each considered WS, the selected sensor nodes are integrated in them properly. For the field assets, the initial data is measured by the assigned sensor nodes. After processing the relevant data from initial one, this data is implemented as target oriented input for the LCIA from the LCI. In this thesis, the automatically collected and digitally communicated data about the elementary flows replaces the costly manually collected data and the uncertain roughly estimated one in conventional LCI. In the early DSS development stages, this collected data is essential for developing the initial conceptual model

[10]. Technically, this dynamically performed real-time data collection is realized by utilizing solutions of Industry 4.0 such as CPPS. Such solution includes sensor nodes that are applied in or to the associated assets, while these sensor nodes are unnecessary integrated as parts of these assets in the SWS concept. The initial data from these sensor nodes is communicated by IoT solutions such as wireless local area networking to reduce infrastructures and to facilitate assets and WS mobility. Then, the data may be processed in big data environment including clouds to feed the EEAM. On a central server or a local one, the EEAM is carrying out the time-dependent LCIA based on the real-time communicated data from the LCI in the SWS. Finally, the results of time-dependent eco-efficiency assessment are visualized in the GUI of computer-based DSS. Such GUI may be available on portable devices to enhance results reachability for the decision-makers.

The framework shown in Fig. 4.4 suggests the development of a conceptual model for each WS. This simplifies the assignment of proper LCI methods and sensor nodes from the SWS concept to enable the real-time data collection by them. As it is thoroughly discussed later in this chapter, the definition of WSs is correlated with the UPs discretization. Furthermore, this can be advantageous for decision-makers not only during the assessment of each UP but also in the development of suitable direct applications for each particular WS. Based on these conceptual models, mathematical models are relaxed to establish the algorithms of LCIA.

The mathematical models in this framework serve the clear description of the process by representative dynamic UPs row vectors and containing matrices that are based on ordered levels of sets for all included elementary flows. In addition, a proper compatible static characterization factor column vectors are provided for the studied CSFs. The impacts in this assessment are the linear products of multiplying the elementary flow magnitude in a specific unit with its characterization factor of that impact per that exact unit. Moreover, the eco-efficiency mathematical models are provided on the relevant CSF levels to dynamically describe this impact based on the time-dependent economic and ecological ones.

Based on these mathematical models, computerized ones are developed to enable a time-dependent eco-efficiency impact assessment within the EEAM. As a DSS for the LCIA, the EEAM illuminates the direct cost and carbon footprint for each WS, a selection of them, as well as the entire process in its facility. Based on the results concluded from the mathematical models, the information about assessed impacts is provided. This information is then transformed within the computerized model and handled to create an understanding from the different associated perspectives. This includes the understanding of impact distribution and drivers descriptions on the different process levels. By the GUI of EEAM as a computer-based DSS, the sought knowledge about studied KRIs is provided to decision-makers. It includes statistical and visual presentations of direct cost, carbon footprint, and eco-efficiency on various CSF levels. Moreover, such presented knowledge assists the decision-makers in developing and implementing suitable direct applications in the form of SDs based on the gained business wisdom [78].

In their original frameworks, there is a difference between the starting points of RAMI 4.0 and eco-efficiency framework. On the one hand, data layers in RAMI 4.0 start from initial raw data and end by aimed business model [2, 128]. On the other hand, the eco-efficiency assessment framework is going the opposite way by starting from defining the goal and scope based on reality [152]. This is expected, while RAMI 4.0 is a generic framework that deals with various types of data for unspecified goals at the beginning. On the other hand, eco-efficiency framework starts as target oriented approach dealing with particular relevant data types. Adopted from Fig. 4.1, the global validations of both EEAM and SWS are illustrated in Fig. 4.4 as dashed gray arrows.

Decision-making media

From the thorough state-of-the-art review, it is concluded that this type of DSSs is associated with multidisciplinary aspects. After clarifying the suggested framework, it is important to assign the generated DSSs to the relevant management environment, which may be distinguished by its media, as Fig. 4.5 shows.

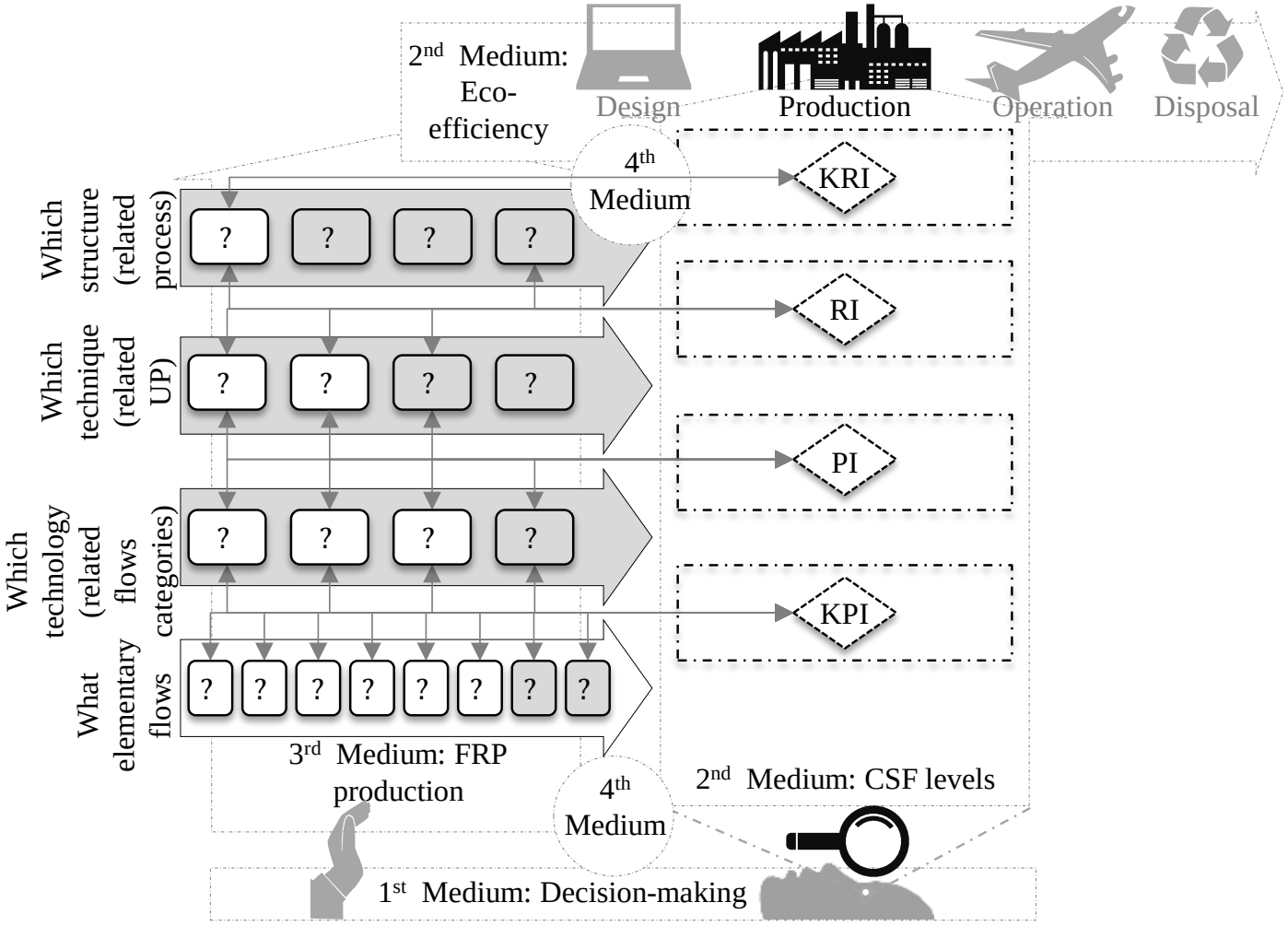

Figure 4.5 Four media associated with the DSSs in this thesis

When it comes to the DSSs introduced by this thesis, there are four media in Fig. 4.5 that should be taken into account. In management, changes can be in the form of applied or forced developments and deteriorations. These changes are taking a place in a medium, impacting another, detected as well as effected by a third one, and represented by a fourth medium. On the selected levels of a CSF, assessing the impacts of such changes is essential to determine how efficient developments or severe deteriorations are.

First, there is the decision-making medium by which a change can be applied, detected, and affected, which is represented as the 1st medium in Fig. 4.5. This medium is generic and applicable for several aspects such as economic and ecological ones regardless the change nature or the system to which it is applied. In practice, this management medium may include DSSs to evaluate the changes. They also assist in determining the problems or opportunities by presenting the assessment results to the decision-makers. The second medium is the CSFs themselves, by which the measurable change impact is assessed. These CSFs may cover several aspects and levels that should be clearly defined within transparent goal and scope definitions in clear system boundaries. As it is shown as the 2nd medium in Fig. 4.5, CSFs can be studied in various life-cycle stages. Third, there is the medium of studied product system as the process where these changes are applied and in which the CSFs are assessed. In practice, a FRP manufacturing process is characterized based on the produced structure, applied

technique, utilized technologies, and relevant elementary flows, as they are illustrated within the 3rd medium in Fig. 4.5. Finally, there is the 4th combining medium, in which the complexity of correlating these media is simplified to a certain degree for the selected group of decision-makers. Concluded from chapter 3, these four media are crucial for the time-dependent eco-efficiency assessment in this thesis. As it is shaded in Fig. 4.5, not all sectors and scenarios are covered in this thesis.

4.1.2 Assessment Conceptual Modeling

As it is mentioned in chapter 3, a process can be described by text, mathematical symbols, graphical visualization, or a combination of them. However, a generic conceptual model of mainly graphical visualizations is established for the time-dependent assessment in this thesis. Such model is essential to reduce the complexity of reality and to provide an understandable complicated illustration of the relevant aspects within a system boundary. Therefore, the visualization of assessment model and eco-efficiency conceptual model is developed here.

Visualization of assessment model

The first step in conceptual modeling can be the visualization of the assessment goals and scope. While goal achievement can be assessed by CSFs, the scope may be represented by their system boundaries. Moreover, the different levels of a CSF can be described to facilitate the assessment throughout different KDD layers. To enable a comprehensive representation of a selected KRI, its other CSF levels are classified by different criteria and categories. In this thesis, the eco-efficiency is defined to be related to both direct cost and carbon footprint. Therefore, the global process eco-efficiency is considered as a KRI in this thesis. However, the total process direct cost and carbon footprint themselves are also assessed as KRIs. The global impact magnitude of any of these three KRIs can be aggregated from all domestic impacts of each domain element in Fig. 4.6.

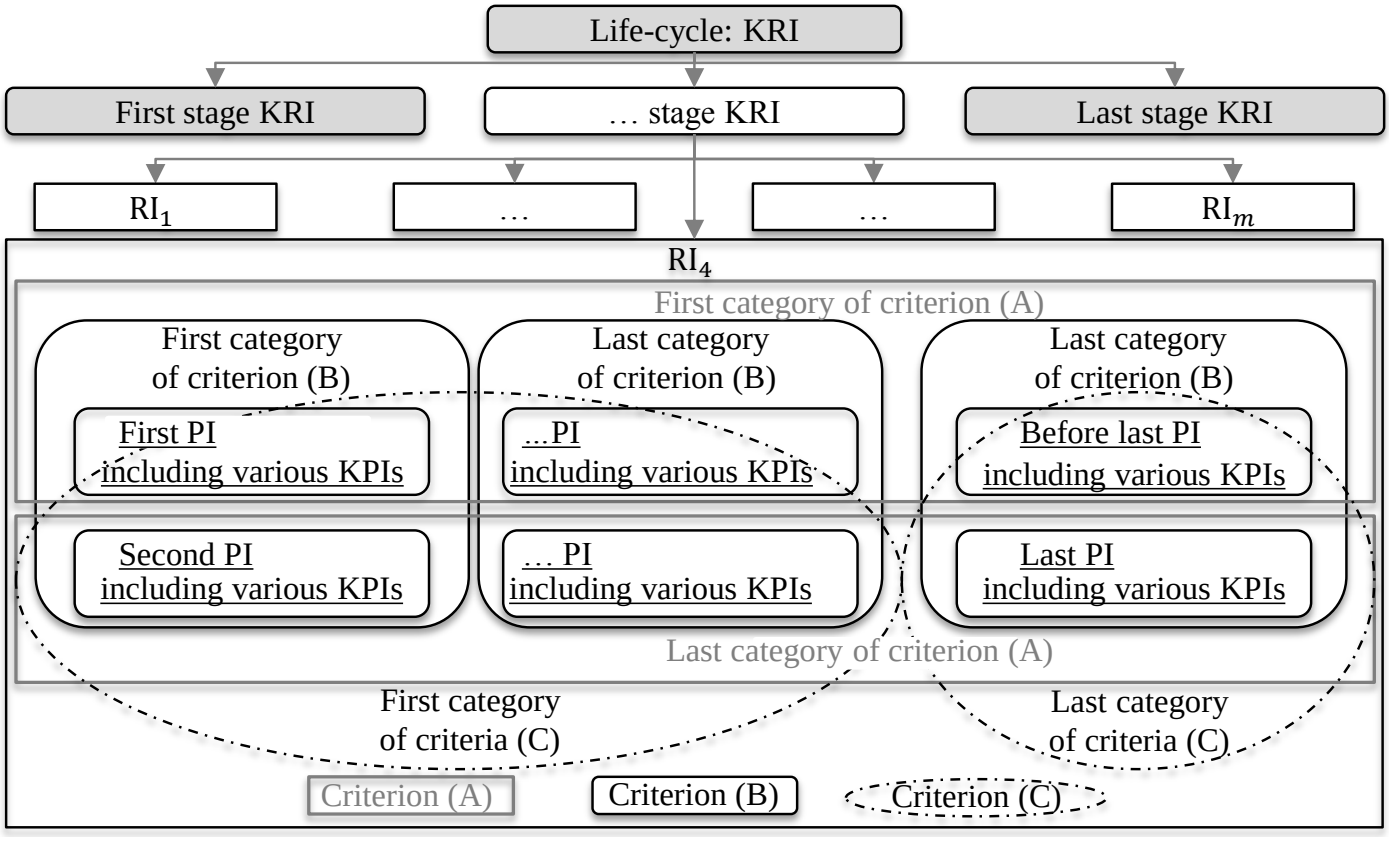

Figure 4.6 Aggregation of a global KRI impact as a product of domestic impacts

In Fig. 4.6, a KRI can be assessed for the entire life-cycle of a functional unit [152]. Due to the freedom of defining and allocating the CSF levels, the assessment of direct cost and carbon footprint in a single life-cycle stage is considered as a KRI here. In this work, not all life-cycle stages are studied, as the are shaded in Fig. 4.6. In this visualized conceptual model, a selected KRI can be broken down into different classes. These classes are defined to be clustered under the various CSF levels. These impact classes are represented by the intersection domains of the criteria and categories, as they are illustrated in Fig. 4.6. On the lowest CSFs level, KPIs are oriented to domains that are contained in distinguishable categories and criteria, as Fig. 4.8 later shows.

Here, it is essential to clearly define the life-cycle coverage of the adopted characterization factors in order to understand the resulted impacts of their elementary flows. In the assessment, a characterization factor describes the impact of a defined life-cycle period for each used unit from its elementary flow type. As it is mentioned in chapter 3, a characterization factor may cover its equivalent from a cradle-to-gate, gate-to-gate, gate-to-grave, or a cradle-to-grave impacts. In literature, there is a common lack of such clear definition in the assessment studies. In practice, this covering variaty may lead to a significant deviation in the values of the same characterization factors from the different possible perspectives. Now, the life-cycle of an assessed product is related to the life-cycles of its elementary flows but not identical to them. Therefore, Fig. 4.7 illustrates the differences between these perspectives on the relevant life-cycles qualitatively.

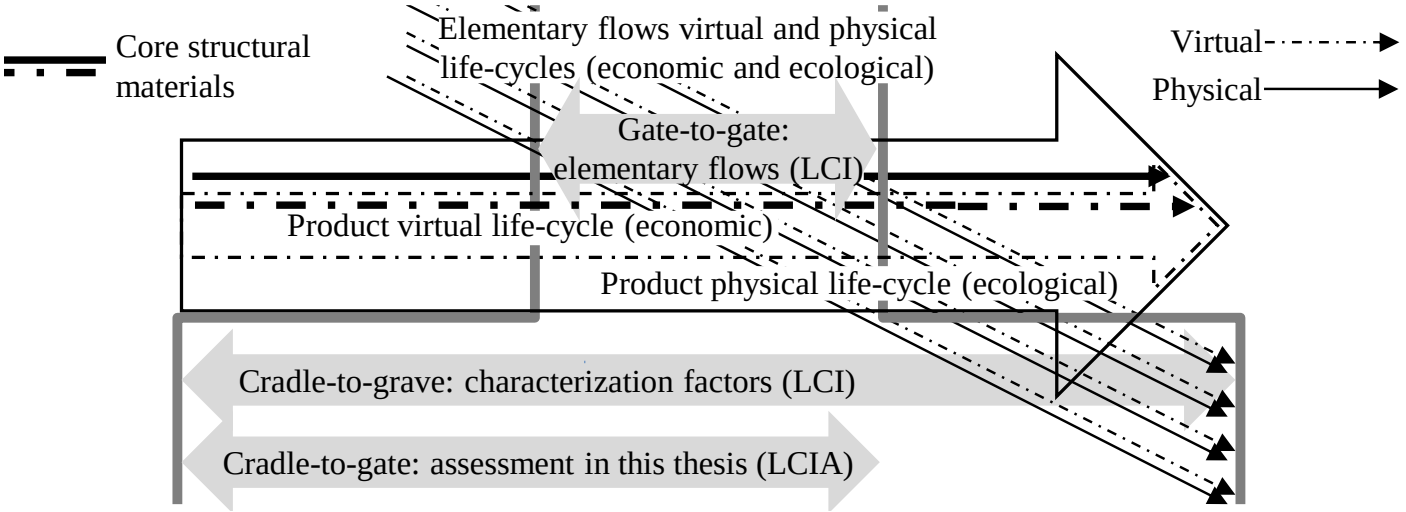

Figure 4.7 Simplified life-cycle scope of the product and its elementary flows

Fig. 4.7 suggests that each elementary flow has a distinguishable life-cycle. Similar to the approach in Fig. 3.28, virtual and physical life-cycle phases are assumed for each elementary flow. In Fig. 4.7, the life-cycle of each considered elementary flow has an intersection with the product life-cycle, otherwise it is irrelevant for the assessment. For the studied FRPs, the core structural materials are represented by the fat horizontal arrows within the product physical and virtual life-cycles in Fig. 4.7. Other elementary flows join these core structural materials in the assessed product system and leave the product life-cycle after that. Ancillaries, equipment, labor, facility, and electricity are examples of such elementary flows, which are represented by the slanting thin arrows in Fig. 4.7.

While a wide range of possible approaches may be adopted based on Fig. 4.7, a cradle-to-gate LCIA is carried out for the direct impacts of a FRP structure in this thesis. As Fig. 4.7 shows, the concluded cradle-to-gate LCIA in this work is a result of combining a gate-to-gate LCI from the real-time process data collection of relevant direct elementary flows and a cradle-to-grave LCI of their characterization factors in Appx. B. This gate starts at the time when the real-time LCI begins collecting the data from its product system. The time, at which the considered LCI gate ends, is the temporal point when the elementary flows measurement ends.

However, this LCIA is clearly not a cradle-to-grave, while the direct elementary flows post to the gate-to-gate LCI are not covered. For instance, assembling, operation, and disposal must have similar LCI in order to have such a cradle-to-grave scope for the direct impacts. In this thesis, the assessment focuses only on the direct cost and carbon footprint of the manufacturing stage, which are arguably excluding the economic and ecological impacts of the early development stages within the product virtual life-cycle. Yet, such early impacts may still be considered as indirect ones in the LCIA of the manufacturing stage. Therefore, such early economic as well as ecological impact equivalents from the development stages in Fig. 3.28 can be considered in future works, whenever the reliable required data is collected from these associated stages. Still, the economic and ecological characterization factors of the considered elementary flows in this work are covering their early life-cycles. Again, it is essential here to distinguish between the product early life-cycle stages, which are not included here, and the early life-cycle stages of the assessed elementary flows, which are covered in the characterization factors in this thesis, as they are discussed thoroughly in Appx. B. Therefore, this work is considered as a cradle-to-gate assessment. Unlike Fig. 3.28, Fig. 4.7 shows identical economic and ecological life-cycle phases, while it hypothesizes that the ecological impacts exist in the virtual life-cycles as well.

As it is previously mentioned in chapter 3, applying cradle-to-grave or at least cradle-to-gate approaches for the characterization factors is common in assessing the product economic impacts. For instance, the useful life in years and salvage of equipment items are considered within the economic characterization factors in the manufacturing stage, although these impacts occur temporally after the assessed stage. Similarly, the ecological impacts of such equipment can be considered for its entire life-cycle from cradle-to-grave, which is adopted in this work. However, data-based assessments for different life-cycle stages of all implemented elementary flows are unavailable in literature and not doable in the limited thesis scope. Now, the realization of time-dependent eco-efficiency assessments about the impacts of all related life-cycle stages for the considered elementary flows can be one of the outlooks from this work. Despite this attempt to have accurate characterization factors, these parameters are still roughly assumed within Eq. 5.30 and Eq. 5.31 by Appx. B, due to the lack of reliable initial data. In conclusion, the novel approach in Fig. 4.7 may be modified to consider flexible selection of stages. Still, the main target of this approach is to standardize such clear definition in every assessment in future studies.

Based on understanding Fig. 4.6, an aggregation relation can be derived for the global impact θ of each KRI. For the direct cost and direct carbon footprint, the representative global impact θ is the summation of all domestic impacts θ_{RI} on the RI level. These RIs can be assigned to the related UPs. Here, it is essential to cover all sub-domains in order to achieve sufficient representation, as it is described in Eq. 4.1.

$$\theta_{KRI} = \sum \theta_{RI} \tag{4.1}$$

In which, these impacts on all levels are assumed to have a unified measuring unit, that enables this summing operation and all following ones. The same approach is adopted in Eq. 4.2 to calculate the impact θ_{RI} on the RI level, which is the summation of all impacts θ_{PI} from the PI level.

$$\theta_{RI} = \sum \theta_{PI} \tag{4.2}$$

Moreover, the impact θ_{PI} on the PI level can be also calculated in Eq. 4.3 as the summation of all impacts θ_{KPI} from the KPI level, while in this work the KPIs are associated with the elementary flows.

$$\theta_{PI} = \sum \theta_{KPI} \tag{4.3}$$

The impact θ_{KPI} on the KPI level for each elementary flow is; however, the product of flow magnitude in a measurement unit and its characterization factor provided per that measurement unit. For example, the fiber magnitude in a specific measurement unit of an exact type in the process is an elementary flow. On the other hand, the price and carbon footprint equivalent of each unit from it are respectively the economic and ecological characterization factors of this elementary flow. It is essential to mention that the relation between KRI, RIs, PIs and KPIs is assumed as a linear summation. This can differ for other KRIs with different possible correlating approaches. However, the discussion of these possibilities is beyond the scope of this thesis. The generic conceptual model in Fig. 4.6, and mathematical ones in Eq. 4.1, Eq. 4.2, and Eq. 4.3 are applied to the bottom-up assessment in this thesis.

Eco-efficiency conceptual model

As Fig. 4.6, Eq. 4.1, Eq. 4.2, and Eq. 4.3 previously show, the global impact θ for a selected KRI from a specific life-cycle stage of a functional unit can be broken down into impact classes. In this thesis, FRP structures are considered as the functional units, while the manufacturing within production is the solely assessed life-cycle stage by the developed DSSs. For the example of parametrized case study in chapter 5, a selection of manufacturing UPs is considered for a single structure of an aircraft vertical stabilizer rib.

In Fig. 4.6, this thesis introduces a comprehensive conceptual model for the manufacturing impact categories that can be implemented to handles both economic and ecological aspects. Now, the impact classes can be categorized due to their association with various elementary flows α_j and the functional unit. In which, α represents the magnitude of any input or output elementary flow in physical unit and the index j represents its type, while all indexes in this work are real numbers $\mathbb{R}$.

Here, it is hypothesized to have direct, indirect, recurring, nonrecurring, fixed, and variable impacts, which are categories that are contained in three main criteria. The first criterion is to be direct or indirect, which depends on the impact typology and its association with functional unit. The second one is to be recurring or nonrecurring, which is a temporal distinguish. The third criterion is to be fixed or variable, while this is about the correlation between the impact magnitude and the functional units number and its direct elementary flows magnitudes. Hence, these impact categories are defined in Tab. 4.1.

Table 4.1 Impact categories, examples, and associations, based on understanding [66, 93, 187, 333]

Category definition	Examples from FRPs manufacturing	Association
Direct: assessable relation with the functional unit	Fiber, matrix, core material, ancillaries, and direct labor	Direct can be fixed, variable, recurring, and nonrecurring
Indirect: no direct association with the functional unit	Interest, facility rent, administration, labor wage, and training	Indirect can be fixed, variable, recurring, and nonrecurring
Recurring: temporal association with specific events	Materials that purchased regularly, rent, wages	Recurring impact can be fixed, variable, direct, and indirect
Nonrecurring: no temporal association with the functional unit	Pre-production planning, equipment acquisition, and interest	Nonrecurring impact can be fixed, direct, and indirect
Fixed: qualitative but not quantitative association with functional unit	Engineering design, production plan, and equipment acquisition	Fixed can be recurring, nonrecurring, direct, and indirect
Variable: quantitative relation with the involved elementary flows	Materials and dedicated labor in manufacturing each functional unit	Variable impact can be recurring, direct, and indirect

From the intersections between these criteria and their categories, domains of impacts are distinguished, as it is previously illustrated in Fig. 4.6. Based on the assessment goal and scope, coverage and cut-off-criteria of these impact classes can be defined [152], as they are shaded in Fig. 4.8.

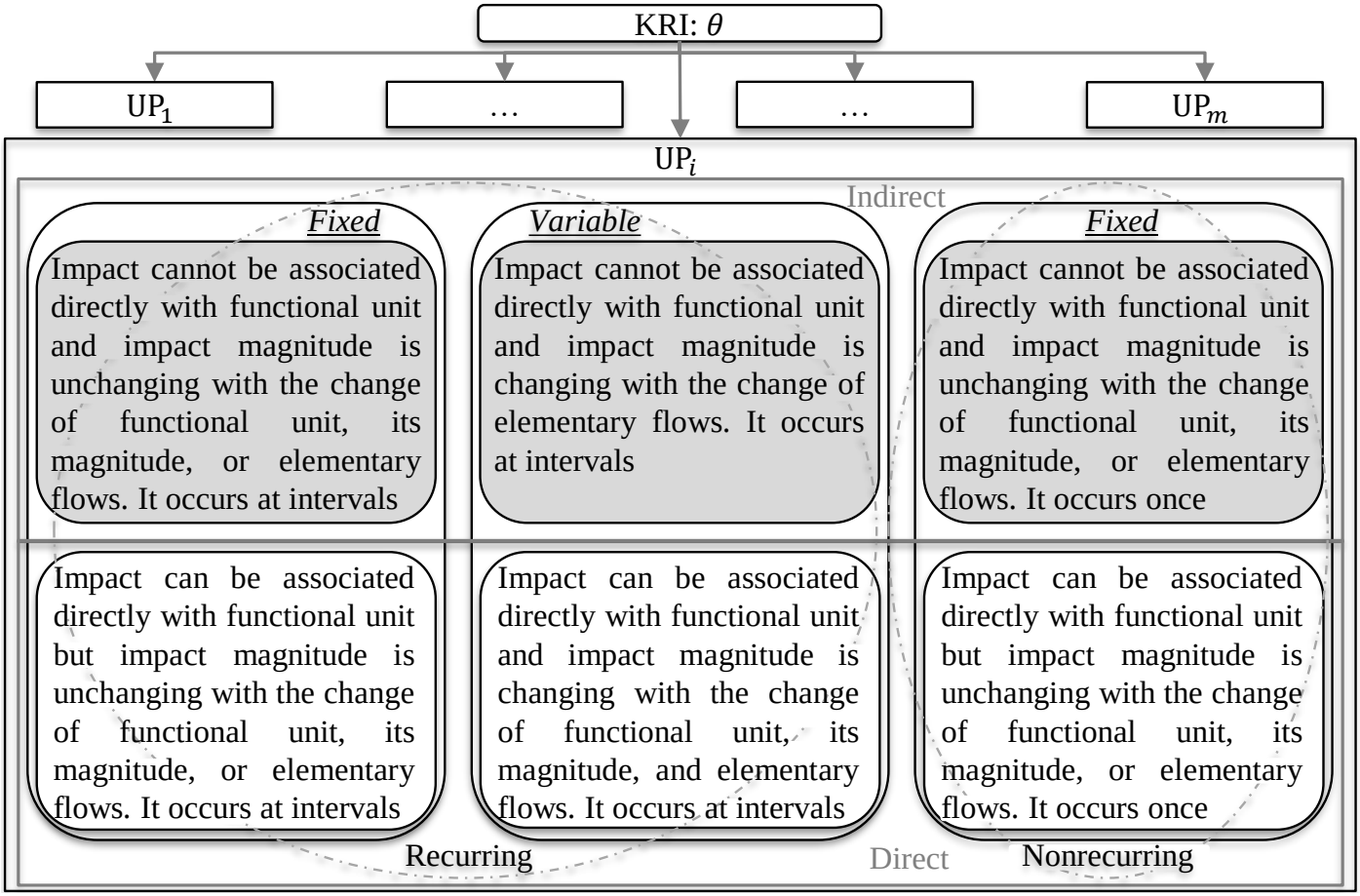

Figure 4.8 Conceptual model of the global impact break-down, based on understanding [66, 93, 187, 211, 333]

Although the previously introduced Fig. 4.6 illustrates the entire life-cycle, the impact θ of a KRI in Fig. 4.8 is reduced to a single assessed life-cycle stage. In which, the index i represents the UP sequence. In general, these domains contain portions of the impacts for various elementary flows that may occur in multiple of them simultaneously. To facilitate understanding this novel illustration in Fig. 4.8, examples of associated impacts are shown later for both economic and ecological aspects within Fig. 4.28 and Fig. 4.29 respectively. As it is shown in Fig. 4.8, this thesis covers only the direct impacts. Therefore, only three direct impact classes are considered from the six intersection domains between the categories in Fig. 4.8, which are the fixed recurring, variable recurring, and fixed nonrecurring. These exact impact classes are reflected in the coverage of selected characterization factors in this thesis, while the global impact is the summation of these domains in this thesis.

4.1.3 Process Equilibrium

After establishing the comprehensive conceptual model, a mathematical model is derived based on it. However, such process mathematical model leans on a set of hypotheses including the equilibrium of production process. Another hypothesis is the possibility of breaking the process model down into discretized UPs that contain all associated elementary flows in their mathematical models. This is essential to allocate the impacts to their causing UPs in general and to their driving elementary flows in specific. However, such discretization is subjected to the interpretation of activities clustering and to the determination of intermediate flows.

Process equilibrium in production

A process can be represented by its elementary flows that are contained in an input flows matrix $[X]$ and an output one $[Y]$ [151]. In Eq. 4.4, a production is described mathematically as an input to output process [284].

$$[Y] = \hat{F}([X]) \tag{4.4}$$

As Fig. 4.9 shows, the transformation of inputs $[X]$ into outputs $[Y]$ is realized by a global production function $\hat{F}$ [284].

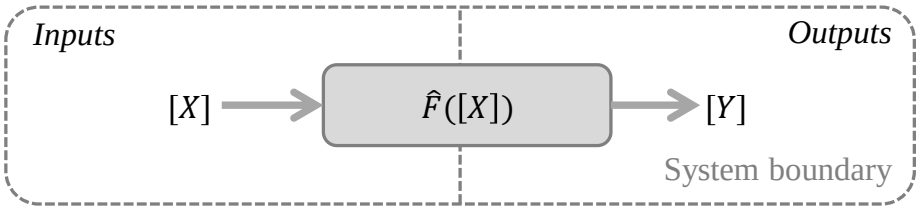

Figure 4.9 Functionality of production process within its boundary, adapted from [85]

In Fig. 4.9, the global process function $\hat{F}$ is representing all functions f of different activities, that contribute to the effort of turning the supplied inputs into the desired outputs. Besides the physical description of the production process, there is the functional description of it. According to Dyckhoff and Spengler, a production process can be modeled by a set of vectors that represents its elementary input and output flows [85]. While the process my be discretized into UPs, the global function $\hat{F}$ can be represented by domestic ones $\hat{F}_i$ for these UPs i, while the UPs i are defined within the sequence range of $i = 1, \cdots, m$. In each UP i, multi physical inputs $v_{i\rho} = \{X_i\}_\rho$ and outputs $u_{i\tau} = \{Y_i\}_\tau$ are involved, as Eq. 4.5 suggests.

$$\{X_i\} = \{v_1, v_2, \cdots, v_{N_{in}}\} \quad \text{and} \quad \{Y_i\} = \{u_1, u_2, \cdots, u_{N_{out}}\} \tag{4.5}$$

In which, the input index value is set as $\rho = 1, \cdots, N_{in}$ for the input elementary flows $v_{i\rho} = \{X_i\}_\rho$ and the output index is set as $\tau = 1, \cdots, N_{out}$ for the output elementary flows $u_{i\tau} = \{Y_i\}_\tau$. Here, these vectors represent distinguishable parts of the process such as its UPs i. In practice, there may be a type variety between the input elementary flows $v_{i\rho} = \{X_i\}_\rho$ in the different UPs i. Similarly, the output elementary flows $u_{i\tau} = \{Y_i\}_\tau$ may also differ between the studied UPs i. As a result, the vector dimensions N_{in} and N_{out} of both $\{X_i\}$ and $\{Y_i\}$ respectively may differ between the various UPs i. As it is explained in Fig. 4.10, not all elementary flows are necessarily applied to every UP i. Such dimension variation leads to an inconsistency in the vectors, which disables deriving a global matrix from them. Therefore, the highest achievable dimension N_{in} is to be adopted in every $\{X_i\}$, to have identical vector dimension in all UPs i. This highest dimension of N_{in} is a result of combining all possible input elementary flow types ρ occurring in all vectors $\{X_i\}$. Within a vector $\{X_i\}$, the non-existing input elementary flow types ρ are substituted by the value of „*zero*“ based on data collection results, in which $v_\rho = 0$. Similarly, the highest achievable dimension N_{out} is adopted in every output vector $\{Y_i\}$.

Hence, the unified input representative vectors of $\{X_i\}$ with the highest possible dimension of ρ and the similarly derived output vectors $\{Y_i\}$ with the highest dimension of τ are used to describe every UP i. These vectors and the matrices, which are generated based on them, are generically shown in Fig. 4.10. As Fig. 4.10 shows, functions f that are represented by $\hat{F}_i$ in each UP$_i$ are converting the inputs $v_{i\rho} = \{X_i\}_\rho$ into outputs $u_{i\tau} = \{Y_i\}_\tau$.

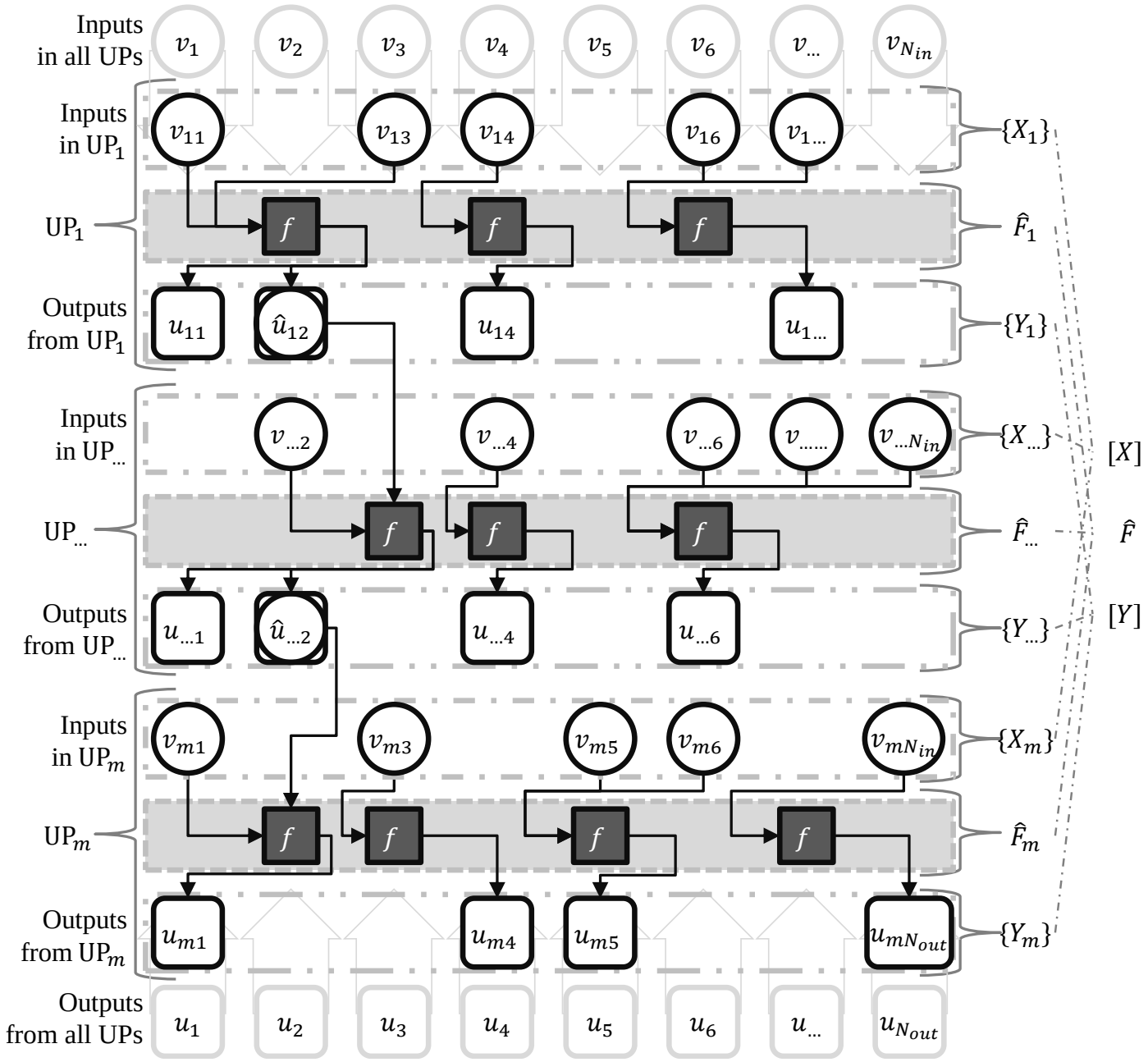

Figure 4.10 Inputs, outputs, intermediates, and functionalities of production process

As it is shown on the right side of Fig. 4.10, these domestic groups of functions in $\hat{F}_i$ can be represented for all UPs in a holistic function $\hat{F}$, while the vectors of inputs $\{X_i\}$ and outputs $\{Y_i\}$ are gathered in the matrices of inputs $[X]$ and outputs $[Y]$ respectively. As it is shaded in Fig. 4.10, the nature of these functions f is beyond the scope of this thesis. Moreover, Fig. 4.10 illustrates the intermediate flows $\hat{u}_{i\tau} = \{\hat{Y}_i\}_\tau$, which exist solely between the UPs in a discretized process [152]. These intermediate flows are outputs of a UP, which are also used as input flows in following UPs. In practice, these intermediate flows can be any matter or energy that flow from a UP to another. On the other hand, the intermediate products are defined as product phases that are processed through the various transformation functions $\hat{F}_i$ in different UPs i [151]. However, these flows are represented mainly by the intermediate products known as semi-finished products in the FRP manufacturing. Thus, each semi-finished product is used solely in the following UP in the FRP manufacturing, as it is explained later in the discretization theory. However, not every UP i necessarily produces a semi-finished product, while the last UP_m is normally producing the finished one. Moreover, other UPs i may have no product related output such as the preparing UP. In addition to the hypothesis of process equilibrium, the physical balance between

both input and output flows is also hypothesized. For this thesis, Fig. 4.10 describes the linearly connected UPs with no consideration of the back-coupling impacts.

Physical equilibrium in production

As a part of the comprehensive assessment framework, the definition of matter, energy, and information flows is included in the technical dimension of the process system boundary [24, 105]. However, the information in this thesis is indirectly addressed within the impacts θ of the assessed CSFs. As it is hypothesized previously in Fig. 4.4, the information stages are correlated with the assessment and not the process in this thesis. All other information types, that are unrelated to the assessment, are assumed to be irrelevant or unchanging. Hence, the information is separated and excluded from the process elementary flows here. Therefore, the elementary flows can be either matter or energy [152].

For a production process $\hat{F}([X])$, it is hypothesized that each UP i is limited spatially to its WS i within the factory. This spatial boundary is essential to define the associated elementary flows as well as their cut-off-criteria. Therefore, a control volume as a spatial boundary within the facility layout is to be defined [81]. Besides the spatial dimension of each WS, it is essential to define the geographical boundary of the assessed process such as the country and city [151]. This geographical boundary is decisive for characterizing the various impact factors, as Appx. B shows.

For a totally efficient production, the outputs in terms of energy and material are equal to the inputs from each of them respectively [284]. From management point of view, no remaining energy or material is expected within the entire control volume after the process ends in an ideal production. In practice, FRP manufacturing includes an exothermic reaction. However, such thermal emission as an environmental aspect is beyond the scope of this thesis, while carbon footprint is the only considered environmental impact. Here, any mass-energy conservation in this process is also neglected, while it has no direct association with direct cost and carbon footprint. Moreover, it is assumed that both net mass and net energy changes in the control volume of a production system go back to their initial value of „*zero*“ when the process ends. However, this assumption of absolute input and output equilibrium is true for a failure free process. In such case, all inputs $[X]$ and outputs $[Y]$ are assumed to be in an ideal process and subjected to rational decision-making as well.

Arguably, the mass and energy change may include some items of investments that are unnecessarily leaving the system when the process ends from management point of view. Nonetheless, such investments are distinguished from the direct elementary flows as they are previously illustrated in Fig. 4.8. In this thesis, they are either covered by the characterization factors or considered as irrelevant for the assessed CSFs. Hence, the equilibrium in this work is applied solely to the assessed elementary flows. Based on the hypothesis of an absolute equilibrium in this work, it can be concluded that within the control volume of a product system Eq. 4.6 is applied.

$$\text{Material}_{IN} = \text{Material}_{OUT} \quad \text{and} \quad \text{Energy}_{IN} = \text{Energy}_{OUT} \tag{4.6}$$

In which, the material inputs are represented by Material_{IN}, while their outputs are the Material_{OUT}. Similarly, the energy inputs are notated by Energy_{IN}, whereas their outputs are represented by Energy_{OUT} in Eq. 4.6. Based on these equilibrium theories, the assessed process are mathematically modeled later in this chapter.

4.1.4 Modeling Parameters and Boundaries

In the mathematical modeling, elementary flows and their characterization factors for the various considered types are the core parameters for the time-dependent eco-efficiency assessment. Besides the classification of these elementary flows α_j, their allocation within the temporal and spatial boundaries is discussed in this section.

Classification of elementary flows

To have a comprehensive description of both input and output elementary flows, the symbol α_j represents the element of a universal set J. This universal set J includes all input and output elementary flows of v_ρ and u_τ respectively for $\alpha_j \in J$ with $j = 1, \cdots, N$ and $N = N_{in} + N_{out}$. Here, tuples may be implemented to cluster the elementary flows instead of the sets. However, the sequence of elements in tuples is fixed, while it is random in sets. On the other hand, tuples may have the same element repeated more than once, while a set has no element repetition. Although tuples are advantageous for establishing computerized models, the mathematical model in this thesis adopts ordered universal set, supersets, sets, and subsets to cluster the elementary flows and allow no elements repetition. Moreover, a union of two supersets, sets, or subsets has the element order of the first one followed by the order of the following one respectively. This is applied for the case of multiple unions as well. These predefinitions of special ordered set forms facilitates the generation of vectors and matrices in the mathematical modeling as well as the data processing in the computerized modeling. Both elementary flow sides of inputs $v_\rho \in J$ with $\rho = 1, \cdots, N_{in}$ and outputs $u_\tau \in J$ with $\tau = 1, \cdots, N_{out}$ are represented by the universal elementary flows $\alpha_j \in J$ with $j = 1, \cdots, N$ and $N = N_{in} + N_{out}$. In which, N is the maximum dimension of all types considered from both input and output types.

Based on the conceptual model in Fig. 4.10, dedicated mathematical models are derived to cluster the elementary flows. Hence, the extensive representation of the elementary flows α_{ij} includes both input flow types $v_{i\rho}$ as well as output flow types $u_{i\tau}$ in all UPs i with $i = 1, \cdots, m$. As Eq. 4.7 shows, all relevant input and output flows can be represented within their supersets of V and U respectively.

$$V = \{v_{11}, \cdots, v_{1N_{in}}, \cdots, v_{m1}, \cdots, v_{mN_{in}}\} \quad \text{and} \quad U = \{u_{11}, \cdots, u_{1N_{out}}, \cdots, u_{m1}, \cdots, u_{mN_{out}}\} \tag{4.7}$$

These supersets for inputs V and outputs U are contained in the universal set J, as it is shown in Eq. 4.8.

$$V \subseteq J \quad \text{and} \quad U \subseteq J \tag{4.8}$$

In Eq. 4.9, the input and output supersets V and U are respectively derived from the process matrices $[X]$ and $[Y]$ from Eq. 4.4.

$$[X] \in V^{m \times N_{in}} \quad \text{and} \quad [Y] \in U^{m \times N_{out}} \tag{4.9}$$

In which, $[X] = [v_{i\rho}]$ is considered for $i = 1, \ldots, m$ and $\rho = 1, \ldots, N_{in}$ as well as $[X] \in \mathbb{R}^{m \times N_{in}}$, while $\mathbb{R}$ represents the real numbers. Similarly, $[Y] = [u_{i\tau}]$ is considered for $i = 1, \ldots, m$ and $\tau = 1, \ldots, N_{out}$ as well as $[Y] \in \mathbb{R}^{m \times N_{out}}$. As Eq. 4.10 suggests, the universal set J is the union of supersets V and U.

$$V \cup U = J \tag{4.10}$$

From this universal set J, an elementary flows representing matrix $[A]$, that contains all elementary flows α_{ij}, can be interpreted in Eq. 4.11.

$$[A] \in J^{m \times N} \tag{4.11}$$

In which, $[A] = [\alpha_{ij}]$ is considered for $i = 1, \ldots, m$ and $j = 1, \ldots, N$ as well as $[A] \in \mathbb{R}^{m \times N}$. Except for the intermediate flows in the superset $\hat{U}$, no elementary flow α_{ij} is allowed to be duplicated in both V and U, as it is stated in Eq. 4.12.

$$U \cap V = \hat{U} \tag{4.12}$$

In Eq. 4.13, this superset $\hat{U}$ for the entire process is also derived from the intermediate matrix $[\hat{Y}]$.

$$[\hat{Y}] \in \hat{U}^{m \times N_{out}} \tag{4.13}$$

Again, $[\hat{Y}] = [\hat{u}_{i\tau}]$ is considered for $i = 1, \ldots, m$ and $\tau = 1, \ldots, N_{out}$ as well as $[\hat{Y}] \in \mathbb{R}^{m \times N_{out}}$.

For the various UPs i in a studied process, the approach of Eq. 4.9 can be also applied to the UP level, as Eq. 4.14 suggests.

$$\{X_i\} \in V_i^{1 \times N_{in}} \quad \text{and} \quad \{Y_i\} \in U_i^{1 \times N_{out}} \tag{4.14}$$

In which, the row vector $\{X_i\} = \{v_\rho\}$ is considered for $\rho = 1, \ldots, N_{in}$ as well as $\{X_i\} \in \mathbb{R}^{m \times N_{in}}$, while $\{Y_i\} = \{u_\tau\}$ is considered for $\tau = 1, \ldots, N_{out}$ as well as $\{Y_i\} \in \mathbb{R}^{m \times N_{out}}$. Similar to Eq. 4.10, the set J_i is the union of V_i and U_i, as Eq. 4.15 explains.

$$V_i \cup U_i = J_i \tag{4.15}$$

As a result, the cardinality of the set V_i is equal to the dimension of the vector $\{X_i\}$. As it is previously explained, an approach of adopting the highest possible dimension for all vectors $\{X_i\}$ of the different UPs i is applied. Based on that, the highest possible cardinality of set V_i is also adopted. Under these circumstances, the non-existing elements are substituted by the value of „*zero*“.

By combining these input sets V_i together and combining the output sets U_i together from all UPs i, the representing supersets V and U can be formed respectively, as Eq. 4.16 shows.

$$V_1 \cup V_{\ldots} \cup V_m = V \quad \text{and} \quad U_1 \cup U_{\ldots} \cup U_m = U \tag{4.16}$$

Unlike the case in Eq. 4.12, no elementary flow α_{ij} is allowed to be duplicated in both V_i and U_i on UP level, while no identical flow types can enter and leave the same sufficient UP i, as it is stated in Eq. 4.17.

$$U_i \cap V_i = \emptyset \tag{4.17}$$

In the case of different UPs $i = 1, \ldots, m$, output elementary flow $u_{x_1 j}$ of UP $i = x_1$ may be an input elementary flow $v_{x_2 j}$ but for a following UP $i = x_2$, as it is discussed thoroughly later in this chapter. Therefore, it is concluded that for the output set U_{x_1} of UP $i = x_1$ and the input set V_{x_2} of a specific following UP $i = x_2$ with

$x_2 > x_1$, common intermediate flows are represented by the set $\hat{U}_{x_1}$, as Eq. 4.18 shows.

$$U_{x_1} \cap V_{x_2} = \hat{U}_{x_1} \tag{4.18}$$

To facilitate the data collection and processing, each of these supersets including V and U is broken down into further sets and subsets based on a comprehensive understanding of the process. These sets and subsets are defined for the manufacturing of FRP based on relevant technical and assessment aspects [13].

From technical point of view, both input superset V and output superset U can be split further into two main sets. As it is discussed previously as a part of the physical equilibrium in production, these sets are the matter main set μ as well as the energy main set. The material main set μ consists of all matters in both input and output elementary flows. While the input matter flows are represented by the set $V^{[\mu]}$, the output matter flows are represented by the set $U^{[\mu]}$, as Eq. 4.19 explains. In this thesis, the notation of square brackets [] is also implemented to distinguish the orienting upper notation from other mathematical operations.

$$\begin{aligned} V^{[\mu]} &\subseteq \mu \\ V^{[\mu]} &\subseteq V \\ U^{[\mu]} &\subseteq \mu \\ U^{[\mu]} &\subseteq U \\ U^{[\mu]} \cup V^{[\mu]} &= \mu \end{aligned} \tag{4.19}$$

Based on the approach in Eq. 4.19, all energy elementary flows $\alpha_j \in J^{[\epsilon]}$ are combined in the main set ϵ. In Eq. 4.20, the elements of this main set are split into two sets to represent the input energy flows $V^{[\epsilon]}$ and output ones $U^{[\epsilon]}$.

$$\begin{aligned} V^{[\epsilon]} &\subseteq \epsilon \\ V^{[\epsilon]} &\subseteq V \\ U^{[\epsilon]} &\subseteq \epsilon \\ U^{[\epsilon]} &\subseteq U \\ U^{[\epsilon]} \cup V^{[\epsilon]} &= \epsilon \end{aligned} \tag{4.20}$$

However, the semi-finished products, which are combined in the intermediate flows superset $\hat{U}$, are special cases of matter elementary flows $\alpha_j \in J^{[\mu]}$. As it is explained previously, they are included in both input superset V and output superset U in Eq. 4.21.

$$\begin{aligned} \hat{U} &\subseteq \mu \\ \hat{U} &\subseteq V \\ \hat{U} &\subseteq U \\ \hat{U} &\subseteq V^{[\mu]} \\ \hat{U} &\subseteq U^{[\mu]} \\ U^{[\mu]} \cap V^{[\mu]} &= \hat{U} \end{aligned} \tag{4.21}$$

A general assumption in this thesis states that there is no energy intermediate flow in FRP manufacturing, as it is explained in Eq. 4.21. This generic classification of elementary flows α_j for all considered types j into sets associated with their physical forms is illustrated in Fig. 4.11.

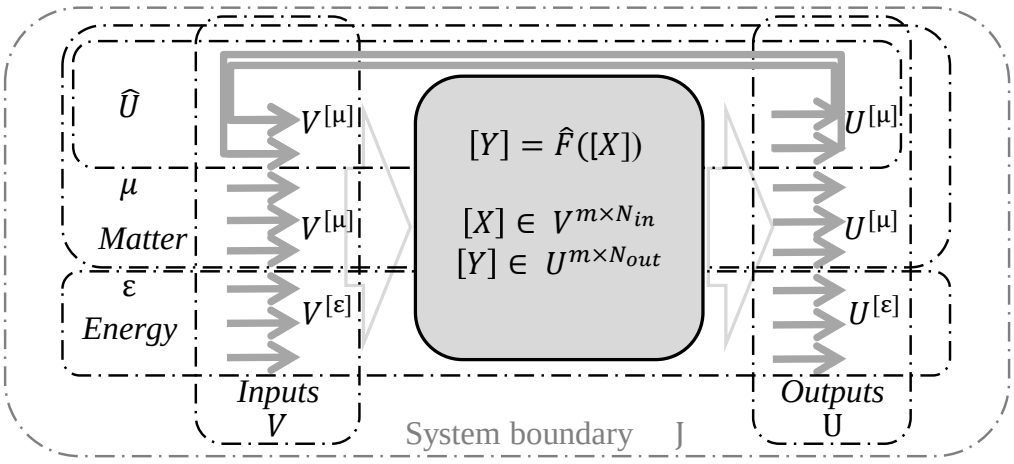

Figure 4.11 Correlation between process universal set, supersets, main sets, and sets

As a generic illustration, Fig. 4.11 is applicable for any production process with no energy intermediate flows. As it is discussed later in this chapter, further classification of each set into subsets $\varphi^{[\Gamma]}$, that represent the elementary flows categories in FRPs manufacturing, is necessary for the LCI and LCIA in this work. Especially for the SWS concept, clustering the assessed elementary flows under such subsets $\varphi^{[\Gamma]}$ is required to select the proper methods and sensor nodes. However, any further classification based on the generic illustration in Fig. 4.11 depends on the process characteristics.

Temporal and spatial allocation of elementary flows

In this thesis, the temporal and spatial dimensions are traced and assigned to every elementary flow α_{ij}. Based on the thorough understanding of the assessed process, the elementary flows α_{ij} in each UP i are defined within the technical system boundary. Generally, a time point t_a in the temporal allocation t is the process beginning point. At this start point t_a, the very first function f of UP $i = 1$ in the process $\hat{F}$ is launched. This production function $\hat{F}$ is accomplished after that at the time point t_b. This happens when the final function f is ended or reached its steady state. For one process, it is logical that $t_a < t_b$, while $\hat{F}$ takes a place in a time duration Δt_{tot} that lays between these two temporal points of process beginning t_a and its end t_b.

Technically, the temporal allocation $t^{[\alpha_j]}$ of an elementary flow α_j is meant to be any point in time within the entire process duration Δt_{tot}. At the very beginning of $\hat{F}$, the first input elementary flow v_ρ arrives at temporal allocation $t_a = \min_{v_\rho} t_a^{[v_\rho]}$. This is considered to be the lowest value or the „*zero*“ start point of duration Δt_{tot} in temporal allocation t. On the other hand, the departure of the last output elementary flow u_τ occurs at the highest temporal allocation value as $t_b = \max_{u_\tau} t_b^{[u_\tau]}$. However, it is also possible to have an input, that ends the process by stop flowing to it at the time of $t_b = \max_{v_\rho} t_b^{[v_\rho]}$. Hence, the process total time Δt_{tot} can be described by the temporal difference between the arrival time $t_a = \min_{v_\rho} t_a^{[v_\rho]}$ of the first elementary flow α_j, which is logically an input v_ρ, and the departure time $t_b = \max_{u_\tau} t_b^{[u_\tau]}$ of the last elementary flow α_j, which may be an output u_τ, as Eq. 4.22 shows.

$$\Delta t_{tot} = t_b - t_a \tag{4.22}$$

This arrival temporal allocation t_a is specified as a temporal point in the standard synchronized official time at the process geographical location, which is described by (hours:minutes:seconds). Hence, the temporal allocation t of any elementary flow α_j is measured as a cumulative time passing rate in seconds (s) from t_a, which can be converted to the standard synchronized official time as well.

Based on the discretization of different UPs, a temporal boundary of each UP i is the duration between time points t_{i_a} and t_{i_b} of the first occurring elementary flow and the last one of it respectively. In which, t_{i_a} is the temporal start of the UP i and t_{i_b} is the temporal end of it, as Eq. 4.23 suggests.

$$\Delta t_i = t_{i_b} - t_{i_a} \tag{4.23}$$

In practice, some activities within the UPs may be performed after the product release time such as system preparing and cleaning. Such activities can be either considered at the beginning of a process or at its end. However, the consideration of such activities to the just released product or the process of the following one is subjected to interpretation. In this thesis, such temporarily unconnected preparing activities are considered at the beginning as well as the end within UP_1, as it is explained later in the UP discretization.

Moreover, a duration $\Delta t^{[v_\rho]}$ between the arrival time $t_a^{[v_\rho]}$ of any selected input elementary flow v_ρ and the time point $t_b^{[v_\rho]}$ of its departure or conversion from the product system can be formulated in Eq. 4.24.

$$\Delta t^{[v_\rho]} = t_b^{[v_\rho]} - t_a^{[v_\rho]} \tag{4.24}$$

However, such a temporal difference in Eq. 4.24 can be generally applied for any input or output elementary flow α_j, as it is shown in Eq. 4.25.

$$\Delta t^{[\alpha_j]} = t_b^{[\alpha_j]} - t_a^{[\alpha_j]} \tag{4.25}$$

The description in Eq. 4.25 is enabled by the real-time data collection in this thesis.

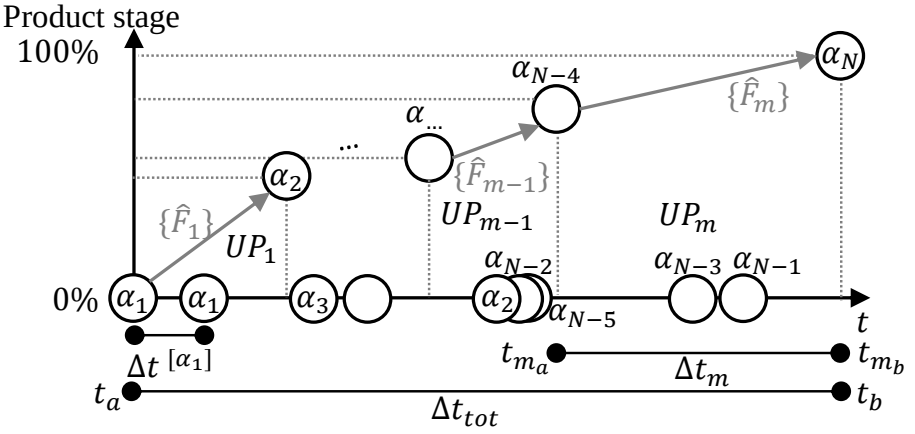

Figure 4.12 Exemplary temporal allocation t of elementary flows α_j

This definition of temporal allocation t for exemplary elementary flows is illustrated in Fig. 4.12. It is essential to mention that Δt_{tot} in Fig. 4.12 may include wasted, down, and break times that contain no functions f. Furthermore, some activities f may be simultaneously performed totally or partially. Therefore, the total process time Δt_{tot} of a process function $\hat{F}$ is not necessarily equal to the summation of all functions durations. To achieve the systematic temporal tracking of the assessed elementary flows α_j, it is essential to assign their occurrences to standard temporal points t, that are counted from the process beginning at $t_a = \min_{v_\rho} t_a^{[v_\rho]}$ or in the synchronized official time.

In this thesis, the temporal allocation t shown in Fig. 4.12 aims to track the changes occur in the magnitude of each assessed elementary flow α_j over time t. Now, the flow existence may be traced by its type identification j throughout the process duration Δt_{tot}.

Similar to the approach of determining the temporal allocation t, each elementary flow α_j has a definable spatial allocation s within two- or three-spatial dimensions over the course of entire process duration Δt_{tot}. These spots draw a virtual spatial path $\Delta s^{[\alpha_j]}$ for each elementary flow α_j during $\Delta t^{[\alpha_j]}$. From considering flows such as the energy ones $\alpha_j \in J^{[\epsilon]}$, it is obvious that some elementary flows α_j are physically untraceable or traceable only by sophisticated sensor nodes. Therefore, the path $\Delta s^{[\alpha_j]}$ can; however, be determined initially by tracking the carriers of these elementary flows α_j. Practically, such carriers are following fixed or slightly mobile supply lines in the case of energy $\alpha_j \in J^{[\epsilon]}$ and flexible but traceable moving labors or tools in the case of materials $\alpha_j \in J^{[\mu]}$. Generally, uniformly repeated paths $\Delta s^{[\alpha_j]}$ of elementary flows α_j are common in a high maturity industrial process, whereas management tools are applied to assure that in such optimized process.

Considering the magnitude of each elementary flow α_j, it is flowing through its path $\Delta s^{[\alpha_j]}$ in different WSs and changing within them. To facilitate the determination of each path $\Delta s^{[\alpha_j]}$, a coordination standard is to be adopted. Therefore, a 2- or 3-dimensional Cartesian coordinate can be applied with an arbitrary point as origin $s = 0$. This coordinate may be defined for each elementary flow path $\Delta s^{[\alpha_j]}$ from predefined reference. Alternatively, all paths of different flows can be determined from the same origin $s = 0$, as Fig. 4.13 shows.

Moreover, each WS may be described as a set of workspaces (WSP) to facilitate breaking its control volume into sub-spaces if required. In practice, this elementary flow path $\Delta s^{[\alpha_j]}$ is not necessarily fixed, especially in manually performed UPs i. In this thesis, it is hypothesized that a single spot s, as a point on, an area in, or a volume of 2 or 3-dimensional space, can be determined to identify the allocation of an elementary flow α_j. These definable spatial spots s can be allocated within the WS or on a flow path $\Delta s^{[\alpha_j]}$ toward the WS. At a specific temporal allocation t, the magnitude of flow α_j can be measured in its definable spatial allocation spots s. However, the path $\Delta s^{[\alpha_j]}$ including all spatial allocations s of a single elementary flow α_j can be described as a route. This definition of the spatial allocation s is illustrated in Fig. 4.13.

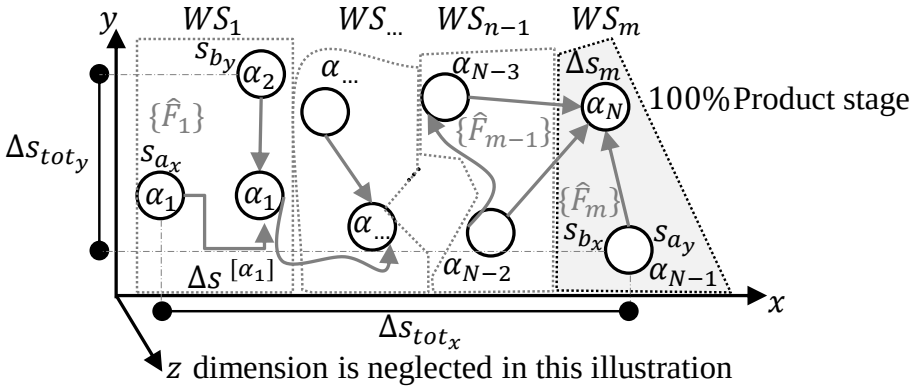

Figure 4.13 Exemplary spatial allocation s of elementary flows α_j in 2-dimensional plane

As the exemplary illustration in Fig. 4.13 shows, the WS can have the form of any 2 or 3-dimensional close shape control volume that matches the technical boundary definition of the studied process. Similar to the process total time Δt_{tot}, the process total space Δs_{tot} can be identified. It is described as the difference between the location $s_a = \min_{\alpha_j} s_a^{[\alpha_j]}$ of an elementary flow α_j closest spot to the origin $s = 0$ and the location $s_b = \max_{\alpha_j} s_b^{[\alpha_j]}$ of geometrically farthest elementary flow α_j from the origin $s = 0$. This geometrical difference should be identified in every included dimension, while the exemplary illustration in Fig. 4.13 covers the facility area in both Δs_{tot_x} and Δs_{tot_y}.

In reality, the space Δs of a WS in all considered dimensions is more than the area or volume required for all elementary flow paths $\Delta s^{[\alpha_j]}$. This deviation is a result of various operation associated reasons and space inefficient utilization. Yet, the flow path $\Delta s^{[\alpha_j]}$ describes the spatial allocation s of an elementary flow α_j throughout its existing duration $\Delta t^{[\alpha_j]}$ within the process. In this thesis, such allocations of spatial spot s and temporal point t of each assessed elementary flow α_j are essential to allocate the sensor nodes in order to realize the real-time data collection. In every WS, a 2-dimensional plane of small areas (similar to the chessboard) can be defined. Based on the smallest coverage area of the implemented sensor nodes, the size of plane units can be defined. On this plane, the paths of all relevant elementary flows $\Delta s^{[\alpha_j]}$ are virtually allocated, while these paths are drawn as actual and possible routes.

As it is mentioned previously, the importance of spatial allocation s is to measure the changes occurring in the magnitude of an elementary flow α_j related to their spatial allocation over time. Consequentially, both temporal and spatial allocations should provide a unique assignment of each measured elementary flow α_j by the SWS. Hence, the questions about; when and where each elementary flow is arriving, how its magnitude and probably type identity are changing, and whether it is departing the WS or not, are answered with temporal and spatial allocations.

4.1.5 Process Mathematical Modeling

As a part of representing a process, mathematical modeling is applied in converting the concepts into a set of algorithms. These algorithms are the cornerstone of any computerized DSS for time-dependent eco-efficiency assessment. In this work, the mathematical models are utilized in the discretization of UPs, creation of generalized process matrix, description of FRP manufacturing, and establishment of the assessment matrix. Now, this requires a clear description of all associated elementary flows α_j and their characterization factors λ_j.

Discretization of UPs

In modeling, any discretization of a holistic process depends on the assessment goal and the served decision-making level. In this work, the comprehensive mathematical generalization model of the entire assessed process is discretized into a set of models, which are representing the different UPs. This approach matches the goals of time-dependent eco-efficiency assessment, while the UP level provides a sufficient detail level [10, 264]. Such UPs may be distinguished whenever logic stepped evolutions of the outcomes can be sensed as intermediate products [151]. As it is mentioned previously, there are activities within each UP where domestic functions f are carried out [264]. Now, Fig. 4.14 illustrates the relation between the process levels.

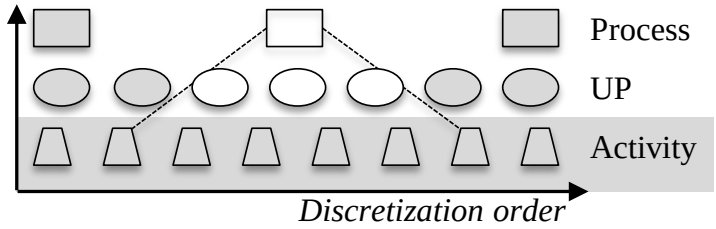

Figure 4.14 Exemplary process levels and discretization

In a previous work, an activity modeling approach and the nature of exemplary activities have been discussed. Although there may be further detailed abstraction levels, an activity is the lowest sufficient level for the eco-efficiency assessment, as Fig. 4.14 shows. Unlike the UPs, no intermediate product occurs between

activities, while product related outputs are unmeasurable for every activity on this level. Therefore, it has been hypothesized that activity inputs are in equilibrium with its outputs [264].

As it is unshaded in Fig. 4.14, the considered level of abstraction is the UP in this thesis, while any further discussion about the activity level is beyond the scope. Although the nature of such activities is beyond the scope of this thesis, it is still essential to mention that any UP is a set of these activities. Practically, the definition and discretization of UPs are based on clustering these activities in a technical, spatial, temporal, or logical content. Furthermore, it is also possible to combine some or all of these aspects to define a UP. The technical aspect describes the allocation and affiliation of intermediate products, which facilitates distinguishing the various UPs in a process. However, not every UP necessarily generates an intermediate product, as it is explained before. Practically, each UP takes a place within a spatial system boundary such as the WS. Still, in reality some WSs are utilized to perform more than a UP. Therefore, an additional temporal distinguishing characteristic is required, at least in the form of a sequence definition. Such sequence may have a temporal nature, especially when the UPs are performed in the same WS. However, this sequence is unnecessarily temporal and may be logical or spatial, whenever various WSs are involved. This may be the case of activities that are performed simultaneously for various UPs of the same process in different WSs. Therefore, the generalized illustration in Fig. 4.14 suggests a discretization sequence and not necessarily a temporal assignment. Nonetheless, some activities may lack of technical, spatial, or even temporal correlation but still have a logical affiliation from decision-making point of view. Therefore, these four system boundary aspects are implemented to distinguish the different UPs in the process of FRP manufacturing.

It is essential to mention that a global impact θ of a process can be related to its main output, which is the demanded product. Here, the finished FRP structure u_{mS} is the physical transition result of all intermediate semi-finished products $\hat{u}_{iP} = [\hat{Y}]_{i\tau}$. Like all other outputs, these intermediate products depend on the input elementary flows $\{X_i\} = \{v_\rho\}$ of their UP as well as their associated UP function $\hat{F}_i$. Based on the discretization of the holistic process function $\hat{F}$ into domestic functions in each UPs $\hat{F}_i$, the global process mathematical model can be split into a set of UP mathematical models $\hat{F}_i(\{X_i\})$, as Fig. 4.15 suggests.

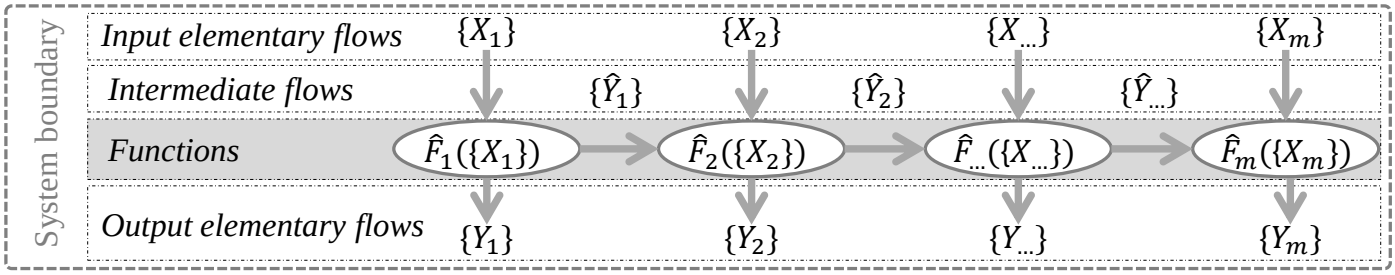

Figure 4.15 Simplified illustration of input, output, and intermediate flows

In FRP manufacturing, no intermediate products $\hat{u}_{ij}$ other than the semi-finished structures $\hat{u}_{iP}$ may be extracted from each UP i. Therefore, semi-finished structures $\hat{u}_{iP}$ are the only elements in the intermediate vector $\{\hat{Y}_i\}$ of each relevant UP i, as Eq. 4.26 explains.

$$\{\hat{Y}_i\} = \hat{u}_{iP} \tag{4.26}$$

However, activities of preparing various assets in FRP manufacturing may be separated from other core activities of transforming these semi-finished products $\hat{u}_{iP}$. Hence, preparation activities can be either integrated in other UPs or separated and clustered in a unique UP. The separation of these activities in a preparing UP serves the thorough assessment of these activities. For example, a previous study shows that preparing has the third largest

direct cost impact in manufacturing CFRP wing ribs, while another internal study of Denkhaus and Hilmer has assigned around 43 % of the direct cost to the preparing UP in CFRP manufacturing [13, 73]. Another reason for the separation of preparing activities in a unique UP is the technical difficulties in enhancing the DoA of these activities in the aerospace industry, while they represent a bottleneck for such attempts. Nonetheless, the adopted case study from the EVo-platform has an automated preparing initially. Still, such advanced manufacturing plant is not common in the production of FRP structures within the aerospace industry. In practice, preparing activities can be; therefore, only logically separated from other ones. However, it is still an exceptional UP that may share WSs with other UPs and may also have an uncontentious and unconnected temporal boundary. Therefore, preparing is the only UP i with outputs unrelated directly to the structure u_{mS} as a final product, whereas no semi-finished structure $\hat{u}_{iP}$ occurs as an output from it. In this general adopted definition, the crucial activities of vacuum bagging in some FRP manufacturing techniques are considered as a part of the preparing UP. Other activities of roll installation, cleaning, mold coating, and several other preparations of various assets are also assumed to be a part of this UP.

Semi-finished structures $\hat{u}_{iP} = \{\hat{Y}_i\}$ have been defined as the transformation stages of raw materials to cuts $\hat{u}_{2P} = \{\hat{Y}_2\}$, a preform $\hat{u}_{3P} = \{\hat{Y}_3\}$, a trimmed preform $\hat{u}_{4P} = \{\hat{Y}_4\}$, an impregnated form $\hat{u}_{5P} = \{\hat{Y}_5\}$, and a consolidated form $\hat{u}_{6P} = \{\hat{Y}_6\}$. From UP_7, the final demanded FRP structure u_{7S} is released based on all these stages [13].

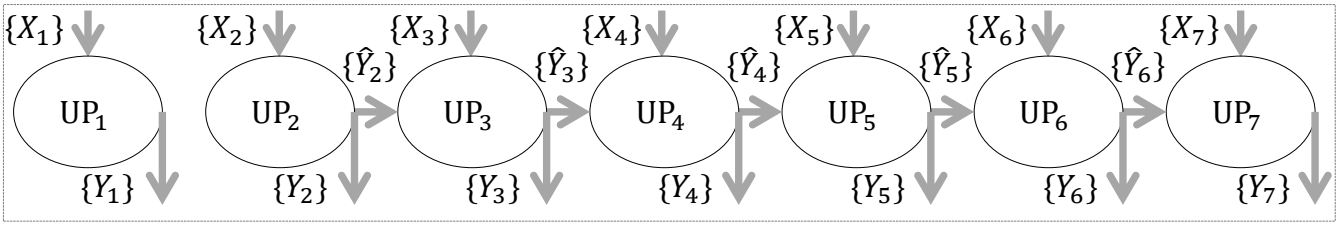

Figure 4.16 Exemplary elementary flows and intermediate flows in FRP manufacturing

In Fig. 4.16, UP_1 is considered as preparing, UP_2 is cutting, UP_3 is preforming, UP_4 is trimming, UP_5 is infusion, UP_6 is curing, and UP_7 is demolding. Linguistically, these terms are describing their main functions without neglecting the significance of other possibly included ones. The sequence of UPs for the FRP manufacturing in this model is addressing the requirement of studied RTM technique in the selected case study. Regardless its sequence, this generic list of UPs in Fig. 4.16 may be totally or partially applicable for a wide range of the techniques from Appx. A.

As it is discussed before, the preparing UP_1 is the only UP with all its outputs $u_{1\tau}$ unrelated directly to the final structure u_{7S}. Moreover, the final demolding UP_7 has no intermediate product as an outcome, while its main output is the demanded FRP structure u_{7S}, as Eq. 4.27 illustrates.

$$\hat{u}_{1P} = 0 \quad \text{and} \quad \hat{u}_{7P} = 0 \tag{4.27}$$

Hence, the unconnected activities or clusters of them within UP_1 may be distinguished by alphabetical order such as UP_{1A}, UP_{1B}, and so on. Practically, the core structural materials including fiber, matrix, and core materials are not processed as inputs in such physically independent preparing activities [264], although they may be handled in them. These core structural materials and other input as well as output types are discussed later in this chapter. As the final product of the sequentially last UP $i = m = 7$, the FRP structure u_{7S} is unconsidered as intermediate flow $\hat{u}_{i\tau}$, while no UP with the sequence of $i = m + 1$ exists within the assessment scope. As it is mentioned previously, not all intermediate flows are necessarily intermediate products. For

instance, reusable ancillaries are also outputs of a UP $i = x_1$ that can be applied as inputs in following UPs $i = x_2$ in which $x_2 > x_1$. Moreover, reusable ancillaries can be handled by a closed-loop recycling between the different UPs as well. However, these reusable ancillaries are excluded from the assessment and considered within the cut-of-criteria, as it is further discussed later in this chapter.

In practice, the transportation activities represent a critical subject to any discretization theory. Transportation of elementary flows α_j between the WSs may include significant activities with decisive impacts within the process, especially for spatially unconnected WSs [138]. However, in this thesis the spatial system boundary is assigned only to the WSs. Unless it is otherwise stated, WSs are assumed to be connected with negligible transportation efforts.

Generalized mathematical process matrix

In this thesis, a mathematical generalization approach is adopted. Theoretically, selected properties can be held for a wide range of elements to be logically clustered and mathematically modeled, although a verification is performed for a selected number of cases only [47]. Therefore, neither all possible production scenarios, nor the entire manufacturing techniques, nor every UP must be covered to validate the hypotheses of this work. For such validation, a selection of UPs from a manufacturing technique is to be sufficient. It is hypothesized in this thesis that production input and output elements can be modeled in a process matrix. Such matrix represents all associated properties of these elements. To have a goal oriented model, these properties are selected to be all parameters that serve the aimed time-dependent eco-efficiency assessment.

In order to have effective and efficient models, these parameters should be correlated with their unique elementary flows as well as characterization factors. In any production process, the elementary flows α_j are not distinguished only by their type j but also by their temporal and spatial allocations within the assessed UPs i. In this thesis, the assessment of all KRIs, which are the eco-efficiency, direct cost, and carbon footprint, requires only three main parameter groups, which are the elementary flows, characterization factors, and the constants of sales revenue excluding all non-process costs.

Not to be confused with the element properties, the process model has its mathematical characteristics known as the model properties. One of these model properties is the superposition, while a model fulfills that if its inputs and outputs are determinable. Moreover, the net output of multiple inputs should be equal to summing the outputs of these individual inputs. The second property is the model homogeneity, in which the scaling of an input is supposed to be reflected as an identical scaling to its output. According to Dorf and Bishop, a system that satisfies both superposition and homogeneity is a linear system [77]. In general, all matrices in this work are fulfilling these properties. In the mathematical modeling, all indexes in this work are real numbers $\mathbb{R}$.

In process assessment, an impact θ can be assessed on various CSF levels. For each elementary flow of type j in a UP i, its impact θ_{ij} can be calculated as the product of multiplying the magnitude of that elementary flow α_{ij} and its associated characterization factor λ_{ij}, as it is illustrated in Eq. 4.28.

$$\theta_{ij} = \alpha_{ij}\lambda_{ij} \tag{4.28}$$

In Eq. 4.28, the magnitude of each elementary flow α_{ij} has to be measured by a specific unit from the international system. On the other side, its characterization factor λ_{ij} should be expressed per that unit. Moreover, a characterization factor λ_j of any elementary flow type j can be provided as a given value or calculated as a function of several variables, as Eq. 5.30, Eq. 5.31, and Appx. B show.

In the mathematical assessment model within this thesis, the results of both input and output flows are assessed by the same impact units. To assess the impact θ of a selected KRI, a model with specified N number of unknowns can be used to transfer the schematic process diagram from Fig. 4.10 into a solvable mathematical model in Eq. 4.29.

$$a_1\lambda_1 + a_2\lambda_2 + \cdots + a_N\lambda_N = \theta_1 + \theta_2 + \cdots + \theta_N \tag{4.29}$$

Here, the magnitudes of process elementary flows from types j are represented by the variables α_j. In Eq. 4.29, the characterization factors λ_j should fulfill the defined boundaries for the assessed impact θ_j of each elementary flow type j in which $j = 1, \cdots, N$. To assess the impacts θ_j of the selected KRIs on any level of the process hierarchy, m number of linear equations can be modeled. In this thesis, these models represent the UPs and their associated N number of elementary flow types j. While the impacts θ_{ij} of the different types j of elementary flows α_{ij} in a single UP i are homogeneous and represented by an identical impact unit, the summation of them in that UP can be expressed based on Eq. 4.3 as θ_i, which is explained in Eq. 4.30.

$$\theta_i = \sum_{j=1}^{N} \theta_{ij} \tag{4.30}$$

For the entire process including its various UPs, Eq. 4.29 can be expanded in Eq. 4.31.

$$\begin{aligned} \alpha_{11}\lambda_{11} + \alpha_{12}\lambda_{12} + \cdots + \alpha_{1N}\lambda_{1N} &= \theta_1 \\ \alpha_{21}\lambda_{21} + \alpha_{22}\lambda_{22} + \cdots + \alpha_{2N}\lambda_{2N} &= \theta_2 \\ \vdots & \\ \alpha_{m1}\lambda_{m1} + \alpha_{m2}\lambda_{m2} + \cdots + \alpha_{mN}\lambda_{mN} &= \theta_m \end{aligned} \tag{4.31}$$

For m number of UPs i and N number of elementary flow types j, the total value θ of impacts θ_i for an assessed KRI can be computed based on Eq. 4.1 in Eq. 4.32.

$$\theta = \sum_{i=1}^{m} \theta_i \tag{4.32}$$

In Eq. 4.32, the impact value for the entire assessed process is a real number $\mathbb{R}$, while θ_i is the impact value in each UP i for $i = 1, \cdots, m$. The elementary flows α_{ij}, as unknown variables in Eq. 4.31, are then described based on Eq. 4.11 by the matrix $[A] = [\alpha_{ij}]$ with $(m \times N)$ in Eq. 4.33.

$$[A] = \begin{bmatrix} \alpha_{11} & \cdots & \alpha_{1N} \\ \vdots & \ddots & \vdots \\ \alpha_{m1} & \cdots & \alpha_{mN} \end{bmatrix} \tag{4.33}$$

Similar to that approach in Eq. 4.33, the characterization factors λ_{ij} of all assessed α_{ij} can be represented by the matrix $[\hat{\Lambda}] = [\lambda_{ij}]$ with $(N \times m)$, as Eq. 4.34 shows.

$$[\hat{\Lambda}] = \begin{bmatrix} \lambda_{11} & \cdots & \lambda_{1m} \\ \vdots & \ddots & \vdots \\ \lambda_{N1} & \cdots & \lambda_{Nm} \end{bmatrix} \tag{4.34}$$

Technically, a characterization factor λ_{ij} is describing the impact equivalent of a type j per its unit, regardless in which UP i this flow occurs. Therefore the equality of a characterization factor λ among the UPs in matrix $[\hat{\Lambda}] = [\lambda_{ij}]$ leads to the reduction of this matrix from Eq. 4.34 into the column vector $[\Lambda]$ with $(N \times 1)$ in Eq. 4.35.

$$[\Lambda] = \begin{bmatrix} \lambda_1 \\ \vdots \\ \lambda_N \end{bmatrix} \tag{4.35}$$

Similar to Eq. 4.35, the input elementary flows in the matrix $[X]$ have their specified characterization factors within the column vector $[\Lambda]^{[X]}$ with $(N_{in} \times 1)$ in Eq. 4.36.

$$[\Lambda]^{[X]} = \begin{bmatrix} \lambda_1 \\ \vdots \\ \lambda_{N_{in}} \end{bmatrix} \tag{4.36}$$

This approach is also applied to the impact of output elementary flows in the matrix $[Y]$ with $(N_{out} \times 1)$, as Eq. 4.37 shows.

$$[\Lambda]^{[Y]} = \begin{bmatrix} \lambda_1 \\ \vdots \\ \lambda_{N_{out}} \end{bmatrix} \tag{4.37}$$

Now, the value of impact θ for the entire assessed process can be calculated in Eq. 4.38.

$$[\theta] = [A][\Lambda] \tag{4.38}$$

In which, $[\theta] = [\theta_i]$ is considered for $i = 1, \ldots, m$. Here, Eq. 4.38 is applicable to assess the impact of input elementary flows in $[X]$ in Eq. 4.39.

$$[\theta^{[X]}] = [X][\Lambda^{[X]}] \tag{4.39}$$

This is also applicable to calculate the total outputs impact $[\theta^{[Y]}]$ in Eq. 4.40.

$$[\theta^{[Y]}] = [Y][\Lambda^{[Y]}] \tag{4.40}$$

In the next section, both input and output matrices, which are represented by $[X]$ and $[Y]$ in Eq. 4.39 and Eq. 4.40 respectively, are introduced. These previously introduced equations are essential for the assessment of impacts θ for both economic and ecological selected KRIs in this thesis, which are namely the direct cost δ and carbon footprint β. Based on these mathematical models for both impacts, the eco-efficiency assessment model is mathematically described later in this chapter.

Production process matrix

For the entire considered process, matrices of inputs $[X]$ and outputs $[Y]$ are combining all vectors of their elements from all UPs i based on Eq. 4.9. On the one hand, the input flows are represented by the matrix $[X] = [v_{i\rho}]$, that contains input vectors $\{X_i\} = [X]_i$ from all UPs in $i = 1, \cdots, m$. On the other hand, the output flows are represented by the matrix $[Y] = [u_{i\tau}]$, that contains output vectors $\{X_i\} = [X]_i$ from all UPs. These comprehensive matrices of $[X]$ and $[Y]$ are describing the entire manufacturing process in the aimed assessment,

as they are shown in Eq. 4.41.

$$[X] = \begin{bmatrix} v_{11} & \cdots & v_{1N_{in}} \\ \vdots & \ddots & \vdots \\ v_{m1} & \cdots & v_{mN_{in}} \end{bmatrix} \quad \text{and} \quad [Y] = \begin{bmatrix} u_{11} & \cdots & u_{1N_{out}} \\ \vdots & \ddots & \vdots \\ u_{m1} & \cdots & u_{mN_{out}} \end{bmatrix} \tag{4.41}$$

To build the DSSs in this thesis, mathematical models that include vectors and matrices for the inputs and outputs in each UP and the entire process are established. These vectors should have identical dimension of $(1 \times N)$ to make any addition or subtraction operations between them possible. To achieve that, a vector $\{A_i^{[X]}\}$ is representing all input flows $v_{i\rho}$ in that UP i. This input vector $\{A_i^{[X]}\}$ has a different dimension compared to the conventional input vector $\{X_i\}$. Similarly, the dimension of suggested output vector $\{A_i^{[Y]}\}$ is also nonidentical with the one in conventional $\{Y_i\}$. In this vector $\{A_i^{[X]}\}$, the dimensions of both input vector $\{X_i\}$ and output vector $\{Y_i\}$ are combined. Nonetheless, the values of all outputs $u_{i\tau}$ are substituted by „*zero*“ in $\{A_i^{[X]}\}$ to have an input representing vector, as Eq. 4.42 explains.

$$\{A_i^{[X]}\} = \{v_1, v_2, \cdots, v_{N_{in}}, u_1, u_2, \cdots, u_{N_{out}}\} = \{\alpha_{a_1}, \alpha_{a_2}, \cdots, \alpha_{a_{N_{in}}}, 0, 0, \cdots, 0\} \tag{4.42}$$

The same approach is then applied to establish a vector $\{A_i^{[Y]}\}$, that represents all output flows $u_{i\tau}$. Therefore, the values of all inputs $v_{i\rho}$ are substituted by the value of „*zero*“ in this case, as it is illustrated in Eq. 4.43.

$$\{A_i^{[Y]}\} = \{v_1, v_2, \cdots, v_{N_{in}}, u_1, u_2, \cdots, u_{N_{out}}\} = \{0, 0, \cdots, 0, \alpha_{b_1}, \alpha_{b_2}, \cdots, \alpha_{b_{N_{out}}}\} \tag{4.43}$$

In which, the elementary flows α_j are represented for the special cases of Eq. 4.42 and Eq. 4.43 as $\alpha_{a_\rho} = v_\rho$ and $\alpha_{b_\tau} = u_\tau$ respectively, before unifying the index of universal flow type $N = N_{in} + N_{out}$ for all elementary flows as $j = 1, \cdots, N$. Based on that, input and output matrices are modeled for the entire process as $[A^{[X]}]$ and $[A^{[Y]}]$ respectively. They cover all UPs i and have an identical dimension of $(m \times N)$. By combining $[A^{[X]}]$ with $[A^{[Y]}]$, all elementary flows α_{ij} are described by the matrix $[A] = [\alpha_{ij}]$ with $(m \times N)$. As Eq. 4.44 illustrates, both input matrix $[X]$ and output matrix $[Y]$ are combined in the elementary flow matrix $[A]$.

$$[A] = [A^{[X]}] + [A^{[Y]}] = [X, Y] = \begin{bmatrix} \alpha_{11} & \cdots & \alpha_{1N} \\ \vdots & \ddots & \vdots \\ \alpha_{m1} & \cdots & \alpha_{mN} \end{bmatrix} \tag{4.44}$$

In Eq. 4.44, every elementary flow α_{ij} is assigned to its UP $i = 1, \cdots, m$ and its type $j = 1, \cdots, N$. As a complex system, the production process can be also represented by an output-input matrix $[Z]$. This matrix $[Z]$ is described as the difference between the process output matrix $[A^{[Y]}]$ and the input one $[A^{[X]}]$ [85], as Eq. 4.45 shows.

$$[Z] = [A^{[Y]}] - [A^{[X]}] \tag{4.45}$$

The relation in Eq. 4.45 can be applied on the elementary flow level, as Eq. 4.46 suggests.

$$z_{ij} = u_{ij} - v_{ij} \tag{4.46}$$

In which, the element z_{ij} is the net output of an elementary flow in the process, that is covering both input and output flows from the same type j for all UPs i [85]. Based on that, $[Z] = [z_{ij}]$ can be expressed in Eq. 4.47.

$$[Z] = \begin{bmatrix} z_{11} & \cdots & z_{1N} \\ \vdots & \ddots & \vdots \\ z_{m1} & \cdots & z_{mN} \end{bmatrix} \tag{4.47}$$

Above all, z_{ij} may represent any type $j = 1, \cdots, N$ of input or output flows in any UP $i = 1, \cdots, m$. The relation between these elementary flows within these matrices of $[Z]$, $[A^{[X]}]$, and $[A^{[Y]}]$ can be described then as Eq. 4.48 suggests [85].

$$\begin{bmatrix} z_{11} & \cdots & z_{1N} \\ \vdots & \ddots & \vdots \\ z_{m1} & \cdots & z_{mN} \end{bmatrix} = \begin{bmatrix} 0 & \cdots & 0 & u_{11} & \cdots & u_{1N_{out}} \\ \vdots & \ddots & \vdots & \vdots & \ddots & \vdots \\ 0 & \cdots & 0 & u_{m1} & \cdots & u_{mN_{out}} \end{bmatrix} - \begin{bmatrix} v_{11} & \cdots & v_{1N_{in}} & 0 & \cdots & 0 \\ \vdots & \ddots & \vdots & \vdots & \ddots & \vdots \\ v_{m1} & \cdots & v_{mN_{in}} & 0 & \cdots & 0 \end{bmatrix} \tag{4.48}$$

Eq. 4.48 represents a comprehensive consideration of all relevant input flows in $[A^{[X]}]$ as well as output flows in $[A^{[Y]}]$. In general, this process model can be further detailed to cover lower abstraction levels. For instance, the process $[Z]$ can be split into discrete UPs represented by the vectors $\{Z_i\}$. Although each UP i can be broken down into a set of activities, the lowest considered discretization level is the UP in this thesis. Similar to the matrix $[A]$, the description of elementary flows in matrix $[Z]$ should cover all associated types of j. However, the process assessed in this thesis consists of several UPs. Therefore, the considered flows α_{ij} should represent all assessed UPs i. For these UPs, the representing process matrix $[Z]$ can be derived as $\{Z_i\}$. Based on Fig. 4.14, the relation can be illustrated in Fig. 4.17.

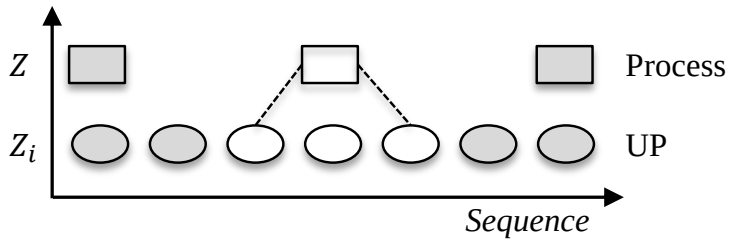

Figure 4.17 UPs within a process as a product system

Hence, a vector $\{Z_i\}$ for each single UP is expressed as Eq. 4.49 illustrates.

$$\{Z_i\} = \{A_i^{[Y]}\} - \{A_i^{[X]}\} \tag{4.49}$$

In this thesis, all possible types j of elementary flows $j > 0$ are considered in every UP model. The implemented elementary flows α_j are to have the value of $\alpha_j > 0$, whereas the inapplicable elementary flows α_j are still listed in the process representing vectors $\{X_i\}$ and $\{Y_i\}$. In spite of that, they are still substituted with the value of „*zero*“ as $\alpha_{ij} = 0$ in any UP i whenever they are irrelevant. This understanding of associated levels is used to identify all relevant elementary flows α_{ij} and the required characterization factors λ_j for assessing the studied FRP manufacturing technique in this section.

Elementary flows α_j in FRP manufacturing

The preliminary conceptual and mathematical models in Fig. 4.9 and Eq. 4.10 respectively state that the process consists of input and output elementary flows. Based on Fig. 3.21, input elementary flows in FRP manufacturing contain the categories of fiber, matrix, core, and ancillary materials, semi-finished products, equipment and facility energy, equipment and labor performances, and utilized facility. On the other hand, this process produces the FRP desired structure, semi-finished products, FRP, fiber wastes, core material wastes, and ancillary wastes, reusable ancillaries, and thermally emitted energy, as categories of its physical output elementary flows [13].

As it is suggested previously in this chapter, these categories are represented by dedicated subsets $\varphi^{[\Gamma]}$ here. Hence, each of these subset is considered as $[\Upsilon^{[\Gamma]}] \in \varphi^{[\Gamma]^{m\times n}}$ for $[\Upsilon^{[\Gamma]}] = [\alpha_{i\Gamma_l}]$. In that subset, the elementary flow type l in its subset type Γ has the following range of $\Gamma = 1,\ldots,p$ for all considered categories and the range of $l = 1,\ldots,n$ for these elementary flows in each category with a maximum p categories and a maximum n elementary flow types. Theoretically, all possible elementary flow types Γ_l in a category subset $\varphi^{[\Gamma]}$ are clustered to be measurable by a single unique unit. However, some exceptions are discussed later in this chapter. Here, the cardinality of each subset $\varphi^{[\Gamma]}$ is defined based on the various possible types and elements of elementary flows within that subset. The distinguishing of possible types Γ_l is also associated with the variety of eco-efficiency characterization factors λ_{Γ_l}. In other words, an elementary flow with a unique economic or ecological characterization factor should have a separated type Γ_l in its subset $\alpha_{\Gamma_l} \in \varphi^{[\Gamma]}$. For the entire elementary flow types Γ_l in a subset $\varphi^{[\Gamma]}$, the eco-efficiency characterization factors λ_{Γ_l} should be measured by a single unique unit if possible. Here, some exceptions are applied again, as it is discussed later in this chapter. The subsets definition can be based on the criteria listed later in Tab. 4.2 and Tab. 4.3.

In Fig. 4.18, a description of these categories for all UPs i in the FRP manufacturing process is illustrated based on Fig. 4.11. Some of the manufacturing techniques, that are covered by these generic categories, are discussed in Appx. A. Although not all categories are necessarily occurring in every UP i, in Fig. 4.18 all subsets $\varphi_i^{[\Gamma]}$ are considered in the exemplary UP i to provide a generic illustration.

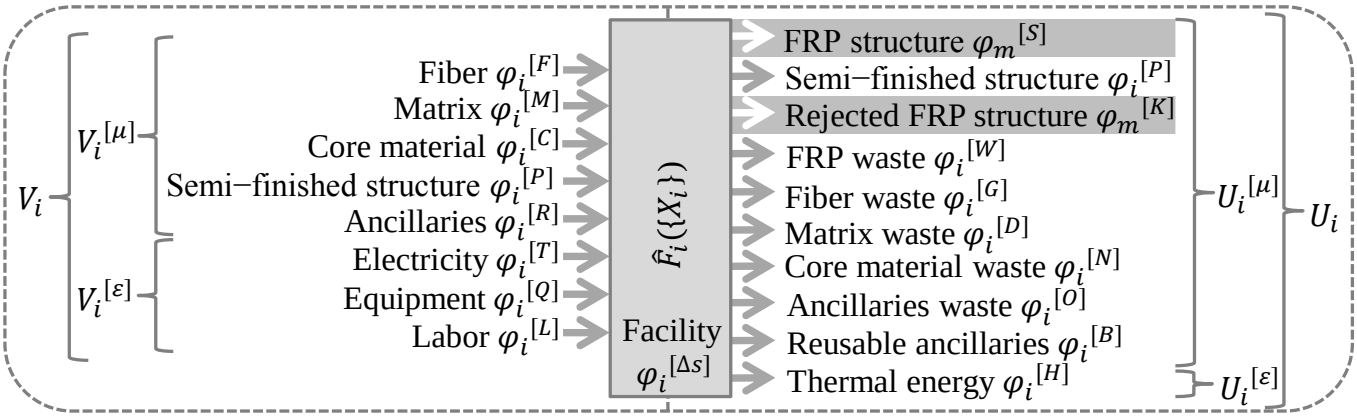

Figure 4.18 Categorization of elementary flows α_j in UPs of FRP manufacturing

For each demanded FRP structure $\varphi^{[S]}$ in Fig. 4.18, the categories of fiber $\varphi^{[F]}$, matrix $\varphi^{[M]}$, and core material $\varphi^{[C]}$ are its physical substances, which are also known as the core structural materials. These substances are physically converted into the various stages of semi-finished FRP structures $\varphi^{[P]}$. As it is shown in Fig. 4.18, the subset of semi-finished FRP structures $\varphi^{[P]}$ is the only one occurring on both input and output sides. It is essential to mention that both $\varphi^{[S]}$ and $\varphi^{[K]}$ are normally relevant only for the final UP_7 according to Fig. 4.16. Therefore, for each category type Γ in Fig. 4.18, a subset $\varphi^{[\Gamma]}$ is defined. In it, all category related elementary flows α_{Γ_l} are included. Initially, the subset $\varphi^{[\Gamma]}$ has a value of $\varphi^{[\Gamma]} = \emptyset$ prior to the identification of the first

element as included elementary flow type $j = \Gamma_1$. The elementary flows $\alpha_j = \alpha_{\Gamma_l}$ within each subset can be defined as Eq. 4.50 shows.

$$\alpha_{\Gamma_l} \in \varphi^{[\Gamma]} \quad \text{and} \quad \varphi^{[\Gamma]} = \{\alpha_{\Gamma_1}, \cdots, \alpha_{\Gamma_n}\} \tag{4.50}$$

In which, n is the maximum index of elementary flow types l in that category Γ. This cardinality n is diverse between the different subsets $\varphi^{[\Gamma]}$ due to the magnitude of possible types belonging to that category Γ, as it is explained later in Tab. 4.2 and Tab. 4.3. A maximum definable magnitude p of the different category types Γ is hypothesized for any assessed process. As Fig. 4.18 shows, in FRP manufacturing the magnitude of set types Γ is $p = 18$ including the semi-finished products once as well as the facility. Within a process, every category subset $\varphi^{[\Gamma]}$ of type Γ has elements Γ_l with a maximum index of Γ_n. Here, the subset elementary flow type l can be representing input or output types as $\Gamma_{l_{in}} = \Gamma_1, \ldots, \Gamma_{n_{in}}$ or $\Gamma_{l_{out}} = \Gamma_1, \ldots, \Gamma_{n_{out}}$ respectively.

Based on Fig. 4.18, the category types Γ in FRP manufacturing from both input and output sides are notated by their letters from Fig. 4.18 in Eq. 4.51.

$$\Gamma \in \{F, M, C, P, R, T, Q, L, \Delta s, S, K, W, G, D, N, O, B\} \tag{4.51}$$

In this thesis these capital letters of category types Γ are also used to describe the indexes of elementary flow type as a part of its specific category in the form of α_{Γ_l}. In this context, Γ and l notate the category and exact elementary flow type within it respectively. As it is mentioned previously, thermal energy $\Gamma = H$ is beyond the scope of this thesis. Therefore, the magnitude of generic subset types Γ is reduced to $p = 17$.

From these subsets $\varphi^{[\Gamma]}$, a vector for the elements of each subset can be derived in Eq. 4.52.

$$\{\Upsilon^{[\Gamma]}\} \in \varphi_i^{[\Gamma]^{1\times n}} \tag{4.52}$$

In which, $\{\Upsilon^{[\Gamma]}\}$ is the vector that includes all elementary flows α_{Γ_l} of the representative category subset $\varphi_i^{[\Gamma]}$, so that vector dimension n is equal to subset cardinality. Moreover, the highest possible dimension in the different assessed UPs i is adopted in this representative vector $\{\Upsilon^{[\Gamma]}\}$.

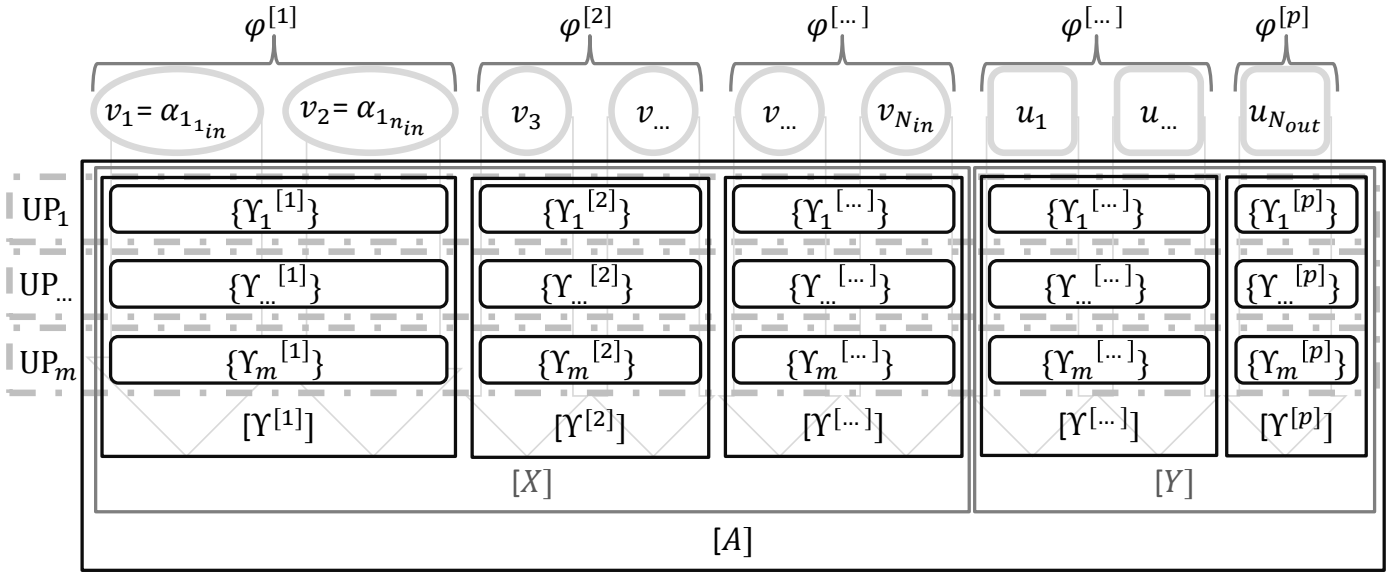

Figure 4.19 Process mathematical model elements in this thesis

For the elementary flows of every category in each UP, a representative vector is considered as $\{\Upsilon_i^{[\Gamma]}\} = \{\Upsilon^{[\Gamma]}\}$. These vectors $\{\Upsilon_i^{[\Gamma]}\}$ from all m included UPs are combined in a matrix $[\Upsilon^{[\Gamma]}]$, that represents the

elementary flows of that subset $\varphi^{[\Gamma]}$ throughout all UPs i in that process, as Eq. 4.53 explains.

$$[\Upsilon^{[\Gamma]}] \in \varphi^{[\Gamma]^{m\times n}} \tag{4.53}$$

For the generic subset types Γ, the correlations between subsets $\varphi_i^{[\Gamma]}$, $\varphi^{[\Gamma]}$, vectors $\{\Upsilon_i^{[\Gamma]}\}$, matrices $[\Upsilon^{[\Gamma]}]$, and their elementary flows $\alpha_{\Gamma_l} \in \varphi^{[\Gamma]}$ throughout process UPs i are illustrated in Fig. 4.19. While the generic model in Fig. 4.10 is dedicated to describe the elementary flows, Fig. 4.19 is visualizing a generic conceptual model for their subsets and the derived vectors.

To have better understanding of them, the criteria of clustering and defining these various subsets $\varphi^{[\Gamma]}$ are explained in Tab. 4.2 and Tab. 4.3 for the input and output categories respectively. Except the excluded thermal energy output, all the categories from Fig. 4.18 are described and distinguished within Tab. 4.2 and Tab. 4.3 for the input subsets $\varphi^{[\Gamma]} \subseteq V$ and output ones $\varphi^{[\Gamma]} \subseteq U$ respectively for the entire FRPs manufacturing process.

Table 4.2 Subsets of input flows in FRPs manufacturing $\varphi^{[\Gamma]} \subseteq V$

Category	Vector	Definition	$\Gamma_{l_{in}}$ criteria of	Affiliation
Fiber	$\{\Upsilon_i^{[F]}\} \in \varphi_i^{[F]^{1\times n}}$	It includes all possible fiber material types and elements as input elementary flows $v_{i\rho} = v_{i,F_{l_{in}}}$, that are or might be used in FRP manufacturing. Here, prepreg is considered as fiber although it technically includes matrix as well.	Substances; Specifications; Orientations; Suppliers	$\varphi^{[F]} \subseteq V^{[\mu]}$ $\varphi^{[F]} \subseteq V$ $\varphi_i^{[F]} = \{v_{i,F_1}, \cdots, v_{i,F_{n_{in}}}\}$
Matrix	$\{\Upsilon_i^{[M]}\} \in \varphi_i^{[M]^{1\times n}}$	It includes all possible matrix material types and elements as input elementary flows $v_{i\rho} = v_{i,M_{l_{in}}}$, that are or might be used in FRP manufacturing. Its elements include all hardener, accelerators, and any other related chemical substances.	Substances; Specifications; Mixtures; Suppliers	$\varphi^{[M]} \subseteq V^{[\mu]}$ $\varphi^{[M]} \subseteq V$ $\varphi_i^{[M]} = \{v_{i,M_1}, \cdots, v_{i,M_{n_{in}}}\}$
Core material	$\{\Upsilon_i^{[C]}\} \in \varphi_i^{[C]^{1\times n}}$	It includes all possible core material types and elements as input elementary flows $v_{i\rho} = v_{i,C_{l_{in}}}$, that are or might be used in FRP manufacturing. Here, any material other than the matrix or fiber, that is integrated in the structure during manufacturing, is considered as core material. Hybrid, wood, and honeycomb structures for instance are included.	Substances; Specifications; Orientations; Suppliers	$\varphi^{[C]} \subseteq V^{[\mu]}$ $\varphi^{[C]} \subseteq V$ $\varphi_i^{[C]} = \{v_{i,C_1}, \cdots, v_{i,C_{n_{in}}}\}$
Semi-finished structure	$\{\Upsilon_i^{[P]}\} \in \varphi_i^{[P]^{1\times n}}$	It includes all possibly produced semi-finished structure types and elements as input elementary flow, that are generated by the UP x_1 within FRP manufacturing and received in a following UP x_2 as input, while $x_2 > x_1$.	Specifications; UPs	$\varphi^{[P]} \subseteq V^{[\mu]}$ $\varphi^{[P]} \subseteq V$ $\varphi_i^{[P]} = \{v_{i,P_1}, \cdots, v_{i,P_{n_{in}}}\}$

Category	$\{\Upsilon_i^{[\Gamma]}\} \in \varphi_i^{[\Gamma]^{1\times n}}$	Definition	Criteria of type Γ_l	Affiliation
Ancillaries	$\{\Upsilon_i^{[R]}\} \in \varphi_i^{[R]^{1\times n}}$	It includes all possible ancillary material types and elements as input elementary flows $v_{i\rho} = v_{i,R_{l_{in}}}$, that are or might be used in FRP manufacturing. This category includes elements that have various measurement units. Moreover, the ancillary input $\varphi^{[R]}$ from each type has the summed magnitude of its wasted as well as reusable materials, that are represented by $\varphi^{[O]}$ and $\varphi^{[B]}$ respectively in Tab. 4.3.	Substances; Specifications; Suppliers	$\varphi^{[R]} \subseteq V^{[\mu]}$ $\varphi^{[R]} \subseteq V$ $\varphi_i^{[R]} = \{v_{i,R_1}, \cdots, v_{i,R_{n_{in}}}\}$
Electricity	$\{\Upsilon_i^{[T]}\} \in \varphi_i^{[T]^{1\times n}}$	It includes an implemented electricity as input elementary flow $v_{i\rho} = v_{i,T_{l_{in}}}$, that is or might be used in the FRP manufacturing. It is used as a process energy to operate the equipment and facility [151].	Suppliers; Affiliation	$\varphi^{[T]} \subseteq V^{[\epsilon]}$ $\varphi^{[T]} \subseteq V$ $\varphi_i^{[T]} = \{v_{i,T_1}, \cdots, v_{i,T_{n_{in}}}\}$
Equipment	$\{\Upsilon_i^{[Q]}\} \in \varphi_i^{[Q]^{1\times n}}$	It includes all possible equipment types and elements as input elementary flows $v_{i\rho} = v_{i,Q_{l_{in}}}$, that are or might be used in FRP manufacturing. The equipment can either be operated by electricity or labor mechanical energy. Under this subset all molds, tools, and machines are considered.	Functionalities; Capacities; Suppliers	$\varphi^{[Q]} \subseteq V^{[\epsilon]}$ $\varphi^{[Q]} \subseteq V$ $\varphi_i^{[Q]} = \{v_{i,Q_1}, \cdots, v_{i,Q_{n_{in}}}\}$
Labor	$\{\Upsilon_i^{[L]}\} \in \varphi_i^{[L]^{1\times n}}$	It includes workforce labors and their ranks as input elementary flows $v_{i\rho} = v_{i,L_{l_{in}}}$, that are or might be used in the FRP manufacturing.	Ranking	$\varphi^{[L]} \subseteq V^{[\epsilon]}$ $\varphi^{[L]} \subseteq V$ $\varphi_i^{[L]} = \{v_{i,L_1}, \cdots, v_{i,L_{n_{in}}}\}$
Facility	$\{\Upsilon_i^{[\Delta s]}\} \in \varphi_i^{[\Delta s]^{1\times n}}$	It includes every implemented space for specifiable durations. Facility is studied here as an energy conversion control volume. Therefore, it may be considered figuratively as an energy.	Location; Temporal allocation; Services	$\varphi^{[\Delta s]} \subseteq V^{[\epsilon]}$ $\varphi^{[\Delta s]} \subseteq V$ $\varphi_i^{[\Delta s]} = \{v_{i,\Delta s_1}, \cdots, v_{i,\Delta s_{n_{in}}}\}$

In Tab. 4.2, an explanation of input element types $\Gamma_{l_{in}}$ in each input subset $\varphi^{[\Gamma]} \subseteq V$ and this subset affiliations with the predefined generic supersets and sets is provided. Each subset $\varphi^{[\Gamma]} \subseteq V$ is obviously affiliated with the input supersets V as well as the material or the energy input sets, which are represented by $V^{[\mu]}$ and $V^{[\epsilon]}$ respectively. Tab. 4.2 is describing the possible applied input elementary flows $v_{\Gamma_{l_{in}}}$, that have been concluded from briefly studying the FRP manufacturing techniques in Appx. A. Again, each subset has its own value for maximum index of elementary flow types n based on the covered flow types l by it. However, the implementation of these input elementary flows v_ρ may vary between the different manufacturing techniques and manufactured structures. For instance, core materials from $\varphi^{[C]}$ are not implemented in every FRP structure.

Furthermore, a matrix input from $\varphi^{[M]}$ is usually not used for the techniques where the prepreg materials are applied. Although it contains both matrix and fiber, prepreg is considered as fiber within $\varphi^{[F]}$ in Tab. 4.2. These input subsets $\varphi^{[\Gamma]} \subseteq V$ from Tab. 4.2 are united in Eq. 4.54 to form the superset of input elementary flows V.

$$\varphi^{[F]} \cup \varphi^{[M]} \cup \varphi^{[C]} \cup \varphi^{[P]} \cup \varphi^{[R]} \cup \varphi^{[T]} \cup \varphi^{[Q]} \cup \varphi^{[L]} \cup \varphi^{[\Delta s]} = V \tag{4.54}$$

Similar to Tab. 4.2, all relevant output flows $u_{\Gamma_{l_{out}}}$ are categorized within the subsets $\varphi^{[\Gamma]} \subseteq U$ in Tab. 4.3.

Table 4.3 Subsets of output flows in FRPs manufacturing $\varphi^{[\Gamma]} \subseteq U$

Category	Vector	Definition	$\Gamma_{l_{out}}$ criteria	Affiliation
FRP structure	$\{\Upsilon_i^{[S]}\} \in \varphi_i^{[S]^{1\times n}}$	In this thesis, FRP product is represented by a single desired structure $\{\Upsilon_m^{[S]}\} = u_{mS}$, that matches predefined quality requirements as functional unit, while it appears at UP_m.	Specifications; UP $i = m$; Predefinition	$\varphi^{[S]} \subseteq U^{[\mu]}$ $\varphi^{[S]} \subseteq U$ $\varphi_i^{[S]} = \{u_{i,S_1}, \cdots, u_{i,S_{n_{out}}}\}$
Semi-finished structure	$\{\Upsilon_i^{[P]}\} \in \varphi_i^{[P]^{1\times n}}$	It includes all possibly produced semi-finished structure types and elements as output elementary flows, that might be generated by the UPs within FRP manufacturing. Here, only the desired semi-finished structures are recognized as intermediate products.	Specifications; UPs $i \neq m$; Predefinition	$\varphi^{[P]} \subseteq U^{[\mu]}$ $\varphi^{[P]} \subseteq U$ $\varphi_i^{[P]} = \{u_{i,P_1}, \cdots, u_{i,P_{n_{out}}}\}$
Rejected FRP structure	$\{\Upsilon_i^{[K]}\} \in \varphi_i^{[K]^{1\times n}}$	It includes all possibly produced defect structures, that cannot match the predefined quality requirements as output elementary flow $u_{i\tau} = u_{mK}$.	Specifications; Predefinition	$\varphi^{[K]} \subseteq U^{[\mu]}$ $\varphi^{[K]} \subseteq U$ $\varphi_i^{[K]} = \{u_{i,K_1}, \cdots, u_{i,K_{n_{out}}}\}$
FRP waste	$\{\Upsilon_i^{[W]}\} \in \varphi_i^{[W]^{1\times n}}$	It includes all possibly wasted pieces and fragments from finished FRP as output elementary flow. An example of that is the waste due to machining.	Specifications; Predefinition	$\varphi^{[W]} \subseteq U^{[\mu]}$ $\varphi^{[W]} \subseteq U$ $\varphi_i^{[W]} = \{u_{i,W_1}, \cdots, u_{i,W_{n_{out}}}\}$
Fiber waste	$\{\Upsilon_i^{[G]}\} \in \varphi_i^{[G]^{1\times n}}$	It includes all possibly wasted fiber material types and elements as output elementary flows $u_{F_{l_{out}}}$ The types and elements of fiber input materials are repeated here, while wastes are associated naturally with their inputs.	Specifications; Substances; Orientations; Suppliers; Stages	$\varphi^{[G]} \subseteq U^{[\mu]}$ $\varphi^{[G]} \subseteq U$ $\varphi_i^{[G]} = \{u_{i,G_1}, \cdots, u_{i,G_{n_{out}}}\}$
Matrix waste	$\{\Upsilon_i^{[D]}\} \in \varphi_i^{[D]^{1\times n}}$	It includes all possibly wasted matrix material types and elements as output elementary flow, that are naturally associated with the matrix input materials.	Specifications; Substances; Mixtures; Suppliers; Stages	$\varphi^{[D]} \subseteq U^{[\mu]}$ $\varphi^{[D]} \subseteq U$ $\varphi_i^{[D]} = \{u_{i,D_1}, \cdots, u_{i,D_{n_{out}}}\}$

Category	$\{\Upsilon_i^{[\Gamma]}\} \in \varphi^{[\Gamma]^{1\times n}}$	Definition	Criteria of type Γ_l	Affiliation
Core material waste	$\{\Upsilon_i^{[N]}\} \in \varphi_i^{[N]^{1\times n}}$	It includes all possibly wasted core material types and elements as output elementary flow. The types and elements of core core input materials are relevant here as well.	Specifications; Substances; Orientations; Suppliers; Stages	$\varphi^{[N]} \subseteq U^{[\mu]}$ $\varphi^{[N]} \subseteq U$ $\varphi_i^{[N]} = \{u_{i,N_1}, \cdots, u_{i,N_{n_{out}}}\}$
Ancillaries waste	$\{\Upsilon_i^{[O]}\} \in \varphi_i^{[O]^{1\times n}}$	It is a set that includes all possibly wasted ancillary types and elements as output elementary flows. The types and elements of ancillaries input materials are associated with this output subset as well.	Substances; Specifications; Suppliers; Stages	$\varphi^{[O]} \subseteq U^{[\mu]}$ $\varphi^{[O]} \subseteq U$ $\varphi_i^{[O]} = \{u_{i,O_1}, \cdots, u_{i,O_{n_{out}}}\}$
Reusable ancillaries	$\{\Upsilon_i^{[B]}\} \in \varphi_i^{[B]^{1\times n}}$	It includes all possibly reusable ancillary types and elements as output elementary flows. The types and elements of ancillaries input materials are repeated here as well.	Specifications; Substances; Suppliers	$\varphi^{[B]} \subseteq U^{[\mu]}$ $\varphi^{[B]} \subseteq U$ $\varphi_i^{[B]} = \{u_{i,B_1}, \cdots, u_{i,B_{n_{out}}}\}$

These output subsets $\varphi^{[\Gamma]} \subseteq U$ are united in Eq. 4.55 to form the elementary flows output superset U.

$$\varphi^{[S]} \cup \varphi^{[P]} \cup \varphi^{[K]} \cup \varphi^{[W]} \cup \varphi^{[G]} \cup \varphi^{[D]} \cup \varphi^{[N]} \cup \varphi^{[O]} \cup \varphi^{[B]} = U \tag{4.55}$$

Now, Tab. 4.2 and Tab. 4.3 provide comprehensive representations of possible input elementary flows v_ρ and output ones u_τ in selected techniques for the FRP structure manufacturing.

In each subset $\varphi^{[\Gamma]}$, its elementary flow types Γ_l are defined based on a set of associated criteria. As they are shown in Tab. 4.2 and Tab. 4.3, these criteria include several aspects such as substances, specifications, orientations, suppliers, stages, UPs, mixtures, functionalities, capacities, and ranking. System boundary definition plays here a decisive role in determining the included elementary flows α_j and the cut-off-criteria. The system boundary implies the definition of assessed KRIs and the associated elementary flows α_j based on that. In this thesis, every output FRP structure u_{mS} is assumed to be a reference flow that fulfills the requirements of ideal produced functional unit, while no rejected FRP structure occurs $u_{mK} = 0$. As it is mentioned previously, all possible elementary flow types Γ_l in each category $\varphi^{[\Gamma]}$ are measured by a single unique unit. Nonetheless, ancillary associated categories have exceptions to this rule. According to the system boundary definition, all elementary flows α_j occur within temporal and spatial dimensions.

As it is explained later, all relevant parameters about any initial or added elementary flow must be also considered in the implemented DBs. In this thesis, these relevant parameters include the initial data required for the real-time data collection, which are included in the SWS-DB. After defining the elementary flows and cluster them generically to their subsets, it is required to have similar clear generic definition of their characterization factors to enable the realization of the assessment mathematical and computerized models.

Characterization factors λ_j in manufacturing FRP structures

In this thesis, the generic scope of both input and output flows is defined in Tab. 4.2 and Tab. 4.3. In Tab. 4.4, the characterization factors for the input categories from Tab. 4.2 are listed. These input subsets $\varphi^{[\Gamma]} \subseteq V$ are associated briefly with their eco-efficiency characterization factors λ_ρ in Tab. 4.4.

Table 4.4 Input subsets $\varphi^{[\Gamma]} \subseteq V$ and their eco-efficiency characterization factors λ_ρ in FRPs manufacturing

Input subsets $\varphi^{[\Gamma]} \subseteq V$	Economic characterization factor γ_ρ in monetary unit (€)	Ecological characterization factor ε_ρ in physical unit (kg CO_2)
Fiber $\varphi^{[F]}$	Material price in (€/kg)	Material equivalent in (kg CO_2/kg)
Matrix $\varphi^{[M]}$	Material price in (€/kg)	Material equivalent in (kg CO_2/kg)
Core material $\varphi^{[C]}$	Material price in (€/kg)	Material equivalent in (kg CO_2/kg)
Ancillaries $\varphi^{[R]}$	Material price in (€/m^2), (€/kg), (€/liter), (€/piece)	Material equivalent in (kg CO_2/m^2), (kg CO_2/kg), (kg CO_2/liter), (kg CO_2/piece)
Electricity $\varphi^{[T]}$	Electricity price in (€/kWh)	Electricity equivalent in (kg CO_2/kWh)
Equipment $\varphi^{[Q]}$	Equipment expenses in (€/s)	Equipment burden in (kg CO_2/s)
Labor $\varphi^{[L]}$	Labor direct expenses in (€/s)	Labor direct burden in (kg CO_2/s)
Facility occupation $\varphi^{[\Delta s]}$	Facility expenses in (€/s × m^2)	Facility burden in (kg CO_2/s × m^2)

As it is discussed previously in Fig. 4.7, it is essential to define the considered life-cycle by every implemented characterization factor. In Tab. 4.4, all characterization factors are representing their cradle-to-grave equivalents. As it is shown in Tab. 4.4, it is hypothesized in this thesis that the labor working time, the facility occupation, and the equipment operation have ecological impacts. Further details about these characterization factors in Tab. 4.4 are provided in Appx. B. Similar to Tab. 4.4, the characterization factors λ_τ for the output subsets $\varphi^{[\Gamma]} \subseteq U$ are defined in Tab. 4.5.

Table 4.5 Output subsets $\varphi^{[\Gamma]} \subseteq U$ and their eco-efficiency characterization factors λ_τ in FRPs manufacturing

Output subsets $\varphi^{[\Gamma]} \subseteq U$	Economic characterization factor γ_τ in monetary unit (€)	Ecological characterization factor ε_τ in physical unit (kg CO_2)
Desired structure $\varphi^{[S]}$	Structure cost in (€/piece)	Structure impact in (kg CO_2/piece)
Rejected structure $\varphi^{[K]}$	Structure cost in (€/piece)	Structure impact in (kg CO_2/piece)
FRP fragment waste $\varphi^{[W]}$	Waste disposal in (€/kg)	Waste disposal (kg CO_2/kg)
Fiber waste $\varphi^{[G]}$	Waste disposal in (€/kg)	Waste disposal (kg CO_2/kg)
Matrix waste $\varphi^{[D]}$	Waste disposal in (€/kg)	Waste disposal (kg CO_2/kg)
Core material waste $\varphi^{[N]}$	Waste disposal in (€/kg)	Waste disposal (kg CO_2/kg)
Ancillaries waste $\varphi^{[O]}$	Waste disposal in (€/m^2), (€/kg), (€/liter), (€/piece)	Waste disposal (kg CO_2/m^2), (kg CO_2/kg), (kg CO_2/liter), (kg CO_2/piece)
Reusable ancillaries $\varphi^{[B]}$	Retrieved cost (€/m^2), (€/kg), (€/liter), (€/piece)	Redeemed impact in (kg CO_2/m^2), (kg CO_2/kg), (kg CO_2/liter), (kg CO_2/piece)

Unlike Tab. 4.4, fulfilling the hypothesis from Fig. 4.7 requires an interpretation in Tab. 4.5. The FRP structure impact from its cradle-to-gate life-cycle is equal to the impact of the entire assessed process in this work, while its gate-to-grave impact is beyond the scope of this thesis. Theoretically, the rejected structure can be treated like the desired one in this case. However, this work considers an ideal process with no rejected structures. As it is explained later, the semi-finished products have equal impacts on both sides of the process, whereas their impacts are negligible. While the categorization factors for initial materials of fiber, matrix, core substances, and ancillaries in Tab. 4.4 include their cradle-to-grave equivalents, their wastes in Tab. 4.5 have only their own particular gate-to-grave impacts. This is also the case of the FRP fragments waste, while it consists of core structural materials. These gate-to-grave impacts for material wastes are associated with the wastes themselves, while they are represented mainly by their disposal. In this work, no re-usability scenarios for any elementary flow are discussed. As it is explained later, the reusable ancillaries are excluded from the assessment by considering them as initial unused materials in the early LCI. For every considered elementary flow in the parametrization case study, the impact equivalents are aggregated carefully in Appx. B to avoid the unwanted redundant or neglected impacts.

In Tab. 4.4 and Tab. 4.5, the eco-efficiency characterization factors λ_j are represented in specific units. It is hypothesized here that the determination of the possible elementary flow types l as cardinality of each subset $\varphi^{[\Gamma]}$ is influenced by the the number of various considered eco-efficiency characterization factors λ_l in that category subset. Therefore, any elementary flow α_j with a unique economic or ecological characterization factor value is representing a particular elementary flow type j. For instance, fiber types with various prices are considered as unique elementary flows, although they may have identical carbon footprint equivalent. Still, multi elementary flows may be defined for a single characterization factor. For example, the electricity flows are distinguished for the different involved equipment or facility types, although the electricity itself has identical values for their economic and ecological characterization factors.

Now, the value of an eco-efficiency characterization factor λ_j depends on various parameters, which might be considered as initial data $\hat{\lambda}_j$ for it. As they are discussed previously in Fig. 4.8, the impact classes, that include the direct impact categories of fixed recurring, variable recurring, or fixed nonrecurring, are applied to calculate or assume the characterization factors of each elementary flow type j. Nonetheless, these characterization factors λ_j are considered as given constants in this thesis, as they are shown for the parameterizing case study later in chapter 5 within Eq. 5.30 as well as Eq. 5.31. Therefore, the calculation equations of these characterization factors λ_j are considered to be beyond the scope of the work. Nonetheless, the equations and assumptions of calculating these economic and ecological characterization factors λ_j, which are represented by γ_j and ε_j respectively, are still provided in Appx. B.

In conclusion, the column vector of all economic characterization factors γ_j and the one of all ecological ones ε_j are distinguished based on the previously discussed Eq. 4.37. On the one hand, the column vector, that includes all input economic characterization factors γ_j, is defined as $[\check{\Lambda}^{[X]}]$ in Eq. 4.56.

$$[\check{\Lambda}^{[X]}] = \begin{bmatrix} \gamma_1 \\ \vdots \\ \gamma_{N_{in}} \end{bmatrix} \tag{4.56}$$

On the other hand, the column vector of all input ecological factors ε_j is defined as $[\check{\check{\Lambda}}^{[X]}]$ in Eq. 4.57.

$$[\check{\check{\Lambda}}^{[X]}] = \begin{bmatrix} \varepsilon_1 \\ \vdots \\ \varepsilon_{N_{in}} \end{bmatrix} \tag{4.57}$$

Similar to Eq. 4.56 and Eq. 4.57, the vectors of output characterization factors $[\check{\Lambda}^{[Y]}]$ and $[\check{\check{\Lambda}}^{[Y]}]$, as well as the combination of both inputs and outputs in $[\check{\Lambda}^{[A]}]$ and $[\check{\check{\Lambda}}^{[A]}]$ can be derived if required. For the LCIA computerized model, the initial data of characterization factors are covered by the EEAM-DB, as it is explained later in this chapter. While both elementary flows and their characterization factors are clearly modeled, the mathematical assessment model can be derived.

Assessment matrix

Based on the categories definition in Tab. 4.2 and Tab. 4.3 and the UPs discretization in Fig. 4.16, the generic input representing matrix $[A^{[X]}]$ for FRPs manufacturing can be described in Eq. 4.58.

$$[A^{[X]}] = \begin{bmatrix} \{\Upsilon_1^{[F]}\}\{\Upsilon_1^{[M]}\}\{\Upsilon_1^{[C]}\} & 0 & \{\Upsilon_1^{[R]}\}\{\Upsilon_1^{[T]}\}\{\Upsilon_1^{[Q]}\}\{\Upsilon_1^{[L]}\}\{\Upsilon_1^{[\Delta s]}\} & 0 & 0 & 0 & 0 & 0 & 0 & 0 & 0 \\ \{\Upsilon_2^{[F]}\}\{\Upsilon_2^{[M]}\}\{\Upsilon_2^{[C]}\} & 0 & \{\Upsilon_2^{[R]}\}\{\Upsilon_2^{[T]}\}\{\Upsilon_2^{[Q]}\}\{\Upsilon_2^{[L]}\}\{\Upsilon_2^{[\Delta s]}\} & 0 & 0 & 0 & 0 & 0 & 0 & 0 & 0 \\ \{\Upsilon_3^{[F]}\}\{\Upsilon_3^{[M]}\}\{\Upsilon_3^{[C]}\}\{\Upsilon_3^{[P]}\}\{\Upsilon_3^{[R]}\}\{\Upsilon_3^{[T]}\}\{\Upsilon_3^{[Q]}\}\{\Upsilon_3^{[L]}\}\{\Upsilon_3^{[\Delta s]}\} & 0 & 0 & 0 & 0 & 0 & 0 & 0 & 0 & 0 \\ \{\Upsilon_4^{[F]}\}\{\Upsilon_4^{[M]}\}\{\Upsilon_4^{[C]}\}\{\Upsilon_4^{[P]}\}\{\Upsilon_4^{[R]}\}\{\Upsilon_4^{[T]}\}\{\Upsilon_4^{[Q]}\}\{\Upsilon_4^{[L]}\}\{\Upsilon_4^{[\Delta s]}\} & 0 & 0 & 0 & 0 & 0 & 0 & 0 & 0 & 0 \\ \{\Upsilon_5^{[F]}\}\{\Upsilon_5^{[M]}\}\{\Upsilon_5^{[C]}\}\{\Upsilon_5^{[P]}\}\{\Upsilon_5^{[R]}\}\{\Upsilon_5^{[T]}\}\{\Upsilon_5^{[Q]}\}\{\Upsilon_5^{[L]}\}\{\Upsilon_5^{[\Delta s]}\} & 0 & 0 & 0 & 0 & 0 & 0 & 0 & 0 & 0 \\ \{\Upsilon_6^{[F]}\}\{\Upsilon_6^{[M]}\}\{\Upsilon_6^{[C]}\}\{\Upsilon_6^{[P]}\}\{\Upsilon_6^{[R]}\}\{\Upsilon_6^{[T]}\}\{\Upsilon_6^{[Q]}\}\{\Upsilon_6^{[L]}\}\{\Upsilon_6^{[\Delta s]}\} & 0 & 0 & 0 & 0 & 0 & 0 & 0 & 0 & 0 \\ \{\Upsilon_7^{[F]}\}\{\Upsilon_7^{[M]}\}\{\Upsilon_7^{[C]}\}\{\Upsilon_7^{[P]}\}\{\Upsilon_7^{[R]}\}\{\Upsilon_7^{[T]}\}\{\Upsilon_7^{[Q]}\}\{\Upsilon_7^{[L]}\}\{\Upsilon_7^{[\Delta s]}\} & 0 & 0 & 0 & 0 & 0 & 0 & 0 & 0 & 0 \end{bmatrix} \tag{4.58}$$

Although several restrictions may be applied to the generic input matrix $[A^{[X]}]$, they are neglected in Eq. 4.58 to keep this generic matrix applicable for other relevant techniques and scenarios. Still, only one restriction regarding the semi-finished structures is considered in Eq. 4.58. As it is illustrated previously in Fig. 4.16, no semi-finished structure occurs as an input for neither the preparing UP_1 nor the cutting UP_2. Considering the fiber, its inputs may be considered solely in the cutting UP_2, while the matrix inputs enter the product system only through the infusion UP_5. However, these two examples of possible restrictions and many others are not applied to Eq. 4.58. Similar to Eq. 4.58, the generic output matrix $[A^{[Y]}]$ can be described in Eq. 4.59.

$$[A^{[Y]}] = \begin{bmatrix} 0 & 0 & 0 & 0 & 0 & 0 & 0 & 0 & 0 & 0 & 0 & 0 & \{\Upsilon_1^{[W]}\}\{\Upsilon_1^{[G]}\}\{\Upsilon_1^{[D]}\}\{\Upsilon_1^{[N]}\}\{\Upsilon_1^{[O]}\}\{\Upsilon_1^{[B]}\} \\ 0 & 0 & 0 & 0 & 0 & 0 & 0 & 0 & 0 & 0 & \{\Upsilon_2^{[P]}\} & 0 & \{\Upsilon_2^{[W]}\}\{\Upsilon_2^{[G]}\}\{\Upsilon_2^{[D]}\}\{\Upsilon_2^{[N]}\}\{\Upsilon_2^{[O]}\}\{\Upsilon_2^{[B]}\} \\ 0 & 0 & 0 & 0 & 0 & 0 & 0 & 0 & 0 & 0 & \{\Upsilon_3^{[P]}\} & 0 & \{\Upsilon_3^{[W]}\}\{\Upsilon_3^{[G]}\}\{\Upsilon_3^{[D]}\}\{\Upsilon_3^{[N]}\}\{\Upsilon_3^{[O]}\}\{\Upsilon_3^{[B]}\} \\ 0 & 0 & 0 & 0 & 0 & 0 & 0 & 0 & 0 & 0 & \{\Upsilon_4^{[P]}\} & 0 & \{\Upsilon_4^{[W]}\}\{\Upsilon_4^{[G]}\}\{\Upsilon_4^{[D]}\}\{\Upsilon_4^{[N]}\}\{\Upsilon_4^{[O]}\}\{\Upsilon_4^{[B]}\} \\ 0 & 0 & 0 & 0 & 0 & 0 & 0 & 0 & 0 & 0 & \{\Upsilon_5^{[P]}\} & 0 & \{\Upsilon_5^{[W]}\}\{\Upsilon_5^{[G]}\}\{\Upsilon_5^{[D]}\}\{\Upsilon_5^{[N]}\}\{\Upsilon_5^{[O]}\}\{\Upsilon_5^{[B]}\} \\ 0 & 0 & 0 & 0 & 0 & 0 & 0 & 0 & 0 & 0 & \{\Upsilon_6^{[P]}\} & 0 & \{\Upsilon_6^{[W]}\}\{\Upsilon_6^{[G]}\}\{\Upsilon_6^{[D]}\}\{\Upsilon_6^{[N]}\}\{\Upsilon_6^{[O]}\}\{\Upsilon_6^{[B]}\} \\ 0 & 0 & 0 & 0 & 0 & 0 & 0 & 0 & 0 & \{\Upsilon_7^{[S]}\} & 0 & 0 & \{\Upsilon_7^{[W]}\}\{\Upsilon_7^{[G]}\}\{\Upsilon_7^{[D]}\}\{\Upsilon_7^{[N]}\}\{\Upsilon_7^{[O]}\}\{\Upsilon_7^{[B]}\} \end{bmatrix} \tag{4.59}$$

In Eq. 4.59, only three main restrictions are applied to the generic output representing matrix $[A^{[Y]}]$. First, no FRP structures may occur before the last UP_i for $i = m = 7$. The second restriction is about the semi-finished structures, while no intermediate product is produced by the first and last UPs. Due to their nonidentical allocations in $[A^{[X]}]$ and $[A^{[Y]}]$, these semi-finished products are disabling the direct application of Eq. 4.45 on

the UP i level here. However, the semi-finished products are still eliminated based on their global magnitude from all UPs i. Therefore, the impacts of these intermediate products are neglected later based on Eq. 4.45, as it is stated later in Eq. 4.72. The third restriction is about the rejected FRP structures, while the assessed process in this thesis is assumed to be technically ideal in producing only desired FRP structures and no rejected ones. Further assumptions and restrictions are discussed later in this chapter and in chapter 5 for the selected case study. For instance, these restrictions may include that no wastes can occur before their initial material inputs. Nonetheless, Eq. 4.58 and Eq. 4.59 may be combined, modified, or both to have proper process mathematical models.

From the process mathematical models in Eq. 4.58 and Eq. 4.59, the impacts of both matrices can be calculated, as Eq. 4.39 and Eq. 4.40 previously suggest. Due to the previously discussed equilibrium, the assessed impacts on both sides can be described on the process level in Eq. 4.60.

$$[\theta^{[X]}] = [\theta^{[Y]}] \quad \text{which can be expressed as} \quad [A^{[X]}][\Lambda^{[X]}] = [A^{[Y]}][\Lambda^{[Y]}] \tag{4.60}$$

After neglecting the intermediate products and the desired as well as rejected structures, this equilibrium is also applicable on the UP level, while Eq. 4.61 is applied to assess this level.

$$\{\theta_i^{[X]}\} = \{\theta_i^{[Y]}\} \quad \text{which can be expressed as} \quad \{A_i^{[X]}\}[\Lambda^{[X]}] = \{A_i^{[Y]}\}[\Lambda^{[Y]}] \tag{4.61}$$

Now, the matrix $[A]$ from Eq. 4.44 has the dimension of $(m \times N)$ for all elementary flows α_{ij} from all types j in every UPs i. Each elementary flow type j has a single unique characterization factor λ_j in the column vector $[\Lambda]$ from Eq. 4.35, which has the dimension of $(N \times 1)$. These mathematical models for the process elementary flows and their characterization factors can be reproduced to assess the total impact $[\theta] = \theta$ by Eq. 4.62.

$$\begin{bmatrix} \alpha_{11} & \cdots & \alpha_{1N} \\ \vdots & \ddots & \vdots \\ \alpha_{m1} & \cdots & \alpha_{mN} \end{bmatrix} \begin{bmatrix} \lambda_1 \\ \vdots \\ \lambda_N \end{bmatrix} = \begin{bmatrix} \theta_1 \\ \vdots \\ \theta_m \end{bmatrix} \tag{4.62}$$

In which, $[A]$ is carefully modified to avoid redundant or neglected impacts, as the case study in chapter 5 shows. For that reason, the column vector $[\theta]$ has a dimension of $(m \times 1)$ with an impact value θ_i for each UP i. Based on Eq. 4.30, the UP impact θ_i is calculated by summing all impacts θ_j of elementary flow types j within that UP i. Now, the global process impact θ can be calculated based on Eq. 4.32 in Eq. 4.63.

$$\sum_{i=1}^{m} \sum_{j=1}^{N} \theta_{ij} = \sum_{i=1}^{m} \theta_i = \theta \tag{4.63}$$

It can be concluded that the total impact of a process CSF in this assessment is the summation of all unique impacts from the elementary flows of types j in all UPs i. Specifically on the operational level in Fig. 4.3, this assessment model in Eq. 4.63 is based on its lowest possible impact level represented by θ_{ij} for each elementary flow α_{ij} in every UP i. Moreover, its highest impact level θ is represented by the global eco-efficiency ξ, direct cost δ, and carbon footprint β of the entire process $[A]$. Nonetheless, these results are useful in providing the knowledge for assisting various management levels including the tactical and strategic, as it is mentioned previously. Between the lowest detected impact of θ_{ij} and the highest detected one θ, there are the impacts of all elementary flows in each UP i as θ_i, the impacts of the subsets as $\theta_{i\Gamma}$ in UP i, as well as the total subset impact in the entire process as θ_Γ. These mathematical models, such as Eq. 4.32, enable the assessment of the

considered CSFs including the eco-efficiency, direct cost, and carbon footprint on the various CSF levels, as Fig. 4.20 shows.

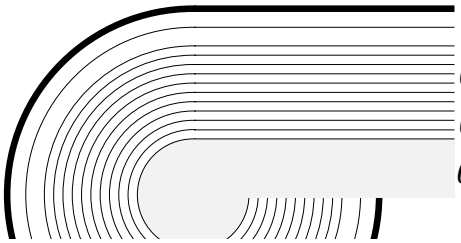

Figure 4.20 Assessment of CSF levels

In addition, the determination of the elementary flows α_{ij} prior to the assessment is significant for the decision-making regarding the KPIs of other CSFs on operation level. Although the elementary flows α_{ij} are distinguished clearly from their characterization factors λ_j, they may dependent of each other in reality. For example, the magnitude of a used elementary flow is decisive to its purchasing prices. This dependency causes a confusion, that leads to mixing both parameters as a single one in many studies. However, any dependency between elementary flows α_{ij} and their characterization factors λ_j is handled case wise, while distinguishing them is the general norm.

4.2 DSS for Real-Time Data Collection

In this thesis, the real-time data collection is realized by the concept of SWS. In it, sensor nodes are assigned to collect the associated initial data based on carefully selected data collection methods. After summarizing the hypotheses of SWS under a generic concept, these sensor nodes and their sensing methods are illustrated.

4.2.1 Concept of Smart-Work-Station (SWS)

The SWS is a cornerstone in enabling a time-dependent eco-efficiency assessment by providing every required data to determine the elementary flows within relevant WSs in real-time. To enable the assignment of proper sensor nodes in the novel concept of SWS, a generic model is studied. Moreover, the SWSs realization in selected composite manufacturing techniques is discussed here.

SWS hypotheses

Based on understanding the production process in Fig. 4.9, the concept of SWS is developed to realize the automated real-time LCI for all assessment relevant elementary flows. While the information flow is excluded, the remaining material and energy flows in Eq. 4.19 and Eq. 4.20 are theoretically measurable by their physical units. In Tab. 4.2, considering the labor work, equipment performance, and facility occupation as energy relevant flows is a working hypothesis that enables the consideration of the physical equilibrium theory in the process. It also enables assessing both economic and ecological impacts of these categories. Based on the process physical equilibrium in Eq. 4.6, it is concluded that measuring selected process inputs or outputs can be sufficient in determining their representative ones on the other side of the equation, which is stated in the process equilibrium within Eq. 4.60. After studying the possible utilized and generated input and output elementary flows in the FRPs manufacturing in Tab. 4.2 and Tab. 4.3 respectively, exact methods and sensor nodes are suggested in Tab. 4.8 and Tab. 4.9 for the real-time automated LCI by the SWS concept. The comprehensive

process models in this work, such as Eq. 4.44, Eq. 4.58, and Eq. 4.59 among others, are enabling the assignment of collected data about these elementary flows in real-time.

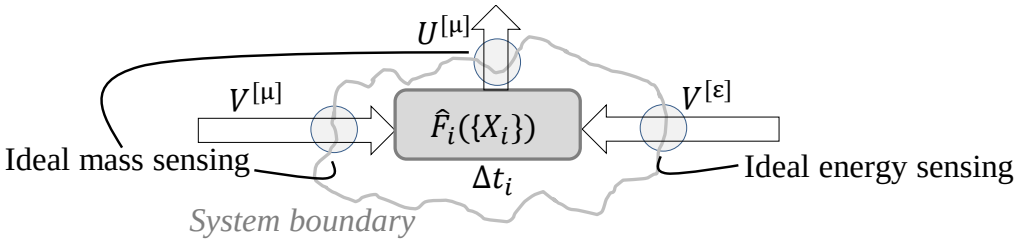

Figure 4.21 Principle of SWS

Still, ideal sensing methods and sensor nodes should be selected for each of these relevant elementary flows, while developing such methods and sensor nodes has been covered sufficiently in literature. Hence, the initial principle of SWS is derived in Fig. 4.21. In addition, the spatial and temporal allocations of the elementary flows, which have been introduced by Fig. 4.12 and Fig. 4.13 previously, are essential to assign the proper data collection method for each categories sensor nodes, as Fig. 4.21 shows.

Although it is excluded from the process elementary flows, the term information and the symbol I may be implemented to describe any decision generation phase. In this work, information is limited to the assessment knowledge stages. In Fig. 4.22, two main levels of associated information can be suggested. They include input information flow I_a and its output flow I_b.

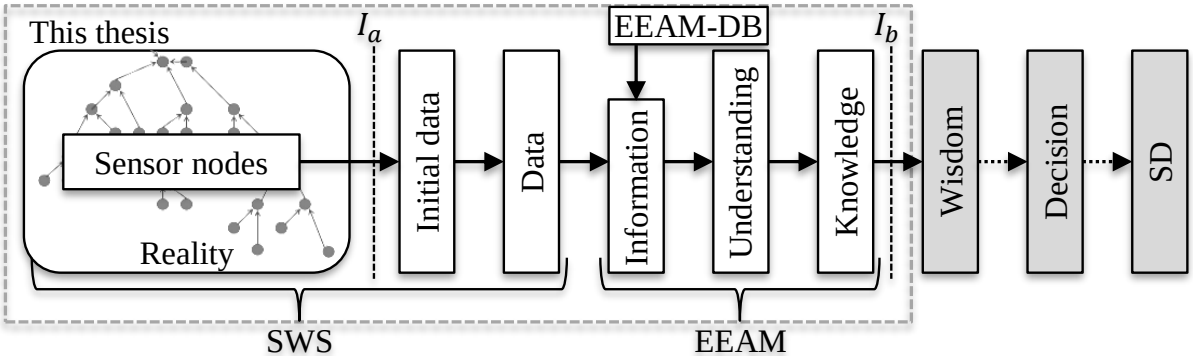

Figure 4.22 Input and output information flows in time-dependent eco-efficiency assessment

By adopting the previously introduced conceptual model in Fig. 4.4, the evolution stages of information I from the reality all the way to SD results are illustrated in Fig. 4.22. These evolution stages are achieved by applying suitable solutions from the Industry 4.0 in the data collection, communication, mining, and storage. As it is previously mentioned, the assessment related input information I_a is about the elementary flows α as well as characterization factors λ of both material and energy inputs. This input information stage of I_a may be considered as the initial data $\hat{\alpha}_{ij}$. For the SWS, the input information I_a about relevant elementary flows α_{ij} is a set of initial data parameters, that are contributing to the type identification j, magnitude determination α_j, its temporal allocation t, and its spatial allocation s. Moreover, these four main parameters are deduced by the SWS from their initial data $\hat{\alpha}_{ij}$ in this thesis. While they are considered as given constants in this work, the characterization factors λ_j can be considered as data in EEAM-DB, while their parameters as initial data $\hat{\lambda}_j$ are handled by Appx. B. As it is discussed within the UP discretization, the UPs i are differentiated in the concept of SWS based on the spatial and temporal occurrence of their elementary flows α_{ij}. On the other hand, the output information stage I_b expected from this thesis is the knowledge about assessed KRIs including the global eco-efficiency ξ, direct cost δ, and carbon footprint β, which are deduced by the EEAM, as Fig. 4.22 explains.

The concept of SWS suggests that by assigning the proper sensor nodes in predefined spatial allocations s, the required initial data $\hat{\alpha}_j$ for the assessment of specific KRIs can be automatically collected in timestamps t. From these sensor nodes, the collected initial data $\hat{\alpha}_j$ about the associated elementary flows α_j can be processed by a computerized model. This concept contributes to realizing the DSSs, that undertake selected decision-making steps. These included steps have been discussed previously in Fig. 4.1. Conventionally, many of these steps are performed partially or completely by the decision-makers and not by DSSs. For instance, the elementary flow initial data $\hat{\alpha}_j$ is usually gathered or at least processed by the data collection clerk. It is hypothesized here that a process such as the manufacturing of FRP structures can be broken down into discretized UPs in a comprehensive conceptual model, such as Fig. 4.16. This model is developed for the time-dependent eco-efficiency assessment of direct cost δ and carbon footprint β. In such conceptual model, all relevant elementary flows α_j can be identified and determined to assess the KRIs. As they are introduced previously in Fig. 4.18, these elementary flow subsets are defined in that conceptual model for the selected techniques. After defining these categories, their elementary flows are assigned to temporal and spatial allocations within the system boundary of their containing UPs, as Fig. 4.10 has shown before. By determining all spatial spots s along the temporal duration $\Delta t^{[\alpha_j]}$ of every associated elementary flow α_j, a path $\Delta s^{[\alpha_j]}$ for every one of them is virtually drawn as a route in that conceptual model, as it is illustrated previously in Fig. 4.12 and Fig. 4.13 respectively. This work provides a comprehensive conceptual model that covers the technical, spatial, and temporal boundaries of the process, UPs, and their elementary flows. Based on it, a generic concept can be established for collecting the initial data that is required to identify, measure, and allocate each associated elementary flow temporally as well spatially.

Hence, the initial data is processed throughout the CSF layers from Fig. 4.20. The first step is to provide the data about relevant elementary flows α_j, which is required for the assessment of the selected CSFs. Unlike the conventional approaches, this data collection is performed automatically and in real-time in this concept. Therefore, the by SWS collected initial data $\hat{\alpha}_j$ is processed to determine the elementary flows α_{ij}. From this determination of α_{ij} and the given data about the characterization factors λ_j, the economic and ecological impacts θ_{ij} as KPIs can be calculated. As it is suggested in Fig. 4.20, PI may be the impact of each category $\theta_{i\Gamma}$ in every UP i. By the the developed models, the impacts θ_i on UP level can be aggregated and represented as RI to the decision-makers in adjustable manners. Alternatively, RIs may be represented by the global impact of each category θ_Γ. Finally, the selected KRIs of eco-efficiency, direct cost, and carbon footprint in the process are assessed. After realizing the SWS, the advanced EEAM has the capability of illustrating the time-dependent eco-efficiency assessment results on the various levels of the selected CSFs. Moreover, it offers adjustable combination possibilities to cover the various perspectives of different decision-makers selectively.

SWS for selected FRPs manufacturing techniques

After setting the general hypotheses of the SWS concept, they are applied to the FRPs manufacturing process. This necessitates adapting the generic concept to the unique requirements of the studied techniques. As it is summarized in Appx. A, there is a wide range of applicable techniques in FRPs manufacturing. However, there are common relevant process features for some techniques. This is also the case of the discussed manufacturing technique in this work. These characteristics are impacting not only the definition of elementary flow types j and their cut-off-criteria that are associated with the technique but also the states of both material and energy applied in the process. These states are crucial for the selection of proper sensor nodes in the SWS .

For many input and output materials $\varphi^{[\Gamma]} \subseteq J^{[\mu]}$, the substances in each material are decisive for the identification of these elementary flows and for clustering them in unique subsets $\varphi^{[\Gamma]}$. Technically, material

elementary flows $\alpha_j \in J^{[\mu]}$ are determined in various matter states. In manufacturing FRP structures, each type j should have a single matter state during the measurement. For instance, fiber subset $\varphi^{[F]}$ includes various substances such as glass and carbon fibers with liquefiable binders in some cases, that are in the solid status during the measurement. The matrix materials subset $\varphi^{[M]}$ includes substances such as resins, hardeners, and accelerators. This distinguishing based on these substances is essential to list the ancillaries in a subset $\varphi^{[R]}$ as well. The same approach is applied to cluster material output elementary flows $u_\tau \subseteq U^{[\mu]}$ based on their substances including the wastes. While in any process matters can be either solid, liquid, or gaseous [46], the elementary flow subsets are sorted under these states in Tab. 4.6.

Table 4.6 States of relevant material elementary flow subsets $\varphi^{[\Gamma]} \subseteq J^{[\mu]}$

Solid	Liquid	Gas
• Fiber material $\varphi^{[F]}$ • Core material $\varphi^{[C]}$ • Ancillaries $\varphi^{[R]}$ • FRP desired structure $\varphi^{[S]}$ • Semi-finished structure $\varphi^{[P]}$ • FRP fragment waste $\varphi^{[W]}$ • Fiber waste $\varphi^{[G]}$ • Core material waste $\varphi^{[N]}$ • Ancillaries waste $\varphi^{[O]}$ • Reusable ancillaries $\varphi^{[B]}$	• Matrix $\varphi^{[M]}$ • Ancillaries $\varphi^{[R]}$ • Matrix waste $\varphi^{[D]}$ • Ancillaries waste $\varphi^{[O]}$ • Reusable ancillaries $\varphi^{[B]}$	• Ancillaries $\varphi^{[R]}$ • Ancillaries waste $\varphi^{[D]}$ • Reusable ancillaries $\varphi^{[B]}$

However, the relevant material elementary flow subsets $\varphi^{[\Gamma]} \subseteq J^{[\mu]}$ listed in Tab. 4.6 are covering all applicable FRPs manufacturing techniques in various industries with different maturity levels. Nonetheless, the case study in this thesis contains only solid materials, as they are listed later in chapter 5.

Technically, the FRP manufacturing process contains technically transformations of four energy forms including electrical, mechanical, thermal, and chemical energies [134]. However, only the electrical and mechanical forms are implemented as input elementary flow subsets $\varphi^{[\Gamma]} \subseteq V^{[\epsilon]}$. On the other hand, only the thermal energy form is generated as an output elementary flow $\varphi^{[\Gamma]} \subseteq U^{[\epsilon]}$, which is previously excluded from this study. While the sorting of material elementary flow subsets $\varphi^{[\Gamma]} \subseteq J^{[\mu]}$ to their states is clear without a need for interpretation, the energy elementary flow subsets $\varphi^{[\Gamma]} \subseteq J^{[\epsilon]}$ are clustered under three relevant states in this thesis. Electrical and mechanical energies are the common relevant forms for the assessment in FRPs manufacturing. However, it is essential to consider the energy conversion as a state that contains the forms exchange. The consideration of conversion is crucial for the equipment, while such machines have the functionality of converting one energy form to another. Moreover, facility is considered exceptionally within this state as the conversion control volume. These energy states are listed in Tab. 4.7.

Table 4.7 States of relevant energy elementary flow subsets $\varphi^{[\Gamma]} \subseteq J^{[\epsilon]}$

Electrical	Mechanical	Conversion
• Equipment electricity $\varphi^{[T]}$ • Facility electricity $\varphi^{[T]}$	• Labor $\varphi^{[L]}$	• Equipment $\varphi^{[Q]}$ • Facility $\varphi^{[\Delta s]}$

In Tab. 4.7, the electricity consumptions of equipment and facility are separated from each other. However, they are both including various types in the same subset $\varphi^{[T]}$. Furthermore, labor work $\varphi^{[L]} \subseteq V^{[\epsilon]}$ is considered under the category of mechanical energy in this thesis. On the other hand, the equipment performance is considered in this thesis as a conversion of energy between different forms. Therefore, the operation impact of each equipment type is assessed based on the duration of its occupation $\Delta t^{[\alpha_j]}$. This is also the case with calculating the direct labor impacts, while labor ranking is covered by their characterization factors.

4.2.2 Real-Time Life-Cycle Inventory Analysis (LCI) by Sensor Nodes in SWS

First, the implementation of SWS concept in FRPs manufacturing process is introduced for the selected techniques. This SWS concept enables collecting the eco-efficiency associated data automatically and in real-time. Therefrom, the term "smart-work-station" is implemented to describe the concept, which has been developed to define the required sensor nodes for the data collection [6, 7]. These sensor nodes serve the identification, magnitude measurement, and temporal as well as spatial assignment of relevant elementary flows.

Generic sensor nodes in SWS

After describing the states of the relevant elementary flows α_j, the available sensor nodes are studied and rated to select the proper combination of them in realizing the SWS. The concept of SWS adopts a set of existing measurement technologies and improves them to serve the novel time-dependent eco-efficiency assessment [6]. For the identification of elementary flow types, methods of identification (MI) as well as sensor nodes for identification (SI) are suggested by the SWS. Similarly, the measurement of their magnitudes is realized through methods of magnitude measuring (MM) and sensor nodes for magnitude measuring (SM). Moreover, theses MIs, MMs, SIs, and SMs are enabling the determination of the temporal and spatial allocations of these elementary flows. While the methods describe how to collect the data, the sensor nodes are the hardware to realize the collection with.

To identify the type j of an elementary flow or measure its magnitude α_j, several methods can be adopted. Some of these MIs and MMs are valid for a single elementary flow type j in a subset $\varphi^{[\Gamma]}$ or the entire subset. They may be also applicable for several subsets. These MIs or MMs require the SIs or SMs respectively to gather the required signals or initial data $\hat{\alpha}$. Methods such as visual recognition, person identifier, barcode or quick response (QR) scanning, radio-frequency identification, person markers tracking, person wearable tracker, person thermal detection, dedicated identification, weight measurement, person count, labor optical and thermal allocation, or energy measurement may be implemented as MIs and MMs to realize the SWS. Moreover, selected sensor nodes can be applied to perform these MIs and MMs. For instance, cameras or imaging sensors for barcode reader or QR code reader, reading device for radio-frequency identification, optical motion capture system, miniature internal sensor, thermal IR camera, electricity meter, and digital scale are examples of possibly implemented SIs and SMs for the MIs and MMs [6, 7]. Therefore, these relevant methods and their sensor nodes are listed and clustered later in this chapter. The combination of some of these MIs, MMs, SIs, and SMs is shown for a simplified exemplary WS in Fig. 4.23 and Fig. 4.24.

In Fig. 4.23, the optical or thermal identification of labor $\varphi^{[L]}$ and magnitude determination of their work time is illustrated. Fig. 4.23 shows schematically the concept of determining labor $\varphi^{[L]}$ as an input elementary flow in FRP manufacturing for an exemplary WS. At a WSP within the WS, labors carry out the manual process

steps. For this purpose, labors must move around and within the WSP to perform manual activities accordingly in order to achieve the desired result with or without equipment.

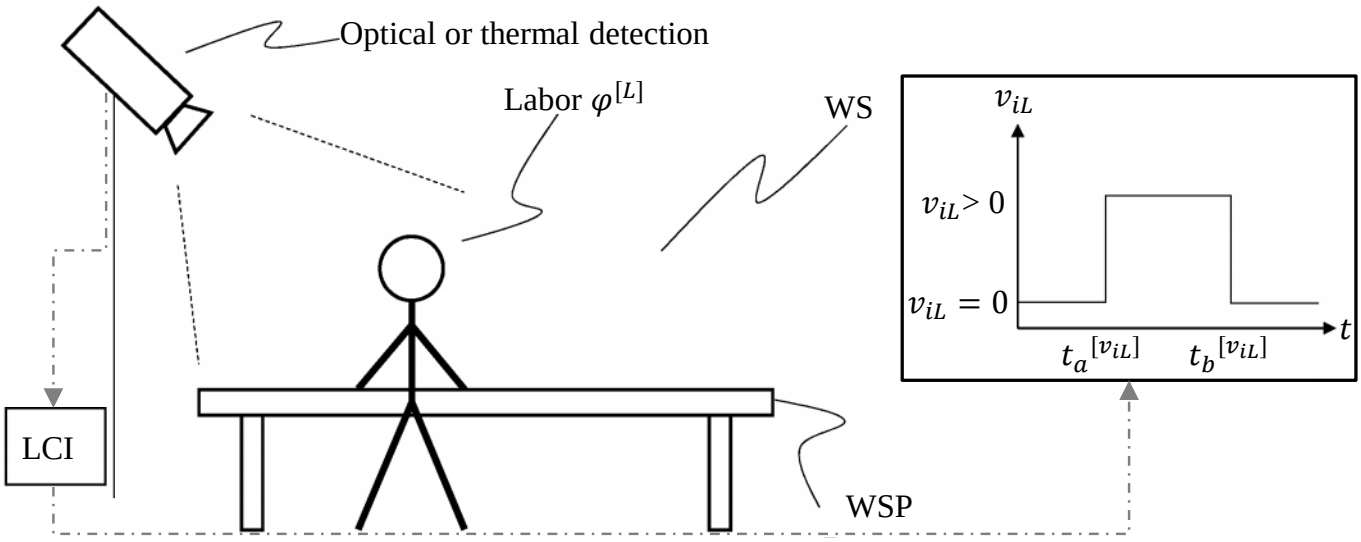

Figure 4.23 Exemplary labor SWS, adapted from [7]

Like all other relevant elementary flows α_j in the SWS, labor activities and motions are continuously detected with timestamps, by optical or thermal detection. This measurement is realized after processing the initial data $\hat{\alpha}_L$ in the LCI of SWS, as Fig. 4.23 shows. In this LCI, both labor temporal and spatial allocations in the UP within its WS are tracked as well. The SWS computerized model enables determining the duration $\Delta t^{[v_{iL}]}$ and the spatial path $\Delta s^{[v_{iL}]}$ of labor movement or activity within predefined WSPs. Hence, it is measured from the beginning at $t_a^{[v_{iL}]}$ to the end at $t_b^{[v_{iL}]}$. Therefrom, the labor activity diagram over time can be visualized, as it is shown on the right side of Fig. 4.23. Based on assuming that all activities should be target oriented and intentional, any activity or movement in a WS is labor relevant whenever it has the value of $v_{iL} > 0$. Moreover, detailed explanations for thermal and optical detection are provided later in Tab. 4.8 and Tab. 4.9.

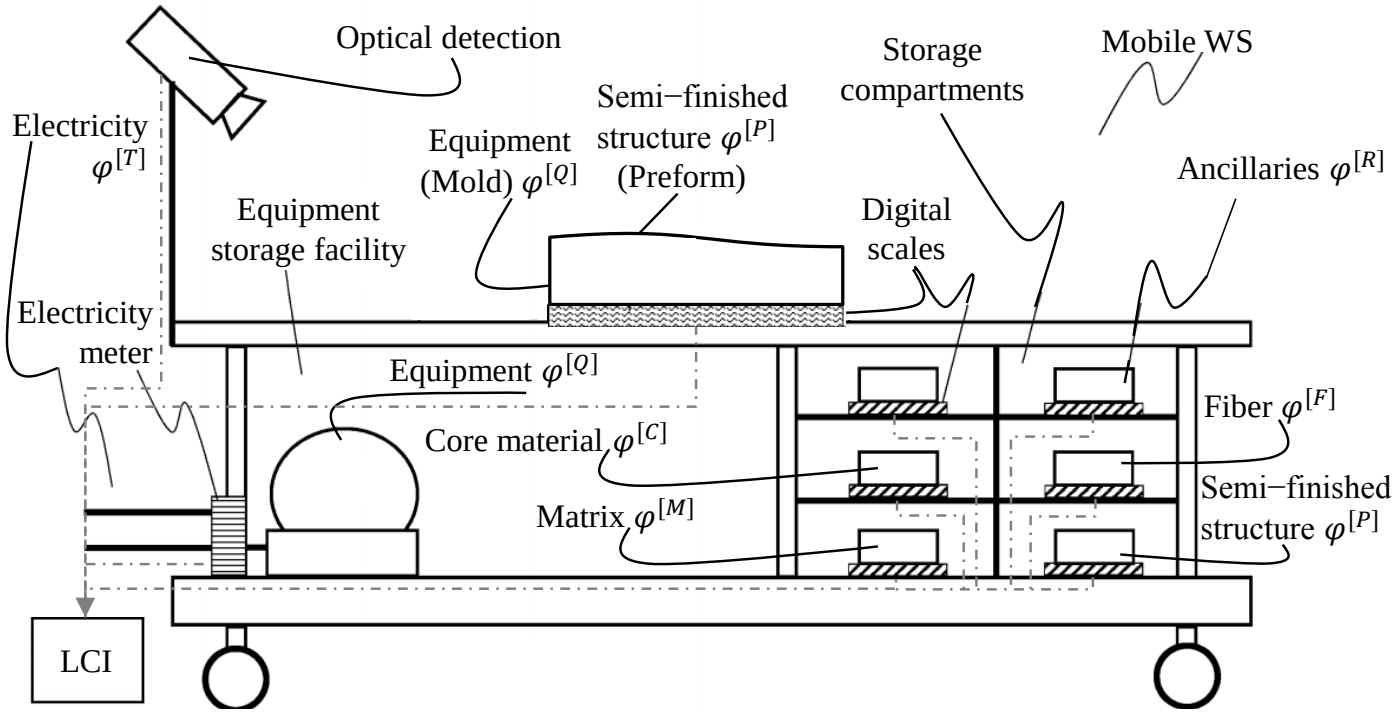

Figure 4.24 Exemplary SWS, adapted from [7]

Similar to the simplified example of labor $\varphi^{[L]}$ in Fig. 4.23, Fig. 4.24 illustrates further elementary flows $\varphi^{[\Gamma]}$ within the generic concept of SWS. This exemplary WS is common in preforming UP_3 for several FRPs manufacturing techniques. Fig. 4.24 shows an example of mobile WS, that contains storage compartments for materials and equipment on the lower phase. On the upper phase activities are performed with different DoA. For labor $\varphi^{[L]}$, the concept in Fig. 4.23 is applicable here as well. In FRP manufacturing process, fiber $\varphi^{[F]}$ or fiber cuts $\varphi^{[P]}$, matrix $\varphi^{[M]}$, and ancillaries $\varphi^{[R]}$, can be stored in that storage phase in their specific compartments. Each dedicated compartment has an integrated digital scale that determines the material weight instantly in real-time. Similar to all other SIs and SMs in the SWS, every digital scale including its software solution is serving the LCI. From real-time weight measurement, every dedicated scale is providing the initial data $\hat{\alpha}_j$ to calculate the material mass flow over time.

In the case of dedicated digital scales in a mature process, no further identification is required while the materials in each compartment are predefined. On the other hand, a digital scale is integrated underneath the work surface. Unlike the dedicated ones, such universal scale requires material identification by proper MIs and their realization in SIs to identify it while measurement. By removing an individual material from its dedicated compartment, the difference between remaining or returned mass at $t_b^{[v_{ij}]}$ on the one hand and the initial mass at $t_a^{[v_{ij}]}$ on the other hand is calculated. This determines the magnitude of the consumed material in each UP i or activity. For core structural materials including $\varphi^{[F]}$, $\varphi^{[M]}$, $\varphi^{[C]}$, and $\varphi^{[P]}$, such calculation can be useful to calculate the wastes for predefined or measured final structure substances. This exemplary mobile WS also has a storage compartment for exemplary equipment v_{iQ} such as vacuum pump or any other proper electrically powered machines. As Fig. 4.24 shows, any electrical equipment is connected to a power source. The electricity, that is required to carry out a UP or an activity in it, is measured by an electricity meter. With the help of dedicated meters, the consumed electrical energy is measured for every equipment during its operation time $\Delta t^{[v_{iQ}]}$. The electricity meters measure not only the energy consumption of each equipment but also the total electricity during the entire UP i.

In this example of preforming UP_3 in Fig. 4.24, the mobile WS has the upper space as a WSP that contains a preforming mold on it. On the mold surface, for example, fiber layers or cuts as semi-finished products $\varphi^{[P]}$ can be manually or automatically preformed. Another semi-finished product from preforming these layers in UP_3, which is the preform $\varphi^{[P]}$, is produced. Hence, this exemplary SWS collects the initial data for labor $\varphi^{[L]}$, fiber $\varphi^{[F]}$ or fiber cuts $\varphi^{[P]}$, if applicable core material $\varphi^{[C]}$ or their cuts $\varphi^{[P]}$, ancillaries $\varphi^{[R]}$, equipment $\varphi^{[Q]}$, and electricity $\varphi^{[T]}$ in real-time. Besides that, the spatially and temporally assigned data from all associated subsets $\varphi^{[\Gamma]}$ can be implemented to identify and measure facility occupation $\varphi^{[\Delta s]}$. Furthermore, both Fig. 4.24 and Fig. 4.23 suggest proper setups of implemented MIs, MMs, SIs, and SMs for specific case studies.

For the SWS as a real-time data collection concept in production, the DoA is an important aspect that should be considered. As it has been discussed previously in chapter 3, the DoA varies based on other aspects such as the implemented techniques, applied technologies in them and their TRLs, as well as process maturity. Therefore, scenarios with different DoA have been considered in developing the SWS concept. This has led to achieve an approach that is applicable for any DoA. In Fig. 4.25, two examples of a fully-automated preforming UP_3 in the EVo-platform and a semi-automated conventional one are subjected to the concept of SWS.

The preforming UP_3 is selected here, while it is a proper example of a UP with different possible DoA. While a high DoA is commonly applied to UP_3 in automotive industry, the DoA of this UP varies between the different scenarios in aerospace industry. Nowadays, the semi-automated conventional preforming, that is shown on the right side of Fig. 4.25, is commonly applied in aerospace and wind energy sectors. From the highly-automated EVo-platform, the fully-automated preforming UP_3 is selected.

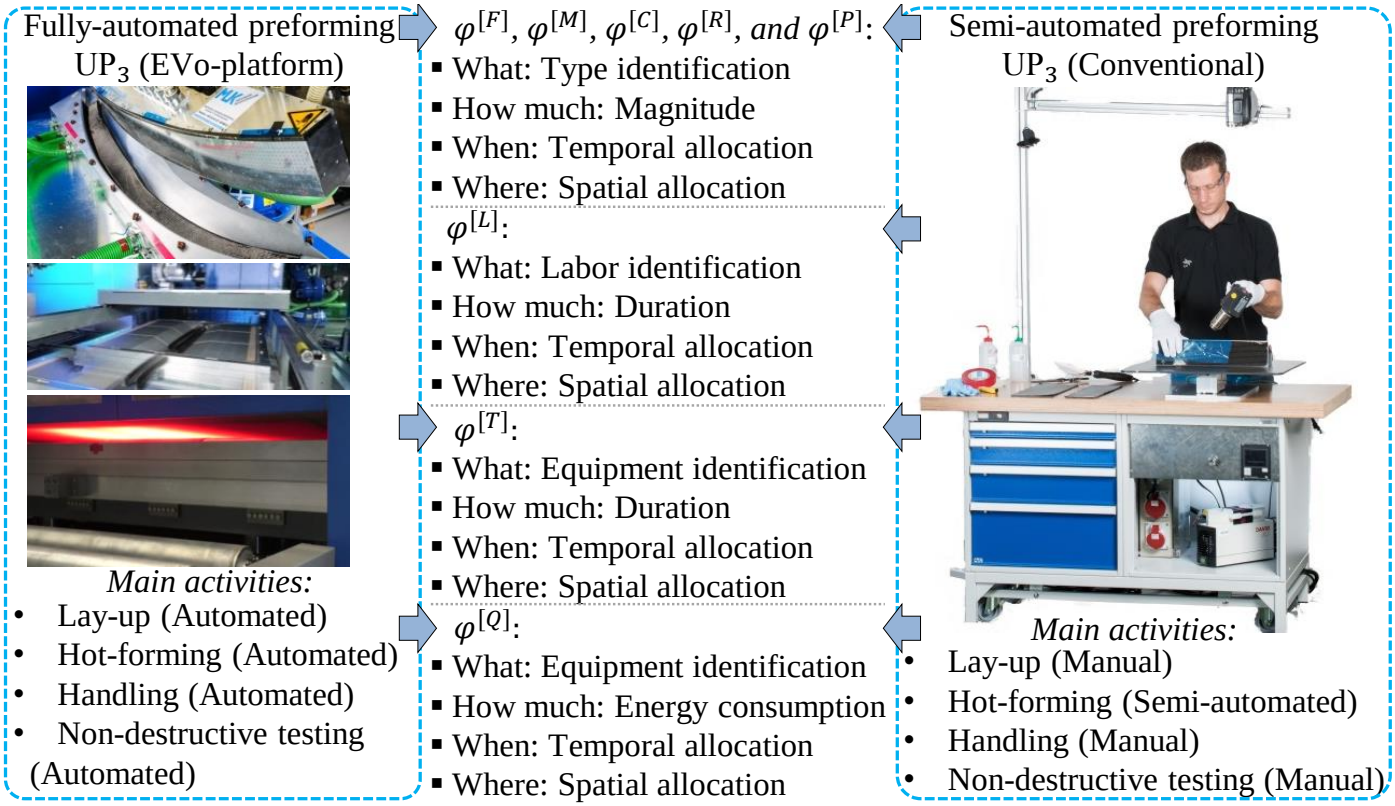

Figure 4.25 Two examples of implementing SWS in preforming UP_3 with different DoA

It includes a lay-up, preforming or hot-forming, preform handling, and non-destructive testing, as it is illustrated on the left side of Fig. 4.25. On the other side, the discussed conventional preforming UP_3 includes manual lay-up, preform handling, and non-destructive testing. However, it includes a semi-automated hot-forming. In this hot-forming, a heating device is operated manually to heat the preform. As it is shown on the left side of Fig. 4.25, the concept of SWS can be applied to the preforming in the EVo-platform. For this fully-automated UP_3, the elementary flow type j, its magnitude α_j, as well as its temporal t and spatial s allocations are determined by the SWS. Similar to the approach in Fig. 4.24, several MIs, MMs, SIs, and SMs are implemented here. This approach with material inputs such as $\varphi^{[F]}$, $\varphi^{[M]}$, $\varphi^{[C]}$, and $\varphi^{[P]}$ is applicable for the conventional preforming with low DoA on the right side of Fig. 4.25 as well.

From the previous definition of equipment, it is obvious that a fully-automated process is equipped with machines in general. On the other hand, a manual process is served by tools only. Hence, a semi-automated one may have both machines and tools. Here, molds are applicable regardless the adopted DoA. However, all these instrument types are considered here as equipment and combined under the subset $\varphi^{[Q]}$. While different types of electrical machines are implemented on both sides of Fig. 4.25, the operation duration and performance of each equipment type are measured by electricity meters. For both examples, dedicated meters are implemented as SI and SM. The same meters are also used in measuring the total and machines electricity consumptions on both sides of Fig. 4.25. While preforming is a fully-automated UP in the EVo-platform, no labor work is required. Therefore, MIs, MMs, SIs, and SMs for labor subset $\varphi^{[L]}$ are applied only in the UPs with manual activities. Further detailed explanation of the implemented MIs, MMs, SIs, and SMs is provided later in this chapter.

Elementary flow identification

In the SWS, it is crucial to identify the type j of each assessment relevant elementary flow α_j. For the identification tasks, MIs are defined in Tab. 4.8 as a novel approach in tracking the required initial data about every included elementary flow. Moreover, commercially available sensor nodes are suggested in the same table to facilitate the realization. These MIs and SIs have some practical pros and cons that can be stated in order to rate them. As it is explained in Tab. 4.8, some sensor nodes as SI-(sort) can be directly used or modified to be implemented for more than a method as MI-(sort). Thus, these sorts are distinguished by unique numbers and letters, whereas the numbers are randomly selected. While they are all based on available solutions, the functionalities of relevant MIs and SIs have been discussed thoroughly in literature. Therefore, only the pros and cons of them in the context of SWS concept are discussed in Tab. 4.8. However, these methods are listed regardless their sort sequence.

Table 4.8 Assigning available solutions to required MIs and realize them by proper SIs

MI	SI	Description and rating: pros and cons
Equipment dedicated identification: MI-(6)	Dedicated electricity meter: SI-(4)	The main research subjects associated with MI-(6) are the equipment monitoring and energy assessment. In literature, these issues have been studied by the scholars in various fields. They include the works of Herrmann and Kara, Kreitlein et al., Lenz et al., Hibino and Yanaga, Bauerdick et al., Zhabelova and Vayatkin, Bharath et al., Higgins et al., Tan et al., Ruzzelli et al., Zhao et al., as well as May and Kiritsis [30, 35, 134, 136, 137, 190, 216, 268, 302, 351]. In modern FRPs production and specifically the studied techniques from Appx. A, every equipment type is operated either by electrical or mechanical energy in the form of manual labor work. As it has been stated previously, any electrical equipment is considered as a machine, while a manually operated one is a tool in this thesis. Therefore, machines are connected to electricity supply points. Each source point is to be provided by dedicated electricity meter to monitor the machine performance. Hence, each one can be identified by its dedicated electricity meter. Therefore, no additional contribution to the existing energy assessment systems is provided in the SWS concept, while they are directly integrated and implemented.

MI	SI	Description and rating: pros and cons
Visual recognition (object optical detection): MI-(1)	Imaging sensor (digital camera): SI-(1)	The functionality of MI-(1) and its implementation in the SWS concept are thoroughly discussed in the internal previous work of Schachinger and Al-Lami [271]. Moreover, this method has been also studied in works of Howard et al., Liu et al., Redmon et al., Ren et al., Han et al., Rosten et al., Kalal et al., Mei et al., Levin and Weiss, Lin et al., Russakovsky et al., Sheikh et al., Wang et al., Prasad et al., and Brumitt et al. [43, 127, 146, 162, 194, 198, 200, 220, 243, 249, 252, 262, 266, 286, 329]. The imaging sensors as SIs have been thoroughly studied and developed in the works of Danna and Newman, Harkin, Mendis et al., Yang et al., Fan et al., Kawahito, Wilder et al., Yamazato et al., and El Gamal and Eltoukhy [70, 92, 99, 130, 168, 221, 336, 347, 348]. MI-(1) may be applied for every matter elementary flow $\alpha_j \in J^{[\mu]}$, whenever it is possible. This MI has the advantage of requiring no tags or stickers. However, this MI requires proper AI technologies such as machine learning to realize it. In addition, a DB, that includes the visual characteristics of each relevant elementary flow α_j, is needed. In practice, not all material flows $\alpha_j \in J^{[\mu]}$ in the FRP manufacturing can be detected by this method. Moreover, aspects such as the angle, distance, lightning, and clearness of camera visualization are crucial for MI-(1) [271]. Due to work regulations in Germany, any method that enables the personnel identification in production is generally prohibited [138, 328]. In addition to material flows, this type of recognition may be applied to identify the tools. Similarly, molds can be recognized visually. Moreover, a machine can be detected as object by this method as well. However, this identification requires advanced AI algorithms that combine the machine identification and its performance determination simultaneously. This combination is required while not every machine in the WS must be actively utilized in the assessed UP. Although AI algorithms and software implemented in MI-(1) are sophisticated, the SIs can be any inexpensive digital cameras that have the suitable quality and specification [271].
Facility identification: MI-(8)	All applied sensors	Facility observation including its identification in MI-(8) has been studied in literature for various applications in different fields. Study cases of activity recognition and facility utilization in laboratories, hotels, and homes have been discussed by several scholars. They include for instance the works of Logan et al., Drira et al., Storf et al., Chahuara et al., Puvanasvaran et al., Wren and Tapia, Wilson and Atkeson, Abowd et al., Intille et al., Brumitt et al., Schmidt et al., Richardson et al., and Holmquist et al. [1, 43, 50, 81, 143, 155, 201, 245, 254, 276, 299, 339, 346]. The identification of a facility as WS, in which a UP is taking a place, can be realized through the spatial assignment s of all associated elementary flows by all used sensor nodes during the assessed UP. It is hypothesized here that where no elementary flow occurs no facility is utilized, which is acceptable for the assessment of direct impacts.

MI	SI	Description and rating: pros and cons
Person detection: MI-(2)	Imaging sensors (cameras): SI-(1)	Similar to MI-(1), MI-(2) has been discussed in several studies including the works of Lefloch, Kim et al., Wang and Aghdasi, Noone et al., Albiol et al., García et al., Hashimoto et al., Moeslund et al., Ganapathi, and Bregler [14, 40, 111, 113, 131, 171, 189, 224, 231, 327]. Compared to MI-(1), SI(1) is implemented differently in MI-(2). According to the works of Fleck et al., Foken and Stiefelhagen, Teixeira and Savvides, Tanner et al., Bamji, Burbano et al., and Ramaswamy et al., the identification and counting of human is realized through a 3-dimensional visual scanning [27, 45, 106, 107, 246, 303, 306]. In this thesis, MI-(2) is applied to distinguish human from other objects within the WS. Practically, there are commercially available hardware and software solutions that operate with AI algorithms to serve this MI. Nonetheless, the price of such solution may be higher than the normal digital cameras. Moreover, SI-(1) can be also implemented to identify the labor motion through the hand detection as an object (with and without gloves). This is useful for determining the spatial path $\Delta s^{[v_{iL}]}$ of human activities in small spots s that contain only a part of the entire human body [271]. Advanced person optical detection may have the capability of revealing the identity of labor. This may be useful to rank them and select the proper characterization factors. However, due to regulation in some countries including Germany, no personalized data about employees is allowed to be collected [138, 328]. In some commercially available solutions, MI-(2) can be; however, realized by imaging sensors SI-(1) that detect people without saving images, which may accommodate such regulations. Therefore, this type of imaging sensors SI-(1) is adopted in the SWS.
Bar- or QR-code scanning: MI-(3)	Imaging sensor (camera): SI-(1) and coded sticker: SI-(1a)	In Schachinger and Al-Lami work, the consideration of MI-(3) in the SWS concept has been also covered [271]. In addition, MI-(3) has been discussed and enhanced in previous works of Ohbuchi et al., Soon, Ruppert et al., Collins Jr, John III, and others [61, 158, 235, 265, 297]. In the SWS concept, MI-(3) is applied whenever it is necessary. In some cases, MI-(3) is required to overcome the difficulties of using MI-(1). For instance, liquid substances in containing vessels may be identified by the implementation of MI-(3). Therefore, it is more suitable than MI-(1) especially for optically indistinguishable objects such as liquid containing vessels and fiber layers. Therefore, the proper QR- or bar-codes are allocated as stickers SI-(1a) on the surfaces of such objects. The implementation of these SI-(1a) should have minor impact on the process activities. The position of these stickers SI-(1a) on the object surfaces is critical, while the imaging sensor nodes SI-(1) should be faced effectively toward them [297]. Similar to MI-(1), this method can be also applied to identify the nonelectrical equipment known as tools. For many elementary flows, this method has the disadvantage of depending on stickers SI-(1a). Practically, it can be physically impossible or very laborious to mount them on the object surfaces. However, AI algorithms implemented in this method are available, while SI-(1) can be any inexpensive digital camera with the suitable quality. A simultaneous application of the same SI-(1) in serving multiple methods such as MI-(1), MI-(2), and MI-(3) is theoretically possible [6, 7, 271, 297].

MI	SI	Description and rating: pros and cons
Person thermal detection: MI-(5)	Thermal sensors (IR-camera): SI-(3)	MI-(5) has been studied for different applications by many scholars such as Han and Bhanu in more than a work, Teutsch et al., Kumar et al., Torresan et al., Al-Habaibeh and Parkin, Fernandez-Caballero et al., Rudol and Patrick, Goubet et al., Jones and Plassmann, Pavlidis et al., and O'Kane [5, 101, 118, 125, 126, 160, 182, 236, 239, 263, 307, 313]. In his thesis, Hilmer has implemented this method to document labor activities for the assessment purposes [138]. MI-(5) is applied here to detect the human body based on its temperature [236]. Therefore, the IR-camera SI-(3) is set to detect predefined temperature range that covers the human body considering its surroundings such as room temperature and clothes [313]. The main technical disadvantage of MI-(5) is the difficulty in distinguishing human body from other objects with close temperatures. This is the case when no aspects other than the temperature are considered. Another technical problem is the variation of body temperature on different body parts as well as clothing and health impacts [160, 239]. This method is effective only in detecting a human body within specific range of room temperature. Generally, this method is unable of directly revealing the labor identity, which is a disadvantage for selecting the proper characterization factor from multiple alternatives when required. However, this is a feature that matches the legal terms for data collection in some countries such as Germany [138].
Material and tool identification: MI-(7)	Dedicated digital scale: SI-(5)	In general, implementation of digital scales SI-(5) is a common approach in different fields. In literature, this method has been discussed by scholars such as Ting et al., Shih, Bruns, Naito and Utsunomiya, Schmidt et al., Richardson et al., Prabuwono et al., Holmquist et al., and Chang et al. [44, 55, 143, 227, 242, 254, 276, 287, 311]. In some process cases, a material elementary flow $\alpha_j \in J^{[\mu]}$ must appear repetitively in a unique spatial spot s in its path $\Delta s^{[\alpha_j]}$ within the WS. In that spatial spot s both identification and magnitude measurements are associated with a single material flow $\alpha_j \in J^{[\mu]}$ [276]. For instance, each material is stored in a unique compartment in a mature production. Such compartments are considered as this unique spot s. This method can be applied for dedicated temporary storage in the WS, as it is explained previously in Fig. 4.24. Moreover, some materials $\alpha_j \in J^{[\mu]}$ in solid, liquid, or liquefied gas forms must flow from, throughout, or to a specific spatial spot s in a predefined temporal point t. Such spots s can be also equipped with dedicated digital scales SI-(5) for that specific material elementary flow α_j. Example for that is the matrix $\varphi^{[M]}$ in the infusion vessel. Moreover, tools may be also detected from the weight deviation occurs to the storage container or trolley. In MI-(7) tool may be recognized by its missing weight. Furthermore, the absence duration of each tool is measured and associated with the utilization time of it, which serves as a MM in this case. However, there are technical difficulties in applying this type of tracking for tools with very similar weights. Technically, the departure of more than a tool item simultaneously may disable the recognition as well. This MI-(7) may be applied to validate other methods that measure the tools utilizing duration.

As it is illustrated in Tab. 4.8, the same imaging sensors SI-(1) can be theoretically utilized as SIs to realize multiple MIs. This is possible whenever the proper setup and AI algorithms are implemented. These MIs include MI-(1), MI-(2), and MI-(3). Still, this combination is not realized in the current version of SWS.

However, not all relevant and possible MIs and SIs are covered by Tab. 4.8 or implemented in the current version of SWS. For instance, 3-dimensional laser scanning may be implemented instead of the optical detection [38, 180, 181, 256]. Due to the laborious identification setups associated with it, this 3-dimensional laser scanning method has been excluded from the studied solutions in Tab. 4.8. In addition, the radio-frequency identification is a common method for tracking objects that has been studied and developed by many scholars such as Angerer et al., Want, and Kwon et al. [19, 184, 330]. It has the advantage of being independent from optical restrictions such as lightning, angles, clearance, etc. Its main disadvantage is the necessity of integrating or attaching the identification chips or tags to the object. Therefore, the implementation of this method is physically difficult or in many cases inapplicable and practically effortful in FRP manufacturing. Yet, this method has been excluded from this thesis and replaced by other identification methods. Another example is the person markers tracking, which has been studied by Chan et al. in their work. For identifying and tracking the motion of a labor, wearable marked dress and capturing system can be used. For instance, this method is common in movies production within the film industry. It provides a detailed description of the body motion of a person in real-time [53]. Therefore, such a functionality is much beyond the simple task of people identification or work time measurement. Moreover, the enforcement of wearing marked dress is practically and organizationally uncomfortable. Therefore, this method is excluded from this work. Furthermore, person wearable tracker is discussed in different fields by Nietner, Gao et al., Tapia, Roetenberg et al., as well as Soehren and Bye [112, 229, 260, 295, 305]. For tracking the motion of labor, wearable miniature inertial sensors can be implemented. This method provides a detailed description of people motion in real-time. It can be set to provide the labor identity, which is advantageous for the selection of proper characterization factors in some cases. Moreover, this method can be easily used to personalize the collected data, while applying it is controversial due to the German work regulation. Therefore, it is excluded from the methods applied in the SWS.

In general, any method that contradicts with the goal of SWS as an automated labor-free data collection concept is also excluded. As it is mentioned before, all SIs are measuring in unified timestamps to associate the elementary flow type j with its temporal allocation t. Moreover, SIs are assigned in predefined spatial spots s, which accomplish both required allocations. By the selected MIs and SIs from Tab. 4.8, the input information except the one about elementary flow magnitude a_j is made available.

Elementary flow magnitude measurement

To measure the magnitude α_j of each relevant elementary flow type j in FRP manufacturing, there are several MMs and SMs that can be applied. For the measurement tasks, MMs are defined in Tab. 4.9 as a novel approach in tracking the required initial data about every included elementary flow. Moreover, commercially available sensor nodes are suggested in the same table to facilitate the realization. These MMs and SMs have some practical pros and cons that can be stated in order to rate them. Similar to the SIs, some existing SMs may be directly implemented or modified to be implemented in realizing more than a MM. For the measurement of elementary flow magnitude α_j, selected MMs and SMs, which may be a set of already defined SIs, are listed and their pros and cons are also discussed in Tab. 4.9.

Table 4.9 Assigning available solutions to required MMs and realize them by proper SMs

MM	SM	Description and rating: pros and cons
Material weight measurement: MM-(1)	Digital scale: SI-(5)	To realize a real-time weight measurement, digital scales SI-(5) are applied. The weight measurement technique can be implemented to sense material mass by the equation Mass=Weight/Gravity. These scales can measure solid as well as in-vessels contained liquid or liquefied matters. For each elementary flow α_j, there is a flow path $\Delta s^{[\alpha_j]}$ that consists of spatial spots s, as it is explained in Fig. 4.13. However, not all these spatial spots s can be predefined, while changes can occur in that path $\Delta s^{[\alpha_j]}$. Furthermore, more than one elementary flow α_j may flow through a shared spatial spot s. Therefore, spots s, that are uniquely associated with a single elementary flow α_j, can be equipped with a digital scale SI-(5) dedicated to that elementary flow α_j. However, the size and surface of each spot s are carefully designed and realized to match the technical boundaries [55, 143, 254, 276]. Whenever such a spatial spot s is indefinable for a single elementary flow α_j, a common spatial spot s for multi elementary flows α is to be looked for. Such a common spatial spot s can be implemented in determining the mass of different elementary flow types j, if the temporal allocation t of each elementary flow α_j is unique and definable. This is, for instance, the case of lay-up activity over the mold within WSP, as Fig. 4.24 and Fig. 4.25 show. Therefore, the combination of MI-(1) or MI-(3) with MM-(1) facilitates realizing it.
Persons count: MM-(2)	Imaging sensors (cameras): SI-(1)	The number of persons can be recognized through a single or multiple cameras SI-(1). These solutions may serve both the person detection and counting methods, which are the MI-(2) and MM-(2) respectively. Here, it is essential to distinguish between person identification, persons counting, and labor work time measurement. Therefore, the methods MI-(2), MM-(2), and MM-(3) are implemented to serve these three aspects respectively. In MM-(2), only the counting of people is discussed. In practice, there are available SI-(1) with AI solutions, that serve all of these three methods by recognizing, counting, and measuring the duration of persons existence within the WS [171]. Based on that, it is concluded that MM-(2) depends on MI-(2).
Optical material item count: MM-(12)	Imaging sensors (cameras): SI-(1)	Similar to the persons counting in MM-(2), the number of items can be determined in MM-(12). While MI-(1) recognize an item, this method is useful for counting the magnitude of various items. For instance, it may count the FRP desired or rejected structures, FRP semi-finished structures as well as some ancillaries,that are used as pieces. In other words, any elementary flow with predefined shape per piece can be covered by MM-(12), whenever this method is technically applicable. Here, the pros and cons of applying MI-(1) are reflected on this method as well. In MM-(12), elementary flow items can be counted by a single camera or multiple of them. However, these cameras SI-(1) should operated by proper AI algorithms to match items characteristics. In practice, the same cameras may serve both visual recognition in MI-(1) and item counting in MM-(12) simultaneously.

MM	SM	Description and rating: pros and cons
Optical labor work duration measurement: MM-(3)	Multi imaging sensors (cameras): SI-(1)	In addition to person detection MI-(2) and counting MM-(2), the work duration of each labor is measured by a 3-dimensional optical scanning in MM-(3). Moreover, MM-(3) provides the spatial allocation combined with the temporal one. Here it is essential to distinguish between person detection and tracking. On the one hand, the first term is implemented for the identification of labor as MI. On the other hand, tracking is implemented here to determine the temporal duration and spatial path of the detected object [162, 243]. As it is mentioned previously, several scholars have studied the object detection. However, others such as Prasad et al. and Kalal et al. have covered all required aspects including detection, learning, and tracking [162, 243]. Therefore, these three stages of optical tracking are covered by MM-(3) to measure the labor work time. The main disadvantage of MM-(3) occurs when the detected spatial spot is covering only a part of the human body. Based on some available solutions of 3-dimensional optical scanning, it is difficult to detect a person if only a part of the body is sensed. From process modeling perspective, this can be the case of a very small WSP. Therefore, it is clear that MM-(3) depends on MI-(2) and MM-(2). To realize all of these methods, advanced imaging sensors SI-(1) can be used.
Thermal labor work measurement: MM-(8)	Thermal sensors (IR-camera): SI-(3)	As an alternative to MM-(3), thermal detection can be implemented to measure the work time duration of a labor in MM-(8). As it is mentioned previously in Tab. 4.8, MI-(5) and SI-(3) have been studied in literature. In this work, MM-(8) depends and is based on MI-(5), while no measurement can be realized without the human body thermal recognition. The thermal sensors, or as they are also called IR-cameras SI-(3), are implemented in detecting the labor work duration based on real-time detection of human body temperature MI-(5) in the WS. Temporal and spatial allocations of a labor or only part of his body can be detected too. Based on that, the occurrence time of a person is measured [138]. Nonetheless, this method is incapable of counting persons in the current version of SWS, which is an aspect that may be addressed in future versions.
Equipment performance time measurement: MM-(4)	Dedicated electricity meter: SI-(4)	As Tab. 4.8 explains, the equipment operating duration and energy consumption have been studied in literature. As it is discussed previously, equipment can be split into three groups. In MM-(4), only the machines are considered, while they are electrically operated. In the SWS, all machines are supplied with energy through dedicated electricity meters SI-(4). Therefore, their operating duration $\Delta t^{[v_i Q]}$ can be concluded from their performance based on measuring their electricity consumption. This is also discussed again in MM-(5). However, it is obvious that some machines have no, or as it is called a „*zero*“, performance with „*nonzero*“ power consumption. For such machines, the „*zero*“-performance consumption is to be defined. It is concluded here, that MM-(4) is associated with MI-(6) and MM-(5), while they are both realized by SI-(4).

MM	SM	Description and rating: pros and cons
Equipment bar- or QR-code time measurement: MM-(9)	Imaging sensors (cameras): SI-(1) and coded sticker: SI-(1a)	As it is discussed previously in this table, MM-(4) is applicable only to electrically operated equipment known as machines in this thesis. However, the operating time $\Delta t^{[v_i Q]}$ of two other groups of equipment is still to be measured. Therefore, MMs other that MM-(4) are suggested for both tools and molds. MM-(9) is one of these methods, which is based on MI-(3). Now, tools and molds operating duration may be concluded from their appearance as an occupation time. Practically, MM-(9) implements sophisticated AI algorithms that interpret the collected data from the imaging sensors SI-(1) about the visible coded stickers SI-(1a) and determine the tools operating durations. In addition, imaging sensors SI-(1) should be set up to cover all possible tracking angles. However, manually operated tools are moving objects within randomly covered surfaces. Furthermore, many of these tools have small surfaces. Therefore, it is difficult to guarantee a visual coverage of the coded stickers SI-(1a). On the other hand, molds are usually stationed on predefined positions, which enable prober SI-(1) and SI-(1a) setup. Therefore, MM-(9) is implemented to measure the operating duration $\Delta t^{[v_i Q]}$ of molds and possibly to monitor the tools in their container or trolley but not in a WS.
Equipment optical time measurement: MM-(10)	Imaging sensor (camera): SI-(1)	In MM-(10), tools are optically detected by the visual recognition. Here, it is essential to decide whether each tool item separately or the overall tools kit is studied. However, MM-(10) implementation depends on the capability of visually recognizing these tools in predefined spatial points s within their path $\Delta s^{[v_i Q]}$. The spatial points s can be observed by the imaging sensors SI-(1). These points s should be associated with the operating duration $\Delta t^{[v_i Q]}$, while spots s related to $t_a^{[v_i Q]}$ and $t_b^{[v_i Q]}$ are to be specified. For a high maturity process, a tools container can include such spots for each item as dedicated marked or foam cut storages. In that case, a tool item in such process leaves the container at the beginning $t_a^{[v_i Q]}$ of that operating duration $\Delta t^{[v_i Q]}$ and turns back at its end $t_b^{[v_i Q]}$, as Fig. 4.12 previously explains. This method is; however, associated with and depending on MI-(1).
Process duration: MM-(6)	All sensor nodes (SIs and SMs)	Based on the timestamps t of the collected initial data $\hat{\alpha}_{ij}$, the process duration Δt_{tot} as well as the duration of each UP Δt_i can be determined in MM-(6). This is realized through subjecting every collected initial data $\hat{\alpha}_{ij}$ from all SIs and SMs to a temporal allocation t. These timestamps t are unified and synchronized for all SIs and SMs in the system to enable their temporal correlation [192]. Hence, each collected initial data $\hat{\alpha}_j$ is to be assigned to a point of time t in the standard synchronized official time at the process geographical location. Based on that, the earliest time point t of initial data $\hat{\alpha}_{ij}$ collected about the first elementary flow α_{ij} in the assessed UP i is considered as the UP i beginning time t_{i_a}, as Fig. 4.12 previously shows. Similar to that, the temporal allocation t of latest initial data $\hat{\alpha}_{ij}$ about the last elementary flow α_{ij} is considered as the end t_{i_b} of that UP i. Therefrom, Δt_i and similarly Δt_{tot} can be calculated by Eq. 4.23. However, time assignment interval depends on the measurement frequency. MM-(6) depends on all other implemented MIs and MMs.

MM	SM	Description and rating: pros and cons
Equipment operating time based on weight measurement: MM-(11)	Dedicated digital scale: SI-(5)	Besides MM-(9) and MM-(10), the weight measurement in MM-(11) may be applied to measure the operating time of tools and molds. Similar to MM-(10), MM-(11) is only applicable for mature processes with planned activities, as it is explained previously in chapter 3. In such process, tools and molds are departing their containers or storages before performing the planned activities and then returning back to their specific compartments after them. Therefore, MM-(11) suggests two possible solutions. On the one hand, a dedicated weight sensor is to be integrated in the predefined compartment of each tool item. This first solution assumes that every item in the tools kit has its own containing place or compartment. Such weight sensor can be any pressure based signal generator and not necessarily a digital scale. In this solution, weight magnitude of each item is irrelevant, while only item existence and disappearance are decisive. The second solution is realized by integrating dedicated digital scales for the entire tools kit container or for each layer of it. For each tool item, the departure of it from storage container or trolley is recognized by its missing specific weight. Furthermore, the absence duration is measured to calculate the operating time $\Delta t^{[v_i Q]}$. However, there are technical difficulties in applying this second solution for tools with very similar specific weights. For instance, a simultaneous departure or arrival of more than an item can hinder this solution, as it is discussed before for MI-(7) in Tab. 4.8. Therefore, the second solution can be applied to validate other methods, but not as a standalone method. In conclusion, it is obvious that MM-(11) is associated with MI-(7) and depends on it.
Equipment operation energy: MM-(5)	Dedicated electricity meter: SI-(4)	Besides measuring the operating time of electrically operated machines, the electricity consumption itself should be measured. As it has been mentioned previously in Tab. 4.8, an energy consumption assessment has been thoroughly studied in literature. In MM-(5), the equipment operating energy is measured by electricity meters SI-(4). In addition to their use in MI-(6) and MM-(4), the same meters SI-(4) can serve MM-(5) as well. While all machines are supplied with energy through dedicated electricity meters SI-(4), the consumption of each one can be directly measured. Moreover, the overall electricity consumed by all machines is also measured by these meters SI-(4). In this work, commercially available sensor nodes SI-(4) are implemented in the SWS.

It is noticeable from Tab. 4.8 and Tab. 4.9 that the same SIs are utilized as SMs. In addition to the MMs and SMs discussed in Tab. 4.9, other methods and their sensor nodes may be adopted in the SWS. In practice, the selection of a sensor node for measuring material magnitude is based on the material state. For instance, liquid and gas materials can be measured by mass flow sensors [108, 133]. Such sensors provide the measurement to compute their mass flow based on their density [316]. However, digital scales SI-(5) are solely applied to the measurement of all materials within the current version of the SWS. This thesis intends to implement existing sensor nodes from various fields to serve the time-dependent eco-efficiency assessment for FRPs production in general and the real-time data collection in specific. It means that the initial technologies and functionalities of these sensor nodes remain outside the scope of this work, while they may be protected by their owners or inventors. Nonetheless, commercial hardware and software solutions are used to accommodate such legal aspects, while computerized models are developed internally to communicate these sensor nodes in real-time.

Based on the previously illustrated LCI procedures in Fig. 3.15 within chapter 3, the SWS functionalities are integrated in these procedures to achieve the real-time LCI, as Fig. 4.26 suggests.

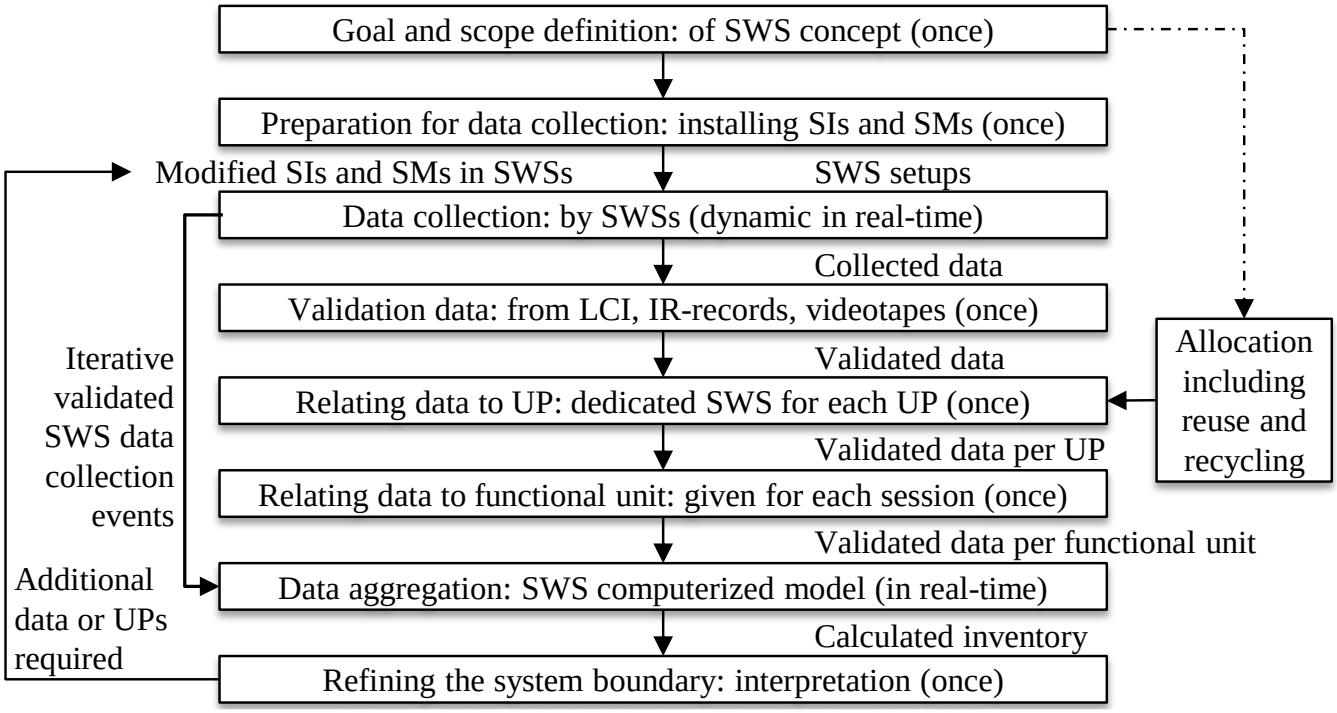

Figure 4.26 SWS integration within LCI procedures

Fig. 4.26 modifies the conventional procedures of LCI to serve the SWS requirements and integrates the SWS functionalities to perform the real-time LCI by the SWS sensor nodes. As Fig. 4.26 shows, goal and scope definition, preparation, and validation are performed only once. Then validated data is collected from each SWS, which is dedicated spatially and temporally to its UP. While the SWS concept is generic for any functional unit with measurable elementary flows, such product is predefined before assessing any process. With the help of real-time data processing, data aggregation is performed automatically by the computerized model of SWS. Based on the validation results and the interpretation between various development phases, the system boundary is refined to include or exclude some data. Based on such refining, the methods as well as their sensor nodes are modified to realize the proper SWS setup. In this thesis, a selection of MIs and SIs from Tab. 4.8 as well as MMs and SMs from Tab. 4.9 is adopted. These methods and sensor nodes are then implemented in realizing SWS for the case study in chapter 5.

Temporal and spatial assignment

The concept of SWS is based on two main cornerstones. These are the real-time and on-site capabilities in data collection. As it has been discussed before in chapter 3, real-time is associated with some technical aspects. These aspects include the data collection and processing frequencies, which are also called time intervals, as well as the synchronization between different sensor nodes. This time interval is crucial in both data collection from each sensor node and its following processing, which may take a place in an assigned server or cloud. However, there is a wide range of methods and sensor nodes combined in Tab. 4.8 and Tab. 4.9 to realize the SWS concept. These MIs, MMs, SIs, and SMs are subjected to restricted data collection and processing frequencies due to their technical limitations. Each method is correlated with processing frequency, that is based on the capabilities of its commercially available sensors. This leads to a deviation in the frequencies between these different adopted methods in the SWS concept.

In practice, the lowest frequency is the most crucial one, while it decides the highest possible frequency of the time-dependent eco-efficiency assessment. In other words, it is technically impossible to realize a time-dependent assessment with a frequency that is higher than its lowest data collection frequency. As a real-time concept, the time interval of data collection in the SWS is to be minimized to the lowest possible period. However, results frequency is less critical for the time-dependent assessment, while decision-makers are used to receive delayed results due to the processing and preparation efforts. Therefore, conventional approaches are still have much longer time interval in comparison to the approximately seconds to minutes delay required in the novel approach of time-dependent assessment. While such temporal allocation t plays a decisive role in performing many MIs and MMs, a time interval is selected based on the sensor nodes restrictions in each case study. In this standard time interval, the initial data $\hat{\alpha}$ is updated from the sensor nodes. For all measured elementary flows α_j, unified timestamps are provided. This offers a temporal correlation between the initial data $\hat{\alpha}$ from all sensor nodes, which is required for a sufficient data processing. For the different UPs in the process, each UP i has also temporal allocation and duration in a predefined sequence within the process.

On the other hand, the on-site approach is obvious in the SWS concept, while the data must be collected from the WSs. However, such application is associated with the assessed elementary flows α_{ij}, as it is previously illustrated in Fig. 4.13. In practice, the sensor nodes are set up to collect the data of each flow α_{ij} on its path $\Delta s^{[\alpha_j]}$. Therefore, the sensor nodes can be either installed on these paths $\Delta s^{[\alpha_j]}$ or on other spatial spots s, that are correlated with these paths. Again, this depends on the different available commercial solutions and their setups. To distinguish between the different UPs, this spatial allocation s is defined holistically by identifying the WS of each UP i, to which the sensor nodes belong. The SWS concept also suggests an independent SWS_i for each spatially distinguishable UP i.

Nonetheless, the selection of exact applied methods and sensor nodes in each case study is the most decisive aspect to that time interval and spatial allocation. Regardless the initial planning and executing efficiency, the spatial and temporal allocations of WSs are assessed and assigned to the elementary flows α_{ij} neutrally as they are, whereas many production operating aspects may impact such type of efficiency. However, this subject is beyond the scope of this thesis. The SMs are measuring the magnitude of elementary flows α_{ij} in timestamps t to associate these magnitudes with their types j, while the types are determined by the SIs. Moreover, these SMs are assigned in predefined spatial spots s for the same purpose. Therefore, all elements of input information flow I_α are made available to process them for the assessment model EEAM. These methods and sensor nodes for both identification and magnitude measurement of the elementary flows α_{ij} are associated with the form of these flows, which is either matter or energy.

Technically, the uniqueness of temporal as well as spatial allocation is crucial for many MIs and MMs. To reduce the amount of implemented SIs and SMs in an efficient SWS_i, the behavior of elementary flows α_{ij} throughout their possible spatial allocation paths can be determined. Based on these determinations, the most sufficient spatial allocations for the SIs and SMs are defined. In the early conceptual modeling of a SWS_i, SIs and SMs have been installed to measure the elementary flow α_{ij} in different spatial spots. Only if a change occurs to that elementary flow α_{ij} between these spots on its path $\Delta s^{[\alpha_j]}$, then a sensor node is required post to that change spot. Here, it is essential to mention that only magnitude change is considered here. In this work, no change in elementary flow type is expected or considered during the same measurement session of the same elementary flow α_j, while this restriction has been carefully covered by the SWS concept previously.

However, some elementary flow types j may have no unique temporal and spatial allocations within the system boundary of the WS. In this case, this system boundary is expanded to cover any unique temporal and spatial allocation of this type j all the way to its initial sources. For instance, material elementary flows can be tracked from their storages. However, this is applicable only when no quantitative or qualitative changes occur

on these matters during the transportation from these storages to the WS. This is applied also in energy case to the electricity supply lines, whereas meters may be installed far from the WS, whenever no measurement deviation occurs. More examples and details about some functionalities within the SWS have been provided in the previous works of Al-Lami, Al-Lami et al., Schachinger and Al-Lami, as well as Rudolf and Al-Lami [6, 7, 11, 264, 271].

4.3 DSSs for Time-Dependent Eco-Efficiency Assessment

After a thorough explanation of the SWS as a real-time data collection concept, the thesis contribution to the time-dependent eco-efficiency assessment model is discussed in this section. It includes the eco-efficiency assessment model and it covers the economic and ecological aspects separately as well. Then, the subject of real-time data processing is discussed to explain the involved data structures and DBs. In this work, the EEAM is implemented as a DSS to realize the time-dependent assessment. Therefore, the functionality and structure of EEAM are illustrated. Moreover, it is essential to understand the EEAM mathematical model. In the last part of this section, the validation approach of eco-efficiency assessment is studied.

4.3.1 Eco-Efficiency Models

The eco-efficiency ξ has been thoroughly studied previously in chapter 3. In this thesis, the eco-efficiency ξ is the ratio between the retained earnings and produced ecological burden. On the one hand, the retained earnings represent the gained economic benefit in this thesis. Initially, such profit is meant to reflect that benefit throughout the entire life-cycle. On the other hand, the ecological burden is considering the life-cycle in its entity as well. Technically, several impact categories are contained in the ecological burden. However, only the global warming is considered in this work. From each of these holistic aspects, a domestic KRI can be defined and assessed separately. In a limited scope, retained earnings r and ecological burdens β can be studied from a selective point of view in a cradle-to-gate or even a gate-to-gate assessment, as Eq. 4.64 suggests.

$$\xi = r/\beta \tag{4.64}$$

As it is shown in Eq. 4.65, eco-efficiency ξ is the ratio between retained earnings of process outputs $r^{[Y]}$ and produced burden of process inputs $\beta^{[X]}$.

$$\xi = \frac{r^{[Y]}}{\beta^{[X]}} \tag{4.65}$$

However, this can be redefined based on the equilibrium in Eq. 4.60. For the considered life-cycle phase, an impact θ is to be determined in both aspects. Therefore, direct cost δ and carbon footprint β are respectively describing the economic and ecological impacts θ of the assessed case study. Still, increasing the benefit without direct cost or carbon footprint reduction increases the value of ξ in Eq. 4.65 but it is enhancing no eco-efficiency whatsoever. In other words, SDs must seek the reduction of both ecological and economic impacts or one of them when the second one is constant. Although they are excluded from the thesis scope, some special cases for such general SDs are discussed later in chapter 6 and chapter 7.

As it is mentioned previously, the assignment of CSFs and their levels may be subjected to different perspectives and interpretations. However, these CSF levels are considered for the clustered impacts of elementary flows, their subsets, the including UPs, and the total process in this thesis.

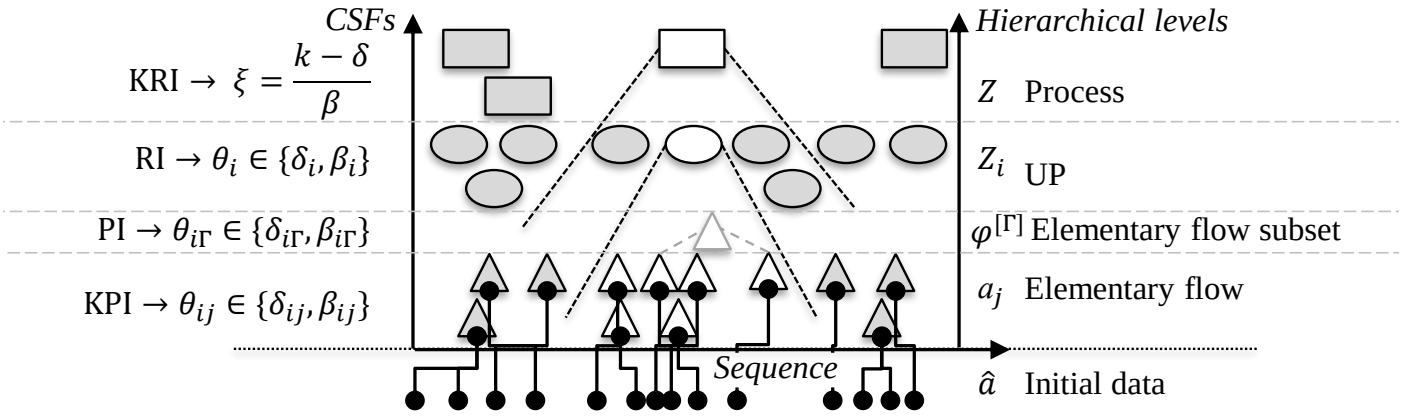

Figure 4.27 Process hierarchical levels and CSFs

Based on Fig. 4.14 and Fig. 4.20, Fig. 4.27 summarizes some of the possible forms of layered time-dependent eco-efficiency assessment, while other combinations of these layers and parts of them are still possible within the EEAM, as chapter 6 later shows.

Economic benefit model

For the eco-efficiency assessment, the retained earnings r are the output economic benefit of the selected life-cycle phase, which can be calculated by Eq. 4.66.

$$r = sr - c - \delta \tag{4.66}$$

With r = retained earnings in monetary unit (€); sr = sales revenue (€); c = all other indirect and non-process costs from other considered life-cycle stages (€); δ = direct cost of process (€).
Here, both sr and c are allocated in other life-cycle stages, which are beyond the scope of the time-dependent assessment in production. Therefore, these retained earnings r are; however, reduced in this thesis to be based solely on the impact of direct cost δ. While all other variables, that are affiliated with the retained earnings r, are beyond the scope of the thesis and treated as given constants. For simplicity, a constant value k is assumed to represent both sr and c in Eq. 4.67.

$$k = sr - c \tag{4.67}$$

k is describing the total sales revenue excluding all non-process costs as a given constant in monetary unit (€). This assumption from Eq. 4.67 is then applied to Eq. 4.66 in order to focus on the direct cost δ of the assessed process in this thesis, as it is explained in Eq. 4.68.

$$r = k - \delta \tag{4.68}$$

Such constant k possibly exists in reality, while some original equipment manufacturers offer their subcontracting suppliers such magnitude of total sales revenue excluding all non-process costs. Nonetheless, these constants have different values when an assessment is carried out on the UP i level. First, the sales revenue sr_i represents the market value of the semi-finished product $\hat{u}_{iP}$ generated by the UP i. Second, c_i represents all other indirect and non-process costs from other considered life-cycle stages associated with that $\hat{u}_{iP}$ and not necessarily the final finished product u_{mS}. Finally, the retained earnings r_i vary between the UPs as a result of

the first and second conditions, while UP_{x1} may have different retained earnings than UP_{x2}. Therefore, each UP i has its constant k_i that is calculated as $k_i = sr_i - c_i$ based on Eq. 4.67.

For any elementary flow α_{ij} from any type j in UP i, its direct cost δ_{ij} can be calculated as it is shown in Eq. 4.69.

$$\delta_{ij} = \alpha_{ij}\gamma_{ij} \tag{4.69}$$

With δ_{ij} = direct cost of elementary flow α_{ij} in monetary values; α_{ij} = magnitude of elementary flow of type j in physical units; γ_{ij} = economic characterization factor in monetary unit per each physical unit.
Analog to Eq. 4.28, the elementary flow α_{ij} is measured by its specific unit, while its economic characterization factor γ_{ij} is expressed by the price per that unit. Technically, these economic characterization factors γ_{ij} may vary based on the goal and scope of the assessment. Based on the hypothesis stated previously in Fig. 4.6 as a part of the conceptual modeling, the economic impact of direct cost δ can be modeled as well. The direct cost δ of the manufacturing process is a part of numerous economic impacts from the life-cycles of the elementary flows as well as the product itself including the different phases and their belonging processes. This direct cost δ may be simplified in Fig. 4.28.

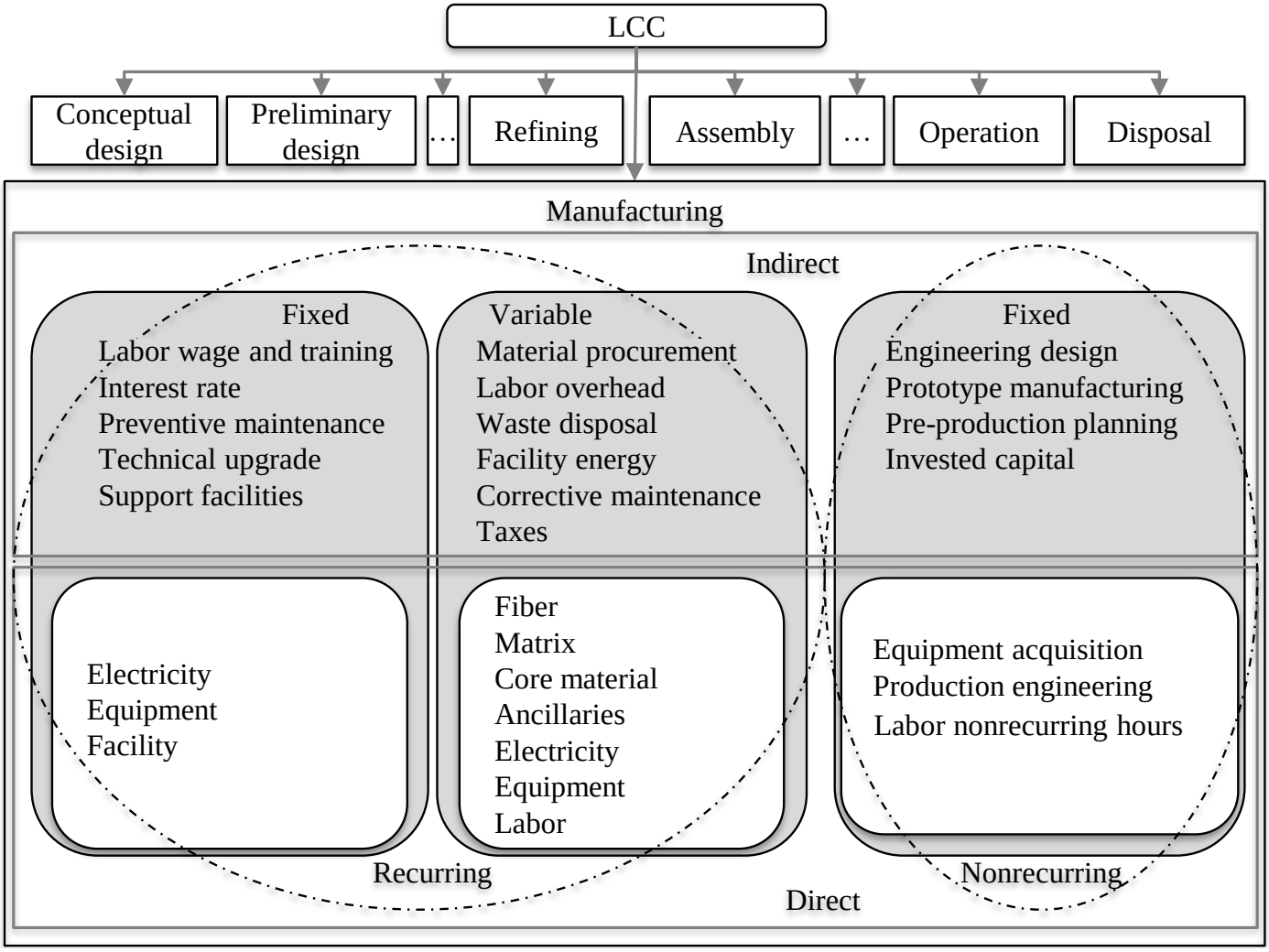

Figure 4.28 Categorization of economic impacts within LCC: direct cost in manufacturing

In practice, there are several methods, approaches, and even standards, which may be adopted in breaking down a KRI [324]. Regardless of the adopted approach, no fraction of that KRI is to be neglected or redundantly over considered in the assessment. Moreover, unless it is clearly declared in the goal and scope of the assessment,

every neglected category should be considered in the cut-off-criteria [152]. The same approach of classifying the economic impacts δ_Γ of input elementary flow sets $\varphi^{[\Gamma]} \subseteq V$ can be applied to assess the economic impacts δ_Γ of output elementary flow sets $\varphi^{[\Gamma]} \subseteq U$.

The economic impact represented by the direct cost δ is calculated by the summation of its categories in Fig. 4.28. Each category is associated with several parameters to measure the related economic characterization factors γ. These factors γ are calculated with a predefined level of detail based on initial data about them $\hat{\gamma}$. Such parameters $\hat{\gamma}$ are provided in a specific set of temporal, geographical, and technical boundaries. That includes decisive issues such as transport, amount, storage, insurance, purchase, check and approval, as well as taxes [170]. The in Appx. B listed parameters are implemented in calculating each economic factor γ, as Eq. 5.30 in chapter 5 later shows. In practice, these factors are dynamic in their nature, whereas the time value of money, discount rate of supplied elementary flows, transportation, tax rates, wage rates, and many other aspects may be considered. However, the values of different economic characterization factors γ_{ij} are considered as static given values in this thesis.

Ecological burden model

As it is the case of direct cost δ, the ecological burden β is required to assess the cradle-to-gate eco-efficiency ξ. Here, the ecological burden of an elementary flow α_{ij}, which is represented by its carbon footprint β_{ij}, is calculated in Eq. 4.70.

$$\beta_{ij} = \alpha_{ij}\varepsilon_{ij} \tag{4.70}$$

As it is previously hypothesized, the break-down conceptual model of the global impact θ

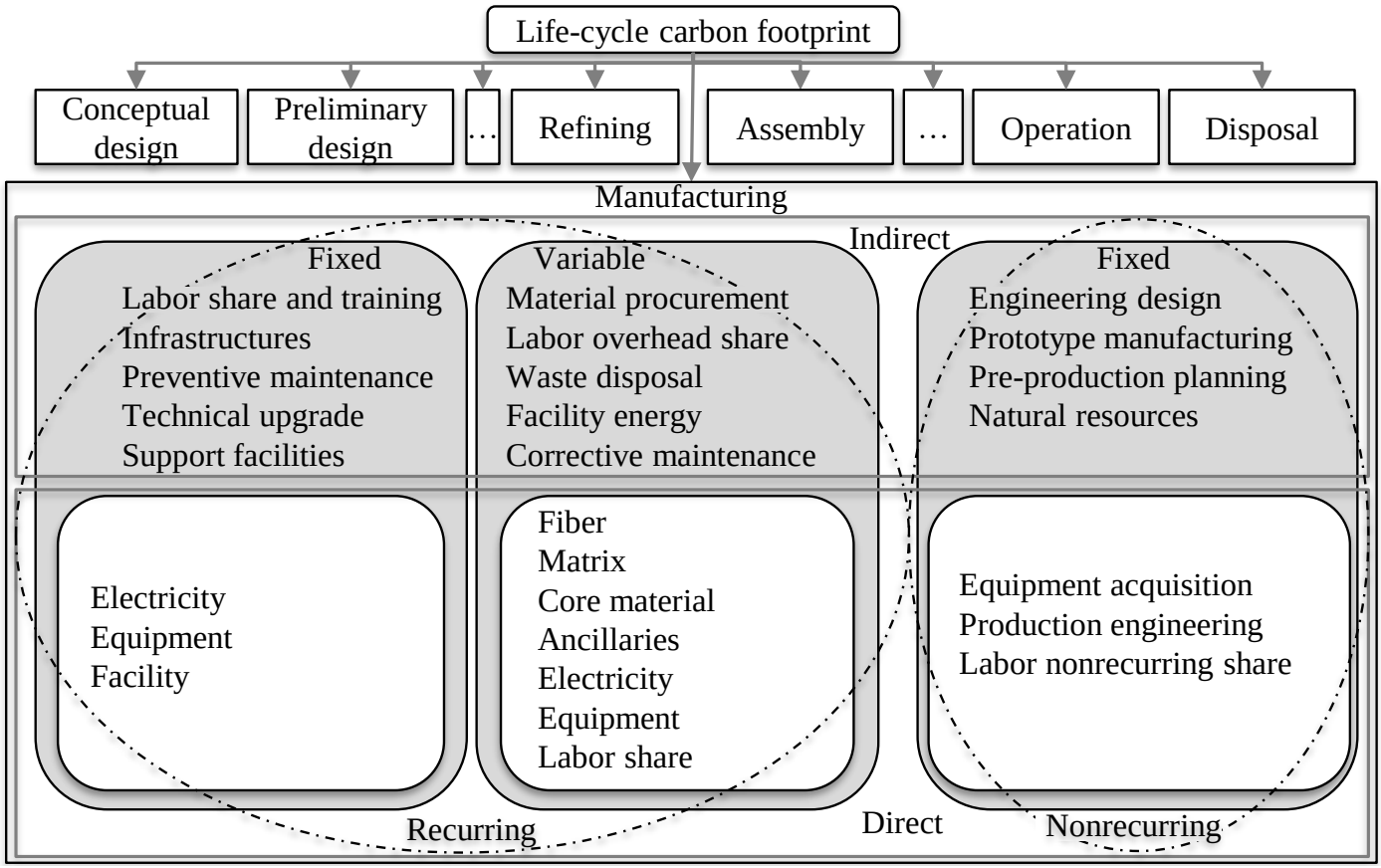

Figure 4.29 Categorization of carbon footprint

in Fig. 4.8 is applicable for the carbon footprint β as well. This suggests a novel approach of categorizing the ecological burden in the same economic categories, as Fig. 4.29 explains. Similar to the approach in Fig. 4.28, Fig. 4.29 categorizes the carbon footprint β into direct, indirect, recurring, nonrecurring, fixed, and variable impacts. In literature, the indirect as well as direct ecological impacts β of labor work are rarely considered in the subject of LCA [73]. For example, each employee has a carbon footprint per day including food, transportation, water usage, and other activities, which may be related to the direct work hours in producing the demanded product. On the other hand, the working in office to prepare the production environment is also related with these activities and other ones such as computer usage.

Similar to the economic characterization factors γ_{ij}, the values of ecological ones ε_{ij} in the EEAM-DB are provided within Eq. 5.31 in chapter 5 and explained in Appx. B. These factors ε are derived from initial data associated with them $\hat{\varepsilon}$. Again, including the output subsets in Fig. 4.28 and Fig. 4.29 or considering them in separated illustrations is possible. Based on the economic and ecological assessment models, the eco-efficiency can be calculated based on Eq. 4.65, as it is illustrated in Eq. 4.71.

$$\xi = \frac{k - [A][\check{\Lambda}^{[A]}]}{[A][\check{\check{\Lambda}}^{[A]}]} \tag{4.71}$$

While both economic and ecological units such as (€) and (kg CO_2) respectively are dimensionally inhomogeneous, the final value can be represented only in the unit of (€/kg CO_2).

Furthermore, the detailed mathematical models of assessing the direct cost of the process and its carbon footprint are provided later in this chapter as a part of describing the EEAM mathematical model.

4.3.2 Data Processing

In its general meaning, information I is a global term that covers all facts acquired or available about a subject in different fields [76, 223, 337]. Technically, it is not necessarily relevant to the assessed KRIs directly or indirectly. However, only the relevant information I is determined and discussed in this work. Now, input information flows I_a are assumed to include all existing initial data that needs to be retrieved by the SWS as an information retrieval system [223]. On the other hand, output information flows I_b are assumed to be the results of time-dependent assessment. These output knowledge flows I_b are generated by the EEAM based on the initial data. In this work, the initial data is gathered and processed into information by the SWS, as it is previously shown in Fig. 4.22. Here, the initial collected data about elementary flows $\hat{\alpha}$ is processed by the SWS. The initial data about the characterization factors $\hat{\lambda}$ is; however, stored and structured in the EEAM-DB. Nonetheless, the characterization factors λ are given as constants in this thesis. Still, some initial data parameters of selected characterization factors are provided later in Appx. B.

Assessment data structure

In order to achieve the data layers in Fig. 4.4, the initial data $\hat{\alpha}$ of every relevant elementary flow is gathered in the SWS-DB. On the other hand, the initial data parameters for their characterization factors $\hat{\lambda}$ are collected in the EEAM-DB. Technically, signals from the sensor nodes are generally preprocessed in models that are provided by their developers as software solutions. These signals are communicated continuously in real-time by these computer-based models and converted into initial data $\hat{\alpha}$. As a part of the SWS concept, the SWS computerized model is connecting these different software solutions and gathering the initial data $\hat{\alpha}$ in unified timestamps. Here, data structures are adopted to handle the elementary flows α_j within SWS-DB and the

characterization factors λ_j within the EEAM-DB. However, the covered parameters of initial data are associated with the included manufacturing techniques in this thesis. While the efficient DBs utilization is supported in the computerized models of this work, the context expansion of data coverage is also enhanced by version based DBs. This aims to include all possible case studies and their process scenarios from various projects.

SWS-DB for elementary flows α_j and their initial data $\hat{\alpha}_j$

In order to identify an elementary flow α_j, it is required to have a DB that includes the parameters of all possible types j, their identifications j, and their relevant characteristics. Practically, all these parameters of initial data $\hat{\alpha}$ are gathered in the SWS-DB. This SWS-DB covers data evolution stages in Fig. 4.22 from the signals to the assessment inputs. The SWS-DB requires the inputs initial data to carry out the real-time LCI and provides data as outputs for the time-dependent LCIA. To be covered by the SWS-DB, the initial data should be necessary for the identification or measurement. Technically, such parameters depend on the selected methods and sensor nodes. In the SWS-DB, the initial data $\hat{\alpha}$ covers different criteria, that are associated with the real-time measuring methods and sensor nodes.

As it is previously mentioned, an elementary flow α_j is an element in its containing subset $\varphi^{[\Gamma]}$. The element order in each subset $\varphi^{[\Gamma]}$ is associated with the elementary flow types j. Here, each single flow α_j has a unique identification number (ID) formed as the subset number followed by the elementary flow order within it as $(\varphi^{[\Gamma]}j)$. Again, the sets are exceptionally considered to have ordered elements of elementary flows in this thesis. Although the component j is ideally expressed in single digits, in this thesis the digit dimension is expanded to cover the different subsets $\varphi^{[\Gamma]}$ and the types j as $10 < \varphi^{[\Gamma]} < 999$ and $01 < j < 999$. Still, more digits might be thinkable when the types j in $\varphi^{[\Gamma]}$ exceeded the 999 variables. The relevant characteristics as initial data $\hat{\alpha}$ for each SI or SM are adopted from understanding the functionality of these sensors.

Within the SWS-DB, a generic structure is introduced for all possible elementary flows α_j. This structure is realized by considering the different classification criteria of all possible elementary flows α_j in its category $\varphi^{[\Gamma]}$. In the SWS, SIs are generating their relevant initial data $\hat{\alpha}$ to be processed by the SWS computerized model. Simultaneously, the associated SMs are measuring the magnitudes of these identified elementary flows α_j. These SMs are also sending their initial data $\hat{\alpha}$ to the model for processing and interpretation. Based on processed data, the EEAM is parameterized with identification oriented magnitude measurement of the relevant elementary flows α_{ij}.

In this work, the SWS computerized model consists of five main software modules. The first module is processing the collected initial data for the visual recognition MI-(1) and QR-code scanning MI-(3) from the digital cameras. As it is discussed in the previous work of Schachinger and Al-Lami, the visual recognition MI-(1) and QR-code scanning MI-(3) lean on an internally developed computerized model that requires initial data, which is included in the SWS-DB. This module is monitoring the digital camera inputs and identifying the relevant elementary flows in real-time based on the SWS-DB inputs then assign them in the SWS-DB outputs. Therefore, this module is considered as the most sophisticated one in the SWS computerized model [271]. In addition, the IR-camera related MIs and MMs have been developed internally to detect and measure the labor work. This module is partially processing the data generated by the IR-camera based on its software settings and its provided application programming interface. However, other MIs and MMs are operating mainly in the supplier software solutions such as all the digital scale and the electricity meter related methods. Therefore, the third module is collecting the initial data from the digital electricity meter through similar application programming interface. In the fourth one, the initial data from the digital scales software is collected through its interface, while all these modules follow unified timestamps. The fifth module communicates with the four

previous ones and brings the final data of all discussed elementary flows together with unified timestamps after allocating them to their types.

In the SWS-DB, materials can be distinguished due to their matter forms into the simplified solid, liquid and gaseous states. For a material subset $\varphi^{[\Gamma]} \subseteq J^{[\mu]}$, this exact classification criterion is essential to define the proper sensor nodes, as it is previously explained. Furthermore, the previously discussed MIs and SIs from Tab. 4.8 are assigned for each subset of matter elementary flow $\varphi^{[\Gamma]} \subseteq J^{[\mu]}$ according to its form based on Tab. 4.6. In Tab. 4.10, these subsets $\varphi^{[\Gamma]}$ and their belonging elementary flows α_j are assigned to their IDs:$(\varphi^{[\Gamma]} j)$. They are also related to the appropriate MIs as well as SIs. Therefore, the identification numbers of the exact elementary flow types j are replaced by stars $(**)$ to represent their possible variables in Tab. 4.10 and Tab. 4.11.

Table 4.10 ID:$(\varphi^{[\Gamma]} j)$, MIs, and SIs for matter elementary flows $\alpha_j \in \varphi^{[\Gamma]}, \varphi^{[\Gamma]} \subseteq J^{[\mu]}$

State	$\varphi^{[\Gamma]} \subseteq J^{[\mu]}$	ID:$(\varphi^{[\Gamma]} j)$	MIs * described below	SIs * described below
Solid	Fiber material $\varphi^{[F]}$	60∗∗ or 80∗∗	MI-(7, 1, or 3)	SI-(5, 1, or 1 and 1a)
	Core material $\varphi^{[C]}$	100∗∗	MI-(7, 1, or 3)	SI-(5, 1, or 1 and 1a)
	Ancillaries $\varphi^{[R]}$	90∗∗	MI-(7, 1, or 3)	SI-(5, 1, or 1 and 1a)
	FRP desired structure $\varphi^{[S]}$	16∗∗	MI-(1)	SI-(1)
	FRP semi-finished structures $\varphi^{[P]}$	17∗∗	MI-(1)	SI-(1)
	FRP fragment waste $\varphi^{[W]}$	19∗∗	MI-(7 or 1)	SI-(5 or 1)
	Fiber waste $\varphi^{[G]}$	65∗∗ or 85∗∗	MI-(7 or 1)	SI-(5 or 1)
	Core material waste $\varphi^{[N]}$	105∗∗	MI-(7 or 1)	SI-(5 or 1)
	Ancillaries waste $\varphi^{[O]}$	95∗∗	MI-(7 or 1)	SI-(5 or 1)
	Reusable ancillaries $\varphi^{[B]}$	90∗∗	MI-(7, 1, or 3)	SI-(5, 1, or 1 and 1a)
Liquid	Matrix $\varphi^{[M]}$	70∗∗	MI-(7)	SI-(5)
	Ancillaries $\varphi^{[R]}$	90∗∗	MI-(3)	SI-(1 and 1a)
	Matrix waste $\varphi^{[D]}$	75∗∗	MI-(7)	SI-(5)
	Ancillaries waste $\varphi^{[O]}$	95∗∗	MI-(3)	SI-(1 and 1a)
	Reusable ancillaries $\varphi^{[B]}$	90∗∗	MI-(3)	SI-(1 and 1a)
Gas	Ancillaries $\varphi^{[R]}$	90∗∗	MI-(3)	SI-(1 and 1a)
	Ancillaries waste $\varphi^{[O]}$	95∗∗	MI-(3)	SI-(1 and 1a)
	Reusable ancillaries $\varphi^{[B]}$	90∗∗	MI-(3)	SI-(1 and 1a)

* MI-(1): visual recognition MI-(3): bar- or QR-code scanning MI-(7): material and tool identification SI-(1): imaging sensor (digital camera) SI-(1a): coded sticker SI-(5): dedicated digital scale

Here, the subsets of input elementary flows are recognized with a number that is followed by a „*zero*“. For instance, the matrix subset $\varphi^{[M]}$ is identified by ID:70∗∗. On the other hand, their waste types as output subsets $u_\tau \in \varphi^{[\Gamma]}$ are identified with numbers followed by the number 5. For example, matrix wastes in $\varphi^{[D]}$ have the identification of ID:75∗∗ in the SWS-DB. However, reusable ancillaries $\varphi^{[B]}$ are exceptionally identified like input flow subsets. As it is shown in Tab. 4.10, the fiber subset $\varphi^{[F]}$ is distinguished into dry-fiber with the ID:60∗∗ or prepregs with the ID:80∗∗.

Similar to the approach in Tab. 4.10, the energy elementary flows $\alpha_j \in J^{[\epsilon]}$ are identified and listed due to their various forms in the SWS-DB. For each elementary flow $\alpha_j \in J^{[\epsilon]}$, an identification number ID:$(\varphi^{[\Gamma]}j)$ is stipulated. Each ID:$(\varphi^{[\Gamma]}j)$ is assigned to a unique elementary type j, while each energy type j should have a single energy form during the measurement. Furthermore, the MIs and their applied SIs are assigned to each subset of energy elementary flow $\varphi^{[\Gamma]} \subseteq J^{[\epsilon]}$ in Tab. 4.11.

Table 4.11 ID: $(\varphi^{[\Gamma]}j)$, MIs, and SIs for energy elementary flows $\alpha_j \in \varphi^{[\Gamma]}, \varphi^{[\Gamma]} \subseteq J^{[\epsilon]}$

State	$\varphi^{[\Gamma]} \subseteq J^{[\epsilon]}$	ID:$(\varphi^{[\Gamma]}j)$	MI * described below	SI * described below
Electrical	Electricity $\varphi^{[T]}$	10**	MI-(6)	SI-(4)
Mechanical	Labor $\varphi^{[L]}$	20**	MI-(5 or 2)	SI-(3 or 1)
Conversion	Equipment $\varphi^{[Q]}$	40**	MI-(6, 7, 1, or 3)	SI-(4, 5, 1, or 1 and 1a)
	Facility $\varphi^{[\Delta s]}$	30**	All	All

* MI-(1): visual recognition MI-(2): person detection MI-(3): bar- or QR-code scanning MI-(5): person thermal detection MI-(6): equipment dedicated identification MI-(7): material and tool identification SI-(1): imaging sensor (digital camera) SI-(1a): coded sticker SI-(3): thermal sensors (IR-camera) SI-(4): dedicated electricity meter SI-(5): dedicated digital scale

The selected energy states in Tab. 4.11 are distinguished based on the previously discussed forms in Tab. 4.7. In Tab. 4.11, both equipment and facility electricity consumptions are considered in the assignment of suitable MIs and SIs under the electrical state. However, a facility consumption has an ID:$(\varphi^{[T]}\varphi^{[\Delta s]}j)$, while the equipment electricity consumption ID is structured similarly as ID:$(\varphi^{[T]}\varphi^{[Q]}j)$. For ID simplicity, the „*zeros*“ in facility and equipment subsets identifications can be eliminated in this special case of electricity consumptions. Nonetheless, the facility electricity consumption may be combined partially or totally with its occupation impact in the characterization factor $\lambda_{\Delta s}$.

In this thesis in general and specifically in Tab. 4.11, the main functionality of equipment is assumed to be the energy conversion from a state to another. Based on that assumption, any equipment performance is considered under the conversion criterion. Based on another assumption in Tab. 4.7, the labor work is handled as mechanical energy. The total occupation time Δt_{tot} of the entire facility area Δs_{tot} is calculated by measuring the used area during the occurrence of every associated elementary flow α_j in it. As it has been previously illuminated, an inefficient facility utilization is to be covered as well. Exceptionally, $\varphi^{[\Delta s]}$ is considered within energy conversion category. In this thesis, the SWS$_i$ is implemented to determine all associated elementary flows α_{ij} of the various UPs i in FRP manufacturing process in real-time.

By all SWSs, the relevant variables of matrix $[A]$ are determined dynamically based on the gathered initial data $\hat{\alpha}_{ij}$. To keep up with the dynamic expansion and development of SWS-DB structure and coverage, a version control is adopted. In its current version, the SWS-DB is implementing different DB solutions including MySQL as an open-source relational DB management system [271]. However, a combination of case based selected SIs and SMs from Tab. 4.10 and Tab. 4.11 is selected for the studied process, as it is explained later in chapter 5.

EEAM-DB for characterization factors λ_j and their initial data $\hat{\lambda}_j$

To enable the communication between the EEAM and SWS, the EEAM-DB and SWS-DB should be compatible. Therefore, the previously introduced IDs are adopted in the EEAM-DB, which accommodate the SWS-DB structure as well. However, the EEAM-DB is enhanced to include the characterization factors λ_j and some

major parameters affiliated with them as initial data $\hat{\lambda}_j$. Unlike the elementary flow initial data $\hat{\alpha}_j$, the initial data of a characterization factor $\hat{\lambda}_j$ is independent of the assessed process. Therefore, the initial data $\hat{\lambda}_j$ is collected from suppliers, literature, or assumed based on previous knowledge about similar factors. Moreover, initial data $\hat{\lambda}_j$ can be associated with various life-cycle stages, based on the goal and scope of the assessment. In a visionary perspective that is discussed later as an outlook in chapter 7, the concept of SWS may be adoptable to provide the initial data $\hat{\lambda}_j$ for such characterization factors λ_j in other product systems. For the cradle-to-gate approach adopted in this thesis, the consideration of prior life-cycle stages by the characterization factors λ_j is essential. For instance, the economic characterization factor γ_j of an elementary flow α_j should represent the final price including all economic impacts throughout its previous life-cycle stages. This is also the case of its ecological characterization factor ε_j.

Table 4.12 Structure of EEAM-DB for parameters associated with selected subsets $\varphi^{[\Gamma]}$

$\varphi^{[\Gamma]}$	ID:($\varphi^{[\Gamma]}j$)	Associated SWS(s)$_i$	α_j definition in English	α_j definition in German	α_j measurement unit	α_j electricity unit	α_j time unit	α_j price per unit	α_j disposal cost per unit	α_j mass per unit	α_j cradle-to-gate kg CO_2 per unit	α_j gate-to-grave kg CO_2 per unit	Equipment replacement price	Residual value	Equipment cradle-to-gate kg CO_2	Equipment end-of-life kg CO_2	Equipment operation life in years	Equipment annual maintenance expenses	Equipment total annual operating hours
$\varphi^{[F]}$	60** or 80**	Y	Y	Y	Y	N	N	Y	N	Y	Y	N	N	N	N	N	N	N	N
$\varphi^{[M]}$	70**	Y	Y	Y	Y	N	N	Y	N	Y	Y	N	N	N	N	N	N	N	N
$\varphi^{[C]}$	100**	Y	Y	Y	Y	N	N	Y	N	Y	Y	N	N	N	N	N	N	N	N
$\varphi^{[R]}$	90**	Y	Y	Y	Y	N	N	Y	N	Y	Y	N	N	N	N	N	N	N	N
$\varphi^{[T]}$	10**	Y	Y	Y	Y	Y	N	Y	N	N	Y	N	N	N	N	N	N	N	N
$\varphi^{[Q]}$	40**	Y	Y	Y	Y	Y	Y	Y	N	N	Y	Y	Y	Y	Y	Y	Y	Y	Y
$\varphi^{[L]}$	20**	Y	Y	Y	Y	N	Y	Y	N	N	Y	N	N	N	N	N	N	N	N
$\varphi^{[\Delta s]}$	30**	Y	Y	Y	Y	Y	Y	Y	N	N	Y	N	N	N	N	N	N	N	N
$\varphi^{[G]}$	65** or 85**	Y	Y	Y	Y	N	N	N	Y	Y	N	Y	N	N	N	N	N	N	N

To illustrate the EEAM-DB structure, Tab. 4.12 provides a generic illustration. However, only a selection of subsets is shown in it. The reason behind such limitation is associated with the case study limited requirements, as it is discussed later in this chapter as a part of the assessment mathematical model. Tab. 4.12 shows the relation between the parameters and subsets $\varphi^{[\Gamma]}$ by the simplified (Y) and (N), which represent positive and negative associations respectively. Tab. 4.12 is covering relevant parameters required for calculating direct characterization factors λ_j of measured elementary flows α_j such as price and disposal cost per unit and cradle-to-gate as well as gate-to-grave kg CO_2 per unit. Furthermore, initial data parameters $\hat{\lambda}_j$ about other characterization factors λ_j are also provided to cover the various included impact categories. These categories

have been discussed before in Fig. 4.28 and Fig. 4.29 sufficiently. In addition, the EEAM-DB structure provides general knowledge including determining the associated SWSs with that elementary flow α_j. A short description of each elementary flow α_j is provided in English and German. Alternatively, further or other languages can be added to assure clear understanding of each input in that EEAM-DB. However, this description is more useful for the manual utilization of the EEAM.

For every elementary flow α_j, the measurement unit is provided in the EEAM-DB to assure compatibility with the gathered data by the SWS. For some subsets $\varphi^{[\Gamma]}$ such as electricity $\varphi^{[T]}$, equipment $\varphi^{[Q]}$, and facility $\varphi^{[\Delta s]}$, the electricity measurement unit is provided. In practice, such unit is unified for all subsets as Kilowatt hours (kWh). Time measurement unit is also relevant for subsets such as $\varphi^{[Q]}$, $\varphi^{[L]}$, and $\varphi^{[\Delta s]}$. Again, the time is measured by a unified unit described as (hours:minutes:seconds), which is also described as (hh:mm:ss). Time is then converted to the standard unit of seconds (s). Additional parameters, such as mass per measurement unit, are provided for matter subsets $\varphi^{[\Gamma]} \subseteq J^{[\mu]}$ as well. There are various initial parameters $\hat{\lambda}_j$ that may be required for the impact assessment of equipment in subset $\varphi^{[Q]}$. For instance, equipment replacement price, cradle-to-gate CO_2 equivalent of it, its annual maintenance expenses, its residual value, its end-of-life CO_2, its operation life in years, and total operating hours per each year are stated in the EEAM-DB. Based on previous studies, parameters associated with about 455 elementary flows λ_j within clearly distinguished subsets $\varphi^{[\Gamma]}$ are listed in the EEAM-DB. These studies include for example processes deduced from internally assessed manufacturing of FRP structures.

While the assessment of an impact θ_j is a product of its categorization factor λ_j and its elementary flow magnitude α_j, it is essential to define which classes of the economic and ecological impacts are to be considered in that factor λ_j. Hence, it is possible to assess a single class or a selection of direct impacts such as fixed recurring impact, variable recurring impact, and fixed nonrecurring impact. Due to the lack of data about many of the aspects required to calculate the impact in some classes, assumptions are adopted. However, any assumption has an impact on the result accuracy, as it is discussed later in this chapter. Therefore, a reduced assessment that covers only the impacts with available data is generally preferred. In the EEAM-DB, every quantitative value is referenced to its source or marked as assumption, while such assumptions are further explained and justified in many cases.

In addition, dependencies between elementary flows α_{ij} and characterization factors λ_{ij} are handled case wise in the EEAM-DB as a factor within the associated category. Example of that is the material price variation when purchasing different amounts such as fiber and matrix. Besides the associated characterization factors λ_j, the EEAM-DB has the functionality of saving the results from previous assessments. This serves the decision-makers in achieving enhanced knowledge. Such results are necessary for performing assessments of later life-cycle stages. However, such results should be clearly associated with their case studies and assessment boundaries. Therefore, the description of significant system boundary parameters is manually added to the results in the EEAM-DB. To simplify the communication with internal and external partners, comma-separated values, or as they are also called .csv format, are adopted to realize the EEAM-DB in its current version.

4.3.3 Time-Dependent Computer-Based Eco-Efficiency Assessment Model (EEAM)

The DSSs are implemented to assess the process and provide the decision-makers with monetary and physical unit values of economic and ecological impacts respectively [156]. In practice, DSSs can be realized based on LCA and LCCA frameworks in the form of computer-based software [174]. Examples of such DDS have been previously mentioned in chapter 3. These assessment software solutions depend on universal ecological DBs, that are established based on the results of associated previous assessments [25]. They all cover the

entire life-cycle as well as a wide range of ecological impact categories such as climate change, human health, resources, and ecosystem quality [159]. In this thesis; however, the EEAM is implemented as a DSS that has been developed internally to assess the FRP production. In this section, the EEAM functionality and structure, its mathematical model for LCIA, and time-dependent assessment in it are introduced.

EEAM functionality and structure

The EEAM has been developed by DLR as a DSS for the simplified LCA within previous works [10, 13]. On the one side, the EEAM is similar to other existing software solutions by being an eco-efficiency DSS that covers both ecological and economic impacts. This model is designed to handle the production of FRP in specific. The EEAM is a bottom-up and activity-based direct δ cost and carbon footprint β assessment model. Despite the fact that EEAM has the advantage of offering detailed assessment for the various manufacturing techniques of numerous FRP structures in $\varphi^{[S]}$, the EEAM handles only a single ecological impact category as well as an economic one. Unlike other commercially available software such as GaBi, Umberto, and SimaPro, the EEAM is not capable of covering neither multiple ecological impact categories, nor life-cycle stages, or even non-FRP products. In the current version of EEAM, only the climate change is considered as an ecological impact by assessing the carbon footprint β. Moreover, it assesses only the production process as simplified cradle-to-gate or gate-to-gate LCA [152]. During its development, several programming languages have been tried and implemented in the EEAM. However, python has been adopted as a programming language based on a rating scheme in a previous work [10]. In its current version, the EEAM is usable under both Windows or Linux operating systems.

As a LCIA model, the EEAM communicates with the different data sources required to calculate direct cost δ and carbon footprint β to derive the process eco-efficiency ξ. To address the CSF levels introduced previously in Fig. 4.20, the EEAM provides detailed assessment on each level. Besides assessing the total impact θ, the EEAM assesses the direct cost δ_i and carbon footprint β_i of each UP i. Moreover, it provides the same assessment on the subset and elementary flow levels. For better understanding, the conventional functionalities of EEAM are shown in Fig. 4.30.

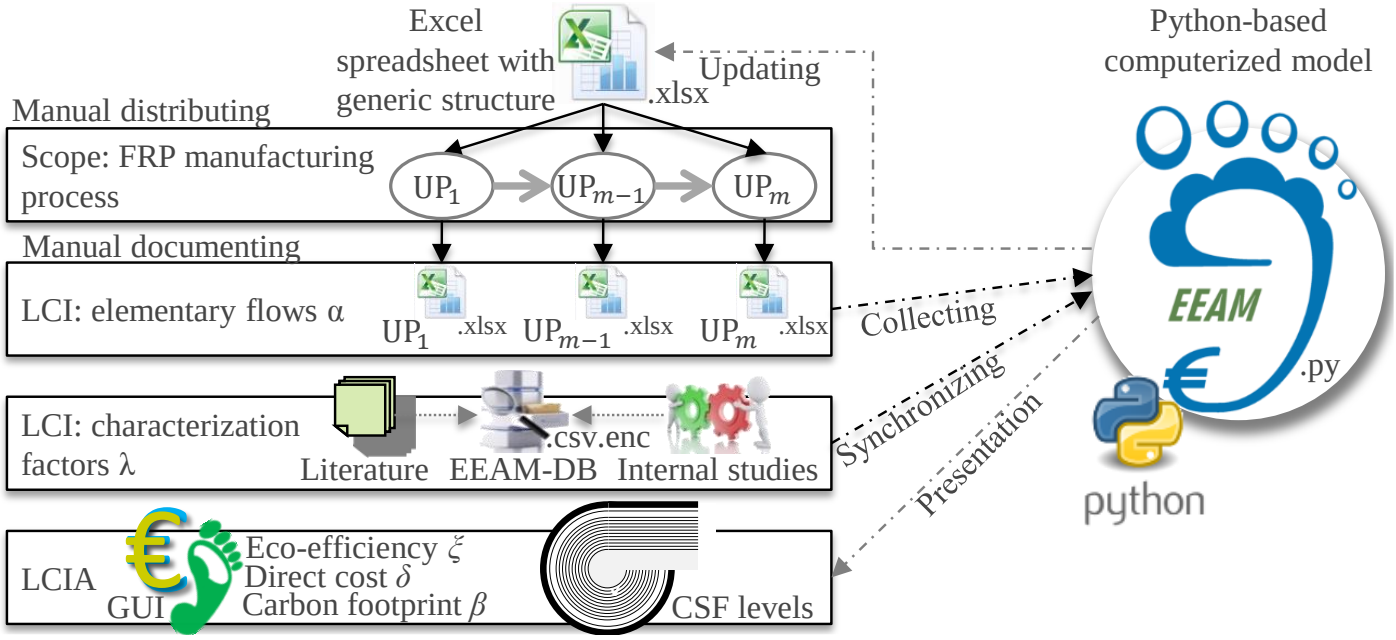

Figure 4.30 Conventional functionalities of EEAM [13]

As Fig. 4.30 illustrates, the main functionalities in the EEAM are the data collecting, updating, synchronizing, and presenting. In addition, the user has to perform predefined tasks in order to enable the assessment by this conventional EEAM. The EEAM functionalities are illustrated with dashed arrows in Fig. 4.30. While the data flow to the python-based EEAM in (.py) file format is distinguished by black dashed arrows, data flow from the tool is shown in gray ones. Elementary flows α, as process parameters that are collected by conventional LCI, are categorized within a generic structure in the EEAM-DB and accordingly in a standard data collection sheet derived from it. Due to the scope definition of FRPs production processes as sets of UPs, data from each UP may be collected manually in such separated Microsoft Excel-spreadsheets in (.xlsx) file format. As a user-friendly model, the EEAM commissions its user to perform confined tasks. In Fig. 4.30, these user tasks are illustrated with solid black arrows. They include distributing m number of Excel-spreadsheet in the WSs to collect the process relevant data from every included UP i.

As a part of that conventional LCI, users document the process parameters in these sheets based on a given system boundary definition. In practice, such Excel-spreadsheets facilitate the data collection task for any data collection clerk including decision-makers as well as field labors, while Microsoft Excel is a common tool. This spreadsheet is structured as a generic table of inputs from all UPs i, while the data collection clerk should only fill that table out in the predefined fields. Moreover, its data structure is compatible with the EEAM-DB in Tab. 4.12. Similar to the EEAM-DB, these spreadsheets are covering a wide range of production techniques for different FRP structures. However, the EEAM-DB has encrypted comma-separated values file format (.csv.enc) for safer communication in the case of confidential data, while the spreadsheets are in Microsoft Excel open spreadsheet file format (.xlsx). Besides the data structure of various elementary flows α_j within the Excel-spreadsheet itself, the magnitude, directory allocation, and order of these sheets are reflecting the process model as ordered UPs i.

As Fig. 4.30 shows, a folder is dedicated to include these Excel-spreadsheets in accordance with the assessment scope. This folder preexists within the EEAM directory in Windows or Linux operating systems. For a single structure, these spreadsheets are to be pasted by the user directly in that folder and named after their UPs started by their i value as (i_UP English term). For multiple structures in an assembly, sub-folders can be added and named after the structures they represent, while assembling UPs may be pasted directly in that preexisting folder. These folders and there structures represent the process modeling including the UPs sequence, that is stated by the i value of each sheet [10]. As a part of the updating process shown in Fig. 4.30, these sheets are automatically modernized from the most recent version of EEAM-DB. On the other hand, characterization factors λ can be optionally modified by the user based on available internal or external studies. These factors λ are adjusted manually in the existing EEAM-DB and synchronized automatically for future EEAM assessment sessions.

Finally, the user needs to start the assessment session by activating the EEAM, whereas no extra process modeling is required. The EEAM collects the associated data of elementary flows α and characterization factors λ with predefined assignments to their subsets $\varphi^{[\Gamma]}$, including UPs i, impact categories, as well as their multiple structures or processes if applicable. In the EEAM, the assessment is conducted through the correlation between the spreadsheets and EEAM-DB by the python-based computerized model. This model connects the spreadsheets, collects the inputs from them, synchronizes their data with the EEAM-DB, and calculates the outputs. As a LCIA model, the EEAM reports the eco-efficiency ξ, direct cost δ, and carbon footprint β statistically and visually in its GUI. To fulfill the targeted decision support details in Fig. 4.20, all results can be produced on the different CSF levels selectively on the EEAM GUI by its user. Technically, all functionalities represented by dashed arrows in Fig. 4.30 are performed automatically whenever an assessment session is activated by the user in the EEAM. However, the conventional functionalities of EEAM are further enhanced in

this thesis to enable this computerized model of performing a time-dependent assessment. Based on Fig. 4.30, the functionalities of the time-dependent EEAM and its correlation with the SWSs are illustrated in Fig. 4.31.

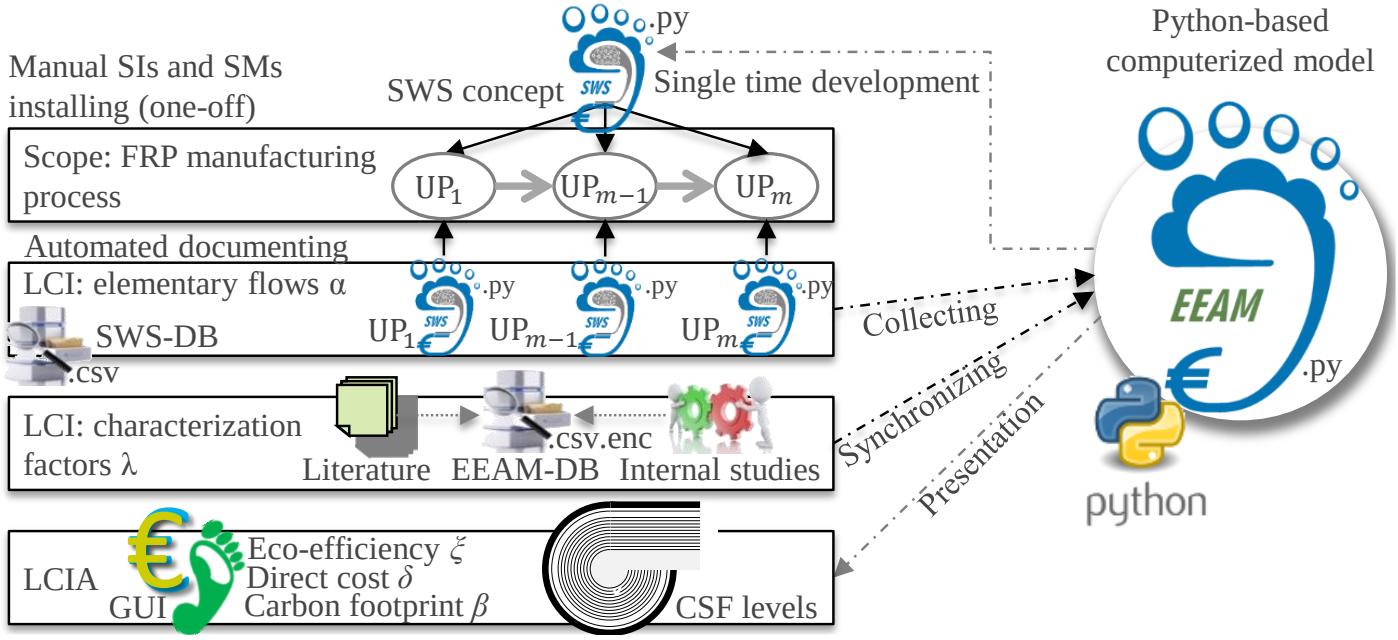

Figure 4.31 Functionalities of EEAM with integrated SWS

Compared to the conventional functionalities of EEAM in Fig. 4.30, the time-dependent EEAM replaces the manually performed LCI of elementary flows α by the SWSs as an automated real-time data collection. This is realized by installing the SIs and SMs of different SWSs for the included UPs i. For each UP i, a SWS_i is to be initially developed and designed based on the SWS concept. These sensor nodes are supplying the SWS computerized model with the initial data, while this model is also python-based. The initial data is interpreted by the SWS computerized model to generate the required output for the EEAM. As far as the file format is concerned, the SWS computerized model has a (.py) python format, whereas the SWS-DB is in comma-separated values format (.csv). For better understanding, the development of SWSs and the installation of their SIs and SMs are further explained for the selected case study in chapter 5.

For various elementary flows α_{ij} or their subsets $\varphi^{[\Gamma]}$, an illustration may include several charts with unified timestamps on the horizontal axis. In each part, the vertical axis is adjusted to the minimum and maximum range, that suits the collected data for optical clarity. For the studied impacts, visualizations are realized by line graphs and area charts as well as pie and bar charts mainly. The time-dependent assessment can be effectively illustrated by line graphs of the cumulative impact values. Depending on the level of impacts, several line graphs may be included in one illustration. However, they still have unified timestamps on the horizontal axis, as it is the case of line graphs. Alternatively, a suitable single area chart with multiple lines can be implemented. For the results as time-independent assessment, pie and bar charts are sufficient for the visualization [13]. Whenever required, the values and shares in percentage can be attached to each assessed category in the charts for better results visualization. Further optical illustrations such as product pictures and process location can be added to the EEAM GUI. In addition to these illustrations, all results can be represented statistically in tables and as unique values in the GUI [10].

By the integration of SWS in EEAM, its data collection tasks have been entirely automated. Therefore, no data collection clerk is required to perform a data collection in the assessment anymore. However, user interference is still required for the one-off tasks of installing the initial SWSs, adding new elementary flows α or characterization factors λ, and manually adjusting them. Combined with the SWSs, the EEAM is automatically

activated for the sake of time-dependent eco-efficiency assessment. However, the time interval of this frequent activation is selected by the decision-makers within the technically possible range. In this regard, the SIs and SMs play here a decisive role in such time interval. To accommodate the time-dependency aspect, the mathematical model behind the time-dependent EEAM is also advanced to enable such dynamic assessment.

Mathematical model of LCIA in EEAM

Based on the previously discussed physical as well as process impact equilibriums in Eq. 4.6 and Eq. 4.60, the impacts on both input and output sides, which are represented by $\theta^{[X]}$ and $\theta^{[Y]}$ respectively, are theoretically equal. This impact equilibrium can be illustrated for the various input and output vectors $\{\Upsilon^{[\Gamma]}\} \in \varphi^{[\Gamma]^{1\times n}}$ by the impact equilibrium equation of $\{\theta^{[X]}\}^\intercal = \{\theta^{[Y]}\}^\intercal$, as Eq. 4.72 shows in details.

$$\{\theta_P\} + \{\theta_F\} + \{\theta_M\} + \{\theta_C\} + \{\theta_R\} + \{\theta_T\} + \{\theta_Q\} + \{\theta_L\} + \{\theta_{\Delta s}\} = \{\theta_S\} + \{\theta_P\} + \{\theta_K\} + \{\theta_W\} + \{\theta_G\} + \{\theta_D\} + \{\theta_N\} + \{\theta_O\} + \{\theta_B\} \quad (4.72)$$

For the entire process, the impacts of all semi-finished structures $\{\theta_P\}$ on the input side are equal to their impacts on the output side. While they are identical on both sides, these impacts have the net value of $\{\theta_P\} = 0$ for the entire process including all UPs. This is a result of applying the process matrix $[Z] = [z_{ij}]$ based on these elementary flow matrices of $[A^{[Y]}]$ and $[A^{[X]}]$, as it is shown in Eq. 4.45 before. Nonetheless, the impact of each semi-finished structure θ_{iP} from a single UP i is considered as the main output of that UP i. Therefore, θ_{iP} is calculated as the result of entire UP i and never neglected on the UP i level. On the input side, the impacts of all elementary flow subsets including fiber $\{\theta_F\}$, matrix $\{\theta_M\}$, core material $\{\theta_C\}$, ancillaries $\{\theta_R\}$, electricity $\{\theta_T\}$, equipment $\{\theta_Q\}$, labor $\{\theta_L\}$, and facility $\{\theta_{\Delta s}\}$ are assessed based on the elementary flows α_j provided by the SWS and characterization factors λ_j from the EEAM-DB.

In Eq. 4.72, the impacts vector of the desired FRP finished structures $\{\theta_S\}$ is representing a single impact from the last UP $i = m$, while $\{\theta_S\} = \theta_{mS}$. In practice, no FRP finished structure may occur before that last UP of $i = m$. Still, the impact of rejected FRP structure $\{\theta_K\}$ is equal to „*zero*“, while an ideal process with no rejected product is previously assumed. Moreover, the impact of FRP waste $\{\theta_W\} = \theta_{mW}$ is an output of the last UP $i = m$, like the FRP finished structure $\{\theta_S\}$. However, these impacts $\{\theta_W\}$ lay beyond the scope of cradle-to-gate assessment. Therefore, the impact of FRP waste θ_{mW} is also neglected in this work.

The impacts of matrix, core material, and ancillaries wastes, represented by $\{\theta_D\}$, $\{\theta_N\}$, and $\{\theta_O\}$ are irrelevant for the selected assessment case study in chapter 5. On the other hand, the impacts of fiber waste $\{\theta_G\}$ are included in that case study. While these impacts are included as a part of the process, a negative sign is assigned to them on the output side for mathematical correctness. However, the impacts of them are associated with the process itself. In the case of waste impact consideration, the impacts of $\{\theta_G\}$ are extruded from their input elementary flows in this case study and considered as $\{-\theta_G\}$, while cradle-to-grave characterization factors are adopted.

Still, the wastes from core structural materials including fiber $\varphi^{[F]}$, matrix $\varphi^{[M]}$, and core material $\varphi^{[C]}$ can be considered as the magnitude difference between their originating initial input materials and their share in the structure. These wastes may have the same characterization impacts as their initial elementary flows or unique ones based on the scope of these factors. To put it more simply, the waste economic or ecological impact itself is not significant to the eco-efficiency assessment in the first case, while it is already covered by the impact of its originating input elementary flow. In the second case, the waste impacts are to be calculated separately and

not as a part of their initial elementary flows. Nonetheless, the determination of waste portion from its initial input is possible in the early real-time LCI before LCIA. In other words, any core structural material can be either in the product or wasted during the process, as Eq. 4.73 suggests.

$$\alpha_{waste} = \alpha_{initial} - \alpha_{product} \tag{4.73}$$

However, two major assumptions are hypothesized before adopting Eq. 4.73. First, none of these core structural material wastes may be reusable in the assessed process, due to the lack of data about re-usability scenarios. Practically, this is a common case in manufacturing identical structures, while re-usability is associated with different products in FRP manufacturing. This makes re-usability assessment beyond the scope of this thesis. Second, the wastes allocation to each UP i is measured locally by applying Eq. 4.73 on the UP level.

As far as ancillaries are concerned, the impact of utilized and wasted ancillaries $\{\theta_O\}$ in the process is the result of subtracting the impact of reusable ancillaries $\{\theta_B\}$ in the process from the impact of their initial inputs $\{\theta_R\}$, which is measurable by the real-time magnitude tracing. However, it is possible to assume that these impact differences are all considered within the consumed elementary flows $\{\theta_O\}$, as Eq. 4.74 shows.

$$\theta_O = \theta_R - \theta_B \tag{4.74}$$

The logic behind this assumption in the SWS is its capability of measuring the consumed or as they are also called wasted ancillaries $\varphi^{[O]}$. The impacts of consumed ancillaries include all associated impacts in other covered life-cycle stages such as the disposal. In the early LCI, the SWS determines the consumed ancillaries $\varphi^{[O]}$ and provides the EEAM with their magnitude as inputs. Now, the impact of a semi-finished structure $\varphi^{[P]}$ or a FRP desired structure $\varphi^{[S]}$ is cumulative. This implies that they are cumulative results of all prior UPs, that are considered as input to their post one. Based on these previous assumptions and conclusions, the impact matrices in Eq. 4.72 can be expressed differently for the case study of this thesis, as Eq. 4.75 suggests.

$$\{\theta_F\} + \{\theta_M\} + \{\theta_C\} + \{\theta_O\} + \{\theta_T\} + \{\theta_Q\} + \{\theta_L\} + \{\theta_{[\Delta s]}\} = \{\theta_S\} - \{\theta_G\} \tag{4.75}$$

As it has been hypothesized previously, the only unknown in Eq. 4.75 is the impact of FRP finished structure $\{\theta_S\} = \theta_{mS}$, which is equivalent to the impacts of the entire process. Similarly, this approach can be applied on the UP level i to assess the impact of its semi-finished structure θ_{iP}. In assessing both economic direct cost δ as well as ecological carbon footprint β, the impact classifications illustrated in Fig. 4.28 and Fig. 4.29 are respectively applied. In the framework introduced by this thesis, a gate-to-gate or a cradle-to-gate LCIA can be performed. The distinction between these two LCIAs depends on the adopted classes and life-cycle stages within the considered characterization factors λ_j. Now, the adopted scope of categories in both economic and ecological aspects is reflected on the definition of their characterization factors in the EEAM-DB, that is represented by γ_j and ε_j respectively. Based on Eq. 4.75, the economic impact of the desired FRP structure δ_S can be derived as Eq. 4.76 suggests.

$$\delta_S = \{\delta_F\} + \{\delta_M\} + \{\delta_C\} + \{\delta_O\} + \{\delta_T\} + \{\delta_Q\} + \{\delta_L\} + \{\delta_{[\Delta s]}\} + \{\delta_G\} \tag{4.76}$$

In this thesis, the EEAM is capable of assessing all impacts on the right side of Eq. 4.76 based on the determination of their elementary flows done by the SWS, while their economic characterization factors are provided in the EEAM-DB. This process impact is equal to the economic impact of the desired FRP structure δ_S on the left side of Eq. 4.76, which is a required KRI for the eco-efficiency assessment.

Similarly, the ecological impact of the desired FRP structure β_S can be calculated in Eq. 4.77 based on Eq. 4.75.

$$\beta_S = \{\beta_F\} + \{\beta_M\} + \{\beta_C\} + \{\beta_O\} + \{\beta_T\} + \{\beta_Q\} + \{\beta_L\} + \{\beta_{[\Delta s]}\} + \{\beta_G\} \tag{4.77}$$

Now, the equilibrium in both Eq. 4.76 and Eq. 4.77 is between the entire process impact and the impact of all produced functional units. In other words, the impact of each structure from the identical functional units manufactured by the process is equal to the manufacturing process impact divided by products magnitude. In that case, these produced structures as functional units in $\varphi^{[S]}$ must be absolutely identical. Nonetheless, the FRP structure is represented by a single desired product u_{mS} that matches predefined quality requirements in this thesis.

Although these total impacts of the manufacturing, regardless of the created products number from it, are what this eco-efficiency assessment aims to address, the determination of each structure impact is useful to the assessment of post life-cycle stages. Based on Eq. 4.69 and Eq. 4.70, Eq. 4.78 states the relation between these characterization factors λ_S and the process output product u_{mS}.

$$\delta_{mS} = u_{mS}\gamma_S \quad \text{and} \quad \beta_{mS} = u_{mS}\varepsilon_S \tag{4.78}$$

Similarly, the characterization factors λ_P of each semi-finished structures $\hat{u}_{iP}$ from a UP i are explained in Eq. 4.79.

$$\delta_{iP} = \hat{u}_{iP}\gamma_P \quad \text{and} \quad \beta_{iP} = \hat{u}_{iP}\varepsilon_P \tag{4.79}$$

However, the impact of a semi-finished product $\hat{u}_{iP}$ is equivalent to the impacts of all previous UPs not only the last one. Moreover, such determination of unit impact from Eq. 4.78 and Eq. 4.79 may be used to identify the impact of each physical unit such as kg or m^2 from that manufactured structure, which is useful for the comparison with other studies. On UP i level, Eq. 4.76 can be modified and applied as Eq. 4.80 shows.

$$\delta_i = \{\delta_{iF}\} + \{\delta_{iG}\} + \{\delta_{iM}\} + \{\delta_{iC}\} + \{\delta_{iO}\} + \{\delta_{iT}\} + \{\delta_{iQ}\} + \{\delta_{iL}\} + \{\delta_{[i\Delta s]}\} \tag{4.80}$$

This is also applied to the ecological impact in Eq. 4.77, as Eq. 4.81 shows.

$$\beta_i = \{\beta_{iF}\} + \{\beta_{iG}\} + \{\beta_{iM}\} + \{\beta_{iC}\} + \{\beta_{iO}\} + \{\beta_{iT}\} + \{\beta_{iQ}\} + \{\beta_{iL}\} + \{\beta_{[i\Delta s]}\} \tag{4.81}$$

These impacts in Eq. 4.76 and Eq. 4.77 as well as Eq. 4.80 and Eq. 4.81 are implemented in assessing the time-dependent eco-efficiency of the process and each UP in it.

Time-dependent assessment in EEAM

In the EEAM, the dynamic time-dependent assessment is realized by subjecting the mathematical models of LCIA to the time dimension. Based on Eq. 4.76 and Eq. 4.77, the eco-efficiency ξ in Eq. 4.71 of the assessed process can be rewritten as Eq. 4.82 suggests.

$$\xi = \frac{k - \delta_S}{\beta_S} = \frac{k - \delta^{[A]}}{\beta^{[A]}} \tag{4.82}$$

In spite of its nature as a dynamic parameter, the total revenue without non-process costs k is assumed to be constant during the considered UP i. In other words, a manufacturer is rewarded by a market known k for each successful activity performed. Therefore, a cumulative value of not necessarily linear parameters is calculated for the performed UPs i. Nonetheless, in this thesis a set of constants k_i is roughly estimated for each UP i.

The associated parameters for the time-dependent eco-efficiency include the total of sales excluding all non-process costs k, the economic and ecological characterization factor vectors from Eq. 4.56 and Eq. 4.57, which are represented by $[\check{\Lambda}^{[X]}]$ and $[\check{\check{\Lambda}}^{[X]}]$ respectively, as well as the dynamic elementary flow matrix $[A]_t$, as Eq. 4.83 explains.

$$\xi_t = \frac{k - [A]_t[\check{\Lambda}^{[A]}]}{[A]_t[\check{\check{\Lambda}}^{[A]}]} \tag{4.83}$$

In which, ξ_t or $\xi(t)$ is the time-dependent cumulative eco-efficiency in monetary unit (€/s) per physical unit (kg CO_2/s) at the same time t. As it is mentioned before, the time-dependency of both characterization factor vectors $[\check{\Lambda}^{[X]}]$ and $[\check{\check{\Lambda}}^{[X]}]$ is beyond the scope of this thesis, while they are studied as static given parameters. Moreover, the total of sales revenue excluding non-process costs k is also dealt with as a constant. Therefore, these values are considered as time-independent constants. As it is mentioned previously in Eq. 4.76 and Eq. 4.77, the impacts of selected inputs and outputs are covered, which necessitate including their elementary flows within the matrix $[A]$. However, many other flows, which were originally included, have been excluded due to the previously explained reasons. Considering the mathematical modeling, it is essential to state that the time-dependency of eco-efficiency assessment is applied here to describe the process state of impacts as non-transient part for prior times. Moreover, the time-dependent impact in this thesis describes the cumulative one of considered process up to that temporal point. Likewise, a time-dependent assessment of a single KRI impact θ_t can be derived in Eq. 4.84.

$$\theta_t = [A]_t[\Lambda^{[A]}] \tag{4.84}$$

Eq. 4.84 is then applied to assess the economic impact δ_t and the ecological one β_t at time t in Eq. 4.85.

$$\delta_t = [A]_t[\check{\Lambda}^{[A]}] \quad \text{and} \quad \beta_t = [A]_t[\check{\check{\Lambda}}^{[A]}] \tag{4.85}$$

Now, the time-dependent global eco-efficiency ξ for the entire process in Eq. 4.82 can be also assessed as ξ_i for a single UP i, as Eq. 4.86 illustrates.

$$\xi_i = \frac{k_i - \delta_i}{\beta_i} = \frac{k_i - \delta^{[A_i]}}{\beta^{[A_i]}} \tag{4.86}$$

For economic impact δ_i in a UP i, Eq. 4.87 can be adopted to dynamically assess δ_{i_t} from the measured vector $\{A_i\}_t$ in real-time by each SWS_i and all associated characterization factors $[\check{\Lambda}^{[A]}]$ in Eq. 4.56.

$$\delta_{i_t} = \{\alpha_{i1_t} \cdots \alpha_{iN_t}\} \begin{bmatrix} \gamma_1 \\ \vdots \\ \gamma_N \end{bmatrix} \tag{4.87}$$

In the same way, the ecological impact β_i of a UP i can be assessed dynamically as $\beta_i(t)$ in Eq. 4.88.

$$\beta_{i_t} = \{\alpha_{i1_t} \cdots \alpha_{iN_t}\} \begin{bmatrix} \varepsilon_1 \\ \vdots \\ \varepsilon_N \end{bmatrix} \tag{4.88}$$

After all, the values of characterization factors are provided in the EEAM-DB. In the EEAM, Eq. 4.87 and Eq. 4.88 are applied as a time-dependent assessment for any temporal point $t_i = t_{i_a}, \cdots, t_{i_b}$ in the discussed UP i, as it is previously illustrated in Fig. 4.12.

In this work, the correlation between all SWS_i and the EEAM enables the time-dependent eco-efficiency assessment for the entire process and on UP_i level as well, as Fig. 4.32 shows.

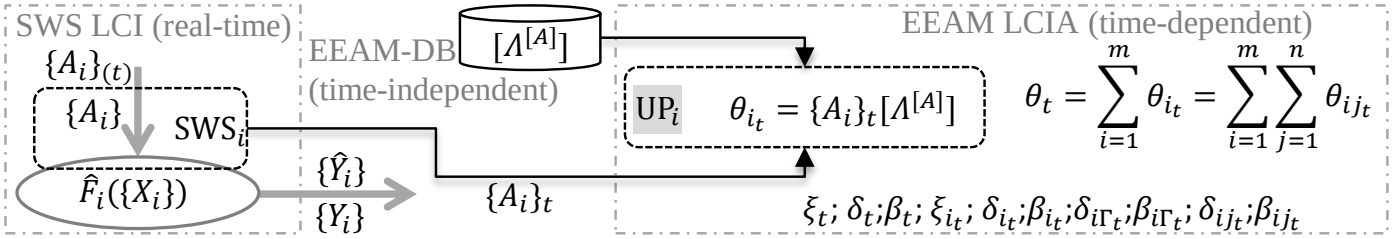

Figure 4.32 Correlation of EEAM and SWS_i in assessing a UP_i

As Fig. 4.32 illustrates, the real-time LCI, which is carried out by every SWS_i, provides the EEAM model with the elementary flow parameters within the dynamic vector $\{A_i\}_t$. Simultaneously, the EEAM-DB is supplying the EEAM with the static characterization factors in their input vectors $[\Lambda^{[A]}]$.

4.3.4 Model Validation Framework

In this section, the validation of eco-efficiency assessment is carried out through a validation approach. This includes the validation of both DSSs of SWS and time-dependent EEAM. In addition, the adopted validation steps are checked themselves by interpretation checks.

Validation approach

Critical thinking is the fuel of innovation. It is the reason behind establishing such DSSs that serve the time-dependent eco-efficiency assessment in this thesis. Now, a DSS should be critically evaluated to sustain decision-makers confidence in it [234]. Throughout the DSSs development, uncertainties in different model levels may be leading to deviations in results. To minimize such deviation, validation steps are to be systematically adopted on each of these modeling levels to enhance the results accuracy. In practice, credibility of a concept may be validated by comparing its functionalities or results with similar examples from comparable concepts. However, the SWS concept and the time-dependent capability of EEAM are novel approaches. Thus, no direct comparison is possible for the validation of this work results. Therefore, the validation in this work focuses on the accuracy assurance on various information levels. Here, the previously discussed model evolution framework in Fig. 4.1 and Fig. 4.4 include validation stages that assure the model reliability and data quality. For the associated themes in this thesis, these validation stages are illustrated in Fig. 4.33 to be adopted in the generated DSSs.

According to the framework in Fig. 4.33, the final goal is to validate the generated computerized model with the reality. This starts when the representation accuracy of that initial reality in the developed conceptual model is qualified. Then, the mathematical model is verified based on the qualified conceptual model.

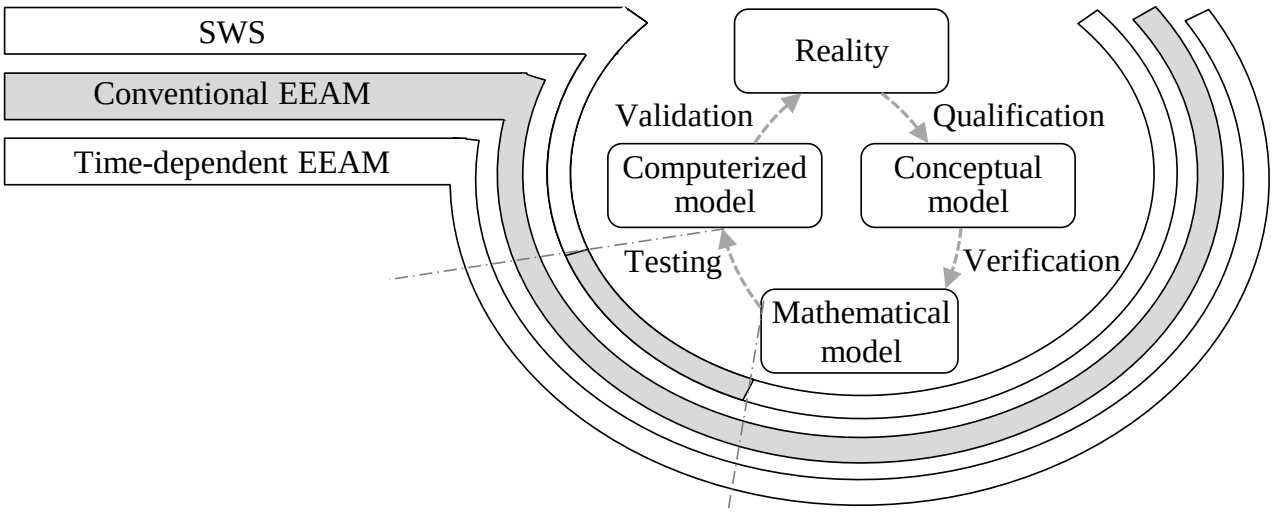

Figure 4.33 Model validation framework for the time-dependent assessment

Finally, an accurate representation of the mathematical model is assured in the computerized model by testing it. Although single direction arrows are shown in Fig. 4.33, these steps are practically serving the double-sided iterative model developments. To put it more simply, the various model levels may be revalidated with each other and reinterpreted until the aimed reliability within an accepted uncertainty margin is reached. Iteratively, the results of time-dependent eco-efficiency assessment are validated and the DSSs themselves are potentially optimized in these steps. As far as this thesis is concerned, there are three validation tasks that are described by surrounding frames in Fig. 4.33. First, there is the validation of the entire time-dependent EEAM, which is suggested generally in Fig. 4.1 and specifically in Fig. 4.4. Therefore, all validation steps are applied to the time-dependent EEAM including both DSSs in this thesis. Then, there is the validation of conventional static EEAM as a DSS, which has been discussed thoroughly in previous works [10, 13, 233]. For this reason, no validation is performed again for the conventional EEAM in this work, which is the meaning of a completely shaded surrounding frame in Fig. 4.33. As it is communicated by the surrounding frame in Fig. 4.4, a thorough validation for the SWS is carried out here. However, models testing is excluded from the validation of SWS, while it is beyond the work scope, as it is shaded in Fig. 4.33. In practice, testing of such sensor nodes is carried out externally by their developers.

Validation of real-time SWS

As it is suggested in Fig. 4.33, all validation steps except testing are applied to the adopted methods and sensor nodes in all SWS_i. Tab. 4.13 assigns the validation steps generically to methods and sensor nodes.

Table 4.13 Assigning the validation steps to the SWS methods as well as sensor nodes

		Qualification	Verification	Testing	Validation
Methods	MIs	Yes	Yes	No	No
	MMs	Yes	Yes	No	No
Sensor nodes	SIs	No	No	n/a	Yes
	SMs	No	No	n/a	Yes

With a simplified yes, no, or not applicable (n/a) answer, the two groups of methods and similarly sensor nodes are subjected to the validation steps in Tab. 4.13. Technically, adopted MIs and MMs provide conceptual

and mathematical solutions. On the other hand, SIs and SMs are hardware devices, which are installed in real system and operated by computerized models. Therefore, not only the sensor nodes as hardware are meant by their therm in Tab. 4.13, but also the computerized models operating them and their provided results. Thus, both qualification and verification are associated with the MIs and MMs, while testing and validation are related to the SIs and SMs. In spite of that, testing is excluded from this work.

As it has been discussed previously, the SWS concept provides a comprehensive conceptual model that assigns the methods and their sensor nodes properly in the WSs. Yet, it is essential to assure the coverage of all relevant elementary flows α_{ij} by adopting suitable MIs and MMs in the SWS concept. This has been proven previously in Tab. 4.10 and Tab. 4.11. As it is discussed within these tables, some MIs and MMs can be utilized as validation methods for other ones, while detailed examples for qualification and verification for all MIs and MMs are provided within Appx. C.

For verification, appropriate videotapes, conventional LCI, IR-records, and audits may be implemented. These verification solutions are applicable for any process under specified conditions. For instance, videotaping is prohibited in manually performed processes in countries such as Germany, due to labor anonymity regulations [138]. Nonetheless, labor work can be documented by IR-records for mathematical method verification, while other automated processes may be simply videotaped. Conventional LCI and audits are also very common applicable solutions for such verification, whereas conventional LCI has been covered thoroughly in previous works [8, 10, 12, 13]. Now, both qualification and verification are time consuming and costly. However, they are required only for newly installed SWSs. In other words, such validation steps are repeated until the associated models are approved with an acceptable inaccuracy margin, while such approval may be provided due to time and resource limitation or relatively low inaccuracy.

In conclusion, videotapes and IR-records are performed and then manually analyzed for a conventional LCI to validate the SIs and SMs results on the computerized model level. In comparison to conventional written LCI, videotaping and IR-recording have the advantage of permanent documentation for various associated UPs, activities, and their optically or thermally detectable elementary flows in clear spatial and temporal allocations. Similar to the qualification and verification, the validation is performed only to approve the results. Once these outputs from the SWS computerized models are validated, no further validation is required unless a change occurs to the assessed process. Moreover, a revalidation is required only for changed activities or UPs in the event of process changes. Such validation steps are carried out once, directly after each SWS_i is set up.

Validation of time-dependent EEAM

Based on the definitions of validation and uncertainty in chapter 3, it is obvious that uncertain results should be avoided by validating the DSSs in all their model levels. However, the uncertainty is unavoidable theoretically but still reducible, especially in a complicated model of a complex reality. Thus, it is essential to understand the reason behind validation and its expected impact on the results. In other words, uncertainty is the reason behind results deviation, which may be reduced by a sufficient validation. For that reason, Fig. 4.34 provides an exemplary neutralized illustration for possible uncertainty deviation and validation correction on the different CSF levels from Fig. 4.20.

It is hypothesized in Fig. 4.34 that the uncertainty in a level leads to a deviation in all following ones as well as the final results. This is the case as far as these model levels are developed in consistency. For instance, falsely neglecting a UP i, elementary flow α, or a characterization factor λ in the conceptual model leads to excluding it from all following levels. For each assessed CSF, a deviation margin may occur on each model level. This leads to changes in the values of studied parameters in all associated levels.

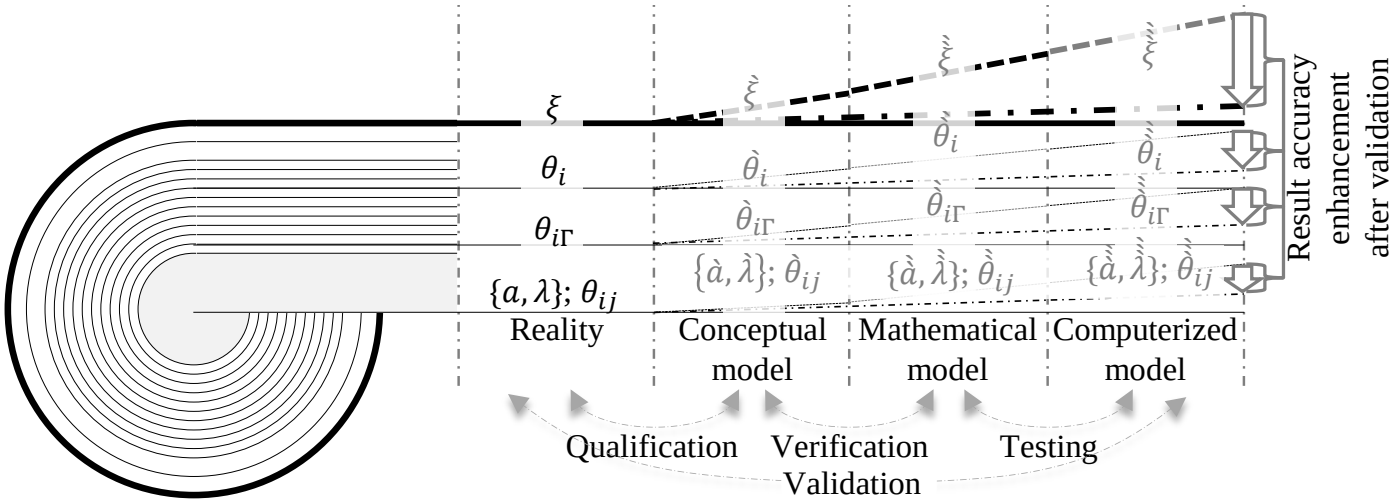

Figure 4.34 Qualitative illustration of exemplary results uncertainty and validation impact

First, the values deviated from reality because of uncertainty in conceptual model are marked by a single grave accent in Fig. 4.34. From the mathematical model uncertainty, its deviated values are marked by double grave accents, while the deviated values caused by the computerized model are distinguished in Fig. 4.34 by triple grave accents. With regard to the validation impact on the CSFs values, an enhancement in accuracy is expected on the results after carrying out a sufficient validation. However, such accuracy enhancement is assumed to make the deviated values get closer to the initial ones in reality but not necessarily meet them entirely. Which is the result accuracy enhancement arrows show on the right side of Fig. 4.34. In Fig. 4.34, it is assumed that the higher the level of uncertainty the severer its impact on the results will be. For instance, a wrong mathematical model of an elementary flow impact calculation leads theoretically to a smaller deviation in this work than a wrong eco-efficiency assessment equation with comparable falsehood. With regard to Fig. 4.34, no quantitative exact values are meant by the sizing of this illustration.

In order to achieve a sufficient reality deduction, the first validation step is to qualify the conceptual model in this work. Based on the thorough analysis of the real problem, that the time-dependent EEAM intends to solve, as well as the goal and scope of this DSS, the conceptual model may represent all relevant aspects of reality more accurately. As it is mentioned before in this chapter as well as chapter 3, no complicated model can address all possible aspects of a complex reality such as the one discussed here. For instance, each characterization factor λ is subjected to numerous external factors such as economic, political, and environmental changes. In practice, every elementary flow α in the process may suffer such unexpected deviations as well. However, the goal of model qualification is to assure the accurate representation of selected reality aspects under the predefined boundaries and assumptions.

Now, such qualification is already considered in the development phases of this scientific work, which has led to the accurate representations in the final versions of various associated illustrations in this chapter. Practically, a conceptual process model should cover all UPs i, as Fig. 4.16 shows. It qualitatively identifies the elementary flow subsets $\varphi^{[\Gamma]}$, as Fig. 4.18 suggests. Based on the assessment scope, the considered characterization factors λ as well as their resulting impact categories of fixed recurring, variable recurring, and fixed nonrecurring should be clearly illustrated, as Fig. 4.28 and Fig. 4.29 do. It should also sufficiently assign all these elementary flows α_{ij} and characterization factors λ_j to their UPs i without neglecting or repeating any, which is illustrated for the selected case study later in chapter 5. Such conceptual model may be visualized for clarity, which it is the case for all major ones in this work. This visualized model is compared to the reality iteratively to assure the accurate representation.

Practically, four main qualification steps are applied. First, process model including all UPs i is qualified with reality by documented observation in the form of LCI extracted from appropriate process videotaping and IR-recording that cover both temporal and spatial allocations of UPs i as well. Second, the models of elementary flow subsets $\varphi^{[\Gamma]}$ are also qualified with reality to assure the consideration of all relevant flows α_{ij}. This qualification is realized by detailed conventional LCI sessions based on process videotaping and IR-recording that cover both temporal and spatial allocations of flows α_{ij} as well. Third, the assignment of elementary flows α_{ij} is modeled as a list by the manufacturing experts. Then, this assignment is also qualified to assure that the elementary flow types j are allocated to their UPs i and not missed or repeated. This can be addressed by the same LCI. Finally, the cut-off-criteria identification is qualified and documented in the form of system boundaries to clarify the assessment scope for decision-makers. Such cut-off-criteria are communicated throughout this work in terms of excluded life-cycle stages, processes, elementary flows, characterization factors, as well as impact categories.

Nonetheless, some of these qualification steps have been performed already in a previous work [13], while the time-dependency can be irrelevant for some aspects. In addition, the verification of the mathematical models in the conventional static EEAM is sufficient to verify the time-dependent EEAM except for the equations of dynamic assessment. Therefore, these time-dependency mathematical models are verified in this work. Similarly, the testing is performed only for these dynamic functionalities in EEAM computerized model.

Interpretation checks

As it is mentioned before, the critical thinking is essential to enhance credibility of the novel time-dependent eco-efficiency assessment in this thesis. In order to increase the reliability of the compiled results, a comprehensive multidisciplinary interpreting evaluation is required. This has been also suggested before in Fig. 4.1. While the validation steps aim to enhance the accuracy of models and reduce their outputs deviation, interpretation checks examine the sufficiency of the validation itself. Therefore, a set of iterative checks is performed after identifying the significant issues. They include completeness, sensitivity, and consistency checks [151]. Although these checks have been already covered by previous works [8, 10, 13], it is useful to reconsider them for the novel time-dependent eco-efficiency assessment in this work.

The completeness check examines the availability and entirety of validation inputs. All inputs should be identified, while their consequences on the results as well as the evaluation are to be considered too. Thus, the completeness check is applied to every relevant validation step in Fig. 4.33. Based on that check, the validation steps and accordingly their models are enhanced iteratively. In this work, Fig. 4.34 has introduced a novel illustration that serves, the completeness check, among others.

After examining the inputs completeness, outputs of the time-dependent EEAM are evaluated in the sensitivity check. It includes ensuring the reliability of final results by evaluating the data allocation and calculation methods as well as uncertainty [151]. Fig. 4.34 has covered this check, while it is accomplished by evaluating the results of each modeling level. If possible, it may compare the final compiled results with associated ones from comparable external and internal studies. The deviation in different results is determined after performing each optimization cycle in order to minimize the deviation and detect its margin.

In the consistency check, the appropriateness of selected methods, collected data, and assumptions is ensured. This has been covered thoroughly as a part of validating both time-dependent EEAM and real-time SWS before in this chapter. This includes checking the consistency of implemented characterization factors regarding temporal and geographical boundaries. Based on these checks, conclusions, limitations, and recommendations are made available to the decision-makers as well as the DSSs developers [151].

Chapter 5

Parameterizing Case Study

As it has been mentioned previously, the parametrization case study in this thesis aims to validate the applicability of introduced framework, concept, and DSSs from chapter 4. As a part of that, the EVo-platform and the manufactured structure of aircraft vertical stabilizer ribs are described. Then, selected UPs i in the EVo-platform are modeled, while applied SIs and SMs from Tab. 4.8 and Tab. 4.9 are assigned to these UPs.

5.1 Case Study of Endkonturnahe Volumenbauteile (EVo)-Platform

In this section, the EVo-platform and the produced structure of the vertical stabilizer rib are described.

5.1.1 EVo-Platform Description

The time-dependent eco-efficiency assessment can be applied to any FRPs production process from the wide range of covered techniques in Appx. A. However, several criteria have been adopted to select the proper process and the suitable FRP structure from aerospace industry as a case study. First, the data availability is essential for the selection, while the possibility of data collection is a prerequisite for the time-dependent eco-efficiency assessment. Second, the entire assessed process should be freely investigated. In other words, it must be accessible and not confidential in order to enable publishing the scientific work about it. Third, the process maturity should be high enough to provide acceptable deviations by process iteration, while repeating the experiments is essential for the validation. Fourth, it should be technically possible and allowed to turn all associated WSs into SWSs. Fifth, the process may consist of activities with various DoA to prove the applicability of the developed DSSs. Nonetheless, a process scenario with high DoA may be more close-to-industry and can be useful for realizing a closed-loop control system based on the eco-efficiency time-dependent assessment in future works.

Within the center for lightweight production technology inside the city of Stade in Germany, the EVo-platform has been built to develop and test the cutting edge technologies in highly-automated FRPs manufacturing. It aims to provide an advanced close-to-industry plant for the research and development to convert ideas into high TRL technologies. This platform for high volume production of components near to net shape addresses both high production rates and final contour issues via automation. As it is explained later, the high production volume is achieved by enhancing the DoA and realize fully-automated activities in the majority of UPs i. In the EVo-platform, the RTM technique is adopted. As far as the infusion time is concerned, the RTM has a noticeable advantage among other techniques. According to a previous internal study, the EVo-platform is able of manufacturing up to 100,000 complex structures yearly. Moreover, this platform utilizes advanced trimming technologies that are implemented to reach the final structure contour before infusion. Such technologies eliminate the need for machining after demolding [123, 251, 314, 315].

The EVo-platform is containing all its relevant UPs *i* in a compact facility, that is spatially optimized to serve specifically the aerospace and automotive industries [314]. In addition, it can manufacture a wide range of FRPs and hybrid structures with various complexity degrees as well as functionalities. By applying some operational adjustments in this platform, it may be used in manufacturing different structures continuously. Although the EVo-platform is fully-automated for the most part of it, some of its activities may still be performed manually. This enables the realization of the SWS concept in different DoA, which is useful to validate various MIs, MMs, SIs, and SMs. The EVo-platform can be controlled from an on-site operator room stationed above it or remotely. These controlling possibilities are applied for carrying out any process in the entire platform or a selected part of it. This provides an advantageous freedom in planning the processes in various research and development projects. Nonetheless, such modification possibilities are subjected to restrict safety norms and regulations. As it is explained later, the EVo-platform leans on a central controlling system that enables the signals and orders communication and exchange between all its devices. Considering these technical features, the EVo-platform is adopted in this thesis as a case study for manufacturing commercial aircraft vertical stabilizer ribs made of CFRP, while it fulfills the previously listed case study criteria.

5.1.2 Aircraft Vertical Stabilizer Ribs Manufacturing by EVo-Platform

From a project for automated RTM manufacturing, a design for a rib in a commercial aircraft vertical stabilizer is selected in this thesis. This rib is developed to be within a set in the vertical stabilizer box, as it is simply illustrated in Fig. 5.1.

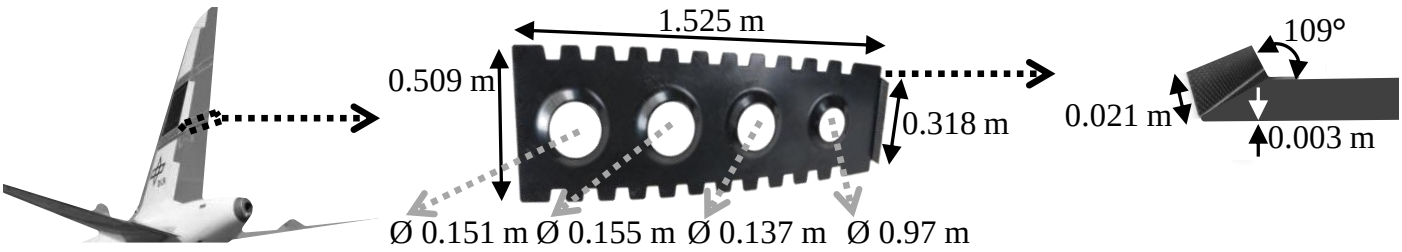

Figure 5.1 Geometry of the vertical stabilizer rib within an exemplary aircraft

Due to its geometry and functionality as a load transmission structure, the vertical stabilizer rib can be classified as a complex primary FRPs structure. In aerospace industry, these ribs are manufactured in high volume within series production. In practice, there are several possible process scenarios that may be applied to manufacture the aimed vertical stabilizer ribs. However, the DoA in EVo-platform is predefined to have a proper validation case study, which is unnecessarily the optimum industrial scenario. Technically, some activities may have adjustable durations based on the selected execution programs, which can enable more efficient scenarios. In spite of the high production volume as a result of the short process time, the selected scenario has relatively long activities durations. For the data collection and validation in this scientific work, this scenario enables better tracking in every UP.

5.2 EVo-Platform Process Models

As it is discussed thoroughly in chapter 4 as well as chapter 3, the conceptual, mathematical, as well as computerized models are essential for the DSSs in this work. Therefore, the conceptual model, that addresses all relevant aspects of the EVo-platform, is introduced here. Consequently, the mathematical model for assessing the case study is discussed too. Now, the time-dependent EEAM and real-time SWS are applicable for any

FRPs production as generic DSSs. Thus, expansions in the EEAM-DB and SWS-DB are required to adopt them in this case study, as it is discussed later.

5.2.1 EVo-Platform Manufacturing Conceptual Model

For the selected case study of EVo-platform, its UPs i and their elementary flows α_{ij} are modeled in visualized conceptual models, which are subjected to the goal and scope definition.

UPs i in EVo-platform

Previous studies on the EVo-platform have provided different perspectives on its conceptual model. Now, such variation in definitions is common due to the differences in the goals and scopes of each study. According to Torstrick-von der Lieth, the manufacturing process in the EVo-platform consists of four segments that contain various activities. These segments are the ply preparation, preforming, infusion, and curing [314]. In this thesis, the EVo-platform process is redefined based on Fig. 4.16 to include the following UPs i and their qualitative DoA:
UP_1: Preparing (semi-automated); UP_2: Cutting (fully-automated); UP_3: Preforming (fully-automated);
UP_4: Trimming (fully-automated); UP_5: Infusion (fully-automated); UP_6: Curing (fully-automated);
UP_7: Demolding (fully-automated).
Based on this definition, the UPs i are assigned to a simplified illustration of the EVo-platform in Fig. 5.2.

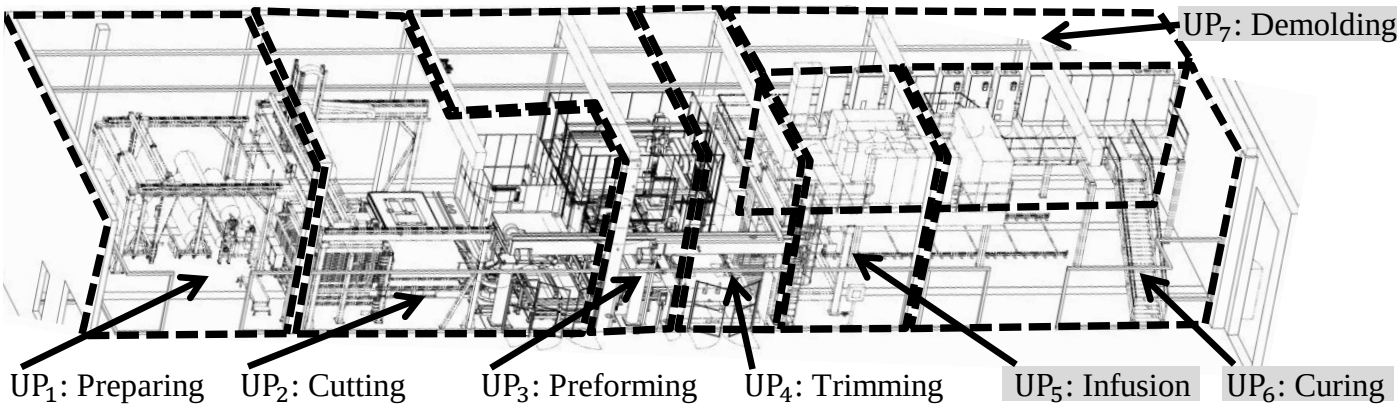

Figure 5.2 EVo-platform and its UPs i, affiliated with [314]

The EVo-platform is developed in efficient facility utilization, as the compact plant in Fig. 5.2 shows. Within these UPs i, activities are also redefined to match the new discretization. However, in this thesis only the first four UPs i including preparing UP_1, cutting UP_2, preforming UP_3, and trimming UP_4 are considered for the parameterization, which are unshaded in Fig. 5.2. For describing their UPs, all associated activities and their elementary flows are discussed here.

As a part of the preparing UP_1, the release film roll $v_{2,9017}$ is transported manually by labors $v_{1,2001} \in \varphi^{[L]}$ to the paternoster roll storage $v_{1,4096} \in \varphi^{[Q]}$ in WS_1. This activity ends when the material roll is placed on the paternoster storage $v_{1,4096}$ and the labors $v_{1,2001}$ leave WS_1. As it has been mentioned previously in Fig. 4.16 within chapter 4, the release film and the fiber materials are considered as inputs in the cutting UP_2 and not preparing UP_1, while no change occurs in them during the preparing. Then, the paternoster storage $v_{1,4096}$ is automatically transporting the rolls to the unwinder $v_{1,4097} \in \varphi^{[Q]}$ and turns back to its initial position. The unwinder $v_{1,4097}$ scrolls the roll down and unwinds the material. In a series production scenario, the roll is scrolled up only when it has no more material. In the EVo-platform, the unwinder $v_{1,4097}$ is capable of sensing

the material magnitude to compare it with the required cut areas. Thus, it scrolls the roll automatically up and orders a replacement in such cases. These activities of preparing are clustered as the first part UP_{1A}.

After the first cutting session is finished, the second part of UP_1 starts. First, the uncut release film is rolled up from the cutter table by the unwinder $v_{1,4097}$. Then, the paternoster storage $v_{1,4096}$ turns the release film roll back to one of its racks. After that, the empty paternoster storage $v_{1,4096}$ turns back to its initial position. The roll can be left on the rack if further projects are planned and free racks are still available. After removing the release film roll, the fiber roll of $v_{2,6014} \in \varphi^{[F]}$ is carried by labors to WS_1 and transported by the paternoster storage $v_{1,4096}$. In practice, the fiber roll is handled by the same activities, which are clustered under UP_{1A}. Still, UP_{1B} activities are temporally unconnected to the previous UP_{1A}. After the second cutting sessions, the fiber roll can be turned back automatically by $v_{1,4096}$. Then, the roll is manually carried by labors $v_{1,2001}$ away from WS_1 at the process end. This third preparing part of UP_{1C} is carried out to set WS_1 back to its initial condition. It is obvious that these activities of UP_1 are required only once for each roll and not per product. This means that if a structure requires multiple material types of fiber or ancillaries, these steps must be repeated to exchange the rolls in this scenario. However, one of the paternoster storage $v_{1,4096}$ advantages is reducing the repetition of these activities, while the racks can store the required rolls of multiple materials. Moreover, the ply storage $v_{2,40100}$ in UP_2 is capable of storing large magnitude of cuts from various materials in its shelves. Although some activities may be performed to prepare the matrix substances, the preparing UP_1 here is studied only for the selected UPs i. These UPs exclude the infusion and its related matrix preparation. Moreover, any preparation activities of setting up the entire facility for a production are not measured in this UP_1 here. Such labor activities are generally considered in the characterization factors as production engineering for the associated equipment and facilities, as Fig. 4.28 and Fig. 4.29 suggest previously in chapter 4.

In the cutting UP_2, the release film and fiber elementary flows are entering this UP_2 as rolls. For each cutting session, the cutter $v_{2,4098} \in \varphi^{[Q]}$ is pulling the roll to its cutting table. Simultaneously, the unwinder $v_{1,4097}$ is down scrolling that roll. Therefore, both UP_1 and UP_2 have limited parallel activities by the unwinder $v_{1,4097}$ and the cutter $v_{2,4098}$. Then, the cutter $v_{2,4098}$ stops pulling as far as the required ply area is already on the cutting table. The first cutting session in UP_{2A} is dedicated to the release film $v_{2,9017}$, while it is temporally unconnected to the other fiber cutting sessions in UP_{2B}. Here, a single layer of the release film $v_{2,9017} \in \varphi^{[R]}$ is cut, whereas it is the only implemented ancillary in this case study. Arguably, cutting the release film $v_{2,9017} \in \varphi^{[R]}$ might be considered as a preparing activity. Still, this work is considering it in cutting UP_2. For the assessed rib, each cutting session for the fiber $v_{2,6014} \in \varphi^{[F]}$ can produce two cuts $\hat{u}_{2,17141} \in \varphi^{[P]}$ of the six required ones. In general, the structure geometry and cutter size play a decisive role in defining the cuts magnitude per session. This cutting session is then repeated until all cuts $\hat{u}_{2,17141}$ are produced, whereas three sessions are sufficient for each rib in this case study. In the EVo-platform, the cuts of fiber and release film can be stored in the ply storage $v_{2,40100} \in \varphi^{[Q]}$ to enable the correct lay-up sequence. Therefore, the ply storage $v_{2,40100}$ opens a dedicated shelf, while the collector of ply storage $v_{2,40100} \in \varphi^{[Q]}$ picks the layers and transports them to that shelf. In this case study, both collector and ply storage systems are considered as one machine $v_{2,40100}$. After both ply storage shelf and collector $v_{2,40100}$ turn back to their initial positions, the cutter $v_{2,4098}$ rolls more material on the cutting table and pushes the wastes $u_{2,6514} \in \varphi^{[G]}$ in a bin. For the limited sessions in this case study, the fiber and release film cuts are stationed on the draping table directly from the ply storage $v_{2,40100}$. This draping table has sufficient area for the total seven cuts and it is located next to the draping robot $v_{3,40101}$ in WS_3. While rolling down the already installed materials by the cutter requires no unwinder activation, the unwinder $v_{1,4097}$ occupation is neglected here. Similar to UP_1, if no enough material is on the roll anymore, the cutter $v_{2,4098}$ pulls the rest back to be scrolled up based on the unwinder orders. In a series production, this exact activity is

required only once for each roll and not repeated by each cutting session. Unlike many other case studies, no cutting papers as ancillaries are required in this specific scenario.

In preforming UP_3, the draping robot $v_{3,40101} \in \varphi^{[Q]}$ is transporting the cuts $\hat{u}_{2,17141}$ from the draping table to the surface of the consolidation mold $v_{3,40103} \in \varphi^{[Q]}$ according to the assigned sequences and orientations. Then, the draping robot $v_{3,40101}$ turns back to its initial position. After that, the mold $v_{3,40103}$ with all layers on it is rolling to the membrane press $v_{3,40102} \in \varphi^{[Q]}$. Whenever the mold has its proper position within the press $v_{3,40102}$, the consolidation process starts following the given durations, pressures, and temperatures required for that exact preform $\hat{u}_{3,17142} \in \varphi^{[P]}$. The membrane press $v_{3,40102}$ operates in this case study with a maximum temperature of around 180 °C under a pressure of up to 1.8 bar. As soon as the consolidation is finished, the mold $v_{3,40103}$ moves with the preform $\hat{u}_{3,17142}$ out of the press $v_{3,40102}$ toward WS_4.

In trimming UP_4, the consolidation mold $v_{3,40103}$ is rolling sideways on a carrier to the trimming WS_4. Then, it is transported by the lower part of the handling robot $v_{4,40104}$. To simplify the assessment in WS_4, two different (in and out) transportation devices are combined under the term handling robot $v_{4,40104}$, which are the upper handling robot stationed on its chain and the lower rolling chain. The same consolidation mold $v_{3,40103}$ is used as a trimming mold $v_{4,40103} \in \varphi^{[Q]}$ in this case study. Then, the trimming portal $v_{4,40105}$ opens its door to the mold $v_{4,40103}$. After going on a lower level, the mold on its carrier is entering the trimming portal $v_{4,40105}$. The mold carrier is lowering down and the portal door closes. After that, the mold may rotate to any proper angle. As a part of the trimming portal $v_{4,40105}$, a robot head is moving down and starts trimming the rib preform $\hat{u}_{3,17142}$ by an ultrasonic knife installed on its head. After the trimming job is done, another picking device, that is installed on the side of the robot head, removes the consolidated waste $u_{4,65141} \in \varphi^{[G]}$ as well as the release film $v_{2,9017}$ and drops them in separated bins. In this case, the consolidated waste $u_{4,65141} \in \varphi^{[G]}$ is distinguished from the non-consolidated one $u_{2,6514} \in \varphi^{[G]}$. Although the re-usability of fiber waste $\varphi^{[G]}$ is beyond the scope of this thesis, distinguishing between the different fiber waste forms is useful to provide the decision-makers with better process understanding regarding possible SDs. Technically, fiber waste $u_{2,6514} \in \varphi^{[G]}$ has different physical characteristics in comparison to the consolidated fiber waste $u_{4,65141} \in \varphi^{[G]}$. Then, the trimming robot head moves up and turns back to its initial position. If it rotates to a new position, the mold carrier should be rotating back to its initial position before rising up again. After the portal door opens, the mold $v_{4,40103}$ slides out of it and moves outside the portal. The final activity in UP_4 is done when the handling robot picks the trimmed preform as the final product in this case study $u_{4,17143} \in \varphi^{[S]}$ and sends it to the next WS.

As it is explained earlier, all further activities are beyond the scope of this case study. For simplicity, the total used magnitudes of ancillaries such as the release film $v_{2,9017}$ are considered as inputs without the differentiation of their wastes or reusable substances. All UPs i within the EVo-platform are taking a place in an air conditioned facility, that is considered as a set of input elementary flows for the assessment. Moreover, several quality assurance activities are carried out automatically by the involved machines, while they are merged in machines performances and not separately discussed here. Later in this chapter, a comprehensive illustration of all involved mentioned machines is introduced as a part of the elementary flows description.

Elementary flows α_{ij} of selected UPs i in EVo-platform

Based on the generic illustration in Fig. 4.18, a description of all relevant elementary flow subsets $\varphi^{[\Gamma]}$ is provided for the selected UPs i of the EVo-platform within Fig. 5.3. For the considered UPs i, the fiber $v_{2,6014} \in \varphi^{[F]}$ is the only core structural material in this case study, whereas no matrix is considered. Consequently, the fiber wastes $\varphi^{[G]}$ are the only wasted materials in this case study.

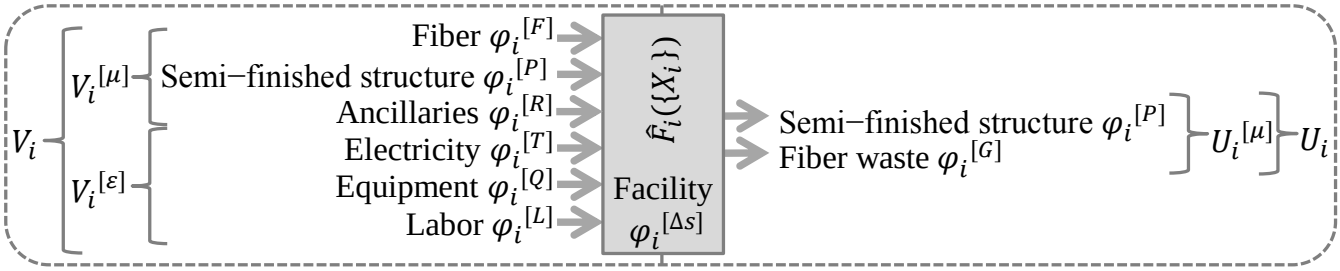

Figure 5.3 Subsets $\varphi^{[\Gamma]}$ relevant for the selected UPs i in EVo-platform

The used fiber for the experiments in this work is produced by HEXCEL®. This material roll has the width of 1.304 m, length of 104 m, fiber surface mass of 0.375 kg/m^2, and total weight of 54.08 kg including the core bar. The semi-finished structures in this case study are the cuts $\hat{u}_{2,17141} \in \varphi^{[P]}$ and preform $\hat{u}_{3,17142} \in \varphi^{[P]}$. In this case study, trimming UP$_4$ is the highest discussed UP$_m$ with $m = 4$. Therefore, the previously introduced conditions for the final UP$_7$ in Fig. 4.16 are applied to trimming UP$_4$ in this case study. To put it more simply, the final outcome of the assessed process is the trimmed preform $u_{4,17143} \in \varphi^{[S]}$. As an industrial process with high DoA, the EVo-platform requires very limited ancillaries $\varphi^{[R]}$ in general. For the selected UPs i in specific, only a single ancillary is implemented, which is the release film $v_{2,9017} \in \varphi^{[R]}$. Manufactured by Airtech Europe Sarl, the used release film is made of polyolefine. Certified for the manufacturing of components in commercial aircraft and wind energy industries, this release film is usable in a temperature below 121 °C.

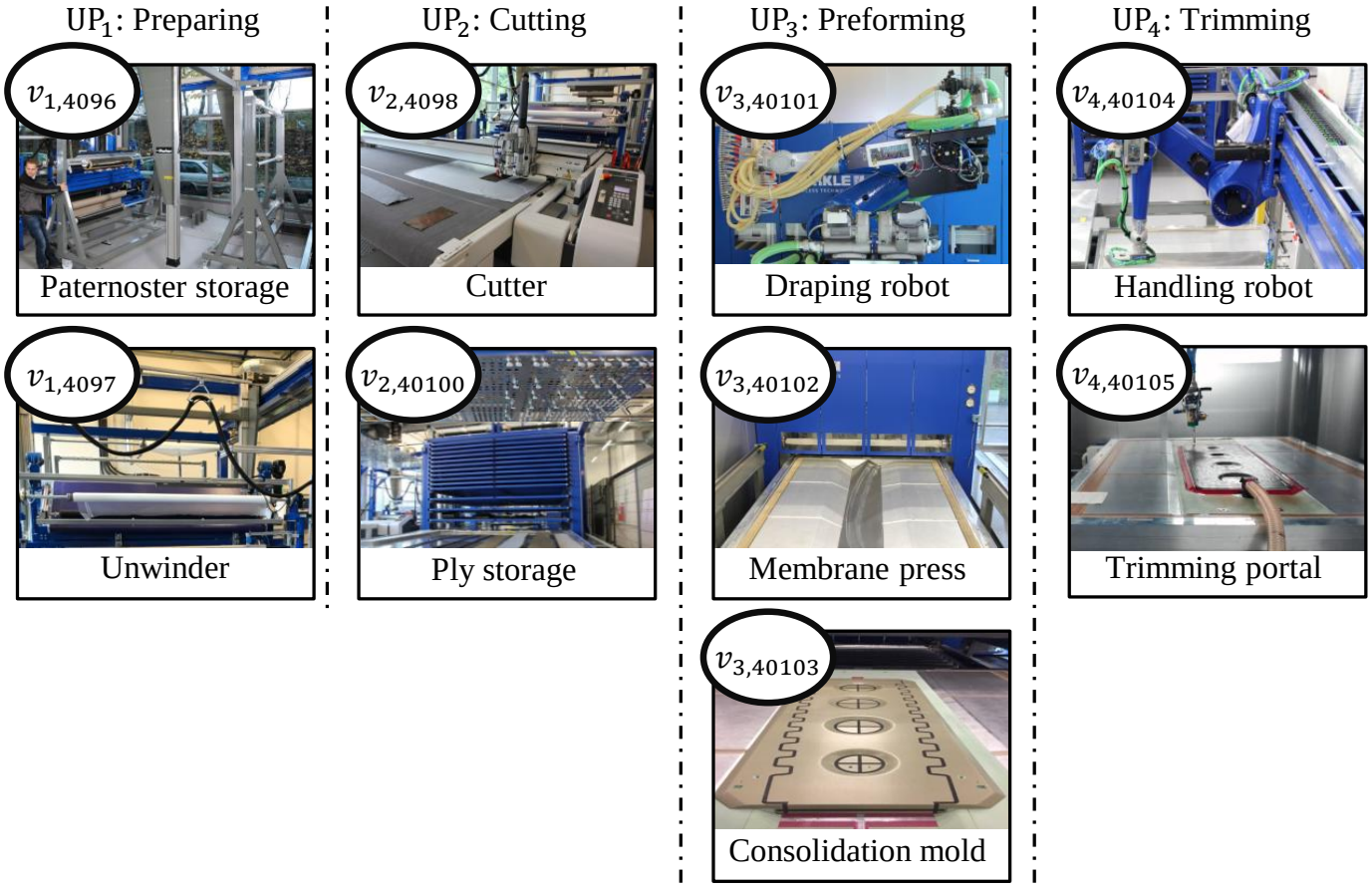

Figure 5.4 Machines as input flows $v_{ij} \in \varphi^{[Q]}$ in considered UPs i of EVo-platform

Understanding the relevant equipment types $v_{ij} \in \varphi^{[Q]}$ of the assessed UPs i plays a decisive role in assessing a high DoA facility such as the EVo-platform. Within the boundary of this case study, only the machines and a single mold are implemented as elementary flows from equipment subset $\varphi^{[Q]}$. The difference between these

types of equipment and their belonging subsystems is subjected to many factors. For instance, transporting robots may be considered as separated machines or as a part of others. Nonetheless, previously established definitions by the developing team of the EVo-platform are adopted for distinguishing the machine and mold types in this thesis [315], as Fig. 5.4 shows. The EVo-platform has a paternoster material storage $v_{1,4096}$ with exchangeable layers for six rolls with maximum width of more than 3 m. This enables the handling of different materials of fibers or ancillaries simultaneously. This paternoster storage $v_{1,4096}$ is supported by a specialized unwinder $v_{1,4097}$ to scroll the rolls up and down automatically. The EVo-platform also includes an automated cutter $v_{2,4098}$ that is capable of handling areas of around (3.2×2.7 m) with variable tools for cutting, punching, grinding, and plotting [10]. The ply storage collector $v_{2,40100}$ is mounted above the cutter $v_{2,4098}$. This collector has a track to reach the ply storage as well as the table of draping next to the draping robot $v_{3,40101}$. In practice, the cuts can be stored in the ply storage $v_{2,40100}$ temporary for better orientation and efficient cutting. The draping robot $v_{3,40101}$ contains various devices, that serve different manufacturing scenarios. For instance, it has a track, a linear axis, optical detection of ply positioning, an active draping-gripper, and a local electric binder activator. It picks the cuts delivered on the draping table after detecting them optically. This robot $v_{3,40101}$ lays these cuts on the mold $v_{3,40103}$, which is positioned on a track heading toward the membrane press $v_{3,40102}$.

The membrane press $v_{3,40102}$ itself contains a list of devices. As a main device, the membrane press itself carries out hot-forming and consolidation of the sub-preforms with the capacity of (2×2.5 m). In addition, there are other devices such as the IR heating device, the vacuum and additional air pressure pumps, as well as the system of automated membrane feeding. The mold $v_{3,40103}$ specifications depend highly on the case study, while in this case study the same mold is implemented in both preforming and trimming. As the main machine in UP_4, the trimming portal $v_{4,40105}$ trims the preforms into final net shape before infusion and curing. The trimming portal $v_{4,40105}$ has an ultrasonic knife, a referencing system, a laser system for topology scan, as well as a laser-controlled safety housing. In UP_4, the handling robot $v_{4,40104}$ picks the trimmed preform and transports it to the infusion station, which is beyond the scope of this work.

The EVo-platform has non-destructive inspection systems, that are integrated within some of the previously mentioned machines [315]. In practice, these machines contain wear components that are routinely changed in the preventive maintenance. For the cutter $v_{2,4098}$, the cutting knife is an example of such wear components. For the membrane press $v_{3,40102}$, the forming membrane is one of these components, while ultrasonic knives in the trimming portal $v_{4,40105}$ belong to them too. However, the impacts of such components are considered within the characterization factors as a part of the maintenance to investment ratio of each equipment. In this case study, two labors $v_{1,2001} \in \varphi^{[L]}$ are required to transport the fiber and release film rolls on 3 m carriers. In the EVo-platform, the WSs boundaries with the surroundings are defined by the safety partitioning fences around the plant. Boundaries between the WSs themselves are based on the UPs allocation, as Fig. 5.2 shows before.

5.2.2 EVo-Platform Mathematical Process Model

The mathematical model for assessing the selected UPs i is generically established based on the previously introduced ones including Eq. 4.62 and Eq. 4.63 from chapter 4. Then, the eco-efficiency is assessed as Eq. 4.83 suggests. The selected case study, which consists of the four UPs i, includes various elementary flows α_{ij}. These elementary flows α_{ij} are determined for the parametrization in each UP i. In UP_1, the paternoster storage $v_{1,4096} \in \varphi^{[Q]}$, unwinder $v_{1,4097} \in \varphi^{[Q]}$, labor $v_{1,2001} \in \varphi^{[L]}$, WS_1 facility $v_{1,3001} \in \varphi^{[\Delta s]}$, and electricity consumption $v_{1,1001} \in \varphi^{[T]}$ of that facility and each equipment represented by $v_{1,1031}$, $v_{1,10496}$, and $v_{1,10497}$ are considered. For UP_2, the associated elementary flows α_{ij} include the cutter $v_{2,4098} \in \varphi^{[Q]}$, ply storage $v_{2,40100} \in \varphi^{[Q]}$, fiber $v_{2,6014} \in \varphi^{[F]}$, release film $v_{2,9017} \in \varphi^{[R]}$, fiber waste $u_{2,6514} \in \varphi^{[G]}$, WS_2 facility

$v_{2,3002} \in \varphi^{[\Delta s]}$, and all electricity inputs $v_{2,1001} \in \varphi^{[T]}$ including $v_{2,1032}$, $v_{2,10498}$ and $v_{2,104100}$. In this case study, UP_3 includes the elementary flows α_{ij} of the draping robot $v_{3,40101} \in \varphi^{[Q]}$, membrane press $v_{3,40102} \in \varphi^{[Q]}$, mold $v_{3,40103} \in \varphi^{[Q]}$, WS_3 facility $v_{3,3003} \in \varphi^{[\Delta s]}$, and total electricity consumption $v_{3,1001} \in \varphi^{[T]}$ including $v_{3,1033}$, $v_{3,104101}$, $v_{3,104102}$. In UP_4, the considered elementary flows α_{ij} consist of the chain robot $v_{4,40104} \in \varphi^{[Q]}$, trimming portal $v_{4,40105} \in \varphi^{[Q]}$, mold $v_{4,40103} \in \varphi^{[Q]}$, consolidate fiber waste $u_{4,65141} \in \varphi^{[G]}$, WS_4 facility $v_{4,3004} \in \varphi^{[\Delta s]}$, and total electricity consumption $v_{4,1001} \in \varphi^{[T]}$ including $v_{4,1034}$, $v_{4,104104}$, $v_{4,104105}$.

Based on this, the adjusted process matrix $[A]$ is described by Eq. 5.1.

$$[A] = \begin{bmatrix} \Upsilon^{[T]} & [\Upsilon^{[L]}] & [\Upsilon^{[\Delta s]}] & [\Upsilon^{[Q]}] & [\Upsilon^{[F]}] & [\Upsilon^{[R]}] & [\Upsilon^{[G]}] \end{bmatrix} \tag{5.1}$$

As it is mentioned previously in chapter 4, the sequence of categories is adjustable in $[A]$. For the outputs, impacts of $[\Upsilon^{[P]}]$ and $[\Upsilon^{[S]}]$ are equal to the entire process in the assessment, while they can be neglected in $[A]$. Therefore, the input ones are illustrated based on their ID sequence followed by the only considered output category in Eq. 5.1. Based on the previously introduced Fig. 4.19 in chapter 4, further mathematical equations can be derived from the global matrix $[A]$ in Eq. 5.1 of the case study. The first category is electricity, which is represented by the column vector and the matrix $[\Upsilon^{[T]}]$ shown in Eq. 5.2.

$$[\Upsilon^{[T]}] = \begin{bmatrix} v_{1,1001} \\ v_{2,1001} \\ v_{3,1001} \\ v_{4,1001} \end{bmatrix} = \begin{bmatrix} v_{1,1031} & 0 & 0 & 0 & v_{1,10496} & v_{1,10497} \\ 0 & v_{2,1032} & 0 & 0 & 0 & 0 \\ 0 & 0 & v_{3,1033} & 0 & 0 & 0 \\ 0 & 0 & 0 & v_{4,1034} & 0 & 0 \\ 0 & 0 & 0 & 0 & 0 & 0 \\ v_{2,10498} & v_{2,104100} & 0 & 0 & 0 & 0 \\ 0 & 0 & v_{3,104101} & v_{3,104102} & 0 & 0 \\ 0 & 0 & 0 & 0 & v_{4,104104} & v_{4,104105} \end{bmatrix} \tag{5.2}$$

Therefore, the subset $\varphi^{[T]}$ represents the electricity category in this case study containing $\{v_{1,1031}, v_{2,1032}, v_{3,1033}, v_{4,1034}\}$, which are the „*zero*" performance electricity consumptions in all WS_i and $\{v_{1,10496}, v_{1,10497}, v_{2,10498}, v_{2,104100}, v_{3,104101}, v_{3,104102}, v_{4,104104}, v_{4,104105}\}$, which are the electricity consumptions of the machines $\{v_{1,4096}, v_{1,4097}, v_{2,4098}, v_{2,40100}, v_{3,40101}, v_{3,40102}, v_{4,40104}, v_{4,40105}\}$ respectively, while $[\Upsilon^{[T]}] \in \varphi^{[T]^{m \times n}}$. The second category is labor, which is represented by the column vector $[\Upsilon^{[L]}]$, that is discussed in Eq. 5.3.

$$[\Upsilon^{[L]}] = \begin{bmatrix} v_{1,2001} \\ 0 \\ 0 \\ 0 \end{bmatrix} \tag{5.3}$$

While labor work is relevant for UP_1 only, the subset $\varphi^{[L]}$ contains a single element of $\varphi^{[L]} = \{v_{1,2001}\}$ in this case study, in which $[\Upsilon^{[L]}] \in \varphi^{[L]^{m \times 1}}$. The facility is represented by the matrix $[\Upsilon^{[\Delta s]}]$ in Eq. 5.4.

$$[\Upsilon^{[\Delta s]}] = \begin{bmatrix} v_{1,3001} & 0 & 0 & 0 \\ 0 & v_{2,3002} & 0 & 0 \\ 0 & 0 & v_{3,3003} & 0 \\ 0 & 0 & 0 & v_{4,3004} \end{bmatrix} \tag{5.4}$$

As Eq. 5.4 shows, each UP i consists of a single „*nonzero*“ element from $[\Upsilon^{[\Delta s]}]$. Here, subset $\varphi^{[\Delta s]}$ contains only four elements as $\varphi^{[\Delta s]} = \{v_{1,3001}, v_{2,3002}, v_{3,3003}, v_{4,3004}\}$, while $[\Upsilon^{[\Delta s]}] \in \varphi^{[\Delta s]^{m\times n}}$. The reason behind distinguishing the facility elements between the different UPs i is their distinguishable characterization factors λ_j due to the area differences. In comparison, the electricity column vector $[\Upsilon^{[T]}]$ has the same characterization factors λ_j in every UP i. For the equipment subset $\varphi^{[Q]}$ including both machines and the mold in this case study, a matrix $[\Upsilon^{[Q]}]$ is derived from Eq. 5.1 in Eq. 5.5.

$$[\Upsilon^{[Q]}] = \begin{bmatrix} v_{1,4096} & v_{1,4097} & 0 & 0 & 0 & 0 & 0 & 0 & 0 \\ 0 & 0 & v_{2,4098} & v_{2,40100} & 0 & 0 & 0 & 0 & 0 \\ 0 & 0 & 0 & 0 & v_{3,40101} & v_{3,40102} & v_{3,40103} & 0 & 0 \\ 0 & 0 & 0 & 0 & 0 & 0 & v_{4,40103} & v_{4,40104} & v_{4,40105} \end{bmatrix} \tag{5.5}$$

Based on Eq. 5.5, subset $\varphi^{[Q]}$ contains ten elements as $\varphi^{[Q]} = \{v_{1,4096}, v_{1,4097}, v_{2,4098}, v_{2,40100}, v_{3,40101}, v_{3,40102}, v_{3,40103}, v_{4,40103}, v_{4,40104}, v_{4,40105}\}$, while the mold $v_{i,40103}$ appears in both UP_3 and UP_4. The fiber category is represented by the column vector $[\Upsilon^{[F]}]$ in Eq. 5.6.

$$[\Upsilon^{[F]}] = \begin{bmatrix} 0 \\ v_{2,6014} \\ 0 \\ 0 \end{bmatrix} \tag{5.6}$$

This subset of $\varphi^{[F]}$ includes a single element as $\varphi^{[F]} = \{v_{2,6014}\}$ in this case study, while $[\Upsilon^{[F]}] \in \varphi^{[F]^{m\times 1}}$. Moreover, the ancillaries category is represented by the column vector $[\Upsilon^{[R]}]$ in Eq. 5.7.

$$[\Upsilon^{[R]}] = \begin{bmatrix} 0 \\ v_{2,9017} \\ 0 \\ 0 \end{bmatrix} \tag{5.7}$$

Again, the subset $\varphi^{[R]}$ represents this category, which consists of a single element of $\varphi^{[R]} = \{v_{2,9017}\}$ in this case study, while $[\Upsilon^{[R]}] \in \varphi^{[R]^{m\times 1}}$. Finally, the last considered category is fiber waste represented by $[\Upsilon^{[G]}]$ in Eq. 5.8.

$$[\Upsilon^{[G]}] = \begin{bmatrix} 0 & 0 \\ u_{2,6514} & 0 \\ 0 & 0 \\ 0 & u_{4,65141} \end{bmatrix} \tag{5.8}$$

As Eq. 5.8 shows, two UPs i consist of a single „*nonzero*“ element from $[\Upsilon^{[G]}]$ in each. Here, subset $\varphi^{[G]}$ contains only two „*nonzero*“ in total as $\varphi^{[G]} = \{u_{2,6514}, u_{4,65141}\}$, while $[\Upsilon^{[G]}] \in \varphi^{[G]^{m\times n}}$.

On the UP i level, Eq. 5.1 can be also split into four vectors of $\{A_i\}$, that represent each UP i separately. For UP_1, Eq. 5.9 provides the comprehensive illustration of all associated row vectors $\{\Upsilon_1^{[\Gamma]}\}$.

$$\{A_1\} = \{\{\Upsilon_1^{[T]}\} \quad \{\Upsilon_1^{[L]}\} \quad \{\Upsilon_1^{[\Delta s]}\} \quad \{\Upsilon_1^{[Q]}\} \quad \{\Upsilon_1^{[F]}\} \quad \{\Upsilon_1^{[R]}\} \quad \{\Upsilon_1^{[G]}\}\} \tag{5.9}$$

The vectors $\{\Upsilon_1^{[T]}\}$, $\{\Upsilon_1^{[L]}\}$, $\{\Upsilon_1^{[\Delta s]}\}$, and $\{\Upsilon_1^{[Q]}\}$ are described in Eq. 5.10, Eq. 5.11, Eq. 5.12, and Eq. 5.13 respectively, while $\{\Upsilon_1^{[F]}\}$, $\{\Upsilon_1^{[R]}\}$, and $\{\Upsilon_1^{[G]}\}$ have only „*zero*“ value elements in UP_1.

$$\{\Upsilon_1^{[T]}\} = v_{1,1001} = \begin{Bmatrix} v_{1,1031} & 0 & 0 & 0 & v_{1,10496} & v_{1,10497} \\ 0 & 0 & 0 & 0 & 0 & 0 \end{Bmatrix} \tag{5.10}$$

$$\{\Upsilon_1^{[L]}\} = v_{1,2001} \tag{5.11}$$

$$\{\Upsilon_1^{[\Delta s]}\} = \{v_{1,3001} \quad 0 \quad 0 \quad 0\} \tag{5.12}$$

$$\{\Upsilon_1^{[Q]}\} = \{v_{1,4096} \quad v_{1,4097} \quad 0 \quad 0 \quad 0 \quad 0 \quad 0 \quad 0 \quad 0\} \tag{5.13}$$

The same approach of Eq. 5.9 is adopted to represent UP_2 in Eq. 5.14.

$$\{A_2\} = \{\{\Upsilon_2^{[T]}\} \quad \{\Upsilon_2^{[L]}\} \quad \{\Upsilon_2^{[\Delta s]}\} \quad \{\Upsilon_2^{[Q]}\} \quad \{\Upsilon_2^{[F]}\} \quad \{\Upsilon_2^{[R]}\} \quad \{\Upsilon_2^{[G]}\}\} \tag{5.14}$$

In which, the vectors $\{\Upsilon_2^{[T]}\}$, $\{\Upsilon_2^{[\Delta s]}\}$, $\{\Upsilon_2^{[Q]}\}$, $\{\Upsilon_2^{[F]}\}$, $\{\Upsilon_2^{[R]}\}$, and $\{\Upsilon_2^{[G]}\}$ are described in Eq. 5.15, Eq. 5.16, Eq. 5.17, Eq. 5.18, Eq. 5.19, and Eq. 5.20 respectively, while $\{\Upsilon_2^{[L]}\}$ has only „*zero*“ elements in UP_2.

$$\{\Upsilon_2^{[T]}\} = v_{2,1001} = \begin{Bmatrix} 0 & v_{2,1032} & 0 & 0 & 0 & 0 \\ v_{2,10498} & v_{2,104100} & 0 & 0 & 0 & 0 \end{Bmatrix} \tag{5.15}$$

$$\{\Upsilon_2^{[\Delta s]}\} = \{0 \quad v_{2,3002} \quad 0 \quad 0\} \tag{5.16}$$

$$\{\Upsilon_2^{[Q]}\} = \{0 \quad 0 \quad v_{2,4098} \quad v_{2,40100} \quad 0 \quad 0 \quad 0 \quad 0 \quad 0\} \tag{5.17}$$

$$\{\Upsilon_2^{[F]}\} = v_{2,6014} \tag{5.18}$$

$$\{\Upsilon_2^{[R]}\} = v_{2,9017} \tag{5.19}$$

$$\{\Upsilon_2^{[G]}\} = \{u_{2,6514} \quad 0\} \tag{5.20}$$

In Eq. 5.21, UP_3 is described by $\{A_3\}$ with its row vectors $\{\Upsilon_3^{[\Gamma]}\}$.

$$\{A_3\} = \{\{\Upsilon_3^{[T]}\} \quad \{\Upsilon_3^{[L]}\} \quad \{\Upsilon_3^{[\Delta s]}\} \quad \{\Upsilon_3^{[Q]}\} \quad \{\Upsilon_3^{[F]}\} \quad \{\Upsilon_3^{[R]}\} \quad \{\Upsilon_3^{[G]}\}\} \tag{5.21}$$

The vectors $\{\Upsilon_3^{[T]}\}$, $\{\Upsilon_3^{[\Delta s]}\}$, and $\{\Upsilon_3^{[Q]}\}$ are described in Eq. 5.22, Eq. 5.23, and Eq. 5.24 respectively, while $\{\Upsilon_3^{[L]}\}$, $\{\Upsilon_3^{[F]}\}$, $\{\Upsilon_3^{[R]}\}$, and $\{\Upsilon_3^{[G]}\}$ have only „*zero*“ value elements.

$$\{\Upsilon_3^{[T]}\} = v_{3,1001} = \begin{Bmatrix} 0 & 0 & v_{3,1033} & 0 & 0 & 0 \\ 0 & 0 & v_{3,104101} & v_{3,104102} & 0 & 0 \end{Bmatrix} \tag{5.22}$$

$$\{\Upsilon_3^{[\Delta s]}\} = \{0 \quad 0 \quad v_{3,3003} \quad 0\} \tag{5.23}$$

$$\{\Upsilon_3^{[Q]}\} = \{0 \quad 0 \quad 0 \quad 0 \quad v_{3,40101} \quad v_{3,40102} \quad v_{3,40103} \quad 0 \quad 0\} \tag{5.24}$$

In Eq. 5.25, UP_4 is described as $\{A_4\}$ by its row vectors $\{\Upsilon_4^{[\Gamma]}\}$.

$$\{A_4\} = \{\{\Upsilon_4^{[T]}\} \quad \{\Upsilon_4^{[L]}\} \quad \{\Upsilon_4^{[\Delta s]}\} \quad \{\Upsilon_2^{[Q]}\} \quad \{\Upsilon_4^{[F]}\} \quad \{\Upsilon_4^{[R]}\} \quad \{\Upsilon_4^{[G]}\}\} \tag{5.25}$$

In which, the vectors $\{\Upsilon_4^{[T]}\}$, $\{\Upsilon_4^{[\Delta s]}\}$, $\{\Upsilon_4^{[Q]}\}$, and $\{\Upsilon_3^{[G]}\}$ are described in Eq. 5.26, Eq. 5.27, Eq. 5.28, and Eq. 5.29 respectively, while $\{\Upsilon_4^{[L]}\}$, $\{\Upsilon_4^{[F]}\}$, and $\{\Upsilon_4^{[R]}\}$ have only „*zero*“ elements in UP_4.

$$\{\Upsilon_4^{[T]}\} = v_{4,1001} = \begin{Bmatrix} 0 & 0 & 0 & v_{4,1034} & 0 & 0 \\ 0 & 0 & 0 & 0 & v_{4,104104} & v_{4,104105} \end{Bmatrix} \tag{5.26}$$

$$\{\Upsilon_4^{[\Delta s]}\} = \{0 \quad 0 \quad 0 \quad v_{4,3004}\} \tag{5.27}$$

$$\{\Upsilon_4^{[Q]}\} = \{0 \quad 0 \quad 0 \quad 0 \quad 0 \quad 0 \quad v_{4,40103} \quad v_{4,40104} \quad v_{4,40105}\} \tag{5.28}$$

$$\{\Upsilon_4^{[G]}\} = \{0 \quad u_{4,65141}\} \tag{5.29}$$

These mathematical extracted models are essential for enabling a multilevel time-dependent eco-efficiency assessment of various covered CSFs.

5.3 SWS and EEAM for EVo-Platform

To apply the time-dependent eco-efficiency assessment to the case study, both real-time SWS and time-dependent EEAM must be adapted to it by the proper methods, sensor nodes, SWS-DB, and EEAM-DB.

5.3.1 SWS Sensor Nodes in EVo-Platform

In this section, the adopted MIs and MMs in the studied UPs i within the EVo-platform are defined. Moreover, the appropriate SIs and SMs to realize these methods are described.

MIs and MMs in EVo-platform

The SWS concept is applied to the WSs to turn them into SWSs by proper MIs, MMs, SIs, and SMs. In this case study, each UP i is performed in spatially and temporally allocated WSs. Therefore, four SWSs have been assigned to this case study, which are the preparing SWS_1, cutting SWS_2, preforming SWS_3, and trimming SWS_4. Based on Tab. 4.8 and Tab. 4.9, the assigned MIs and MMs are listed for each SWS_i in Tab. 5.1.

While MI-(5) is insufficient in distinguishing between multiple labors in the current version of SWS, both MI-(2) and MI-(5) are combined to identify the labors $v_{1,2001} \in \varphi^{[L]}$ in this work. MI-(3) is utilized to identify the fiber or ancillary rolls in SWS_1.

Table 5.1 Assigned MIs and MMs in the SWS_i of the case study *

Method	SWS_1	SWS_2	SWS_3	SWS_4
MIs	MI-(2); MI-(3); MI-(5); MI-(6); MI-(8)	MI-(1); MI-(6); MI-(7); MI-(8)	MI-(6); MI-(7); MI-(8)	MI-(1); MI-(6); MI-(7); MI-(8)
MMs	MM-(1); MM-(2); MM-(3); MM-(4); MM-(5); MM-(6); MM-(7); MM-(8)	MM-(1); MM-(4); MM-(5); MM-(6); MM-(7)	MM-(1); MM-(4); MM-(5); MM-(6); MM-(7)	MM-(1); MM-(4); MM-(5); MM-(6); MM-(7)

* MI-(1): visual recognition MI-(2): person detection MI-(3): bar- or QR-code scanning MI-(5): person thermal detection MI-(6): equipment dedicated identification MI-(7): material and tool identification MI-(8): facility identification MM-(1): material weight measurement MM-(2): persons count MM-(3): optical labor work measurement MM-(4): equipment time measurement MM-(5): equipment operation energy MM-(6): process duration MM-(7): facility occupation MM-(8): thermal labor work measurement

Although, MI-(7) may replace MI-(3) in SWS_1 for a predefined material on a specified rack in the paternoster storage, MI-(3) is preferred because of its capability in covering multiple fiber types in future case studies within the EVo-platform. MI-(3) is also used for identifying ancillaries and their variants such as the rolls of release film $v_{2,9017} \in \varphi^{[R]}$. MI-(6) is applied for every established SWS_i in the EVo-platform, while several machines are implemented. Similar to MI-(6), MI-(8) is applied in identifying the facilities of all SWS_i in this case study. For the magnitude determination, MM-(1) is applied to track materials magnitude changes throughout the assessed UPs i. Nonetheless, MM-(1) is combined with MI-(3) to determine the rolls weight in SWS_1. While MI-(2) is applied to identify the labors $v_{1,2001}$, MM-(2) and MM-(3) are used to count them and determine their work duration. For the validation, MM-(8) is also used to determine the labor work duration based on the thermal measurement, while the labor count of two labors is predefined. For the various machines used in every considered SWS_i, MM-(4) and MM-(5) are applied to measure the performance duration and electricity consumption of each machine respectively. In addition, MM-(6) is applied to every considered UP i to determine their durations. Based on the facility identification from MI-(8) and process duration from MM-(6), MM-(7) is similarly applied to all SWS_i to determine the facility occupation time. To validate the wasted fiber $u_{2,6514}$ measurement in SWS_2, the fiber cuts $\hat{u}_{2,17141} \in \varphi^{[P]}$ are measured by MM-(1), while the input from material roll is already measured by SWS_1. In SWS_3, only intermediate flows are entering in the form of material, which requires no additional distinguishing method other than MI-(7). Methods in SWS_4 are identical to the ones implemented in SWS_2. In SWS_4, MI-(1) has been included due to the need for distinguishing the wastes from trimming UP_4. It is clear in Tab. 5.1 that any SWS_i with manual activities requires further MIs and MMs compared to fully-automated ones.

SIs and SMs in EVo-platform

Based on defining the required methods in Tab. 5.1, the proper SIs and SMs are selected and allocated for the case study in Fig. 5.5. To convert the included WSs into SWSs, five types of sensor nodes have been utilized. These types are listed on the left side of Fig. 5.5, while pictures of commercially available solutions are shown too. As it is shown on the right side of Fig. 5.5, these sensor nodes are set up within each associated SWS_i to fulfill the methods suggested before in Tab. 5.1. In addition, the allocation of each sensor node is distinguished by a number to provide more explanation of that exact setup.

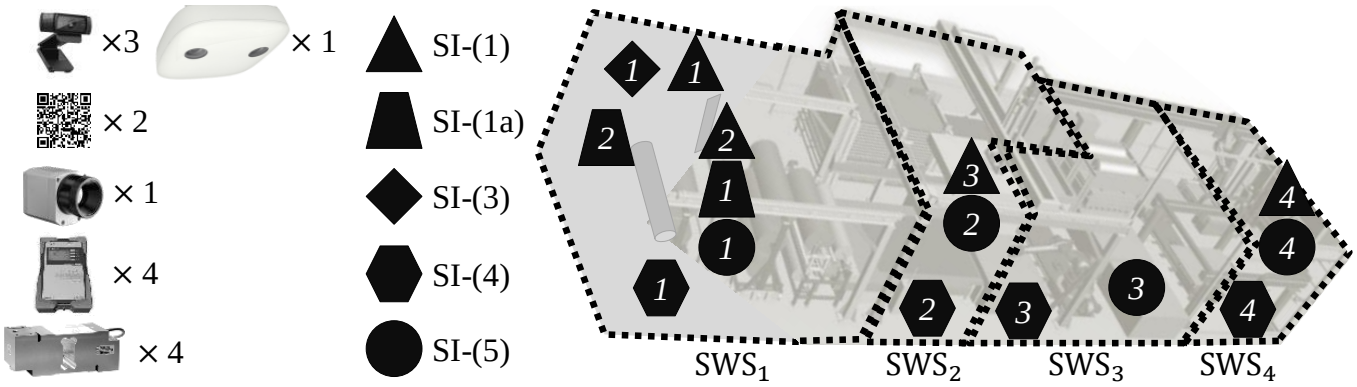

Figure 5.5 SIs and SMs in SWSs of EVo-platform *

* SI-(1): imaging sensor (digital camera) SI-(1a): coded sticker SI-(3): thermal sensors (IR-camera) SI-(4): dedicated electricity meter SI-(5): dedicated digital scale

They include four SI-(1) of two types, two SI-(1a) sets, single SI-(3), four SI-(4) channels, and four SI-(5) sets, which have been discussed thoroughly in Tab. 4.8 and Tab. 4.9 before. For MI-(2) in SWS_1, the person identification is realized by a 3-dimensional visual scanning camera from HELLA AGLAIA Mobile Vision company. The advanced people sensor, that is shown as a white colored two lenses camera on the left side of Fig. 5.5, is mounted above SWS_1 and projected to cover its entire area. Distinguished by number „*1*“ of SI-(1), this camera is implemented to realize MI-(2), MM-(2), and MM-(3) in SWS_1. In SWS_1, SI-(3) is represented by a single IR-camera from the company optris® to serve both MI-(5) and MM-(8). This IR-camera is mounted next to the 3-dimensional visual scanning camera to carry out a surveillance on the same spectrum for the validation. To realize MI-(3) in SWS_1, a digital web cam SI-(1) is set up on the paternoster storage racks to observe the rolls tip, whereas two sets of QR-coded stickers SI-(1a) are taped with various angles on the bars of both fiber and release film rolls. As it is shown on the left side of Fig. 5.5, web cams have been selected for this method. In SWS_1, the same rack is stationed on two digital scales SI-(5) under the carriers of both roll sides. As the left side of Fig. 5.5 shows, a high sensitivity digital scale with measurement amplifier has been selected to serve MM-(1) in SWS_1. Therefore, a single-point load cell for a maximum load of 50 kg is installed beneath each side of the carrier. On the right side of Fig. 5.5, both scales are mentioned by number „*1*“ of SI-(5). More details about the implementation of SI-(1), SI-(1a), and SI-(5) in serving MI-(1), MI-(3), MI-(7), and MM-(1) have been introduced in a previous work [271]. To serve MI-(6), MM-(4), and MM-(5), dedicated SI-(4) from the company A. Eberle is implemented. Here, Fig. 5.5 shows four electricity meters, while each is stationed in a SWS_i. However, this type of sensor nodes may be installed far away from the SWS_i at the central electricity distributer or on its supply lines, as it has been explained as a part of the temporal and spatial assignment in chapter 4. In this case study, a single SI-(4) with multiple channels on the WS_i electricity supply lines within the central distributer is applied. The numbers in Fig. 5.5 from „*1*“ to „*4*“ refer in this case to the measurement main channels installed on the supply lines in the distributer. Using a single SI-(4) with multiple channels is technically sufficient and requires less sensor connecting efforts. To serve MI-(8), MM-(6), and MM-(7), all previously mentioned SIs and SMs are utilized.

For MI-(1) in SWS_2, the same type of web cam from SWS_1 is implemented. This SI-(1) is installed as a part of the lower surface of ply storage collector $v_{2,40100}$. For this case study, only a single type of fiber $v_{2,6014}$ and similarly a release film $v_{2,9017}$ are collected by $v_{2,40100}$. Therefore, optically distinguishing both materials by MI-(1) is possible due to their unique optical characteristics in the SWS-DB such as the different colors [271]. Combined with MI-(1), a single digital scale is mounted to measure the weight of picked materials by the collector $v_{2,40100}$ as a realization for MM-(1). Instead of the ply storage collector $v_{2,40100}$, these SI-(1)

and SI-(5) may be installed to each shelf in the ply storage $v_{2,40100}$. While this requires more sensor nodes to deliver the same results, this approach has been neglected in this work. Similar to their setups in SWS_1, MI-(6), MM-(4), and MM-(5) are realized in SWS_2 by channels of the same central electricity meter, which covers the machines in this WS. MI-(8), MM-(6), and MM-(7) are served by all sensors in SWS_2.

In SWS_3, similar sensor nodes to SWS_2 are applied. However, MI-(1) is not required for SWS_3. MI-(7) and MM-(1) are realized by four units from the digital scale of 50 kg capacity numbered as „*3*“ in Fig. 5.5, which are mounted under the draping table. MI-(7) and MM-(1) may be also realized by one 200 kg capacity single point load cell, which may be integrated in the draping robot head. The reason of requiring this high load capacity is the weight of the head attached to the draping $v_{3,40101}$ itself. However, the downside of implementing such scale is the proportional relationship between the load increase and accuracy decrease in a digital scale. Another technical problem with this approach is the impact of head angle on the weight measurement. Therefore, the scales under the draping table are technically more sufficient in this case. The approaches with MI-(8), MM-(4), MM-(5), MM-(6), and MM-(7) in SWS_3 are identical to those in SWS_2. In this case study, no additional waste is caused by the preforming UP_3 within SWS_3.

In general, the setups in SWS_4 are identical to those in SWS_2, while the trimmed preform $u_{4,17143}$ is optically identified. Nonetheless, there are several approaches that may be adopted in SWS_4. For instance, the fiber waste $u_{4,65141}$ in SWS_4 is also measured by a dedicated scale SI-(5) for the waste bin. Moreover, the consolidated fiber waste $u_{4,65141}$ can be determined by subtracting the output trimmed preform $u_{4,17143} \in \varphi^{[S]}$ out of SWS_4 from the initial preform $\hat{u}_{3,17142} \in \varphi^{[P]}$. In this work, the approaches adopted in setting up all SIs and SMs in the included SWS_i from SWS_1 to SWS_4 are based on the conditions and system boundaries within this specific case study. In other words, alternative approaches are still thinkable as far as they satisfy these conditions and boundaries. Yet, these setups are crucial for selecting the required modifications especially in the SWS-DB.

5.3.2 Databases (DBs) for EVo-Platform

For this case study, both SWS-DB and EEAM-DB are modified and enhanced. This includes the definition of data required for the SWS-DB and all relevant characterization factors within the EEAM-DB.

SWS-DB for EVo-platform

In the SWS-DB, the initial data parameters of relevant elementary flows $\hat{\alpha}_{ij}$ are modified to serve the selected MIs, MMs, SIs, SMs, and their setups. As it has been discussed previously in the works of Schachinger and Al-Lami as well as Rudolf and Al-Lami, some of these parameters should be processed to generate the required inputs in the SWS-DB. Such processing activities are associated with initial data preparation tools [264, 271]. However, only limited examples are described in this thesis, while these types of SWS-DB inputs are either discussed in the previous works or provided by the SIs and SMs suppliers. In Tab. 5.2, selected examples of the SWS-DB initial data elements for some elementary flows in this case study are listed.

From the SWS_i results, the required inputs for the time-dependent assessment about the magnitudes of associated elementary flow types j are provided in real-time. In the SWS-DB, the initial data $\hat{\alpha}_{ij}$ and interpreted data α_{ij} about each elementary flow type j are assigned to their temporal and spatial allocations. The temporal allocation t includes the timestamps of initial data, that is gathered from any sensor node. Due to the time delay by sensor nodes and data processing, the data collection is limited to the minimum possible time interval of $\Delta t = 1$ s.

Table 5.2 Examples of initial data $\hat{\alpha}_{ij}$ for the SIs and SMs

α_j *	SWS-DB for SIs and SMs
$v_{1,2001}$	Human temperature range for SI-(3) and work areas for SI-(3) and SI-(1)
$v_{2,3002}$	Electricity meter identification for SI-(4)
$v_{1,4096}$	Electricity meter identification for SI-(4)
$v_{2,6014}$	QR-code ID and multi angle pictures for SI-(1) and scale identification for SI-(5)
$v_{2,9017}$	QR-code ID and multi angle pictures for SI-(1) and scale identification for SI-(5)
$u_{2,6514}$	Dedicated scale identification for SI-(5)

* $v_{1,2001}$ = labor $v_{2,3002}$ = WS_2 $v_{1,4096}$ = paternoster storage $v_{2,6014}$ = fiber $v_{1,9017}$ = release film $u_{2,6514}$ = fiber waste

EEAM-DB for EVo-platform

Although the characterization factors λ_{ij} are considered as given values, these parameters are crucial for the assessment. While several research works are dedicated to study them, the brief discussion of these parameters in Appx. B aims to clarify the origin of them for the selected case study.

$$\begin{bmatrix} \text{Electricity} \\ \text{Labor} \\ \text{Facility WS}_1 \\ \text{Facility WS}_2 \\ \text{Facility WS}_3 \\ \text{Facility WS}_4 \\ \text{Paternoster storage} \\ \text{Unwinder} \\ \text{Cutter} \\ \text{Ply storage} \\ \text{Draping robot} \\ \text{Membrane press} \\ \text{Mold} \\ \text{Handling robot} \\ \text{Trimming portal} \\ \text{Fiber} \\ \text{Release film} \\ \text{Fiber waste} \\ \text{Fiber consolidated waste} \end{bmatrix} \begin{bmatrix} \gamma_{1001} \\ \gamma_{2001} \\ \gamma_{3001} \\ \gamma_{3002} \\ \gamma_{3003} \\ \gamma_{3004} \\ \gamma_{4096} \\ \gamma_{4097} \\ \gamma_{4098} \\ \gamma_{40100} \\ \gamma_{40101} \\ \gamma_{40102} \\ \gamma_{40103} \\ \gamma_{40104} \\ \gamma_{40105} \\ \gamma_{6014} \\ \gamma_{9017} \\ \gamma_{6514} \\ \gamma_{65141} \end{bmatrix} = \begin{bmatrix} 8.55 \times 10^{-2}\,€/\text{kW} \\ 2.639 \times 10^{-2}\,€/\text{s} \\ 1.389 \times 10^{-4}\,€/\text{s} \\ 2.339 \times 10^{-4}\,€/\text{s} \\ 1.402 \times 10^{-4}\,€/\text{s} \\ 2.072 \times 10^{-4}\,€/\text{s} \\ 1.449 \times 10^{-3}\,€/\text{s} \\ 1.05 \times 10^{-3}\,€/\text{s} \\ 6.107 \times 10^{-3}\,€/\text{s} \\ 5.956 \times 10^{-3}\,€/\text{s} \\ 4.863 \times 10^{-3}\,€/\text{s} \\ 6.978 \times 10^{-3}\,€/\text{s} \\ 1.649 \times 10^{-3}\,€/\text{s} \\ 2.753 \times 10^{-3}\,€/\text{s} \\ 7.591 \times 10^{-3}\,€/\text{s} \\ 88.857\,€/\text{kg} \\ 90.086\,€/\text{kg} \\ 5\,€/\text{kg} \\ 5\,€/\text{kg} \end{bmatrix} = [\check{\Lambda}^{[A]}] \tag{5.30}$$

It is essential to mention that the given values in Eq. 5.30 are mainly assumed and not approved by the elementary flows suppliers. In practice, many of these characterization factors are calculated based on other parameters, as they have been discussed in chapter 4 before. Therefore, they are reviewed briefly here. The economic characterization factors γ_j are provided as givens in Eq. 5.30, whereas further details about their origins are discussed in Appx. B. In practice, such economic characterization factors γ_j are made available for the decision-makers in a production facility within internal records. Therefore, the internal research for

appropriate values of these parameters is less laborious and more accurate in the assessment of an industrial process.

For the assessment of carbon footprint β_{ij} of each elementary flow α_{ij}, an ecological characterization factor ε_j is to be selected or calculated. For the labor $\varphi^{[L]}$, facility $\varphi^{[\Delta s]}$, and equipment $\varphi^{[Q]}$ as inputs, the uncommon approach of considering their ecological factors is adopted in this thesis.

$$\begin{array}{r|c|c|l}
\text{Electricity} & \varepsilon_{1001} & 0.474\,\text{kg}\,CO_2/\text{kWh} & \\
\text{Labor} & \varepsilon_{2001} & 1.139\times10^{-4}\,\text{kg}\,CO_2/\text{s} & \\
\text{Facility WS}_1 & \varepsilon_{3001} & 1.099\times10^{-3}\,\text{kg}\,CO_2/\text{s} & \\
\text{Facility WS}_2 & \varepsilon_{3002} & 1.851\times10^{-3}\,\text{kg}\,CO_2/\text{s} & \\
\text{Facility WS}_3 & \varepsilon_{3003} & 1.109\times10^{-3}\,\text{kg}\,CO_2/\text{s} & \\
\text{Facility WS}_4 & \varepsilon_{3004} & 1.64\times10^{-3}\,\text{kg}\,CO_2/\text{s} & \\
\text{Paternoster storage} & \varepsilon_{4096} & 3.75\times10^{-5}\,\text{kg}\,CO_2/\text{s} & \\
\text{Unwinder} & \varepsilon_{4097} & 1.694\times10^{-5}\,\text{kg}\,CO_2/\text{s} & \\
\text{Cutter} & \varepsilon_{4098} & 1.035\times10^{-4}\,\text{kg}\,CO_2/\text{s} & \\
\text{Ply storage} & \varepsilon_{40100} & 1.242\times10^{-4}\,\text{kg}\,CO_2/\text{s} & = [\check{\check{\Lambda}}^{[A]}] \\
\text{Draping robot} & \varepsilon_{40101} & 3.562\times10^{-4}\,\text{kg}\,CO_2/\text{s} & \\
\text{Membrane press} & \varepsilon_{40102} & 2.386\times10^{-4}\,\text{kg}\,CO_2/\text{s} & \\
\text{Mold} & \varepsilon_{40103} & 3.708\times10^{-5}\,\text{kg}\,CO_2/\text{s} & \\
\text{Handling robot} & \varepsilon_{40104} & 2.365\times10^{-4}\,\text{kg}\,CO_2/\text{s} & \\
\text{Trimming portal} & \varepsilon_{40105} & 2.545\times10^{-4}\,\text{kg}\,CO_2/\text{s} & \\
\text{Fiber} & \varepsilon_{6014} & 46.8\,\text{kg}\,CO_2/\text{kg} & \\
\text{Release film} & \varepsilon_{9017} & 2.683\,\text{kg}\,CO_2/\text{kg} & \\
\text{Fiber waste} & \varepsilon_{6514} & 1.25\times10^{-2}\,\text{kg}\,CO_2/\text{kg} & \\
\text{Fiber consolidated waste} & \varepsilon_{65141} & 1.25\times10^{-2}\,\text{kg}\,CO_2/\text{kg} &
\end{array} \tag{5.31}$$

The ecological characterization factors ε_{ij} are provided as given constants in Eq. 5.31, while further details about them are discussed in Appx. B. Again, the given values in Eq. 5.31 are based on relevant studies and assumptions, while they are not provided or approved by the elementary flows suppliers.

In order to calculate the eco-efficiency ξ, the total of sale revenue excluding all non-process costs is to be estimated as a given constant k in the monetary unit of €. For the studied case of all covered UPs i within the EVo-platform, the produced semi-finished structure of trimmed preform has a roughly estimated k =500 €. This represents the expected value that a customer is welling to pay for the offered trimmed preform $u_{4,17143} \in \varphi^{[S]}$ excluding all non-process costs. To put it more simply, a FRPs supplier is expected to have this total revenue excluding all non-process costs, while including the direct costs from performing all considered UPs i from UP_1 up to UP_4. As it is explained in Appx. B, the constants of k_1 =50 €, k_2 =300 €, k_3 =75 €, and k_4 =75 € are assumed for each single UP i without considering its prior ones.

Chapter 6

Results and Discussion

In this chapter, the results of time-dependent eco-efficiency assessment as output information from the DSSs are obtained. Including both visual and statistical aspects, these results provide decision-makers with sufficient presentation of the economic and ecological impacts on the various selected CSF levels. After presenting these results, they are validated. In this chapter, the discussion section comes after illustrating the entire results to have better conclusions.

6.1 LCI and LCIA Results

The main result of this work is the realization of time-dependent eco-efficiency assessment. In other words, the results of the selected case study are relevant for the validation of this approach. As Fig. 6.1 shows, the introduced framework for time-dependent eco-efficiency assessment in Fig. 4.1 within chapter 4 has been fulfilled.

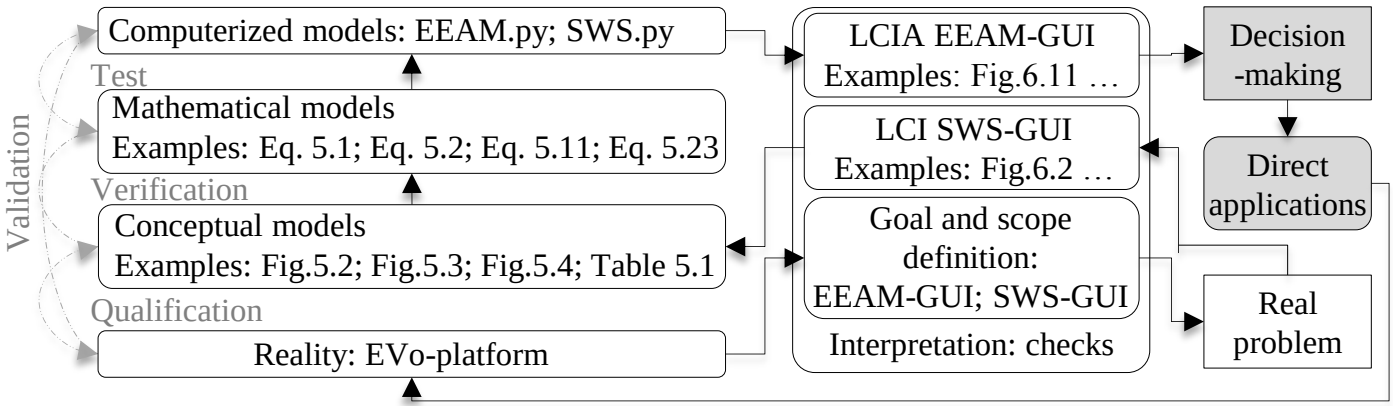

Figure 6.1 Results of adopting the framework for time-dependent eco-efficiency assessment

Fig. 6.1 lists the associated results from this chapter as well as the previous one to their stages within the adopted framework. This section includes presenting the results from real-time data collection as well as time-dependent direct cost, carbon footprint, and eco-efficiency assessment on various CFS levels.

6.1.1 Real-Time LCI Results

To understand the conducted results from all SWS_i, the structures and forms of these results are explained. Then these results from each SWS_i are separately presented. Finally, examples of real-time results from randomly selected temporal points t are provided.

SWS results structure

The SWSs provide the associated data about included elementary flows α_{ij} from every covered UP i in real-time. For all included UPs from UP_1 up to UP_4, the measured elementary flows α_{ij} are illustrated visually. From the various available illustration types, the area charts and line graphs are selected to show the continuous change over time. The elementary flows within the subsets $\varphi^{[T]}$, $\varphi^{[Q]}$, $\varphi^{[L]}$, and $\varphi^{[\Delta s]}$ are represented by noncumulative values in all following illustrations of the relevant UPs i in Fig. 6.2, Fig. 6.3, Fig. 6.4, and Fig. 6.5. On the other hand, material elementary flows within the subsets $\varphi^{[F]}$, $\varphi^{[R]}$ and $\varphi^{[G]}$ are represented by cumulative values in these illustrations. Practically, the cumulative total mass is a more common representation, that is easier to interpret. Nonetheless, any illustration may be switched between cumulative and noncumulative modes based on decision-makers demands. Although the elementary flows and their subsets are described by there mathematical nomenclature in the results within this thesis for more efficient visualization, they are also presented for the decision-makers by their full description in the associated illustrations.

In these figures, the horizontal axis represents the unified timestamps for all considered elementary flows α_{ij}. On the vertical axis, each elementary flow α_{ij} is represented by a separated section that covers its value range by the proper unit. Going top-down, the first section is dedicated to the total electricity consumption in each UP. The value range of electricity varies between the UPs i, while it is measured in kW. This section is followed by the ones that represent equipment types separately. Arranged by their IDs, each equipment type section has the maximum utilization range of $\alpha_{ij} = 1$ and the minimum one of $\alpha_{ij} = 0$. After the elementary flows from $\varphi^{[Q]}$, the labor category $\varphi^{[L]}$ is shown. In this case study, a single labor elementary flow of production technicians $v_{i,2001}$ is applied in UP_1 only. In this case study, the maximum amount of labors is $\alpha_{ij} = 2$, while the minimum one is $\alpha_{ij} = 0$. Here, all manual activities in UP_1 requires two labors. In all figures, the next section is dedicated to represent the facility occupation $\varphi^{[\Delta s]}$ of every WS_i in its UP i. For the sake of clear visualization, the separated illustration of each electricity consumption has a unique vertical axis that occurs after each relevant elementary flow from equipment or facility subsets.

In the last sections of associated figures, the material elementary flows of $v_{i,6014} \in \varphi^{[F]}$, $v_{i,9017} \in \varphi^{[R]}$, $u_{i,6514} \in \varphi^{[G]}$, and $u_{i,65141} \in \varphi^{[G]}$ are represented if applicable. These materials are measured by the cumulative mass unit of kg in the proper range. In addition, intermediate flows are also illustrated to provide the decision-makers with advanced understanding of the process.

Table 6.1 Start and end temporal points as well as their standard synchronized times of every UP_i

UP Description	UP_i	t_{i_a} at standard time	t_{i_b} at standard time
Preparing part A	UP_{1A}	t_{1A_a} =0 s at 14:00:10	t_{1A_b} =159 s at 14:02:49
Cutting part A	UP_{2A}	t_{2A_a} =116 s at 14:02:06	t_{2A_b} =268 s at 14:04:38
Preparing part B	UP_{1B}	t_{1B_a} =269 s at 14:04:39	t_{1B_b} =522 s at 14:08:52
Cutting part B	UP_{2B}	t_{2B_a} =478 s at 14:08:08	t_{2B_b} =4034 s at 15:07:24
Preforming	UP_3	t_{3_a} =4035 s at 15:07:25	t_{3_b} =5041 s at 15:24:11
Trimming	UP_4	t_{4_a} =5042 s at 15:24:12	t_{4_b} =7319 s at 16:02:09
Preparing part C	UP_{1C}	t_{1C_a} =7320 s at 16:02:10	t_{1C_b} =7482 s at 16:04:52

To generate the statistical results, the parametrized mathematical models provide cumulative values of the elementary flows between two selected temporal points. These points may be starting from the beginning of

entire process at t_a or the start of a selected UP i at t_{i_a}. Similarly, this cumulative presentation may end at t_b, t_{i_b}, or any selected temporal point t. Now, the values of elementary flows α_{ij} in the matrix $[A]_t$ at a selected time point t can be determined based on Eq. 5.1 an its contained matrices of Eq. 5.2, Eq. 5.3, Eq. 5.4, Eq. 5.5, Eq. 5.6, Eq. 5.7, and Eq. 5.8. Moreover, each UP i can have its time-dependent vector $\{A_i\}_t$ based on its separated representing row vector in that matrix $[A]_t$, as the vectors $\{A_i\}$ in Eq. 5.9, Eq. 5.14, Eq. 5.21, and Eq. 5.25 previously suggest.

Here, the significant temporal points, such as the beginning t_{i_a} and the end t_{i_b} of every UP_i, may be crucial to understand the results. Therefore, these temporal points are listed in Tab. 6.1. The adopted manufacturing process has been carried out in the city of Stade in Germany, while the selected representative experiment has took a place on Thursday October 17, 2019.

SWS_1 results

For UP_1, Fig. 6.2 shows the behaviors of all associated elementary flows including the total electricity consumption in UP_1 as $v_{1,1001}$, paternoster storage $v_{1,4096}$, paternoster storage consumption $v_{1,10496}$, unwinder $v_{1,4097}$, unwinder electricity $v_{1,10497}$, labor $v_{1,2001}$, air conditioned facility of WS_1 as $v_{1,3001}$, and WS_1 electricity $v_{1,1031}$.

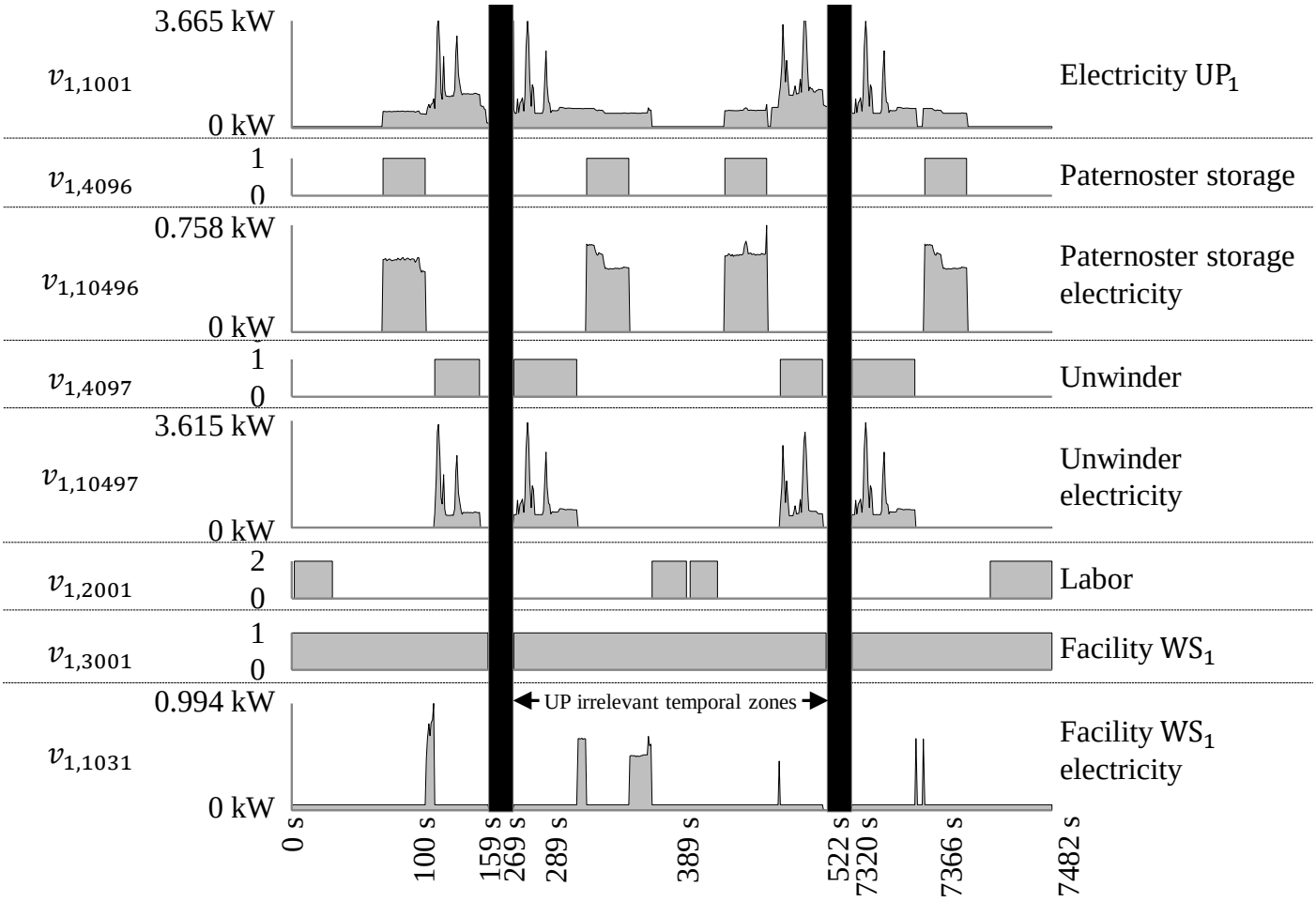

Figure 6.2 Real-time data collection of elementary flows α_{1j} by SWS_1 in UP_1

Including three temporally unconnected clusters of activities, UP_1 is split into UP_{1A}, UP_{1B}, and UP_{1C}, as they are separated by black shaded columns in Fig. 6.2. From the temporal point of t_{1A_a} =0 s at 14:00:10 in the standard synchronized official time at the city of Stade in Germany, the previously explained preparing activities in UP_{1A} start. This part ends in t_{1A_b} =159 s at 14:02:49, as the unwinder $v_{1,4097}$ finishes scrolling

down the release film roll $v_{2,9017}$. After the first cutting session, the second part UP_{1B} starts in t_{1B_a} =269 s at 14:04:39 to install the fiber roll $v_{2,6014}$. This part UP_{1B} ends in t_{1B_b} =522 s at 14:08:52.

At the end of UP_4, further preparing activities under the third part UP_{1C} take a place to set the WS_1 back to its initial status. Arguably, these activities under UP_{1C} may occur directly after the cutting UP_2. However, UP_{1C} occurs after UP_4 in the selected scenario of this case study. This third part UP_{1C} starts in t_{1C_a} =7320 s at 16:02:10 by rolling up the rest of fiber $v_{2,6014}$. Then, this roll is carried away by two labors $v_{1,2001}$ leaving the WS_1 in t_{1C_b} =7482 s at 16:04:52, as Fig. 6.2 shows. In UP_1, facility electricity $v_{1,1031}$ is illustrated with relatively small consumption. This consumption is associated with to non-equipment safety systems for human-machine collaboration, while heating and lighting impacts are covered by the facility characterization factors in all WS_i.

SWS_2 results

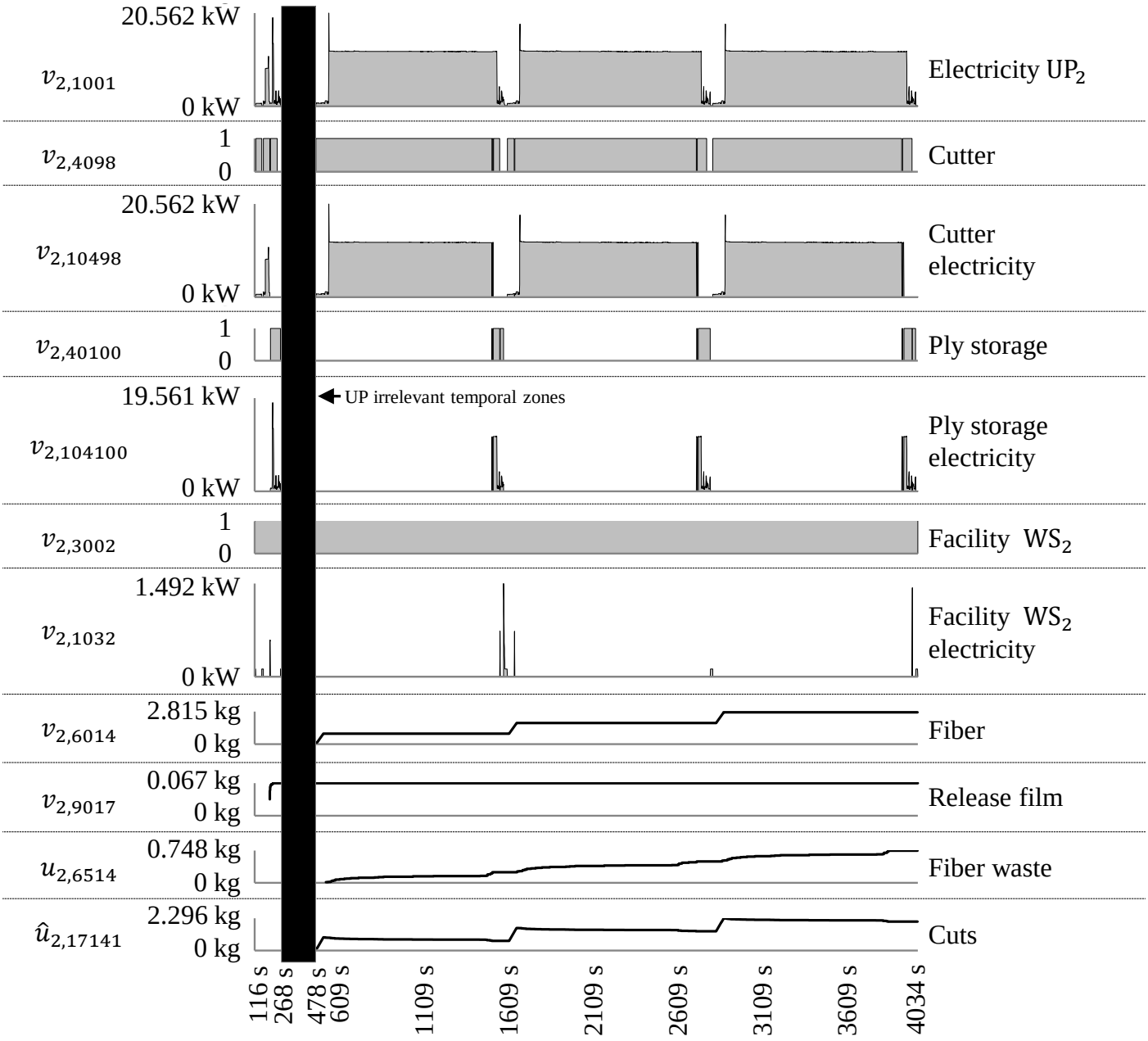

Figure 6.3 Real-time data collection of elementary flows α_{2j} by SWS_2 in UP_2

In UP_2, the same approach is adopted to illustrate the measured elementary flows α_{2j} visually within Fig. 6.3. Here, UP_2 is split into two parts, while these two parts of UP_{2A} and UP_{2B} are separated by the main

portion of UP_{1B}. In Fig. 6.3, UP_2 starts in t_{2A_a} =116 s at 14:02:06 when the cutter $v_{2,4098}$ begins pulling the release film $v_{2,6014}$ from its roll and ends when the release film ply cutting is finished in t_{2A_b} =268 s at 14:04:38. Technically, this first cutting activity of pulling the release film by cutter $v_{2,4098}$ runs simultaneously to the roll down scrolling by the unwinder $v_{1,4097}$ as the last activity of UP_{1A}. In the second part UP_{2B}, time duration between t_{2B_a} =478 s at 14:08:08 and t_{1B_b} =522 s at 14:08:52 includes activities of both UPs as well. As it has been discussed previously in chapter 4, this is the case of simultaneously carried out UPs i in different spatial WSs. From a temporal perspective, UP_2 ends in t_{2B_b} =4034 s at 15:07:24. In Fig. 6.3, three distinguishable cutting sessions are carried out in UP_{2B} after the unique release film cutting session in UP_{2A}. Each session in UP_{2B} includes the cutting of two cuts $\hat{u}_{2,17141}$ by the cutter $v_{2,4098}$. On the other hand, a single ply of the release film $v_{2,9017}$ is cut by the cutter $v_{2,4098}$ from its roll in UP_{2A}. As it is stated before, material elementary flows are shown as cumulative values. In this scenario, fiber waste $u_{2,6514}$ of each session occurs directly after the fiber $v_{2,6014}$ of that session, whenever this fiber completely enters the system.

SWS_3 results

After UP_2, the real-time data collection of UP_3 is illustrated in Fig. 6.4.

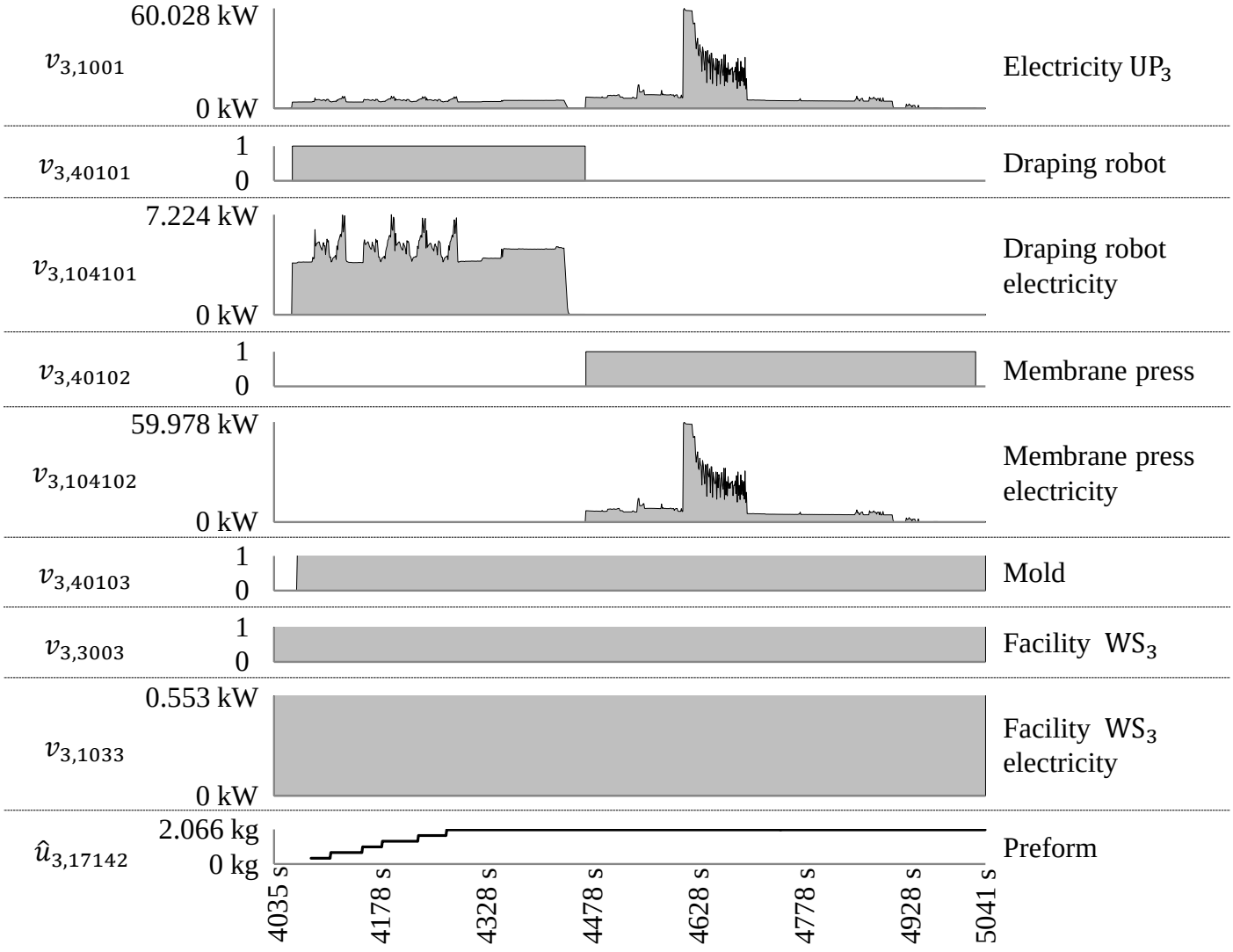

Figure 6.4 Real-time data collection of elementary flows α_{3j} by SWS_3 in UP_3

UP_3 starts right after UP_2 in t_{3_a} =4035 s at 15:07:25. It includes a very short pause for safety checks at the beginning. After laying up all six cuts $\hat{u}_{2,17141}$ on the consolidation mold $v_{3,40103}$ by the draping robot

$v_{3,40101}$, the robot $v_{3,40101}$ travels back on its track to its stationary spot. Then, the mold $v_{3,40103}$ rolls inside the membrane press $v_{3,40102}$. This membrane press $v_{3,40102}$ allocates this mold in its proper position before the consolidation activity starts. The electricity consumptions of the draping robot $v_{3,104101}$, membrane press $v_{3,104102}$, and WS_3 $v_{3,1033}$ are illustrated in Fig. 6.4. Then, the cuts $\hat{u}_{2,17141}$ are consolidated into a preform $\hat{u}_{3,17142}$. Followed by another very short pause after this activity, UP_3 ends in t_{3_b} =5041 s at 15:24:11. As Fig. 6.4 shows, UP_3 includes pauses that are associated mainly with the system cooling and safety reasons.

SWS_4 results

Finally, the real-time data collection of all associated elementary flows α_{4j} in UP_4 is illustrated visually in Fig. 6.5.

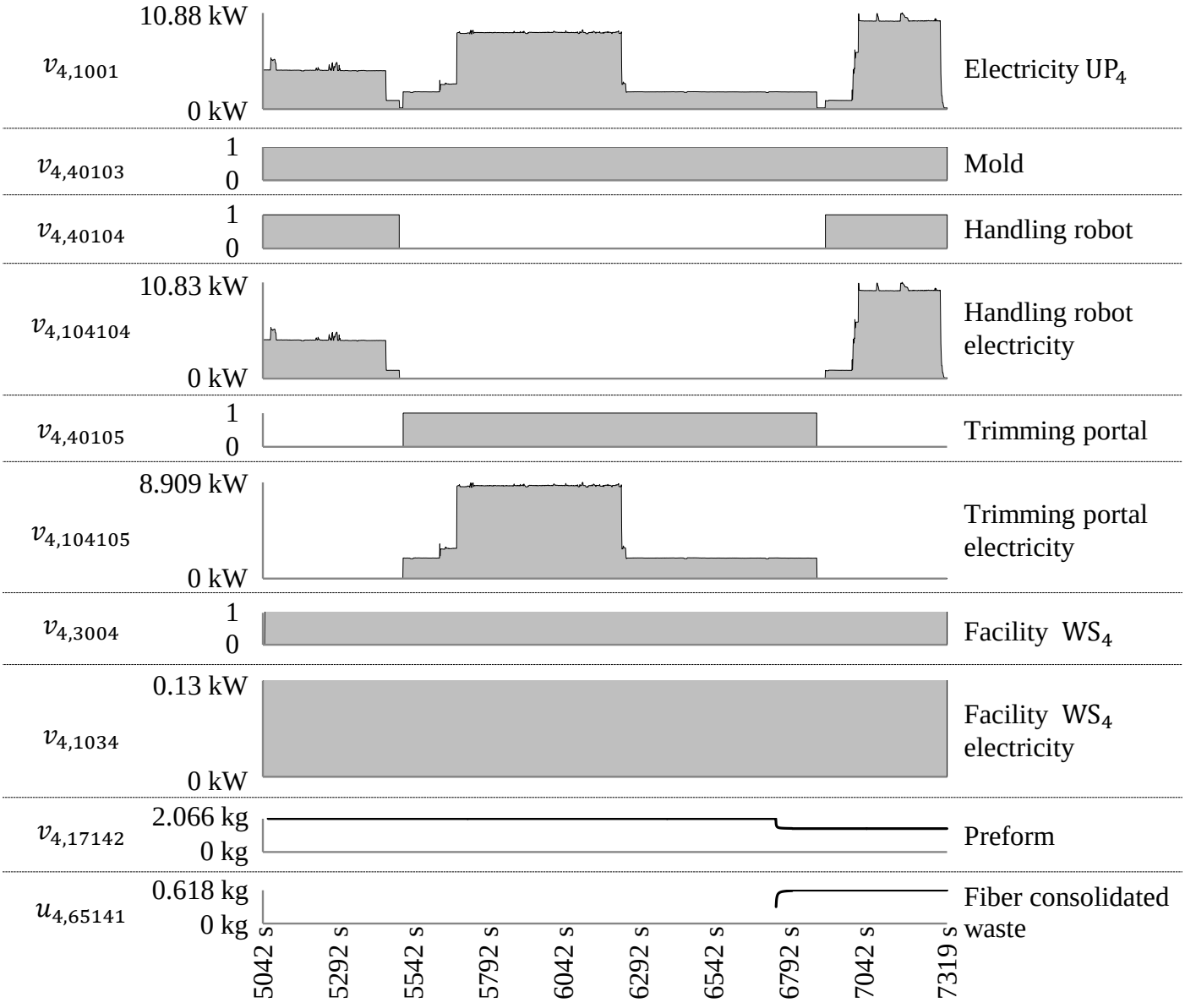

Figure 6.5 Real-time data collection of elementary flows α_{4j} by SWS_4 in UP_4

Starting in t_{4_a} =5042 s at 15:24:12, UP_4 begins right after UP_3 when the consolidation mold $v_{3,40103}$ moves to WS_4 from WS_3. As it has been mentioned before, the consolidation mold $v_{3,40103}$ is also utilized as a trimming mold $v_{4,40103}$ in this case study. The trimming mold $v_{4,40103}$ is transported by the ground track of the chain robot $v_{4,40104}$ to the trimming portal $v_{4,40105}$. In a secured environment within the trimming portal $v_{4,40105}$, the preform $\hat{u}_{3,17142}$ as an input $v_{4,17142}$ to UP_4 is turned into a trimmed preform $u_{4,17143}$ as the final output of

all considered UPs. Fig. 6.5 illustrates the electricity consumptions of the chain robot $v_{4,104104}$, trimming portal $v_{4,104105}$, and WS_4 $v_{4,1034}$. Moreover, consolidated fiber waste $u_{4,65141}$ is also generated by UP_4. As Fig. 6.5 shows, the fiber consolidated waste $u_{4,65141}$ is dropped in the bin as one load, while the preform behavior as an input to UP_4 is based on the waste measurement. The trimmed preform $u_{4,17143}$ is then transported by the upper chain robot $v_{4,40104}$ to WS_5 in t_{4_b} =7319 s at 16:02:09. However, UP_5 is beyond the scope of this case study, while the third part of UP_1, which is defined as UP_{1C}, ends in t_{1C_b} =7482 s at 16:04:52. As it is mentioned previously, UP_{1C} starts right after UP_4.

Real-time results of selected temporal points t

Based on the previously introduced matrix in Eq. 5.1, the time-independent results of real-time data collection at $t = \Delta t_{tot}$ are illustrated for $[A]_t$ in Eq. 6.1. Eq. 6.1 states the cumulative values from the process starts at t_{1A_a} =0 s until its end at t_{1C_b} =7482 s from all studied UPs i.

$$[A]_{t=7482\,\mathrm{s}} = \left[[\Upsilon^{[T]}]_{t=7482\,\mathrm{s}} \; [\Upsilon^{[L]}]_{t=7482\,\mathrm{s}} \; [\Upsilon^{[\Delta s]}]_{t=7482\,\mathrm{s}} \; [\Upsilon^{[Q]}]_{t=7482\,\mathrm{s}} \; [\Upsilon^{[F]}]_{t=7482\,\mathrm{s}} \; [\Upsilon^{[R]}]_{t=7482\,\mathrm{s}} \; [\Upsilon^{[G]}]_{t=7482\,\mathrm{s}} \right] \tag{6.1}$$

$$[\Upsilon^{[T]}]_{t=7482\,\mathrm{s}} = \begin{bmatrix} 0.013 & 0 & 0 & 0 & 0.02 & 0.045 \\ 0 & 0.005 & 0 & 0 & 0 & 0 \\ 0 & 0 & 0.015 & 0 & 0 & 0 \\ 0 & 0 & 0 & 0.033 & 0 & 0 \\ 0 & 0 & 0 & 0 & 0 & 0 \\ 10.409 & 0.333 & 0 & 0 & 0 & 0 \\ 0 & 0 & 0.497 & 1.348 & 0 & 0 \\ 0 & 0 & 0 & 0 & 1.329 & 1.763 \end{bmatrix}_{t=7482\,\mathrm{s}}^{\text{in kWh}} \tag{6.2}$$

$$[\Upsilon^{[L]}]_{t=7482\,\mathrm{s}} = \begin{bmatrix} 270 \\ 0 \\ 0 \\ 0 \end{bmatrix}_{t=7482\,\mathrm{s}}^{\text{in s}} \tag{6.3}$$

$$[\Upsilon^{[\Delta s]}]_{t=7482\,\mathrm{s}} = \begin{bmatrix} 577 & 0 & 0 & 0 \\ 0 & 3710 & 0 & 0 \\ 0 & 0 & 1008 & 0 \\ 0 & 0 & 0 & 2278 \end{bmatrix}_{t=7482\,\mathrm{s}}^{\text{in s}} \tag{6.4}$$

$$[\Upsilon^{[Q]}]_{t=7482\,\mathrm{s}} = \begin{bmatrix} 140 & 176 & 0 & 0 & 0 & 0 & 0 & 0 & 0 \\ 0 & 0 & 3544 & 272 & 0 & 0 & 0 & 0 & 0 \\ 0 & 0 & 0 & 0 & 415 & 552 & 967 & 0 & 0 \\ 0 & 0 & 0 & 0 & 0 & 0 & 2278 & 861 & 1377 \end{bmatrix}_{t=7482\,\mathrm{s}}^{\text{in s}} \tag{6.5}$$

$$[\Upsilon^{[F]}]_{t=7482\,\mathrm{s}} = \begin{bmatrix} 0 \\ 2.815 \\ 0 \\ 0 \end{bmatrix}_{t=7482\,\mathrm{s}}^{\text{in kg}} \tag{6.6}$$

$$[\Upsilon^{[R]}]_{t=7482\,\mathrm{s}} = \begin{bmatrix} 0 \\ 0.067 \\ 0 \\ 0 \end{bmatrix}^{\text{in kg}}_{t=7482\,\mathrm{s}} \tag{6.7}$$

$$[\Upsilon^{[G]}]_{t=7482\,\mathrm{s}} = \begin{bmatrix} 0 & 0 \\ 0.748 & 0 \\ 0 & 0 \\ 0 & 0.618 \end{bmatrix}^{\text{in kg}}_{t=7482\,\mathrm{s}} \tag{6.8}$$

As Eq. 6.3 shows, the only UP i, that contains labor work, is UP_1. This UP has the labor $v_{1,2001}$ with a total working time of 270 s for both labors. Facility subset $\varphi_i^{[\Delta s]}$ includes $v_{1,3001}$, $v_{2,3002}$, $v_{3,3003}$, and $v_{4,3004}$, that represent WS_1, WS_2, WS_3, and WS_4 respectively. In the selected case study of EVo-platform, these facilities have various sizes with different total areas, as they are discussed in Appx. B. As it is written in Eq. 6.4, WS_2 as $v_{2,3002}$ has the highest occupation duration of 3710 s, which is a result of the selected cutting speed in the case study. The second longest facility occupation duration is represented by $v_{4,3004}$ in WS_4, which is equal to 2278 s. This duration is also associated with the trimming speed selected in the case study. The fiber subset $\varphi_i^{[F]}$ is represented by the single applied fiber input solely in UP_2 as $v_{2,6014}$ with a total magnitude of around 2.815 kg. In this case study, ancillaries subset $\varphi_i^{[R]}$ has also the single input of release film $v_{2,9017}$ with a total magnitude of around 0.067 kg that occurs solely in UP_2 too. Electricity subset $\varphi_i^{[T]}$ varies between the assessed UPs i. While $\varphi_1^{[T]}$ has the lowest value of totally consumed 0.078 kWh, this low electricity consumption is a result of equipment performance and utilizing duration in UP_1. The electricity $v_{2,1001}$ in UP_2 has the highest total consumption of around 10.748 kWh as the summation of different consumptions in that UP, due to the long duration of machines utilization in UP_2 as well as the performance of these machines. In UP_3, electricity subset $\varphi_3^{[T]}$ represents the second lowest consumption with a total amount of 1.859 kWh. Despite the high peak energy of 60 kW in Fig. 6.4, UP_3 electricity consumption is relatively low due to the short duration of machines operation. The electricity $\varphi_4^{[T]}$ in UP_4 has a total amount of 3.124 kWh, which ranks UP_4 as the second highest electricity consuming UP i.

Fiber wastes are generated in UP_2 and UP_4 as $u_{2,6514}$ and $u_{4,65141}$ respectively. From both UP_2 and UP_4, a total fiber waste of around 1.366 kg is measured. Therefore, the fiber magnitude in the core structural material can be calculated as 1.449 kg in the finished product, which is equal to around 51.5 % of the total fiber input $v_{2,6014}$. Therefore, the waste portion is about 48.5 %, which is common in FRPs manufacturing [13]. However, adopting other scenarios including fiber reusing ones may decrease this waste magnitude in this case study.

To demonstrate the real-time data collection capabilities, elementary flow values α_{ij} from two exemplary temporal points t are presented here. The time points of t=100 s and t=1000 s are randomly selected and shown in Eq. 6.9 and Eq. 6.14 respectively. Based on these global matrices in Eq. 6.9 and Eq. 6.14, sub-matrices are derived for each category $[\Upsilon^{[\Gamma]}]$, as they are illustrated previously in chapter 5.

$$[A]_{t=100\,\mathrm{s}} = \left[[\Upsilon^{[T]}]_{t=100\,\mathrm{s}} \; [\Upsilon^{[L]}]_{t=100\,\mathrm{s}} \; [\Upsilon^{[\Delta s]}]_{t=100\,\mathrm{s}} \; [\Upsilon^{[Q]}]_{t=100\,\mathrm{s}} \; [\Upsilon^{[F]}]_{t=100\,\mathrm{s}} \; [\Upsilon^{[R]}]_{t=100\,\mathrm{s}} \; [\Upsilon^{[G]}]_{t=100\,\mathrm{s}} \right] \tag{6.9}$$

$$[\Upsilon^{[T]}]_{t=100\,\mathrm{s}} = \begin{bmatrix} 0.001 & 0 & 0 & 0 & 0.004 & 0 \\ 0 & 0 & 0 & 0 & 0 & 0 \\ 0 & 0 & 0 & 0 & 0 & 0 \\ 0 & 0 & 0 & 0 & 0 & 0 \\ 0 & 0 & 0 & 0 & 0 & 0 \\ 0 & 0 & 0 & 0 & 0 & 0 \\ 0 & 0 & 0 & 0 & 0 & 0 \\ 0 & 0 & 0 & 0 & 0 & 0 \end{bmatrix}^{\text{in kWh}}_{t=100\,\mathrm{s}} \tag{6.10}$$

$$[\Upsilon^{[L]}]_{t=100\,\mathrm{s}} = \begin{bmatrix} 64 \\ 0 \\ 0 \\ 0 \end{bmatrix}^{\text{in s}}_{t=100\,\mathrm{s}} \tag{6.11}$$

$$[\Upsilon^{[\Delta s]}]_{t=100\,\mathrm{s}} = \begin{bmatrix} 101 & 0 & 0 & 0 \\ 0 & 0 & 0 & 0 \\ 0 & 0 & 0 & 0 \\ 0 & 0 & 0 & 0 \end{bmatrix}^{\text{in s}}_{t=100\,\mathrm{s}} \tag{6.12}$$

$$[\Upsilon^{[Q]}]_{t=100\,\mathrm{s}} = \begin{bmatrix} 27 & 0 & 0 & 0 & 0 & 0 & 0 & 0 & 0 \\ 0 & 0 & 0 & 0 & 0 & 0 & 0 & 0 & 0 \\ 0 & 0 & 0 & 0 & 0 & 0 & 0 & 0 & 0 \\ 0 & 0 & 0 & 0 & 0 & 0 & 0 & 0 & 0 \end{bmatrix}^{\text{in s}}_{t=100\,\mathrm{s}} \tag{6.13}$$

Nonetheless, $[\Upsilon^{[F]}]_{t=100\,\mathrm{s}}$, $[\Upsilon^{[R]}]_{t=100\,\mathrm{s}}$, and $[\Upsilon^{[G]}]_{t=100\,\mathrm{s}}$ have only „*zero*“ value elements at $t = 100\,\mathrm{s}$. At the randomly selected temporal point of t=1000 s, Eq. 6.14 demonstrates the elementary flows α_{ij} similarly.

$$[A]_{t=1000\,\mathrm{s}} = \left[[\Upsilon^{[T]}]_{t=1000\,\mathrm{s}} \; [\Upsilon^{[L]}]_{t=1000\,\mathrm{s}} \; [\Upsilon^{[\Delta s]}]_{t=1000\,\mathrm{s}} \; [\Upsilon^{[Q]}]_{t=1000\,\mathrm{s}} \; [\Upsilon^{[F]}]_{t=1000\,\mathrm{s}} \; [\Upsilon^{[R]}]_{t=1000\,\mathrm{s}} \; [\Upsilon^{[G]}]_{t=1000\,\mathrm{s}} \right] \tag{6.14}$$

$$[\Upsilon^{[T]}]_{t=1000\,\mathrm{s}} = \begin{bmatrix} 0.011 & 0 & 0 & 0 & 0.015 & 0.032 \\ 0 & 0.001 & 0 & 0 & 0 & 0 \\ 0 & 0 & 0 & 0 & 0 & 0 \\ 0 & 0 & 0 & 0 & 0 & 0 \\ 0 & 0 & 0 & 0 & 0 & 0 \\ 1.582 & 0.047 & 0 & 0 & 0 & 0 \\ 0 & 0 & 0 & 0 & 0 & 0 \\ 0 & 0 & 0 & 0 & 0 & 0 \end{bmatrix}^{\text{in kWh}}_{t=1000\,\mathrm{s}} \tag{6.15}$$

$$[\Upsilon^{[L]}]_{t=1000\,\mathrm{s}} = \begin{bmatrix} 168 \\ 0 \\ 0 \\ 0 \end{bmatrix}^{\text{in s}}_{t=1000\,\mathrm{s}} \tag{6.16}$$

$$[\Upsilon^{[\Delta s]}]_{t=1000\,\mathrm{s}} = \begin{bmatrix} 414 & 0 & 0 & 0 \\ 0 & 677 & 0 & 0 \\ 0 & 0 & 0 & 0 \\ 0 & 0 & 0 & 0 \end{bmatrix}_{t=1000\,\mathrm{s}}^{\text{in s}} \tag{6.17}$$

$$[\Upsilon^{[Q]}]_{t=1000\,\mathrm{s}} = \begin{bmatrix} 105 & 124 & 0 & 0 & 0 & 0 & 0 & 0 & 0 \\ 0 & 0 & 0 & 638 & 60 & 0 & 0 & 0 & 0 \\ 0 & 0 & 0 & 0 & 0 & 0 & 0 & 0 & 0 \\ 0 & 0 & 0 & 0 & 0 & 0 & 0 & 0 & 0 \end{bmatrix}_{t=1000\,\mathrm{s}}^{\text{in s}} \tag{6.18}$$

$$[\Upsilon^{[F]}]_{t=1000\,\mathrm{s}} = \begin{bmatrix} 0 \\ 0.941 \\ 0 \\ 0 \end{bmatrix}_{t=1000\,\mathrm{s}}^{\text{in kg}} \tag{6.19}$$

$$[\Upsilon^{[R]}]_{t=1000\,\mathrm{s}} = \begin{bmatrix} 0 \\ 0.067 \\ 0 \\ 0 \end{bmatrix}_{t=1000\,\mathrm{s}}^{\text{in kg}} \tag{6.20}$$

$$[\Upsilon^{[G]}]_{t=1000\,\mathrm{s}} = \begin{bmatrix} 0 & 0 \\ 0.145 & 0 \\ 0 & 0 \\ 0 & 0 \end{bmatrix}_{t=1000\,\mathrm{s}}^{\text{in kg}} \tag{6.21}$$

In addition to the discrete illustration of various elementary flows α_{ij} and their subsets $\varphi_i^{[\Gamma]}$ in each UP i, global description of these flows α_j and their subsets $\varphi^{[\Gamma]}$ can be provided for the entire process. For the time duration that covers all UPs i from UP_1 up to UP_4 starting in t_{1A_a} =0 s at 14:00:10 and ending in t_{1C_b} =7482 s at 16:04:52, illustrations for the different considered elementary flows are visualized. As a part of that, the labor subset $\varphi^{[L]}$ and the facility subset $\varphi^{[\Delta s]}$ are visualized in Fig. 6.6 for the entire process.

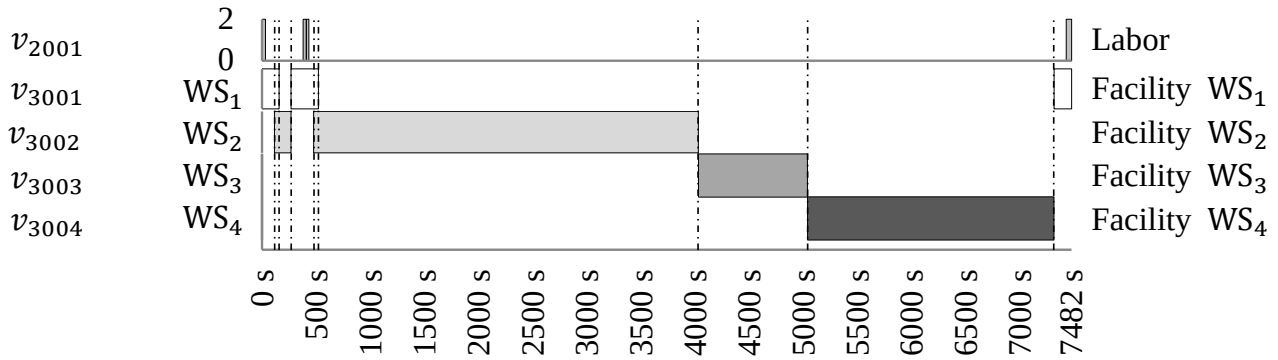

Figure 6.6 Real-time labor and facility flows by all SWSs in 0 s< t <7482 s

For electricity and equipment subsets $\varphi^{[T]}$ and $\varphi^{[Q]}$, Fig. 6.7 visualizes their elementary flows v_j throughout the entire process.

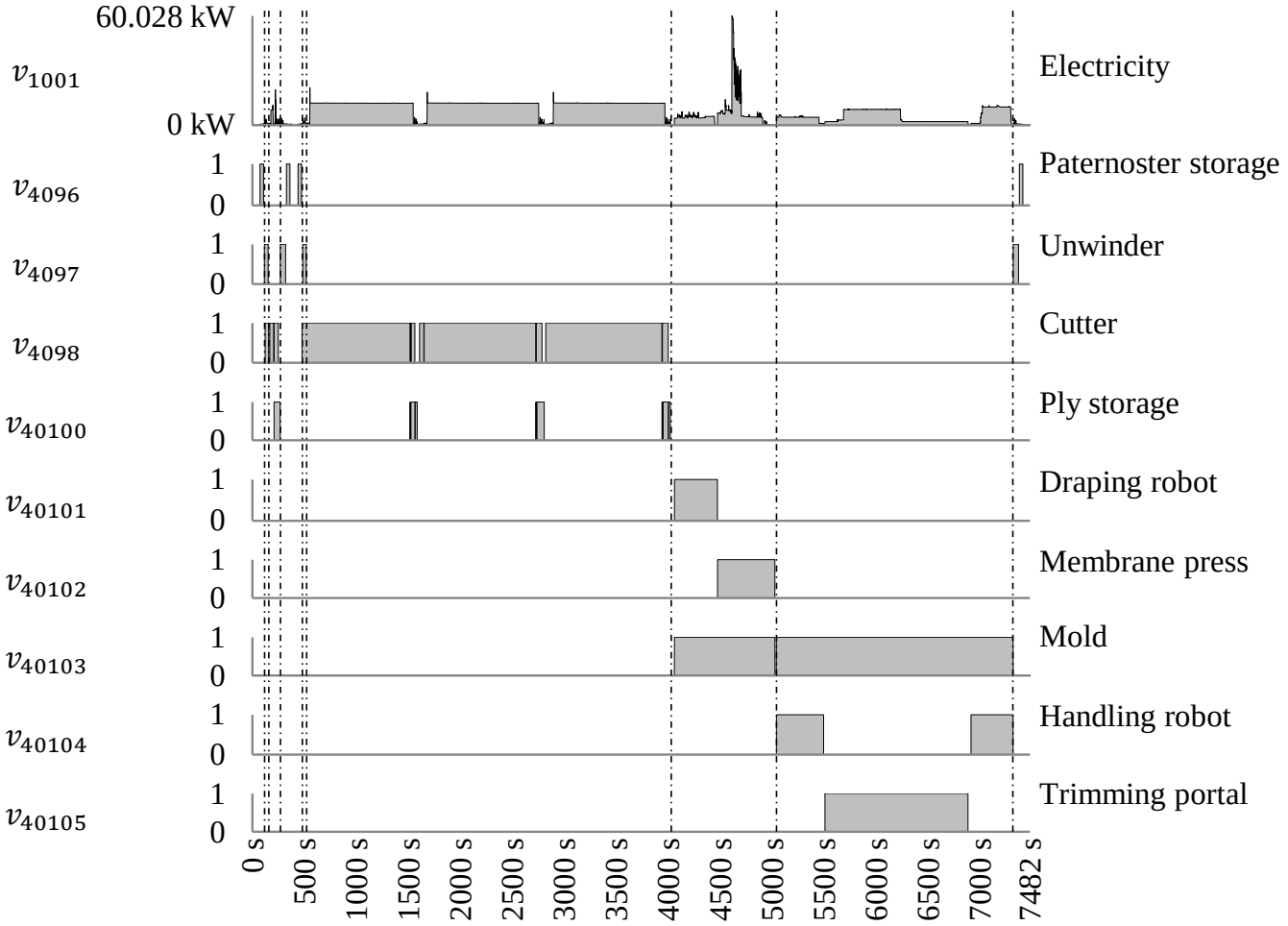

Figure 6.7 Real-time electricity and equipment flows by all SWSs in 0 s< t <7482 s

As Fig. 6.7 shows, the combined electricity consumption v_{1001} has a distinguishable performance in various UPs i. For equipment subset $\varphi^{[Q]}$, the associated input flows v_j are shown in Fig. 6.7 for the entire process as well. Based on the comprehensive illustration of the mathematical model elements from Fig. 4.19 in chapter 4, Fig. 6.7 includes the matrix $[\Upsilon^{[Q]}]$, that covers all equipment items throughout the entire process.

Similarly, the cumulative values of elementary flows within the subsets of fiber $\varphi^{[F]}$, ancillaries $\varphi^{[R]}$, and fiber waste $\varphi^{[G]}$ are shown in Fig. 6.8.

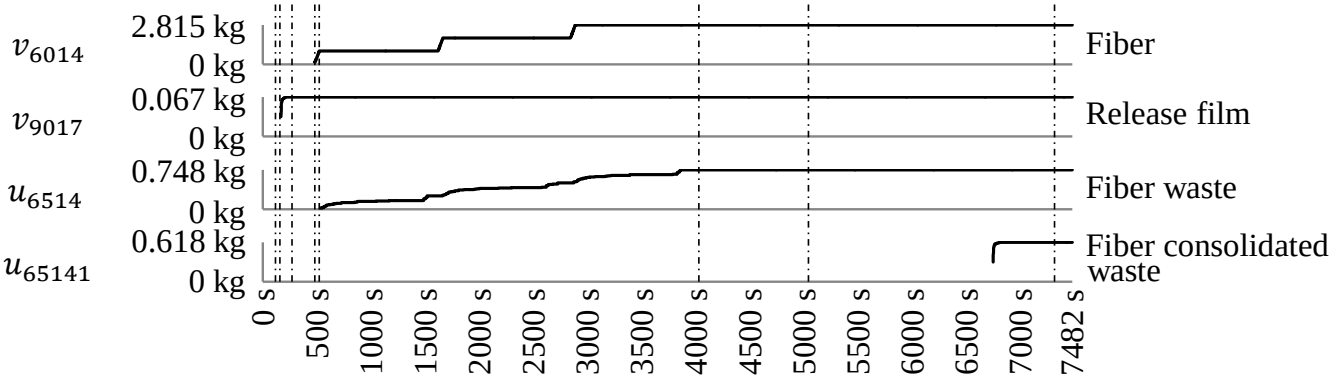

Figure 6.8 Real-time cumulative fiber, ancillaries, and fiber waste flows by all SWSs in 0 s< t <7482 s

In addition, the real-time collected data provides better understanding of the elementary flows ranking in their subsets. For instance, the total operation durations of various equipment types and facilities can be compared.

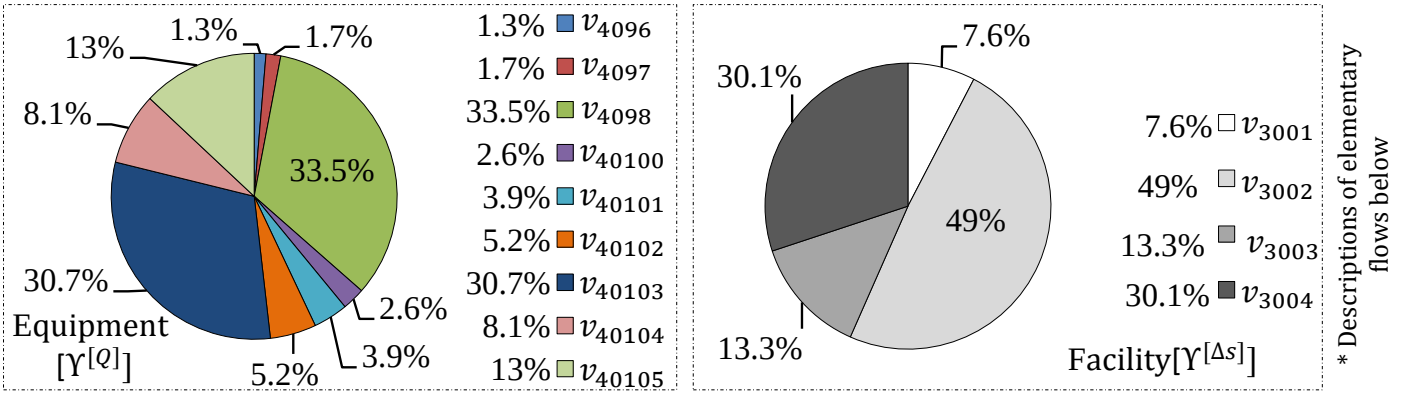

Figure 6.9 Total operation and occupation of equipment and facility flows by all SWSs in 0 s< t <7482 s

* v_{4096} = paternoster storage v_{4097} = unwinder v_{4098} = cutter v_{40100} = ply storage v_{40101} = draping robot v_{40102} = membrane press v_{40103} = mold v_{40104} = handling robot v_{40105} = trimming portal v_{3001} = facility WS_1 v_{3002} = facility WS_2 v_{3003} = facility WS_3 v_{3004} = facility WS_4

As Fig. 6.9 shows, conventional time-independent results can still be illustrated for decision-makers by SWS as a DSS based on the real-time LCI. For decision-makers, the real-time data collection may be implemented in enhancing process efficiency through suitable controlling related SDs for each equipment if applicable. Moreover, a wide range of illustrations can be derived from selecting elements, vectors, matrices, or combination of them based on the comprehensive illustration of mathematical model elements from Fig. 4.19. By the real-time LCI throughout the process duration, a time-dependent assessment is enabled.

6.1.2 Time-Dependent LCIA Results

After going through the characteristics of time-dependent results briefly, these results are shown for every assessed UP. Moreover, the global process results are also presented and discussed.

Brief characteristics of time-dependent results

In this work, a time-dependent assessment of both economic and ecological impacts is performed for every included elementary flow α_{ij}. This is realized on the impact level of θ_{ij}, as it has been shown in Fig. 4.20 within chapter 4. Here, the selected time interval of time-dependent results can be changed, if another assessment rhythm is required. Nonetheless, increasing its frequency is limited to the possible frequency of data collection from the various implemented real-time LCI. As it is mentioned previously, the impacts are illustrated in line graphs for the cumulative impact values on the vertical axis, while the time is shown on the horizontal axis. The impacts θ_{ij_t} of the economic aspect δ_{ij_t} and the ecological one β_{ij_t} are the products of the dynamic elementary flow values α_{ij_t} over time t multiplied by their constant characterization factors γ_j and ε_j respectively. Therefore, the behaviors of these cumulative economic and ecological impacts are identical to their cumulative elementary flow but with different values. Now, the same line graph may describe both economic and ecological impacts, if a proper vertical axis is implemented. Such graphs are used in this chapter to present both aspects.

The eco-efficiency ξ_t and its associated economic and ecological impacts for the case study have been assessed in time-dependent manner within a constant time interval of Δt =1 s. This allows the determination of these impacts at any temporal point t based on the assessment of both economic impacts δ_{ij_t} and ecological ones β_{ij_t} of all included elementary flows α_{ij_t}. The eco-efficiency value of every UP i is shown at selected temporal points t as ξ_{i_t} to demonstrate the DSSs capabilities and to assure an optimized result visualization in this work. Moreover, the time-dependent logarithmic scaled eco-efficiency of each UP i is separately illustrated

for the assumed k_i. This logarithmic scaling is necessary, while the difference is very large in the absolute value of ξ_{i_t} during the UP. To be freed from the assumed constants k_i and their accuracy, the decision-makers are provided with the graphs of time-dependent direct cost to carbon footprint behavior δ_{i_t}/β_{i_t}.

For decision-makers, identifying the temporal allocation of impact drivers is essential to associate them with their activities and technologies in order to define the proper SDs. Moreover, such illustrations are essential to prioritize the activities that need these SDs. However, not every technology has the SD potential, while the next one within the priority list is to be considered in such case. Therefore, the time-dependent total impacts are illustrated by area charts in this work. As it is hypothesized previously in chapter 2, every temporal impact is considered as a non-transient cumulative one in its temporal point.

Moreover, pie and bar charts are utilized to present conventional time-independent results. For the sake of comparing the results of this work with other studies, a unified comparable product should be defined. While the functional units are not identical in the relevant studies, the impact of each kg from a similar structure may be a more sufficient comparing unit. Therefore, the impact results are calculated for a single kg of the structure as well, while the trimmed preform has the weight of around 1.449 kg as the final structure output in this thesis. For the economic assessment, an additional digit is considered in this work to present the statistical results on the level of 1/1000 €. Although the cent is the lowest available momentary coin as the 1/100 of the €, the representation of all impacts on this 1/1000 level is reducing the deviation severity of numbers rounding by keeping them on a lower level than the crucial one. When it comes to rating the impacts of elementary flows, electricity consumptions may be clustered under the total UP consumption for simplicity.

Preparing UP_1 time-dependent results

For UP_1, the time-dependent assessment of elementary flows in this case study covers the economic and ecological impacts of the total electricity consumption in UP_1 as $v_{1,1001}$, paternoster storage $v_{1,4096}$, paternoster storage consumption $v_{1,10496}$, unwinder $v_{1,4097}$, unwinder electricity $v_{1,10497}$, labor $v_{1,2001}$, air conditioned facility of WS_1 as $v_{1,3001}$, and WS_1 electricity $v_{1,1031}$, as Fig. 6.10 shows.

Similar to the elementary flows in Fig. 6.2, the impacts in Fig. 6.10 are split into three discontinuous temporal slots in UP_1. In Fig. 6.10, the labor work $v_{1,2001}$ causes the highest direct cost δ_{ij}. On the other hand, the lowest economic impact causer in UP_1 is the total electricity $\delta_{1,1001}$, while all other electricity consumptions are covered by it. From the equipment subset $\varphi_1^{[Q]}$, the paternoster storage $v_{1,4096}$ has the highest direct cost. As Fig. 6.10 shows, the facility $v_{1,3001}$ has the highest share of carbon footprint β_{ij}. This illuminates the importance of considering the ecological impact of this subset, which has been traditionally neglected in literature. The total electricity $\varphi_1^{[T]}$ is the second ecological impact contributor in UP_1, which is followed by the labor $v_{1,2001}$. Again, the hypothesis of considering labor ecological impact has shown a significant result in UP_1. From the equipment subset $\varphi_1^{[Q]}$, the paternoster storage $v_{1,4096}$ has the highest direct cost and carbon footprint in its subset. In addition, the time-dependent assessment results of total economic and ecological impacts are visualized within Fig. 6.11.

The behavior of direct cost δ_{1_t} in Fig. 6.11 is clearly connected to the occurrence of the labor work $v_{1,2001}$ in Fig. 6.2. The carbon footprint β_{1_1} in Fig. 6.11 is differently impacted by various elementary flows α_{1j}, that have been shown in Fig. 6.2. In Fig. 6.11, a single eco-efficiency value is randomly selected at t =389 s to demonstrate the assessment capabilities. From Fig. 6.11, other eco-efficiency values are interpretable directly from the total economic and ecological impacts. The final eco-efficiency ξ_1 of UP_1 in t_{1C_b} =7482 s at 16:04:52 is equal to $\xi_1 = \dfrac{\text{k} € \text{ - } 7.6 €}{0.71\,\text{kg}\,CO_2}$.

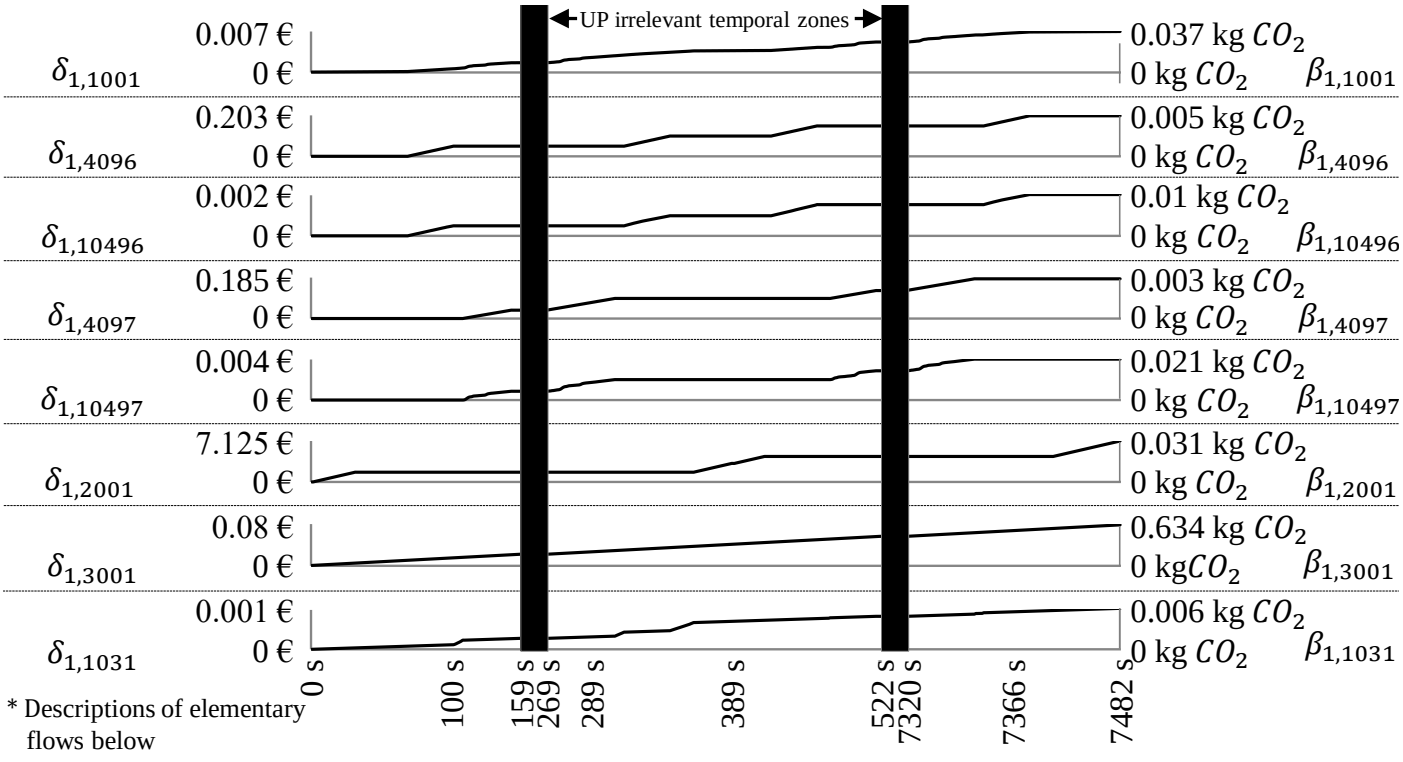

Figure 6.10 Time-dependent cumulative direct cost δ_{1j} and carbon footprint β_{1j} in UP_1

* $v_{1,1001}$ = electricity in UP_1 $v_{1,4096}$ = paternoster storage $v_{1,10496}$ = paternoster storage electricity $v_{1,4097}$ = unwinder $v_{1,10497}$ = unwinder electricity $v_{1,2001}$ = labor $v_{1,3001}$ = facility WS_1 $v_{1,1031}$ = facility WS_1 electricity

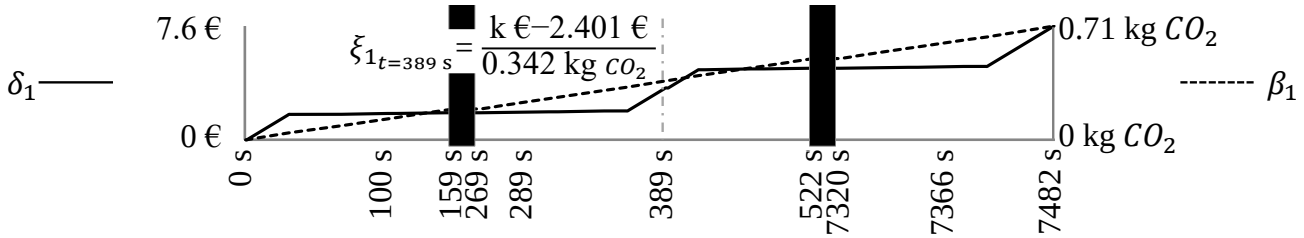

Figure 6.11 Time-dependent total cumulative direct cost δ_{1_t} and carbon footprint β_{1_t} in UP_1

As it is assumed previously in chapter 5, the revenue excluding all non-process costs of preparing UP_1 is around k_1 =50 €, while the eco-efficiency of UP_1 is equal to $\xi_1 = \frac{42.4\ €}{0.71\,\text{kg}\,CO_2}$. For a single kg of CFRP structure, the direct cost from UP_1 in this thesis is calculated as δ_1 = 5.245 €/kg, while the carbon footprint from UP_1 is calculated as $\beta_1 = 0.489\,\text{kg}\,CO_2/\text{kg}$. To understand the eco-efficiency behavior ξ_{1_t} based on the assumed constant of k_1 =50 €, Fig. 6.12 shows the cumulative logarithmic scaled ξ_{1_t} throughout UP_1 duration.

Moreover, a time-dependent direct cost to carbon footprint behavior δ_{1_t}/β_{1_t} in UP_1 is introduced by Fig. 6.13 to enable future assessment capabilities regarding the activities and their technologies. This high ratio of direct cost to carbon footprint δ_{1_t}/β_{1_t} with around 38 at the beginning of UP_1 varies between 5 and 12 after that. Furthermore, the time-dependent direct cost can be solely considered by decision-makers to evaluate selected activities and their technologies within this UP_1 based on the resulting economic impact shown in Fig. 6.14.

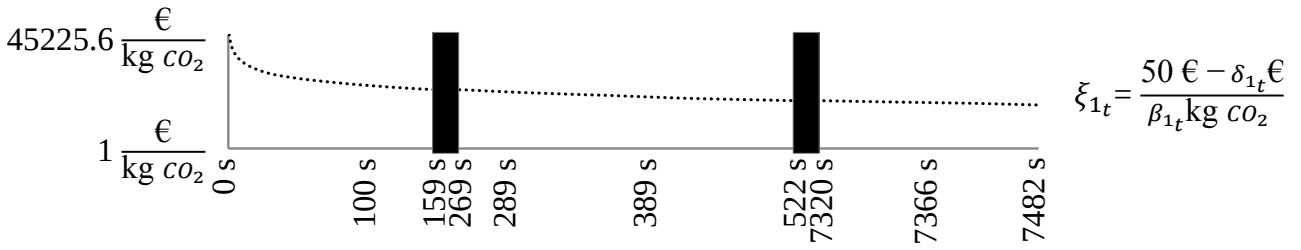

Figure 6.12 Time-dependent logarithmic scaled eco-efficiency ξ_{1_t} in UP_1

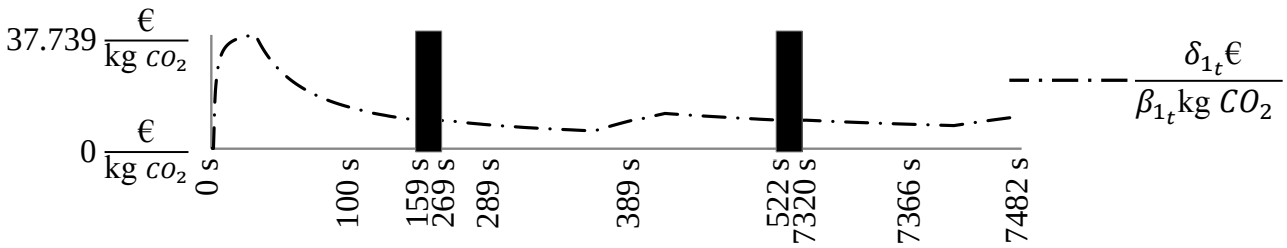

Figure 6.13 Time-dependent direct cost to carbon footprint behavior δ_{1_t}/β_{1_t} in UP_1

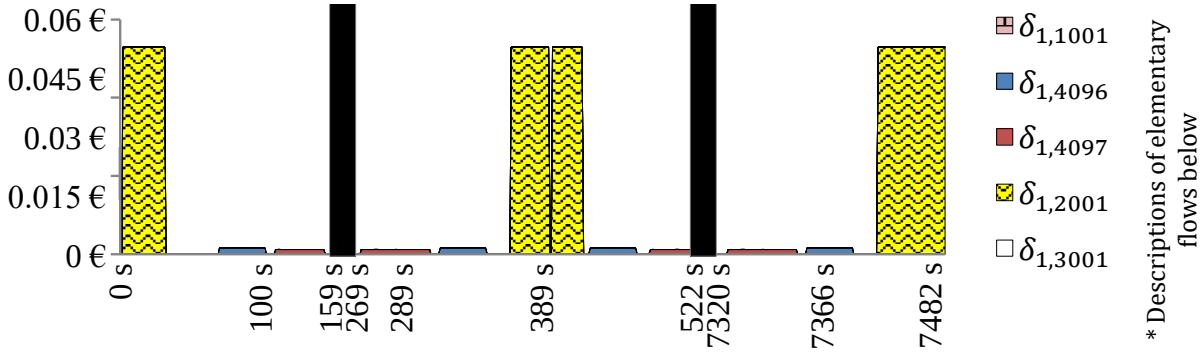

Figure 6.14 Time-dependent total direct cost δ_1 in UP_1

* $v_{1,1001}$ = electricity in UP_1 $v_{1,4096}$ = paternoster storage $v_{1,4097}$ = unwinder $v_{1,2001}$ = labor $v_{1,3001}$ = facility WS_1

Due to their minor economic impact from Fig. 6.10, the direct costs of all electricity consumptions are combined under $v_{1,1001}$.

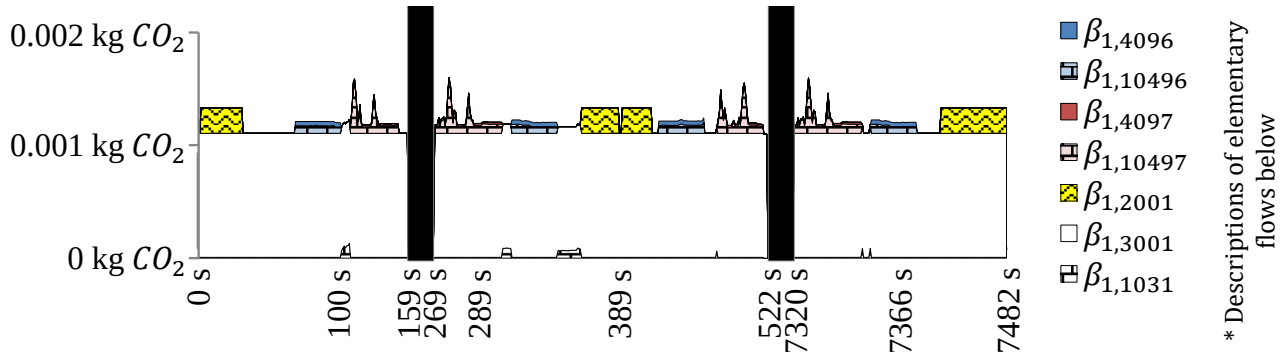

Figure 6.15 Time-dependent total carbon footprint β_1 in UP_1

$v_{1,4096}$ = paternoster storage $v_{1,10496}$ = paternoster storage electricity $v_{1,4097}$ = unwinder $v_{1,10497}$ = unwinder electricity $v_{1,2001}$ = labor $v_{1,3001}$ = facility WS_1 $v_{1,1031}$ = facility WS_1 electricity

Similar to Fig. 6.14, the total ecological impact throughout UP_1 is shown by the area chart in Fig. 6.15. While the electricity consumption contributors are more significant to the carbon footprint, they are presented separately in Fig. 6.15.

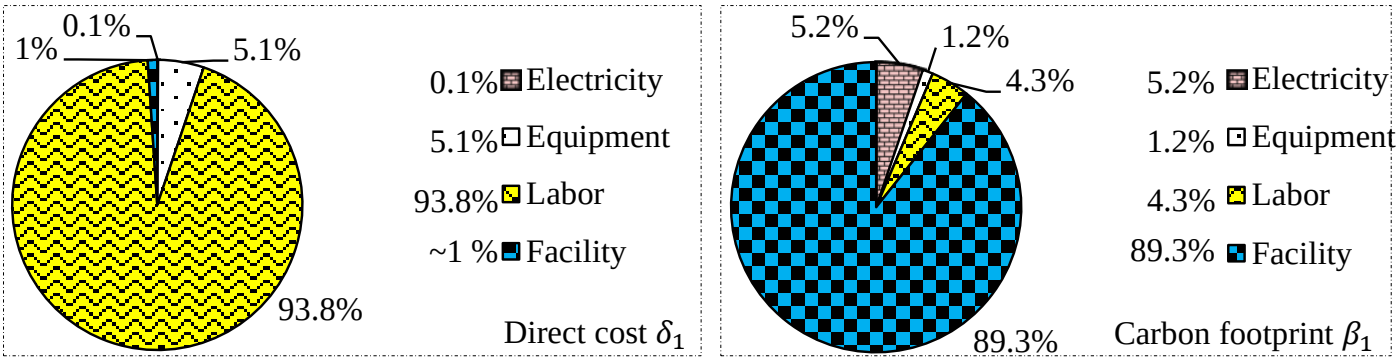

Figure 6.16 Direct cost δ_1 and carbon footprint β_1 contributing subsets in UP_1

For the decision-makers, the total impact results of all assessed elementary flow subsets $\varphi^{[\Gamma]}$ are essential. Therefore, they are shown in the pie charts within Fig. 6.16. As it is illustrated on the left side of Fig. 6.16, the labor subset $\varphi_1^{[L]}$ represented by $v_{1,2001}$ is the dominating direct cost contributor with around 93.8 % from the total δ_1. Despite the relatively short work duration in this scenario, the labor work $v_{1,2001}$ has a very high direct cost due to its high economic characterization factor γ_{2001}. In Fig. 6.16, the equipment subset $\varphi_1^{[Q]}$ has the second highest direct cost of around 5.1 %. The electricity subset $\varphi_1^{[T]}$ has the lowest economic impact in UP_1.

With regard to the carbon footprint β_1, the facility of WS_1 as $v_{1,3001}$ has the highest ecological impact within UP_1. As the right side of Fig. 6.16 shows, the electricity subset $\varphi_1^{[T]}$ is the second highest carbon footprint causer in UP_1. This is associated with the relatively low electricity consumption of UP_1 in comparison to other UPs i, as it has been shown previously in Fig. 6.7. In UP_1, the labor subset $\varphi_1^{[L]}$ is the third largest contributor to the carbon footprint β_1. Again, these results of the contribution to carbon footprint from facility and labor subsets put a light on the importance of considering them in the ecological assessment. The equipment subset $\varphi_1^{[Q]}$ is the lowest carbon footprint producer in Fig. 6.16. It is essential to mention that UP_1 contains no material elementary flows according to the defined system boundary of the selected case study. Therefore, labor and equipment direct costs and facility carbon footprint play the significant role in this UP.

Cutting UP_2 time-dependent results

Similar to UP_1, the results of time-dependent eco-efficiency assessment are visualized for UP_2 within Fig. 6.17. In Fig. 6.17, the fiber $v_{2,6014}$ is the dominating direct cost contributor, while the cutter $v_{2,4098}$ from equipment subset $\varphi^{[Q]}$ is following it by a large margin. Compared to other equipment types, the cutter direct cost $\delta_{2,4098}$ is much higher due to its long operation time, as Eq. 6.5 shows before. On the other hand, the total electricity $\varphi_2^{[T]}$ has a total direct cost $\delta_{2,1001}$ of less than 1 € in UP_2. In this comparison, the separated electricity consumptions of the involved equipment types and facility are excluded, while they are clustered within the total electricity of UP_2. Based on that, the lowest direct cost is associated with the facility of WS_2 represented by $\delta_{2,3002}$. Although WS_1 is considered to have larger area than WS_2, $\delta_{2,3002}$ is much higher than $\delta_{1,3001}$ due to the longer occupation in Eq. 6.4. Although input elementary flows are the targeted assessment flows, the output elementary flow of fiber waste $u_{2,6514}$ is considered as well. After excluding the cost of its initial fiber, the fiber waste from UP_2 has a total economic impact of around 3.741 €, which represents 1.5 % of fiber share and 1.31 % from the total direct cost δ_2 of UP_2. By including the fiber initial cost, the fiber waste costs around 70.23 € in UP_2.

As far as the carbon footprint β_2 is considered, the fiber $\beta_{2,6014}$ is also the dominating contributor in Fig. 6.17, that is followed by the facility $\beta_{2,3002}$ then the total electricity $\beta_{2,1001}$. Again, this illuminates the importance of considering the ecological impact of facility subset, as it is hypothesized previously.

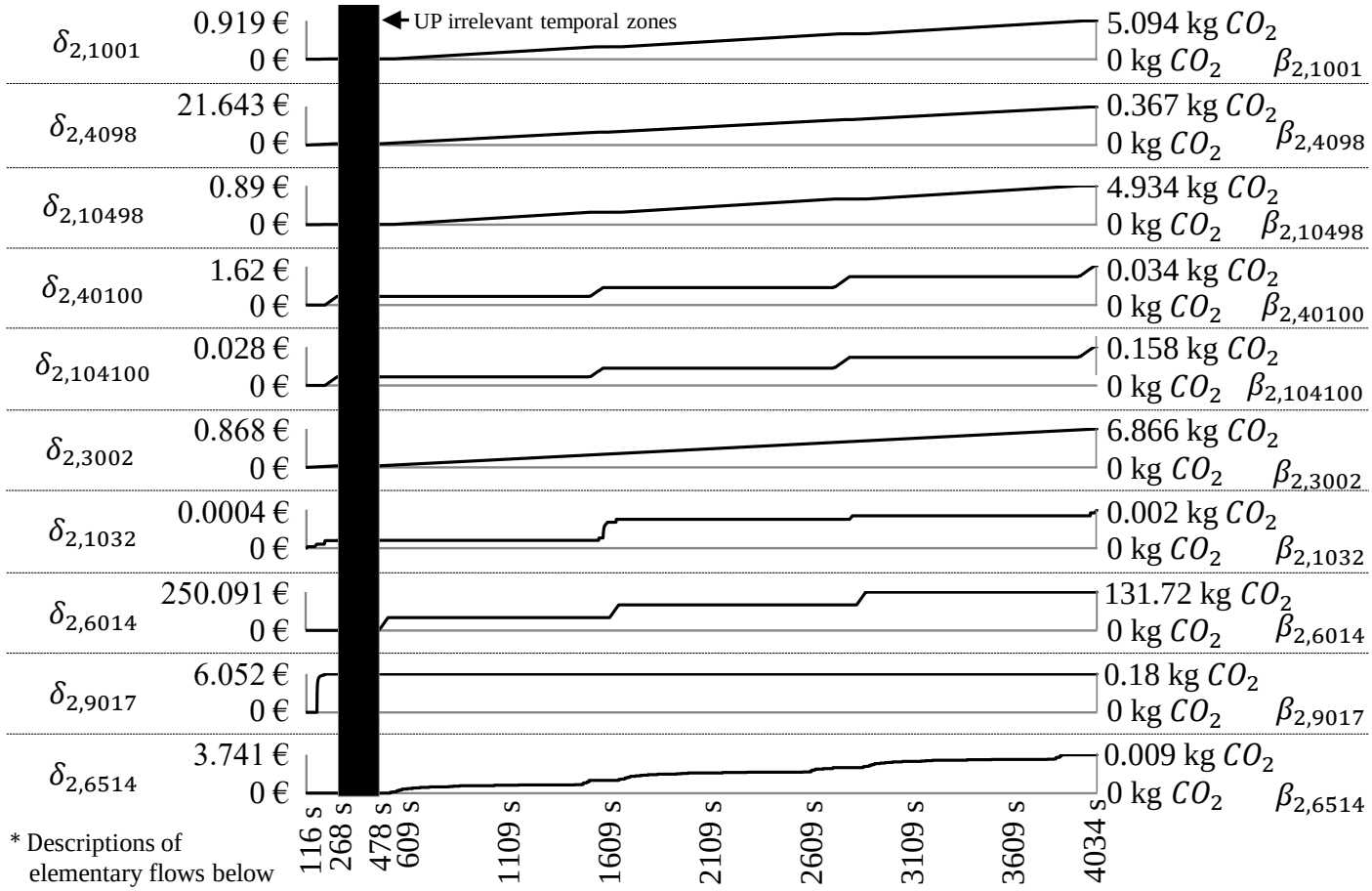

Figure 6.17 Time-dependent cumulative direct cost δ_{2j} and carbon footprint β_{2j} in UP_2

* $v_{2,1001}$ = electricity in UP_2 $v_{2,4098}$ = cutter $v_{2,10498}$ = cutter electricity $v_{2,40100}$ = ply storage $v_{2,104100}$ = ply storage electricity $v_{2,3002}$ = facility WS_2 $v_{2,1032}$ = facility WS_2 electricity $v_{2,6014}$ = fiber $v_{2,9017}$ = release film $u_{2,6514}$ = fiber waste

After excluding the fiber initial carbon footprint, the fiber waste from UP_2 has a total ecological impact of 0.009 kg CO_2, which represents around 0.01 % from the fiber carbon footprint share. By including the carbon footprint of initial fiber, the fiber waste has the ecological impact of around 35.028 kg CO_2. Similar to Fig. 6.11, the time-dependent total cumulative direct cost δ_2 and carbon footprint β_2 in UP_2 are illustrated in Fig. 6.18.

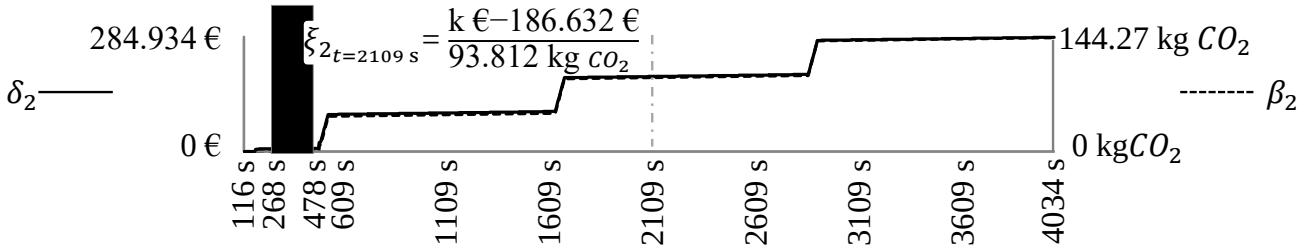

Figure 6.18 Time-dependent total cumulative direct cost δ_{2_t} and carbon footprint β_{2_t} in UP_2

UP_2 has a total direct cost δ_2 of around 284.934 €, while a very small share of that occurs in the first part in UP_{2A}. The direct cost δ_{2_t} in Fig. 6.18 is associated with the behaviors of fiber $v_{2,6014}$ and cutter $v_{2,4098}$ from Fig. 6.3. Similarly, the carbon footprint β_{2_t} in Fig. 6.18 is shaped based mainly on the fiber $v_{2,6014}$ and electricity $\varphi_2^{[T]}$ behaviors. Unlike their behavior in UP_1 within Fig. 6.11, the direct cost and carbon footprint have a clear similarity throughout the entire UP in Fig. 6.18. In Fig. 6.18, a single eco-efficiency value is randomly selected at t =2109 s to demonstrate the assessment capabilities. The results show that the final eco-efficiency ξ_2 of UP_2 is equal to $\xi_2 = \frac{\text{k €} - 284.934\text{ €}}{144.27\text{ kg } CO_2}$. As it is assumed previously

in chapter 5, the constant of cutting UP_2 is around k_2 =300 €. Therefore, the eco-efficiency of UP_2 is calculated as $\xi_2 = \frac{15.066\,€}{144.27\,\mathrm{kg}\,CO_2}$. For a single kg of the CFRP structure, the direct cost from UP_2 in this thesis is calculated as δ_2 = 196.642 €/kg, while the carbon footprint from UP_2 is considered to be β_2 = 99.566 kg CO_2/kg. Nonetheless, other elementary flows are inappropriately visualized in Fig. 6.18 due to the domination of economic and ecological fiber impacts. Therefore, an additional illustration is exceptionally provided in Fig. 6.19 for the direct cost $\delta_{2_t} \setminus (\delta_{2,6014_t}, \delta_{2,6514_t})$ and carbon footprint $\beta_{2_t} \setminus (\beta_{2,6014_t}, \beta_{2,6514_t})$, that are excluding the impacts of fiber $\theta_{2,6014_t}$ and its waste $\theta_{2,6514}$ in UP_2.

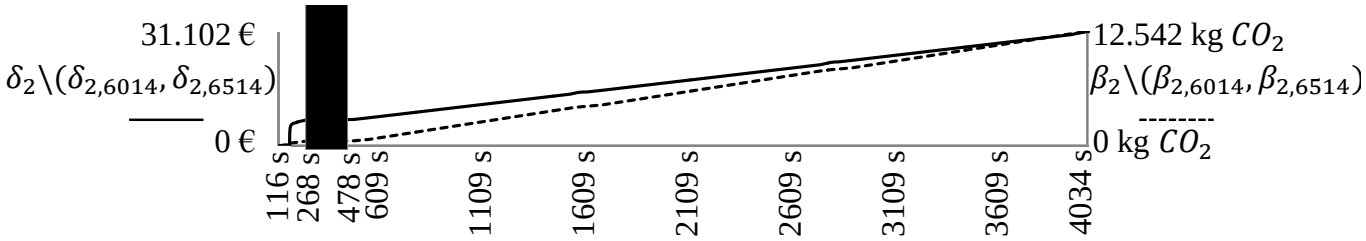

Figure 6.19 Time-dependent total cumulative direct cost and carbon footprint $\theta_{2_t} \setminus (\theta_{2,6014_t}, \theta_{2,6014_t})$

To understand the eco-efficiency behavior ξ_{2_t} based on the assumed revenue excluding all non-process costs of k_2 =300 €, Fig. 6.20 shows the cumulative logarithmic scaled ξ_{2_t} throughout UP_2 duration.

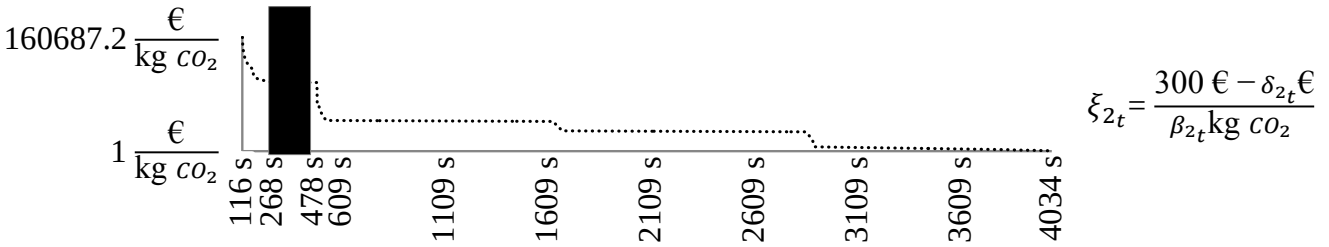

Figure 6.20 Time-dependent logarithmic scaled eco-efficiency ξ_{2_t} in UP_2

Similar to Fig. 6.13, the time-dependent direct cost to carbon footprint behavior δ_{2_t}/β_{2_t} is shown in Fig. 6.21.

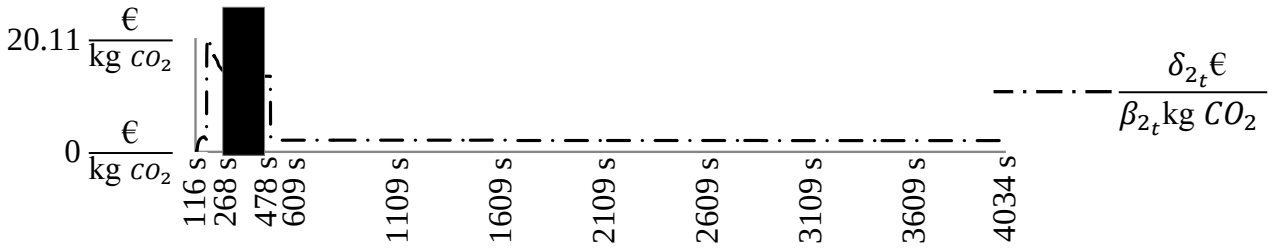

Figure 6.21 Time-dependent direct cost to carbon footprint behavior δ_{2_t}/β_{2_t} in UP_2

The ratio in Fig. 6.21 has a very high value in the time between t =116 s and t =268 s in comparison to the relatively constant ratio of around 2 after that time slot. Moreover, the total time-dependent direct cost and carbon footprint of the elementary flows except the material flows during UP_2 are shown in the area graphs within Fig. 6.22 and Fig. 6.23 respectively.

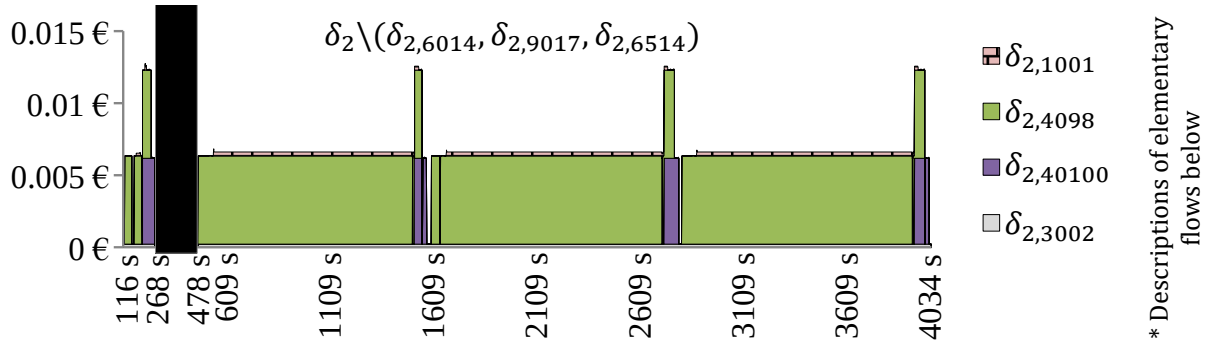

Figure 6.22 Time-dependent total direct cost $\delta_2 \setminus (\delta_{2,6014}, \delta_{2,9017}, \delta_{2,6514})$ in UP_2

* $v_{2,1001}$ = electricity in UP_2 $v_{2,4098}$ = cutter $v_{2,40100}$ = ply storage $v_{2,3002}$ = facility WS_2

In Fig. 6.22 and Fig. 6.23, excluding the impacts of fiber $\theta_{2,6014}$ and its waste $\theta_{2,6514}$ as well as the release film $\theta_{2,9017}$ is necessary to achieve visually understandable illustrations, while the excluded impacts are dominating with large differences.

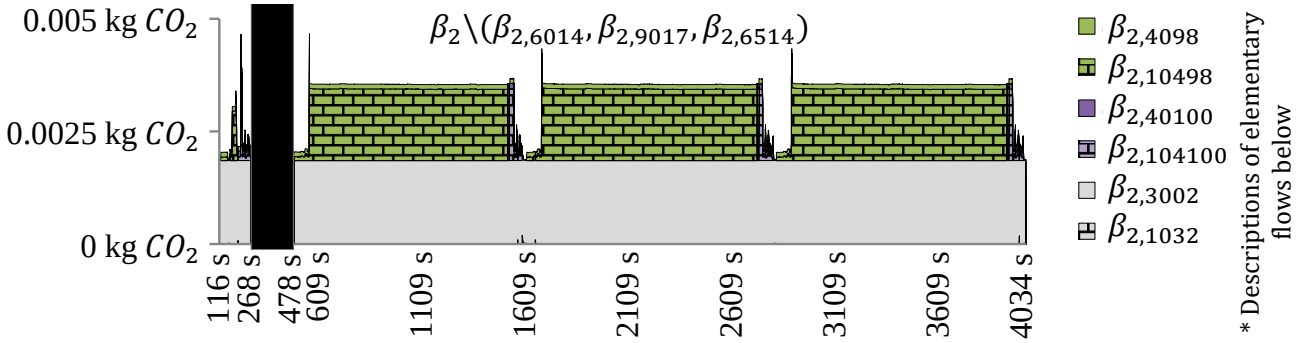

Figure 6.23 Time-dependent total carbon footprint $\beta_2 \setminus (\beta_{2,6014}, \beta_{2,9017}, \beta_{2,6514})$ in UP_2

* $v_{2,4098}$ = cutter $v_{2,10498}$ = cutter electricity $v_{2,40100}$ = ply storage $v_{2,104100}$ = ply storage electricity $v_{2,3002}$ = facility WS_2 $v_{2,1032}$ = facility WS_2 electricity

The total time-independent contributions of direct cost δ_2 and carbon footprint β_2 among the considered subsets $\varphi_2^{[\Gamma]}$ in UP_2 are illustrated in Fig. 6.24.

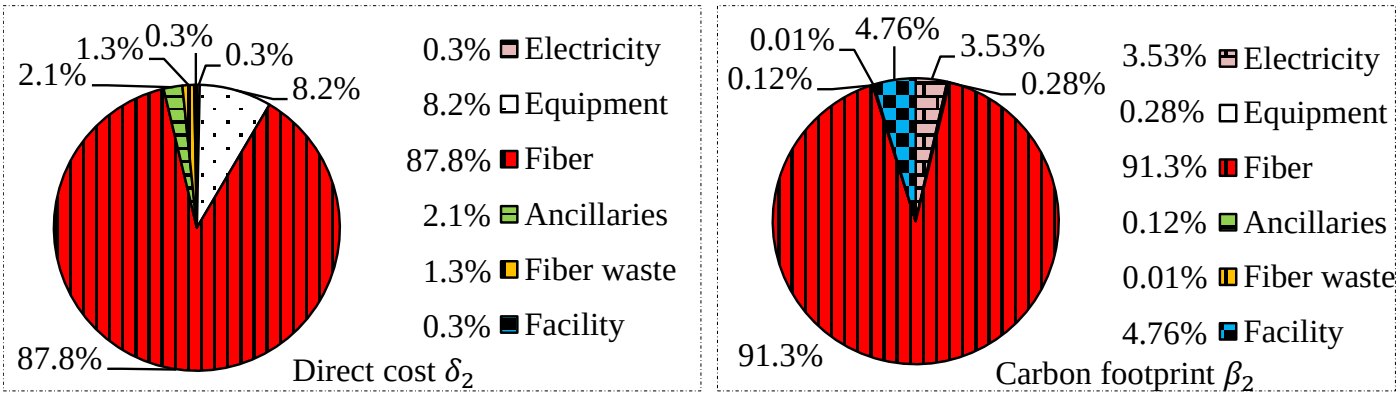

Figure 6.24 Direct cost δ_2 and carbon footprint β_2 contributing subsets in UP_2

As the left part of Fig. 6.24 shows, the fiber subset $\varphi_2^{[F]}$ is the dominating direct cost contributor with a major share of 87.8 %. The dominating fiber direct cost $\delta_{2,6014}$ is associated with its high economic characterization factor γ_{6014}, that is represented by the estimated market price. As Eq. 5.30 in chapter 5 shows, γ_{6014} is the highest economic characterization factor. Moreover, the implemented magnitude of around 2.815 kg is relatively

high in comparison to the release film $v_{2,9017} \in \varphi_2^{[R]}$ with around 0.067 kg as the only other material in this case study. The equipment subset $\varphi_2^{[Q]}$, which is represented by the cutter $v_{2,4098}$ and ply storage $v_{2,40100}$, has the second highest direct cost. Ancillaries subset $\varphi_2^{[R]}$ represented by the release film $v_{2,9017}$ has a relatively low direct cost due to the low applied magnitude.

Turning to the carbon footprint β_2 on the right side of Fig. 6.24, the fiber subset $\varphi_2^{[F]}$ represented by $v_{2,6014}$ is the dominating contributor again. This is also a result of the relatively high ecological characterization factor ε_{6014}, which is the highest among other ones in Eq. 5.31 within chapter 5. The facility subset $\varphi_2^{[\Delta s]}$ comes second in the carbon footprint contribution. When the fiber waste $\varphi_2^{[G]}$ is neglected as an output, both equipment $\varphi_2^{[Q]}$ and ancillaries $\varphi_2^{[R]}$ come last in the contributors to carbon footprint β_2. Due to the domination of economic and ecological fiber impacts $\delta_{2,6014}$ and $\beta_{2,6014}$, the results visualization in Fig. 6.24 can be further simplified by excluding the fiber and its waste impacts and show the contributions of other ones more clearly, as Fig. 6.25 suggests. The decision-makers may require such illustrations to understand the contribution among subsets other that the dominating ones.

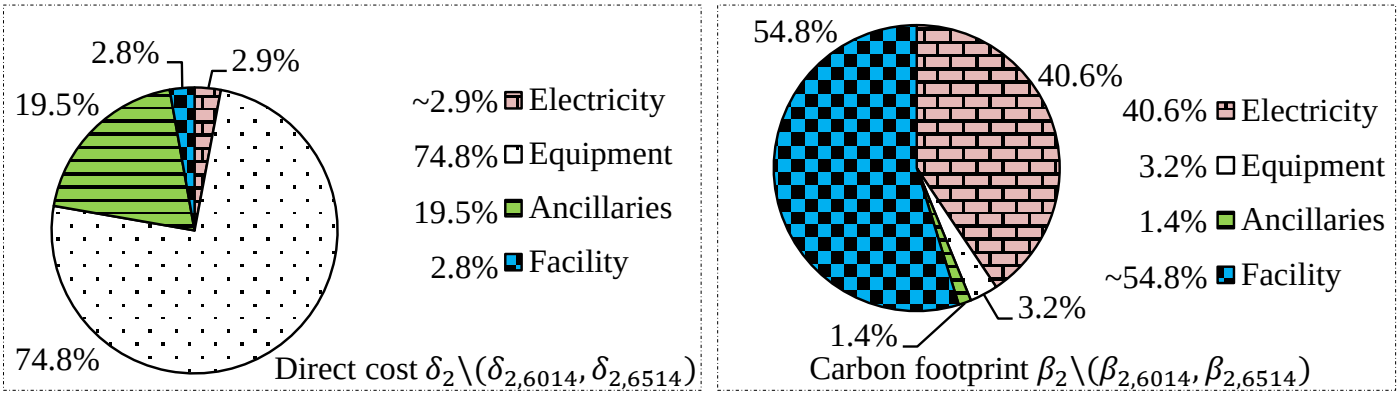

Figure 6.25 Direct cost and carbon footprint $\theta_2 \setminus (\theta_{2,6014}, \theta_{2,6514})$ selected contributing subsets in UP_2

Preforming UP_3 time-dependent results

In Fig. 6.26, the time-dependent cumulative direct cost δ_{3j} and carbon footprint β_{3j} of each considered elementary flow α_{3j} in UP_3 are shown. The membrane press $v_{3,40102}$ has the highest direct cost contribution in Fig. 6.26. Except for the separated electricity consumptions in Fig. 6.26, the lowest direct cost δ_{3j} is caused by the facility $v_{3,3003}$. On the right side of Fig. 6.26, the facility WS_3 has the highest carbon footprint. Except for the electricity of facility WS_3, which is included in the total electricity, the smallest carbon footprint is caused by the mold $v_{3,40103}$. This mold has a relatively low ecological characterization factor ε_{40103} in Eq. 5.31. In Fig. 6.27, the time-dependent total cumulative direct cost δ_3 and carbon footprint β_3 in UP_3 are illustrated.

As Fig. 6.27 shows, the direct cost δ_{3_t} is associated with the utilized equipment types and their electricity. On the other hand, the cumulative carbon footprint β_{3_t} is clearly correlated with the ecological impact, that is caused by the electricity. To demonstrate the time-dependent capability in assessing the eco-efficiency, the randomly selected eco-efficiency value in Fig. 6.27 is set at t =4778 s. The eco-efficiency ξ_3 of UP_3 at t_{3_b} =5041 s is equal to $\xi_3 = \frac{\text{k€ - 7.764 €}}{2.315\,\text{kg}\,CO_2}$, as Fig. 6.27 shows. Based on the previous assumptions in chapter 5, the constant of preforming UP_3 is around k_3 =75 €, which makes the eco-efficiency of UP_3 calculable as $\xi_3 = \frac{67.236\,€}{2.315\,\text{kg}\,CO_2}$. The direct cost from UP_3 in this thesis is calculated as δ_3 = 5.358 €/kg, while the carbon footprint from UP_3 is calculated as $\beta_3 = 1.598\,\text{kg}\,CO_2/\text{kg}$ for a single kg of CFRP structure.

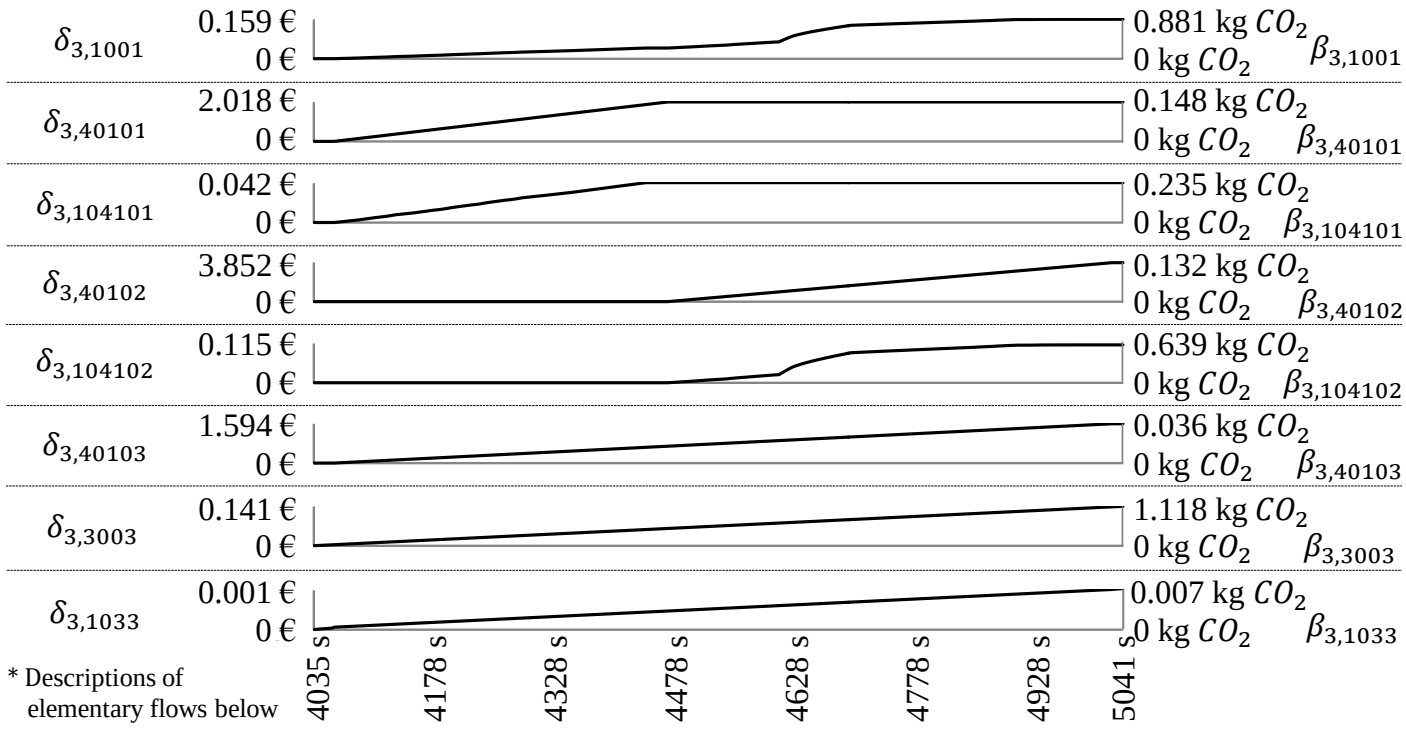

Figure 6.26 Time-dependent cumulative direct cost δ_{3j} and carbon footprint β_{3j} in UP_3

* $v_{3,1001}$ = electricity in UP_3 $v_{3,40101}$ = draping robot $v_{3,104101}$ = draping robot electricity $v_{3,40102}$ = membrane press $v_{3,104102}$ = membrane press electricity $v_{3,40103}$ = mold $v_{3,3003}$ = facility WS_3 $v_{3,1033}$ = facility WS_3 electricity

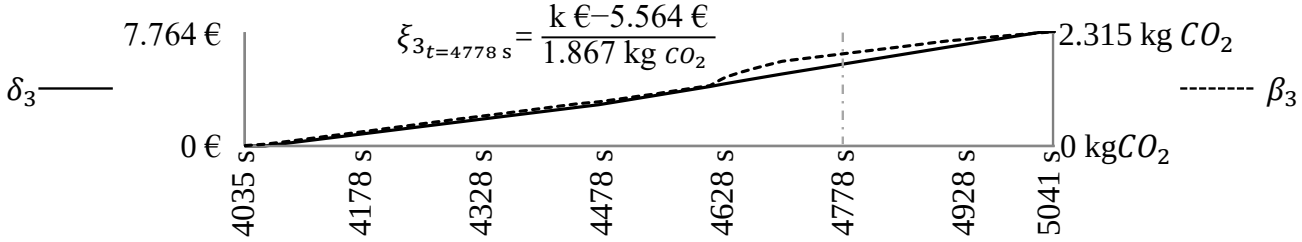

Figure 6.27 Time-dependent total cumulative direct cost δ_{3_t} and carbon footprint β_{3_t} in UP_3

For the time-dependent eco-efficiency of UP_3 throughout its duration, Fig. 6.28 shows its cumulative logarithmic behavior.

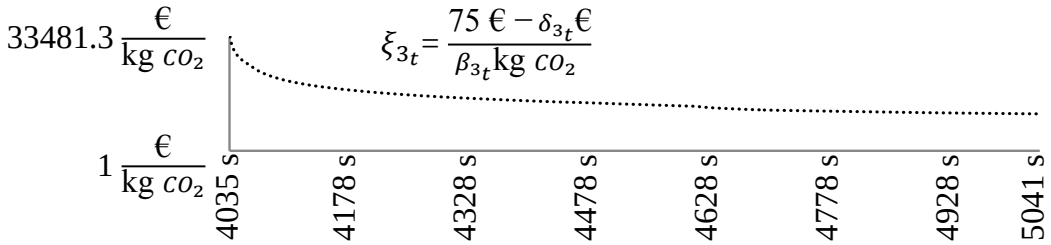

Figure 6.28 Time-dependent logarithmic scaled eco-efficiency ξ_{3_t} in UP_3

Again, this behavior in Fig. 6.28 is associated with the direct cost to carbon footprint behavior δ_{3_t}/β_{3_t}, which can be separately illustrated in Fig. 6.29.

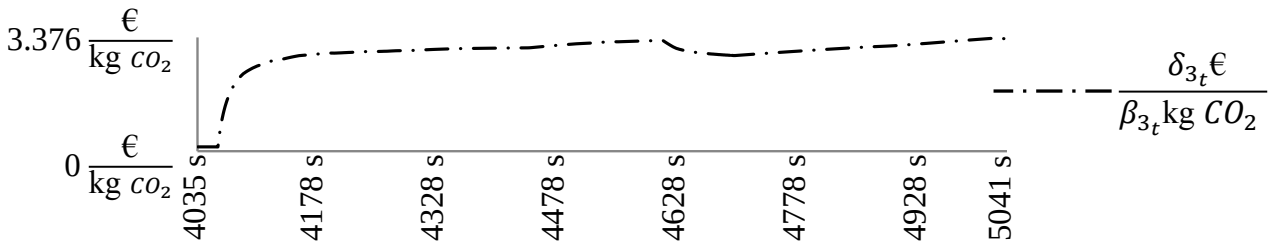

Figure 6.29 Time-dependent direct cost to carbon footprint behavior δ_{3_t}/β_{3_t} in UP_3

From Fig. 6.29, the ratio of δ_{3_t}/β_{3_t} is stable with a value that varies approximately between 2 and 4 except for the beginning of UP_3. Similar to the previous UPs, the total impacts of each relevant elementary flow in θ_{3j} are illustrated by Fig. 6.30 and Fig. 6.31 in time-dependent manner for the sake of allocating them to their activities and associated technologies.

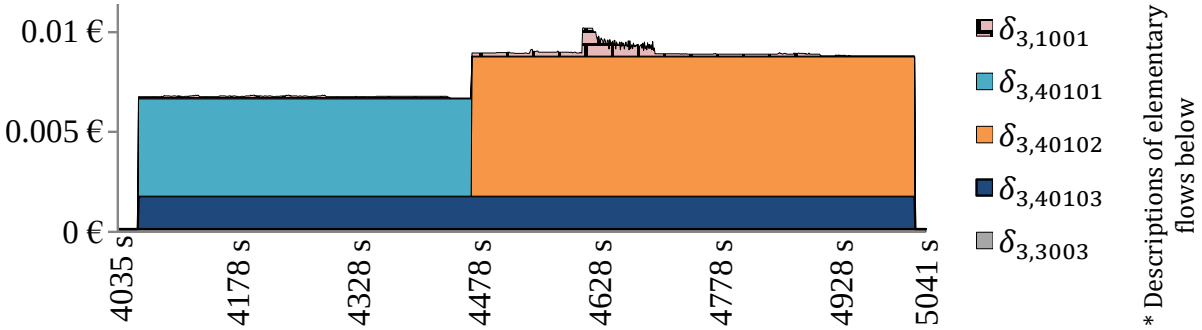

Figure 6.30 Time-dependent total direct cost δ_3 in UP_3

* $v_{3,1001}$ = electricity in UP_3 $v_{3,40101}$ = draping robot $v_{3,40102}$ = membrane press $v_{3,40103}$ = mold $v_{3,3003}$ = facility WS_3

For instance, the activities between t =4614 s and t =4703 s in Fig. 6.30 are behaving differently compared to the other time slots in UP_3.

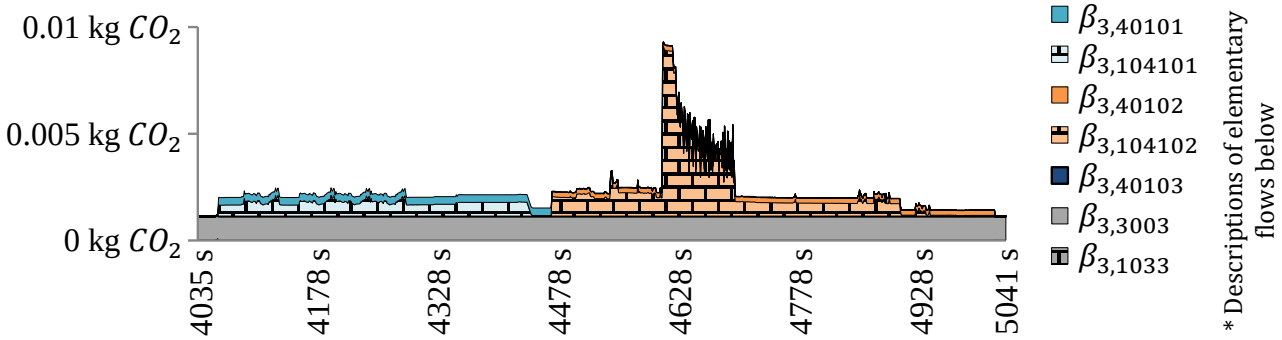

Figure 6.31 Time-dependent total carbon footprint β_3 in UP_3

* $v_{3,40101}$ = draping robot $v_{3,104101}$ = draping robot electricity $v_{3,40102}$ = membrane press $v_{3,104102}$ = membrane press electricity $v_{3,40103}$ = mold $v_{3,3003}$ = facility WS_3 $v_{3,1033}$ = facility WS_3 electricity

In Fig. 6.31, the same period of highest impact in Fig. 6.30 has the highest carbon footprint. This result prioritizes the enhancement of activities in that specific slot for both aspects. Similar to UP_1 and UP_2, the total economic and ecological impacts of all assessed subsets within UP_3 are shown in Fig. 6.32 left and right sides respectively.

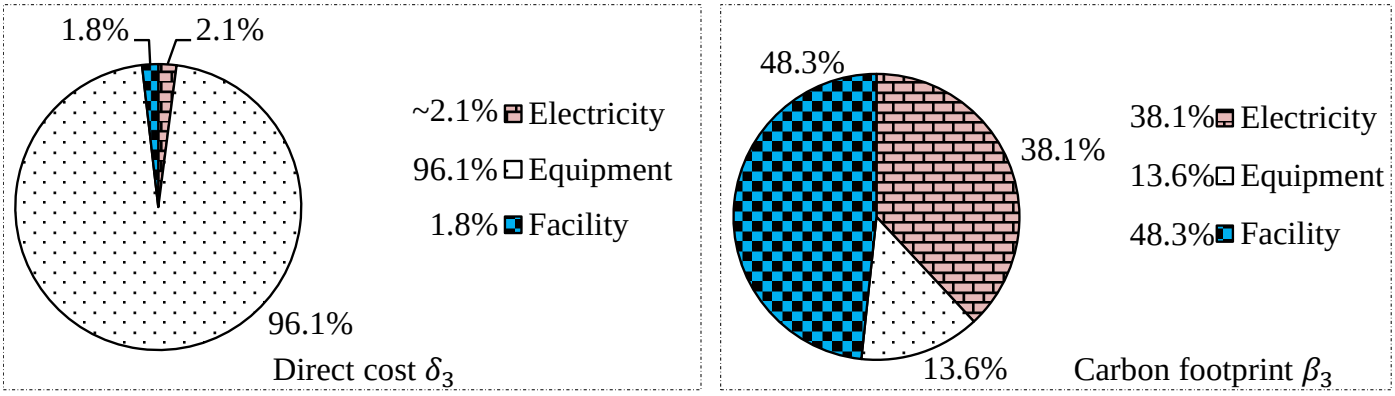

Figure 6.32 Direct cost δ_3 and carbon footprint β_3 contributing subsets in UP_3

On the left side of Fig. 6.32, the equipment subset is dominating the direct cost, while facility has the lowest direct cost. As Fig. 6.32 shows, the carbon footprint is mainly contributed by facility, while electricity comes second. With a total ecological impact of around 61.9 %, the approach of considering both facility and equipment subsets has proved its significance to ecological assessment result in UP_3.

Trimming UP_4 time-dependent results

Similar to the previously illustrated UPs, the assessment results of UP_4 are visualized. In Fig. 6.33, the time-dependent cumulative direct cost δ_{4j} and carbon footprint β_{4j} of all elementary flows in UP_4 are shown.

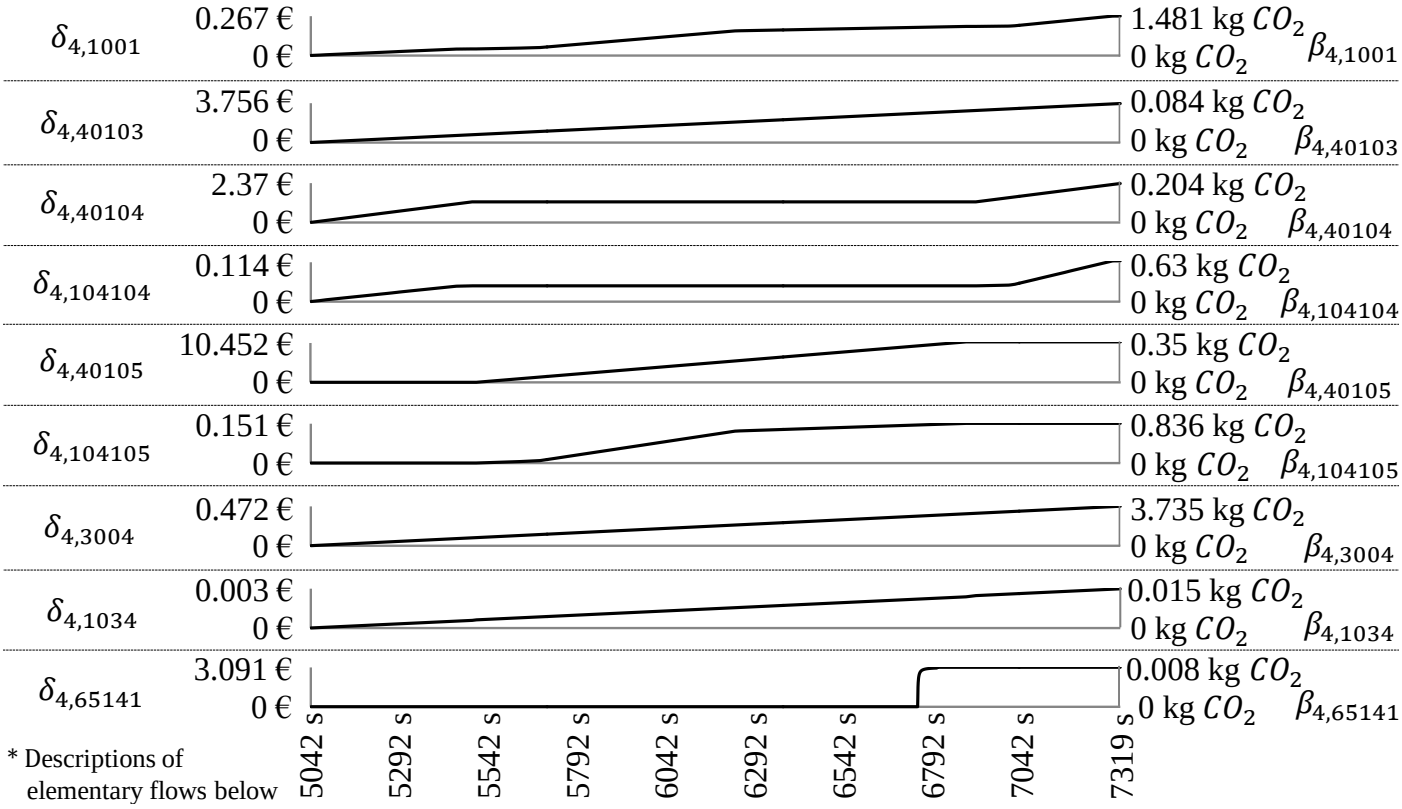

Figure 6.33 Time-dependent cumulative direct cost δ_{4j} and carbon footprint β_{4j} in UP_4

* $v_{4,1001}$ = electricity in UP_4 $v_{4,40103}$ = mold $v_{4,40104}$ = handling robot $v_{4,104104}$ = handling robot electricity $v_{4,40105}$ = trimming portal $v_{4,104105}$ = trimming portal electricity $v_{4,3004}$ = facility WS_4 $v_{4,1034}$ = facility WS_4 electricity $u_{4,65141}$ = fiber consolidated waste

The trimming portal $\delta_{4,40105}$ is the highest direct cost of all elementary flows in this UP_4, while the mold direct cost $\delta_{4,40103}$ comes second. Moreover, the facility $v_{4,3004}$ has the lowest direct cost followed by electricity

$\varphi_4^{[T]}$, when the impacts of separated electricity consumptions are not considered. With reference to the carbon footprint β_{4j} in UP_4, the facility of WS_4 has the highest impact, while total UP_4 electricity comes second. The lowest carbon footprints are coming from the fiber waste, facility WS_4 electricity, and the mold respectively. Similar to the case in UP_2, the fiber waste $u_{4,65141}$ is considered in the results, while it represents around 22 % of the total fiber input $v_{2,6014}$. In addition, the time-dependent assessment results of the total economic and ecological impacts are visualized within Fig. 6.34.

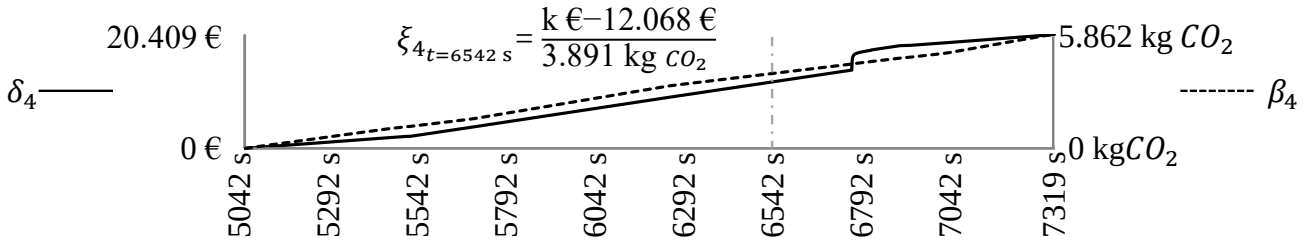

Figure 6.34 Time-dependent total cumulative direct cost δ_{4_t} and carbon footprint β_{4_t} in UP_4

The correlation between the economic impacts of considered equipment types in Fig. 6.33 and the direct cost δ_{4_t} in Fig. 6.34 is clear. On the other hand, the carbon footprint β_4 is shaped by the impacts of facility $\beta_{4,3004}$ and electricity $\beta_{4,1001}$ mainly. In Fig. 6.34, the random eco-efficiency value is selected at t =6542 s. The final eco-efficiency ξ_4 of UP_4 at t_{4_b} =7319 s is equal to $\xi_4 = \frac{\text{k €} - 20.409\text{ €}}{5.862\,\text{kg}\,CO_2}$, as Fig. 6.34 shows. As it is assumed previously, the trimming constant is equal to k_4 =75 €, while the eco-efficiency of UP_4 is considered as $\xi_4 = \frac{54.591\text{ €}}{5.862\,\text{kg}\,CO_2}$. For a single kg of the CFRP structure, the direct cost from UP_4 in this thesis is calculated as δ_4 = 14.085 €/kg, while its carbon footprint from UP_4 is calculated as $\beta_4 = 4.046\,\text{kg}\,CO_2/\text{kg}$. Again, the time-dependent cumulative logarithmic scaled eco-efficiency ξ_{4_t} in UP_4 is shown by Fig. 6.35.

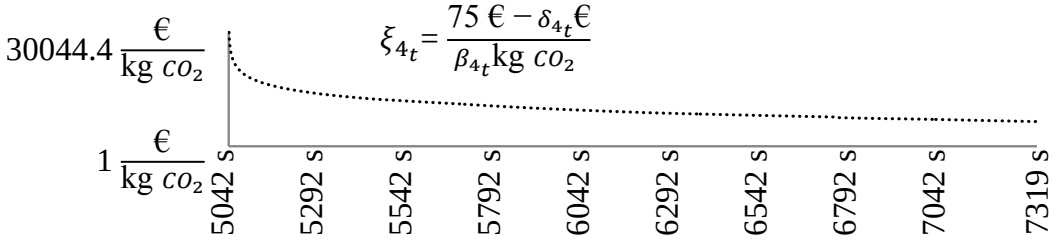

Figure 6.35 Time-dependent logarithmic scaled eco-efficiency ξ_{4_t} in UP_4

Fig. 6.35 shows that UP_4 has similar behavior to UP_3 when it comes to the time-dependent eco-efficiency ξ_{4_t}. The time-dependent direct cost to carbon footprint behavior δ_{4_t}/β_{4_t} in UP_4 is shown in Fig. 6.36, while this ratio δ_{4_t}/β_{4_t} in UP_4 lays between 2 and 4.

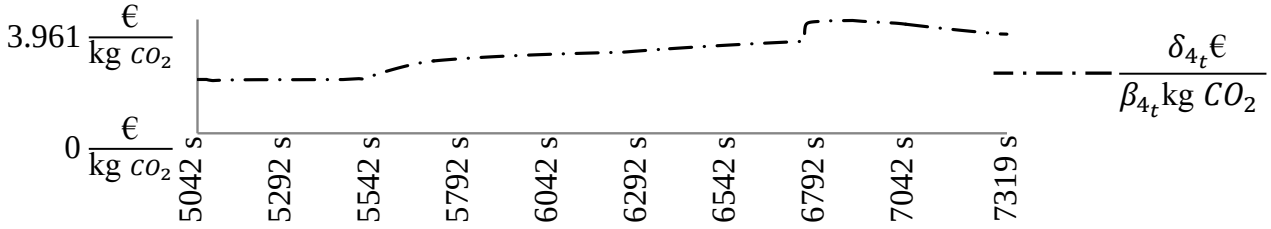

Figure 6.36 Time-dependent direct cost to carbon footprint behavior δ_{4_t}/β_{4_t} in UP_4

Similar to UP_2, the fiber waste output in UP_4 is excluded from the illustrations of the time-dependent total direct cost and carbon footprint in Fig. 6.37 and Fig. 6.38 respectively.

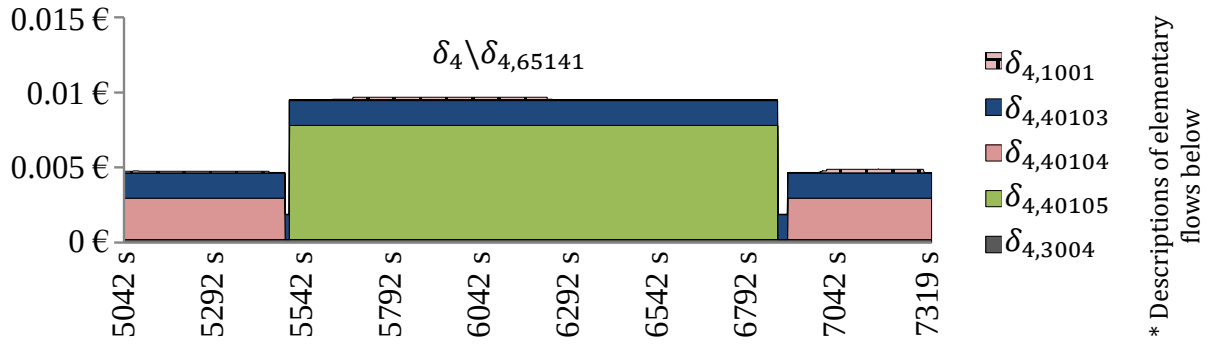

Figure 6.37 Time-dependent total direct cost $\delta_4 \setminus \delta_{4,65141}$ in UP_4

* $v_{4,1001}$ = electricity in UP_4 $v_{4,40103}$ = mold $v_{4,40104}$ = handling robot $v_{4,40105}$ = trimming portal $v_{4,3004}$ = facility WS_4

In Fig. 6.37, a clear economic enhancement priority exists in activities within time period between t =5509 s and t =6885 s. Similarly, Fig. 6.38 shows the ecological impacts of the elementary flows excluding the fiber waste to achieve a clear visualization.

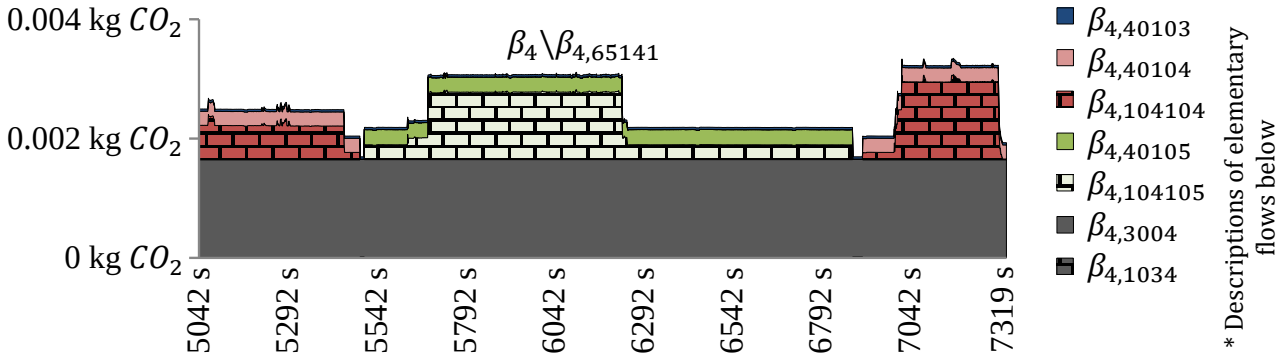

Figure 6.38 Time-dependent total carbon footprint $\beta_{4_t} \setminus \beta_{4,65141}$ in UP_4

* $v_{4,40103}$ = mold $v_{4,40104}$ = handling robot $v_{4,104104}$ = handling robot electricity $v_{4,40105}$ = trimming portal $v_{4,104105}$ = trimming portal electricity $v_{4,3004}$ = facility WS_4 $v_{4,1034}$ = facility WS_4 electricity

In Fig. 6.38, a clear ecological enhancement priority exists in the activities within the time period between t =7042 s and t =7319 s. Moreover, the total contributions of direct cost δ_4 and carbon footprint β_4 among the considered subsets $\varphi_4^{[\Gamma]}$ in UP_4 are illustrated in Fig. 6.39.

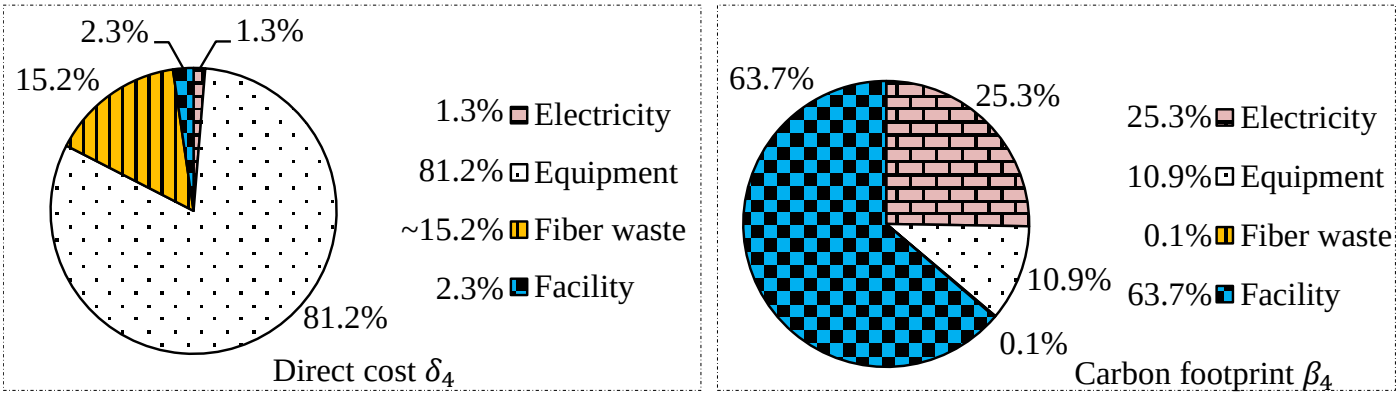

Figure 6.39 Direct cost δ_4 and carbon footprint β_4 contributing subsets in UP_4

Here, only three input subsets $\varphi_4^{[\Gamma]}$ exist in UP_4. As it is illustrated on the left side of Fig. 6.39, equipment subset $\varphi_4^{[Q]}$ has the dominating share of direct cost δ_4 in UP_4. Both facility and electricity have a minor combined direct cost of around 3.6 % from the total economic impact. On the right side of Fig. 6.39, facility

subset has the largest ecological impact, while electricity subset comes at second. The last contributor to the carbon footprint is the fiber waste, while the impact of initial fiber is excluded from it.

Process time-dependent visual results

The eco-efficiency of the entire process including all considered UPs i is calculated to be $\xi = \xi_{t=7482s} \approx \frac{\text{k€ - 320.71 €}}{153.16\,\text{kg}\,CO_2}$. As it is assumed previously in chapter 5, the revenue excluding all non-process costs of the total process including all UPs i is around k =500 €. Therefore, the total eco-efficiency at t =7482 s is calculated as $\xi \approx \frac{179.29\,€}{153.16\,\text{kg}\,CO_2}$. For a single kg of the assessed CFRP structure, the direct cost from the entire process in this thesis is calculated as $\delta \approx 221.33$ €/kg, while its carbon footprint is equal to $\beta \approx 105.7\,\text{kg}\,CO_2$/kg. Similar to the approach of tracing the cumulative logarithmic scaled eco-efficiency in every UP, Fig. 6.40 illustrates it for the entire process throughout its duration.

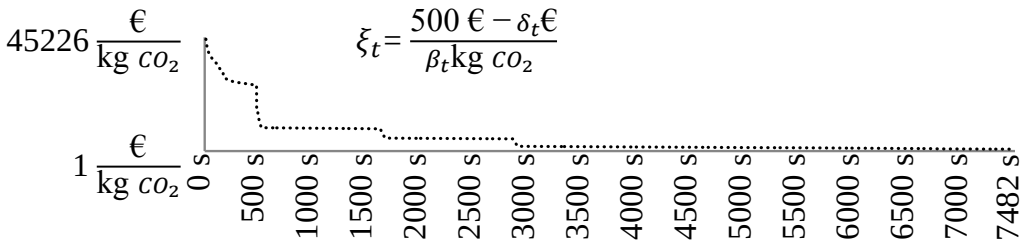

Figure 6.40 Time-dependent cumulative logarithmic scaled eco-efficiency ξ_t in the entire process

Moreover, the time-dependent direct cost to carbon footprint ratio δ_t/β_t in the entire process is visualized in Fig. 6.41.

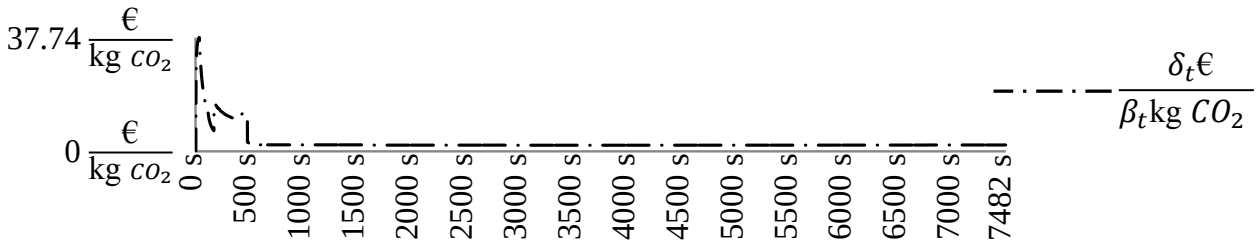

Figure 6.41 Time-dependent direct cost to carbon footprint behavior δ_t/β_t in the entire process

Except for the process beginning, the ratio in Fig. 6.41 is almost constant with the value of around 2 after t =500 s. For better visualization, Fig. 6.42 represents the time-dependent total direct cost $\delta_t \setminus (\delta_{6014}, \delta_{9017}, \delta_{6514}, \delta_{65141})$ excluding all materials in the entire process. For the same reason as Fig. 6.42, Fig. 6.43 represents the time-dependent total carbon footprint $\beta_t \setminus (\beta_{6014}, \beta_{9017}, \beta_{6514}, \beta_{65141})$ excluding all materials in the entire process.

From Fig. 6.42 and Fig. 6.43, technologies throughout the process may be evaluated based on their local impacts within the duration of their activities as well as global impacts on the entire process in future detailed works. In future works, the back-coupling impacts of each technology change may be also studied during the entire process based on the time-dependent assessment capabilities from this thesis. From these time-dependent results, conventional time-independent illustrations of the final values can be derived. For instance, the direct cost distribution among all UPs i and elementary flows α_j or their subsets $\varphi^{[\Gamma]}$ within them can be visualized in Fig. 6.44.

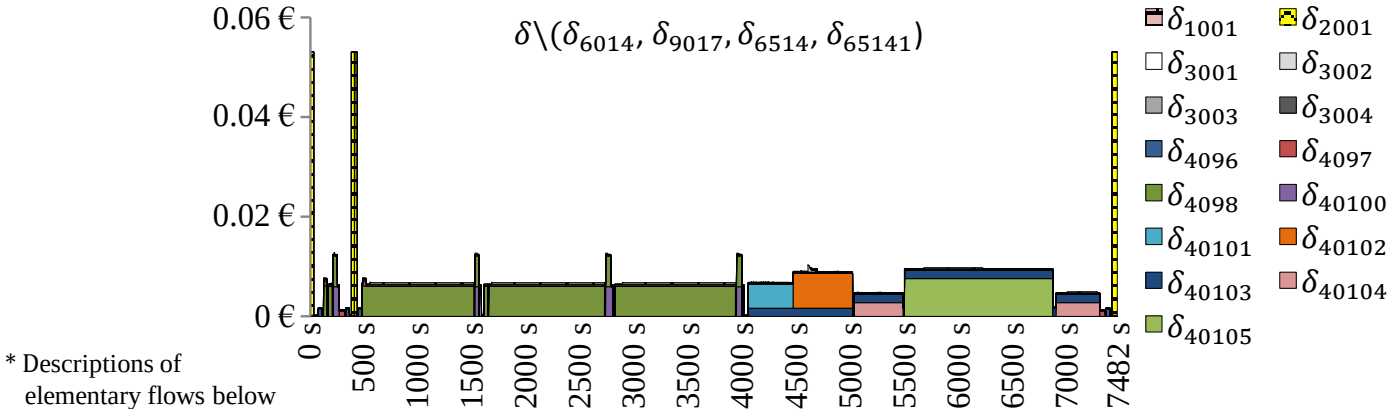

Figure 6.42 Time-dependent total direct cost $\delta \setminus (\delta_{6014}, \delta_{9017}, \delta_{6514}, \delta_{65141})$ in the entire process

* v_{1001} = electricity v_{2001} = labor v_{3001} = facility WS_1 v_{3002} = facility WS_2 v_{3003} = facility WS_3 v_{3004} = facility WS_4 v_{4096} = paternoster storage v_{4097} = unwinder v_{4098} = cutter v_{40100} = ply storage v_{40101} = draping robot v_{40102} = membrane press v_{40103} = mold v_{40104} = handling robot v_{40105} = trimming portal

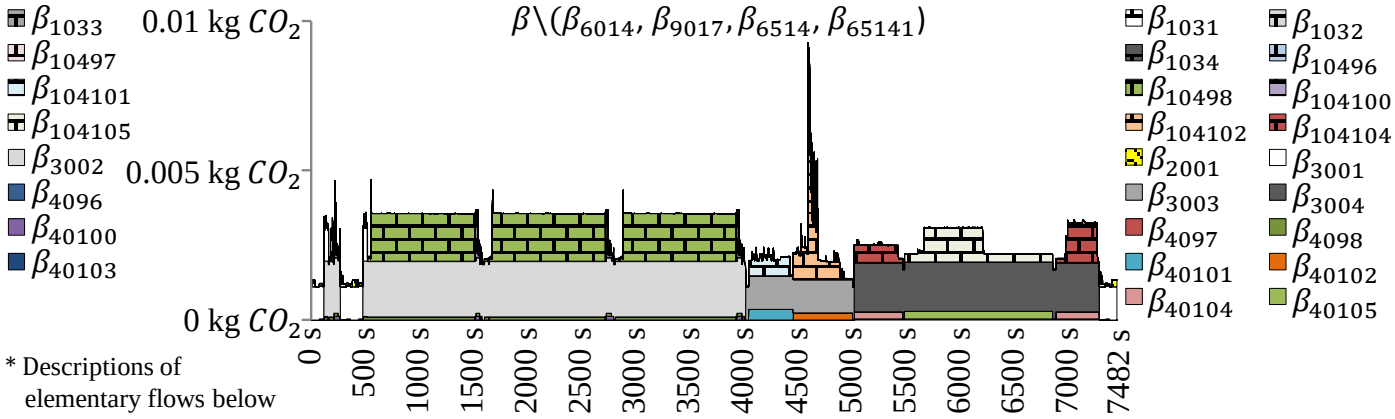

Figure 6.43 Time-dependent total carbon footprint $\beta_t \setminus (\beta_{6014}, \beta_{9017}, \beta_{6514}, \beta_{65141})$ in the entire process

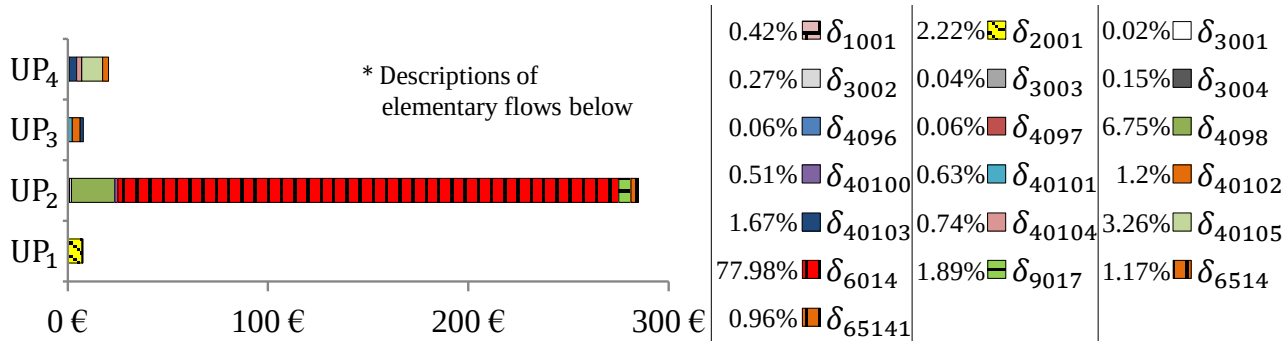

Figure 6.44 Direct cost δ of UPs and elementary flows for the entire process

Similar to Fig. 6.44, the distribution of carbon footprint β can be illustrated in Fig. 6.45.

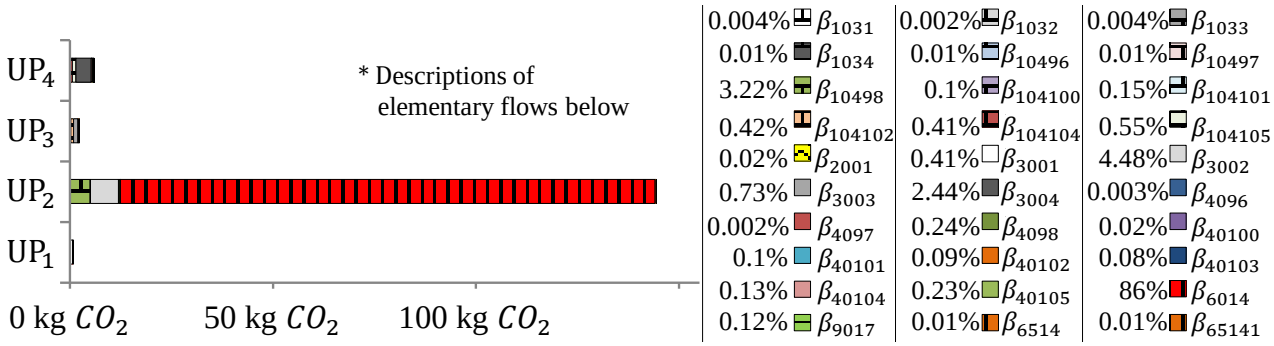

Figure 6.45 Carbon footprint β of UPs and elementary flows for entire process

* v_{1031} = facility WS_1 electricity v_{1032} = facility WS_2 electricity v_{1033} = facility WS_3 electricity v_{1034} = facility WS_4 electricity v_{2001} = labor v_{3001} = facility WS_1 v_{3002} = facility WS_2 v_{3003} = facility WS_3 v_{3004} = facility WS_4 v_{4096} = paternoster storage v_{10496} = paternoster storage electricity v_{4097} = unwinder v_{10497} = unwinder electricity v_{4098} = cutter v_{10498} = cutter electricity v_{40100} = ply storage v_{104100} = ply storage electricity v_{40101} = draping robot v_{104101} = draping robot electricity v_{40102} = membrane press v_{104102} = membrane press electricity v_{40103} = mold v_{40104} = handling robot v_{104104} = handling robot electricity v_{40105} = trimming portal v_{104105} = trimming portal electricity u_{6014} = fiber v_{9017} = release film u_{6514} = fiber waste u_{65141} = fiber consolidated waste

Due to the minor ecological impact of some elementary flows in Fig. 6.45, the digits of share percentages are increased for better visualization. For the entire process, total contributions of direct cost δ and carbon footprint β among the considered subsets are illustrated on the left and right sides of Fig. 6.46 respectively.

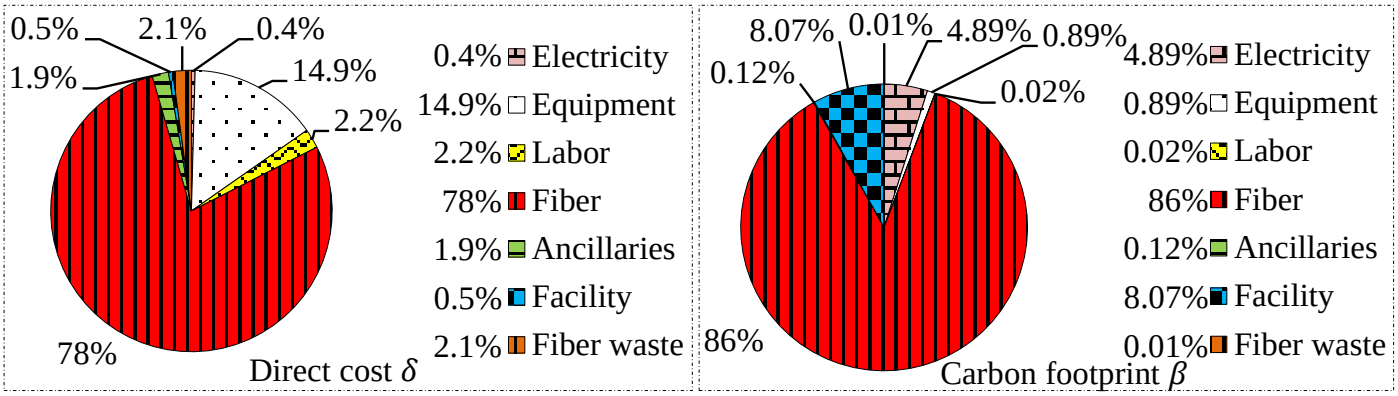

Figure 6.46 Direct cost and carbon footprint of elementary flow subsets in the entire process

This conventional visualization in Fig. 6.46 illustrates the time-independent drivers of both aspects.

Process time-dependent statistical economic results

In addition to the visualized results, the statistical ones can be presented to decision-makers by the developed DSSs. Therefore, the same previously selected temporal points at t =7482 s, t =100 s, and t =1000 s are respectively selected to validate the DSSs capabilities of assessing the cumulative non-transient direct cost. While the UPs are covered by the process matrix at each point, no need for separating their statistical results is sensed. Here, the time-dependent economic assessment can be realized based on Eq. 6.1 and Eq. 5.30 from chapter 5 for the entire process including all selected UPs i. Therefore, Eq. 6.22 shows the entire economic impact of all four UPs from the beginning of UP_1 in t_{1A_a} =0 s at 14:00:10 until the end in t_{1C_b} =7482 s at 16:04:52.

$$\delta_{t=7482\,\mathrm{s}} = \delta = \delta_{T_{t=7482\,\mathrm{s}}} + \delta_{L_{t=7482\,\mathrm{s}}} + \delta_{\Delta s_{t=7482\,\mathrm{s}}} + \delta_{Q_{t=7482\,\mathrm{s}}} + \delta_{F_{t=7482\,\mathrm{s}}} + \delta_{R_{t=7482\,\mathrm{s}}} + \delta_{G_{t=7482\,\mathrm{s}}} \tag{6.22}$$

Similar to the previous approach of handling each subset separately, the time-dependent direct cost is presented for each subset at the selected temporal point.

$$\delta_{T_{t=7482\,\mathrm{s}}} = \begin{bmatrix} 0.013 & 0 & 0 & 0 & 0.02 & 0.045 \\ 0 & 0.005 & 0 & 0 & 0 & 0 \\ 0 & 0 & 0.015 & 0 & 0 & 0 \\ 0 & 0 & 0 & 0.033 & 0 & 0 \\ 0 & 0 & 0 & 0 & 0 & 0 \\ 10.409 & 0.333 & 0 & 0 & 0 & 0 \\ 0 & 0 & 0.497 & 1.348 & 0 & 0 \\ 0 & 0 & 0 & 0 & 1.329 & 1.763 \end{bmatrix}^{\text{in kWh}}_{t=7482\,\mathrm{s}} \begin{bmatrix} 8.55\times10^{-2}\,€/\mathrm{kW} \\ 8.55\times10^{-2}\,€/\mathrm{kW} \\ 8.55\times10^{-2}\,€/\mathrm{kW} \\ 8.55\times10^{-2}\,€/\mathrm{kW} \\ 8.55\times10^{-2}\,€/\mathrm{kW} \\ 8.55\times10^{-2}\,€/\mathrm{kW} \\ 8.55\times10^{-2}\,€/\mathrm{kW} \\ 8.55\times10^{-2}\,€/\mathrm{kW} \\ 8.55\times10^{-2}\,€/\mathrm{kW} \\ 8.55\times10^{-2}\,€/\mathrm{kW} \\ 8.55\times10^{-2}\,€/\mathrm{kW} \end{bmatrix} = 1.352\,€ \tag{6.23}$$

$$\delta_{L_{t=7482\,\mathrm{s}}} = \begin{bmatrix} 270 \\ 0 \\ 0 \\ 0 \end{bmatrix}^{\text{in s}}_{t=7482\,\mathrm{s}} \times 2.639\times10^{-2}\,€/\mathrm{s} = 7.125\,€ \tag{6.24}$$

$$\delta_{\Delta s_{t=7482\,\mathrm{s}}} = \begin{bmatrix} 577 & 0 & 0 & 0 \\ 0 & 3710 & 0 & 0 \\ 0 & 0 & 1008 & 0 \\ 0 & 0 & 0 & 2278 \end{bmatrix}^{\text{in s}}_{t=7482\,\mathrm{s}} \begin{bmatrix} 1.389\times10^{-4}\,€/\mathrm{s} \\ 2.339\times10^{-4}\,€/\mathrm{s} \\ 1.402\times10^{-4}\,€/\mathrm{s} \\ 2.072\times10^{-4}\,€/\mathrm{s} \end{bmatrix} = 1.561\,€ \tag{6.25}$$

$$\delta_{Q_{t=7482\,\mathrm{s}}} = \begin{bmatrix} 140 & 176 & 0 & 0 & 0 & 0 & 0 & 0 & 0 \\ 0 & 0 & 3544 & 272 & 0 & 0 & 0 & 0 & 0 \\ 0 & 0 & 0 & 0 & 415 & 552 & 967 & 0 & 0 \\ 0 & 0 & 0 & 0 & 0 & 0 & 2278 & 861 & 1377 \end{bmatrix}^{\text{in s}}_{t=7482\,\mathrm{s}} \begin{bmatrix} 1.449\times10^{-3}\,€/\mathrm{s} \\ 1.05\times10^{-3}\,€/\mathrm{s} \\ 6.107\times10^{-3}\,€/\mathrm{s} \\ 5.956\times10^{-3}\,€/\mathrm{s} \\ 4.863\times10^{-3}\,€/\mathrm{s} \\ 6.978\times10^{-3}\,€/\mathrm{s} \\ 1.649\times10^{-3}\,€/\mathrm{s} \\ 2.753\times10^{-3}\,€/\mathrm{s} \\ 7.591\times10^{-3}\,€/\mathrm{s} \end{bmatrix} = 47.693\,€ \tag{6.26}$$

$$\delta_{F_{t=7482\,\mathrm{s}}} = \begin{bmatrix} 0 \\ 2.815 \\ 0 \\ 0 \end{bmatrix}^{\text{in kg}}_{t=7482\,\mathrm{s}} \times 88.857\,€/\mathrm{kg} = 250.091\,€ \tag{6.27}$$

$$\delta_{R_{t=7482\,\mathrm{s}}} = \begin{bmatrix} 0 \\ 0.067 \\ 0 \\ 0 \end{bmatrix}^{\text{in kg}}_{t=7482\,\mathrm{s}} \times 90.086\,€/\mathrm{kg} = 6.052\,€ \tag{6.28}$$

$$\delta_{G_{t=7482\,\mathrm{s}}} = \begin{bmatrix} 0 & 0 \\ 0.748 & 0 \\ 0 & 0 \\ 0 & 0.618 \end{bmatrix}_{t=7482\,\mathrm{s}}^{\text{in kg}} \begin{bmatrix} 5\,€/\mathrm{kg} \\ 5\,€/\mathrm{kg} \end{bmatrix} = 6.833\,€ \tag{6.29}$$

$$\delta_{t=7482\,\mathrm{s}} = \delta = 1.352\,€ + 7.125\,€ + 1.561\,€ + 47.693\,€ + 250.091\,€ + 6.052\,€ + 6.833\,€ \approx 320.71\,€ \tag{6.30}$$

As it is shown in Eq. 6.30, the total direct cost δ of the entire process at the end of it when t_{1C_b} =7482 s is around 320.707 €. Not only on UP i level, the time-dependent eco-efficiency assessment capabilities offer the observation of KRIs behaviors for the entire process at any selected time such as the temporal points of t =100 s and t =1000 s in Eq. 6.31 and Eq. 6.37 respectively.

$$\delta_{t=100\,\mathrm{s}} = \delta_{T_{t=100\,\mathrm{s}}} + \delta_{L_{t=100\,\mathrm{s}}} + \delta_{\Delta s_{t=100\,\mathrm{s}}} + \delta_{Q_{t=100\,\mathrm{s}}} + \delta_{F_{t=100\,\mathrm{s}}} + \delta_{R_{t=100\,\mathrm{s}}} + \delta_{G_{t=100\,\mathrm{s}}} \tag{6.31}$$

$$\delta_{T_{t=100\,\mathrm{s}}} = \begin{bmatrix} 0.001 & 0 & 0 & 0 & 0.004 & 0 \\ 0 & 0 & 0 & 0 & 0 & 0 \\ 0 & 0 & 0 & 0 & 0 & 0 \\ 0 & 0 & 0 & 0 & 0 & 0 \end{bmatrix}_{t=100\,\mathrm{s}}^{\text{in kWh}} \begin{bmatrix} 8.55\times10^{-2}\,€/\mathrm{kW} \\ 8.55\times10^{-2}\,€/\mathrm{kW} \\ 8.55\times10^{-2}\,€/\mathrm{kW} \\ 8.55\times10^{-2}\,€/\mathrm{kW} \\ 8.55\times10^{-2}\,€/\mathrm{kW} \\ 8.55\times10^{-2}\,€/\mathrm{kW} \\ 8.55\times10^{-2}\,€/\mathrm{kW} \\ 8.55\times10^{-2}\,€/\mathrm{kW} \\ 8.55\times10^{-2}\,€/\mathrm{kW} \\ 8.55\times10^{-2}\,€/\mathrm{kW} \\ 8.55\times10^{-2}\,€/\mathrm{kW} \end{bmatrix} = 4.504\times10^{-4}\,€ \tag{6.32}$$

$$\delta_{L_{t=100\,\mathrm{s}}} = \begin{bmatrix} 64 \\ 0 \\ 0 \\ 0 \end{bmatrix}_{t=100\,\mathrm{s}}^{\text{in s}} \times 2.639\times10^{-2}\,€/\mathrm{s} = 1.689\,€ \tag{6.33}$$

$$\delta_{\Delta s_{t=100\,\mathrm{s}}} = \begin{bmatrix} 101 & 0 & 0 & 0 \\ 0 & 0 & 0 & 0 \\ 0 & 0 & 0 & 0 \\ 0 & 0 & 0 & 0 \end{bmatrix}_{t=100\,\mathrm{s}}^{\text{in s}} \begin{bmatrix} 1.389\times10^{-4}\,€/\mathrm{s} \\ 2.339\times10^{-4}\,€/\mathrm{s} \\ 1.402\times10^{-4}\,€/\mathrm{s} \\ 2.072\times10^{-4}\,€/\mathrm{s} \end{bmatrix} = 0.014\,€ \tag{6.34}$$

$$\delta_{Q_{t=100\,\mathrm{s}}} = \begin{bmatrix} 27 & 0 & 0 & 0 & 0 & 0 & 0 & 0 & 0 \\ 0 & 0 & 0 & 0 & 0 & 0 & 0 & 0 & 0 \\ 0 & 0 & 0 & 0 & 0 & 0 & 0 & 0 & 0 \\ 0 & 0 & 0 & 0 & 0 & 0 & 0 & 0 & 0 \end{bmatrix}^{\text{in s}}_{t=100\,\mathrm{s}} \begin{bmatrix} 1.449\times10^{-3}\,€/\mathrm{s} \\ 1.05\times10^{-3}\,€/\mathrm{s} \\ 6.107\times10^{-3}\,€/\mathrm{s} \\ 5.956\times10^{-3}\,€/\mathrm{s} \\ 4.863\times10^{-3}\,€/\mathrm{s} \\ 6.978\times10^{-3}\,€/\mathrm{s} \\ 1.649\times10^{-3}\,€/\mathrm{s} \\ 2.753\times10^{-3}\,€/\mathrm{s} \\ 7.591\times10^{-3}\,€/\mathrm{s} \end{bmatrix} = 0.039\,€ \tag{6.35}$$

As it is mentioned previously, $[\Upsilon^{[F]}]_{t=100\,\mathrm{s}}$, $[\Upsilon^{[R]}]_{t=100\,\mathrm{s}}$, and $[\Upsilon^{[G]}]_{t=100\,\mathrm{s}}$ have no direct costs δ_{ij} at this temporal point, while they contain only „*zero*“ value elements at $_{t=100\,\mathrm{s}}$.

$$\delta_{t=100\,\mathrm{s}} = 4.504\times10^{-4}\,€ + 1.689\,€ + 0.014\,€ + 0.039\,€ + 0 + 0 + 0 = 1.742\,€ \tag{6.36}$$

Based on the collected data from all associated SWS_i at the selected temporal point of t =100 s, Eq. 6.36 provides the decision-makers with an economic time-dependent total impact. The same approach of Eq. 6.31 is adopted in Eq. 6.37 to assess the economic impact at the randomly selected temporal point of t =1000 s.

$$\delta_{t=1000\,\mathrm{s}} = \delta_{T_{t=1000\,\mathrm{s}}} + \delta_{L_{t=1000\,\mathrm{s}}} + \delta_{\Delta s_{t=1000\,\mathrm{s}}} + \delta_{Q_{t=1000\,\mathrm{s}}} + \delta_{F_{t=1000\,\mathrm{s}}} + \delta_{R_{t=1000\,\mathrm{s}}} + \delta_{G_{t=1000\,\mathrm{s}}} \tag{6.37}$$

$$\delta_{T_{t=1000\,\mathrm{s}}} = \begin{bmatrix} 0.011 & 0 & 0 & 0 & 0.015 & 0.032 \\ 0 & 0.001 & 0 & 0 & 0 & 0 \\ 0 & 0 & 0 & 0 & 0 & 0 \\ 0 & 0 & 0 & 0 & 0 & 0 \end{bmatrix} \begin{bmatrix} 0 & 0 & 0 & 0 & 0 & 0 \\ 1.582 & 0.047 & 0 & 0 & 0 & 0 \\ 0 & 0 & 0 & 0 & 0 & 0 \\ 0 & 0 & 0 & 0 & 0 & 0 \end{bmatrix}^{\text{in kWh}}_{t=1000\,\mathrm{s}} \begin{bmatrix} 8.55\times10^{-2}\,€/\mathrm{kW} \\ 8.55\times10^{-2}\,€/\mathrm{kW} \\ 8.55\times10^{-2}\,€/\mathrm{kW} \\ 8.55\times10^{-2}\,€/\mathrm{kW} \\ 8.55\times10^{-2}\,€/\mathrm{kW} \\ 8.55\times10^{-2}\,€/\mathrm{kW} \\ 8.55\times10^{-2}\,€/\mathrm{kW} \\ 8.55\times10^{-2}\,€/\mathrm{kW} \\ 8.55\times10^{-2}\,€/\mathrm{kW} \\ 8.55\times10^{-2}\,€/\mathrm{kW} \\ 8.55\times10^{-2}\,€/\mathrm{kW} \end{bmatrix} = 0.144\,€ \tag{6.38}$$

$$\delta_{L_{t=1000\,\mathrm{s}}} = \begin{bmatrix} 168 \\ 0 \\ 0 \\ 0 \end{bmatrix}^{\text{in s}}_{t=1000\,\mathrm{s}} \times 2.639\times10^{-2}\,€/\mathrm{s} = 4.433\,€ \tag{6.39}$$

$$\delta_{\Delta s_{t=1000\,\mathrm{s}}} = \begin{bmatrix} 414 & 0 & 0 & 0 \\ 0 & 677 & 0 & 0 \\ 0 & 0 & 0 & 0 \\ 0 & 0 & 0 & 0 \end{bmatrix}^{\text{in s}}_{t=1000\,\mathrm{s}} \begin{bmatrix} 1.389\times10^{-4}\,€/\mathrm{s} \\ 2.339\times10^{-4}\,€/\mathrm{s} \\ 1.402\times10^{-4}\,€/\mathrm{s} \\ 2.072\times10^{-4}\,€/\mathrm{s} \end{bmatrix} = 0.216\,€ \tag{6.40}$$

$$\delta_{Q_{t=1000\,\mathrm{s}}} = \begin{bmatrix} 105 & 124 & 0 & 0 & 0 & 0 & 0 & 0 & 0 \\ 0 & 0 & 0 & 638 & 60 & 0 & 0 & 0 & 0 \\ 0 & 0 & 0 & 0 & 0 & 0 & 0 & 0 & 0 \\ 0 & 0 & 0 & 0 & 0 & 0 & 0 & 0 & 0 \end{bmatrix}^{\text{in s}}_{t=1000\,\mathrm{s}} \begin{bmatrix} 1.449\times10^{-3}\,€/\mathrm{s} \\ 1.05\times10^{-3}\,€/\mathrm{s} \\ 6.107\times10^{-3}\,€/\mathrm{s} \\ 5.956\times10^{-3}\,€/\mathrm{s} \\ 4.863\times10^{-3}\,€/\mathrm{s} \\ 6.978\times10^{-3}\,€/\mathrm{s} \\ 1.649\times10^{-3}\,€/\mathrm{s} \\ 2.753\times10^{-3}\,€/\mathrm{s} \\ 7.591\times10^{-3}\,€/\mathrm{s} \end{bmatrix} = 4.536\,€ \tag{6.41}$$

$$\delta_{F_{t=1000\,\mathrm{s}}} = \begin{bmatrix} 0 \\ 0.941 \\ 0 \\ 0 \end{bmatrix}^{\text{in kg}}_{t=1000\,\mathrm{s}} \times 88.857\,€/\mathrm{kg} = 83.639\,€ \tag{6.42}$$

$$\delta_{R_{t=1000\,\mathrm{s}}} = \begin{bmatrix} 0 \\ 0.067 \\ 0 \\ 0 \end{bmatrix}^{\text{in kg}}_{t=1000\,\mathrm{s}} \times 90.086\,€/\mathrm{kg} = 6.052\,€ \tag{6.43}$$

$$\delta_{G_{t=1000\,\mathrm{s}}} = \begin{bmatrix} 0 & 0 \\ 0.145 & 0 \\ 0 & 0 \\ 0 & 0 \end{bmatrix}^{\text{in kg}}_{t=1000\,\mathrm{s}} \begin{bmatrix} 5\,€/\mathrm{kg} \\ 5\,€/\mathrm{kg} \end{bmatrix} = 0.725\,€ \tag{6.44}$$

$$\delta_{t=1000\,\mathrm{s}} = 0.144\,€ + 4.433\,€ + 0.216\,€ + 4.536\,€ + 83.639\,€ + 6.052\,€ + 0.725\,€ = 99.745\,€ \tag{6.45}$$

These cumulative statistical assessment at these selected temporal points can be applied for any other time points to accommodate the decision-makers demands in building a comprehensive dynamic knowledge of their process.

Process time-dependent statistical ecological results

The same previously discussed approaches are adopted to assess the ecological time-dependent impacts for the entire process at t =7482 s, t =100 s, and t =1000 s based on Eq. 5.31 from chapter 5. These time-dependent total ecological assessments of t =7482 s, t =100 s, and t =1000 s are stated statistically in Eq. 6.46, Eq. 6.55, and Eq. 6.61 respectively.

$$\beta_{t=7482\,\mathrm{s}} = \beta = \beta_{T_{t=7482\,\mathrm{s}}} + \beta_{L_{t=7482\,\mathrm{s}}} + \beta_{\Delta s_{t=7482\,\mathrm{s}}} + \beta_{Q_{t=7482\,\mathrm{s}}} + \beta_{F_{t=7482\,\mathrm{s}}} + \beta_{R_{t=7482\,\mathrm{s}}} + \beta_{G_{t=7482\,\mathrm{s}}} \tag{6.46}$$

$$\beta_{T_{t=7482\,\mathrm{s}}} = \begin{bmatrix} 0.013 & 0 & 0 & 0 & 0.02 & 0.045 \\ 0 & 0.005 & 0 & 0 & 0 & 0 \\ 0 & 0 & 0.015 & 0 & 0 & 0 \\ 0 & 0 & 0 & 0.033 & 0 & 0 \\ 0 & 0 & 0 & 0 & 0 & 0 \\ 10.409 & 0.333 & 0 & 0 & 0 & 0 \\ 0 & 0 & 0.497 & 1.348 & 0 & 0 \\ 0 & 0 & 0 & 0 & 1.329 & 1.763 \end{bmatrix}^{\text{in kWh}}_{t=7482\,\mathrm{s}} \begin{bmatrix} 0.474\,\mathrm{kg}\,CO_2/\mathrm{kWh} \\ 0.474\,\mathrm{kg}\,CO_2/\mathrm{kWh} \\ 0.474\,\mathrm{kg}\,CO_2/\mathrm{kWh} \\ 0.474\,\mathrm{kg}\,CO_2/\mathrm{kWh} \\ 0.474\,\mathrm{kg}\,CO_2/\mathrm{kWh} \\ 0.474\,\mathrm{kg}\,CO_2/\mathrm{kWh} \\ 0.474\,\mathrm{kg}\,CO_2/\mathrm{kWh} \\ 0.474\,\mathrm{kg}\,CO_2/\mathrm{kWh} \\ 0.474\,\mathrm{kg}\,CO_2/\mathrm{kWh} \\ 0.474\,\mathrm{kg}\,CO_2/\mathrm{kWh} \\ 0.474\,\mathrm{kg}\,CO_2/\mathrm{kWh} \\ 0.474\,\mathrm{kg}\,CO_2/\mathrm{kWh} \end{bmatrix} = 7.494\,\mathrm{kg}\,CO_2 \tag{6.47}$$

$$\beta_{L_{t=7482\,\mathrm{s}}} = \begin{bmatrix} 270 \\ 0 \\ 0 \\ 0 \end{bmatrix}^{\text{in s}}_{t=7482\,\mathrm{s}} \times 1.139 \times 10^{-4}\,\mathrm{kg}\,CO_2/\mathrm{s} = 0.031\,\mathrm{kg}\,CO_2 \tag{6.48}$$

$$\beta_{\Delta s_{t=7482\,\mathrm{s}}} = \begin{bmatrix} 577 & 0 & 0 & 0 \\ 0 & 3710 & 0 & 0 \\ 0 & 0 & 1008 & 0 \\ 0 & 0 & 0 & 2278 \end{bmatrix}^{\text{in s}}_{t=7482\,\mathrm{s}} \begin{bmatrix} 1.099 \times 10^{-3}\,\mathrm{kg}\,CO_2/\mathrm{s} \\ 1.851 \times 10^{-3}\,\mathrm{kg}\,CO_2/\mathrm{s} \\ 1.109 \times 10^{-3}\,\mathrm{kg}\,CO_2/\mathrm{s} \\ 1.64 \times 10^{-3}\,\mathrm{kg}\,CO_2/\mathrm{s} \end{bmatrix} = 12.354\,\mathrm{kg}\,CO_2 \tag{6.49}$$

$$\beta_{Q_{t=7482\,\mathrm{s}}} = \begin{bmatrix} 140 & 176 & 0 & 0 & 0 & 0 & 0 & 0 & 0 \\ 0 & 0 & 3544 & 272 & 0 & 0 & 0 & 0 & 0 \\ 0 & 0 & 0 & 0 & 415 & 552 & 967 & 0 & 0 \\ 0 & 0 & 0 & 0 & 0 & 0 & 2278 & 861 & 1377 \end{bmatrix}^{\text{in s}}_{t=7482\,\mathrm{s}} \begin{bmatrix} 3.75 \times 10^{-5}\,\mathrm{kg}\,CO_2/\mathrm{s} \\ 1.694 \times 10^{-5}\,\mathrm{kg}\,CO_2/\mathrm{s} \\ 1.035 \times 10^{-4}\,\mathrm{kg}\,CO_2/\mathrm{s} \\ 1.242 \times 10^{-4}\,\mathrm{kg}\,CO_2/\mathrm{s} \\ 3.562 \times 10^{-4}\,\mathrm{kg}\,CO_2/\mathrm{s} \\ 2.386 \times 10^{-4}\,\mathrm{kg}\,CO_2/\mathrm{s} \\ 3.708 \times 10^{-5}\,\mathrm{kg}\,CO_2/\mathrm{s} \\ 2.365 \times 10^{-4}\,\mathrm{kg}\,CO_2/\mathrm{s} \\ 2.545 \times 10^{-4}\,\mathrm{kg}\,CO_2/\mathrm{s} \end{bmatrix} = 1.363\,\mathrm{kg}\,CO_2 \tag{6.50}$$

$$\beta_{F_{t=7482\,\mathrm{s}}} = \begin{bmatrix} 0 \\ 2.815 \\ 0 \\ 0 \end{bmatrix}^{\text{in kg}}_{t=7482\,\mathrm{s}} \times 46.8\,\mathrm{kg}\,CO_2/\mathrm{kg} = 131.72\,\mathrm{kg}\,CO_2 \tag{6.51}$$

$$\beta_{R_{t=7482\,\mathrm{s}}} = \begin{bmatrix} 0 \\ 0.067 \\ 0 \\ 0 \end{bmatrix}_{t=7482\,\mathrm{s}}^{\text{in kg}} \times 2.67\,\mathrm{kg}\,CO_2/\mathrm{kg} = 0.18\,\mathrm{kg}\,CO_2 \tag{6.52}$$

$$\beta_{G_{t=7482\,\mathrm{s}}} = \begin{bmatrix} 0 & 0 \\ 0.748 & 0 \\ 0 & 0 \\ 0 & 0.618 \end{bmatrix}_{t=7482\,\mathrm{s}}^{\text{in kg}} \begin{bmatrix} 1.25\times10^{-2}\,\mathrm{kg}\,CO_2/\mathrm{kg} \\ 1.25\times10^{-2}\,\mathrm{kg}\,CO_2/\mathrm{kg} \end{bmatrix} = 0.017\,\mathrm{kg}\,CO_2 \tag{6.53}$$

$$\begin{aligned} \beta_{t=7482\,\mathrm{s}} = \beta = {} & 7.494\,\mathrm{kg}\,CO_2 + 0.031\,\mathrm{kg}\,CO_2 + 12.354\,\mathrm{kg}\,CO_2 + 1.363\,\mathrm{kg}\,CO_2 \\ & + 131.72\,\mathrm{kg}\,CO_2 + 0.18\,\mathrm{kg}\,CO_2 + 0.017\,\mathrm{kg}\,CO_2 \approx 153.16\,\mathrm{kg}\,CO_2 \end{aligned} \tag{6.54}$$

In Eq. 6.54, the total ecological impact of the considered process at its end t =7482 s is statistically shown. Similarly, the cumulative ecological impact of the considered process at t =100 s is shown in Eq. 6.55.

$$\beta_{t=100\,\mathrm{s}} = \beta_{T_{t=100\,\mathrm{s}}} + \beta_{L_{t=100\,\mathrm{s}}} + \beta_{\Delta s_{t=100\,\mathrm{s}}} + \beta_{Q_{t=100\,\mathrm{s}}} + \beta_{F_{t=100\,\mathrm{s}}} + \beta_{R_{t=100\,\mathrm{s}}} + \beta_{G_{t=100\,\mathrm{s}}} \tag{6.55}$$

$$\beta_{T_{t=100\,\mathrm{s}}} = \begin{bmatrix} 0.001 & 0 & 0 & 0 & 0.004 & 0 & 0 & 0 & 0 & 0 & 0 & 0 \\ 0 & 0 & 0 & 0 & 0 & 0 & 0 & 0 & 0 & 0 & 0 & 0 \\ 0 & 0 & 0 & 0 & 0 & 0 & 0 & 0 & 0 & 0 & 0 & 0 \\ 0 & 0 & 0 & 0 & 0 & 0 & 0 & 0 & 0 & 0 & 0 & 0 \end{bmatrix}_{t=100\,\mathrm{s}}^{\text{in kWh}} \begin{bmatrix} 0.474\,\mathrm{kg}\,CO_2/\mathrm{kWh} \\ 0.474\,\mathrm{kg}\,CO_2/\mathrm{kWh} \\ 0.474\,\mathrm{kg}\,CO_2/\mathrm{kWh} \\ 0.474\,\mathrm{kg}\,CO_2/\mathrm{kWh} \\ 0.474\,\mathrm{kg}\,CO_2/\mathrm{kWh} \\ 0.474\,\mathrm{kg}\,CO_2/\mathrm{kWh} \\ 0.474\,\mathrm{kg}\,CO_2/\mathrm{kWh} \\ 0.474\,\mathrm{kg}\,CO_2/\mathrm{kWh} \\ 0.474\,\mathrm{kg}\,CO_2/\mathrm{kWh} \\ 0.474\,\mathrm{kg}\,CO_2/\mathrm{kWh} \\ 0.474\,\mathrm{kg}\,CO_2/\mathrm{kWh} \\ 0.474\,\mathrm{kg}\,CO_2/\mathrm{kWh} \end{bmatrix} \approx 0.003\,\mathrm{kg}\,CO_2 \tag{6.56}$$

$$\beta_{L_{t=100\,\mathrm{s}}} = \begin{bmatrix} 64 \\ 0 \\ 0 \\ 0 \end{bmatrix}_{t=100\,\mathrm{s}}^{\text{in s}} \times 1.139\times10^{-4}\,\mathrm{kg}\,CO_2/\mathrm{s} = 0.007\,\mathrm{kg}\,CO_2 \tag{6.57}$$

$$\beta_{\Delta s_{t=100\,\mathrm{s}}} = \begin{bmatrix} 101 & 0 & 0 & 0 \\ 0 & 0 & 0 & 0 \\ 0 & 0 & 0 & 0 \\ 0 & 0 & 0 & 0 \end{bmatrix}_{t=100\,\mathrm{s}}^{\text{in s}} \begin{bmatrix} 1.099\times10^{-3}\,\mathrm{kg}\,CO_2/\mathrm{s} \\ 1.851\times10^{-3}\,\mathrm{kg}\,CO_2/\mathrm{s} \\ 1.109\times10^{-3}\,\mathrm{kg}\,CO_2/\mathrm{s} \\ 1.64\times10^{-3}\,\mathrm{kg}\,CO_2/\mathrm{s} \end{bmatrix} = 0.111\,\mathrm{kg}\,CO_2 \tag{6.58}$$

$$\beta_{Q_{t=100\,\mathrm{s}}} = \begin{bmatrix} 27 & 0 & 0 & 0 & 0 & 0 & 0 & 0 & 0 \\ 0 & 0 & 0 & 0 & 0 & 0 & 0 & 0 & 0 \\ 0 & 0 & 0 & 0 & 0 & 0 & 0 & 0 & 0 \\ 0 & 0 & 0 & 0 & 0 & 0 & 0 & 0 & 0 \end{bmatrix}_{t=100\,\mathrm{s}}^{\text{in s}} \begin{bmatrix} 3.75\times10^{-5}\,\mathrm{kg}\,CO_2/\mathrm{s} \\ 1.694\times10^{-5}\,\mathrm{kg}\,CO_2/\mathrm{s} \\ 1.035\times10^{-4}\,\mathrm{kg}\,CO_2/\mathrm{s} \\ 1.242\times10^{-4}\,\mathrm{kg}\,CO_2/\mathrm{s} \\ 3.562\times10^{-4}\,\mathrm{kg}\,CO_2/\mathrm{s} \\ 2.386\times10^{-4}\,\mathrm{kg}\,CO_2/\mathrm{s} \\ 3.708\times10^{-5}\,\mathrm{kg}\,CO_2/\mathrm{s} \\ 2.365\times10^{-4}\,\mathrm{kg}\,CO_2/\mathrm{s} \\ 2.545\times10^{-4}\,\mathrm{kg}\,CO_2/\mathrm{s} \end{bmatrix} = 0.001\,\mathrm{kg}\,CO_2 \tag{6.59}$$

Nonetheless, $[\Upsilon^{[F]}]_{t=100\,\mathrm{s}}$, $[\Upsilon^{[R]}]_{t=100\,\mathrm{s}}$, and $[\Upsilon^{[G]}]_{t=100\,\mathrm{s}}$ have no carbon footprint β_{ij} at $t = 100\,\mathrm{s}$, while they have only „*zero*“ value elements at that temporal point.

$$\beta_{t=100\,\mathrm{s}} = 0.003\,\mathrm{kg}\,CO_2 + 0.007\,\mathrm{kg}\,CO_2 + 0.111\,\mathrm{kg}\,CO_2 + 0.001\,\mathrm{kg}\,CO_2 + 0 + 0 + 0 = 0.122\,\mathrm{kg}\,CO_2 \tag{6.60}$$

The time-dependent cumulative ecological impact of the considered process at the randomly selected time point of t =100 s is calculated by Eq. 6.60. By the same approach, the time-dependent ecological impact of the entire considered process at the randomly selected temporal point of t =1000 s is statistically shown in Eq. 6.61.

$$\beta_{t=1000\,\mathrm{s}} = \beta_{T_{t=1000\,\mathrm{s}}} + \beta_{L_{t=1000\,\mathrm{s}}} + \beta_{\Delta s_{t=1000\,\mathrm{s}}} + \beta_{Q_{t=1000\,\mathrm{s}}} + \beta_{F_{t=1000\,\mathrm{s}}} + \beta_{R_{t=1000\,\mathrm{s}}} + \beta_{G_{t=1000\,\mathrm{s}}} \tag{6.61}$$

$$\beta_{T_{t=1000\,\mathrm{s}}} = \begin{bmatrix} 0.011 & 0 & 0 & 0 & 0.015 & 0.032 \\ 0 & 0.001 & 0 & 0 & 0 & 0 \\ 0 & 0 & 0 & 0 & 0 & 0 \\ 0 & 0 & 0 & 0 & 0 & 0 \\ & 0 & 0 & 0 & 0 & 0 & 0 \\ & 1.582 & 0.047 & 0 & 0 & 0 & 0 \\ & 0 & 0 & 0 & 0 & 0 & 0 \\ & 0 & 0 & 0 & 0 & 0 & 0 \end{bmatrix}_{t=1000\,\mathrm{s}}^{\text{in kWh}} \begin{bmatrix} 0.474\,\mathrm{kg}\,CO_2/\mathrm{kWh} \\ 0.474\,\mathrm{kg}\,CO_2/\mathrm{kWh} \\ 0.474\,\mathrm{kg}\,CO_2/\mathrm{kWh} \\ 0.474\,\mathrm{kg}\,CO_2/\mathrm{kWh} \\ 0.474\,\mathrm{kg}\,CO_2/\mathrm{kWh} \\ 0.474\,\mathrm{kg}\,CO_2/\mathrm{kWh} \\ 0.474\,\mathrm{kg}\,CO_2/\mathrm{kWh} \\ 0.474\,\mathrm{kg}\,CO_2/\mathrm{kWh} \\ 0.474\,\mathrm{kg}\,CO_2/\mathrm{kWh} \\ 0.474\,\mathrm{kg}\,CO_2/\mathrm{kWh} \\ 0.474\,\mathrm{kg}\,CO_2/\mathrm{kWh} \\ 0.474\,\mathrm{kg}\,CO_2/\mathrm{kWh} \end{bmatrix} = 0.8\,\mathrm{kg}\,CO_2 \tag{6.62}$$

$$\beta_{L_{t=1000\,\mathrm{s}}} = \begin{bmatrix} 168 \\ 0 \\ 0 \\ 0 \end{bmatrix}_{t=1000\,\mathrm{s}}^{\text{in s}} \times 1.139\times10^{-4}\,\mathrm{kg}\,CO_2/\mathrm{s} = 0.019\,\mathrm{kg}\,CO_2 \tag{6.63}$$

$$\beta_{\Delta s_{t=1000\,\mathrm{s}}} = \begin{bmatrix} 414 & 0 & 0 & 0 \\ 0 & 677 & 0 & 0 \\ 0 & 0 & 0 & 0 \\ 0 & 0 & 0 & 0 \end{bmatrix}_{t=1000\,\mathrm{s}}^{\text{in s}} \begin{bmatrix} 1.099\times10^{-3}\,\mathrm{kg}\,CO_2/\mathrm{s} \\ 1.851\times10^{-3}\,\mathrm{kg}\,CO_2/\mathrm{s} \\ 1.109\times10^{-3}\,\mathrm{kg}\,CO_2/\mathrm{s} \\ 1.64\times10^{-3}\,\mathrm{kg}\,CO_2/\mathrm{s} \end{bmatrix} = 1.708\,\mathrm{kg}\,CO_2 \tag{6.64}$$

$$\beta_{Q_{t=1000\,\mathrm{s}}} = \begin{bmatrix} 105 & 124 & 0 & 0 & 0 & 0 & 0 & 0 & 0 \\ 0 & 0 & 0 & 638 & 60 & 0 & 0 & 0 & 0 \\ 0 & 0 & 0 & 0 & 0 & 0 & 0 & 0 & 0 \\ 0 & 0 & 0 & 0 & 0 & 0 & 0 & 0 & 0 \end{bmatrix}^{\text{in s}}_{t=1000\,\mathrm{s}} \begin{bmatrix} 3.75\times10^{-5}\,\mathrm{kg}\,CO_2/\mathrm{s} \\ 1.694\times10^{-5}\,\mathrm{kg}\,CO_2/\mathrm{s} \\ 1.035\times10^{-4}\,\mathrm{kg}\,CO_2/\mathrm{s} \\ 1.242\times10^{-4}\,\mathrm{kg}\,CO_2/\mathrm{s} \\ 3.562\times10^{-4}\,\mathrm{kg}\,CO_2/\mathrm{s} \\ 2.386\times10^{-4}\,\mathrm{kg}\,CO_2/\mathrm{s} \\ 3.708\times10^{-5}\,\mathrm{kg}\,CO_2/\mathrm{s} \\ 2.365\times10^{-4}\,\mathrm{kg}\,CO_2/\mathrm{s} \\ 2.545\times10^{-4}\,\mathrm{kg}\,CO_2/\mathrm{s} \end{bmatrix} = 0.08\,\mathrm{kg}\,CO_2 \tag{6.65}$$

$$\beta_{F_{t=1000\,\mathrm{s}}} = \begin{bmatrix} 0 \\ 0.941 \\ 0 \\ 0 \end{bmatrix}^{\text{in kg}}_{t=1000\,\mathrm{s}} \times 46.8\,\mathrm{kg}\,CO_2/\mathrm{kg} = 44.051\,\mathrm{kg}\,CO_2 \tag{6.66}$$

$$\beta_{R_{t=1000\,\mathrm{s}}} = \begin{bmatrix} 0 \\ 0.067 \\ 0 \\ 0 \end{bmatrix}^{\text{in kg}}_{t=1000\,\mathrm{s}} \times 2.67\,\mathrm{kg}\,CO_2/\mathrm{kg} = 0.18\,\mathrm{kg}\,CO_2 \tag{6.67}$$

$$\beta_{G_{t=1000\,\mathrm{s}}} = \begin{bmatrix} 0 & 0 \\ 0.145 & 0 \\ 0 & 0 \\ 0 & 0 \end{bmatrix}^{\text{in kg}}_{t=1000\,\mathrm{s}} \begin{bmatrix} 1.25\times10^{-2}\,\mathrm{kg}\,CO_2/\mathrm{kg} \\ 1.25\times10^{-2}\,\mathrm{kg}\,CO_2/\mathrm{kg} \end{bmatrix} = 0.002\,\mathrm{kg}\,CO_2 \tag{6.68}$$

$$\begin{aligned} \beta_{t=1000\,\mathrm{s}} &= 0.8\,\mathrm{kg}\,CO_2 + 0.019\,\mathrm{kg}\,CO_2 + 1.708\,\mathrm{kg}\,CO_2 + 0.08\,\mathrm{kg}\,CO_2 \\ &+44.051\,\mathrm{kg}\,CO_2 + 0.18\,\mathrm{kg}\,CO_2 + 0.002\,\mathrm{kg}\,CO_2 = 46.84\,\mathrm{kg}\,CO_2 \end{aligned} \tag{6.69}$$

Although these various visualization and statistical forms provide different assessment perspectives, further ones can be generated for selected subsets, elementary flows, UPs, temporal periods, or combinations of them. Based on the comprehensive model from Fig. 4.19 in chapter 4, decision-makers can select and adjust the statistical or visual presentation of time-dependent results in the EEAM.

6.2 Results Validation

The validation is a continuous process that follows each step in this work. In other words, each correction effort in any stage is logically a part of such validation efforts. This consists of validating the time-dependent eco-efficiency assessment as well as the SWS real-time data collection. Validations in this work have been applied to the results as well as the framework. In every modeling stage within this work, each validation has led to significant changes by considering new aspects and subjects or modifying existing ones. Although some of the validation activities seem to be common sense, mentioning them is essential to assure performing them sufficiently and carefully.

6.2.1 Outputs Validation

As it is mentioned previously, the purpose of assessing the selected case study is to examine the capabilities of the introduced DSSs for time-dependent eco-efficiency assessment. From the conducted results, the studied levels of CSFs in Fig. 4.20 are provided in visual and statistical forms to the decision-makers, as Fig. 6.47 shows.

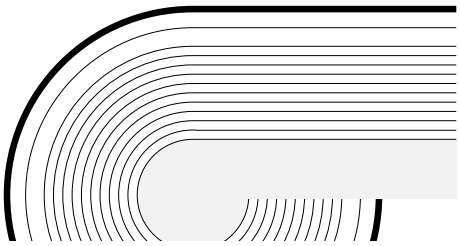

$\xi_t; \delta_t; \beta_t$	Fig.6.40; Eq.6.30; Eq.6.36; Eq.6.54; Eq.6.60 …
$\xi_{i_t}; \delta_{i_t}; \beta_{i_t}$	Fig.6.11; Fig.6.12; Fig.6.18; Fig.6.27; Fig.6.28 …
$\theta_{i\Gamma_t} \in \{\delta_{i\Gamma_t}, \beta_{i\Gamma_t}\}$	Fig.6.16; Fig.6.25; Fig.6.32; Eq.6.30; Eq.6.45 …
$\theta_{ij_t} \in \{\delta_{ij_t}, \beta_{ij_t}\}$	Fig.6.10; Fig.6.14; Fig.6.15; Fig.6.17; Fig.6.31 …
$\{a_t, \lambda_t\}$	Fig.6.2; Fig.6.3; Fig.6.4; Eq.6.5; Eq.6.6 …

Figure 6.47 Assessment results of associated CSF levels of the case study

In Fig. 6.47, only randomly selected examples of relevant figures and equations, as conceptual and mathematical models of assessing the listed CSF levels, are shown on the right side, while many others can be found in this chapter. As it is shown in Fig. 4.33 before, the comprehensive validation is carried out through four stages including the conceptual model qualification, the verification of the mathematical model, the computerized model testing, and finally the validation of the DSSs results based on the reality. As Fig. 4.34 shows before, these stages of validation aim to increase the results accuracy and get them as close as possible to reality.

Qualification of conceptual model

This validation stage aims to assure that the conceptual model matches the considered aspects in the reality. As it has been discussed in Fig. 3.24 within chapter 3, a complex system has no valid comprehensive representing model other than itself, while the reality is considered as a complex system in this thesis. Therefore, a boundary definition plays a crucial role in limiting the considered aspects. For the case study and based on the generic illustration in Fig. 4.18, a description of all relevant elementary flow subsets has been provided for the selected UPs of EVo-platform within Fig. 5.3. This conceptual model has been validated in this work to assure the coverage of all relevant elementary flow subsets from the real process. Based on performed audits and videotapes of assessed UPs i, the conceptual model has been qualified as Fig. 6.48 shows.

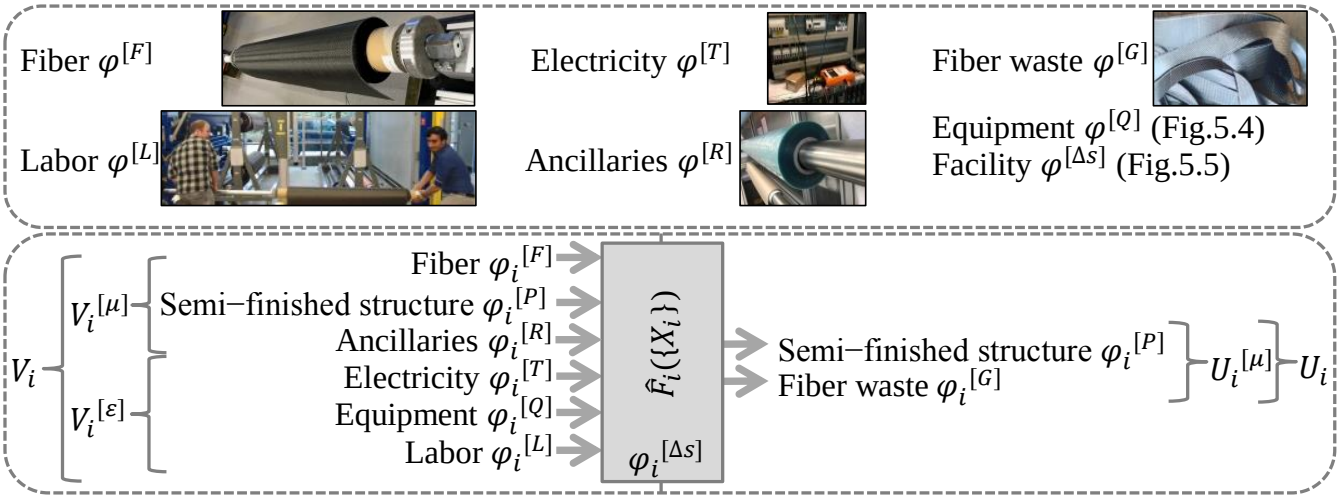

Figure 6.48 Conceptual model qualification of the case study

On the upper side of Fig. 6.48, examples from the documentation for model qualification are shown. This qualification is also applied to the model in Fig. 5.4. However, Fig. 5.4 includes actual qualifying pictures from the early validation loops. Similarly, the facility subset is split into various elementary flows that represent the covered WSs in Fig. 5.2 and Fig. 5.5, while these conceptual models are qualified later in Fig. 6.51. In addition, audits, videotapes, IR-records, and feedbacks from the EVo-platform team have been implemented iteratively in qualifying the conceptual modeling stage.

Verification of mathematical model

Both model types, that are describing the process as well as calculating the impacts, have been verified. As the main process describing matrix, the mathematical model in Eq. 5.1 can be verified based on the qualified conceptual model Fig. 5.3, as the correlation lines in Fig. 6.49 show.

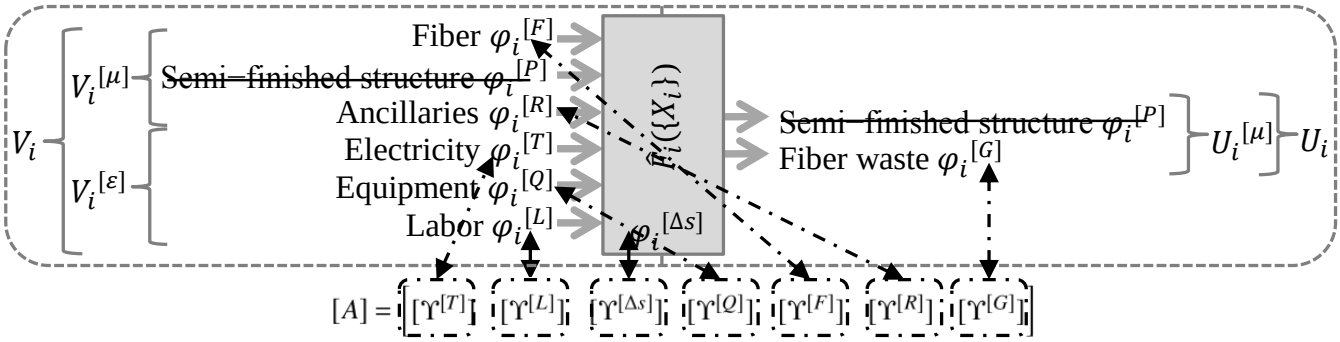

Figure 6.49 Mathematical model verification of included subsets $\varphi^{[\Gamma]}$ in the case study

In which, semi-finished subsets on both sides can be neglected in Fig. 6.49. Nonetheless, both subsets of equipment and facility contain multiple elementary flows. Therefore, the mathematical models of both subsets are verified in Fig. 6.50 and Fig. 6.51 respectively to assure a sufficient representation of input elementary flows.

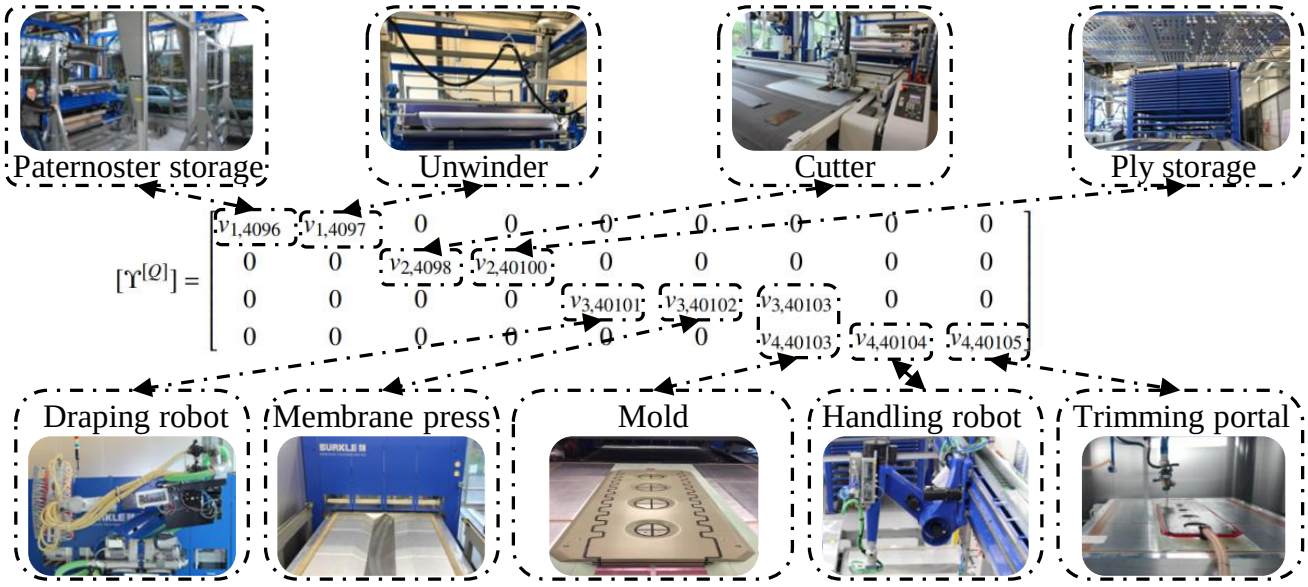

Figure 6.50 Mathematical model verification of the equipment matrix $[\Upsilon^{[Q]}]$

Based on the mathematical model in Eq. 5.5 and the qualified conceptual one in Fig. 5.4, the verification is performed and illustrated in Fig. 6.50. Similarly, the facility mathematical model in Eq. 5.4 and its electricity consumption as a part of Eq. 5.2 are verified in Fig. 6.51 based on the qualified conceptual model from Fig. 5.2.

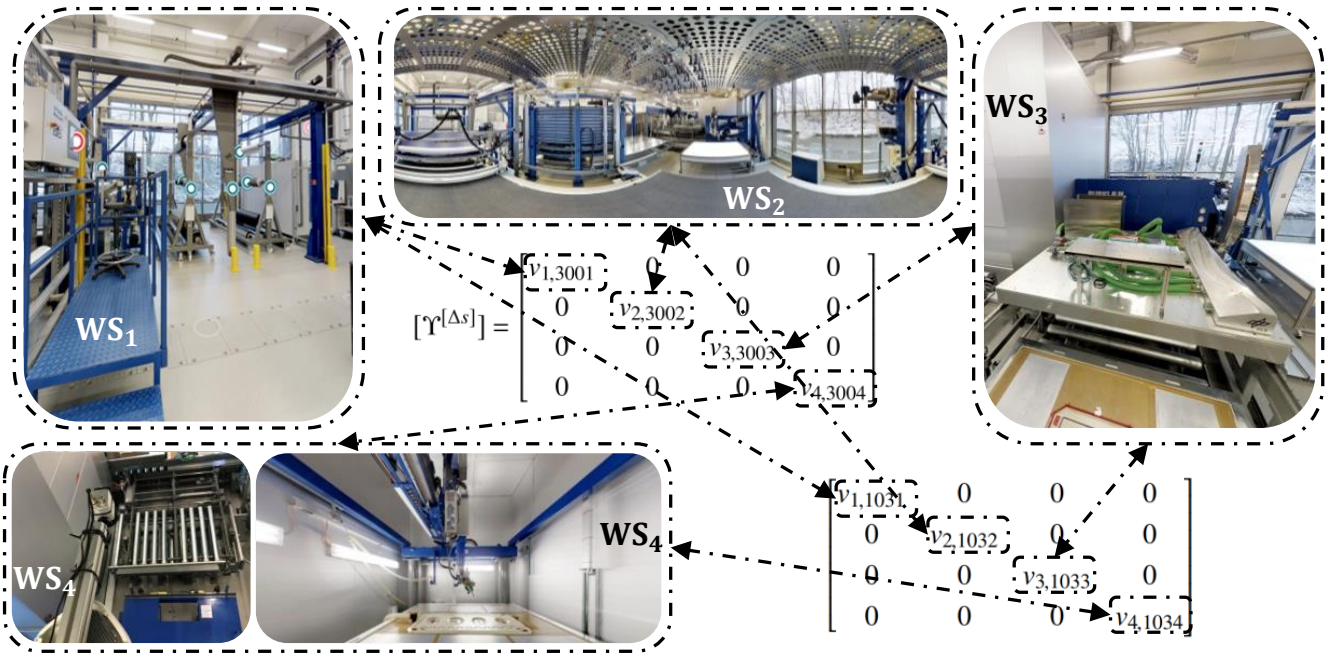

Figure 6.51 Mathematical model verification of facility matrix $[\Upsilon^{[\Delta s]}]$ and a part of the electricity matrix $[\Upsilon^{[T]}]$

To verify the mathematical model of equipment consumption in Eq. 5.5, it has been correlated with its conceptual model from Fig. 5.4, as Fig. 6.52 shows.

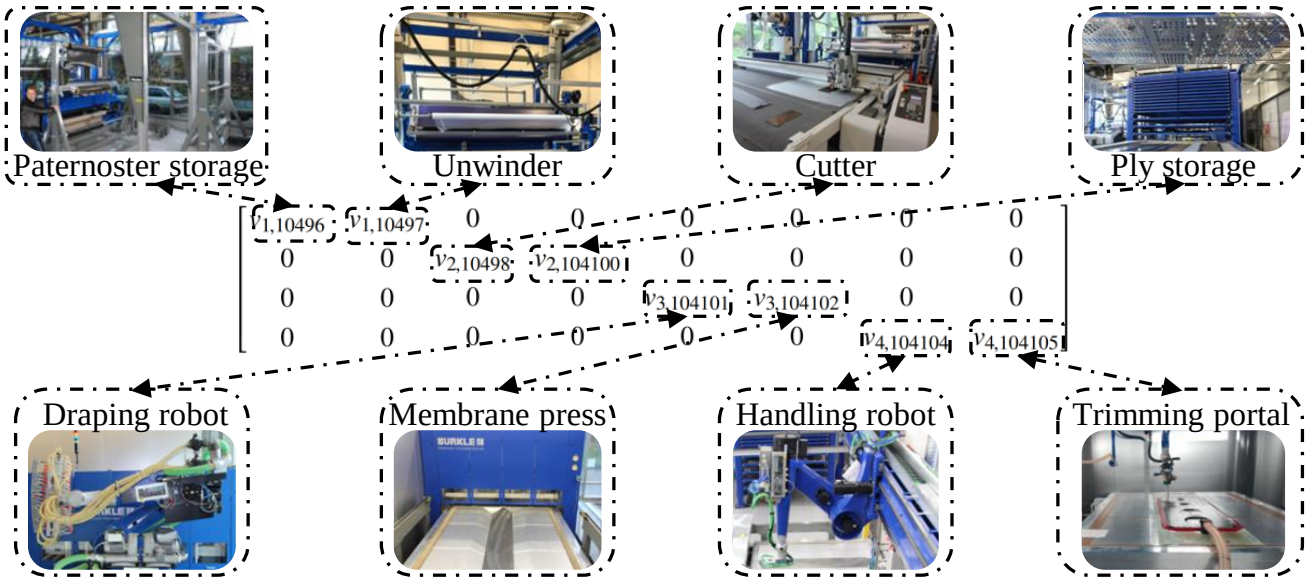

Figure 6.52 Mathematical model verification of the equipment related electricity matrix $[\Upsilon^{[T]}]$

Moreover, the consistency of implemented characterization factors λ, including the economic and ecological ones, is checked to verify the assessment mathematical models. As a part of that, a validation of these factors has been performed based on a selection of comparable works, as it is discussed in Appx. B.

Test of computer-based DSS

The test activities of validation aims to assure the results accuracy from the implemented software solutions as DSSs in this work. The conventional and time-dependent assessment functionalities of EEAM as a computerized model have been partially validated in the previous works of Al-Lami et al., Riech and Hilmer, Nothdurft and Hilmer, Rudolf and Al-Lami, as well as Schachinger and Al-Lami [13, 233, 255, 264, 271].

In this work, the LCIA functionalities of EEAM have been tested by cheeking selected exemplary results based on conventional calculation methods. Although the test of SWS sensor nodes and their operation software solutions is considered to be beyond the scope of this thesis according to Fig. 4.33, limited test activities are carried out to validate the computerized models of SWS. In the SWS computerized model, the timestamps of collected data are tested. A simple comparison, between the start to end time of each measurement session in (hh:mm:ss) on the one hand and the total measurement duration on the other hand, is performed to detect any deviation as a part of the SWS testing. However, the outputs of some software solutions for the sensor nodes have shown some insufficiency in limited cases. While some deviations in the timestamps of collected initial data occur in very limited preparation experiments, such experiments have been repeated. Still, further enhancements are required and planned to achieve more software stability. As it is mentioned before, the current SWS version requires a user-friendly GUIs, that is also planed in future works. Such GUI may be developed to have the capability of warning the user whenever a data deviation is occurred. In practice, some of the purchased sensor nodes have problems regarding temporal allocations of real-time collected data, that have led to the deviations in timestamps. Some operating software solutions of these sensor nodes correct such failure by repeating the most recent amount or calculating the mean value of the last range of recent values to fill the data gap.

To validate the masses of fiber cuts $\hat{u}_{2,17141}$ and fiber wastes from $u_{2,6514}$ as well as $u_{4,65141}$, the preform $\hat{u}_{3,17142}$ and the trimmed preform $u_{4,17143}$ have been remeasured by portable digital scales to assure the accuracy of SWS results regarding the initial fiber and its wastes in UP_2 and UP_4. The deviations of these masses have been neglected, while they are lower that the lowest considered mass digit of $1/1000\,\text{kg}$. In this work, the selected digits are a result of having very small impacts of some elementary flows. Moreover, rounding the numbers is leading to a deviation in the results and inconsistency in some values and percentage representations, while this is a well known problem in many DSSs. Such inconsistency in the digits level of $1/1000$ occurs in several occasions within the illustrated results. For instance, Fig. 6.17 is showing a total electricity impact of $\delta_{2,1001} = 0.919\,€$ although it is the summation of $\delta_{2,10498} + \delta_{2,104100} + \delta_{2,1302} = 0.89 + 0.028 + 0.0004 = 0.918€$. After looking for this specific rounding deviation in the computerized assessment model, these rounded numbers have originally the values of $\delta_{2,10498} + \delta_{2,104100} + \delta_{2,1302} = 0.890 + 0.0285 + 0.0004 = 0.9189€$ which is correctly rounded as $\delta_{2,1001} = 0.919\,€$. However, this $0.1\,\%$ deviation is considered within the previously mentioned inaccuracy margin, which has been expected.

DSSs results validation

In this work, Fig. 4.34 has introduced a novel illustration that serves completeness, among other checks. To validate the SWS results, the process has been documented by authorized videotapes as well as IR-records. Based on interpreting and analyzing them, a conventional LCI has been performed. From this LCI, it has been concluded that temporal deviations are occurring in the SWS_i measurements within a margin of 1 s. From iterating this validation, it has been found that the conventional LCI itself is insufficient to validate such high frequency results, while the check process may have such deviations due to the manual analyses. In other words, the conventional LCI lacks the capability of validating the time-dependency aspects, while it is only sufficient for the validation of time-independent assessment results. For instance, the implementation of thermal labor work measurement MM-(8) to validate the optical one MM-(3) shows identical results in that 1 s margin, whereas it is a real-time LCI and not a conventional one.

As it is mentioned before, the validation activities have been performed throughout the development of this thesis in general and the DSSs in specific. Therefore, selected examples of result accuracy enhancements can

be presented based on understanding the previous illustrations of Fig. 4.20 and Fig. 4.34 in chapter 4. On the one hand, iterative reworking throughout the suggested framework has been performed to enhance the results accuracy. For instance, the total direct cost of the assessed structure has been initially calculated as 312.15 €. After adjusting the assumptions as a results of validation, this result has been alternated by the currently adopted direct cost of 320.71 €. At the same time, the carbon footprint has been initially calculated to be 145.31 kg CO_2 before the validation, while this validation has led to conduct the current impact of 153.16 kg CO_2.

To fulfill the completeness check, it is challenging to find studies with comparable results due to the differences regarding their functional units, industry applications, assessment scope, applied techniques, their DoA, and adopted characterization factors. Nonetheless, such relatively low accuracy comparisons are still useful for validating the conducted results. While a wide range of studies may be considered for such validation, works with available data about comparable techniques with relevant UPs and similar discretization approaches have been selected. Here, the completeness check examines the availability and entirety of validation inputs. However, this lack of sufficient studies for validating the results of time-dependent assessment in general and the case study of EVo-platform in specific has been sensed.

As it has been explained before, the validation studies have been selected from internally performed works due to the comparable system boundaries and close assumptions. Moreover, the data availability is a crucial criteria in selecting these studies, while having both economic and ecological assessments in the same study is preferred. Therefore, the direct cost results of the selected works have been converted to the direct cost δ of each 1 kg in the year 2019 with the consideration of inflation, in order to fulfill the consistency check and have comparable values in Tab. 6.2.

Table 6.2 Validation studies for direct cost results δ of 1 kg CFRP structure

Scholars	Functional unit	Scope	Boundaries	δ (2019)
Denkhaus and Hilmer [73]	L-profile	Manufacturing by low DoA RTM technique	Universal; Germany; 2014	889.74 €/kg
Al-Lami et al. [13]	Wing-box rib	Manufacturing by very low DoA autoclave technique	Aerospace; Germany; 2016	607.36 €/kg

In Tab. 6.2, the questions about the functional units, the study scope within its life-cycle, the technical, geographical, and temporal boundaries, as well as the total economic impacts are answered for the selected studies. From Tab. 6.2, the deviation between the results of these studies is expected. Here, the variations in the DoA, the production rates, and the characterization factors may be behind this noticeable results deviation. In comparison to them, the manufactured preformed structure has the direct cost of around 221.3 €/kg from the assessed four UPs in this thesis. However, such a direct comparison between the total manufacturing costs in Tab. 6.2 and the one of the four selected UPs in this thesis is unrealistic. Therefore, a comparison between the UPs of these internally performed works and the UPs of this work is carried out in Tab. 6.3 for each manufactured kg of the CFRP structures.

While some UPs in Tab. 6.3 have relatively close direct costs such as in trimming UP_4, others vary significantly. On this level of CSFs, the assessment results can be validated only when the validating studies have unified aspects such as identical system boundaries and assumptions. As Tab. 6.3 shows, the work of Denkhaus and Hilmer considers the trimming activities as a part of other UPs, while this illuminates the importance of adopting unified UPs discretization approach. Despite that the paper of Al-Lami et al. includes no trimming as well, the finishing UP in that work has a comparable function. Here, the total direct costs from

Table 6.3 UPs direct cost δ_i comparison of each 1 kg from the CFRP structures

Scholars	Preparing δ_1	Cutting δ_2	Preforming δ_3	Trimming δ_4	δ_1+δ_2+δ_3+δ_4
Denkhaus and Hilmer [73]	378.47 €	117.26 €	28.3 €		524.03 €
Al-Lami et al. [13]	94.16 €	228.33 €	133.8 €	12.73 €	469.02 €
This thesis	5.2 €	196.6 €	5.4 €	14.1 €	221.3 €

all these UPs for both considered validation works of Denkhaus and Hilmer as well as Al-Lami et al. have a deviation of around 11 %.

While the functional units, the study scope within its life-cycle, as well as the technical, geographical, and temporal boundaries are shown previously in Tab. 6.2, the ecological results from the same works of Denkhaus and Hilmer as well as Al-Lami et al. are calculated as 44.09 kg CO_2/kg and 109 kg CO_2/kg respectively [13, 73]. Based on that, there is a clear difference in the total ecological impacts between the selected studies. Again, the comparison of these results with the ones of this work is only realistic if the same UPs are considered, while Tab. 6.4 provides this comparison.

Table 6.4 UPs carbon footprint β_i comparison of each 1 kg from the CFRP structures

Scholars	Preparing β_1	Cutting β_2	Preforming β_3	Trimming β_4	β_1+β_2+β_3+β_4
Denkhaus and Hilmer [73]	2.14 kg CO_2	7.62 kg CO_2	0.09 kg CO_2	-	9.86 kg CO_2
Al-Lami et al. [13]	1.37 kg CO_2	76.39 kg CO_2	2.47 kg CO_2	0.12 kg CO_2	80.35 kg CO_2
This thesis	0.49 kg CO_2	99.57 kg CO_2	1.6 kg CO_2	4.05 kg CO_2	105.7 kg CO_2

When it comes to the ecological impacts for the studied UPs in Tab. 6.4, the results from the works of Denkhaus and Hilmer as well as Al-Lami et al. show a significant deviation of around 88 % between them [13, 73]. Again the deviations in Tab. 6.4 are related to the functional units, industry applications, assessment scope, applied techniques, their DoA, and the adopted characterization factors. Moreover, the discretization and allocation approaches are crucial here.

In conclusion, the direct cost of the selected UPs from this thesis represents about 42 % and 47 % of the assessed economic impacts of comparable UPs from the works of Denkhaus and Hilmer as well as Al-Lami et al. respectively [13, 73]. Considering the high DoA and process maturity of the EVo-platform, such cost reduction is expected. Due to the variety in UPs functions, their discretization approach, and the allocation of elementary flows in these studies, the impact comparison on UPs level within Tab. 6.3 is insufficient, while the difference margins are noticeable in most UPs. The difference between the ecological impact of this thesis and the one from Denkhaus and Hilmer work for the selected UPs is about 91 %, which is a result of the significantly high impact in this work. While the system boundaries are comparable between this work and the paper of Al-Lami et al., the deviation of around 24 % is understandable for all the previously mentioned case differences. The selected ecological characterization factor and impact allocation of fiber are decisive here, while the factor is set by Denkhaus and Hilmer to be around 2 kg [73]. In Tab. 6.4, the high ecological impact from the assessed process in this work is associated with the selected fiber ecological characterization factor as well as the novel consideration of facility, equipment, and labor subsets. This raises the question about the need

for sensitivity checks that introduce the results of the ecological impacts from this work for alternated fiber ecological factor and neglected facility, equipment, and labor environmental impacts.

6.3 Results Discussion

In this discussion, the framework of time-dependent eco-efficiency assessment as well as the two generated DSSs are debated.

6.3.1 Framework Review

The introduced framework of time-dependent eco-efficiency assessment is a generic approach that may be applied to any functional unit in any of its life-cycle stages. Therefore, this framework can be adopted to generate specialized DSSs for real-time LCI and time-dependent LCIA for further case studies. As Fig. 4.5 shows before, it combines different perspectives and integrates them to achieve its DSSs. In addition, the work hypotheses in this study lead to a new vision by considering the exact same elementary flows in both economic and ecological assessments. While other studies concentrate on a specific economic or ecological aspect and handle it, this thesis illuminates the importance of combining both in one KRI. It is essential to mention that the main goal of this thesis exceeds the assessment of the selected case study, while it aims to validate the applicability of the suggested framework and DSSs.

Considering the previously studied criteria within Tab. 3.4, this work contributes to all mentioned ones by providing a time-dependent eco-efficiency assessment. This assessment covers all relevant direct elementary flows by the SWS as a comprehensive automated real-time data collection concept. By the clear goal and scope definition, knowledge processing, data mining, as well as conceptual, mathematical, and computerized models, this thesis achieves the aimed goals by a novel iterative framework for the assessment and validation. As it has been discussed previously by Fig. 3.2 and Fig. 3.4 within chapter 3, this work contributes directly to the recognition and definition of the problem, while generating the SDs or direct applications is beyond the work scope. However, any scientific work is expected to have a clear implementation potential. Therefore, some SD suggestions may be briefly mentioned in the following discussion sections. Still, no dedicated works are performed to validate these suggested SDs, while the framework and its developed DSSs from this thesis can be implemented to facilitate such validations in future studies.

The time-dependent assessment results are assisting the decision-makers on the operational level mainly. These results are crucial for the realization of timely manner controlling, especially in the dynamically modified process scenarios within mass customization for instance. Moreover, further possible applications of such time-dependent DSSs are discussed later as outlooks within chapter 7. While the time-dependent assessment illuminates the impacts per time, it offers detailed results that go deeper than the UP itself. Hence, the UPs discretization illuminates the impacts of clustered activities, while these activities are unnecessarily temporally connected.

As it is discussed previously by Fig. 3.22, the studied techniques are UP associated, while selecting them is commonly based on the impacts they have within their associated UPs. This work adopts the definition of preparing as a separated UP, while the preparing UP_1 and its activities are relevant for some decision-makers as a distinguished cluster. However, these preparing activities may be distributed throughout the entire assessed process, as it is the case in this work. Despite that the activity level is considered as the relevant one for technology development, no activity discretization is discussed in this thesis. However, a previous work of

Rudolf and Al-Lami has been carried out to discuss this subject [264]. Nonetheless, the time-dependent capability enables such further discretization in future works if required.

As it is illustrated in Fig. 3.10, the functional unit itself and its fulfillment of the eco-efficiency are always the most significant KRIs. Theoretically, an absolutely-nonexistent product has the minimum possible impacts of „*zero*“ direct cost and carbon footprint. Therefore, structure characteristics and quality are to be fulfilled by the decision-makers with the most possibly optimized eco-efficiency. Taking Fig. 3.28 into consideration, a manufacturing process is effected by other life-cycle stages while affecting others. Therefore, selecting the proper techniques or technologies in the manufacturing or production in general must consider not only the time-dependent results but also the possible global impacts throughout the entire life-cycle. Moreover, the local back-coupling impacts of these technologies and techniques within the process or the global ones throughout the entire life-cycle are to be studied thoroughly in future works with the help of the time-dependent assessment framework and DSSs from this work. In practice, such back-coupling impacts are expected, while any technology change in an activity or more is alternating the impacts in them directly and may be effecting others indirectly.

6.3.2 SWS Results Review

To discuss the SWS, both its concept and results are to be reviewed. This includes the revision of LCI in each SWS_i.

Discussing SWS concept

To have a limited study scope, it has been assumed that no rejected structures are manufactured and the process is technically ideal. However, these assumptions are not the norms in reality. In an industrial process, rejected structures are less than the desired ones, but they are still existing. Similarly, it is impossible to have a problem-free process at least for a long term. Therefore, such reality deviations should be covered in future versions of the SWS concept. To put it more simply, process deviations as well as their failures can be assessed in time-dependent approach as a part of the activities in UPs i. Including these aspects in future versions of the suggested DSSs provides a realistic and transparent assessment for the decision-makers in order to establish effective SDs. Based on this thesis, product quality may be considered as a crucial aspect side-by-side with the assessed KRIs in future works, while the need for such capabilities has been sensed.

In reality, real-time is a feature that is somehow difficult to realize, while a time delay must exist even when it is very minor. Therefore, an absolute real-time data collection is technically impossible, but the term is still common for near real-time approaches. Based on the previously generated and discussed results, the visualizations of SWS results have a clear development potential. In the current visualization forms, illustrations are unclear unless a zoom function is implemented for some cases, especially for long temporal durations on the horizontal axis. Moreover, the enrichment of SWS-DB may be laborious for newly considered techniques or scenarios and their elementary flows, as it is concluded from previous works [264, 271]. However, a significant portion of initial process data is likely to be common within the same industry. Here, inputs are mainly field and not case or manufacturer specific. Therefore, it is essential to generate a sufficient SWS-DB in a field with a clear potential for SWS implementation in it. This can be investigated by dedicated field market studies in various industries. However, such field market studies are beyond the thesis scope.

Discussing SWS visualized and statistical results

The SWS results are discussed for all applied SWS_i in this case study. When it comes to SWS_1 results, the different range of electricity elementary flows in Fig. 6.2 may cause a visual interpretation confusion. Nonetheless, using the same range for all of them will make the value of facility WS_1 electricity $v_{1,1031}$ almost invisible in some temporal points. To assist in finding the suitable SDs for reducing the electricity consumptions, the used range variants in Fig. 6.2, Fig. 6.3, Fig. 6.4, and Fig. 6.5 may be preferred for decision-makers, that are focusing on such SDs. In general, the labor work $v_{1,2001}$ provides no detailed description of efforts quantification, while the SWS only detects whether a person is in the WS or not. This labor time measurement leans on the hypothesis that everyone in the WS is working for the assessed process, which is true for the case study but not every possible scenario. According to the operating team of EVo-platform, the possibilities of further time reduction are limited in the activities within UP_1. Considering the adopted scenario, the labor work $v_{1,2001}$ may be slightly improved by further training, while equipment types including $v_{1,4096}$ and $v_{1,4097}$ are operating with the highest safe speed.

SWS_2 results in Fig. 6.3 have both cumulative and noncumulative forms, while material mass is commonly described cumulatively. However, enabling a unified form may still be preferable for some decision-makers. In Fig. 6.3, adding the intermediate flow of cuts $\hat{u}_{2,17141}$ can be considered as redundant illustration, while it is a logical result of subtracting the fiber waste $u_{2,6514}$ from the initial fiber $v_{2,6014}$. Nonetheless, comprehensive illustrations for all possible input, output, and intermediate flows are useful for better process understanding and facilitated SDs regarding each elementary flow of them. Considering activities durations, the ones performed by the cutter $v_{2,4098}$ have a clear reduction potential. However, the selected operating program has safer characteristics for the case study. Moreover, activity acceleration may have negative impacts on electricity consumptions and equipment useful life. In UP_2, the facility electricity consumption is noticeably related to the collector $v_{2,40100}$ operation. While the cutter $v_{2,4098}$ is utilized as a manually operated machine in some projects, the collector $v_{2,40100}$ is a critical machine for labor safety in WS_2. Therefore, safety devices for motion detection and alarms in this facility are activated whenever the collector $v_{2,40100}$ is operating, which may be the reason behind this noticeable correlation in Fig. 6.3.

The results of SWS_3 in Fig. 6.4 include the preform $\hat{u}_{3,17142}$ as an intermediate flow, which may be irrelevant directly for the assessment. Although its magnitude is calculable as the direct summation of all cuts, presenting its additive process may be useful for better understanding of the applied technologies. Moreover, the installation of portable digital scales to measure these material elementary flows has very limited setting up efforts in comparison to some other ones. This is a motivation to perform such data collection for validation purposes. In general, the activity acceleration may be a solution in many cases. However, the time reduction in UP_3 may require new technologies especially within the membrane press, while such technologies may have very different characterization factors that can increase the impacts significantly. The continuous electricity consumption of WS_3 is associated with the standard safety devices, while they assure that no manual activities are done during equipment operation.

SWS_4 results in Fig. 6.5 represent the flows of input preform from UP_3 $v_{4,17142}$ and its fiber consolidated waste $u_{4,65141}$ simultaneously. Here, the illustration of the final trimmed preform $u_{4,17143}$ may replace these two graphs or be added to them. Similar to WS_3, WS_4 has almost constant electricity consumptions due to the laser-controlled safety housing. This visualization of the minor electricity consumption of the facility WS_4 is an unnecessary presentation for some decision-makers. However, such visualization may be useful for others especially when such consumptions from all WSs are to be compared. Based on the technical feedback of the operating team, trimming activities within the portal $v_{4,40105}$ can be accelerated. Similar to the case in other

UPs i, such acceleration may increase the electricity consumption of associated devices and has an impact on their useful life. Nonetheless, every activity acceleration in all UPs i is leading to reducing facility occupation and logically facility electricity consumption, if no unchanged activity is simultaneously performed in that exact WS_i.

For all UPs i in Fig. 6.7, the correlation between electricity consumption and machine utilization is clear, while this is an obvious result of measuring the machine performance based on its consumption. In practice, some equipment types are obligatory occupied for a process even when they are not operating. This may be a result of the facility or process characteristics. However, such dependency is not covered in this work, whereas this may be a crucial subject for future studies. From all SWS_i, the real-time data collection of elementary flows can relate their behaviors with the applied technologies in all activities as time slots. Based on these SWS results, bottleneck activities can be prioritized, while proper SDs for efficiency enhancement may be possibly applied to their technologies. Here, elementary flow efficiency enhancement can include the reduction of materials waste, labor work time, electricity consumption, and equipment operation time. As it is mentioned before, the efficiency is again unequal to eco-efficiency but it is a way to enhance eco-efficiency. For instance, Fig. 6.9 assists the decision-makers, who are concerned about equipment operation development, in prioritizing their efforts toward effective SDs for the most significant equipment types.

6.3.3 EEAM Results Review

Similar to the SWS, the EEAM capabilities and results may be separately discussed. It is essential to mention that this thesis handles the selected case study of UPs from the manufacturing process of vertical stabilizer ribs as a validation assessment. Although direct applications such as SDs are beyond the thesis scope, limited unvalidated suggestions about such SDs are provided to illuminate the usefulness of the conducted results.

Discussing EEAM capabilities

In the time-dependent assessment, the EEAM provides dynamic perspectives of the impacts from considered process elementary flows. However, the time-dependency is associated theoretically with the characterization factors as well, while a comprehensive absolute time-dependent assessment must cover the dynamic nature of these parameters as well. Still, this is beyond the scope of this thesis. Especially in assessing the eco-efficiency ξ_t by the suggested calculation in Eq. 4.83, the time-dependency is theoretically applicable to the total sales revenue excluding all non-process costs k. Technically, such dynamic k_t varies throughout the process based on the performed activities and the quality of that performance in each UP. To put it more simply, no enterprise is willing to offer any performance for free in a profitable case. Simultaneously, customers are not willing to pay for nothing in similar profitable cases. However, the study of how much each activity is worth for the different qualities and scenarios requires dedicated investigations, which are beyond the scope of this work.

After evaluating the DSSs results in this chapter, it can be concluded that the results visualization in this thesis is sufficient for a scientific work. However, further functionalities must be included within the EEAM in general and within its GUI in specific to fulfill the decision-makers demands. As it is mentioned previously, selecting the proper functionalities in the future is associated with identifying the fields and sectors that these DSSs are to be developed for. Whether these time-dependent assessment capabilities have a better potential in other sectors is still an open question.

As it is previously suggested in Fig. 4.5 within chapter 4, there are four media that are associated with the generated DSSs and their outcomes in this thesis. The first medium in this work contains the decision-makers

that are concerned about production aspects especially on the operation level. The second medium in this work has been covered by the CSF levels for the eco-efficiency and its aspects within manufacturing, which are represented by the collected initial data up to the generated knowledge. While the third medium is the selected UPs of preparing, cutting, preforming and trimming from the manufacturing, the product is a CFRP structure of a vertical stabilizer rib manufactured by the preforming technique and the selected technologies with high DoA. Finally, the fourth medium in Fig. 4.5 is represented by the integrated framework, that brings all these media together to achieve the sufficient knowledge aimed from the developed DSSs.

Discussing EEAM visualized and statistical results

The UPs i have distinguishable behaviors regarding both direct cost δ_i and carbon footprint β_i. When it comes to UP_1, it is clear from Fig. 6.10 that the labor direct cost $\delta_{1,2001}$ is the highest economic impact with a noticeably high margin. Further automation is not a new solution for labor work reduction in the EVo-Platform, while a fully-automated preparing with machine performed roll transportation is already realized in other scenarios. However, selecting a scenario with some manually performed activities is significant to the validation of this thesis framework and its DSSs for various DoA. In practice, many FRPs production activities are still carried out manually in aerospace industry among others.

Fig. 6.11 shows the different behaviors of cumulative direct cost and carbon footprint in UP_1. The clear correlation between the labor and the direct cost as well as the total electricity consumption and the carbon footprint in Fig. 6.11 directs the decision-makers to handle these elementary flows discreetly in UP_1. The behavior of eco-efficiency within Fig. 6.12 is related to the assumption of having a constant k throughout the entire UP. The descending curve of time-dependent logarithmic scaled eco-efficiency ξ_{i_t} in Fig. 6.12 is a logical result of subtracting an increasing variable from a larger constant and divide their outcome over another much smaller increasing variable throughout the UP duration. This is also the case of the descending curves in Fig. 6.20, Fig. 6.28, and Fig. 6.35 for UP_2, UP_3, and UP_4 respectively. While the eco-efficiency in Eq. 4.83 is calculated for a constant k, the illustration of it is a new approach that should be further investigated. This time-dependent eco-efficiency ξ_{i_t} contains two unique units of € for the direct cost and $\mathrm{kg}\,CO_2$ for the carbon footprint. For UP_1, a calculated eco-efficiency of $\xi_1 = 59.72\,\frac{€}{\mathrm{kg}\,CO_2}$ is the simplified absolute final impact.

For better understanding, the temporal ratio of direct cost to carbon footprint in Fig. 6.13 may be required, while the logarithmic scaled eco-efficiency graph provides a complex visualization. Therefore, the ratio in Fig. 6.13 assists the decision-makers in identifying the bias to eco-efficiency aspects, by understanding this behavior in the associated time slots. This can be crucial for orienting the focus of SDs. This novel assessment visualization is also provided for the ratios of the other three UPs in Fig. 6.21, Fig. 6.29, and Fig. 6.36. Theoretically, the ratio itself is supposed to vary slightly throughout the process, while all elementary flows have both economic and ecological impacts in this thesis. However, this ratio may still have radical deviations at some temporal points. In such situations, activities and their technologies within this deviation time slots are to be prioritized for thorough investigations. For instance, this ratio of UP_1 in Fig. 6.13 has a clear high values in the first 100 s that are going between 5 and 12 after that. Here, the goal of any SD must be decreasing one or both impacts and not having a constant ratio.

Practically, SDs are realized through technologies or managerial developments on the lowest activity level. Therefore, decision-makers need to correlate the assessed impacts with their causing activities, whenever the SDs on UP level are insufficient any further. This correlation is one of the advantages gained by a time-dependent assessment. Such relation can be interpreted from the visualization of time-dependent total direct cost and carbon footprint of UP_1 in Fig. 6.14 and Fig. 6.15 respectively. As Fig. 6.14 and Fig. 6.15 show, manual

activities have significant temporal impacts on both aspects during UP_1. Moreover, both of these time-dependent impacts of relevant elementary flows are similarly visualized for all other UPs including Fig. 6.22 and Fig. 6.23 for UP_2, Fig. 6.30 and Fig. 6.31 for UP_3, as well as Fig. 6.37 and Fig. 6.38 for UP_4. Despite of the importance of illustrating the impacts in these different time-dependent forms, any further decision-making steps based on these illustrations are beyond the scope of this thesis.

Although the time-dependent eco-efficiency assessment is the core output of this work, decision-makers may still need the conventional time-independent visualization of global impact drivers, that are shown in Fig. 6.16 for UP_1. Especially on higher managerial levels, such global impact illustration is relevant, while neither UPs and their activities nor the related techniques and technologies are commonly discussed on such high management levels. Therefore, similar time-independent impact visualizations have been provided in Fig. 6.24 as well as Fig. 6.25 for UP_2, in Fig. 6.32 for UP_3, and in Fig. 6.39 for UP_4.

Similar to UP_1, UP_2 impacts are shown in Fig. 6.17. While Eq. 4.73 previously suggests that initial fiber direct cost $\delta_{2,6014}$ and its carbon footprint $\beta_{2,6014}$ cover the wasted portion of it as well, the waste direct cost $\delta_{2,6514}$ and its carbon footprint $\beta_{2,6514}$ include only the disposal expenses and ecological impact respectively. However, the fiber waste final impacts including the ones from their initial materials are also provided statistically to illuminate the significance of this output elementary flow. However, providing the time-dependent impacts of this inclusive fiber waste in Fig. 6.17 is thinkable. According to the operating team of EVo-platform, the selected cutting scenario is much slower than the highest possible one. Adopting such advanced scenario may eliminate about 80 % of the cutting duration in this work. Still, the selected relatively slow scenario is more appropriate for validating the applicability of the scientific framework for the first time in this thesis.

Unlike UP_1, both direct cost δ_{2_t} and carbon footprint β_{2_t} in Fig. 6.18 have similar behaviors that are associated with the dominating fiber impacts $\theta_{2,6014}$. In addition to the relatively high material magnitude, this fiber type has very high economic and ecological characterization factors, which are causing this domination. While the decision-makers need a better understanding of the impacts from other flows, Fig. 6.19 excludes the fiber and its waste impacts. From tracing back the slight deviation between both impacts with the help of Fig. 6.17, it is concluded that the economic impact of release film is causing that deviation in the direct cost line graph within Fig. 6.19. Here, the concluded final eco-efficiency of this UP_2 can be simplified as $\xi_2 = 0.104 \frac{€}{\mathrm{kg}\,CO_2}$, which is very low in comparison to ξ_1. The cumulative time-dependent logarithmic scaled eco-efficiency of UP_2 in Fig. 6.20 differs from the one of UP_1 in Fig. 6.12, while the assumed $k_2 = 300\,€$ constant is much higher than $k_1 = 50\,€$ and the materials have significant impacts in UP_2.

When it comes to the ratio of direct cost to carbon footprint in UP_2, the ratio line in Fig. 6.21 has a noticeable peak at the first part UP_{2A} and another one at the beginning of UP_{2B}. As it is mentioned before, the materials have significant impacts in UP_2. Here, the first peak is related to the release film occurrence, while the second one is clearly fiber associated. As they are listed in Eq. 5.30 and Eq. 5.31, the release film $v_{2,9017}$ has a relatively high economic characterization factor and a low ecological one in comparison to the fiber $v_{2,6014}$, which has them both relatively high. These reasons cause the noticeable deviations in the ratio behavior in Fig. 6.21, which has a mostly constant value of around 2 throughout the rest of UP_2. From Fig. 6.13 and Fig. 6.21, the ratio trend of around 2 in UP_2 is lower than the one of 5 to 12 in UP_1, which shows that the carbon footprint is generally more significant for UP_2.

While the material domination on both impacts hinders any clear visualization of other elementary flows, Fig. 6.22 and Fig. 6.23 respectively visualize the time-dependent total direct cost and carbon footprint excluding these elementary flows in UP_2. Here, it is concluded that the cutter utilization time and its electricity consump-

tion are leading both impacts respectively. While the suggested acceleration of cutting activities can sufficiently reduce the direct cost, it indirectly decreases the carbon footprint through reducing the facility occupation as well. Again, the conventional time-independent subset impacts in Fig. 6.24 are dominated by the fiber input. Although these dominating impacts must be illustrated, some decision-makers may be concerned about the hidden ones in Fig. 6.24. Therefore, Fig. 6.25 is a possible visualization solution.

Considering UP_3, the decision-makers can identify the cumulative time-dependent impact of each elementary flow in Fig. 6.26. While UP_3 is carried out by a set of fully-automated activities and no material inputs, the impacts are caused by the machines and their electricity consumptions, the mold, as well as the facility and its electricity consumption. As Fig. 6.26 shows, the impacts of the elementary flows from a same subset, such as the subsets of equipment and electricity, have clear relatively close impacts with reasonable differences. This may be a distinguishing feature for fully-automated UPs with no materials. From Fig. 6.27, both direct cost and carbon footprint behave similarly until the moment when electricity consumption of membrane press $v_{3,104102}$ radically increases, which impacts the carbon footprint β_{3_t} significantly.

The concluded final eco-efficiency of this UP_3 can be simplified as $\xi_3 = 29.044 \frac{€}{\mathrm{kg}\,CO_2}$, which is between the values of ξ_1 and ξ_2. The behavior of time-dependent cumulative logarithmic scaled eco-efficiency ξ_{3_t} of UP_3 in Fig. 6.28 is similar to the one from UP_1 in Fig. 6.12. For the ratio of direct cost to carbon footprint in UP_3, the line graph in Fig. 6.29 has a unique behavior after the UP beginning and when the press electricity consumption $v_{3,104102}$ radically increases. This low ratio of δ_{3_t}/β_{3_t} at the very beginning of UP_3 is related to the previously mentioned pause. However, this ratio is between 2 and 4 except for the begging of UP_3, which is closer to the ratio range in UP_2 than the one in UP_1. The time-dependent total direct cost and carbon footprint of UP_3, which are shown in Fig. 6.30 and Fig. 6.31 respectively, are both pointing to the membrane press $v_{3,40102}$ due to its utilization time and electricity consumption. However, the impacts of the draping robot $v_{3,40101}$ are also noticeable in both illustrations.

Technically, the membrane press activities have a limited development potential unless core technology changes are applied, which requires dedicated studies for such SDs. On the other hand, the draping robot is to be studied thoroughly, while this robot moves on a long track between its stations. Although having shorter travel can reduce both impacts, technical and safety aspects may hinder such change in the EVo-platform. Fig. 6.32 visualizes the time-independent impacts of studied subsets, in which the facility ecological impact $\beta_{3,3003}$ is noticeable. While this subset is rarely considered in conventional ecological assessments, its impact in this thesis should be further investigated. Here, the selected characterization factor of facility ecological impact can be further studied to optimize the assumptions in Appx. B.

In UP_4, the direct cost of trimming portal $\delta_{4,40105}$ and the carbon footprint of WS_4 facility $\beta_{4,3004}$ are the leading impacts in Fig. 6.33. While all equipment types have relatively low direct costs, the waste disposal expenses $\delta_{4,65141}$ are noticeable in UP_4. The behaviors of time-dependent direct cost and carbon footprint during UP_4 within Fig. 6.34 are similar to the ones in Fig. 6.27 for UP_3. Here, a clear deviation in δ_{4_t} is associated with relatively high waste disposal expenses. The calculated final eco-efficiency of UP_4 may be also simplified to be $\xi_4 = 9.313 \frac{€}{\mathrm{kg}\,CO_2}$, which is much lower than ξ_1 and ξ_3, but much higher than ξ_2. The time-dependent logarithmic scaled eco-efficiency ξ_{4_t} in Fig. 6.35 behaves closely to ξ_{3_t} in Fig. 6.28 and similarly to ξ_{1_t} in Fig. 6.12. While both UP_4 and UP_3 have close characteristics in being fully-automated and they have identical constants of $k_3 = k_4 = 75\,€$, the close behavior of ξ_{4_t} and ξ_{3_t} is logical.

In Fig. 6.36, the noticeable changing ratio of direct cost to carbon footprint in UP_4 may be associated with the direct costs of the handling robot $\delta_{4,40104}$ and the consolidated fiber waste $\delta_{4,65141}$, that are shown in Fig. 6.33. The time-dependent direct cost and carbon footprint impacts of the selected elementary flows

excluding the fiber waste in UP_4, which are shown in Fig. 6.37 and Fig. 6.38 respectively, are bringing the light to the importance of accelerating the activities within the trimming portal $v_{4,40105}$. According to the operating team of EVo-platform, faster trimming scenarios are technically possible. Again, any acceleration is indirectly reducing the carbon footprint through facility and its electricity consumption. However, such acceleration is not necessarily reducing the equipment electricity consumption. Fig. 6.39 shows the domination of the economic impact of the equipment subset over the direct cost and the ecological impact of the facility subset over the carbon footprint in UP_4, while this UP has only an output material but no input materials or labor.

Despite the importance of the process discretization, the global view of this process may be essential for some decision-makers on specific managerial levels. All the time-dependent impact visualization forms, that have been studied for each UP i, are also illustrated for the entire case study within Fig. 6.40, Fig. 6.41, Fig. 6.42, and Fig. 6.43. As Fig. 6.40 shows, the time-dependent logarithmic scaled eco-efficiency of the entire process ξ_t combines the behaviors of previous ones of the studied UPs with a similar descending trend at the beginning.

Moreover, the ratio of direct cost to carbon footprint in all UPs i is descending at the process beginning in Fig. 6.41. Except for the behavior until around t =500 s in Fig. 6.41, the ratio has a value of around 2 after that. It is clear here that illustrating the time-dependent direct cost to carbon footprint ratio δ_t/β_t for the entire process is not equal to combining the relevant graphs of UPs ratios in one illustration, while the cumulative impacts are covering all UPs i in Fig. 6.41. Excluding all materials, the time-dependent direct cost and carbon footprint in Fig. 6.42 and Fig. 6.43 respectively are guiding the decision-makers toward the proper focal points for process enhancement. From the time-independent results in Fig. 6.45 and Fig. 6.46, it is obvious that the facility, labor, and equipment elementary flows may have crucial ecological impacts. This subject should be further considered in all future related works, while considering them in the cut-off-criteria of ecological impacts seems to be unrealistic.

Here it is concluded from Fig. 6.46, that despite the importance of the facility, labor, and equipment subsets on their UPs ecological impacts, they are barely significant on the global level due to the fiber impact domination. This also illuminates the significance of adopting time-dependent or at least discretized assessment for sufficient decision-making, while such time-independent illustrations of the entire process are incapable of providing the required understanding of the significant impacts on the UPs level. In other words, conventional assessment results can be misleading on some other levels even when they are correct on another. Hence, time-dependent results introduce new perspectives in understanding the impact behaviors throughout the assessed process. Freed from blaming a subset or a UP, the time-dependent results illuminate when exactly each elementary flow has a noticeable impact. Based on this novel time-dependent assessment, decision-makers can apply direct applications locally within each activity in the assessed UP and not only global ones.

The statistical results for both economic and ecological impacts are selected at random temporal points of t = 100 s and t = 1000 s to demonstrate the DSSs capabilities. In practice, such temporal points or time slots are to be selected carefully to assess a specific technique, technology, or a set of them within defined UP, activity, or multiple ones. Moreover, the introduced time-dependent assessment facilitates an iterative approach in performing that by minimized adjusting efforts in the implemented DSSs. Moreover, the suggested framework and its DSSs may cover a wide range of process scenarios. However, assessing the global impacts of each technology on the entire process is still crucial to understand the global back-coupling impacts as well, while the time-dependent assessment can be used to trace such impacts in their exact temporal allocations.

Although the characterization factors are considered as given constants in this thesis, some impacts are dominating due to their selected factors. For such characterization factors of elementary flows with high impacts, sensitivity checks have been performed to examine their significance. Based on reviewing alternative

research works from Appx. B, the fiber economic and ecological characterization factors have been changed to be 17.9 €/kg and 16.9 kg CO_2/kg respectively in the first sensitivity check. Consequently, the previously introduced impacts distribution among the subsets within Fig. 6.46 is alternated by Fig. 6.53.

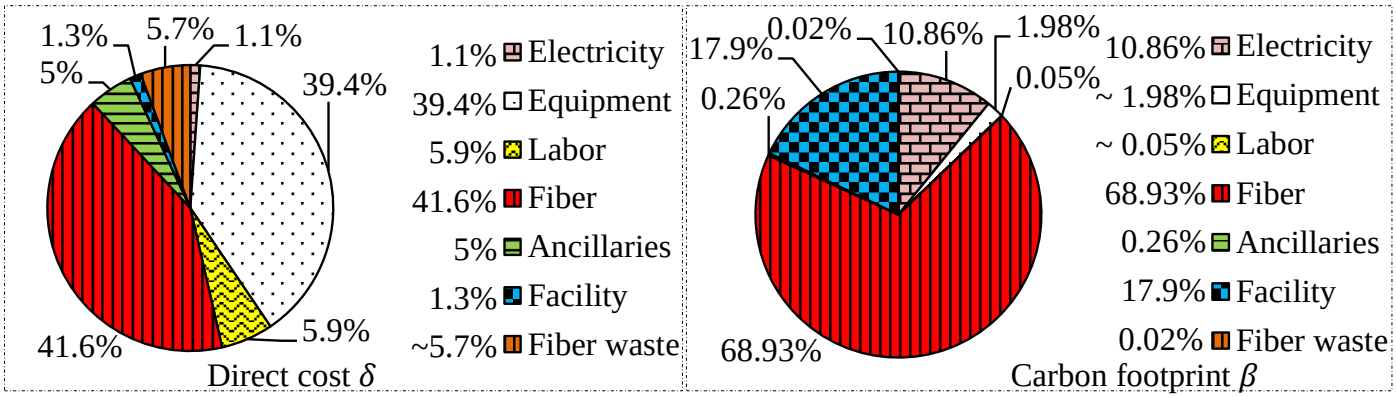

Figure 6.53 Process direct cost and carbon footprint contributors with alternative fiber characterization factors

Despite the significant fiber impact reduction on both aspects, the fiber is still the leading one on both sides of Fig. 6.53. Considering the total impacts as results of this change in fiber factors, a total process direct cost of 120.996 € and a total carbon footprint of 69.004 kg CO_2 are calculated. This significant reduction in the total impacts illuminates the importance of further studies regarding the characterization factors in general and the alternative fiber materials in specific. Such studies may include simulating the variations of these factors as well, while this subject is beyond the scope of this thesis.

In this thesis, it is hypothesized that all elementary flows, that are assessed in the economic approach, are also considered in the ecological one. Here, it is assumed that everything with an economic cost must have an ecological impact as well. While the impacts results of these newly considered subsets on the ecological aspect are significant, they are also examined in the second sensitivity check. Unlike the right side of Fig. 6.46, Fig. 6.54 illustrates the results of excluding the carbon footprint from facility, labor, and equipment for the initial fiber ecological factor on the left side and the alternative one on the right side.

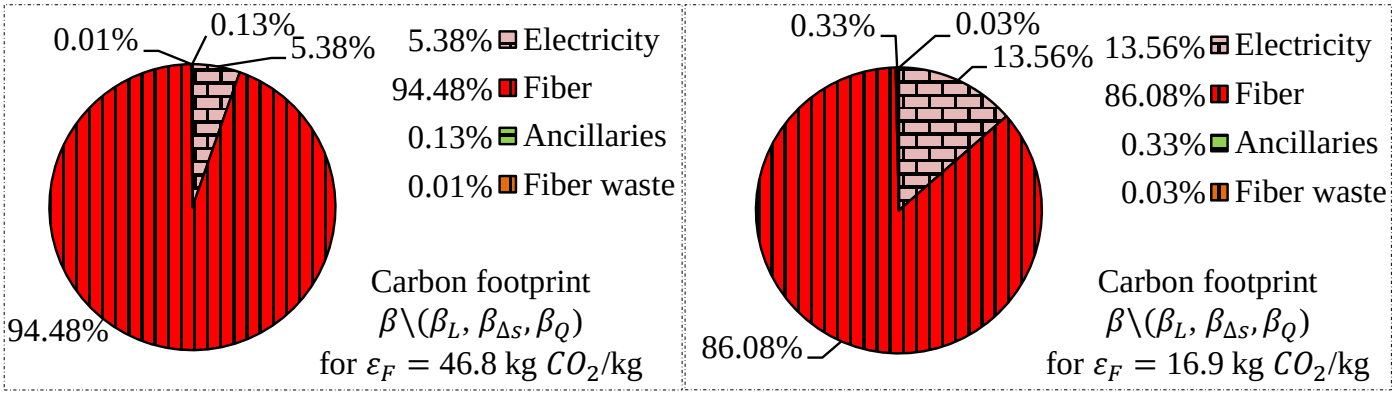

Figure 6.54 Process carbon footprint contributors excluding labor, facility, and equipment

This sensitivity check calculates the carbon footprint of around 96.212 kg CO_2/kg from the assessed case study of unchanged fiber characterization factor and neglected facility, labor, and equipment impacts on the left side of Fig. 6.54. On the right side of Fig. 6.54, the ecological impact of around 38.134 kg CO_2/kg is calculated for the same case but with the alternated fiber ecological factor. Here, the domination of fiber subset is increasing as a result of neglecting these subsets on the global process level.

For the case study of selected UPs from the EVo-platform, there is a lack of sufficient studies related to the eco-efficiency assessment. Here, the EVo-platform represents an advanced close-to-industry process, while a

reduced direct cost is expected by such manufacturing in comparison to the laboratory-based studies in Tab. 6.3. On the other hand, this thesis shows a much higher ecological impact in comparison to the other two studies in general and within cutting UP_2 in Tab. 6.4 in specific. However, this is also expected after considering three new categories including facility, labor, and equipment, which have been neglected traditionally in the ecological assessment. Moreover, cutting duration, which is a result of the selected relatively slow scenario, plays a role in this ecological impact mainly through equipment and facility occupation. Nonetheless, the second sensitivity check leads to comparable ecological impacts of 96.21 kg CO_2/kg and 38.13 kg CO_2/kg, when these categories are neglected with initial and alternative fiber characterization factors respectively. Still, the higher ecological impact of an advanced DoA process with high electricity consumption is logical, when it is compared to a low DoA process with no consideration of labor ecological impacts.

Chapter 7

Conclusion and Outlook

In summary, the eco-efficiency assessment includes the time dimension in its core, while temporal system boundaries have been focused on in literature. However, the necessary time interval of an assessment iteration is still the main question, while the assessment recency is always required. Here, this time-dependency can be a key in providing novel assessment capabilities, when the assessing interval comes closer to real-time. Such time-dependent eco-efficiency assessment capabilities enable studying process variants iteratively, whenever the appropriate framework, concept, and decision support systems (DSSs) are available for assessing these scenarios.

In literature, the time-dependency aspect in eco-efficiency assessment is rarely handled in general, while there is a lack of studies about the production processes for structures made of fiber-reinforced polymers (FRPs) in specific. Here, such approach can enable not only the clear impact allocation to their associated unit processes (UPs), categories, and elementary flows but it can also facilitate establishing an eco-efficiency control system in FRPs production based on identifying the impacts associated time slots, activities, and their technologies. In practice, such controlling should combine the eco-efficiency aspects with other ones such as quality and time to market.

To fulfill the hypotheses from chapter 2, a framework for the time-dependent eco-efficiency assessment has been introduced in this thesis. It serves as a generic approach for any product system within the different life-cycle stages of an assessed functional unit. In this work, an equality in treating both economic and ecological aspects regarding their elementary flows is adopted. In other words, it is hypothesized that every elementary flow should have both impacts. Based on this assumption, the results have shown significant ecological impacts of traditionally neglected categories such as the facility and labor. Moreover, this work suggests an adjustable clear scope of the eco-efficiency assessment based on selecting the considered life-cycle stages of the elementary flows and their characterization factors, as it is suggested previously by Fig. 4.7 in chapter 4. While the time-dependency is applicable for the elementary flows and their characterization factors, this thesis applies it for the flows only.

For the production as a specific phase in the life-cycle of predefined products such as FRP structures, the concept of smart-work-station (SWS) provides a generic real-time data collection approach. It enables an automated determination of the elementary flows, while the characterization factors are given as constants. Although the SWS concept is theoretically applicable for both manufacturing and assembling, this thesis focuses on the manufacturing process only. In this work, the Endkonturnahe Volumenbauteile (EVo)-platform is the adopted case study of a manufacturing plant. In this case study, the identification and measurement methods as well as their sensor nodes are selected from the SWS concept to turn the work stations (WSs) of EVo-platform into SWSs. These SWSs serve as a DSS for real-time life-cycle inventory analysis (LCI). Based on the collected data in real-time, the previously developed eco-efficiency assessment model (EEAM) is further enhanced as another DSS. With the implementation of SWS for real-time LCI, the advanced EEAM

enables a time-dependent life-cycle impact assessment (LCIA) with a defined assessing frequency. The novel visualization of time-dependent direct cost as well as carbon footprint of each elementary flow in every UP is a key for evaluating the applied techniques and their technologies. Moreover, these bottom-up DSSs are based on relatively transparent gray-box models, in which the reasons and results are easily distinguishable. These DSSs provide a multi level description of the studied CSFs with adjustable focal points for the decision-makers on the operational level in specific and on many other levels in general. For the decision-makers on the operation level, several customized products are generated by an adjustable selection of discrete UPs. In such production, a conventional assessment is costly, while each scenario must be assessed separately to provide sufficient results.

While they are product independent, the suggested concept of SWS and the advanced EEAM provide DSSs that may be implemented in carrying out automated production assessments for all comparable products in the SWSs of a smart factory. With the help of these DSSs, this work introduces novel time-dependent visualizations for the total eco-efficiency, direct cost and carbon footprint behaviors, direct cost to carbon footprint ratio, as well as economic and ecological impacts of the elementary flows. Moreover, the developed assessment capability can allocate and determine any impact change whenever a product or process modification is applied. While this thesis covers limited decision-making stages, the process development and control are beyond its scope. Still, some SD suggestions have been provided to demonstrate the usefulness of the conducted results.

In outlook, the generic framework can be implemented in further applications and case studies to generate specialized versions of its DSSs in various fields. This may start by filling shadowed fields in Fig. 4.5 with more associated case studies. In future works, each technology should be allocated to its time slot within a UP in order to assess its local impacts, while its global and back-coupling ones are also assessable.

Based on future results from iterative studies performed by the SWS and EEAM with minimized efforts, the eco-efficiency estimation accuracy in the early phase of product design or process planning can be enhanced. This may be realized when a sufficient amount of results from reliable time-dependent assessments of comparable scenarios is generated. Based on this thesis, the generic concept of SWS for FRPs production can be expanded to cover further life-cycle phases of other FRP structures. Here, assessing the time-dependent eco-efficiency in the structures assembling process may be the next proper product system to cover. Theoretically, the previously suggested identification and measurement methods as well as their sensor nodes in this work are applicable in the assembling process as well. Still, this assumption needs to be validated in future works. Furthermore, functional units other than the FRP structures may be covered by modified versions of the framework and its DSSs. The development of a modified SWS concept for other industries and life-cycle stages such as the maintenance of FRP structures is also possible. However, the deep knowledge about these processes is required to enable the sufficient performance of the suggested framework stages. For future SWS modified versions, selecting the proper industries, products, and processes is subjected to the decision-makers and customers demands.

In addition to the eco-efficiency and its aspects, the work effort and ergonomics may be significant KRIs for the decision-makers in manually performed activities. Therefore, they have to be covered in future SWS versions by specialized measurement methods and sensor nodes to enable the time-dependent assessment of them as well. From the SWS results in general and specifically the real-time identification of elementary flows, the UPs and activities can be described and modeled dynamically based on the interpreted correlations between these elementary flows. To achieve that in the future, solutions from the field of artificial intelligence (AI) can be implemented to enhance the required additional data processing algorithms and functionalities within the SWS. For instance, the activity of transporting the rolls to WS_1 can be automatically identified when labors are detected and the roll is positioned on its rack. Such activity identification capability can play a significant role in generating the digital procedure guides for a production as well as auditing them automatically. Adopting the

time-dependent eco-efficiency assessment in identifying the data-based impacts of all elementary flows related to the focal functional unit can be one of the outlooks from this work. The concept of SWS may be adoptable to provide the initial data for such characterization factors in other product systems. This can be significant, especially when it is applied to the life-cycle stages prior to the assessed one. For instance, the production of the raw input materials such as fiber, matrix, and core material can be assessed with the help of an upgraded SWS concept based on the one introduced in this thesis. Moreover, policy makers can have a role in enhancing such data-based assessment approaches to avoid the uncertainty of assumption based results.

In addition to the SWS, the EEAM can be enhanced to include time-dependent characterization factors as well. Moreover, the direct cost to carbon footprint ratio can be further investigated to conclude a unified aimed value of it on each assessment level. In the future, the EEAM and SWS should be standalone DSSs. In other words, the decision-makers in a field should have versions of these DSSs, that are capable of performing iterative time-dependent assessments for various scenarios with no or very limited adjustment efforts. In the future, these DSSs should cover all process and product variants, that are carried out within the facility to provide a comprehensive assistance for the decision-makers.

Commercializing the next versions of these DSSs can be a sufficient solution for enhancing them and their industrial implementation. However, market studies and business cases are required to answer questions about suitable industries, customer demands, operation models, and systems expenses for the next modifications in the SWS concept. In addition, further comparison capabilities between the assessed process scenarios are to be enhanced in the future EEAM-GUI versions as well. Zooming in and out, choosing specific elementary flows or time slots, and presenting temporal noncumulative results are characteristics that some decision-makers may need in the future EEAM versions. In the EEAM, the sparse matrix may be applied to reduce the data size, while tuples may also replace the sets. Moreover, a better rounding algorithms may be developed to avoid the 0.1 % deviation that has been detected in the results.

In the era of sustainability enhancement and possibly forced regulations of it, suppliers may be obligated to provide products with carbon footprint resume in the future. In such cases, the capability of generating a digital identity documentation about various KRIs including eco-efficiency may be a prerequisite for every product supplier. This necessitates the implementation of such automated time-dependent eco-efficiency DSSs. In a smart factory, advanced controlling systems may be needed to control the process in real-time and to adjust the economic and ecological impacts based on the customer demands. To stay competitive in such case, production technology developers also need a clear time-dependent description for the impacts from their solutions in each UP.

While decreasing both impacts is an obvious goal for any decision-maker, prioritizing one of them in each scenario may be a customization requirement. For instance, some decision-makers may prefer a process scenario with slightly high direct cost, if it offers a reduced carbon footprint. This can be practically based on their will or on authority forced regulations. On the other hands, some decision-makers may prefer the other way around to reduce the cost while having an acceptable environmental burden. Moreover, the introduced DSSs in this work enable future studies about each implemented equipment type and its belonging devices by assessing the time-dependent eco-efficiency of their containing UPs.

In conclusion, this thesis has introduced a framework and DSSs for time-dependent eco-efficiency assessment, that may be implemented to enhance the understanding of various aspects within a wide range of considerable products and processes. However, this thesis includes a single validation case study of selected UPs from manufacturing vertical stabilizer ribs by the EVo-platform for a commercial aircraft in aerospace industry.

Bibliography

[1] Abowd, G. D., Atkeson, C. G., Bobick, A. F., Essa, I. A., MacIntyre, B., Mynatt, E. D., and Starner, T. E. (2000, April 1-6). Living laboratories: the future computing environments group at the Georgia Institute of Technology. In *CHI'00 Extended Abstracts on Human Factors in Computing Systems*, pages 215–216. ACM.

[2] Adolphs, P. (2015). RAMI 4.0: An Architectural Model for Industrie 4.0. Technical report, Plattform Industrie 4.0. https://www.omg.org/news/meetings/tc/berlin-15/special-events/mfg-presentations/adolphs.pdf.

[3] Adolphs, P., Auer, S., Bedenbender, H., Billmann, M., Hankel, M., Heidel, R., and Hoffmeister, M. (2016). Structure of the Administration Shell: Continuation of the Development of the Reference Model for the Industrie 4.0 Component. Technical report, Plattform Industrie4.0: Federal Ministry for Economic Affairs and Energy (BMWi). https://www.academia.edu/35536663/Structure_of_the_Administration_Shell_Continuation_of_the_Development_of_the_Reference_Model_for_the_Industrie_4_0_Componen.

[4] Advani, S. G. and Sozer, E. M. (2010). *Process modeling in composites manufacturing*. CRC Press.

[5] Al-Habaibeh, A. and Parkin, R. (2003). An autonomous low-cost infrared system for the on-line monitoring of manufacturing processes using novelty detection. *The International Journal of Advanced Manufacturing Technology*, 22(3-4):249–258.

[6] Al-Lami, A. (2017). Smart-Work-Station (SWS) – concept of real-time eco-efficiency assessment in composite manufacturing. In *Innovation Report 2017 Institute of Composite Structures and Adaptive System*, pages 62–63.

[7] Al-Lami, A. (2018). Verfahren und Vorrichtung zum Bestimmen der in einen Fertigungsprozess eingebrachten Energie. German pending Patent DE 10 2016 120 555 A1.

[8] Al-Lami, A. and Hilmer, P. (2014). Assessment of composite manufacturing process variation with the help of a process model. [Study thesis, Technical University of Braunschweig].

[9] Al-Lami, A. and Hilmer, P. (2015a). Implementing LEAN and Six-Sigma: a case study in developing the composites production process economically and ecologically. [Study thesis, Technical University of Braunschweig].

[10] Al-Lami, A. and Hilmer, P. (2015b). Life-cycle assessment and life-cycle cost analysis for manufacturing and assembly of complex composite structures. [Master thesis, Technical University of Braunschweig].

[11] Al-Lami, A. and Hilmer, P. (2016, October 26-27). Novel applications in assessing manufacturing and assembly of complex composite structures a pace towards Industry 4.0 in composite manufacturing. In *11th AIRTEC Congress, Munich, Germany*. https://elib.dlr.de/118781/1/Airtec_27.10_v063.pdf.

[12] Al-Lami, A., Hilmer, P., and Kleineberg, M. (2016, August 24-25). Cost modeling in composite manufacturing and assembly. In *7th International Symposium on Composites Manufacturing for High Performance Applications, Braunschweig, Germany*.

[13] Al-Lami, A., Hilmer, P., and Sinapius, M. (2018). Eco-efficiency assessment of manufacturing carbon fiber reinforced polymers (CFRP) in aerospace industry. *Aerospace Science and Technology*, 79:669–678.

[14] Albiol, A., Mora, I., and Naranjo, V. (2001). Real-time high density people counter using morphological tools. *IEEE Transactions on Intelligent Transportation Systems*, 2(4):204–218.

[15] Allison, I. K. (1996). Executive information systems: An evaluation of current UK practice. *International Journal of Information Management*, 16(1):27–38.

[16] Ameri, F. and Dutta, D. (2005). Product lifecycle management: closing the knowledge loops. *Computer-Aided Design and Applications*, 2(5):577–590.

[17] Anderson, C. L. (1987). The production process: Inputs and wastes. *Journal of Environmental Economics and Management*, 14(1):1–12.

[18] Anderson, L. W. and Sosniak, L. A. (1994). *Bloom's Taxonomy*. Univ. Chicago Press.

[19] Angerer, C., Langwieser, R., and Rupp, M. (2010). RFID reader receivers for physical layer collision recovery. *IEEE Transactions on Communications*, 58(12):3526–3537.

[20] Arnott, D. and Pervan, G. (2005). A critical analysis of decision support systems research. *Journal of Information Technology*, 20(2):67–87.

[21] Asiedu, Y. and Gu, P. (1998). Product life cycle cost analysis: state of the art review. *International Journal of Production Research*, 36(4):883–908.

[22] Atkinson, R. (1999). Project management: cost, time and quality, two best guesses and a phenomenon, its time to accept other success criteria. *International Journal of Project Management*, 17(6):337–342.

[23] Attaran, M. (2004). Exploring the relationship between information technology and business process reengineering. *Information & Management*, 41(5):585–596.

[24] Ayres, R. U. and Ayres, L. (2002). *A handbook of industrial ecology*. Elgar Publishing.

[25] Baitz, M., Colodel, C. M., Kupfer, T., Florin, J., Schuller, Oliver; Kokborg, M. K. A. T. D. S. A. S. S. G. J. R. M., and Liedke, A. (2014). GaBi Database & Modelling Principles 2014. Technical report, PE-International. http://www.gabi-software.com/uploads/media/GaBi_Modelling_Principles_2014.pdf.

[26] Bamber, C., Castka, P., Sharp, J., and Motara, Y. (2003). Cross-functional team working for overall equipment effectiveness (OEE). *Journal of Quality in Maintenance Engineering*, 9(3):223–238.

[27] Bamji, C. (2001). CMOS-compatible three-dimensional image sensor IC. US Patent 6,323,942.

[28] Barber, K. D., Dewhurst, F. W., Burns, R., and Rogers, J. (2003). Business-process modelling and simulation for manufacturing management: A practical way forward. *Business Process Management Journal*, 9(4):527–542.

[29] Barnett, M. (2003). Modeling & simulation in business process management. *BP Trends Newsletter, White Papers & Technical Briefs*, 10(1):1–10.

[30] Bauerdick, C. J., Helfert, M., Menz, B., and Abele, E. (2017). A common software framework for energy data based monitoring and controlling for machine power peak reduction and workpiece quality improvements. *Procedia CIRP*, 61:359–364.

[31] Bechtold, J., Kern, A., Lauenstein, C., and Bernhofer, L. (2014). Industry 4.0-The Capgemini Consulting View. *Capgemnini Consulting*, 31:32–33. https://www.academia.edu/10569438/Industry_4_0_The_Capgemini_Consulting_View_Sharpening_the_Picture_beyond_the_Hype.

[32] Becker, T. (2005). *Prozesse in Produktion und Supply Chain Optimieren*. Springer.

[33] Beer, S. (1994). *Decision and Control: The Meaning of Operational Research and Management Cybernetics*. Wiley.

[34] Bellman, R. E. and Zadeh, L. A. (1970). Decision-making in a fuzzy environment. *Management Science*, 17(4):B–141.

[35] Bharath, P., Ananth, N., Vijetha, S., and Prakash, K. J. (2008, November). Wireless automated digital energy meter. In *2008 IEEE International Conference on Sustainable Energy Technologies*, pages 564–567. IEEE.

[36] Björnsson, A. (2014). Enabling Automation of Composite Manufacturing through the Use of Off-The-Shelf Solutions. [PhD thesis. Linköping University].

[37] Bollerslev, T. and Wright, J. H. (2001). High-frequency data, frequency domain inference, and volatility forecasting. *Review of Economics and Statistics*, 83(4):596–602.

[38] Borghese, N. A., Ferrigno, G., Baroni, G., Pedotti, A., Ferrari, S., and Savarè, R. (1998). Autoscan: A flexible and portable 3d scanner. *IEEE Computer Graphics and Applications*, 18(3):38–41.

[39] Brander, M., Tipper, R., Hutchison, C., and Davis, G. (2008). Technical paper: Consequential and attributional approaches to LCA: a guide to policy makers with specific reference to greenhouse gas LCA of biofuels. http://www.globalbioenergy.org/uploads/media/0804_Ecometrica_-_Consequential_and_attributional_approaches_to_LCA.pdf.

[40] Bregler, C. (2007). Motion capture technology for entertainment [in the spotlight]. *IEEE Signal Processing Magazine*, 24(6):160–158.

[41] Breidenich, C., Magraw, D., Rowley, A., and Rubin, J. W. (1998). The Kyoto protocol to the United Nations framework convention on climate change. *American Journal of International Law*, 92(2):315–331.

[42] Brettel, M., Friederichsen, N., Keller, M., and Rosenberg, M. (2014). How virtualization, decentralization and network building change the manufacturing landscape: An Industry 4.0 Perspective. *International Journal of Mechanical, Industrial Science and Engineering*, 8(1):37–44.

[43] Brumitt, B., Meyers, B., Krumm, J., Kern, A., and Shafer, S. (2000). Easyliving: Technologies for intelligent environments. In *Handheld and ubiquitous computing*, pages 97–119. Springer.

[44] Bruns, R. W. (1998). Helical load cell. US Patent 5,714,695.

[45] Burbano, A., Bouaziz, S., and Vasiliu, M. (2015, December). 3D-sensing distributed embedded system for people tracking and counting. In *2015 International Conference on Computational Science and Computational Intelligence (CSCI)*, pages 470–475. IEEE.

[46] Callister, W. D., Rethwisch, D. G., et al. (2007). *Materials Science and Engineering: an introduction*. Wiley.

[47] Carraher, D. W., Martinez, M. V., and Schliemann, A. D. (2008). Early algebra and mathematical generalization. *ZDM*, 40(1):3–22.

[48] Cengel, Y. A. and Boles, M. A. (2008). *Thermodynamics An Engineering Approach*. McGraw-Hill.

[49] Cerdas, F., Thiede, S., Juraschek, M., Turetskyy, A., and Herrmann, C. (2017). Shop-floor life cycle assessment. *Procedia CIRP*, 61:393–398.

[50] Chahuara, P., Fleury, A., Portet, F., and Vacher, M. (2012). Using markov logic network for on-line activity recognition from non-visual home automation sensors. *Ambient Intelligence*, pages 177–192.

[51] Champy, J. and Cohen, L. (1995). *Reengineering Management*. Dunod.

[52] Chan, A. P. and Chan, A. P. (2004). Key performance indicators for measuring construction success. *Benchmarking: an International Journal*, 11(2):203–221.

[53] Chan, J. C., Leung, H., Tang, J. K., and Komura, T. (2011). A virtual reality dance training system using motion capture technology. *IEEE Transactions on Learning Technologies*, 4(2):187–195.

[54] Chang, C. M. (2005). *Engineering Management: challenges in the new millennium*. Pearson Education.

[55] Chang, K., Liu, S., Chu, H., Hsu, J. Y., Chen, C., Lin, T., Chen, C., and Huang, P. (2006, May 7-10). The diet-aware dining table: Observing dietary behaviors over a tabletop surface. In *International Conference on Pervasive Computing, Dublin, Ireland*, pages 366–382. Springer.

[56] Chen, D. and Doumeingts, G. (1996). The GRAI-GIM reference model, architecture and methodology. In *Architectures for Enterprise Integration*, pages 102–126. Springer.

[57] Chorin, A. J., Marsden, J. E., and Marsden, J. E. (1990). *A mathematical Introduction to Fluid Mechanics*. Volume 3. Springer.

[58] Ciroth, A., Theret, J.-P., Fliegner, M., Srocka, M., Bläsig, V., and Duyan, Ö. (2013). Integrating life cycle assessment tools and information with product life cycle management. *11 th Global Conference on Sustainable Manufacturing - Innovative Solutions*, pages 210–212.

[59] Clarke, J. (2002). Device and method for data timestamping. US Patent App. 10/073,261.

[60] Collinge, W. O., Landis, A. E., Jones, A. K., Schaefer, L. A., and Bilec, M. M. (2013). Dynamic life cycle assessment: framework and application to an institutional building. *The International Journal of Life Cycle Assessment*, 18(3):538–552.

[61] Collins Jr, D. A., Aleshire, R. A., Hammer, S. J., and Orwig, W. L. (2004). Checkout device including barcode reading apparatus, scale, and EAS system. US Patent 6,764,010.

[62] Cortés, U., Sànchez-Marrè, M., Ceccaroni, L., R-Roda, I., and Poch, M. (2000). Artificial intelligence and environmental decision support systems. *Applied Intelligence*, 13(1):77–91.

[63] Costanza, R. and Patten, B. C. (1995). Defining and predicting sustainability. *Ecological Economics*, 15(3):193–196.

[64] Cowling, K. and Waterson, M. (1976). Price-cost margins and market structure. *Economica*, 43(171):267–274.

[65] Čuček, L., Klemeš, J. J., and Kravanja, Z. (2012). A review of footprint analysis tools for monitoring impacts on sustainability. *Journal of Cleaner Production*, 34:9–20.

[66] Curran, R., Raghunathan, S., and Price, M. (2004). Review of aerospace engineering cost modelling: The genetic causal approach. *Progress in Aerospace Sciences*, 40(8):487–534.

[67] da Silva, C. G., Figueira, J., Lisboa, J., and Barman, S. (2006). An interactive decision support system for an aggregate production planning model based on multiple criteria mixed integer linear programming. *Omega*, 34(2):167–177.

[68] Da Silveira, G., Borenstein, D., and Fogliatto, F. S. (2001). Mass customization: Literature review and research directions. *International Journal of Production Economics*, 72(1):1–13.

[69] Dababneha, O. and Kipouros, T. (2017). A review of aircraft wing mass estimation methods. *Aerospace Science and Technology*, 72:256–266.

[70] Danna, D. and Newman, R. W. (1985). Image sensor assembly. US Patent 4,491,865.

[71] Davies, R. (2015). Industry 4.0: Digitalisation for productivity and growth. Technical report, European Parliamentary Research Service (EPRS).

[72] Davis, W. J., Jackson, R. H., and Jones, A. T. (1989, February). Real-time optimization in the automated manufacturing research facility. In *Progress in Materials Handling and Logistics*, pages 257–274. Springer.

[73] Denkhaus, J. and Hilmer, P. (2014). Economical and Environmental Assessment of CFRP Manufacturing Process Variations with Special Regards to Production Equipment. [Bachelor thesis, Technical University of Braunschweig].

[74] Derwall, J., Guenster, N., Bauer, R., and Koedijk, K. (2005). The eco-efficiency premium puzzle. *Financial Analysts Journal*, 61(2):51–63.

[75] DeSimone, L. D. and Popoff, F. (2000). *Eco-efficiency: the business link to sustainable development*. MIT Press.

[76] Dodig Crnkovic, G. (2012). Information and energy/matter. *Information*, 3:751–755.

[77] Dorf, R. C. and Bishop, R. H. (2008). *Modern control systems*. Pearson.

[78] Dorst, W. (2016). Implementation Strategy Industrie 4.0: Report on the results of the Industrie 4.0 Platform. Technical report, Bundesverband Informationswirtschaft, Telekommunikation und neue Medien e. V. (Bitkom e.V.). https://www.bitkom.org/Bitkom/Publikationen/Implementation-Strategy-Industrie-40-Report-on-the-results-of-the-Industrie-40-Platform.html.

[79] Doumeingts, G. and Chen, D. (1996). Architectures for Enterprise Integration State-of-the-art on models, architectures and methodologies. *IFIP Advances in Information and Communication Technology*, pages 32–59.

[80] Drath, R. and Horch, A. (2014). Industrie 4.0: Hit or hype?[industry forum]. *IEEE Industrial Electronics Magazine*, 8(2):56–58.

[81] Drira, A., Pierreval, H., and Hajri-Gabouj, S. (2007). Facility layout problems: A survey. *Annual Reviews in Control*, 31(2):255–267.

[82] Drucker, P. F. (1986). *Management: Tasks, Responsibilities, Practices*. Talley Books.

[83] Dumitrescu, R. (2010). Entwicklungssystematik zur integration kognitiver funktionen in fortgeschrittene mechatronische systeme. [PhD thesis, Albert-Ludwigs-University of Freiburg].

[84] Dunham, M. H. (2002). *Data mining: Introductory and advanced topics*. Pearson Education India.

[85] Dyckhoff, H. and Spengler, T. S. (2010). *Produktionswirtschaft: Eine Einführung*. Springer.

[86] Dyllick, T. and Hockerts, K. (2002). Beyond the business case for corporate sustainability. *Business Strategy and the Environment*, 11(2):130–141.

[87] Dysert, L. R. (2008). An Introduction to Parametric Estimating. *AACE International Transactions*, page ES31.

[88] Ebbesen, J. B. and Hope, A. (2013). Re-imagining the iron triangle: embedding sustainability into project constraints. *PM World Journal*, 2:1–13.

[89] Ehrenfeld, J. R. (2005). Eco-efficiency. *Journal of Industrial Ecology*, 9(4):6–8.

[90] Eigner, M. (2014). Product Lifecycle Management (PLM). In *Modellbasierte virtuelle Produktentwicklung*, chapter 11, pages 267–300. Springer, Berlin.

[91] Ekvall, T., Azapagic, A., Finnveden, G., Rydberg, T., Weidema, B. P., and Zamagni, A. (2016). Attributional and consequential LCA in the ILCD handbook. *The International Journal of Life Cycle Assessment*, 21(3):293–296.

[92] El Gamal, A. and Eltoukhy, H. (2005). CMOS image sensors. *IEEE Circuits and Devices Magazine*, 21(3):6–20.

[93] El Kelety, I. (2006). Towards a conceptual framework for strategic cost management-the concept, objectives, and instruments. [PhD thesis, Technische Universität Chemnitz].

[94] Ellram, L. M. (1995). Total cost of ownership: an analysis approach for purchasing. *International Journal of Physical Distribution & Logistics Management*, 25(8):4–23.

[95] Erlach, K. (2010). Wertstromdesign–Der Weg zur schlanken Fabrik, 2. aktualisierte Auflage. *Berlin Heidelberg*.

[96] European Environment Agency (EEA) (2012). Total greenhouse gas emissions by sector (%) in EU-27, 2009. Technical report. https://www.eea.europa.eu/data-and-maps/figures/total-greenhouse-gas-emissions-by-sector-in-eu-1.

[97] European Environment Agency (EEA) (2019). European Union emission inventory report 1990-2017: under the UNECE Convention on Long-range Transboundary Air Pollution (LRTAP). Technical report. https://www.eea.europa.eu/publications/european-union-emissions-inventory-report-2017.

[98] Fan, W. and Bifet, A. (2013). Mining big data: current status, and forecast to the future. *ACM sIGKDD Explorations Newsletter*, 14(2):1–5.

[99] Fan, Z., Ho, J. C., Jacobson, Z. A., Razavi, H., and Javey, A. (2008). Large-scale, heterogeneous integration of nanowire arrays for image sensor circuitry. *Proceedings of the National Academy of Sciences*, 105(32):11066–11070.

[100] Fayyad, U., Piatetsky-Shapiro, G., and Smyth, P. (1996). From data mining to knowledge discovery in databases. *AI Magazine*, 17(3):37.

[101] Fernández-Caballero, A., Castillo, J. C., Martínez-Cantos, J., and Martínez-Tomás, R. (2010). Optical flow or image subtraction in human detection from infrared camera on mobile robot. *Robotics and Autonomous Systems*, 58(12):1273–1281.

[102] Ferriter, K. M. and Mathis, R. B. (1989). Automated bill of material. US Patent 4,847,761.

[103] Ferriter, K. M. and Palmer, E. R. (1989). Bill of material interface to CAD/CAM environment. US Patent 4,862,376.

[104] Finkbeiner, M., Schau, E. M., Lehmann, A., and Traverso, M. (2010). Towards life cycle sustainability assessment. *Sustainability*, 2(10):3309–3322.

[105] Finnveden, G., Hauschild, M. Z., Ekvall, T., Guinée, J., Heijungs, R., Hellweg, S., Koehler, A., Pennington, D., and Suh, S. (2009). Recent developments in life cycle assessment. *Journal of Environmental Management*, 91(1):1–21.

[106] Fleck, S., Busch, F., Biber, P., and Straber, W. (2006, June 17-22). 3D surveillance a distributed network of smart cameras for real-time tracking and its visualization in 3D. In *2006 Conference on Computer Vision and Pattern Recognition Workshop (CVPRW'06)*, page 118. IEEE.

[107] Focken, D. and Stiefelhagen, R. (2002). Towards vision-based 3-d people tracking in a smart room. In *Proceedings. Fourth IEEE International Conference on Multimodal Interfaces*, pages 400–405. IEEE.

[108] Freeman, B. S. (1998). Digital phase locked loop signal processing for coriolis mass flow meter. US Patent 5,804,741.

[109] French, S. (2013). Cynefin, statistics and decision analysis. *Journal of the Operational Research Society*, 64(4):547–561.

[110] Frické, M. (2009). The knowledge pyramid: a critique of the dikw hierarchy. *Journal of Information Science*, 35(2):131–142.

[111] Ganapathi, V., Plagemann, C., Koller, D., and Thrun, S. (2010, June). Real time motion capture using a single time-of-flight camera. In *Computer Vision and Pattern Recognition (CVPR), 2010 IEEE Conference on*, pages 755–762. IEEE.

[112] Gao, W., Emaminejad, S., Nyein, H. Y. Y., Challa, S., Chen, K., Peck, A., Fahad, H. M., Ota, H., Shiraki, H., Kiriya, D., et al. (2016). Fully integrated wearable sensor arrays for multiplexed in situ perspiration analysis. *Nature*, 529(7587):509–514.

[113] García, J., Gardel, A., Bravo, I., Lázaro, J. L., Martínez, M., and Rodríguez, D. (2013). Directional people counter based on head tracking. *IEEE Transactions on Industrial Electronics*, 60(9):3991–4000.

[114] Gay, D. (2014). *Composite materials: design and applications*. CRC Press.

[115] Georgescu-Roegen, N. (1970). The economics of production. *The American Economic Review*, 60(2):1–9.

[116] Goedkoop, M., De Schryver, A., Oele, M., Durksz, S., and de Roest, D. (2008). Introduction to LCA with SimaPro 7. *PRé Consultants, The Netherlands*. https://www.pre-sustainability.com/download/SimaPro8IntroductionToLCA.pdf.

[117] Gottmann, J. (2016). *Produktionscontrolling: Wertströme und Kosten optimieren*. Springer.

[118] Goubet, E., Katz, J., and Porikli, F. (2006). Pedestrian tracking using thermal infrared imaging. In *Infrared Technology and Applications XXXII*. Volume 6206, page 62062C. International Society for Optics and Photonics.

[119] Gupta, M. P. K. and Chandrawat, M. S. S. (2012). To improve work force productivity in a medium size manufacturing enterprise by MOST Technique. *IOSR Journal of Engineering*, 2(10):8–15.

[120] Gurumurthy, A. and Kodali, R. (2011). Design of lean manufacturing systems using value stream mapping with simulation: a case study. *Journal of Manufacturing Technology Management*, 22(4):444–473.

[121] Gutowski, T., Dahmus, J., and Thiriez, A. (2006, May). Electrical energy requirements for manufacturing processes. In *13th CIRP international conference on life cycle engineering*. Volume 31, page 623-638. CIRP International Leuven, Belgium.

[122] Gutowski, T., Hoult, D., Dillon, G., Neoh, E.-T., Muter, S., Kim, E., and Tse, M. (1994). Development of a theoretical cost model for advanced composite fabrication. *Composites Manufacturing*, 5(4):231–239.

[123] Hagedorn, C., Torstrick, S., and Reinhard, B. (2015). Optimierung der roboterbasierten feinbesäumung von kohlenstofffaserpreforms im end-konturnahen preformingprozess. [Bachelor thesis, Hamburg University of Applied Sciences].

[124] Hagnell, M. and Åkermo, M. (2015). A composite cost model for the aeronautical industry: Methodology and case study. *Composites Part B: Engineering*, 79:254–261.

[125] Han, J. and Bhanu, B. (2005, September). Human activity recognition in thermal infrared imagery. In *2005 IEEE Computer Society Conference on Computer Vision and Pattern Recognition (CVPR'05)-Workshops*, page 17. IEEE.

[126] Han, J. and Bhanu, B. (2007). Fusion of color and infrared video for moving human detection. *Pattern Recognition*, 40(6):1771–1784.

[127] Han, J., Zhang, D., Cheng, G., Guo, L., and Ren, J. (2014). Object detection in optical remote sensing images based on weakly supervised learning and high-level feature learning. *IEEE Transactions on Geoscience and Remote Sensing*, 53(6):3325–3337.

[128] Hankel, M. and Rexroth, B. (2015). The Reference Architectural Model Industrie 4.0 (RAMI 4.0). Technical report, ZVEI - German Electrical and Electronic Manufacturers' Association. http://przemysl-40.pl/wp-content/uploads/2010-The-Reference-Architectural-Model-Industrie-40.pdf.

[129] Hansen, J., Sato, M., and Ruedy, R. (1997). Radiative forcing and climate response. *Journal of Geophysical Research: Atmospheres*, 102(D6):6831–6864.

[130] Harkin, G. F. (2003). Image sensor. US Patent 6,583,398.

[131] Hashimoto, K., Morinaka, K., Yoshiike, N., Kawaguchi, C., and Matsueda, S. (1997, June). People count system using multi-sensing application. In *Solid State Sensors and Actuators, 1997. TRANSDUCERS'97 Chicago., 1997 International Conference on*. Volume 2, pages 1291–1294. IEEE.

[132] Helminen, R.-R. (2000). Developing tangible measures for eco-efficiency: the case of the Finnish and Swedish pulp and paper industry. *Business Strategy and the Environment*, 9(3):196.

[133] Henry, M., Clarke, D., Archer, N., Bowles, J., Leahy, M., Liu, R., Vignos, J., and Zhou, F. (2000). A self-validating digital coriolis mass-flow meter: an overview. *Control Engineering Practice*, 8(5):487–506.

[134] Herrmann, C. and Kara, S. (2012). *Sustainable Production, Life Cycle Engineering and Management*. Springer.

[135] Hesselbach, J. and Herrmann, C. (2011). *Glocalized Solutions for Sustainability in Manufacturing: Proceedings of the 18th CIRP International Conference on Life Cycle Engineering*. Springer Science.

[136] Hibino, H. and Yanaga, K. (2017). Decision support for energy-saving idle production facility operations in a production line based on an M2M environment. *Procedia CIRP*, 61:399–403.

[137] Higgins, N., Vyatkin, V., Nair, N.-K. C., and Schwarz, K. (2011). Distributed power system automation with iec 61850, iec 61499, and intelligent control. *IEEE Transactions on Systems, Man, and Cybernetics, Part C (Applications and Reviews)*, 41(1):81–92.

[138] Hilmer, P. (2016). Ressourceneffizienz von Fertigungsverfahren für Faserverbundwerkstoffe. [PhD thesis, Technical University of Braunschweig].

[139] Hischier, R., Baitz, M., Bretz, R., Frischknecht, R., Jungbluth, N., Marheineke, T., McKeown, P., Oele, M., Osset, P., Renner, I., et al. (2001). Guidelines for consistent reporting of exchanges/to nature within life cycle inventories (LCI). *The International Journal of Life Cycle Assessment*, 6(4):192.

[140] Hlupic, V. and Robinson, S. (1998, December). Business process modelling and analysis using discrete-event simulation. In *Proceedings of the 30th conference on Winter simulation*, pages 1363–1370. IEEE Computer Society Press.

[141] Hoa, S. V. (2009). *Principles of the manufacturing of composite materials*. DEStech Publications.

[142] Hoegh-Guldberg, O., Jacob, D., and Michael, T. (2018). Impacts of 1.5°C of Global Warming on Natural and Human Systems. Technical report, Intergovernmental Panel on Climate Change (IPCC).

[143] Holmquist, L. E., Gellersen, H.-W., Kortuem, G., Antifakos, S., Michahelles, F., Schiele, B., Beigl, M., and Mazé, R. (2004). Building intelligent environments with smart-its. *IEEE Computer Graphics and Applications*, 24(1):56–64.

[144] Houghton, J., Callander, B., and Varney, S. (1992). *Climate Change 1992: The Supplementary Report to the IPCC Scientific Assessment*. Cambridge University Press.

[145] Houghton, J. T. (1996). *Climate change 1995: The science of climate change: contribution of working group I to the second assessment report of the Intergovernmental Panel on Climate Change*. Volume 2. Cambridge University Press.

[146] Howard, A. G., Zhu, M., Chen, B., Kalenichenko, D., Wang, W., Weyand, T., Andreetto, M., and Adam, H. (2017). Mobilenets: Efficient convolutional neural networks for mobile vision applications. *arXiv preprint arXiv:1704.04861*.

[147] Huppes, G. and Ishikawa, M. (2005). Eco-efficiency and Its xsTerminology. *Journal of Industrial Ecology*, 9(4):43–46.

[148] Inaba, A., Chevassus, S., Cumberlege, T., Hong, E., Kataoka, A., Lohsomboon, P., Mercadie, C., Mungcharoen, T., and Radunsky, K. (2016). Carbon footprint of products. In *Special Types of Life Cycle Assessment*, pages 11–71. Springer.

[149] International Air Transport Association (IATA) and Deutsches Zentrum für Luft- und Raumfahrt e.V. (DLR) and Georgia Institute of Technology (2013). IATA Technology roadmap. Technical report, IATA.

[150] International Organization for Standardization (ISO) (1998). EN ISO 14041 Umweltmanagement, Ökobilanz: Festlegung des Ziels und des Untersuchungsrahmens sowie Sachbilanz.

[151] International Organization for Standardization (ISO) (2006). ISO14044 Environmental management – Life cycle assessment – Requirements and guidelines.

[152] International Organization for Standardization (ISO) (2009). ISO14040: Environmental management – Life cycle assessment – Principles and framework.

[153] International Organization for Standardization (ISO) (2012). DIN EN ISO 14045: Environmental management – Eco-efficiency assessment of product systems – Principles, requirements and guidelines.

[154] International Organization for Standardization (ISO) (2014). DIN CEN ISO/TS 14067: Greenhouse gases – Carbon footprint of products –Requirements and guidelines for quantification and communication.

[155] Intille, S. S., Tapia, E. M., Rondoni, J., Beaudin, J., Kukla, C., Agarwal, S., Bao, L., and Larson, K. (2003, October). Tools for studying behavior and technology in natural settings. In *UbiComp*, pages 157–174. Springer.

[156] Jasch, C. M. (2008). *Environmental and material flow cost accounting: principles and procedures*. Volume 25. Springer Science.

[157] Jensen, C. S. and Snodgrass, R. T. (1999). Temporal data management. *IEEE Transactions on Knowledge and Data Engineering*, 11(1):36–44.

[158] John III, G. C. (2002). Item processing device with barcode reader and integrated RFID interrogator. US Patent 20,020,145,037.

[159] Jolliet, O., Margni, M., Charles, R., Humbert, S., Payet, J., Rebitzer, G., and Rosenbaum, R. (2003). IMPACT 2002+: a new life cycle impact assessment methodology. *The International Journal of Life Cycle Assessment*, 8(6):324.

[160] Jones, B. F. and Plassmann, P. (2002). Digital infrared thermal imaging of human skin. *IEEE Engineering in Medicine and Biology Magazine*, 21(6):41–48.

[161] Jufer, N., Politze, D. P., Bathelt, J., and Kunz, A. (2011). Performance Factory–A new approach of performance assessment for the Factory of the Future. *Estonian Journal of Engineering*, 18(1):42–57.

[162] Kalal, Z., Mikolajczyk, K., and Matas, J. (2011). Tracking-learning-detection. *IEEE Transactions on Pattern Analysis and Machine Intelligence*, 34(7):1409–1422.

[163] Kamin, K. A. and Rachlinski, J. J. (1995). Ex post≠ ex ante: Determining liability in hindsight. *Law and Human Behavior*, 19(1):89.

[164] Kappel, E., Stefaniak, D., and Hühne, C. (2014, June 24-25). Process-induced Distortions in CFRP Manufacturing: A bottle-neck for high-rate Production Scenarios. In *8th CFK Valley Stade Convention*, pages 86–94.

[165] Kärkkäinen, H., Piippo, P., and Tuominen, M. (2001). Ten tools for customer-driven product development in industrial companies. *International Journal of Production Economics*, 69(2):161–176.

[166] Kasai, J. (1999). Life cycle assessment, evaluation method for sustainable development. *JSAE Review*, 20(3):387–394.

[167] Kaufmann, U. H. (2012). *Praxisbuch Lean Six Sigma*. Hanser.

[168] Kawahito, S. (2008). Distance image sensor. US Patent 7,436,496.

[169] Khan, M. E., Khan, F., et al. (2012). A comparative study of white box, black box and grey box testing techniques. *International Journal of Advanced Computer Sciences and Applications*, 3(6):12–1.

[170] Kilger, W. (2013). *Flexible Plankostenrechnung und Deckungsbeitragsrechnung*. Springer.

[171] Kim, J.-W., Choi, K.-S., Choi, B.-D., and Ko, S.-J. (2002, July). Real-time vision-based people counting system for the security door. In *International Technical Conference on Circuits/Systems Computers and Communications*, pages 1416–1419.

[172] Kim, Y. H., Sting, F. J., and Loch, C. H. (2014). Top-down, bottom-up, or both? Toward an integrative perspective on operations strategy formation. *Journal of Operations Management*, 32(7-8):462–474.

[173] Kleineberg, M. (2013). Self-Controlled Composite Processing. In *Adaptive, tolerant and efficient composite structures*, pages 311–316. Springer.

[174] Kloepffer, W. (2008). Life cycle sustainability assessment of products. *The International Journal of Life Cycle Assessment*, 13(2):89.

[175] Klöpffer, W. (2003). *Life-cycle based methods for sustainable product development*. Springer.

[176] Klöpffer, W. and Grahl, B. (2009). *Ökobilanz (LCA): Ein Leitfaden für Ausbildung und Beruf*. Wiley.

[177] Kokubu, K., Campos, M. K. S., Furukawa, Y., and Tachikawa, H. (2009). Material flow cost accounting with ISO 14051. *ISO Management Systems*, 2:15–18.

[178] Kraus, T., Kuhnel, M., and Witten, E. (2014). Composites Market Report 2014. *Federation of Reinforced Plastics, Berlin*.

[179] Krein, A. and Williams, G. (2012). Flightpath 2050: europe's vision for aeronautics. *Innovation for Sustainable Aviation in a Global Environment*, page 63. : Proceedings of the Sixth European Aeronautics Days, Madrid, 30 March-1 April, 2011.

[180] Kriegel, S., Brucker, M., Marton, Z.-C., Bodenmüller, T., and Suppa, M. (2013, November). Combining object modeling and recognition for active scene exploration. In *2013 IEEE/RSJ International Conference on Intelligent Robots and Systems*, pages 2384–2391. IEEE.

[181] Kriegel, S., Rink, C., Bodenmüller, T., and Suppa, M. (2015). Efficient next-best-scan planning for autonomous 3D surface reconstruction of unknown objects. *Journal of Real-Time Image Processing*, 10(4):611–631.

[182] Kumar, S., Marks, T. K., and Jones, M. (2014). Improving person tracking using an inexpensive thermal infrared sensor. In *Proceedings of the IEEE Conference on Computer Vision and Pattern Recognition Workshops*, pages 217–224. IEEE.

[183] Kuosmanen, T. and Kortelainen, M. (2005). Measuring eco-efficiency of production with data envelopment analysis. *Journal of Industrial Ecology*, 9(4):59–72.

[184] Kwon, I., Eo, Y., Bang, H., Choi, K., Jeon, S., Jung, S., Lee, D., and Lee, H. (2008). A single-chip CMOS transceiver for UHF mobile RFID reader. *IEEE Journal of Solid-State Circuits*, 43(3):729–738.

[185] Laney, M. (2011). Sustainable Composites from Natural Materials. [Master thesis, North Carolina State University].

[186] Laring, J., Forsman, M., Kadefors, R., and Örtengren, R. (2002). MTM-based ergonomic workload analysis. *International journal of Industrial ergonomics*, 30(3):135–148.

[187] LeBlanc, D. J. (1976). *Advanced composite cost estimating manual*. Northrop Corporation, Aircraft Division.

[188] Lee, J., Bagheri, B., and Kao, H.-A. (2015). A cyber-physical systems architecture for industry 4.0-based manufacturing systems. *Manufacturing Letters*, 3:18–23.

[189] Lefloch, D., Cheikh, F. A., and Gouton, P. Real-Time People Counting system using Video Camera. [Master thesis, Gjøvik University College].

[190] Lenz, J., Kotschenreuther, J., and Westkaemper, E. (2017). Energy efficiency in machine tool operation by online energy monitoring capturing and analysis. *Procedia CIRP*, 61:365–369.

[191] Leonard, B. (2009). *GAO Cost estimating and assessment guide: best practices for developing and managing capital program costs*. DIANE Publishing. http://www.gao.gov/new.items/d093sp.pdf.

[192] Lerch, R. (2005). *Elektrische Messtechnik*. Volume 1. Springer.

[193] Levasseur, A., Lesage, P., Margni, M., Deschenes, L., and Samson, R. (2010). Considering time in LCA: dynamic LCA and its application to global warming impact assessments. *Environmental Science & Technology*, 44(8):3169–3174.

[194] Levin, A. and Weiss, Y. (2006). Learning to combine bottom-up and top-down segmentation. In *European conference on computer vision*, pages 581–594. Springer.

[195] Lewis, M. and Slack, N. (2003). *Operations management: critical perspectives on business and management*. Volume 1. Taylor.

[196] Li, W. and Kara, S. (2017). Methodology for Monitoring Manufacturing Environment by Using Wireless Sensor Networks (WSN) and the Internet of Things (IoT). *Procedia CIRP*, 61:323–328.

[197] Lim, C. and Mohamed, M. Z. (1999). Criteria of project success: an exploratory re-examination. *International Journal of Project Management*, 17(4):243–248.

[198] Lin, T.-Y., Maire, M., Belongie, S., Hays, J., Perona, P., Ramanan, D., Dollár, P., and Zitnick, C. L. (2014, September). Microsoft coco: Common objects in context. In *European conference on computer vision*, pages 740–755. Springer.

[199] Liu, G., Baniyounes, A., Rasul, M., Amanullah, M., and Khan, M. M. K. (2012). Fuzzy logic based environmental indicator for sustainability assessment of renewable energy system using life cycle assessment. *Procedia Engineering*, 49:35–41.

[200] Liu, W., Anguelov, D., Erhan, D., Szegedy, C., Reed, S., Fu, C.-Y., and Berg, A. C. (2016, October). Ssd: Single shot multibox detector. In *European conference on computer vision*, pages 21–37. Springer.

[201] Logan, B., Healey, J., Philipose, M., Tapia, E. M., and Intille, S. (2007, September). A long-term evaluation of sensing modalities for activity recognition. In *International Conference on Ubiquitous Computing*, pages 483–500. Springer.

[202] Long, A. C. (2005). *Design and manufacture of textile composites*. Elsevier.

[203] Loos, P. (1997). *Produktionslogistik in der chemischen Industrie: Betriebstypologische Merkmale und Informationsstrukturen*. Gabler.

[204] Lu, K. (2010). The future of metals. *Science*, 328(5976):319–320.

[205] Lucke, D., Constantinescu, C., and Westkämper, E. (2008). Smart factory-a step towards the next generation of manufacturing. In *Manufacturing systems and technologies for the new frontier*, pages 115–118. Springer.

[206] Lucke, D. and Wieland, M. (2007). Umfassendes Kontextdatenmodell der Smart Factory als Basis für kontextbezogene Workflow-Anwendungen. *Küpper, Axel (Hrsg.)*, pages 47–51.

[207] Lunenburg, F. C. (2010). THE DECISION MAKING PROCESS. In *National Forum of Educational Administration & Supervision Journal*. 27(4):1–11.

[208] Ma, L., Zhang, W., Fu, H., Guo, Y., Chablat, D., Bennis, F., Sawanoi, A., and Fugiwara, N. (2010). A framework for interactive work design based on motion tracking, simulation, and analysis. *Human Factors and Ergonomics in Manufacturing & Service Industries*, 20(4):339–352.

[209] Madden, K., Young, R., Brady, K., and Hall, J. (2005). Eco-efficiency: Learning Module. Technical report, World Business Council for Sustainable Development, File Winds International.

[210] Mahal, I. and Hossain, M. A. (2015). Activity-Based Costing (ABC)–An Effective Tool for Better Management. *Research Journal of Finance and Accounting*, 6(4):66–74.

[211] Maine, E. and Ashby, M. F. (2000). Cost Estimation and the Vialibity of Metal Foams. *Advanced Engineering Materials*, 2(4):205–209.

[212] Manku, G. S. and Motwani, R. (2002, January). Approximate frequency counts over data streams. In *VLDB'02: Proceedings of the 28th International Conference on Very Large Databases*, pages 346–357. Elsevier.

[213] Marr, B. (2016). Why Everyone Must Get Ready For The 4th Industrial Revolution. *Forbes*.

[214] Marsh, G. (2010). Airbus A350 XWB update. *Reinforced plastics*, 54(6):20–24.

[215] Mårtensson, P., Zenkert, D., and Åkermo, M. (2014, June 22-26). Integral or Differential Design for a Cost Effective Composite Automotive Body Structure. In *16th European Conference on Composite Materials, ECCM 2014, Seville, Spain*.

[216] May, G. and Kiritsis, D. (2017). Business model for energy efficiency in manufacturing. *Procedia CIRP*, 61:410–415.

[217] McAfee, A., Brynjolfsson, E., Davenport, T. H., Patil, D., and Barton, D. (2012). Big data. *The management revolution. Harvard Bus Rev*, 90(10):61–67.

[218] McDonough, W. and Braungart, M. (1998). The next industrial revolution. *The Atlantic Monthly*, 282(4).

[219] McLeod, R. and Schell, G. P. (1998). *Management information systems*. Hall.

[220] Mei, X., Zhou, S. K., and Wu, H. (2006, May). Integrated detection, tracking and recognition for ir video-based vehicle classification. In *2006 IEEE International Conference on Acoustics Speech and Signal Processing Proceedings*, volume 5, pages V–V. IEEE.

[221] Mendis, S. K., Kemeny, S. E., Gee, R. C., Pain, B., Staller, C. O., Kim, Q., and Fossum, E. R. (1997). CMOS active pixel image sensors for highly integrated imaging systems. *IEEE Journal of Solid-State Circuits*, 32(2):187–197.

[222] Mercer, J. H. (1978). West Antarctic ice sheet and CO2 greenhouse effect: a threat of disaster. *Nature*, 271(5643):321–325.

[223] Mizzaro, S. (1997). Relevance: The whole history. *Journal of the American Society for Information Science*, 48(9):810–832.

[224] Moeslund, T. B., Hilton, A., and Krüger, V. (2006). A survey of advances in vision-based human motion capture and analysis. *Computer vision and image understanding*, 104(2-3):90–126.

[225] Möller, A. and Schaltegger, S. (2005). The Sustainability Balanced Scorecard as a Framework for Eco-efficiency Analysis. *Journal of Industrial Ecology*, 9(4):73–83.

[226] Moropoulou, A., Bakolas, A., and Anagnostopoulou, S. (2005). Composite materials in ancient structures. *Cement and concrete composites*, 27(2):295–300.

[227] Naito, K. and Utsunomiya, M. (1986). Load sensor using a piezoelectric SAW device. US Patent 4,623,813.

[228] Neitzel, M., Mitschang, P., and Breuer, U. (2014). *Handbuch Verbundwerkstoffe: Werkstoffe, Verarbeitung, Anwendung*. Hanser.

[229] Nietner, L. F. Shareables: systems for rapid prototyping of IoT devices to broaden participation in engineering design. [PhD thesis, Massachusetts Institute of Technology].

[230] Nill, S. T. Aerospace composite manufacturing cost models as geometric programs. [PhD thesis, Massachusetts Institute of Technology].

[231] Noone, D. R., Bergman, A. S., and Lynch, R. K. (2015). Method and system for people counting using passive infrared detectors. US Patent 9,183,686.

[232] Norris, G. A. (2001). Integrating life cycle cost analysis and LCA. *The International Journal of Life Cycle Assessment*, 6(2):118–120. The international journal of life cycle assessment.

[233] Nothdurft, N. and Hilmer, P. (2016). Integrierte Umweltkostenrechnung von Faserverbundfertigungsprozessen am Beispiel einer CFK-Flügelrippe. [Master thesis, Technical University of Braunschweig].

[234] Oberkampf, W. L., Trucano, T. G., and Hirsch, C. (2004). Verification, validation, and predictive capability in computational engineering and physics. *Applied Mechanics Reviews*, 57(5):345–384.

[235] Ohbuchi, E., Hanaizumi, H., and Hock, L. A. (2004, November). Barcode readers using the camera device in mobile phones. In *2004 International Conference on Cyberworlds*, pages 260–265. IEEE.

[236] O'Kane, B. L. (1992, January). Human target detection using thermal systems. In *Passive Sensors*, volume 2075, page 207507. International Society for Optics and Photonics.

[237] Okun, L. B. (1989). The concept of mass (mass, energy, relativity). *Soviet Physics Uspekhi*, 32(7):629.

[238] Parmenter, D. (2015). *Key performance indicators: developing, implementing, and using winning KPIs*. Wiley.

[239] Pavlidis, I., Levine, J., and Baukol, P. (2000, June). Thermal imaging for anxiety detection. In *Proceedings IEEE Workshop on Computer Vision Beyond the Visible Spectrum: Methods and Applications (Cat. No. PR00640)*, pages 104–109. IEEE.

[240] Pehnt, M. (2006). Dynamic life cycle assessment (LCA) of renewable energy technologies. *Renewable energy*, 31(1):55–71.

[241] Pora, J. (2001). Composite materials in the airbus A380–from history to future. *Proceedings of ICCM13, Plenary lecture, CD-ROM*.

[242] Prabuwono, A. S., Akbar, H., and Usino, W. (2009, January). PC based weight scale system with load cell for product inspection. In *2009 International Conference on Computer Engineering and Technology*, volume 1, pages 343–346. IEEE.

[243] Prasad, D. K., Rajan, D., Rachmawati, L., Rajabally, E., and Quek, C. (2017). Video processing from electro-optical sensors for object detection and tracking in a maritime environment: a survey. *IEEE Transactions on Intelligent Transportation Systems*, 18(8):1993–2016.

[244] PricewaterhouseCoopers (PwC) (2016). 2016 global industry 4.0 survey: What we mean by industry 4.0 / survey key findings / blueprint for digital success. Technical report, PricewaterhouseCoopers (PwC).

[245] Puvanasvaran, A., Mei, C., and Alagendran, V. (2013). Overall equipment efficiency improvement using time study in an aerospace industry. *Procedia Engineering*, 68:271–277.

[246] Ramaswamy, A., Nelson, D. J., and Srinivasan, V. (2007). Methods and apparatus to count people appearing in an image. US Patent 7,203,338.

[247] Raymer, D. P. (2006). *Aircraft design: a conceptual approach and Rds-student, software for aircraft design, sizing, and performance set (AIAA Education)*. AIAA.

[248] Recker, J. (2010). Opportunities and constraints: the current struggle with BPMN. *Business Process Management Journal*, 16(1):181–201.

[249] Redmon, J., Divvala, S., Girshick, R., and Farhadi, A. (2016). You only look once: Unified, real-time object detection. In *Proceedings of the IEEE Conference on Computer Vision and Pattern Recognition*, pages 779–788. IEEE.

[250] Reed, F. M. and Walsh, K. (2002). Enhancing technological capability through supplier development: a study of the UK aerospace industry. *IEEE Transactions on Engineering Management*, 49(3):231–242.

[251] Reinhard, B. and Torstrick, S. (2016, November 24-25). Automated net-shape preforming of maaximus c73 frames. In *Aachen-Dresden-Denkendorf International Textile Conference 2016, Dresden*. Technische Universität Dresden.

[252] Ren, S., He, K., Girshick, R., and Sun, J. (2015). Faster r-cnn: Towards real-time object detection with region proposal networks. In *Advances in neural information processing systems*, pages 91–99.

[253] Ribeiro, J. S. and de Oliveira Gomes, J. (2014). A framework to integrate the End-of-Life Aircraft in Preliminary Design. *Procedia CIRP*, 15:508–513.

[254] Richardson, B., Leydon, K., Fernstrom, M., and Paradiso, J. A. (2004). Z-Tiles: building blocks for modular, pressure-sensing floorspaces. In *CHI'04 extended abstracts on Human factors in computing systems*, pages 1529–1532. ACM.

[255] Riech, S. and Hilmer, P. Modellierung und ökologische Bewertung der Fertigung einer CFK-Flügelrippe mit Umberto. [Master thesis, Technical University of Braunschweig].

[256] Rink, C. and Kriegel, S. (2016). Streaming Monte Carlo pose estimation for autonomous object modeling. In *2016 13th Conference on Computer and Robot Vision (CRV)*, pages 156–163. IEEE.

[257] Roberts, D. (2016). A global roadmap for climate change action: From cop17 in durban to cop21 in paris. *South African Journal of Science*, 112(5-6):1–3.

[258] Robertson, D., Bundy, A., Muetzelfeldt, R., Haggith, M., and Uschold, M. (1991). *Eco-logic: logic-based approaches to ecological modelling*. MIT press.

[259] Roeseler, W. G., Sarh, B., Kismarton, M. U., Quinlivan, J., Sutter, J., and Roberts, D. (2007, July). Composite structures: the first 100 years. In *16th International Conference on Composite Materials, Kyoto, Japan*, pages 1–41. Japan Society for Composite Materials.

[260] Roetenberg, D., Luinge, H., and Slycke, P. (2009). Xsens MVN: full 6DOF human motion tracking using miniature inertial sensors. *Xsens Motion Technologies BV, Tech. Rep*.

[261] Roskam, J. (2006). *Airplane Design: Part I-VIII*. Roskam Aviation and Engineering Corp.

[262] Rosten, E., Porter, R., and Drummond, T. (2008). Faster and better: A machine learning approach to corner detection. *IEEE transactions on pattern analysis and machine intelligence*, 32(1):105–119.

[263] Rudol, P. and Doherty, P. (2008, March). Human body detection and geolocalization for UAV search and rescue missions using color and thermal imagery. In *2008 IEEE Aerospace Conference*, pages 1–8. IEEE.

[264] Rudolf, H.-C. and Al-Lami, A. (2019). Leistungsmessung in der Produktion von Faserverbundbauteilen: Ein generisches Modell zur Abbildung und Bewertung in Bezug auf Kosten, Ressourcen und Umweltverträglichkeit. [Master thesis, Technical University of Clausthal].

[265] Ruppert, J. P., Fish, R. C., Yap, T. A., Ames, R. M., et al. (1997). Portable RF ID tag and barcode reader. US Patent 5,640,002.

[266] Russakovsky, O., Deng, J., Su, H., Krause, J., Satheesh, S., Ma, S., Huang, Z., Karpathy, A., Khosla, A., Bernstein, M., et al. (2015). Imagenet large scale visual recognition challenge. *International Journal of Computer Vision*, 115(3):211–252.

[267] Russell, S., Norvig, P., and Intelligence, A. (1995). *Artificial Intelligence: A modern approach*, volume 25. Hall.

[268] Ruzzelli, A. G., Nicolas, C., Schoofs, A., and O'Hare, G. M. (2010, June). Real-time recognition and profiling of appliances through a single electricity sensor. In *2010 7th Annual IEEE Communications Society Conference on Sensor, Mesh and Ad Hoc Communications and Networks (SECON)*, pages 1–9. IEEE.

[269] Saling, P. (2016). Eco-efficiency Assessment. In *Special Types of Life Cycle Assessment*, pages 115–178. Springer.

[270] Saling, P., Grosse-Sommer, A., Alba-Peréz, A., and Kölsch, D. (2007, May). Using the eco-efficiency analysis and SEEBALANCE in the sustainability assessment of products and processes. In *Sustainable neighbourhood, from Lisbon to Leipzig through research, 4th BMBF-Forum for Sustainability, Leipzig, Germany*, pages 1–8.

[271] Schachinger, A. and Al-Lami, A. Real-Time Life Cycle Assessment in the Production of Composite Structures using Visual Recognition. [Master thesis, FH JOANNEUM].

[272] Schaltegger, S. and Sturm, A. (1992). *Ökologieorientierte Entscheidungen in Unternehmen: Ökologisches Rechnungswesen statt Ökobilanzierung: Notwendigkeit, Kriterien, Konzepte*, volume 1. Haupt.

[273] Scheer, A.-W. (2013). *Industrie 4.0: Wie sehen Produktionsprozesse im Jahr 2020 aus*. IM. https://www.researchgate.net/profile/August_Wilhelm_Scheer/publication/277717764_Industrie_40_-_Wie_sehen_Produktionsprozesse_im_Jahr_2020_aus/links/55ee9e5608ae0af8ee1a1d72/Industrie-40-Wie-sehen-Produktionsprozesse-im-Jahr-2020-aus.pdf.

[274] Schlesinger, S., Crosbie, R. E., Gagné, R. E., Innis, G. S., Lalwani, C. S., Loch, J., Sylvester, R. J., Wright, R. D., Kheir, N., and Bartos, D. (1979). Terminology for model credibility. *Simulation*, 32(3):103–104.

[275] Schmidheiny, S. (1992). *Changing course: A global business perspective on development and the environment*, volume 1. MIT Press.

[276] Schmidt, A., Strohbach, M., Van Laerhoven, K., Friday, A., and Gellersen, H.-W. (2002, September). Context acquisition based on load sensing. In *International Conference on Ubiquitous Computing*, pages 333–350. Springer.

[277] Schmidt, M. and Keil, R. (2002). Stoffstromnetze und ihre Nutzung für mehr Kostentransparenz sowie die Analyse der Umweltwirkung betrieblicher Stoffströme. Technical report, (No. 103) Beiträge der Fachhochschule Pforzheim. https://www.hs-pforzheim.de/fileadmin/user_upload/uploads_redakteur/Forschung/INEC/Dokumente/Publikationen/Beitraege103.pdf.

[278] Schmidt, M. and Nakajima, M. (2013). Material flow cost accounting as an approach to improve resource efficiency in manufacturing companies. *Resources*, 2(3):358–369.

[279] Schmidt, R., Möhring, M., Härting, R.-C., Reichstein, C., Neumaier, P., and Jozinović, P. (2015, June). Industry 4.0-potentials for creating smart products: empirical research results. In *International Conference on Business Information Systems*, pages 16–27. Springer.

[280] Schönemann, M., Kurle, D., Herrmann, C., and Thiede, S. (2016). Multi-product EVSM Simulation. *Procedia CIRP*, 41:334–339.

[281] Schuldt, J. P., Konrath, S. H., and Schwarz, N. (2011). "Global warming"? or "climate change"?? Whether the planet is warming depends on question wording. *Public Opinion Quarterly*, 75(1):115–124.

[282] Schwab, K. (2017). *The fourth industrial revolution*. World Economic Forum.

[283] Scriven, M. (1996). Types of evaluation and types of evaluator. *Evaluation practice*, 17(2):151–161.

[284] Sengupta, J. K. (1982). Efficiency measurement in stochastic input-output systems. *International Journal of Systems Science*, 13(3):273–287.

[285] Serrano, I., Ochoa, C., and Castro, R. D. (2008). Evaluation of value stream mapping in manufacturing system redesign. *International Journal of Production Research*, 46(16):4409–4430.

[286] Sheikh, H. R., Sabir, M. F., and Bovik, A. C. (2006). A statistical evaluation of recent full reference image quality assessment algorithms. *IEEE Transactions on Image Processing*, 15(11):3440–3451.

[287] Shih, B. (2012). Real-time weight measuring system for hospital bed. US Patent App. 13/608,440.

[288] Shim, J. P., Warkentin, M., Courtney, J. F., Power, D. J., Sharda, R., and Carlsson, C. (2002). Past, present, and future of decision support technology. *Decision support systems*, 33(2):111–126.

[289] Simões, C. L., Pinto, L. M. C., Simoes, R., and Bernardo, C. (2013). Integrating environmental and economic life cycle analysis in product development: a material selection case study. *The International Journal of Life Cycle Assessment*, 18(9):1734–1746.

[290] Simon, H. A. (1960). *The new science of management decision*. Harper.

[291] Simon, H. A. (1993). Decision making: Rational, nonrational, and irrational. *Educational Administration Quarterly*, 29(3):392–411.

[292] Smith, B. (2003). The Boeing 777. *Advanced Materials and Processes*, 161(9):41–44.

[293] Snowden, D. J. and Boone, M. E. (2007). A leader's framework for decision making. *Harvard business review*, 85(11):68.

[294] Sobczyk, G. and Yarman, T. (2008). Unification of space-time-matter-energy. *Appl. Comput. Math*, 7(2):255–268.

[295] Soehren, W. and Bye, C. (2005). Human motion identification and measurement system and method. US Patent App. 10/634,931.

[296] Solow, R. M. (1957). Technical change and the aggregate production function. In *The Review of Economics and Statistics*. MIT Press.

[297] Soon, T. J. (2008). QR code. *Synthesis Journal*, 2008:59–78.

[298] Spector, B. I., Sjöstedt, G., and Zartman, I. W. (1994). *Negotiating international regimes: lessons learned from the United Nations Conference on Environment and Development (UNCED)*. Graham & Trotman/Martinus Nijhoff.

[299] Storf, H., Becker, M., and Riedl, M. (2009, April). Rule-based activity recognition framework: Challenges, technique and learning. In *2009 3rd International Conference on Pervasive Computing Technologies for Healthcare*, pages 1–7. IEEE.

[300] Suh, S., Lenzen, M., Treloar, G. J., Hondo, H., Horvath, A., Huppes, G., Jolliet, O., Klann, U., Krewitt, W., Moriguchi, Y., et al. (2004). System boundary selection in life-cycle inventories using hybrid approaches. *Environmental Science & Technology*, 38(3):657–664.

[301] Tajelawi, O. A. and Garbharran, H. L. (2015). MFCA: An Environmental Management Accounting Technique for Optimal Resource Efficiency in Production Processes. *World Academy of Science, Engineering and Technology, International Journal of Social, Behavioral, Educational, Economic, Business and Industrial Engineering*, 9(11):3740–3745.

[302] Tan, Y. S., Ng, Y. T., and Low, J. S. C. (2017). Internet-of-Things Enabled Real-time Monitoring of Energy Efficiency on Manufacturing Shop Floors. *Procedia CIRP*, 61:376–381.

[303] Tanner, R., Studer, M., Zanoli, A., and Hartmann, A. (2008, September). People detection and tracking with tof sensor. In *2008 IEEE Fifth International Conference on Advanced Video and Signal Based Surveillance*, pages 356–361. IEEE.

[304] Tao, F., Zuo, Y., Da Xu, L., Lv, L., and Zhang, L. (2014). Internet of things and bom-based life cycle assessment of energy-saving and emission-reduction of products. *IEEE Transactions on Industrial Informatics*, 10(2):1252–1261.

[305] Tapia, E. M., Intille, S. S., Haskell, W., Larson, K., Wright, J., King, A., and Friedman, R. (2007, October). Real-time recognition of physical activities and their intensities using wireless accelerometers and a heart rate monitor. In *2007 11th IEEE international symposium on wearable computers*, pages 37–40. IEEE.

[306] Teixeira, T. and Savvides, A. (2007, September). Lightweight people counting and localizing in indoor spaces using camera sensor nodes. In *2007 First ACM/IEEE International Conference on Distributed Smart Cameras*, pages 36–43. IEEE.

[307] Teutsch, M., Muller, T., Huber, M., and Beyerer, J. (2014). Low resolution person detection with a moving thermal infrared camera by hot spot classification. In *Proceedings of the IEEE Conference on Computer Vision and Pattern Recognition Workshops*, pages 209–216. IEEE.

[308] The United Nations (UN): The United Nations Framework Convention on Climate Change (UNFCCC) (2009). Kyoto protocol reference manual on accounting of emissions and assigned amounts. Technical report, The United Nations (UN). https://unfccc.int/resource/docs/publications/08_unfccc_kp_ref_manual.pdf.

[309] Thiede, S., Juraschek, M., and Herrmann, C. (2016). Implementing cyber-physical production systems in learning factories. *Procedia CIRP*, 54:7–12.

[310] Timmis, A. J., Hodzic, A., Koh, L., Bonner, M., Soutis, C., Schäfer, A. W., and Dray, L. (2015). Environmental impact assessment of aviation emission reduction through the implementation of composite materials. *The International Journal of Life Cycle Assessment*, 20(2):233–243.

[311] Ting, N. Y., Shee, T. Y., and Choong, L. J. S. (2017). Internet of Things for Real-time Waste Monitoring and Benchmarking: Waste Reduction in Manufacturing Shop Floor. *Procedia CIRP*, 61:382–386.

[312] Töpfer, A. (2008). *Lean Six Sigma: erfolgreiche Kombination von Lean Management, Six Sigma und Design for Six Sigma*. Springer.

[313] Torresan, H., Turgeon, B., Ibarra-Castanedo, C., Hebert, P., and Maldague, X. P. (2004, April). Advanced surveillance systems: combining video and thermal imagery for pedestrian detection. In *Thermosense XXVI*, volume 5405, pages 506–515. International Society for Optics and Photonics.

[314] Torstrick, S., Kruse, F., and Wiedemann, M. (2013, June). RTM processing for net-shaped parts in high quantities. In *CFK-Valley Stade Convention, Stade*, volume 12. DLR. http://www.dlr.de/fa/Portaldata/17/Resources/dokumente/publikationen/EVo-Handout.pdf.

[315] Torstrick, S., Kruse, F., and Wiedemann, M. (2016). EVo: Net Shape RTM Production Line. *Journal of Large-Scale Research Facilities (JLSRF)*, 2:66.

[316] Tränkler, H.-R. and Fischerauer, G. (2014). *Das Ingenieurwissen: Messtechnik*. Springer.

[317] US-Department of Defense (DoD) (2002). COMPOSITE MATERIALS HANDBOOK: VOLUME 3. POLYMER MATRIX COMPOSITES MATERIALS USAGE, DESIGN, AND ANALYSIS. Technical report, US-Department of Defense (DoD).

[318] US-Department of Energy (DOE) (2010). GENERAL GUIDE FOR TECHNICAL ANALYSIS OF COST PROPOSALS FOR ACQUISITION CONTRACTS. Technical report, US-Department of Energy (DOE). http://energy.gov/sites/prod/files/15.4-4_General_Guide_for_Technical_Analysis_of_Cost_Proposals_for_Acquisition_Contracts_0.pdf.

[319] US-Environmental Protection Agency (EPA) (1995). An introduction to environmental accounting as a business management tool: key concepts and terms. Technical report, Office of Pollution Prevention and Toxics. https://www.epa.gov/sites/production/files/2014-01/documents/busmgt.pdf.

[320] Van der Laan, E. and Salomon, M. (1997). Production planning and inventory control with remanufacturing and disposal. *European Journal of Operational Research*, 102(2):264–278.

[321] Van Veen, E. and Wortmann, J. (1992). Generative bill of material processing systems. *Production Planning & Control*, 3(3):314–326.

[322] Varela, L., Araújo, A., Ávila, P., Castro, H., and Putnik, G. (2019). Evaluation of the Relation between Lean Manufacturing, Industry 4.0, and Sustainability. *Sustainability*, 11(5):1439.

[323] Velickov, S. and Solomatine, D. (2000). Predictive data mining: practical examples. In *2nd Joint Workshop on Applied AI in Civil Engineering*.

[324] Verein Deutscher Ingenieure (VDI) (1997). Design engineering methodics Engineering design at optimum cost: Simplified calculation of costs.

[325] Verrey, J., Wakeman, M., Michaud, V., and Månson, J.-A. (2006). Manufacturing cost comparison of thermoplastic and thermoset RTM for an automotive floor pan. *Composites Part A: Applied Science and Manufacturing*, 37(1):9–22.

[326] Volling, T. and Spengler, T. S. (2008). Configuration of Order-Driven Planning Policies. In *Operations Research Proceedings 2007*, pages 441–446. Springer.

[327] Wang, L. and Aghdasi, F. (2012). Method and System for Counting People Using Depth Sensor. US Patent App. 13/683,886.

[328] Wang, Y. and Kobsa, A. (2007). Respecting users' individual privacy constraints in web personalization. In *International Conference on User Modeling, Corfu, Greece*, pages 157–166. Springer.

[329] Wang, Z., Bovik, A. C., Sheikh, H. R., Simoncelli, E. P., et al. (2004). Image quality assessment: from error visibility to structural similarity. *IEEE Transactions on Image Processing*, 13(4):600–612.

[330] Want, R. (2004). Enabling ubiquitous sensing with RFID. *Computer*, (4):84–86.

[331] Watson, H. J., Rainer Jr, R. K., and Koh, C. E. (1991). Executive information systems: a framework for development and a survey of current practices. *MIS Quarterly*, pages 13–30.

[332] Weiss, B. A., Horst, J., and Proctor, F. (2013). Assessment of Real-Time Factory Performance Through the Application of Multi-Relationship Evaluation Design. Technical report. http://nvlpubs.nist.gov/nistpubs/ir/2013/NIST.IR.7911.pdf.

[333] Westkämper, E. (2006). *Einführung in die Organisation der Produktion*. Springer.

[334] Wiedemann, M. and Sinapius, M. (2012). *Adaptive, tolerant and efficient composite structures*. Springer Science.

[335] Wiedmann, T. and Minx, J. (2008). A definition of 'carbon footprint'. *Ecological Economics Research Trends*, 1:1–11.

[336] Wilder, J. and Kosonocky, W. F. (1993). Multiple resolution image sensor. US Patent 5,262,871.

[337] Williams, E. B. et al. (1977). *The Scribner-Bantam English Dictionary*. Scribner.

[338] Williams, T., Bernus, P., and Nemes, L. (1996). The concept of enterprise integration. In *Architectures for enterprise integration*, pages 9–20. Springer.

[339] Wilson, D. H. and Atkeson, C. (2005, May). Simultaneous tracking and activity recognition (STAR) using many anonymous, binary sensors. In *International Conference on Pervasive Computing*, pages 62–79. Springer.

[340] Wilson, M. (2003). Corporate sustainability: What is it and where does it come from. *Ivey Business Journal*, 67(6):1–5.

[341] Winterton, J., Delamare-Le Deist, F., and Stringfellow, E. (2006). *Typology of knowledge, skills and competences: clarification of the concept and prototype*. Office for Official Publications of the European Communities Luxembourg.

[342] Witik, R., Gaille, F., Teuscher, R., Ringwald, H., Michaud, V., and Månson, J.-A. (2011a). Assessing the economic and environmental potential of out of autoclave processing. In *18th International Conference on Composite Materials (ICCM)*. ICCM.

[343] Witik, R. A., Payet, J., Michaud, V., Ludwig, C., and Månson, J.-A. E. (2011b). Assessing the life cycle costs and environmental performance of lightweight materials in automobile applications. *Composites Part A: Applied Science and Manufacturing*, 42(11):1694–1709.

[344] Witten, E., Sauer, M., and Kühnel, M. (2017). Composites-Marktbericht 2017. Technical report. http://www.avk-tv.de/files/20170919_avkccev__marktbericht_2017.pdf.

[345] Woodward, D. G. (1997). Life cycle costing—theory, information acquisition and application. *International journal of project management*, 15(6):335–344.

[346] Wren, C. R. and Tapia, E. M. (2006, May). Toward scalable activity recognition for sensor networks. In *International Symposium on Location-and Context-Awareness*, volume 3987, pages 168–185. Springer.

[347] Yamazato, T., Takai, I., Okada, H., Fujii, T., Yendo, T., Arai, S., Andoh, M., Harada, T., Yasutomi, K., Kagawa, K., et al. (2014). Image-sensor-based visible light communication for automotive applications. *IEEE Communications Magazine*, 52(7):88–97.

[348] Yang, D. X. D., El Gamal, A., Fowler, B., and Tian, H. (1999). A 640× 512 CMOS Image Sensor with Ultra Dynamic Range Floating-Point Pixel-Level ADC. *IEEE ISSCC Digest of Technical Papers, 1999*.

[349] Yousefpour, A., Hojjati, M., and Immarigeon, J.-P. (2004). Fusion bonding/welding of thermoplastic composites. *Journal of Thermoplastic Composite Materials*, 17(4):303–341.

[350] Zandin, K. B. (2002). *MOST work measurement systems*. CRC press.

[351] Zhabelova, G. and Vyatkin, V. (2012). Multiagent smart grid automation architecture based on IEC 61850/61499 intelligent logical nodes. *IEEE Transactions on Industrial Electronics*, 59(5):2351–2362.

Appendix A

FRPs Manufacturing Techniques

	Technique	Description	Process	Mold	Fiber
1	RTM	Matrix is injected by pressure into fiber within a two-side rigid close mold [1]	LCM[14 2]	Close mold with two rigid sides [2]	Diverse fabric forms [2 3]
2	Single-line infusion	Matrix is dragged to evacuated bagged fiber through the same line, from which air has been evacuated [4]	LCM [5]	Open mold with rigid and flexible sides [4]	Unidirectional continuous fiber [5]
3	Differential pressure RTM	It controls fiber volume content during injection process by vacuum [6]	LCM [6]	Open mold with rigid and flexible sides [6 4]	Diverse fabric forms [2 3]
4	Same qualified RTM	Instead of dry fiber prepreg is implemented in RTM [7]	LCM [6]	Same as RTM [2]	Prepreg [6]
5	Compression molding	Bulk and sheet molding compounds are formed by pressing under mold [15 12 24]	LCM [6]	Same as RTM	Long or short fiber [3 8]
6	Hand/wet lay-up	Layers are placed on the one side mold. After curing in open air further layers can be placed, poured, and cured [1 3]	LCM and prepreg	One side open mold or work surface [2 9]	Unidirectional prepreg or dry [2 3]
7	Autoclave	Autoclave is a sealed and isolated vessel with heating, cooling, pressurizing, and vacuuming capabilities [10 2]	LCM and prepreg	Open mold with rigid and flexible sides [10 11]	Prepreg or dry fiber [13 2 3]
8	Vacuum assisted RTM	In addition to pressured matrix, air-evacuated open mold is used in dragging it [9 6]	LCM [2]	Open with rigid and flexible sides [1]	Same as RTM
9	Pultrusion	Fiber is continuously tempered and cured while passing into mold [9 2]	LCM or prepreg [2]	Close mold with two side rigid die [2]	Bare roving or continuous fiber [9 11]
10	Filament winding	Fiber tows are dragged continuously by a rotating mandrel and placed by a cross-feed head. Fiber tow is placed accordingly by adjusting the rotation speed, fiber tension, and cross-feed head position [2 1 9]	LCM or prepreg	One side mandrel [2 9]	Prerpreg tows, dry, or dry that are passed through matrix [2]
11	SCRIMP [31]	Air-evacuated open mold is used in dragging the matrix, while permeable material is laid underneath or above fiber layers [2]	LCM	Open mold with rigid and flexible sides [2]	Same as RTM
12	Automated tape laying	Fiber tape is melted then laid and solidified on mold sequentially by controlled paths [2 9 11]	Prepreg [2 9]	One side mold (mandrel)	Unidirectional fiber [2 9]
13	Automated preforming	Fiber layers are laid up by robot head and preformed by automated membrane press device [16]	LCM or prepreg [16]	One side mold [16]	Unidirectional dry or prepreg [16 22]

[1] Reference: Hoa, S. V. (2009); in the previous Bibliography as [141]

[2] Reference: Advani, S. G. and Sozer, E. M. (2010); in the previous Bibliography as [4]

[3] Reference: Mazumdar, S. K. (2002). Composites Manufacturing-Materials, Product and Process Engineering. CRC Press.

[4] Reference: Herrmann, A. S., Pabsch, A., and Kleineberg, M. (2001). SLI-RTM Fairings for Fairchild Dornier DO 328 Jet. In 22nd SAMPE Europe International Conference, Paris.

	Cost	Geometry	Surfaces	Size	FVF	Industries	Volume
1	Low [2 5]	3D- complex forms [9]	Both sides control [59]	Small to large [30 2]	40-60% [24 6]	Automotive; aerospace [30 9]	5k-100k /year [16]
2	Lower than RTM [10 5]	3D- complex forms [17]	One side control [4]	Small to medium [17]	60% [5]	Aerospace [4]	0.5k/year [4]
3	Higher than RTM: autoclave [2 3 46]	3D- complex forms [6]	Both sides control [6]	Small to large [6]	Up to 65% [6]	Aerospace [6]	2k-5k/year [6]
4	More than RTM [2 5 7]	3D- complex forms [7]	Both sides control [7]	Small to large [7]	40-60% [6]	Aerospace [6]	Close to RTM
5	Very low [2 3 8]	3D- complex forms [12 24]	Rough both sides [2 12]	Small to medium [3]	20-30% [3]	Automotive; construction; others [3 12 15]	15k-150k /year [3]
6	Low cost components [3 9]	Non-complex forms [1]	Adequate control [1]	Small to very large size [1 11]	45% [21]	Construction; marine; others [1]	5k/year
7	Slightly Lower than RTM [10 2 9]	Simple to complex [9 18]	Accurate control [2]	Small to large [2]	Up to 68% [1]	Aerospace [2 1]	0.5k-90k /year (assumed)
8	Lower than RTM [2 3]	3D- less complex [9]	One side controlled [9]	Small to very large size [2]	70% [3]	Automotive; others	5k-15k /year
9	Low cost process [1 2]	Cross-section [9 2 1]	Both sides control [9]	Very long thin forms [2]	20-50% [11]	Construction; others [1]	15k-100k /year [9]
10	Low cost material and relatively equipment [3]	Revolution shapes [1 2 3]	Rough outer moderate inner [24]	Limited to the mandrel and filament winding machine size [1]	50% [24 3]	Tanks; pipes; marine; automotive; aerospace [1]	High: depends on product size
11	Lower than RTM [2 3]	Simple forms such as shells [1]	Poor quality on flexible side [2]	Very large components [1]	70% [3]	Marine; construction; wind energy	5k-15k /year
12	Relatively high [22]	Flat or curved [9]	Smooth net shape [19]	Very large [22 11]	50% [23]	Aerospace [28]	2k/year [28]
13	Low for high production volume [22 28]	Complex forms [20 22]	Controlled net shape on both sides [19 20]	Small to medium [20 23]	-	Aerospace; automotive [20 28]	100k/year [16 20 28]

[5] Reference: Kleineberg, M. (2013); in the previous Bibliography as [173]

[6] Reference: Neitzel, M., Mitschang, P., and Breuer, U. (2014); in the previous Bibliography as [228]

[7] Reference: Black, S. (2010). SQRTM enables net-shape parts. Technical report, Composites World (CW). https://www.compositesworld.com/articles/sqrtm-enables-net-shape-parts.

[8] Reference: Bienick, C., Herrmann, B., and Daley, H. (2003). Method of molding a peripherally encapsulated product under heat and pressure utilizing sheet molding compound (SMC) or bulk molding compound (BMC). US Patent 6,558,596.

[9] Reference: US-Department of Defense (DoD) (2002); in the previous Bibliography as [317]

[10] Reference: Al-Lami, A. and Hilmer, P. (2014); in the previous Bibliography as [8]

	Matrix	Duration	Temperature	Pressure	DoA
1	Low viscosity mostly thermoset [2 5]	Fast: 5-25 min: [2 6]	120 °C [11]	0.2-2 MPa [11]	Partially to fully [2 20]
2	Low viscosity mostly thermoset [5]	Long: preparation [5 6 17]	Autoclave: 100-370 °C [9 2]	0.5-2 MPa [11]	Not automated [26]
3	Low viscosity mostly thermoset [2 5]	Longer than RTM [6]	Autoclave: 100-370 °C [9 2]	Low differential pressure [6]	Similar to RTM except autoclave
4	Pre-impregnated [7]and LCM low viscosity mostly thermoset [7 5]	30-180 min [6]	177 °C [7]	Same as RTM	Same as RTM
5	Very high viscosity thermoset or thermoplastic [2 8]	Very fast 5-6 min [2]	135-165 °C [2]	3.5-15 MPa [2]	Highly [15]
6	Low or high viscosity LCM or prepreg. Thermoset or thermoplastic [9]	Slow [11]	Room temperature or higher [21]	Atmospheric pressure [21]	Manual [1]
7	Low or high viscosity LCM or prepreg. Thermoset or thermoplastic [9]	Slow due to autoclave prepare up to 8 h [11 17]	100-370 °C [2 9]	0.5-2 MPa [2]	Manual bagging [11]
8	Low viscosity mostly thermoset [5 2]	Longer than RTM [5]	Maximum 100 °C [9]	No elevated pressure [9]	Manual bagging [11 2 26]
9	Low viscosity thermoset or high viscosity thermoplastic which is difficult to process [2]	Combined short process [1]	120-180 °C [9]	0.001 MPa [25]	Automated [9]
10	Low viscosity thermoset or high viscosity thermoplastic. In process or after infusion	Relatively fast for small thin structures [1]	Up to 385 °C [3]	Low pressure mainly fiber tensile force	Automated [9]
11	Low viscosity mostly thermoset	Long especially at preparation [2]	Same as Vacuum assisted RTM [1]	Same as Vacuum assisted RTM [1]	Same as Vacuum assisted RTM [2 26]
12	Pre-impregnated thermoset [28]	Relatively fast: 2-150 kg/h [22 2]	450 °C [27]	0.6 MPa [23]	Fully automated [9]
13	Low or high viscosity LCM or prepreg.	Relatively fast: 2-18 min [29]	70-150 °C [29]	2.3 MPa [29]	Fully automated [16]

[11] Reference: Haffner, S. M. (2002). Cost modeling and design for manufacturing guidelines for advanced composite fabrication. [PhD thesis, Massachusetts Institute of Technology].

[12] Reference: Rohrbacher, F., Spain, P. L., and Fahlsing, R. A. (1990). Process for forming a composite structure of thermoplastic polymer and sheet molding compound. US Patent 4,959,189.
[13] Kleineberg, M., Herbeck, L., and Schöppinger, C. (2002, December). Advanced liquid resin infusion-A new perspective for space structures. In European Conference on Spacecraft Structures, Materials and Mechanical Testing, Toulouse, France, pages 1–9.
[14] Abbreviation: Liquid composite molding (LCM)
[15] Reference: Magnaud, H. (2016). Design for success: A design & technology manual for SMC BMC. Technical report, European Alliance for SMC/BMC.
[16] Reference: Torstrick, S., Kruse, F., and Wiedemann, M. (2013, June); in the previous Bibliography as [314]
[17] Reference: Al-Lami, A. and Hilmer, P. (2015b); in the previous Bibliography as [10]
[18] Reference: Hilmer, P. (2016); in the previous Bibliography as [138]
[19] Reference: Willden, K., Metschan, S., Grant, C., and Brown, T. (1992). Composite Fuselage Crown Panel Manufacturing Technology. Technical report, Boeing Commercial Airplanes and Hercules Aerospace.
[20] Reference: Torstrick, S., Kruse, F., and Wiedemann, M. (2016); in the previous Bibliography as [315]
[21] Reference: Abdurohman, K., Satrio, T., & Muzayadah, N. L. (2018, November). A comparison process between hand lay-up, vacuum infusion and vacuum bagging method toward e-glass EW 185/lycal composites. In Journal of Physics Conference Series (Vol. 1130, No. 1, p. 012018).
[22] Reference: Hagnell, M. and Åkermo, M. (2015). A composite cost model for the aeronautical industry: Methodology and case study. Composites Part B: Engineering, 79:254–261.
[23] Reference: Christophe, B., Antoine, K., Marine, L., Denis, C., Antoine, L. D., Alain, B., and Peter, D. (2016). Flax/PP manufacture by automated fibre placement (AFP). Materials and Design, 94:207–213.
[24] Reference: Ermanni, P. (2007). Composites technologien. Skript zur ETH-Vorlesung, 151-0307.
[25] Reference: Sharma, D., McCarty, T. A., Roux, J. A., and Vaughan, J. G. (1998). Investigation of dynamic pressure behavior in a pultrusion die. Journal of Composite Materials, 32(10):929–950.
[26] Reference: Liebers, N., Buggisch, M., Kleineberg, M., and Wiedemann, M. (2015). Autoclave infusion of aerospace ribs based on process monitoring and control by ultrasound sensors.
[26] Reference: Liebers, N., Buggisch, M., Kleineberg, M., and Wiedemann, M. (2015). Autoclave infusion of aerospace ribs based on process monitoring and control by ultrasound sensors.
[27] Reference: Raspall, F., Velu, R., and Vaheed, N. M. (2019). Fabrication of complex 3d composites by fusing automated fiber placement (AFP) and additive manufacturing (AM) technologies. Advanced Manufacturing: Polymer & Composites Science, VOL. 5(1):6–16.
[28] Reference: Schubel, P. J. (2012). Cost modelling in polymer composite applications: Case study–Analysis of existing and automated manufacturing processes for a large wind turbine blade. Composites Part B: Engineering, 43(3):953–960.
[29] Reference: Hagedorn, C., Torstrick, S., and Reinhard, B. (2015); in the previous Bibliography as [123]
[30] Reference: Verrey, J., Wakeman, M., Michaud, V., and Månson, J.-A. (2006); in the previous Bibliography as [325]
[31] Abbreviation: Seaman composite resin infusion molding process (SCRIMP)

Appendix B

Characterization Factors in EEAM

Although the calculations of these characterization factors λ_j can be hidden within a gray- or black-box model that generates them as givens, the insight of how they are calculated is useful for decision-makers. Still, several roughly estimated inputs of calculating these characterization factors λ_j is leading to a possibly gray-box model but not a white-box one. Again, these characterization factors λ_j are mainly based on assumptions due to the lack of reliable data. Nonetheless, they are still considered as givens in this thesis. Based on available data or assumptions, such characterization factors λ_j may cover all associated direct categories including fixed recurring impact ζ_j, variable recurring impact Ψ_j, and fixed nonrecurring impact υ_j. For unavailable given values, simplified equations are implemented to generate these factors λ_j here. These parameters are considered for the year 2019 that consists of total 365 days, in which the average of 30.416 days is in each of its 12 months. Based on the geographical system boundary of the assessed case study, the city of Stade, in which the process is performed, is part of the Lower Saxony state in Germany. In it, total working days of around 251 days are considered in 2019. While production operation has various rhythm models, the time can be split in working shifts. However, a single work shift of 39 working hours/week in a five working days/week is considered for the entire production in this thesis. Therefore, the total of approximately 1957.8 working hours/year is considered not only for 2019 but theoretically any year.

Arguably, such model of a single shift 7.8 working hours/day in a five working days/week is matching the boundaries of laboratory production at DLR and other research and development organizations but not the FRPs industrial manufacturers. Therefore, other models of three or more shifts per day may be also considered in generating the associated characterization factors λ_j. These models offer up to 24 working hours/day in 7 working days/week, which leads to a total working hours of around 8760 working hours/year. However, the production model impact must be carefully taken into consideration. For instance, labor wage differs in most cases between these various shift models and based on the geographical system boundary. In addition, the total useful life of equipment is associated with these models too. However, production rhythms adjustments and their associated calculation models of characterization factors λ_j are integrated in EEAM to enable the assessment of these various scenarios based on the same collected data. Therefore, the first scenario of a single shift of 7.8 working hours/day in a five working days/week is selected in the assessment for simplicity.

Considering the assessment of direct cost δ_{ij} of each elementary flow α_{ij}, an economic characterization factor γ_j is to be selected or calculated. For labor $v_{i,2001} \in \varphi^{[L]}$ as an input, a given value of work time price is given based on an internal calculation by DLR. Technically, the value of labor work in both ecological and economic terms exceeds the final mechanical energy delivered by the labor. However, the value of this work is reflected on the characterization factors λ_L especially when it comes to the economic characterization factor γ_L. At least theoretically, the labor economic characterization factor γ_L depends on the knowledge and experience level of the labor. Including several direct impacts within the spectrum of ζ_j, Ψ_j, and υ_j, the work price per person is considered to be 95 €/h which is equal to around 0.026 €/s. For the economic impact of facility $v_{ij} \in \varphi^{[\Delta s]}$, a rental model is considered in which each quadratic meter is costing around 2.81 €/month $\cdot$ m^2 including all direct economic impacts. In the selected production rhythm, the facility is used for a shift but rented logically for the entire day. Therefore, the total areas of 42.2 m^2 in γ_{3001}, 71.1 m^2 in γ_{3002}, 42.6 m^2 in γ_{3003}, and 63 m^2 in γ_{3004} are considered for WS_1, WS_2, WS_3, and WS_4 respectively. In which, air-conditioning, lightning, and other services are covered by these assumed economic factors. For γ_j of various equipment types $v_{ij} \in \varphi^{[Q]}$,

ζ_j, Ψ_j, and υ_{ij} impact categories are considered. Technically, equipment subset $\varphi^{[Q]}$ contains electrically operated machines, manually used tools, and molds. Not only the values of their characterization factors λ_j are unique for each type, but also the methods of calculating the impacts vary between these equipment classes, as it is discussed later in chapter 5. However, these characterization factors λ_j are all unified to describe the impact per time of utilization for this equipment subset $\varphi^{[Q]}$. In practice, characterization factors λ_j of equipment type may vary based on the operating scenarios as well, as they are discussed in Appx. B. They are effected by aspects such as TRL, process maturity, as well as production rhythm. It is essential to mention that EVo-platform consists of novel technologies from DLR and DLR partners. Therefore, some relevant parameters of such devices are unavailable, while rough assumptions are adopted in such cases. In this case study, a simplified relation of straight-line depreciation is adopted initially in the EEAM,[B1] as Eq. B.1 shows.

$$\gamma_{iQ} = \frac{\text{total investment + (total investment * maintenance rate) - salvage}}{\text{useful life duration}} \tag{B.1}$$

In Eq. B.1, each equipment type has a specific total investment in €, salvage, or as it is also called residual value, in €, maintenance rate as a percentage of its investment, and a useful life in years. This useful life is to be determined based on production rhythm, as it is discussed before. The suggested economic calculation of γ_{iQ} covers the entire life-cycle of an equipment item by assumptions. The total investment in Eq. B.1 includes activities such as transportations and equipment development phase, while an economic impact is cumulative in its nature. To put it more simply, the common approach in price definition is to have no free-of-charge performance. Tab. B.1 introduces the main required parameters of equipment economic characterization factors γ_j.

As it is shown in Tab. B.1, the considered parameters for each equipment type are listed based on collected data. These parameters take all direct impact categories into consideration within simplified values. These roughly estimated values are not necessarily identical to the market available values by equipment providers, while the EVo-platform adopts some novel technologies as modifications to these available machines. Moreover, Tab. B.1 consists the economic impacts from the entire life-cycle of each item as a cradle-to-grave economic characterization factors γ_{iQ}.

Table B.1 Main initial data $\hat{\gamma}_j$ required for economic characterization factors γ_j of elements in equipment subset $\varphi^{[Q]}$

Factor γ_{iQ}	Total investment (€)	salvage (€)	Maintenance (%)	Useful life (h in years)
γ_{4096}	53 k€	3 k€	2 %	9789 h in 5 years
γ_{4097}	30 k€	1 k€	2 %	7831.2 h in 4 years
γ_{4098}	315 k€	20 k€	2 %	13 704.6 h in 7 years
γ_{40100}	215 k€	10.5 k€	2.5 %	9789 h in 5 years
γ_{40101}	175 k€	8 k€	2.5 %	9789 h in 5 years
γ_{40102}	325 k€	10 k€	9 %	13 704.6 h in 7 years
γ_{40103}	12 k€	0.5 k€	1 %	1957.8 h in 1 year
γ_{40104}	100 k€	5 k€	2 %	9789 h in 5 years
γ_{40105}	320 k€	15 k€	5 %	11 746.8 h in 6 years

* v_{4096} = paternoster storage v_{4097} = unwinder v_{4098} = cutter v_{40100} = ply storage v_{40101} = draping robot v_{40102} = membrane press v_{40103} = mold v_{40104} = handling robot v_{40105} = trimming portal

While total investment and salvage vary clearly between the various equipment types, maintenance rate may have common values of around 2 %,[1] unless the technical data suggests other rates. However, the useful life varies in the range of minimum one year to maximum seven years. By considering aspects such as process maturity, TRL, equipment sophistication, market feedback, and field experiences, such life can be estimated. Commonly implemented machines are

expected to have a useful life that is relatively longer than a case customized ones. Moreover, equipment types with novel technologies are expected to have relatively shorter useful life than other simple ones. In the case of mold occupation, it is obvious that the mold impacts are related mainly to its acquisition and maintenance. In practice, each mold can be implemented to carry out specific manufacturing cycles. In practice, molds have short useful life due to the high depreciation per production cycle.

Here, the prices of materials including fiber $v_{2,6014}$ and release film $v_{2,9017}$ per kg are roughly estimated, while no real values are provided in this thesis due to confidentiality of suppliers data. In literature, there is a significant deviation between the fiber price estimations. In their work, Shuaib and Mativenga estimated the carbon fiber price to lay between 15 £/kg and 23 £/kg, which may be converted at the time by exchange rate of 1.17 £/€ in 2017 and subjected to the inflation rate of around 1.02 $\frac{\text{€ in 2017}}{\text{€ in 2019}}$ to around 17.9 €/kg and 28 €/kg in 2019 respectively.[B3] However, the prices in their study are not assigned to a specific industry. In the composites world electronic magazine published in 2014, Jeff Sloan estimated the carbon fiber price for aerospace application to lay between 85 $/kg and 220 $/kg. Considering the exchange rate in 2014 and inflation factor of 0.950 $/€ and 1.04 $\frac{\text{€ in 2014}}{\text{€ in 2019}}$ respectively, carbon fiber has a price of 84 €/kg to 217 €/kg for aerospace applications in 2019.[B4] In his thesis, Hilmer studied similar fiber material with approximate price of around 163.45 €/kg. Internal reports at DLR shows a price range of 83.5 €/kg up to 99.5 €/kg for aerospace qualified non-crimp fabrics from carbon fiber with different orientations and purchased amount in 2016. Considering the inflation, this price range lays between 86.84 €/kg and 103.48 €/kg in 2019. In this thesis, the carbon fiber price is considered to be 88.857 €/kg. As it has been mentioned in chapter 4, the waste characterization factors depend on the adopted impact scope. While all other characterization factors have been considered to contain a cradle-to-grave scope, waste ones have to be treated similarly for results homogeneity. Therefore, fiber waste $u_{2,6014}$ is considered within the fiber input and has different economic and ecological factors than the initial material due to impacts variation in other life-cycle stages. Fiber waste $u_{2,6514}$ has an additional disposal fees of around 5 €/kg. The scenario of no re-usability of fiber cutting waste is adopted in this thesis. However, consolidated fiber waste $u_{4,65141}$ is to be disposed with the same expenses. The same fees of around 5 €/kg are also applied to dispose the release film $v_{2,9017}$, while it has an initial price of around 85.086 €/kg. For electricity, a given price of 0.0855 €/kWh is considered based on the published official reports from 2019.[B2]

In this thesis, a simplified calculation for the equipment ecological equivalent as a product of the impacts in other life-cycle phases, as Eq. B.2 shows.

$$\varepsilon_{iQ} = \frac{\text{design impact} + \text{magnitude (device impact)} + \text{total labor impact} + \text{magnitude (non-recycables impact)} + \text{transportation impact} + \text{magnitude (recyclables impact)}}{\text{useful life duration}} \tag{B.2}$$

In Eq. B.2, total labor work includes production, installation, and maintenance manual activities within the useful life duration are considered. Therefore, rough assumptions are met for these main factors in Eq. B.2. Transportation impact is roughly assumed to sum the impacts of transporting the equipment item to the facility from its manufacturer and from the facility to its disposal or recycling site. Now, the total mass of each machine or mold is applied to calculate the transportation impact. Design ecological impact is traditionally neglected in literature. In reality, the development phase, which can take decades, engages thousands of employees, and requires a wide range of experiments and prototype productions. This phase must have a carbon footprint. By taking a highly simplified example of design, the impact can be

based on considering the basic labor work and computer utilization in such development works for a specific equipment type. For instance, a year of development, that is carried out by a single employee, has the impact of roughly estimated 802.698 kg CO_2/year, while the computer utilization in this duration has an approximate impact of 175 kg CO_2/year . Despite the fact, that research and development projects are carried out practically by large teams for longer durations and with further direct and indirect possible ecological impacts, in this thesis the design impact is highly simplified due to the lack of reliable data about developing each equipment item in specific and elementary flows in general. Therefore, a total approximate design impact of around 977.698 kg CO_2/year · developer is considered in the design phase, while each equipment item is assigned to a unique roughly estimated development duration in working time of a single developer.

In the production, four main impacts are considered. They include the impacts of devices within the equipment as result of the roughly estimated ecological equivalent and their magnitude. The labor work carbon footprint in producing and installing these equipment items is also considered based on roughly estimated work hours for each one. Still, maintenance work is represented only by labor work and considered exceptionally as a part of production. The impact of non-recyclable materials is distinguished from recyclable ones. However, no deep investigations have been carried out to prove the recycle-ability or non-recycle-ability of these materials.

In this cradle-to-grave impact, a roughly estimated transport impact is calculated for a standard distance of 350 km. This distance is assumed for moving every equipment item from its manufacturer to the facility cite and later from the facility to disposal site at the end of its useful life. Based on weight variation, each item has a different transport impact, while the considered equivalent is 1.25×10^{-4} kg CO_2/km · kg for a heavy duty vehicle in road transportation. Paternoster storage $v_{1,4096}$ has a roughly estimated design duration of six working months. For the paternoster storage $v_{1,4096}$ in UP_1, steel components are assumed to have the total mass of around 700 kg, that is totally retrievable by a recycling impact of around 0.39 kg CO_2/kg, six devices with an approximate equivalent of 80 kg CO_2/device, and a total labor work of 120 h with the impact equivalent of 0.41 kg CO_2/h. The unwinder $v_{1,4097}$ is assumed to be designed in three working months and to have 150 kg totally recyclable steel with the same previously considered equivalent. It contains four devices with an approximate equivalent of 40 kg CO_2/device and 20 h with the same labor impact.

Cutter $v_{2,4098}$ is designed in around four working years, as the rough estimation suggests. For the cutter $v_{2,4098}$ in UP_2, the simplified ecological characterization factor ε_{4098} is assumed to contain the equivalents from 200 kg of steel that is totally recyclable, 100 kg of non-recyclable plastic oriented materials with an assumed equivalent of 2.7 kg CO_2/kg, and ten devices with an equivalent of 80 kg CO_2/device. The same approach is adopted to assume an ecological characterization factor of the ply storage $v_{2,40100}$, which has an approximate design phase of two working years. It is assumed to have 50 kg of recyclable steel and the same amount of totally recyclable aluminum, that has an approximate impact equivalent of 2 kg CO_2/kg in the collector system. It contains also a total of 32 small devices with an roughly estimated impact of around 10 kg CO_2/kg for each of them and to require labor work of around 120 h. The ply storage part of $v_{2,40100}$ has a roughly estimated 1280 kg of totally recyclable steel, 17 devices with an equivalent of 80 kg CO_2/device, and requires a total labor work of 140 h. Therefore, the total 1330 kg of totally recyclable steel, 17 devices with an equivalent of 80 kg CO_2/device as well as 32 small devices with an roughly estimated impact of around 10 kg CO_2/kg, 50 kg recyclable aluminum, and total labor work of 160 h are assumed for the entire ply storage $v_{2,40100}$. The draping robot $v_{3,40101}$ with its entire high technology devices is assumed to have a total design phase of 10 working years. For UP_3, draping robot $v_{3,40101}$ and its rail are assumed to contain around 2500 kg of recyclable steel, four devices with an equivalent impact of 400 kg CO_2/device, and total required labor work of 220 h. In this best guess assumption, the membrane press $v_{3,40102}$ has an approximate design phase of eight years and an estimated mass of 4000 kg from totally recyclable steel. The membrane press $v_{3,40102}$ contains an assumed amount of four main devices with an approximate equivalent of 500 kg CO_2/device and required a roughly estimated labor work amount of 520 h.

In UP_3 as well as UP_4, consolidation and trimming mold $v_{i,40103}$ has an approximate design phase of one month and consists of 85 kg totally recyclable aluminum. This mold requires the total amount of 15 h in labor work. In UP_4, chain robot $v_{4,40104}$ has an assumed mass of 2700 kg totally recyclable steel, contains five devices with an equivalent impact of 240 kg CO_2/device, and required a roughly estimated labor work amount of 240 h. Also in UP_4, trimming portal

$v_{4,40105}$ contains a roughly estimated 1000 kg of recyclable steel, 500 kg of recyclable aluminum, and 15 devices with an equivalent impact of 80 kg CO_2/device, while it requires approximately 750 h in labor work.

In literature, carbon footprints equivalents of carbon fiber varies in the different studies. For instance, Zhang has suggested that the characterization factor is to be 22.4 kg CO_2/kg, while Das considers it as 16.9 kg CO_2/kg.[B1] [B5] In his work Wille suggested a fiber ecological characterization factor of about 26.6 kg CO_2/kg, while Nothdurft considers an equivalent of 50 kg CO_2/kg in his work.[B6] In this case study, fiber waste $u_{2,6514}$ has the same previously mentioned re-usability ration of 0 %. However, the equivalent of 100 km transport with an approximate impact of 1.25×10^{-4} kg CO_2/km · kg is roughly assumed for the disposal of both $u_{2,6514}$ and $u_{2,6514}$. In this study, labor work has an ecological impact like all other considered input elementary flows.[B1] This hypothesis is also applied to facility and equipment input flows in this work. These elementary flows have been excluded systematically as irrelevant flows for ecological impact β in the majority of previous internal and external works. This work is examining their ecological impacts based on the available data of their equivalents. Including several direct impacts within the spectrum of ζ_j, Ψ_j, and υ_j, the work ecological impact is considered to be 0.41 kg CO_2/h . For facility $v_{ij} \in \varphi^{[\Delta s]}$, an external study results are adopted in which each quadratic meter has the approximate ecological equivalent of 183.461 kg CO_2/year · m^2.[B7] while energy consumption is around 173 kWh/year · m^2. [B8] [B9] [B10] [B11] In which, air-conditioning, lightning, and other services are covered by this energy consumption, while the adopted factor is 2.603×10^{-5} kg CO_2/m^2 · s.

Therefore, fiber ecological characterization factor ε_{6014} is assumed to be 46.8 kg CO_2/kg based on data for a similar material in a previous work. [B12] In this case study, the release film ecological factor ε_{9017} is assumed to be 2.67 kg CO_2/kg and an additional disposal impact equal to the one of fiber waste . The roughly estimated ecological characterization factors ε_{iQ} of the studied equipment types may be covered in future dedicated works. In practice, there is a lack of reliable ecological characterization factors ε_j even in the industry. Therefore, the difficulties in estimating these parameters may occur even for assessing an industrial process. The constant of performing only the preparing UP_1 is roughly estimated to be around k_1 =50 €. As a material intensive UP i, cutting UP_2 may have a constant of totally k_2 =300 € For preforming UP_3 as a unique performance, a constant of totally k_3 =75 € is assumed. Similarly, a final constant of totally k_4 =75 € is assumed for trimming UP_4 as a field advanced performance with modern technologies. Based on these assumptions, the constant of more than a UP i is the combination of there cumulative constants. However, these given values are based on rough assumptions and not information, while the facilities considered in the case study belong to DLR as nonprofit organization. As a part of adjusting the results of selected works, inflation rates are considered to be around 1.33 (€ in 2002/€ in 2019), 1.07 (€ in 2012/€ in 2019), 1.04 (€ in 2014/€ in 2019), and 1.04 (€ in 2016/€ in 2019). There is a common inhomogeneity problem with the way of calculating the various characterization factors. In practice, investment economical impact consists of all previous impacts, while ecological one considers no development phase.

[B1] Reference: Denkhaus, J. and Hilmer, P. (2014); in the previous Bibliography as [73]

[B2] Reference: erostat (2018). Strompreise nach Art des Benutzers: EUR je kWh. Technical report, European Union (EU): erostat. https://ec.europa.eu/eurostat/de/web/products-datasets/product?code=ten00117

[B3] Reference: Shuaib, N. A. and Mativenga, P. T. (2017). Carbon footprint analysis of fibre reinforced composite recycling processes. Procedia Manufacturing, 7:183–190.

[B4] Reference: Sloan, J. (2014). The vexing economics of carbon fiber manufacturing. Technical report, Composites World.

[B5] Reference: Zhang, X., Yamauchi, M., and Takahashi, J. (2011). Life cycle assessment of cfrp in application of automobile. In 18th International Conference on Composite Material. ICCM.

[B6] Reference: Nothdurft, N. and Hilmer, P. (2016); in the previous Bibliography as [233]

[B7] Reference: Biswas, W. K. (2014). Carbon footprint and embodied energy consumption assessment of building construction works in Western Australia. International Journal of Sustainable Built Environment, 3(2):179–186.

[B8] Reference: Seo, M.-S., Kim, T., Hong, G., and Kim, H. (2016). On-site measurements of CO2 emissions during the construction phase of a building complex. Energies, 9(8):599.

B9 Reference: Kovacic, I. and Zoller, V. (2015). Building life cycle optimization tools for early design phases. Energy, 92:409–419.

B10 Reference: Airaksinen, M. and Matilainen, P. (2011). A carbon footprint of an office building. Energies, 4(8):1197–1210.

B11 Reference: Alwan, Z. and Jones, P. (2014). The importance of embodied energy in carbon footprint assessment. Structural Survey, 32(1):49–60.

B12 Reference: Al-Lami, A., Hilmer, P., and Sinapius, M. (2018); in the previous Bibliography as [13]

Appendix C

MIs and MMs Qualification and Verification

To have a clear understanding of Tab. C.1, the conceptual model qualification aims to assure that MIs and MMs are assigned to the targeted elementary flows α_{ij} in the associated WSs and their WSPs properly. Hence, the spatial allocation and the setup of the sensor nodes of these methods is decisive. On the other hand, verification of the mathematical models aims to guarantee that these elementary flows α_{ij} are identified by MIs and measured by MMs accurately. Accordingly, each method is to be qualified in order to prove whether the concept behind it matches the process reality. Thus, qualification and verification are applied for all MIs and MMs from Tab. 4.8 and Tab. 4.9 respectively, as Tab. C.1 illustrates.

Table C.1 Validation steps of SWS methods

Method	Qualification	Verification
MI-(1)	In visual recognition MI-(1), it is required to assure that this method is capable of covering all relevant UPs i in their temporal and spatial boundaries. This can be achieved by checking the optical coverage of the implemented cameras SI-(1). MI-(3) and MI-(7) may be implemented for such qualification.	Furthermore, all relevant types j must be detectable in MI-(1) mathematical model. This can be verified by a conventional LCI. In practice, such accuracy percentage depends on various aspects of that specific detected object and the SIs setups [271]. In practice, videotapes may be useful verification solution.
MI-(2)	MI-(2) must be capable of detecting the persons in WSs as well as their WSPs. This can be qualified by MI-(5) or photographic documentation by the SI-(1).	The mathematical model behind MI-(2) is verified to assure its compatibility with production environment. IR-records or videotapes (if allowed) can be used for such verification.
MI-(3)	MI-(3) is to be assigned correctly to the targeted elementary flow types j within the relevant UPs i. Therefore, MI-(1), MI-(7), or photographic documentation by SI-(1) can qualify this method.	The mathematical model should match the UP i as well as elementary flow type j specifications. MI-(3) mathematical model is to be correlated with the algorithms of other methods such as MI-(7), MI-(1), as well as videotapes.
MI-(5)	Person thermal detection MI-(5) should be able to cover the WSs and their WSPs. MI-(5) is to be assigned to the relevant UPs i correctly. Here, MI-(2) or LCI based on proper videotape may qualify this method.	The mathematical model of MI-(5) should be matching the WS and WSP conditions. For instance, body and surrounding temperatures should be verified. Here, MI-(2) and videotapes if allowed can be used for such verification.
MI-(6)	MI-(6) should be referring to the machines in their WSs accurately. MI-(6) is qualified by an audit or LCI of assigned SI-(4) and the targeted machines. So, MI-(1) may be implemented in qualifying MI-(6).	The mathematical model of MI-(6) should simply correlate the electricity measurement to the associated machines. Verifying the channels is essential here. Conventional LCI and specifically energy measurement may verify the accuracy of this model.

Method	Qualification	Verification
MI-(7)	Material and tool identification MI-(7) should be assigned correctly to the appropriate spots of relevant elementary flow paths $\Delta s^{[\alpha_j]}$. MI-(1), MI-(3), videotapes, and conventional LCI can be applied to qualify this model.	The mathematical models behind MI-(7) should be verified to measure the weight changes of the correct elementary flow type j properly. This identification model can be verified by videotaping all associated paths.
MI-(8)	Facility identification MI-(8) should be qualified to assure that the WSs are covered comprehensively by all associated methods and their sensor nodes.	The mathematical models should derive the facility utilization areas and durations accurately. An audit or photographic documentation is thinkable here.
MM-(1)	With regard to qualification, material weight measurement MM-(1) is unique because no other SWS method can qualify it.	The accuracy of measuring an elementary flow weight in the mathematical model of MM-(1) may be verified by conventional LCI.
MM-(2)	Persons count MM-(2) is similar to their identification in MI-(2), while all associated WSs and WSPs should be accurately covered. It must distinguish between the different persons, which MI-(5) unable of in the current SWS.	The counting mathematical model should address the WSs and WSPs requirements. Moreover, it must have a sufficient pattern to distinguish different persons. Videotapes and photographic documentation can verify that.
MM-(3)	MM-(3) should accurately cover labors only in the targeted WSs and WSPs with no redundancy or neglect. Optical labor work duration measurement MM-(3) is qualified by MM-(8).	Similar to MM-(2), MM-(3) mathematical model should address the WSs and WSPs requirements. Again, LCI based on videotapes (if allowed) may verify this method as well.
MM-(8)	Again, the correct coverage of WSs and WSPs is crucial here. Likewise, thermal labor work measurement MM-(8) may be qualified by MM-(3).	MM-(3) mathematical model must accurately assign human body occurrences temporally and spatially. A proper videotapes is sufficient for verification here too.
MM-(4)	MM-(4) should cover the operation time of associated machines. In SWS, no other method is qualifying MM-(4).	There is no verification solutions other than using further SI-(4). Videotapes and IR-records may verify operating durations partially.
MM-(9)	MM-(9) must measure the appearance time of a tool or mold. This should cover the entire WSs and WSPs. MM-(9) is qualified through MM-(10) and MM-(11) if applicable.	MM-(9) equations are verified by LCI based on videotapes from these SI-(1). Verifying tools time is more complex sophisticated than molds, due to the tools motion.
MM-(10)	With a functionality similar to MM-(9), MM-(10) can be qualified through MM-(9) and MM-(11) if applicable.	Again, this is verified by LCI based on videotapes from these SI-(1). Like MM-(9), tools and molds comparison is applied here too.
MM-(11)	MM-(11) must measure the utilization durations of correct tools or molds. MM-(11) is qualified through MM-(9) and MM-(10).	MM-(11) algorithms should distinguish between the tools weight accurately. This can be also verified by LCI from videotapes.
MM-(5)	MM-(5) is a common robust method. Still, no other method in SWS can qualify all aspects of this one.	Similar to MM-(4), no verification solutions other than using further SI-(4). Partially, this can be also verified based on videotapes.
MM-(6)	MM-(6) should measure the associated process time accurately. Qualifying all other adopted methods is addressing this one as well.	A proper videotaping (if allowed) of all associated activities in every UP i in relevant WSs and WSPs is verifying the mathematical model.

Method	Qualification	Verification
MM-(7)	MM-(7) is similar to MM-(6), while it should accurately measure areas of relevant WSs and WSPs. Again, qualifying all other adopted methods is addressing this one as well.	A proper videotaping or at least photographic documentation of all associated WSs and WSPs is verifying the mathematical model behind MM-(7) too.

It is concluded from Tab. C.1 that the majority of discussed methods can be qualified by other suggested method. However, material weight measurement MM-(1) and equipment operation energy MM-(5) have exceptionally no qualifying alternatives. In practice, both MM-(1) and MM-(5) are commonly implemented methods with available qualification approaches provided by the manufacturers or suppliers of their hardware as sensor nodes. After qualifying the conceptual models and verifying the mathematical ones of both MIs and MMs, SIs and SMs are validated in Tab. C.2.

Table C.2 Validation of SWS sensor nodes

Method	Validation
SI-(1) in MI-(1)	The data accuracy of SI-(1) is validated by videotaping the considered WSs of the case study.
SI-(1) in MI-(2)	The data accuracy of SI-(1) is validated by a comprehensive videotapes and IR-records in considered WSs of the case study.
SI-(1) and SI-(1a) in MI-(3)	This is validated by a comprehensive videotape in considered WSPs of the case study.
SI-(3) in MI-(5)	IR-records or videotapes (if allowed) are used to perform a detailed LCI here.
SI-(4) in MI-(6)	An audit based on proper photographs is carried out here.
SI-(5) in MI-(7)	A comprehensive LCI that is extracted from proper videotapes is thinkable here.
All sensor nodes in MI-(8)	Photographic documentation that is concluded from the videotapes is implemented to validate the outputs of various sensor nodes regarding this aspect.
SI-(5) in MM-(1)	Only conventional LCI from sensor nodes is applicable here.
SI-(1) in MM-(2)	A proper videotape is sufficient for the validation.
SI-(1) in MM-(3)	IR-record is implemented here.
SI-(3) in MM-(8)	IR-records or videotapes with proper setups are used.
SI-(4) in MM-(4)	Appropriate videotapes or IR-records may validate SI-(4) results here as well.
SI-(1) and SI-(1a) in MM-(9)	Again, a proper videotape is sufficient for the validation of this sensor node.
SI-(1) in MM-(10)	The same videotaping approach is applicable here as well.
SI-(5) in MM-(11)	Videotaping approach is applicable here too.
SI-(4) in MM-(5)	As it is mentioned before, only similar SI-(4) can validate the data of these SMs.
All sensor nodes in MM-(6)	Proper videotapes can be used to establish a detailed LCI regarding the data from all relevant sensor nodes serving this method.
All sensor nodes in MM-(7)	Again, proper photographic documentation or videotapes can be used to establish a detailed LCI to validate the results of all associated sensor nodes serving this method.